

# **The Tungsten-Promoted Dearomatization of *N*-Sulfonyl Pyridinium Salts for Novel Organic Synthesis**

Jonathan David Dabbs  
Mint Hill, North Carolina

B.S., Biochemistry, Grove City College, 2018

A Dissertation Presented to the Graduate Faculty of the University of Virginia in Candidacy for  
the Degree of Doctor of Philosophy

Department of Chemistry

University of Virginia  
November 2023

## Abstract

**Chapter 1:** Previously reported dearomative transformations to pyridine are surveyed. Nucleophilic and electrophilic aromatic substitutions are surveyed first and followed by dearomatization strategies, including Birch reductions, cycloadditions, hydride reductions, and nucleophilic additions to *N*-activated pyridiniums. However, the main approach emphasized is transition metal mediated, which is done *via* hexahapto ( $\eta^6$ ) and dihapto ( $\eta^2$ ) coordination of pyridine to a metal center. The  $\eta^2$  coordination of pyridine to tungsten and molybdenum fragments is specifically explored as the work contained in this thesis herein expands upon these works.

**Chapter 2:** *N*-acetyl pyridinium  $\eta^2$ -bound to a {WTP(NO)(PMe<sub>3</sub>)} ([W]) capably generates a range of selectively functionalized compounds, including tetrahydropyridines, isoquinuclidines, and merocyanine; however, each of these syntheses are plagued with amide rotational isomers visible in NMR spectroscopy. Because an electron-withdrawing group is necessary, sulfonyl *N*-protecting groups are explored herein. Although a [W]-*N*-tosyl pyridinium complex retains chemistry established by the acetyl system, this system promotes a Zincke-like dihydropyridine ring opening that allows the access of terminally functionalized  $\alpha,\gamma$ -dienyl imines and highly functionalized THPs

**Chapter 3:** Due to its efficacy as a cocaine agonist, methylphenidate (MPH) is of interest as a potential therapeutic for cocaine addiction. While numerous derivatives of MPH have been investigated for their potential medicinal value, the functionalization of the piperidine ring has not been explored. The pyridine borane ligand in [W]-pyBH<sub>3</sub> is dearomatized by the metal and can be elaborated to the analogous  $\eta^2$ -mesylpyridinium complex. Installing a methyl phenylacetate moiety at the C2' position *via* a Reformatsky reaction followed by a tandem protonation/nucleophilic addition sequence results in a library of *erythro* MPH analogues functionalized at the piperidyl C5' position. The functional group is added chemoselectively to C5', *cis* to the methyl phenylacetate. Repeating this procedure with an enantioenriched source of the tungsten reagent results in enantioenriched MPH derivatives. All identities of the newly reported compounds are supported by comprehensive 2D NMR and HRMS or crystallographic data. This work was conducted in conjunction with Megan Ericson, who contributed to nucleophile explorations, organic oxidations, and DFT studies.

**Chapter 4:** Despite longstanding use of deuterium for determining organic and biochemical mechanisms, the advent of readily available deuterated materials and new methods of deuterium-hydrogen exchange have led to a resurgence in incorporating deuterium into the Active Pharmaceutical Ingredient of medicines. Due to its abundance in drugs, piperidine is an attractive scaffold for selective deuteration. This work explores the selective syntheses of  $d_0$ - $d_8$  tetrahydropyridine isotopomers by treating a mesylated  $d_x$ -pyridine dihapto-coordinated to [W] with stepwise deuterides and deuterons. These compounds were analyzed *via* Molecular Rotational Resonance (MRR), a highly sensitive technique that distinguishes the various isotopomers and isotopologues by their unique moments of inertia. Deuterated *erythro*-methylphenidate analogues were then generated by this approach. This study demonstrates a general method for synthesizing

libraries of free and substituted deuterated tetrahydropyridines. This work was conducted in conjunction with Martin Holdren and Brooks Pate, who contributed by analyzing deuterated THPs *via* MRR.

**Chapter 5:** The [W]-promoted Zincke-like ring opening process established chapter 2 was further probed with  $\pi$ -donating amine nucleophiles. Primary aliphatic amines were found to generate *N*-alkylated DHPium compounds with a variety of amines *via* a pyridine ring-opening ring-closing nitrogen transplant. Furthermore, novel bicyclic alkaloid scaffolds were accessed from intramolecular ring-closures.

**Chapter 6:** This is a survey of the research described herein, comparing the second generation [W]-*N*-sulfonyl system to the analogous *N*-acetyl system. Potential future extensions for each project are also described as well as novel independent projects.

## Copyright Information

Chapter 3 is a published work which is copyright by the American Chemical Society. This work is reproduced herein in accordance with Section II.1 of the American Chemical Society Journal Publishing Agreement. Chapters 2, 4, and 5 are drafts of future manuscripts and may subsequently be published in whole or part.

**Chapter 3:** Dabbs, J. D.;<sup>#</sup> Ericson, M. N.;<sup>#</sup> Wilde, J. H.; Lombardo, R. F.; Ashcraft, E. C.; Dickie, D. A.; Harman, W. D. The Tungsten-Promoted Synthesis of Piperidyl-Modified *erythro*-Methylphenidate Derivatives. *ACS Cent. Sci.* **2023**, 7 (7), 1775-1783.

<sup>#</sup> joint first authorship

## Acknowledgements

During my time here at UVA, the film adaptation of the book ‘Dune’ came out. Upon the suggestion of my brother, I ended up reading the first book before seeing the movie to both appreciate the film more while also taking a break from the dense reading of chemistry journals and textbooks. While reading, I was struck by the following quote, “The Fremen were supreme in that quality the ancients called ‘spannungsbogen’ -- which is the self-imposed delay between desire for a thing and the act of reaching out to grasp that thing.” The quote references the Fremen, a people native to the harsh desert planet Arrakis who were abundantly resourceful and single-mindedly focused on the decades-long process of transforming their desert planet into a lavish garden. Doing so required grit, ingenuity, and self-denial for a future that they would likely not even get to enjoy the fruits of their labors.

Upon reading this quote, this mindset of patience and short-term self-denial for the prospect of future gain made sense to me as it was what I and, I imagine, many other grad students console themselves with during the dogdays of obtaining their degree. Although obtaining a Ph.D. is gratifying, one frequently feels life passing by as you see your peers around you from high school and college begin their careers, start families, and travel abundantly and lavishly all while laying down their roots in a community they know they can invest in for the long haul. Now, grad schools don’t force you to renounce these things, but they can be difficult to jointly pursue. So how would I console myself when I felt like I was being left behind? With the idea that I too was practicing ‘spannungsbogen,’ and that graduate school would simply be a season of relative ‘blah’ bookended by good times (college and postgrad life) that I just had to grind through like a good TV show with one bad season. What a tremendously stupid outlook. Ultimately, my time here, which I had written-off, has become a time of incredible growth and fulfillment. While, sure, some of this can be attributed to nice hiking nearby, a decent Charlottesville restaurant scene, and mild winters, this is overwhelmingly attributed to the communities of the Harman lab, the UVA Chemistry Department, and Charlottesville as a whole, all of whom played a critical role in supporting me in the pursuit of this degree.

I would be remiss to not begin with thanking Dean. To work with Dean is to be supported in every facet. During the fall/winter of 2020/2022, which was just after the fever dream of the COVID shutdown, I was deeply mired in a post-candidacy slump. My work was both stalled and directionless, and my confidence was plummeting. But Dean’s faith in me never wavered even when my own had grown fractious cracks. My gratitude to Dean stems from both his supportiveness as well as the lab culture he has engendered. The Harman lab strikes a wonderful balance of personalities that spans a broad spectrum of strengths, but that ultimately is characterized as a lab of shared discovery and mutual support. Whether we are getting crushed by Dean in croquet, straining ourselves to think of a movie two actors have both appeared in, or facing down some goblins in D&D, the Harman lab functions as a part-time science factory and a part-time Chuck E. Cheese’s.

This work was greatly contributed to by members of the Harman Lab both past and present. In particular, I’d like to mention Jacob Smith and Justin Wilde, both of whom mentored me in my early days. Thank you for your endless patience, for not losing your cool when I royally screwed up seemingly daily, and for fostering my curiosity with your encouragement. To my fellow 2018

entrant Justin Weatherford-Pratt, watching your star ascend was truly inspiring. You have a chemical instincts that are only matched by your incredible drive, and I sincerely look forward to working together again at St. Jude's. To my first (successful) mentee Megan Ericson, working alongside you was truly a pleasure. There's just a deeper bond between those who have swam in the deep murky depths of pyridine like we have. Few understand the struggles like you! Like Justin, your research has launched into orbit, and seeing you juggle your teaching, research, mentoring, and leadership like an orchestra conductor has been awe-inspiring. To Caleb, my other fellow pyridine coworker, sorry for putting it back on your plate after you thought you escaped! You have taken an unconventional pathway in pursuit of your degree, but you have stepped up and quickly established yourself in the lab. Thank you for your kindness, your willingness to discuss anything (chemistry or otherwise), and your amenability during my late chemist-zilla days. To other members of the Harman Lab (Paolo, Jeremy, Daniel, Mason, Ben, Josh, & undergrads), please understand that each of you are an integral part of the lab and have transformed my experience here for the better, but it's 4:00 AM and I need to start wrapping this up.

Many staff within the Chemistry Department have also been wonderful to work alongside. Earl has likely grown all-too-familiar with me knocking on his office door to let him know that yet another pump in our lab broke. I cannot even begin to calculate the amount of time you saved me by running my HRMS samples, thus sparing me from the nightmare that is acquiring publishable EA data. This thesis will feature numerous crystal structures obtained *via* SC-XRD, none of which would have been acquired/determined without the equal parts determined, kind, and helpful Diane. Her ability to derive a structure from the sorriest excuse of crystals can only be described as a certain magical touch. Her patience and willingness to educate will be sorely missed. I also recall the many times I had to call upon the expertise of Jeff to help with tuning Echo for a  $^{31}\text{P}$  NMR. Sorry for taking so long to learn how to manually tune, Jeff! Thank you for your patience in working with me. I would also like to acknowledge the members of my committee: Drs. Gunnoe, Hilinski, and Pu, for overseeing me through candidacy and through my defense. Thank you for your time and attention as well as your fairness throughout this entire process.

To my wonderful friends from home and from college, (particular thanks to Mark, Zach, Spencer, Dan, Danny, Matt, Sam, Connor, Tim, Schuyler, and Hunter) thank you for the holiday get-togethers, the out-of-the-blue phone calls, the vacations (special shout out to the Faroe Islands: sorry to the locals for those loud Americans from 2019), and encouragement from afar. Many times one finds themselves needing to escape Charlottesville to maintain sanity, and I am unbelievably grateful to each of you for your reminders, overtly or accidentally, that there's a far bigger world outside of the lab, and that tunnel vision is not healthy. And I always look forward to Tuesday night phone calls and the Star Wars/LOTR memes that make the rounds.

Finally, this simply doesn't happen without the most wonderful family. You won't find a group of people who are not familiar with silence and yet more willing to endure listening to my scientific jargon than them. Growing up, when I heard people thanking their 'supportive' friends and family, I conceptualized them receiving an 'atta boy' every now and then and, perhaps, a little bit of financial or material help if needed. What I didn't imagine was them receiving advice on everything from interviewing to cooking tips by phone. Or multi-hour long debrief sessions with Nick about my recent progress in any Stormlight Archive novel. Or entire coolers full of frozen

food to stock up my freezer. Your love and support made you feel close even when you were far away.

To each of you, and to other wonderful unspokens: for your love, efforts, and support on my behalf, I am enduringly and overwhelmingly grateful. How do you thank those to whom you owe so much? How do you thank the sun for rising and providing you with its Light daily? I don't really know. They strike me as equally ridiculous questions due to the tremendous amount of one-way debt owed in each case, and I'm not that insightful. But I would imagine the answer begins with resisting the urge to use has been given to me for personal aggrandizement, and instead using it for the well-being of others. To be a mirror to reflect the Light that has shone for you so that it may shine for others. To much is given, much will be required.

SDG.

## Table of Contents

<b>Abstract</b>	<b>(2-3)</b>
<b>Copyright Information</b>	<b>(4)</b>
<b>Acknowledgements</b>	<b>(5-7)</b>
<b>Table of Contents</b>	<b>(8-10)</b>
<b>List of Abbreviations</b>	<b>(11-12)</b>
<b>List of Figures</b>	<b>(13-14)</b>
<b>List of Tables</b>	<b>(14)</b>
<b>1. A Survey of Organic Transformations <i>via</i> Pyridine Dearomatization</b>	<b>(15-49)</b>
1.1. Introduction	(16-17)
1.2. Pyridine and Applied Dearomatization	(17-19)
1.2.1. Aromaticity	(17)
1.2.2. Alkaloids in Drug Discovery	(18)
1.2.3. Piperidine Synthesis <i>via</i> Ring Closures	(18-19)
1.3. Pyridine Substitution Reactions	(20-23)
1.3.1. Pyridine EAS Reactions	(20)
1.3.2. Pyridine NAS Reactions	(20-21)
1.3.3. Pyridine- <i>N</i> -Oxide Substitution Reactions	(21-23)
1.3.4. Alternative Pyridine Substitution Strategies	(23)
1.4. Pyridine Dearomatization Strategies	(24-27)
1.4.1. Birch Reduction	(24-25)
1.4.2. Hydrogenations/Hydride Additions	(25-26)
1.4.3. Cycloadditions	(26-27)
1.5. Pyridine Dearomatization <i>via</i> Nucleophilic Additions <i>N</i> -Activated Pyridinium Salts	(27-31)
1.5.1. Nucleophilic Additions to <i>N</i> -Acyl Pyridiniums	(27-29)
1.5.2. Nucleophilic Additions to <i>N</i> -Alkyl Pyridiniums	(29-30)
1.5.3. Nucleophilic Additions to <i>N</i> -Heteroatomic Pyridiniums	(30)
1.5.4. Conclusion	(31)
1.6. Transition-Metal Mediated Pyridine Dearomatization	(31-40)
1.6.1. Transition-Metal Catalyzed Pyridine Dearomatization	(31-32)
1.6.2. Pyridine Dearomatization <i>via</i> $\eta^6$ Coordination to a Transition Metal	(32)
1.6.3. Pyridine $\eta^2$ Coordination to a Transition Metal	(33-34)
1.6.4. Pyridine Dearomatization <i>via</i> $\eta^2$ Coordination to a Transition Metal	(34-38)
1.6.5. Featured Chemistry	(38-40)
1.7. References	(40-49)
<b>2. Synthesis of <math>\alpha,\gamma</math>-Dienyl Tosylimines and Highly Functionalized Tetrahydropyridines <i>via</i> a Tungsten <math>\eta^2</math>-<i>N</i>-tosyl Pyridinium Salt</b>	<b>(50-66)</b>
2.1. The Rotamer Problem with [W]- $\eta^2$ - <i>N</i> -Acetyl-Pyridines	(51)
2.2. Alternative Nitrogen Protecting Groups	(52-54)
2.3. Nucleophilic Additions to [W]- $\eta^2$ - <i>N</i> -Tosyl Pyridinium	(54-57)
2.4. DHP Ring Opening	(58-61)
2.5. Protonation to Allyl Complex	(61-62)
2.6. Nucleophilic Additions to Allyls	(63-64)
2.7. Oxidative Liberations	(64-65)
2.8. Conclusions	(65)
2.9. References	(65-66)



<b>3. The Tungsten-Promoted Synthesis of Piperidyl-Modified <i>erythro</i>-Methylphenidate Derivatives</b>	<b>(67-87)</b>
3.1. Introduction	(68-70)
3.2. Generation of Highly Enriched Mesylated Pyridinium Complex	(71-72)
3.3. Aza-Reformatsky Ester Installation	(72-73)
3.4. Chiral Determination of <b>35D</b>	(73-75)
3.5. Protonation of <b>35D</b>	(75-76)
3.6. Nucleophilic Additions to <b>37P</b>	(76-78)
3.7. Oxidative Demetallation of Organics	(78-79)
3.8. MPH THP Hydrogenation	(79-81)
3.9. [W] Enantioenrichemnt for Asymmetric MPH Synthesis	(81-84)
3.10. Conclusions	(84)
3.11. References	(84-87)
<b>4. Syntheses and Quantitative Analyses of Selectively Deuterated Tetrahydropyridine Isotopologues and Isotopomers</b>	<b>(88-113)</b>
4.1. Introduction	(89-91)
4.2. Synthesis of [W] $\eta^2$ -Dihydropyridine Complexes	(91-93)
4.3. Synthesis of [W] $\eta^2$ -Tetrahydropyridine Complexes	(93-94)
4.4. Acid-Promoted Ring-Opening of THP Complexes	(94-95)
4.5. Synthesis of High-Deuterium THP Complexes ( <i>ds-ds</i> )	(95-98)
4.6. Synthesis of Methylphenidate Isotopologues/-mers	(98-99)
4.7. THP Oxidative Demetallations	(100-101)
4.8. MRR Analysis of THPs	(101-106)
4.9. Analysis of MPH THPs	(107)
4.10. Catalytic Hydrogenation of THPs	(107-108)
4.11. Asymmetric Synthesis	(108-109)
4.12. Conclusions	(109-111)
4.13. References	(111-113)
<b>5. Pyridine Nitrogen Transplant <i>via</i> a Tungsten-Promoted Zincke-like Ring-Opening/Ring-Closing Cascade of 2-Aminodihydropyridines</b>	<b>(114-123)</b>
5.1. Introduction: Accessing <i>N</i> -Alkyl Piperidines	(115-116)
5.2. Zincke Ring Opening/Ring Closing Cascade	(116-119)
5.3. Nitrogen Transplants	(119-120)
5.4. Bicyclics	(120-121)
5.5. Iminium Functionalizations	(121-122)
5.6. Discussion	(122)
5.7. Reference	(122-123)
<b>6. Concluding Remarks</b>	<b>(124-130)</b>
6.1. General Comments	(125)
6.2. Summary of Chapter 2	(125-126)
6.3. Novel Piperidine-Containing Drug Analogues	(126)
6.4. Novel Deuterated THPs	(127)
6.5. Functionalizing Linear Amines	(127-128)
6.6. Expanding the Ring Opening/Closing Chemistry	(128-130)
6.7. References	(130)
<b>Appendix A: General Methods</b>	<b>(131-133)</b>
<b>Appendix B: Chapter 2 Data</b>	<b>(134-194)</b>
Compound Synthetic Methodologies and Characterizations	(135-162)
NMR Spectroscopy	(163-190)

SC-XRD Data	(191-194)
<b>Appendix C: Chapter 3 Data</b>	<b>(195-268)</b>
Compound Synthetic Methodologies and Characterizations	(196-222)
NMR Spectroscopy	(223-251)
Computational Methods, DFT Geometry Optimization, and DFT Analysis for <b>35D</b>	(252-255)
Chiral HPLC Parameters	(256)
SC-XRD Data	(257-268)
<b>Appendix D: Chapter 4 Data</b>	<b>(269-381)</b>
Compound Synthetic Methodologies and Characterizations	(270-297)
NMR Spectroscopy	(298-358)
SC-XRD Data	(359-362)
Molecular Rotational Resonance Spectroscopy Results	(363-380)
References	(381)
<b>Appendix E: Chapter 5 Data</b>	<b>(382-410)</b>
Compound Synthetic Methodologies and Characterizations	(383-395)
NMR Spectroscopy	(396-408)
SC-XRD Data	(409-410)

## List of Abbreviations/Symbols

acetonitrile	MeCN
anhydrous magnesium sulfate	MgSO <sub>4</sub>
aqueous sodium bicarbonate	NaHCO <sub>3</sub>
benzoyl	Bz
benzyl chloroformate	Cbz
benzyl magnesium chloride	BnMgCl
coordination diastereomer ratio	c.d.r.
cyclopentadienyl	Cp
dichloroethane	DCE
dichloromethane	DCM
diethyl ether	Et <sub>2</sub> O
diethylzinc	ZnEt <sub>2</sub>
dimethoxyethane	DME
dimethylacetamide	DMA
dimethylzinc	ZnMe <sub>2</sub>
diphenylammonium triflate	DPhAT
dihapto	$\eta^2$
dihydropyridine	DHP
dihydropyridinium	DHPium
ditertbutylpyridine	DTBP
electrophilic aromatic substitution	EAS
ethyl acetate	EtOAc
hard-soft acid/base	HSAB
hexahapto	$\eta^6$
highest occupied molecular orbital	HOMO
isopropylmagnesium bromide	<i>i</i> PrMgBr
kappa- <i>N</i> coordination	$\kappa$ - <i>N</i>
lithium dimethyl malonate	LiDiMM
lowest unoccupied molecular orbital	LUMO
<i>meta</i> -chloroperoxybenzoic acid	mCPBA
methanesulfonic anhydride	Ms <sub>2</sub> O
methanol	MeOH
methyl bromoacetate	MBA
methyl $\alpha$ -phenyl bromoacetate	MAPBA
methylmagnesium bromide	MeMgBr
methyl trimethylsilyl dimethylketene acetal	MTDA
methylvinylketone	MVK
nucleophilic aromatic substitution	NAS
<i>para</i> -toluenesulfonyl	tosyl
propionitrile	EtCN
pyridine borane	pyrb
saturated aq. sodium bicarbonate	NaHCO <sub>3</sub>
singly occupied molecular orbital	SOMO
sodium borodeuteride	NaBD <sub>4</sub>
sodium borohydride	NaBH <sub>4</sub>

sodium cyanide	NaCN
sodium tertbutoxide	NaOtBu
<i>tert</i> -butyloxycarbonyl	boc
tetrahydrofuran	THF
tetrahydropyridine	THP
toluenesulfonyl	Tosyl/Ts
toluenesulfonic anhydride	Ts <sub>2</sub> O
triethylamine	TEA
triflate	-OTf
triflic acid	TfOH
triflic acid-d <sub>1</sub>	TfOD
trifluoroacetyl	TFA
triisopropylsilyl	TIPS
trimethylsilyl cyanide	TMSCN
trimethylsilyl dimethylketene acetal	MTDA
2,3-dichloro-5,6-dicyanobenzoquinone	DDQ
{Wtp(NO)(PMe <sub>3</sub> )}	[W]

## List of Figures

### Chapter 1

Figure 1.1	Pyridine	(17)
Figure 1.2	Piperidine Containing Drugs	(18)
Figure 1.3	Piperidine Synthesis	(19)
Figure 1.4	Pyridine- <i>N</i> -Oxide Chemistry	(22)
Figure 1.5	Pyridine Dearomatization	(25)
Figure 1.6	Nucleophilic Additions to Pyridinium Salts	(28)
Figure 1.7	Pyridine Dearomatization <i>via</i> Metals	(34)
Figure 1.8	Additions to [Mo] $\eta^2$ -Bound Pyridine	(35)
Figure 1.9	Additions to [W] $\eta^2$ -Bound Pyridine	(37)
Figure 1.10	This Work	(39)

### Chapter 2

Figure 2.1	[W]-Pyridine Amide Rotamers	(51)
Figure 2.2	Alternate <i>N</i> -Protecting Groups	(53)
Figure 2.3	1 <sup>st</sup> Nucleophilic Additions	(54)
Figure 2.4	SC-XRD of <b>7P</b>	(55)
Figure 2.5	Additions to Pyridine	(56)
Figure 2.6	Stereochemical assignments of <b>15D</b>	(57)
Figure 2.7	[W]-DHP Ring Opening	(58)
Figure 2.8	SC-XRD of <b>17D</b>	(59)
Figure 2.9	Comparable Ring Openings	(60)
Figure 2.10	DHP Protonation to Allys	(62)
Figure 2.11	[W]-THP Synthesis	(63)
Figure 2.12	THP Organic Synthesis	(64)

### Chapter 3

Figure 3.1	MPH Isomers, MPH Analogues, and This Work	(68)
Figure 3.2	MPH Retrosynthesis <i>via</i> [W] Bound Pyridine	(70)
Figure 3.3	Reformatsky Additions	(72)
Figure 3.4	<i>Erythro/threo</i> Determination <i>via</i> NOESY	(74)
Figure 3.5	SC-XRD of <b>37</b>	(76)
Figure 3.6	Tandem Additions to <b>35D</b>	(77)
Figure 3.7	Oxidative Demetallations	(79)
Figure 3.8	Hydrogenated MPH THPs	(80)
Figure 3.9	NOESY Spectrum of enamine	(81)
Figure 3.10	Asymmetric MPH Synthesis	(82)

### Chapter 4

Figure 4.1	Previous Works & This Work	(90)
Figure 4.2	Additions to [W]-Mesyl Pyridinium	(92)
Figure 4.3	SC-XRD of <b>60D</b> and <b>62</b>	(93)
Figure 4.4	THP Ring Opening	(94)
Figure 4.5	Synthesis and Additions to <i>d</i> <sub>5</sub> - <b>33D</b>	(96)
Figure 4.6	MPH Isotopologues/-mers	(98)

Figure 4.7	Oxidative Demetallations	(100)
Figure 4.8	Isotopic Impurity Pathways	(104)
Figure 4.9	THP Hydrogenations	(108)
Figure 4.10	Asymmetric THP Isotopologue Synthesis	(109)
Figure 4.11	Pyridine Borane Ligands	(110)
<b>Chapter 5</b>		
Figure 5.1	Pyridine Alkylations	(115)
Figure 5.2	Initial Amine Additions	(117)
Figure 5.3	Secondary Amines & Mechanism Proposals	(118)
Figure 5.4	Monoaminations	(120)
Figure 5.5	[W] Bicyclic Ring Closures	(120)
Figure 5.6	SC-XRD of <b>78</b> and <b>79</b>	(121)
Figure 5.7	Iminium Functionalizations	(122)
<b>Chapter 6</b>		
Figure 6.1	This Work	(125)
Figure 6.2	Troxipide Derivatives	(126)
Figure 6.3	Expanding Deuterated THPs	(127)
Figure 6.4	[W]-THP Ring Openings	(128)
Figure 6.5	Expanding Ring Opening/Closing Chemistry	(129)

### List of Tables

Table 4.1	Compounds Detected <i>via</i> MRR for Each Sample	(103)
Table 4.2	<sup>1</sup> H NMR Integrations & MRR data at C2, C3, and C6	(106)
Table 4.3	Deuterium Incorporation at each ring proton for MPH	(107)

# Chapter 1

## A Survey of Organic Transformations *via* Pyridine Dearomatization

## 1.1. Introduction

The widespread implementation of high-throughput screening allows for researchers to rapidly investigate large compound libraries for promising drug leads. This technology, which is capable of screening upwards of 100,000 molecules per day, has drastically increased the demand for molecule libraries to the point that organic synthesis is now the “rate-limiting step of the drug-discovery process.”<sup>1</sup> To meet this demand, synthetic chemists are turning to efficient and reliable chemical reactions capable of swiftly introducing molecular complexity. Brown and Boström determined that 19 of the 20 most commonly used reactions in medicinal chemistry in 2014 were also used in 1984.<sup>2</sup> Areas of chemical space accessible by these reactions heavily overshadow other areas accessible by lesser used reactions, thereby limiting the structural diversity within the field.<sup>3</sup>

Furthermore, many of these commonly utilized reactions, including the Suzuki-Miyaura coupling, Sonogashira coupling, and the Wittig reaction, saturate libraries with compounds rich in  $sp^2$ -hybridized atoms. Drug candidates undergoing clinical trials demonstrate higher rates of attrition when they contain fewer stereocenters and a greater percentage of  $sp^2$ -hybridized atoms due their increased overall flat architecture that promotes less-specific binding to off-targets.<sup>4,5</sup> The pharmaceutical industry is facing declining R&D productivity while also increasingly losing crucial revenue as patents on previously developed drugs expire, thus amounting to an untenable business model for many companies critical for global public health.<sup>6</sup> To summarize, synthetic chemists responsible for assembling molecular and fragment libraries are producing potential drug leads that only reflect a small pocket of the vastness of chemical space, and the products that are produced are flawed in design, resulting in the loss of billions of dollars, decades of wasted time,



and the continued suffering of those afflicted with ailments for which cures and/or treatments remain undeveloped when drug candidates undergoing clinical trials fail.

## 1.2. Pyridine and Applied Dearomatization

### 1.2.1. Aromaticity

Assembling higher quality drug candidate libraries with increased topologically complexity requires the development of novel synthetic tools. Theoretically, the high degree of unsaturation aromatic molecules possess ideally suits them for assembling complex small molecules containing highly functionalized ring scaffolds. The diverse range (Figure 1.1A), abundance, and low cost of aromatic molecules, or arenes, further reinforce this notion. However, arenes are characterized by a state of aromaticity, which is when a molecular ring scaffold contains  $(4n + 2) \pi$  electrons delocalized around continuous coplanar p orbitals of the ring (Figure 1.1B). The delocalized electrons confer notable thermodynamic stability on molecules from resonance.

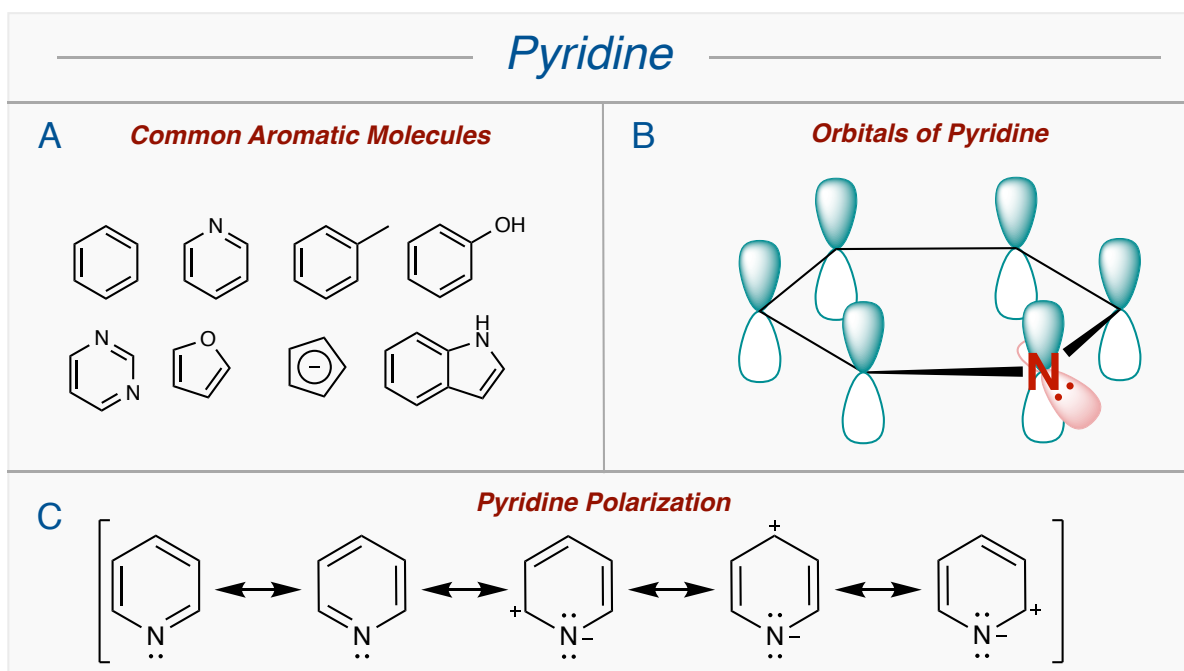


**Figure 1.1:** (A) Several common aromatic molecules. (B) The coplanar p orbitals and lone pair orbital of pyridine. (C) Resonance structures show the electron deficiency on the  $\alpha$  and  $\gamma$  positions, making them susceptible to nucleophilic attack.

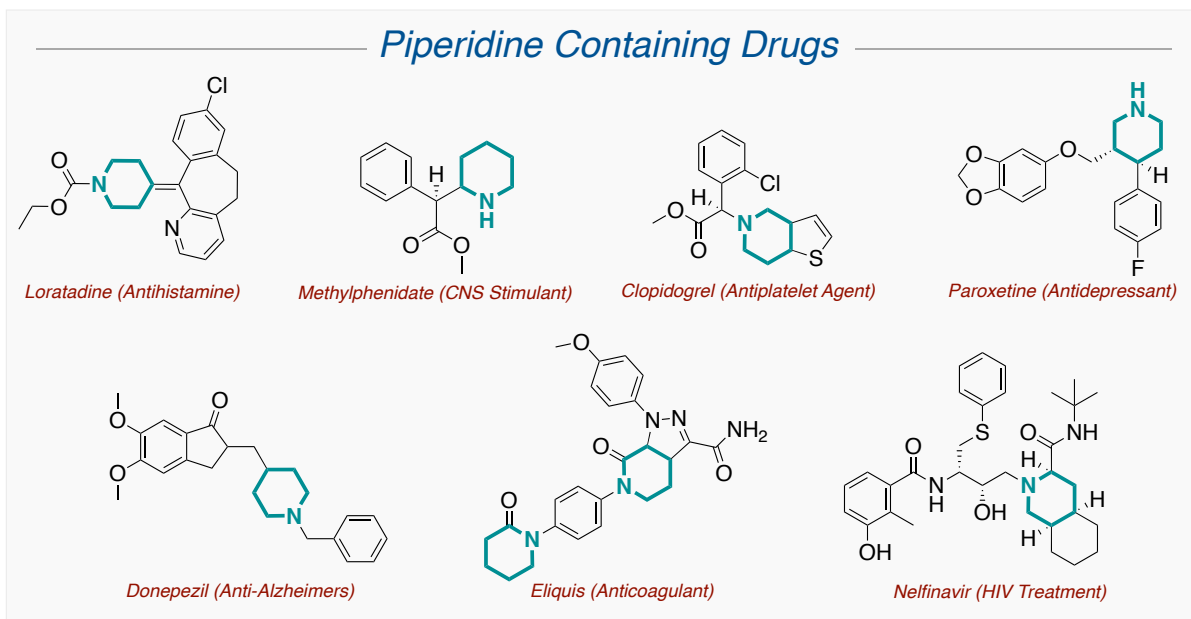


**Figure 1.2:** Piperidine is a commonly occurring moiety in FDA-approved small molecule drugs.

### 1.2.2. Alkaloids in Drug Discovery

When designing molecular libraries for drug-lead screening, the presence of stereocenters and  $sp^3$ -hybridized atoms are important considerations. Another important factor is the type of functionality installed on the small molecule. Nitrogen heterocycles are privileged architectures in pharmaceutical design, and numerous natural products are alkaloids.<sup>7</sup> Of all unique small-molecule drugs in the FDA database, 59% of them contain at least 1 nitrogen heterocycle. The most commonly occurring nitrogen heterocycle in drugs is piperidine, which is prevalent in many different classes of drugs (Figure 1.2). Assembling drug candidate libraries of highly-functionalized alkaloids that are also rich in stereocenters would provide potential drug candidates of exceptional quality as they are comprised of structural features that have correlated with higher degrees of success in clinical trials.

### 1.2.3. Piperidine Synthesis via Ring Closures

There are two primary retrosynthetic approaches for accessing functionalized piperidines: heteroatomic chain ring closures and pyridine dearomatization (Figure 1.3A). Ring closures are

primarily conducted through the intramolecular cyclization of amine chains<sup>8</sup> bearing either a leaving group<sup>9-12</sup> or an alkene (Figure 1.3B).<sup>13</sup> Similar intramolecular cyclizations occur with chains containing a terminal imine group.<sup>14,15</sup> Alternatively, intermolecular cyclizations occur either between terminal amine chains and short carbon substrates<sup>11,16</sup> or carbon chains and short nitrogen substrates.<sup>17-19</sup> Several of these methods utilize transition metal catalysts, including palladium,<sup>20</sup> nickel,<sup>21</sup> iridium,<sup>17</sup> and rhodium<sup>18</sup> while organo- and photocatalytic methods remain underdeveloped. Collectively, these cyclizations, while numerous and well-designed, could be improved upon by a highly modular method capable of highly selective asymmetric synthesis with a wide functional group tolerance.

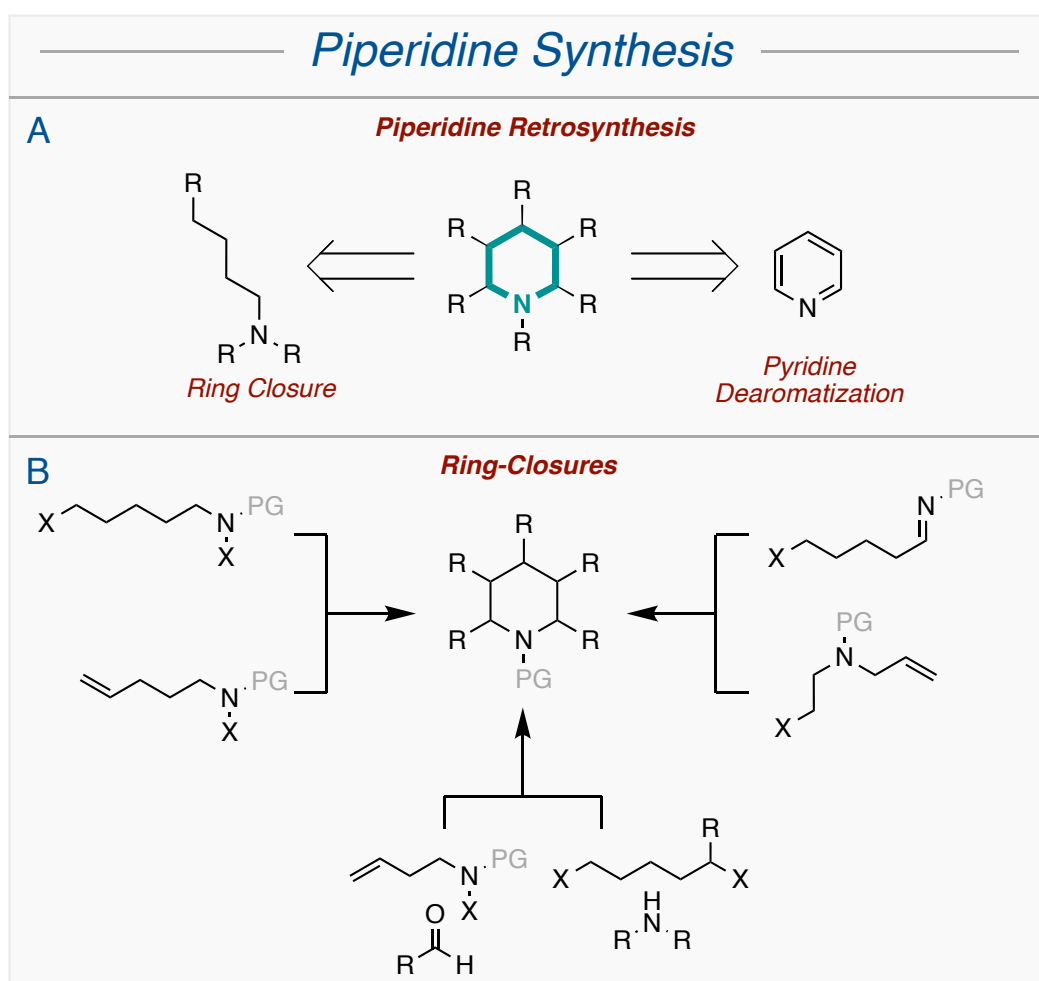


**Figure 1.3:** (A) Piperidine cores can be accessed either via ring closures or pyridine dearomatization methods. (B) Various ring closure strategies for accessing piperidines via inter- and intramolecular cyclizations

### 1.3. Pyridine Substitution Reactions

#### 1.3.1. Pyridine EAS Reactions

Reactions to aromatic molecules are traditionally limited to substitution reactions due to the strong thermodynamic driving force for re-establishing aromaticity, which readily synthesizes functionalized arenes, but not the more saturated and stereocenter-containing ring systems. Electron-rich arenes are conventionally functionalized through electrophilic aromatic substitution (EAS) reactions, which are characterized by electrophilic attack followed by a deprotonation step to restore aromaticity and include halogenations, Friedel-Craft alkylations/acylations, nitrations, and sulfonations.<sup>22</sup> Functionalized pyridines are commonly reduced to piperidines; therefore, a brief survey of pyridine substitution reactions is important for grasping the range of piperidines accessible *via* conventional reactions. Pyridine, being electron-poor, requires an activating group to undergo EAS transformations. For example, nitration only occurs when electron-donating moieties such as halogens, alkoxy groups, and alkyl groups are present on the pyridine ring.<sup>23-26</sup> Pyridine also undergoes halogenations<sup>27,28</sup> at the  $\beta$  position, but they require harsh conditions and/or activating substituents. Despite its electron deficiency, pyridine still displays EAS reactivity, yet this limited reactivity is still often interrupted by the basic lone pair on the nitrogen binding to incoming electrophiles.

#### 1.3.2. Pyridine NAS Reactions

The electron-deficient  $\alpha$  and  $\gamma$  carbons are far more susceptible to functionalization by incoming nucleophiles. Pyridine is susceptible to nucleophilic attack because the electronegative nitrogen atom lowers the energy of the lowest unoccupied molecular orbital (LUMO), which results in it having greater overlap with the highest occupied molecular orbital (HOMO) for the incoming nucleophile as well as increased stability of the newly formed molecular orbital. Like

EAS reactions, nucleophilic aromatic substitution (NAS) reactions are characterized by nucleophilic attack on an arene followed by loss of a leaving group to restore aromaticity. Amines, thiolates, and alkoxides are common nucleophiles in NAS reactions.<sup>29</sup> Another class of NAS reactions uses strong organolithium reagents to alkylate the  $\alpha$  and  $\gamma$  carbons.<sup>30-32</sup> The ensuing hydride loss to restore aromaticity, while rare, demonstrates that unsubstituted pyridine can still undergo functionalization through NAS reactions. Hydride loss was also observed by Shreve and coworkers in their successful additions of amide nucleophiles at the pyridine  $\alpha$  position.<sup>33</sup> Despite these instances of successful hydride loss, hydride is a poor leaving group; therefore, functionalized pyridines with halogens and alkoxy moieties are better suited for this class of reactions.<sup>32,34</sup>

### 1.3.3. Pyridine-*N*-Oxide Substitution Reactions

To circumvent the challenges in traditional EAS or NAS chemistry with pyridine, chemists have turned to pyridine-*N*-oxide. The oxide bound to the nitrogen lone pair drastically alters the electronic properties of the complex and imparts unconventional reactivity (Figure 1.4A). A combination of inductive and resonance effects allows for the addition of electrophiles at the  $\beta$  position in addition to both nucleophiles and electrophiles at the  $\alpha$  and  $\gamma$  positions of pyridine-*N*-oxide (Figure 1.4B). The regioselectivity of the reaction largely depends on the nature of the incoming electrophile or nucleophile. Hard electrophiles and soft or bulky nucleophiles tend to add at the  $\gamma$  position while soft electrophiles and hard nucleophiles add at the  $\alpha$  position, and electrophiles add at the  $\beta$  position under highly acidic conditions (Figure 1.4C). Although pyridine-*N*-oxide is cheap and commercially available, it can be accessed through a number of oxidants including hydrogen peroxide or *meta*-chloroperoxybenzoic acid (mCPBA).<sup>35,36</sup> While rarer than  $\alpha$

and  $\gamma$  functionalizations, EAS brominations and nitrations can occur at the  $\beta$  site under acidic conditions.<sup>29,37</sup>

Additionally, pyridine-*N*-oxide incorporates a wide range of nucleophiles into the pyridine ring. When sterically able to access the  $\alpha$  and  $\gamma$  positions equally, nucleophiles preferentially add  $\alpha > \gamma \gg \beta$ .<sup>29</sup> Both alkyl<sup>38</sup> and aryl<sup>39,40</sup> Grignard reagents add to the  $\alpha$  position in a strong yield

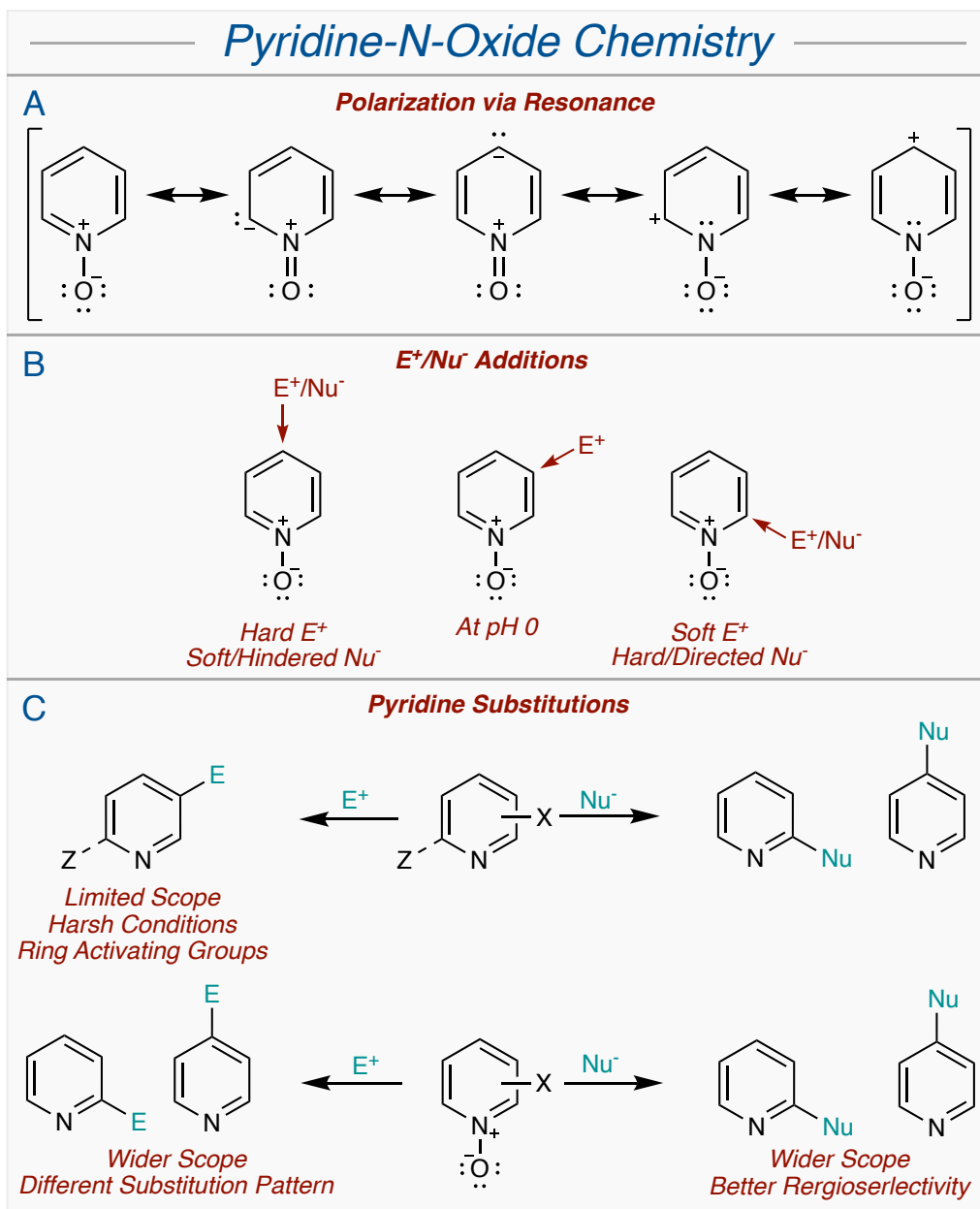


**Figure 1.4:** (A) Resonance structures of pyridine-*N*-oxide. (B) Site of additions to pyridine-*N*-oxide based on resonance. (C) EAS/NAS additions to pyridine and pyridine-*N*-oxide.

while cyanide adds to an *N*-alkoxypyridine compound at both the  $\alpha$  and  $\gamma$  positions.<sup>41</sup> The poor regioselectivity of this reaction prompted Fife and coworkers to explore and report a highly regioselective nitrile addition to pyridine-*N*-oxide (followed by rearomatization) in nearly quantitative yields.<sup>42</sup> In addition to these moieties, NAS reactions also install azides,<sup>43</sup> amines,<sup>36,44</sup> amides,<sup>45</sup> thiols,<sup>46-48</sup> chloride,<sup>49,50</sup> and acetylides<sup>29</sup> in mixtures of  $\alpha$  and  $\gamma$  regioisomers predominantly favoring  $\alpha$  substitution. Nitrogen activation on the pyridine ring is a strategy for NASs that extends far past pyridine-*N*-oxide and includes other *N*-activators such as amines and trialkylsilyls.<sup>36</sup> Pyridine-*N*-oxide also acts as an effective cross coupling partner for pyridine, allowing for the swift introduction of molecular complexity.<sup>51</sup>

#### 1.3.4. Alternative Pyridine Substitution Strategies

An alternative approach to synthesize functionalized pyridine is through transition metal catalysts. Coordination to a transition metal can greatly alter the reactivity of a molecule. Zirconium,<sup>52</sup> yttrium,<sup>53</sup> and rhodium catalysts<sup>54</sup> have been developed which regioselectively alkylate pyridines at C2 with a terminal alkene that rearomatize to produce functionalized pyridines. Palladium also catalyzes the cross coupling of pyridine-*N*-oxide with arenes<sup>55</sup> and various alkenes<sup>56</sup> at C2 of the pyridine. A similar copper-based catalyst prepared by Daugulis and coworkers also arylates various functionalized pyridine-*N*-oxides at C2.<sup>57</sup> Lastly, nickel readily catalyzes the hydroalkynylation of pyridine-*N*-oxide at the *ortho* position to form 2-alkenylpyridines.<sup>58,59</sup> These metal-catalyzed reactions along with NAS and EAS are exceptionally useful for functionalizing pyridine, but the strong thermodynamic driving force to restore aromaticity prevents the formation of stereocenters. Alternatively, dearomatization strategies could provide the synthetic chemist with the necessary tools to reliably access alkaloids.

## 1.4. Pyridine Dearomatization Strategies

While pyridine eschews addition reactions in favor of substitutions, it can be dearomatized through a variety of techniques, allowing for the generation of  $sp^3$ -hybridized atoms and alkaloid scaffolds including piperidines, dihydropyridines (DHPs), tetrahydropyridines (THPs), isoquinuclidines, etc. Once dearomatized, the remaining alkenes are then readily functionalized through well-established alkene addition reactions. With multiple ring atoms reduced to a  $sp^3$ -hybridization, the drive to rearomatization is significantly hindered. Some dearomatization methods are novel to pyridine while others are adaptations of benzene dearomatization methods.

### 1.4.1. Birch Reduction

Benzene can be reductively dearomatized by an industrial reaction known as the Birch reduction. This reaction requires harsh conditions including pyrophoric reducing metals such as  $Na^0$  or  $Li^0$  and cryogenic temperatures due to carrying the reaction out in liquid ammonia, but the resulting 1,4-cyclohexadiene products are resistant to rearomatization.<sup>60</sup> The reducing metal induces a radical around the arene, which forms a radical anionic species. The anion readily protonates upon exposure to an acidic hydrogen, and the radical is converted to yet another anion through another equivalent of  $Na^0$  that similarly accepts another equivalent of acid.<sup>61-63</sup> The Birch reduction was first applied to pyridine by Danishefsky and Cain. A difunctionalized pyridine was reduced to a 1,4-dihydropyridine (1,4-DHP) (Figure 1.5A) under the conventional Birch  $Na^0$ -ammonia-methanol conditions.<sup>64</sup> Donohoe and coworkers furthered this work by using Birch conditions on mono- and disubstituted pyridines containing electron-withdrawing functional groups.<sup>65</sup> Electrophilic alkylation of the pyridine then occurs on the product to yield conjugated 1,2-DHPs resistant to rearomatization. The regioselectivity of the alkylation process depends on the substitution pattern of the pyridine.



## Pyridine Dearomatization

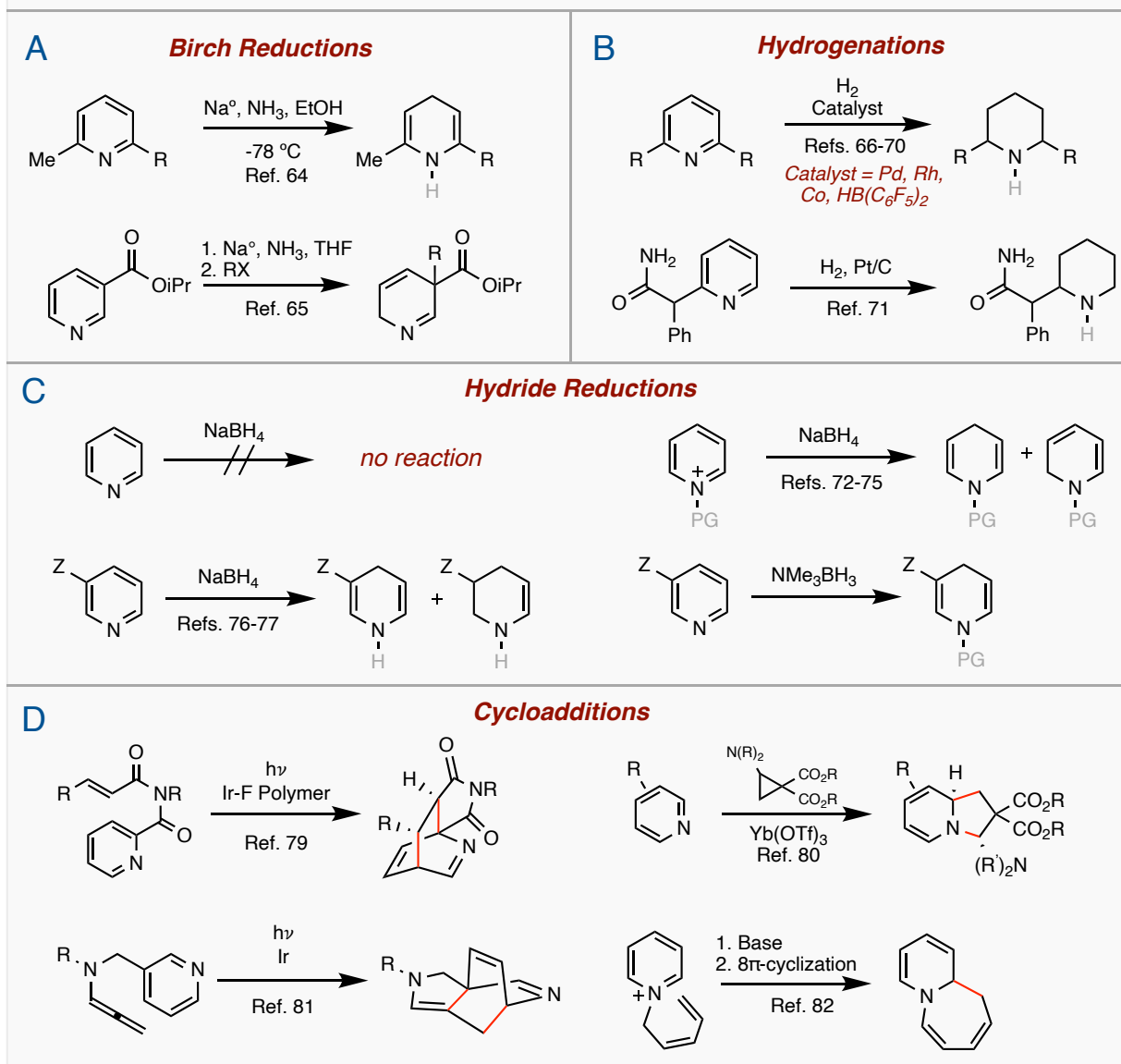


**Figure 1.5:** (A) The Birch Reduction applied to pyridine in the total synthesis of estrone. (B) A variety of catalysts can hydrogenate pyridine. (C) Hydride sources can reduce activated pyridines. (D) Metal-promoted and photocatalytic cycloadditions are preceded with pyridine.

### 1.4.2. Hydrogenations/Hydride Additions

Pyridine are also dearomatized by the reductive incorporation of hydrogen into the ring. The two primary methods for this are catalytic hydrogenations and hydride-mediated reductions (Figure 1.5B & 1.5C). Various pyridines undergo complete catalytic hydrogenations to piperidines

using catalysts including platinum,<sup>66</sup> palladium,<sup>67</sup> rhodium,<sup>68</sup> cobalt nanoparticles,<sup>69</sup> and Piers borane ( $\text{HB}(\text{C}_6\text{F}_5)_2$ ).<sup>70</sup> Of note, platinum catalyzed the hydrogenation of pyridine in the commercial synthesis of methylphenidate.<sup>71</sup> Moderate reducing agents, such as  $\text{NaBH}_4$ , can also dearomatively reduce pyridine. Although simple pyridine will not undergo hydride addition, pyridinium salts activated by the *N*-coordination of a Lewis acid are readily reduced; however, a mixture of 1,2- and 1,4-DHP products is observed.<sup>72-75</sup> Alternatively, 3-substituted pyridines with electron-withdrawing groups also undergo hydride addition, but a mixture of 1,4-DHP and 1,4,5,6-THP is formed.<sup>76,77</sup>

#### 1.4.3. Cycloadditions

Pericyclic reactions have also demonstrated their capacity to dearomatize arenes through multiple strategies. The Woodward-Hoffmann rules dictate that cycloadditions for systems containing  $4n+2$   $\pi$  electrons, or Diels-Alder reactions, are thermally allowed due to orbital symmetry and the lack of energetically unfavorable antarafacial arrangements.<sup>78</sup> Arenes, and pyridine specifically are highly resistant to cycloadditions owing to their resonance stabilization energies. Nevertheless, dearomatizing [4+2] cycloadditions were demonstrated with pyridine in the presence of a recyclable polymer-immobilized Ir(II) photocatalyst (Figure 1.5D).<sup>79</sup> Exposure to visible light excites the photocatalyst to the triplet state, where it catalyzes the regio- and stereoselective intramolecular [4+2] cycloaddition to produce isoquinuclidine products. Various functionalized DHPs can also be produced by [3+2] cycloadditions catalyzed by ytterbium (III) triflate.<sup>80</sup> A range of aminocyclopropanes containing geminal esters binds to the pyridine imine, resulting in a functionalized DHP fused to pyrrolidine (Scheme 1.4). Allenes also undergo intramolecular [4+2] dearomative cycloadditions with pyridine when in the presence of an iridium visible light photocatalyst.<sup>81</sup> Eberbach and coworkers also demonstrated an intramolecular  $8\pi$

electron cycloaddition promoted by the addition of base.<sup>82</sup> While pyridine do capably undergo dearomative cycloadditions, it does so with limited functional group tolerance and even these cannot be applied to free unsubstituted pyridine, and the resulting cycloadducts have not been utilized as piperidine synthons.

### 1.5. Pyridine Dearomatization *via* Nucleophilic Additions to *N*-Activated Pyridinium Salts

The most common method of pyridine dearomatization is through nucleophilic addition reactions to pyridines activated by an *N*-coordinating activator. This strategy is analogous to carrying out NAS reactions on pyridine-*N*-oxide (*vide supra*) with the primary difference being the final product is a functionalized DHP instead of a rearomatized functionalized pyridine. These resulting DHPs feature stereocenters, and thus more sp<sup>3</sup>-hybridized atoms, as well as the ability to undergo further additions on the remaining olefins. This methodology must circumvent several challenges in order to achieve efficient and selective nucleophilic additions. The equilibrium drive greatly favors free pyridine over *N*-coordinated activated pyridine, which is the key intermediate needed for addition to occur. Not only will this both slow the reaction and result in lower yields, but uncoordinated *N*-activator reagent still in solution would likely interfere with the incoming nucleophile. Pabel and coworkers determined that utilizing a triflate counteranion greatly shifted the equilibrium balance towards activated pyridine, thus raising nucleophilic addition yields and shortening reaction times.<sup>83</sup> Various nitrogen activation strategies have been developed with each capable of adding a small to moderate range of nucleophiles to the pyridine ring.

#### 1.5.1. Nucleophilic Additions to *N*-Acyl Pyridiniums

Acyl groups, which are also generally used as nitrogen protecting groups, are a class of widely used pyridine activators that promote nucleophilic additions (Figure 1.6). When bound, reactivity patterns suggest that hard nucleophiles such as methylmagnesium bromide (MeMgBr)

and other Grignard reagents<sup>84</sup> preferentially add at C2 of the (*N*-acyl)-pyridinium while softer nucleophiles, including zinc chlorides, organocuprates,<sup>85</sup> organostannane,<sup>86</sup> phosphite esters, titanium enolates,<sup>87</sup> and zinc chloride reagents favor C4 addition, thus often resulting in mixtures of 1,2- and 1,4-DHPs. Notably, alkenyl and alkynyl Grignard reagents underwent C2 addition exclusively and was utilized in the total synthesis of several alkaloids.<sup>88,89</sup> Furthermore, steric bulk influences regioselectivity as bulky nucleophiles such as isopropylmagnesium bromide (*i*PrMgBr) favor C4 addition. Bulky substituents on the pyridine ring also generally disfavor additions *ipso* and *ortho* relative to the bulky functional group and prefer *meta* and *para* additions instead. Bulky acyl R groups also shift the regioselectivity of both alkyl and aryl Grignards shifts more to C4 addition, yet the regioselectivity of the reaction worsens. Commonly used acyl groups are methylcarbonyl, methoxycarbonyl, phenoxy carbonyl,<sup>90</sup> *tert*-butyloxycarbonyl (boc), and

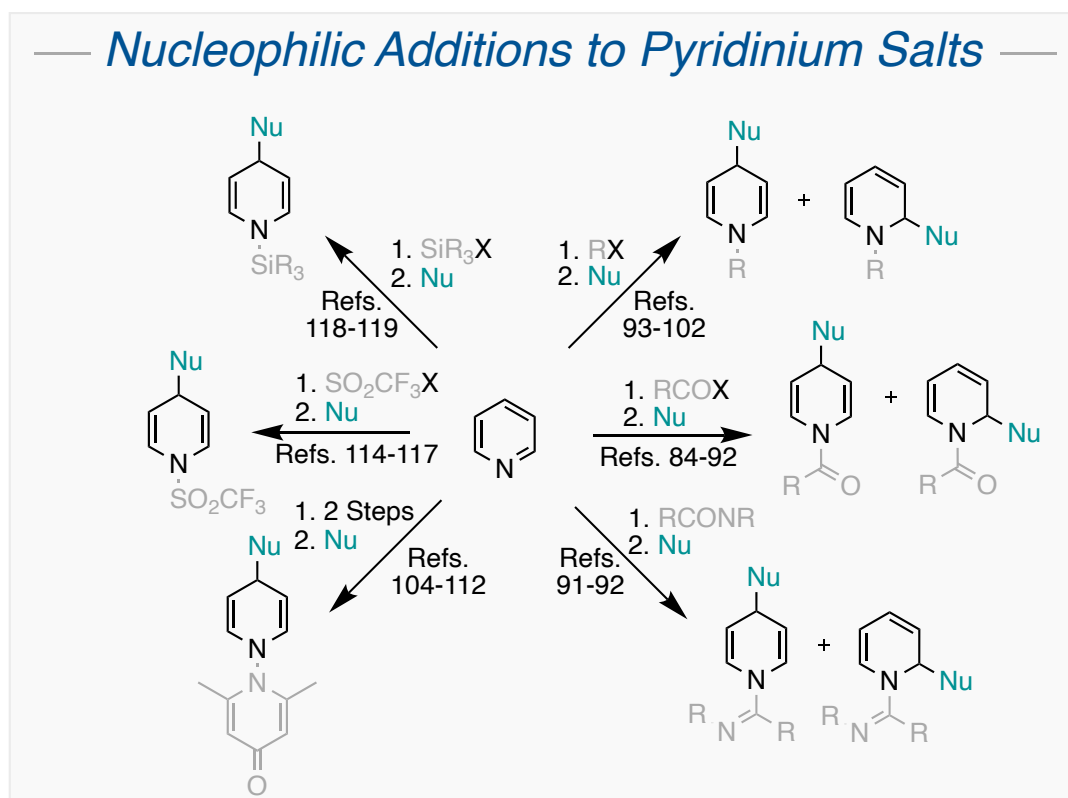


**Figure 1.6:** Various *N*-activators promote a wide array of nucleophilic additions to pyridinium salts. 1,2- and 1,4-DHP products are often produced, and rearomatization is typically an issue.

ethoxycarbonyl. Charette and coworkers demonstrate the same activation/addition method by utilizing an imidoyl activating group structurally analogous to the acyl group (Figure 1.6).<sup>91</sup> Various Grignard reagents added highly regio- and diastereoselectively at C2 when using a chiral (*S*)-valinol-based imidoyl activating group. An electronically analogous imine *N*-activator was also used for incorporating Grignard nucleophiles into C2.<sup>92</sup>

### 1.5.2. Nucleophilic Additions to *N*-Alkyl Pyridiniums

Alkyl groups also comprise another large group of pyridine *N*-activators for dearomatizing nucleophilic additions (Figure 1.6).<sup>36</sup> However, these nucleophilic additions often result in poor yields because the unstable products are challenging to isolate and are susceptible to polymerization upon base addition. Better yields are obtained when the pyridine contains an electron-withdrawing group at C3. Additions generally observed the same patterns previously described above relating to hard-soft acid/base (HSAB) theory and bulkiness. While alkyl Grignard reagents follow this convention and slightly favor C2 addition, the poor regioselectivity of this reaction forms racemized mixtures of 1,2- and 1,4-DHPs.<sup>93-96</sup> However, soft or bulky nucleophiles incorporate nucleophiles at C4, including nucleophiles such as dialkylzincs,<sup>94</sup> alkyl and aromatic organocuprates,<sup>97</sup> electron-rich heterocycles,<sup>98</sup> ketene acetals,<sup>99</sup> enolates,<sup>100</sup> and cyanide.<sup>101,102</sup> Various groups including linear alkyl chains, benzyl groups, benzhydryl groups, triphenylmethyl groups, etc. have been utilized as *N*-binding pyridine alkyl activators. Like with acyl groups, bulky alkyl *N*-activators such as triphenylmethyl kinetically hinder nucleophilic attack at *ortho* carbons, thus promoting C4 addition. Similar to acyl-activators, alkyl activators mostly result in racemized nucleophilic addition product mixtures. Diastereoselectivity can be achieved, but doing so requires introducing a chiral functional group on the ring. Chiral benzyl *N*-

activators result in diastereoselective C2 additions of Grignard reagents<sup>93</sup> while chiral electrophiles result in diastereoselective C4 addition of organocuprates.<sup>85</sup>

### 1.5.3. Nucleophilic Additions to *N*-Heteroatomic Pyridiniums

Although many activators are carbon-based, *N*-bound heteroatomic activators also capably activate pyridine towards nucleophilic additions. Pyridine-*N*-oxides readily promote a range of nucleophilic reactions (*vide supra*), but generally form products through NAS reactions that rearomatize and do not produce stereocenters (Figure 1.6). Although *N-N* pyridinium salts, similarly promote NAS reactions, they also foster dearomatizing nucleophilic additions (Figure 1.6).<sup>36</sup> Amines,<sup>103</sup> amides, pyridones,<sup>104-112</sup> and nitro groups<sup>113</sup> all serve as *N-N* activators. Notably, addition products with (*N*-pyridone)-pyridines are more resistant to rearomatization and can be isolated as DHPs. Successfully added nucleophiles, including Grignard reagents,<sup>105-107</sup> nitriles,<sup>104</sup> enolates,<sup>105,110,111</sup> nitroalkanes,<sup>108</sup> thiols,<sup>112</sup> and phosphites,<sup>109</sup> reportedly add at C4. *N*-triflyl is another class of heteroatom activating group subset that have displayed synthetic versatility (Figure 1.6). They coordinate nucleophiles such as phosphites,<sup>114</sup> enolates,<sup>115</sup> ketene acetals,<sup>116</sup> and electron-rich arenes<sup>117</sup> at C4 with strong regioselectivity owing to the large steric profile of the triflate group. In most cases, the racemized 1,4-DHP products rearomatize to form a functionalized pyridine complex. The final classes of *N*-bound activating groups are trialkylsilyl groups<sup>118,119</sup> (Figure 1.6), which both capably promotes the 1,4 regioselective addition of Grignard reagents and silyl enolates respectively; however, like with other systems, the loose *N*-coordination of the silyl groups promotes facile rearomatization, thus complicating isolation of the DHP addition products.

#### 1.5.4. Conclusion

The vast array of functional groups incorporated into the pyridine ring through these techniques highlights the longstanding usefulness of this approach, yet lingering issues underscore the need for further innovation. As stated previously, many of these nucleophilic reactions with pyridine result in rearomatized functionalized pyridine that lack the chiral carbons and  $sp^3$ -hybridized atoms necessary for improving their druglikeness. Alternatively, while some additions are highly regioselective, most addition reactions yield a mixture 1,2- and 1,4-DHPs that are highly problematic for synthetic chemists. Further still, diastereoselectivity issues of these additions have been addressed by only a few strategies that require bulky chiral *N*-activators or ring substituents that present challenging installations and removals. Another shortcoming is that the list of nucleophiles added by a broader system, such as acyl activators, are not all compatible with every different *N*-activator within the subset. Generally, a single specific *N*-activator installs a small range of nucleophiles, emphasizing the need for a wide range of nucleophiles that add *via* a single robust methodology. Lastly, this multitude of approaches fails to address adding nucleophiles  $\beta$  to the pyridine nitrogen with selectivity. While small-molecule drugs and other compounds exist with  $\beta$  functionalized piperidine from pyridine, the explored chemical space of  $\beta$ -substituted piperidines/DHPs/THPs is far smaller than that of  $\alpha$  and  $\gamma$  additions, which is a direct reflection of the lack of robust techniques for synthesizing this functionalization pattern.

### 1.6. Transition-Metal Mediated Pyridine Dearomatization

#### 1.6.1. Transition-Metal Catalyzed Pyridine Dearomatization

Recently, metal catalysts have offered an alternate approach for the dearomatization of pyridine. The pyridine hydroboration has been conducted *via* magnesium,<sup>120</sup> rhodium,<sup>121</sup> and

iridium<sup>122</sup> catalysts resulting in mixtures of 1,2 and 1,4 hydroboration DHP products. Cobalt, however, catalyzed a highly regioselective 1,4 pyridine hydroboration for a variety of functionalized and pyridines.<sup>123</sup> Similarly, the Delferro lab developed a lanthanide catalyst capable of highly regioselective 1,2 pyridine hydroboration for a wide scope of functionalized pyridines.<sup>124</sup> Yet all of these hydroboration catalysts fail to incorporate new topologically rich functional groups into the pyridine ring.

### 1.6.2. Pyridine Dearomatization via $\eta^6$ Coordination to a Transition-Metal

Classically, transition-metal dearomatization involves the hexahapto ( $\eta^6$ ) coordination of an arene to a stoichiometric transition-metal complex consisting of a 1<sup>st</sup> row d<sup>6</sup> metal, specifically Cr(0) and Mn(I), and strong  $\pi$ -acid ligands like CO.<sup>125,126</sup> An analogous method was developed by Draper and Byrne uses a chromium tricarbonyl  $\eta^6$  pyridine complex.<sup>127</sup> Pyridine is activated for regio- and stereoselective *ortho* additions of various organolithium reagents (Figure 1.7A).<sup>128</sup> Subsequent methylation of the nitrogen produces a 1,2-DHP ligand  $\eta^4$  coordinated to the metal while the functionalized carbon flanks out of the plane of the ring. However, isolation of the DHP ligand requires oxidative decomplexation, which often rearomatizes the product. Chaudret and Jalon report the first synthesized and isolated  $\eta^6$  bound pyridine to a ruthenium complex bearing a Cp\* ligand.<sup>129</sup> This complex is synthesized in high yield, but the pyridine ligand is readily displaced by coordinating solvents, limiting the usefulness of this particular complex. However, Fish and coworkers later emphasized that the  $\eta^6$  bound pyridine to the same ruthenium complex used by Chaudret is the thermodynamic product.<sup>130</sup> At ambient temperatures, a  $\kappa$ -N complex is observed followed by a slow slippage to  $\eta^4$  and then eventually  $\eta^6$  coordination. Although  $\eta^6$  coordination is observed, functionalization of pyridine has not successfully occurred using this approach.



### 1.6.3. Pyridine $\eta^2$ Coordination to a Transition Metal

Alternatively, a variety of transition metals are capable of dihapto ( $\eta^2$ ) binding to arenes. Numerous complexes have been developed from Groups III and IV transition metals scandium,<sup>131</sup> titanium,<sup>132</sup> zirconium, and thorium<sup>133</sup> due to their ability to insert into the C-H bond  $\alpha$  to the pyridine nitrogen.<sup>36</sup> These complexes each contain two sterically bulky cyclopentadienyl (Cp) ligands that donate electron density while also precluding multiple pyridines binding or  $\eta^4$  and  $\eta^6$  coordination modes. An alkyl group, usually a methyl group, is also on the complex and undergoes a  $\sigma$ -bond metathesis with an  $\alpha$  pyridine hydrogen to produce methane gas, a convenient indicator of reaction progress (Figure 1.7B). As this occurs, the  $\kappa$ -N bound pyridine undergoes metalation at the carbon bound to the hydrogen involved in the metathesis to form an  $\eta^2$  pyridine complex.

While these dihapto complexes have been isolated for the metals listed above, the zirconium complex has been utilized for functionalizing pyridine. The zirconium  $\eta^2$  pyridine complex inserts functionalized alkenes and alkynes at the  $\alpha$  pyridine position bound to the metal center.<sup>134</sup> The reaction occurs in chlorinated solvents and a migratory insertion is responsible for the installment of the functional group on the pyridine ring. Various azametallacycles can also be constructed off the *ortho* pyridine position using this method. Chiral zirconium complexes were also developed capable of adding chiral olefins to the pyridine ring with high diastereoselectivity.<sup>135</sup> However, the zirconium metal is not dearomatizing the pyridine, and thus the products are simply functionalized pyridines. Analogous hafnium<sup>136</sup> and tantalum<sup>137</sup> complexes demonstrated the *ortho* silylacylation of pyridines, but they also fail to both dearomatize pyridine and generate stereocenters. The challenge remains to develop a robust

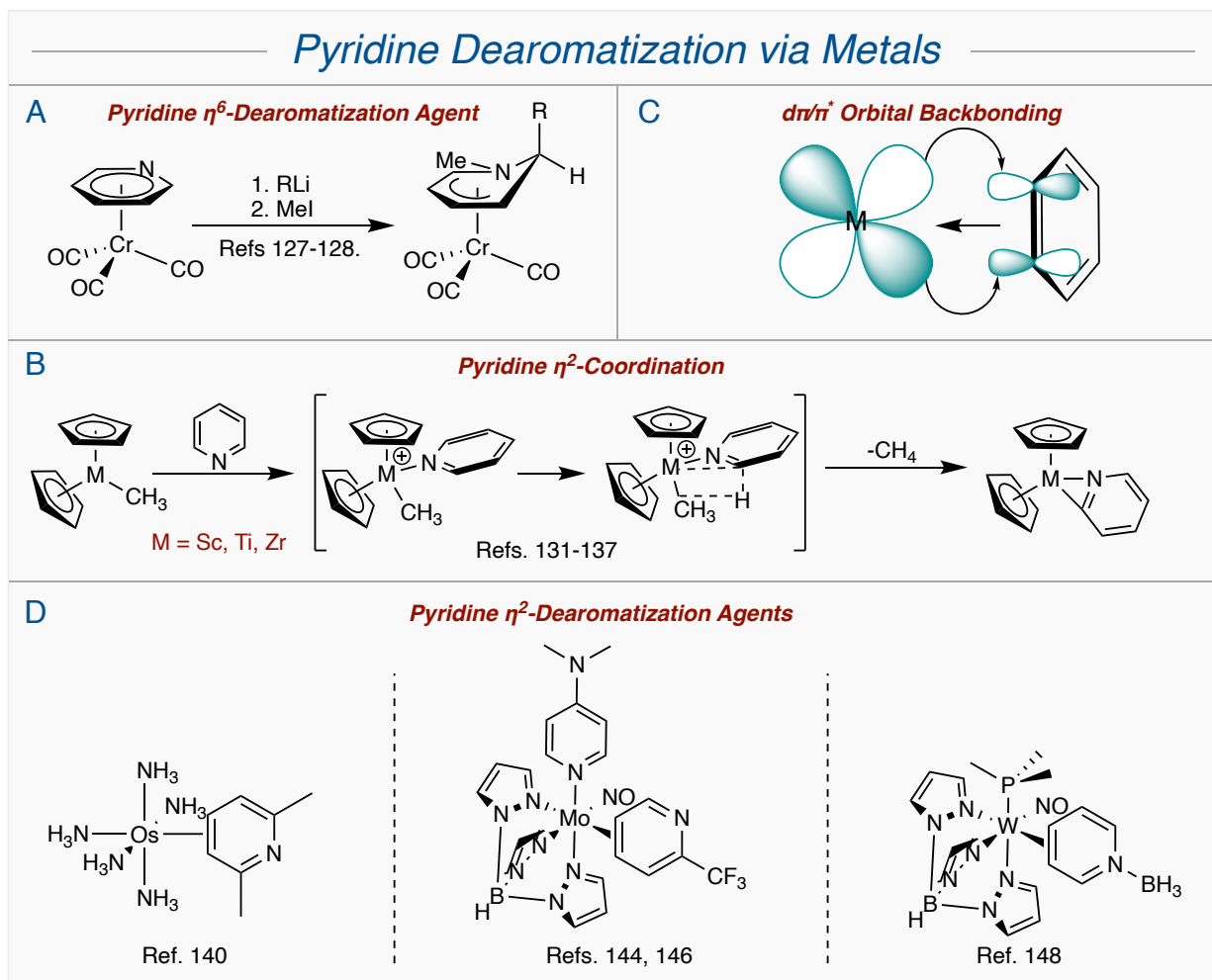


**Figure 1.7:** (A) Pyridine  $\eta^6$ -coordination to electron-deficient chromium activates the pyridine for nucleophilic additions. (B)  $\eta^2$  pyridine complexes are accessed through high valent Sc, Ti, and Zr Cp<sub>2</sub> complexes (C) Metal d orbital backbonds into arene  $\pi^*$  orbital. (D) Os(II), Mo(0), and W(0) pyridine  $\eta^2$ -dearomatization agents.

methodology capable of adding a wide range of functional groups to a pyridine core while selectively developing stereocenters.

#### 1.6.4. Pyridine Dearomatization via $\eta^2$ Coordination to a Transition Metal

Octahedral metal  $\pi$ -bases are capable of backbonding into the  $\pi^*$  orbital of arenes, forming a  $\eta^2$ /metallacyclopropane-like bonding interaction that disrupts aromaticity (Figure 1.7C).<sup>138</sup> The electron-donation from the stoichiometric metal activates each uncoordinated arene-centered alkene for tandem electrophilic/nucleophilic additions. The first generation of  $\eta^2$  dearomatization agents was a pentaammineosmium(II) benzene complex first reported by Harman and Taube.<sup>139</sup> The

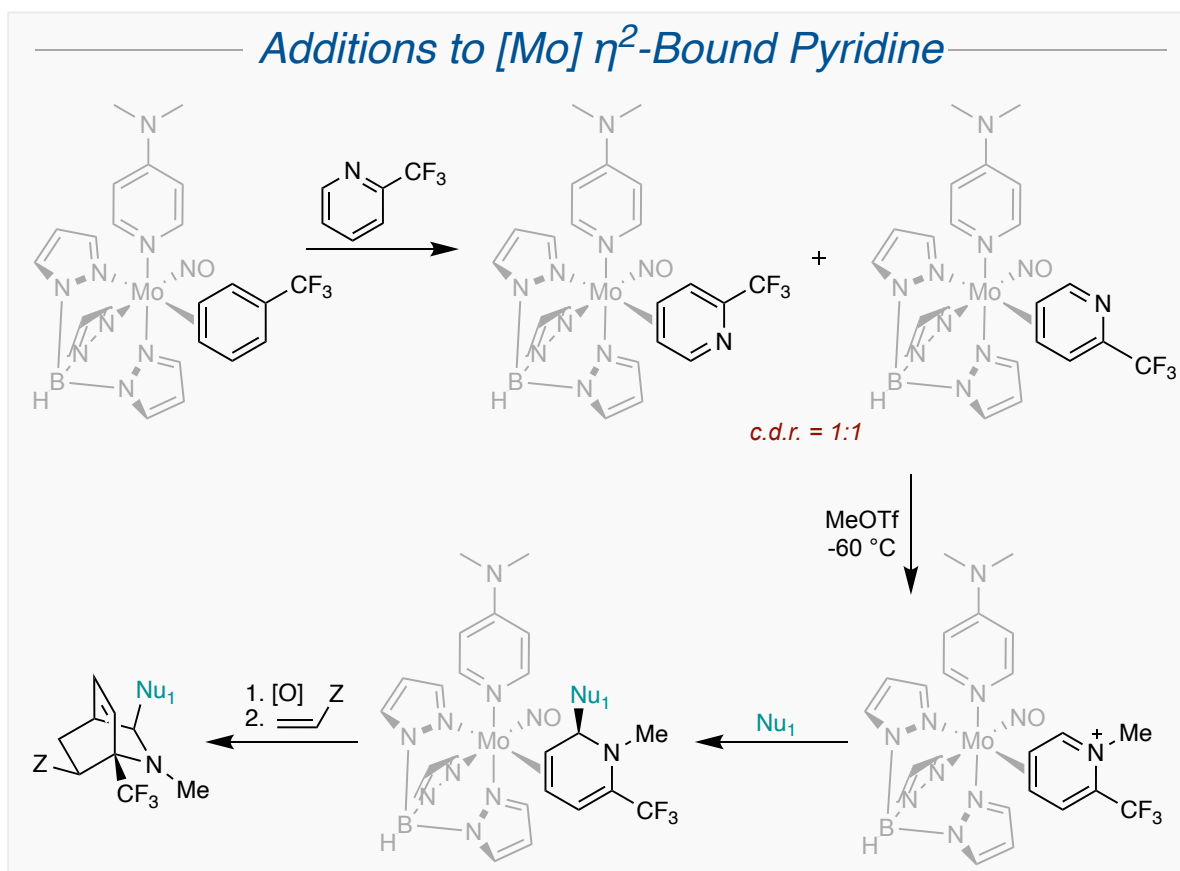


**Figure 1.8:** [Mo]  $\eta^2$  binds to  $\eta^2$ -(2-CF<sub>3</sub>)-pyridine and activates it for methylation/nucleophilic additions. The resulting DHPs can be liberated from the metal and subjected to Diels Alder reactions.

presence of the strong  $\sigma$ -donor amine ligands raise the energy of the  $t_{2g}$  osmium orbitals making them capable of backbonding into high energy arene  $\pi^*$  orbitals. Although an unfunctionalized  $\eta^2$ -osmium pyridine complex was never isolated, 2,6-lutidine was electrochemically observed to be in equilibrium between its  $\eta^2$  and  $\kappa$ -N forms, but subsequent functionalizations were not conducted on this complex (Figure 1.7D).<sup>140</sup>

New  $\eta^2$  dearomatization agents were sought capable of stronger backbonding while reducing both the cost and toxicity issues present with the osmium system. Re(I),<sup>141</sup> Mo(0),<sup>142</sup> and W(0)<sup>143</sup> were selected as  $d_6$  isoelectronic analogues of the osmium complex, and each was optimized with a ligand set consisting of trispyrazolylborate (Tp), a  $\pi$ -acid nitrosyl (NO) or carbonyl (CO), and an ancillary ligand L. While TpRe(CO)(MeIm) dearomatized and

functionalized numerous arenes; however, attempts to coordinate pyridine were underexplored and unsuccessful. Meanwhile,  $\text{TpMo}(\text{NO})(4\text{-DMAP})$  [Mo] readily coordinates a range of substituted pyridines including 2-(trifluoromethyl)pyridine (Figure 1.7D). After methylating the pyridine nitrogen, the  $[\text{Mo}]\text{-}\eta^2\text{-}(N\text{-methyl})\text{-}2\text{-}(\text{trifluoromethyl})\text{pyridinium}$  complex was subjected to a range of nucleophilic additions (Figure 1.8). These include cyanide, amines, dialkylzinc, Barbier, and Grignard additions, all of which occur at C2 *anti* to the [Mo] complex, thus yielding a range of  $\text{Mo } \eta^2\text{-}1,2\text{-DHP}$  complexes.<sup>144</sup> Enantioenriched DHPs, synthesized *via* the enantioenrichment of the [Mo] fragment,<sup>145</sup> were then oxidatively liberated and subjected to Diels-Alder reactions with various dienophiles to form a range of functionalized isoquinuclidines.<sup>146</sup> However, these  $\text{CF}_3\text{-}$ substituted  $[\text{Mo}]\text{-}\eta^2$  DHPs cannot undergo a second tandem electrophile-nucleophile addition as they instead perform a Zincke-like ring opening under acidic conditions, thus precluding the synthesis of highly functionalized THPs and piperidines.

In order to synthesize highly functionalized THPs/piperidines, a tungsten complex capable of dearomatizing pyridine was necessary. As a 3<sup>rd</sup> row transition metal, tungsten backbonds more strongly than molybdenum, and the analogous  $\text{TpW}(\text{NO})(\text{PMe}_3)$  [W] complex has proved both a stronger dearomatization agent of a wider range of arenes as well as stable to a variety of organic reaction conditions.<sup>138,143</sup> A wide range of functionalized pyridines are coordinated and dearomatized by [W].<sup>147</sup> The parent  $[\text{W}]\text{-}(\eta^2\text{-benzene})$  complex (**1**) is an exchange synthon due to its 30 minute half-life before benzene dissociation. When stirred in the presence of a desired pyridine substrate, it can coordinate to the metal. Free pyridine, however, coordinates to [W] *via* the nitrogen ( $\kappa\text{-N}$ ) in order to avoid paying the thermodynamic penalty for dearomatizing pyridine, but this binding mode does not activate the pyridine ligand for additions. Three strategies are

utilized to prevent  $\kappa$ -N coordination: 2,6 steric repulsion,  $\pi$ -donors, and N-blockers. Simply adding alkyl groups at both C2 and C6 (e.g. 2,6-lutidine) will sterically disfavor  $\kappa$ -N binding, and including a  $\pi$ -donor ligand (e.g. alkoxy or amine group) adjacent to the nitrogen makes the nitrogen a worse  $\pi$ -acceptor, also disfavoring  $\kappa$ -N binding. However, coordinating pyridine borane (pyrb) to form a mixture of  $[W]-\eta^2$ -(pyrb) complexes (**2**) proved most effective due to the nonoxidizing

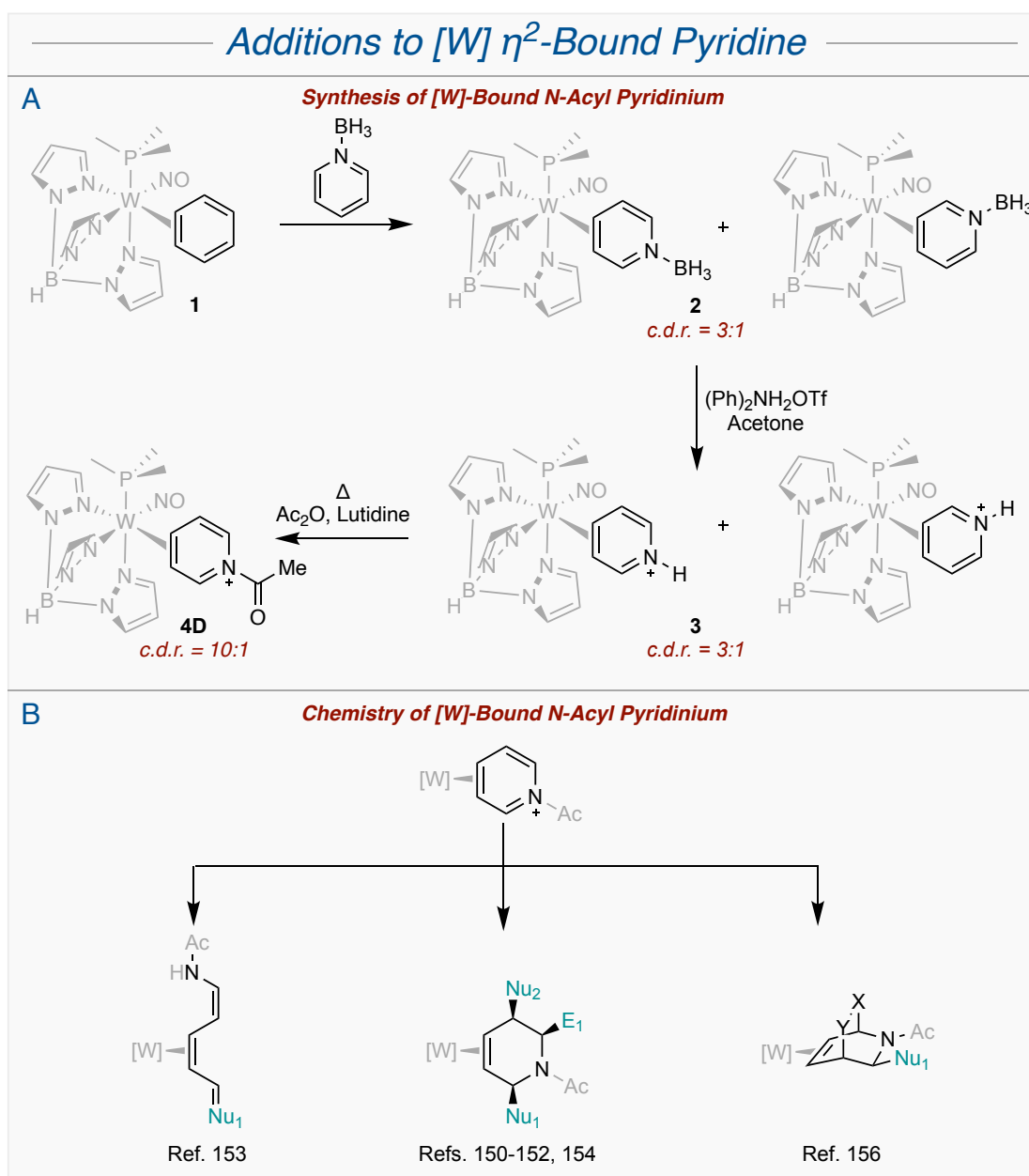


**Figure 1.9:** (A) Synthesis of **4D** from **1** occurs through pyrb. (B) Highly functionalized THPs, merocyanines, and isoquinuclidines can be synthesized from **4D**.

ylide nature of pyrb while simultaneously blocking  $\kappa$ -N coordination. A mixture of coordination diastereomers is produced in a 3:1 ratio of the distal/proximal forms (Figure 1.9A).<sup>148</sup> This mixture can then undergo subsequent protonation (**3**) and N-protection with an array of protecting groups, including acetyl, which allows for the selective synthesis of the **4D** diastereomer when gently heated due to unequal tungsten  $t_{2g}$  orbital thermodynamically preferring to orient carbeniums distal to the  $\text{PMe}_3$  ligand.<sup>148-150</sup>

This parent **4D** pyridinium complex serves as the launchpad for a wide variety of transformations. The iminium carbon is activated *via* resonance for nucleophile incorporation, which is demonstrated with a wide range of nucleophile types (Grignards, dialkylzincs, nitrile, enolates, etc.) exclusively *anti* to the metal at C2, resulting in a range of 2-functionalized  $\eta^2$  DHP complexes.<sup>150</sup> These DHPs can be further transformed *via* tandem electrophile/nucleophile additions to the remaining free alkene to highly functionalized THPs<sup>151,152</sup> or ring opened to various merocyanine complexes (Figure 1.9B).<sup>153</sup> Kosturko and coworkers also demonstrated the Selectfluor®- promoted dialkoxylation of **4D** to various functionalized THPs<sup>154</sup> and that [W]-bound dimethoxypyridine undergoes [4+2] cycloadditions that generate isoquinuclidine cores with varying functionality.<sup>155</sup> Lastly, [4+2] cyclocondensations were demonstrated with DHPs bound to [W], producing functionalized isoquinuclidines.<sup>156</sup> These ground-breaking works, which have expanded the synthetic utility of pyridine while accessing novel druglike chemical space, are plagued with the presence of rotational isomers from the acetyl group.

#### 1.6.5. Featured Chemistry

This work is a continuation of previously outlined chemistry rooted in the transformations of [W]-bound pyridine. Second generation [W]-bound pyridinium salts were developed containing sulfonyl nitrogen protecting groups (Figure 1.10A). In addition to eliminating observable

downstream rotamers, which greatly eased spectroscopic analysis, these complexes retained much of the previously established chemistry, including tandem nucleophile-electrophile-nucleophile additions to form highly functionalized tetrahydropyridines. This approach was applied in the synthesis of piperidyl substituted methylphenidate analogues (Chapter 3) and tetrahydropyridine isotopologues and isotopomers (Chapter 4) (Figure 1.10B). These *N*-sulfonylpyridinium complexes also demonstrated novel reactivity including a Zincke-like ring opening of [W]-DHPs (Chapter 2) and a hitherto unprecedented nitrogen dealkylative ring-opening of [W]-bound

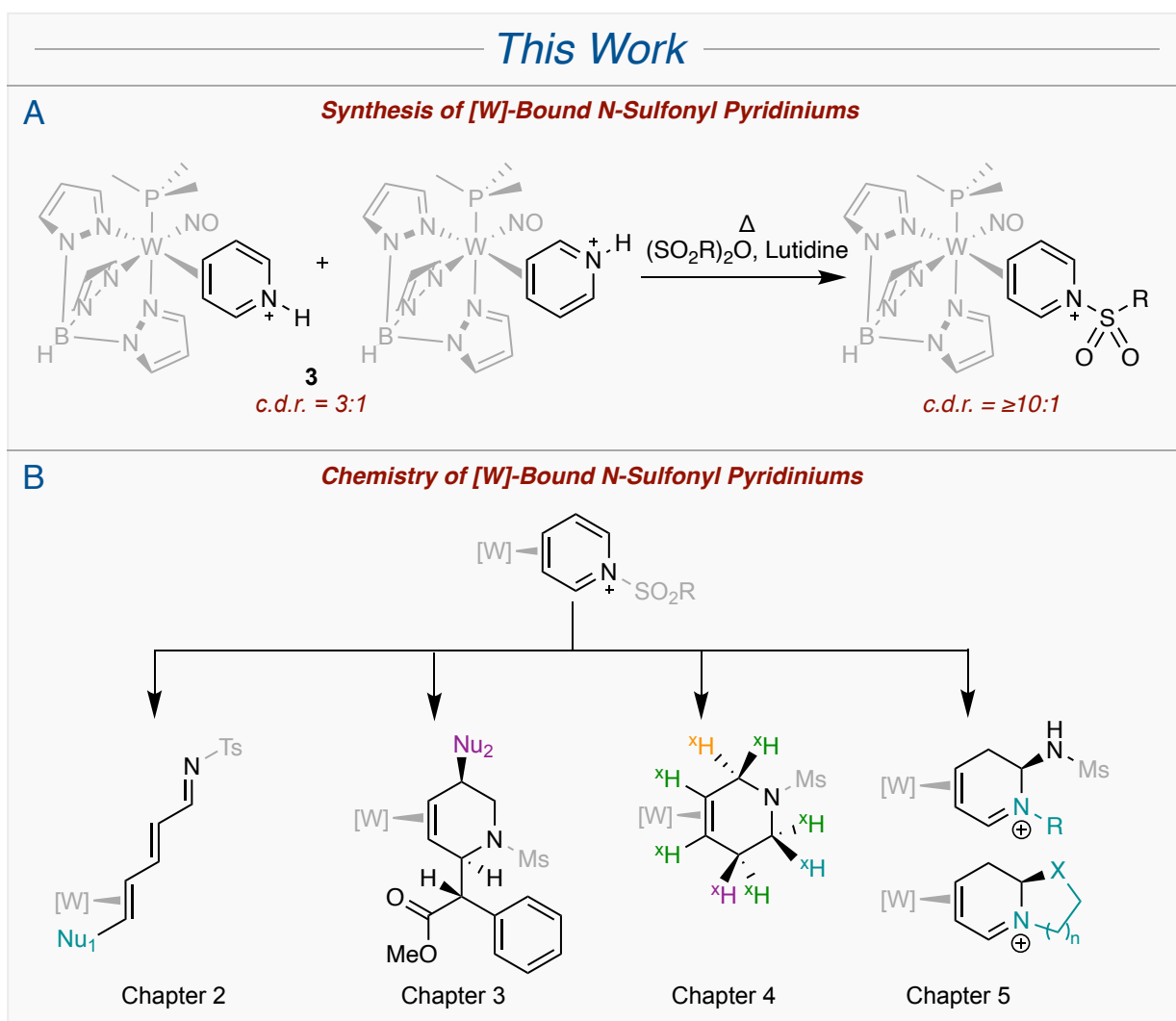


**Figure 1.10:** (A) Synthesis of *N*-sulfonyl pyridinium complexes from **3**. (B) Preview of each subsequent thesis chapter.

tetrahydropyridines (Chapter 5). Together, these findings both explore the capability and demonstrate the synthetic utility of [W]-pyridinium complexes.

## 1.7. References

- (1) Blakemore, D. C.; Castro, L.; Churcher, I.; Rees, D. C.; Thomas, A. W.; Wilson, D. M.; Wood, A. Organic synthesis provides opportunities to transform drug discovery. *Nat. Chem.* **2018**, *10*, 383-394.
- (2) Brown, D. G.; Bostrom, J. Analysis of Past and Present Synthetic Methodologies on Medicinal Chemistry: Where Have All the New Reactions Gone? *J. Med. Chem.* **2016**, *59* (10), 4443-4458.
- (3) Bostrom, J.; Brown, D. G.; Young, R. J.; Keseru, G. M. Expanding the medicinal chemistry synthetic toolbox. *Nat. Rev. Drug Discov.* **2018**, *17* (10), 709-727.
- (4) Lovering, F.; Bikker, J.; Humblet, C. Escape from flatland: increasing saturation as an approach to improving clinical success. *J. Med. Chem.* **2009**, *52* (21), 6752-6756.
- (5) Morley, A. D.; Pugliese, A.; Birchall, K.; Bower, J.; Brennan, P.; Brown, N.; Chapman, T.; Drysdale, M.; Gilbert, I. H.; Hoelder, S.; Jordan, A.; Ley, S. V.; Merritt, A.; Miller, D.; Swarbrick, M. E.; Wyatt, P. G. Fragment-based hit identification: Thinking in 3D. *Drug Discov. Today*: **2013**, *18*, 1221-1227.
- (6) Paul, S. M.; Mytelka, D. S.; Dunwiddie, C. T.; Persinger, C. C.; Munos, B. H.; Lindborg, S. R.; Schacht, A. L. How to improve RD productivity: The pharmaceutical industry's grand challenge. *Nat. Rev. Drug Discov.* **2010**, *9*, 203-214.
- (7) Vitaku, E.; Smith, D. T.; Njardarson, J. T. Analysis of the structural diversity, substitution patterns, and frequency of nitrogen heterocycles among U.S. FDA approved pharmaceuticals. *J. Med. Chem.* **2014**, *57* (24), 10257-10274.
- (8) Gandon, L. A.; Russell, A. G.; Guveli, T.; Brodewolf, A. E.; Kariuki, B. M.; Spencer, N.; Snaith, J. S. Synthesis of 2,4-disubstituted piperidines *via* radical cyclization: unexpected enhancement in diastereoselectivity with tris(trimethylsilyl)silane. *J. Org. Chem.* **2006**, *71* (14), 5198-5207.
- (9) Xu, P.; Zhang, M.; Ingoglia, B.; Allais, C.; Dechert-Schmitt, A. R.; Singer, R. A.; Morken, J. P. Construction of Azacycles by Intramolecular Amination of Organoboronates and Organobis(boronates). *Org. Lett.* **2021**, *23* (9), 3379-3383.
- (10) Xu, F.; Simmons, B.; Reamer, R. A.; Corley, E.; Murry, J.; Tschaen, D. Chlorination/cyclodehydration of amino alcohols with SOCl<sub>2</sub>: an old reaction revisited. *J. Org. Chem.* **2008**, *73* (1), 312-315.
- (11) van Rootselaar, S.; Peterse, E.; Blanco-Ania, D.; Rutjes, F. P. J. T. Stereoselective Mannich Reactions in the Synthesis of Enantiopure Piperidine Alkaloids and Derivatives. *Eur. J. Org. Chem.* **2023**, *26* (22).
- (12) Zhou, Q. H.; Dai, J. Y.; Zhao, W. J.; Zhong, X. Y.; Liu, C. Y.; Luo, W. W.; Li, Z. W.; Li, J. S.; Liu, W. D. Photocatalytic synthesis of azaheterocycle-fused piperidines and pyrrolidines *via* tandem difunctionalization of unactivated alkenes. *Org. Biomol. Chem.* **2023**, *21* (16), 3317-3322.
- (13) Ebule, R.; Mudshinge, S.; Nantz, M. H.; Mashuta, M. S.; Hammond, G. B.; Xu, B. A 5 + 1



- Protic Acid Assisted Aza-Pummerer Approach for Synthesis of 4-Chloropiperidines from Homoallylic Amines. *J. Org. Chem.* **2019**, *84* (6), 3249-3259.
- (14) Shan, C.; Xu, J.; Cao, L.; Liang, C.; Cheng, R.; Yao, X.; Sun, M.; Ye, J. Rapid Synthesis of alpha-Chiral Piperidines *via* a Highly Diastereoselective Continuous Flow Protocol. *Org. Lett.* **2022**, *24* (17), 3205-3210.
- (15) Cui, Z.; Yu, H. J.; Yang, R. F.; Gao, W. Y.; Feng, C. G.; Lin, G. Q. Highly enantioselective arylation of N-tosylalkylaldimines catalyzed by rhodium-diene complexes. *J. Am. Chem. Soc.* **2011**, *133* (32), 12394-12397.
- (16) Liu, G. Q.; Cui, B.; Xu, R.; Li, Y. M. Preparation of trans-2-Substituted-4-halopiperidines and cis-2-Substituted-4-halotetrahydropyrans *via* AlCl<sub>3</sub>-Catalyzed Prins Reaction. *J. Org. Chem.* **2016**, *81* (12), 5144-5161.
- (17) Fujita, K.; Fujii, T.; Yamaguchi, R. CpIr complex-catalyzed N-heterocyclization of primary amines with diols: a new catalytic system for environmentally benign synthesis of cyclic amines. *Org. Lett.* **2004**, *6* (20), 3525-3528.
- (18) Yamada, T.; Sato, M.; Gunji, Y.; Ikeno, T. Efficient Preparation of Optically Pure C2-Symmetrical Cyclic Amines for Chiral Auxiliary. *Synthesis* **2004**, *2004* (09), 1434-1438.
- (19) Ju, Y.; Varma, R. S. Aqueous N-heterocyclization of primary amines and hydrazines with dihalides: microwave-assisted syntheses of N-azacycloalkanes, isoindole, pyrazole, pyrazolidine, and phthalazine derivatives. *J. Org. Chem.* **2006**, *71* (1), 135-141.
- (20) Lu, Z.; Stahl, S. S. Intramolecular Pd(II)-catalyzed aerobic oxidative amination of alkenes: synthesis of six-membered N-heterocycles. *Org. Lett.* **2012**, *14* (5), 1234-1237.
- (21) Li, K.; Li, M. L.; Zhang, Q.; Zhu, S. F.; Zhou, Q. L. Highly Enantioselective Nickel-Catalyzed Intramolecular Hydroalkenylation of N- and O-Tethered 1,6-Dienes To Form Six-Membered Heterocycles. *J. Am. Chem. Soc.* **2018**, *140* (24), 7458-7461.
- (22) Ashenurst, J. Electrophilic Aromatic Substitution: The Six Key Reactions. 2020.
- (23) D Johnson, B. C.; Katritzky, A. R.; Ridgewell, B. J.; Viney, M.; Johnson, C. D.; Chem, A.; Chern Soc, J. *The Mechanism of the Electrophilic Substitution of Heteroaromatic Compounds. Part VI. The Nitration of Pyridines in the 3-Position as Free Bases and as Conjugate Acids*; **1967**.
- (24) D Johnson, B. C.; Katritzky, A. R.; Shakir, N.; Viney, M. *The Mechanism of the Electrophilic Substitution of Heteroaromatic Compounds. Part VIII. The a-, p-, and .y-Nitration of Pyridine I-Oxides*.
- (25) D Johnson, B. C.; Katritzky, A. R.; Viney, M.; Johnson, D.; Ridgewell, B. J.; Paper, p. H.; Hertog, d.; van Weeren, J. W.; Johnson, C. D.; Shakir, N. *The Mechanism of the Electrophilic Substitution of Heteroaromatic Compounds. Part VII. The Nitration of Pyridines in the a-Position and Rules for the Nitration of Substituted Pyridines*; **1963**.
- (26) Katritzky, A. R.; Fan, W. Q. Mechanisms and rates of the electrophilic substitution reactions of heterocycles. **1992**; *34*, 2179-2229.
- (27) Garcia, E. E.; Greco, C. V.; Hunsberger, I. M. Facile Bromination of Pyridine-Type Heterocycles at the β-Position. *J. Am. Chem. Soc.* **2002**, *82* (16), 4430-4431.
- (28) Pearson, D. E.; Hargrove, W. W.; Chow, J. K. T.; Suthers, B. R. The Swamping Catalyst Effect. III. The Halogenation of Pyridine and Picolines. *J. Org. Chem.* **2002**, *26* (3), 789-792.
- (29) John, A. J.; Keith, M. *Heterocycl. Chem.*; Blackwell Publishing Ltd, **2010**.
- (30) Robertson, S. D.; Kennedy, A. R.; Liggat, J. J.; Mulvey, R. E. Facile synthesis of a

- genuinely alkane-soluble but isolable lithium hydride transfer reagent. *Chem. Commun. (Camb.)* **2015**, 51 (25), 5452-5455.
- (31) Zhang, L. H.; Tan, Z. L. Double nucleophilic addition. A new one-pot synthesis of 2-alkyl- and 2-phenyl-5-hydrazinopyridine from pyridine. *Tetrahedron Lett.* **2000**, 41 (17), 3025-3028.
- (32) Rohrbach, S.; Smith, A. J.; Pang, J. H.; Poole, D. L.; Tuttle, T.; Chiba, S.; Murphy, J. A. Concerted Nucleophilic Aromatic Substitution Reactions. *Angew. Chem. Int. Ed. Engl.* **2019**, 58 (46), 16368-16388.
- (33) Shreve, R. N.; Riechers, E. H.; Rubenkoenig, H.; Goodman, A. H. Amination in the heterocyclic series by sodium amide. *Ind. Eng. Chem.* **1940**, 32 (2), 173-178.
- (34) Pang, J. H.; Kaga, A.; Chiba, S. Nucleophilic amination of methoxypyridines by a sodium hydride-iodide composite. *Chem. Commun. (Camb.)* **2018**, 54 (73), 10324-10327.
- (35) Youssif, S. Recent trends in the chemistry of pyridine N-oxide. *Arkivoc* **2001**, 2001 (1), 242-268.
- (36) Bull, J. A.; Mousseau, J. J.; Pelletier, G.; Charette, A. B. Synthesis of pyridine and dihydropyridine derivatives by regio- and stereoselective addition to N-activated pyridines. *American Chemical Society* **2012**, 112, 2642-2713.
- (37) den Hertog, H. J.; Overhoff, J. Pyridine-N-oxide as an intermediate for the preparation of 2- and 4-substituted pyridines. *Recl. Trav. Chim. Pays-Bas* **2010**, 69 (4), 468-473.
- (38) Kato, T.; Yamanaka, H. Reaction of Pyridine and Quinoline N-Oxides with Phenylmagnesium Bromide. *J. Org. Chem.* **1965**, 30 (3), 910-913.
- (39) Webb, T. R. Regioselective Synthesis of 2-Substituted Pyridines Via Grignard Addition to 1-(Alkoxy-carboxy)-Pyridinium Salts. *Tetrahedron Lett.* **1985**, 26 (27), 3191-3194.
- (40) Andersson, H.; Almqvist, F.; Olsson, R. Synthesis of 2-substituted pyridines via a regiospecific alkylation, alkynylation, and arylation of pyridine N-oxides. *Org. Lett.* **2007**, 9 (7), 1335-1337.
- (41) Feely, W. E.; Beavers, E. M. Cyanation of Amine Oxide Salts - a New Synthesis of Cyanopyridines. *J. Am. Chem. Soc.* **1959**, 81 (15), 4004-4007.
- (42) Fife, W. K. Regioselective Cyanation of Pyridine 1-Oxides with Trimethylsilanecarbonitrile - a Modified Reissert-Henze Reaction. *J. Org. Chem.* **1983**, 48 (8), 1375-1377.
- (43) Reddy, K. S.; Iyengar, D. S.; Bhalarao, U. T. The reaction of pyridine N-oxide and its benzoanalogues with arenesulfonyl azides: novel synthesis of tetrazoloazines. *Chem. Lett.* **1983**, 12 (11), 1745-1748.
- (44) Abramovitch, R. A.; Singer, G. M. A Direct Alkyl and Aryl Amination of Heteroaromatic Nitrogen Compounds. *American Chemical Society* **1969**; 91, 5672-5673.
- (45) Medley, J. W.; Movassaghi, M. Direct dehydrative N-pyridinylation of amides. *J. Org. Chem.* **2009**, 74 (3), 1341-1344.
- (46) Bauer, L.; Prachayasittikul, S. Deoxydative substitutions of pyridine 1-oxides by thiols. **1986**, 24, 161-179.
- (47) Prachayasittikul, S.; Bauer, L. The deoxydative substitution reactions of nicotinamide and nicotinic acid N-oxides by 1-adamantanethiol in acetic anhydride. *J. Heterocycl. Chem.* **1985**, 22 (3), 771-775.
- (48) Prachayasittikul, S.; Doss, G.; Bauer, L. Deoxydative substitution of pyridine 1-oxides by thiols. Part XX. Reactions of (2, 3, and 4-phenyl)-, 3-acetamido-, 3-bromo-, 3-acetoxy-, 3-ethoxypyridine 1-oxides with 1-adamantanethiol in acetic anhydride. *J. Heterocycl. Chem.* **1991**, 28 (4), 1051-1060.

- (49) Bremner, D. H.; Dunn, A. D.; Wilson, K. A. The Synthesis of Thienopyridines from Ortho-Halogenated Pyridine-Derivatives. *Synthesis-Stuttgart* **1992**, 1992 (6), 528-530.
- (50) Bremner, D. H.; Dunn, A. D.; Wilson, K. A.; Sturrock, K. R.; Wishart, G. The synthesis of thienopyridines from ortho-halogenated pyridine derivatives. Part 2. *Synthesis* **1998**, 1997, 1095-1097.
- (51) Habib, I.; Singha, K.; Hossain, M. Recent Progress on Pyridine N-Oxide in Organic Transformations: A Review. *ChemistrySelect* **2023**, 8 (5).
- (52) Jordan, R. F.; Taylor, D. F. Zirconium-catalyzed coupling of propene and  $\alpha$ -picoline. *J. Am. Chem. Soc.* **2002**, 124 (2), 778-779.
- (53) Deelman, B.-J.; Stevels, W. M.; Teuben, J. H.; Lakin, M. T.; Spek, A. L. Insertion Chemistry of Yttrium Complex Cp\*2Y(2-pyridyl) and Molecular Structure of an Unexpected CO Insertion Product (Cp\*2Y)<sub>2</sub>( $\mu$ - $\eta^2$ -OC(NC<sub>5</sub>H<sub>4</sub>)<sub>2</sub>). *Organometallics* **2002**, 21 (10), 3881-3891.
- (54) Lewis, J. C.; Bergman, R. G.; Ellman, J. A. Rh(I)-catalyzed alkylation of quinolines and pyridines via C-H bond activation. *J. Am. Chem. Soc.* **2007**, 129 (17), 5332-5333.
- (55) Campeau, L. C.; Schipper, D. J.; Fagnou, K. Site-selective sp<sup>2</sup> and benzylic sp<sup>3</sup> palladium-catalyzed direct arylation. *J. Am. Chem. Soc.* **2008**, 130 (11), 3266-3267.
- (56) Cho, S. H.; Hwang, S. J.; Chang, S. Palladium-catalyzed C-H functionalization of pyridine N-oxides: highly selective alkenylation and direct arylation with unactivated arenes. *J. Am. Chem. Soc.* **2008**, 130 (29), 9254-9256.
- (57) Do, H. Q.; Daugulis, O. Copper-catalyzed arylation of heterocycle C-H bonds. *J. Am. Chem. Soc.* **2007**, 129 (41), 12404-12405.
- (58) Kanyiva, K. S.; Nakao, Y.; Hiyama, T. Nickel-catalyzed addition of pyridine-N-oxides across alkynes. *Angew. Chem. Int. Ed. Engl.* **2007**, 46 (46), 8872-8874.
- (59) Nakao, Y.; Kanyiva, K. S.; Hiyama, T. A strategy for C-H activation of pyridines: direct C-2 selective alkenylation of pyridines by nickel/Lewis acid catalysis. *J. Am. Chem. Soc.* **2008**, 130 (8), 2448-2449.
- (60) Hoffmann, R.; Woodward, R. B. Selection Rules for Concerted Cycloaddition Reactions. *J. Am. Chem. Soc.* **1965**, 87 (9), 2046-&.
- (61) Serrano-Perez, J. J.; de Vleeschouwer, F.; de Proft, F.; Mendive-Tapia, D.; Bearpark, M. J.; Robb, M. A. How the conical intersection seam controls chemical selectivity in the photocycloaddition of ethylene and benzene. *J. Org. Chem.* **2013**, 78 (5), 1874-1886.
- (62) Wilzbach, K. E.; Kaplan, L. Photoaddition of benzene to olefins. II. Stereospecific 1,2 and 1,4 cycloadditions. *J. Am. Chem. Soc.* **2002**, 124 (8), 2073-2074.
- (63) Clifford, S.; Bearpark, M. J.; Bernardi, F.; Olivucci, M.; Robb, M. A.; Smith, B. R. Conical intersection pathways in the photocycloaddition of ethene and benzene: A CASSCF study with MMVB dynamics. *J. Am. Chem. Soc.* **1996**, 118 (31), 7353-7360.
- (64) Danishefsky, S.; Cain, P. An expeditious synthesis of estrone. *J. Steroid Biochem.* **1975**, 6 (3-4), 177-181.
- (65) Donohoe, T. J.; McRiner, A. J.; Sheldrake, P. Partial reduction of electron-deficient pyridines. *Org. Lett.* **2000**, 2 (24), 3861-3863.
- (66) Glorius, F.; Spielkamp, N.; Holle, S.; Goddard, R.; Lehmann, C. W. Efficient asymmetric hydrogenation of pyridines. *Angew. Chem. Int. Ed. Engl.* **2004**, 43 (21), 2850-2852.
- (67) Glorius, F. Asymmetric hydrogenation of aromatic compounds. *Org. Biomol. Chem.* **2005**, 3 (23), 4171-4175.
- (68) Wu, J.; Chen, Z.; Barnard, J. H.; Gunasekar, R.; Pu, C.; Wu, X.; Zhang, S.; Ruan, J.; Xiao,

- J. Synthesis of chiral piperidines from pyridinium salts *via* rhodium-catalysed transfer hydrogenation. *Nat. Catal.* **2022**, 5 (11), 982-992.
- (69) Chen, F.; Li, W.; Sahoo, B.; Kreyenschulte, C.; Agostini, G.; Lund, H.; Junge, K.; Beller, M. Hydrogenation of Pyridines Using a Nitrogen-Modified Titania-Supported Cobalt Catalyst. *Angew. Chem. Int. Ed. Engl.* **2018**, 57 (44), 14488-14492.
- (70) Liu, Y.; Du, H. Metal-free borane-catalyzed highly stereoselective hydrogenation of pyridines. *J. Am. Chem. Soc.* **2013**, 135 (35), 12968-12971.
- (71) Prashad, M. Approaches to the preparation of enantiomerically pure (2R,2' R)-(+)-threo-methylphenidate hydrochloride. *Adv. Synth. Catal.* **2001**, 343 (5), 379-392.
- (72) Lyle, R. E.; Boyce, C. B. Sodium-Borohydride Reduction of Sterically Hindered Pyridinium Salts. *J. Org. Chem.* **1974**, 39 (25), 3708-3711.
- (73) Knaus, E. E.; Redda, K. The sodium borohydride reduction of N-sulfonylpyridinium salts. Synthesis of N-sulfonyl-1,4-(1,2-) dihydropyridines. *Can. J. Chem.* **1977**, 55 (10), 1788-1791.
- (74) Fowler, F. W. Synthesis of 1,2- and 1,4-dihydropyridines. *J. Org. Chem.* **2002**, 37 (9), 1321-1323.
- (75) Mishra, S.; Karabiyikoglu, S.; Fletcher, S. P. Catalytic Enantioselective Synthesis of 3-Piperidines from Arylboronic Acids and Pyridine. *J. Am. Chem. Soc.* **2023**, 145 (26), 14221-14226.
- (76) Kikugawa, Y.; Kuramoto, M.; Saito, I.; Yamada, S. Chemistry of Diborane and Sodium Borohydride. X. The Reduction of 2-or 4-Substituted Pyridines and Quinolines, and 1-or 3-Substituted Isoquinolines with Sodium Borohydride. *Chem. and Pharm. Bull.* **1973**, 21 (9), 1927-1937.
- (77) Zhao, G.; Deo, U. C.; Ganem, B. Selective fowler reductions: asymmetric total syntheses of isofagomine and other 1-azasugars from methyl nicotinate. *Org. Lett.* **2001**, 3 (2), 201-203.
- (78) Wertjes, W. C.; Southgate, E. H.; Sarlah, D. Recent advances in chemical dearomatization of nonactivated arenes. *Chem. Soc. Rev.* **2018**, 47 (21), 7996-8017.
- (79) Ma, J.; Strieth-Kalthoff, F.; Dalton, T.; Freitag, M.; Schwarz, J. L.; Bergander, K.; Daniliuc, C.; Glorius, F. Direct Dearomatization of Pyridines *via* an Energy-Transfer-Catalyzed Intramolecular [4+2] Cycloaddition. *Chem-Us* **2019**, 5 (11), 2854-2864.
- (80) Preindl, J.; Chakrabarty, S.; Waser, J. Dearomatization of electron poor six-membered N-heterocycles through [3 + 2] annulation with aminocyclopropanes. *Chem. Sci.* **2017**, 8 (10), 7112-7118.
- (81) Chiminelli, M.; Serafino, A.; Ruggeri, D.; Marchio, L.; Bigi, F.; Maggi, R.; Malacria, M.; Maestri, G. Visible-Light Promoted Intramolecular para-Cycloadditions on Simple Aromatics. *Angew. Chem. Int. Ed. Engl.* **2023**, 62 (12), e202216817.
- (82) Maier, W.; Eberbach, W.; Fritz, H. Zur Synthese von Derivaten des Pyrido[1,2-a]azepins. *Helv. Chim. Acta* **1991**, 74 (5), 1095-1101.
- (83) Pabel, J.; Hosl, C. E.; Maurus, M.; Ege, M.; Wanner, K. T. Generation of N-acylpyridinium ions from pivaloyl chloride and pyridine derivatives by means of silyl triflates. *J. Org. Chem.* **2000**, 65 (26), 9272-9275.
- (84) Comins, D. L.; Abdullah, A. H. Regioselective Addition of Grignard-Reagents to 1-Acylpyridinium Salts - a Convenient Method for the Synthesis of 4-Alkyl(Aryl)Pyridines. *J. Org. Chem.* **1982**, 47 (22), 4315-4319.
- (85) Mangeney, P.; Gosmini, R.; Raussou, S.; Commercon, M.; Alexakis, A. Preparation and

- Utilization of Chiral Dihydropyridines - Synthesis of Chiral Indoloquinolizines and Benzoquinolizines. *J. Org. Chem.* **1994**, *59* (7), 1877-1888.
- (86) Yamaguchi, R.; Moriyasu, M.; Yoshioka, M.; Kawanisi, M. Reaction of allylic tin reagents with nitrogen heteroaromatics activated by alkyl chloroformates: regioselective synthesis of  $\alpha$ -allylated 1,2-dihydropyridines and change of the regioselectivity depending on methyl substituents at the allylic moiety. *J. Org. Chem.* **2002**, *53* (15), 3507-3512.
- (87) Comins, D. L.; Brown, J. D. Regioselective Addition of Titanium Enolates to 1-Acylpyridinium Salts - a Convenient Synthesis of 4-(2-Oxoalkyl)Pyridines. *Tetrahedron Lett.* **1984**, *25* (31), 3297-3300.
- (88) Nakazono, Y.; Yamaguchi, R.; Kawanisi, M. Synthesis of cis- and trans-2,6-dialkylated piperidines through highly regioselective  $\alpha$ -alkynylation of pyridinium salts and its application to synthesis of ( $\pm$ )-solenopsine A. *Chem. Lett.* **1984**, *13* (7), 1129-1132.
- (89) Yamaguchi, R.; Hata, E.; Matsuki, T.; Kawanisi, M. An efficient regio- and stereoselective synthesis of (+)-monomorine I via the highly regioselective  $\alpha$ -alkynylation of a 1-acylpyridinium salt. *J. Org. Chem.* **2002**, *52* (10), 2094-2096.
- (90) Wang, X.; Kauppi, Anna M.; Olsson, R.; Almqvist, F. Efficient Solution-Phase Parallel Synthesis of 4-Substituted N-Protected Piperidines. *Eur. J. Org. Chem.* **2003**, *2003* (23), 4586-4592.
- (91) Charette, A. B.; Grenon, M.; Lemire, A.; Pourashraf, M.; Martel, J. Practical and highly regio- and stereoselective synthesis of 2-substituted dihydropyridines and piperidines: Application to the synthesis of (-)-coniine. *American Chemical Society* **2001**; *123*, 11829-11830.
- (92) Charette, A. B.; Mathieu, S.; Martel, J. Electrophilic activation of lactams with Tf<sub>2</sub>O and pyridine: expedient synthesis of (+/-)-tetraponerine T4. *Org Lett* **2005**, *7* (24), 5401-5404.
- (93) Barbier, D.; Marazano, C.; Riche, C.; Das, B. C.; Potier, P. An enantioselective access to 1-alkyl-1,2-dihydroisoquinolines and 1-alkyl-, 3-alkyl-, and 1,3-dialkyl-1,2,3,4-tetrahydroisoquinolines. *J. Org. Chem.* **1998**, *63* (6), 1767-1772.
- (94) Donohoe, T. J.; Connolly, M. J.; Walton, L. Regioselective nucleophilic addition to pyridinium salts: a new route to substituted dihydropyridones. *Org. Lett.* **2009**, *11* (23), 5562-5565.
- (95) Lyle, R. E.; White, E. Reaction of organometallic reagents with pyridinium ions. *J. Org. Chem.* **2002**, *36* (6), 772-777.
- (96) Hilgeroth, A.; Baumeister, U. The First Functionalized 6,12-Diazatetrakis-homocubanes. *Angew. Chem. Int. Ed. Engl.* **2000**, *39* (3), 576-578.
- (97) Bennasar, M. L.; Juan, C.; Bosch, J. Addition of organocopper reagents to N-alkylpyridinium salts. A flexible access to polysubstituted dihydropyridines. *Tetrahedron Lett.* **2001**, *42* (4), 585-588.
- (98) Volochnyuk, D. M.; Kostyuk, A. N.; Pinchuk, A. M.; Tolmachev, A. A. Addition of some aminoheterocycles to N-benzyl-3-cyanopyridinium chloride. *Tetrahedron Lett.* **2003**, *44* (2), 391-394.
- (99) Yamada, S.; Misono, T.; Ichikawa, M.; Morita, C. Regio- and stereoselective synthesis of 1,4-dihydropyridines by way of an intramolecular interaction of a thiocarbonyl or carbonyl with a pyridinium nucleus. *Tetrahedron Lett.* **2001**, *57* (43), 8939-8949.
- (100) Wenkert, E.; Angell, E. C.; Drexler, J.; Moeller, P. D. R.; Pyrek, J. S.; Shi, Y. J.; Sultana, M.; Vankar, Y. D. Carbon-carbon bond-forming additions to 1-alkyl-3-acylpyridinium salts. *The J. Org. Chem.* **2002**, *51* (15), 2995-3000.

- (101) Foster, R.; Fyfe, C. A. Nuclear magnetic resonance spectra of intermediates formed by the action of nucleophiles on pyridine and pyridinium ions. *Tetrahedron Lett.* **1969**, 25 (7), 1489-1496.
- (102) Lyle, R. E.; Gauthier, G. J. Reactions of Nucleophiles with Pyridinium Ions . Cyanide Ion Reactions with Some Pyridinium Ions. *Tetrahedron Lett* **1965**, 6 (51), 4615.
- (103) Okamoto, T.; Hirobe, M.; Yabe, E. Reaction of N-aminopyridinium derivatives. VI. Properties of s-triazolo[1,5-a]pyridine ring. *Chem Pharm Bull (Tokyo)* **1966**, 14 (5), 523-528.
- (104) Sammes, M. P.; Lee, C. M.; Katritzky, A. R. Synthetic applications of N–N linked heterocycles. Part 14. The preparation of  $\alpha$ -(4-pyridyl)esters and  $\alpha$ -(4-pyridyl)nitriles by regiospecific attack of ester and nitrile anions on pyridinium salts. *J. Chem. Soc., Perkin Trans. I* **1981**, (0), 2476-2482.
- (105) Katritzky, A. R.; Beltrami, H.; Keay, J. G.; Rogers, D. N.; Sammes, M. P.; Leung, C. W. F.; Lee, C. M. Regiospecific Nucleophilic Attack at the ?-Position of 1-(2,6-Dimethyl-4-oxo-1,4-dihydro-1-pyridyl)pyridinium Compounds; Novel Synthesis of 4-Substituted Pyridines. *Angew. Chem. Int. Ed. Engl.* **1979**, 18 (10), 792-793.
- (106) Katritzky, A. R.; Beltrami, H.; Sammes, M. P. Preparation of 4-Aryl-Pyridines and 4-Heteroaryl-Pyridines - Regiospecific Nucleophilic Attack Gamma to a Quaternary Nitrogen Atom. *J. Chem. Soc., Chem. Commun.* **1979**, (3), 137-137.
- (107) Katritzky, A. R.; Beltrami, H.; Sammes, M. P. Synthetic applications of N-N linked heterocycles. Part 7. The preparation of 4-alkyl- and 4-aryl-pyridines by regiospecific attack of Grignard reagents ? to quaternary nitrogen ? to quaternary nitrogen in N-(2,6-dimethyl-4-oxopyridin-1-yl)pyridinium salts. *J. Chem. Soc., Perkin Trans. I* **1980**, (0), 2480-2484.
- (108) Katritzky, A. R.; Keay, J. G.; Rogers, D. N.; Sammes, M. P.; Leung, C. W. F. Synthetic applications of N–N linked heterocycles. Part 9. Preparation of  $\alpha$ -(4-pyridyl)nitroalkanes and N-(4-pyridyl)azoles by regiospecific attack of nitroalkyl and azolyl anions on N-(2,6-dimethyl-4-oxopyridin-1-yl)pyridinium salts. *J. Chem. Soc., Perkin Trans. I* **1981**, (0), 588-592.
- (109) Katritzky, A. R.; Keay, J. G.; Sammes, M. P. Synthetic applications of N–N linked heterocycles. Part 11. Regiospecific synthesis of dialkyl pyridin-4-yl-, quinolin-4-yl-, and isoquinolin-1-yl-phosphonates. *J. Chem. Soc., Perkin Trans. I* **1981**, (0), 668-671.
- (110) Lee, C. M.; Sammes, M. P.; Katritzky, A. R. Synthetic applications of N-N linked heterocycles. Part 8. Regiospecific synthesis of 4-( $\alpha$ -acylalkyl)pyridines by attack of lithium enolates of ketones  $\gamma$  to N-(2,6-dimethyl-4-oxopyridin-1-yl)pyridinium salts. *J. Chem. Soc., Perkin Trans. I* **1980**, (0), 2458-2462.
- (111) Sammes, M. P.; Leung, C. W. F.; Katritzky, A. R. Synthetic applications of N–N linked heterocycles. Part 16. Reactions between carbanions derived from carbon acids with  $pK_a$  7–14 and N-(2,6-dimethyl-4-oxopyridin-1-yl)pyridinium tetrafluoroborate: synthesis of 4-substituted pyridines, and observation of pyridine ringopening reactions. *J. Chem. Soc., Perkin Trans. I* **1981**, (0), 2835-2839.
- (112) Sammes, M. P.; Leung, C. W. F.; Mak, C. K.; Katritzky, A. R. Synthetic applications of N–N linked heterocycles. Part 12. The preparation of 4-alkylthio- and 4-arylthio-pyridines by regiospecific attack of thioalkoxide ions on N-(4-oxopyridin-1-yl)pyridinium salts. *J. Chem. Soc., Perkin Trans. I* **1981**, (0), 1585-1590.
- (113) Katritzky, A. R.; Scriven, E. F. V.; Majumder, S.; Tu, H. B.; Vakulenko, A. V.;

- Akhmedov, N. G.; Murugan, R. Preparation of cyanopyridines by direct cyanation. *Synthesis-Stuttgart* **2005**, *2005* (6), 993-997.
- (114) Haase, M.; Goerls, H.; Anders, E. Synthesis of PO(OR)<sub>2</sub>- and PR<sub>3</sub><sup>+</sup>-Disubstituted Pyridines via N-(Trifluoromethylsulfonyl)pyridinium Triflates. *Synthesis* **1998**, *1998* (02), 195-200.
- (115) Katritzky, A. R.; Zhang, S.; Kurz, T.; Wang, M.; Steel, P. J. Regiospecific synthesis of 4-(2-oxoalkyl)pyridines. *Org. Lett.* **2001**, *3* (18), 2807-2809.
- (116) Toscano, R. A.; Rosas, R.; Hernandez-Galindo, M. D.; Alvarez-Toledano, C.; Garcia-Mellado, O. Synthesis and structural characterization of tricarbonyl 1-azahexa-1,3,5-triene iron(0) complexes. *Transit. Metal. Chem.* **1998**, *23* (2), 113-116.
- (117) Corey, E. J.; Tian, Y. Selective 4-arylation of pyridines by a nonmetalloorganic process. *Org. Lett.* **2005**, *7* (24), 5535-5537.
- (118) Akiba, K.-y.; Iseki, Y. j.; Wada, M. A Convenient Method for the Regioselective Synthesis of 4-Alkyl(aryl)pyridines Using Pyridinium Salts. *Bull. Chem. Soc. Jpn.* **1984**, *57* (7), 1994-1999.
- (119) Gribble, M. W., Jr.; Guo, S.; Buchwald, S. L. Asymmetric Cu-Catalyzed 1,4-De aromatization of Pyridines and Pyridazines without Preactivation of the Heterocycle or Nucleophile. *J. Am. Chem. Soc.* **2018**, *140* (15), 5057-5060.
- (120) Arrowsmith, M.; Hill, M. S.; Hadlington, T.; Kociok-Kohn, G.; Weetman, C. Magnesium-Catalyzed Hydroboration of Pyridines. *Organometallics* **2011**, *30* (21), 5556-5559.
- (121) Oshima, K.; Ohmura, T.; Suginome, M. Regioselective synthesis of 1,2-dihydropyridines by rhodium-catalyzed hydroboration of pyridines. *J. Am. Chem. Soc.* **2012**, *134* (8), 3699-3702.
- (122) Rodriguez, J.; Conley, M. P. A Heterogeneous Iridium Catalyst for the Hydroboration of Pyridines. *Org. Lett.* **2022**, *24* (25), 4680-4683.
- (123) Pang, M.; Shi, L.-L.; Xie, Y.; Geng, T.; Liu, L.; Liao, R.-Z.; Tung, C.-H.; Wang, W. Cobalt-Catalyzed Selective Dearomatization of Pyridines to N-H 1,4-Dihydropyridines. *ACS Catal.* **2022**, *12* (9), 5013-5021.
- (124) Dudnik, A. S.; Weidner, V. L.; Motta, A.; Delferro, M.; Marks, T. J. Atom-efficient regioselective 1,2-dearomatization of functionalized pyridines by an earth-abundant organolanthanide catalyst. *Nat. Chem.* **2014**, *6* (12), 1100-1107.
- (125) Pape, A. R.; Kaliappan, K. P.; Kundig, E. P. Transition-metal-mediated dearomatization reactions. *Chem Rev* **2000**, *100* (8), 2917-2940.
- (126) Uemura, M.; Miyake, R.; Nakayama, K.; Shiro, M.; Hayashi, Y. Chiral (η<sup>6</sup>-arene)chromium complexes in organic synthesis: stereoselective synthesis of chiral (arene)chromium complexes possessing amine and hydroxy groups and their application to asymmetric reactions. *The Journal of Organic Chemistry* **2002**, *58* (5), 1238-1244.
- (127) Brehieny, C. J.; Long, C. Tricarbonyl(η<sup>6</sup>-pyridine)chromium(0). *Acta Crystallogr.* **1994**, *1669*-1671.
- (128) Davies, S. G.; Shipton, M. R. Preparation and reactivity of η<sup>6</sup>-pyridine tricarbonyl chromium complexes. *J. Chem. Soc., Chem. Commun.* **1989**, *0* (15), 995-996.
- (129) Chaudret, B.; Jalon, F. A. Facile preparation of π-arene complexes of ruthenium [(η<sup>5</sup>-C<sub>5</sub>Me<sub>5</sub>)Ru(arene)]X including a π-pyridine and the first π-furan derivatives. *J. Chem. Soc., Chem. Commun.* **1988**, (11), 711-713.
- (130) Fish, R. H.; Fong, R. H.; Anh, T.; Baralt, E. Heteroaromatic nitrogen ligand studies with

- the ( $\eta^5$ -pentamethylcyclopentadienyl)ruthenium cation:  $\eta^1(\text{N})$  and  $\eta^6 \pi$  bonding modes and factors that influence a nitrogen to  $\pi$  rearrangement. *Organometallics* **2002**, *10* (4), 1209-1212.
- (131) Thompson, M. E.; Baxter, S. M.; Ray Bulls, A.; Burger, B. J.; Nolan, M. C.; Santarsiero, B. D.; Schaefer, W. P.; Bereaw, J. E. "Bond Metathesis" for C-H Bonds of Hydrocarbons and Sc-R (R = H, alkyl, aryl) Bonds of Permethylscandocene Derivatives. Evidence for Noninvolvement of the tt System in Electrophilic Activation of Aromatic and Vinylic C-H Bon. *J. Am. Chem. Soc.* **1987**, *109* (3), 203-219.
- (132) Klei, E.; Teuben, J. H. Reaction of Titanocene Alkyls with Pyridines - a Novel Type of Cyclometallation Reaction. *J. Organomet. Chem.* **1981**, *214* (1), 53-64.
- (133) Jantunen, K. C.; Scott, B. L.; Kiplinger, J. L. A comparative study of the reactivity of Zr(IV), Hf(IV) and Th(IV) metallocene complexes: Thorium is not a Group IV metal after all. *J. Alloys Compd.* **2007**, *444-445* (SPEC. ISS.), 363-368.
- (134) Jordan, R. F.; Taylor, D. F.; Baenziger, N. C. Synthesis and Insertion Chemistry of Cationic Zirconium(IV) Pyridyl Complexes - Productive Sigma-Bond Metathesis. *Organometallics* **1990**, *9* (5), 1546-1557.
- (135) Rodewald, S.; Jordan, R. F. Stereoselective Olefin Insertion Reactions of Chiral (EBI)Zr( $\eta^2$ -pyrid-2-yl)<sup>+</sup> and (EBTHI)Zr( $\eta^2$ -pyrid-2-yl)<sup>+</sup> Complexes. *J. Am. Chem. Soc.* **1994**, *116*, 4491-4492.
- (136) Arnold, J.; Woo, H. G.; Tilley, T. D.; Rheingold, A. L.; Geib, S. J. Reaction of an early-transition metal  $\eta^2$ -silaacyl complex with pyridine. Diastereoselectivity in the formation of a (2-pyridyl)silyl methoxy ligand. *Organometallics* **2002**, *7* (9), 2045-2049.
- (137) Arnold, J.; Don Tilley, T.; Rheingold, A. L.; Geib, S. J.; Arif, A. M. Carbonylation Chemistry of the Tantalum Silyl (775-C<sub>5</sub>Me<sub>5</sub>)Cl<sub>3</sub>TaSiMe<sub>3</sub>. Synthesis, Characterization, and Reaction Chemistry of (775-C<sub>5</sub>Me<sub>5</sub>)Cl<sub>3</sub>Ta(772-COSiMe<sub>3</sub>) and Derivatives. *J. Am. Chem. Soc.* **1989**, *111* (1), 149-164.
- (138) Ha, Y.; Dilsky, S.; Graham, P. M.; Liu, W. J.; Reichart, T. M.; Sabat, M.; Keane, J. M.; Harman, W. D. Development of group 6 dearomatization agents. *Organometallics* **2006**, *25* (21), 5184-5187.
- (139) Harman, W. D.; Taube, H. Reactivity of pentaammineosmium(II) with benzene. *J. Am. Chem. Soc.* **2002**, *109* (6), 1883-1885.
- (140) Cordone, R.; Taube, H. Pentaammineosmium(II).  $\eta^2$ -2,6-lutidine: an intermediate for carbon-hydrogen activation. *J. Am. Chem. Soc.* **2002**, *109* (26), 8101-8102.
- (141) Meiere, S. H.; Brooks, B. C.; Gunnoe, T. B.; Sabat, M.; Harman, W. D. A Promising New Dearomatization Agent: Crystal Structure, Synthesis, and Exchange Reactions of the Versatile Complex TpRe(CO)(1-methylimidazole)( $\eta^2$ -benzene) (Tp = Hydridotris(pyrazolyl)borate). *Organometallics* **2001**, *20* (6), 1038-1040.
- (142) Meiere, S. H.; Keane, J. M.; Gunnoe, T. B.; Sabat, M.; Harman, W. D. Binding and activation of aromatic molecules by a molybdenum pi-base. *J. Am. Chem. Soc.* **2003**, *125* (8), 2024-2025.
- (143) Graham, P. M.; Meiere, S. H.; Sabat, M.; Harman, W. D. Dearomatization of Benzene, Deamidization of N,N-Dimethylformamide, and a Versatile New Tungsten  $\pi$  Base. *Organometallics* **2003**, *22* (22), 4364-4366.
- (144) Wilde, J. H.; Myers, J. T.; Dickie, D. A.; Harman, W. D. Molybdenum-Promoted Dearomatization of Pyridines. *Organometallics* **2020**, *39* (8), 1288-1298.
- (145) Shivokevich, P. J.; Myers, J. T.; Smith, J. A.; Pienkos, J. A.; Dakermanji, S. J.; Pert, E. K.;



- Welch, K. D.; Trindle, C. O.; Harman, W. D. Enantioenriched Molybdenum Dearomatization: Dissociative Substitution with Configurational Stability. *Organometallics* **2018**, *37* (23), 4446-4456.
- (146) Wilde, J. H.; Smith, J. A.; Dickie, D. A.; Harman, W. D. Molybdenum-Promoted Synthesis of Isoquinuclidines with Bridgehead CF<sub>3</sub> Groups. *J. Am. Chem. Soc.* **2019**, *141* (47), 18890-18899.
- (147) Delafuente, D. A.; Kosturko, G. W.; Graham, P. M.; Harman, W. H.; Myers, W. H.; Surendranath, Y.; Klet, R. C.; Welch, K. D.; Trindle, C. O.; Sabat, M.; Harman, W. D. Isomerization dynamics and control of the  $\eta^2/N$  equilibrium for pyridine complexes. *J. Am. Chem. Soc.* **2007**, *129* (2), 406-416.
- (148) Harrison, D. P.; Welch, K. D.; Nielander, A. C.; Sabat, M.; Myers, W. H.; Harman, W. D. Efficient synthesis of an  $\eta^2$ -pyridine complex and a preliminary investigation of the bound heterocycle's reactivity. *J. Am. Chem. Soc.* **2008**, *130* (50), 16844-16845.
- (149) Harrison, D. P.; Nichols-Nielander, A. C.; Zottig, V. E.; Strausberg, L.; Salomon, R. J.; Trindle, C. O.; Sabat, M.; Gunnoe, T. B.; Iovan, D. A.; Myers, W. H.; Harman, W. D. Hyperdistorted Tungsten Allyl Complexes and Their Stereoselective Deprotonation to Form Dihapto-Coordinated Dienes. *Organometallics* **2011**, *30* (9), 2587-2597.
- (150) Harrison, D. P.; Zottig, V. E.; Kosturko, G. W.; Welch, K. D.; Sabat, M.; Myers, W. H.; Harman, W. D. Stereo- and Regioselective Nucleophilic Addition to Dihapto-Coordinated Pyridine Complexes. *Organometallics* **2009**, *28* (19), 5682-5690.
- (151) Harrison, D. P.; Sabat, M.; Myers, W. H.; Harman, W. D. Polarization of the pyridine ring: highly functionalized piperidines from tungsten-pyridine complex. *J. Am. Chem. Soc.* **2010**, *132* (48), 17282-17295.
- (152) Wilde, J. H.; Dickie, D. A.; Harman, W. D. A Highly Divergent Synthesis of 3-Aminotetrahydropyridines. *J. Org. Chem.* **2020**, *85* (12), 8245-8252.
- (153) Harrison, D. P.; Kosturko, G. W.; Ramdeen, V. M.; Nielander, A. C.; Payne, S. J.; Sabat, M.; Myers, W. H.; Harman, W. D. Tungsten-Promoted Pyridine Ring Scission: The Selective Formation of  $\eta^2$ -Cyanine and  $\eta^2$ -Merocyanine Complexes and Their Derivatives. *Organometallics* **2010**, *29* (8), 1909-1915.
- (154) Kosturko, G. W. a. H. D. P. a. S. M. a. M. W. H. a. H. W. D. Selectfluor-mediated dialkoxylation of tungsten  $\eta^2$ -pyridinium complexes. *Organometallics* **2009**, *28* (2), 387-389.
- (155) Kosturko, G. W.; Graham, P. M.; Myers, W. H.; Smith, T. M.; Sabat, M.; Harman, W. D. Tungsten-promoted Diels-Alder cycloaddition of pyridines: Dearomatization of 2,6-dimethoxypyridine generates a potent 2-azadiene synthon. *Organometallics* **2008**, *27* (17), 4513-4522.
- (156) Harrison, D. P.; Iovan, D. A.; Myers, W. H.; Sabat, M.; Wang, S.; Zottig, V. E.; Harman, W. D. [4 + 2] Cyclocondensation reactions of tungsten-dihydropyridine complexes and the generation of tri- and tetrasubstituted piperidines. *J. Am. Chem. Soc.* **2011**, *133* (45), 18378-18387.

## Chapter 2

Synthesis of  $\alpha,\gamma$ -Dienyl Tosylimines and Highly Functionalized  
Tetrahydropyridines *via* a Tungsten  $\eta^2$ -*N*-tosyl Pyridinium Salt

## 2.1. The Rotamer Problem with [W]- $\eta^2$ -*N*-Acetyl-Pyridines

A previously reported [W]-( $\eta^2$ -(*N*-acetyl)-pyridinium) complex (**4D**) was used to synthesize topologically complex tetrahydropyridines (THPs),<sup>1-3</sup> isoquinuclidines,<sup>4</sup> and merocyanines.<sup>5</sup> Despite **4D** demonstrating broad synthetic utility, these products were plagued by the presence of rotational isomers (rotamers) from rotation of the acetyl around the pyridine nitrogen (Figure 2.1B). These rotamers, which can greatly complicate NMR analysis, are not seen for complex **4D** or any of the subsequently generated DHP complexes, but first appear upon protonation of dihydropyridines (DHPs)  $\eta^2$ -bound to the [W] fragment. Rotamers are then observed with the resulting allyl complexes and every subsequent compound.<sup>1,6</sup> An exact determination of whether protonating [W]-DHPs to allyls hinders rapid acetyl rotation to be observable on the NMR timescale or if it initiates slow rotation from a standstill remains unclear. Previous studies report that functionalized enamides have a rotation barrier ranging from 10-18 kcal mol, which is generally low enough for rotation to occur at room temperature.<sup>7</sup> However, it is possible [W] backbonding favors maintaining  $\pi$ -electron conjugation, and thus potential disfavoring ambient rotation, in order for the dearomatized pyridine to be a better  $\pi$ -acid.

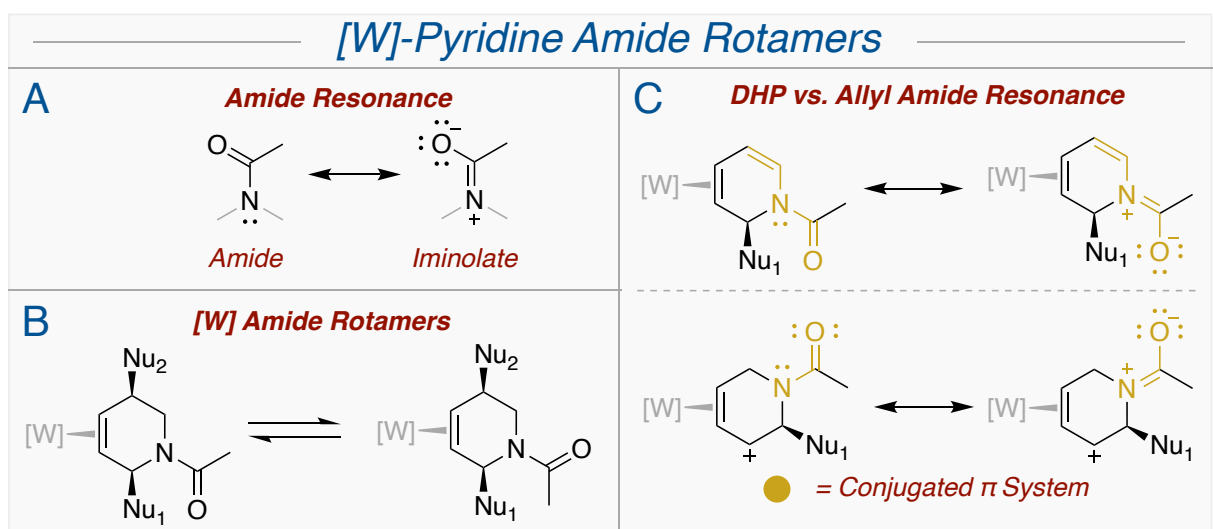


**Figure 2.1:** (A) Resonance forms of an amide. (B) Rotamer forms of [W]-THP complexes. (C) Rotamers of the acetyl system are introduced upon protonation to the  $\eta^3$ -allyl,

## 2.2. Alternative Nitrogen Protecting Groups

Finding an alternative nitrogen protecting group requires overcoming several prerequisite challenges. First, the protecting group must be electron-withdrawing.<sup>8</sup> Compound **3** is synthesized in a 3:1 c.d.r. (*vide supra*), however; this ratio is enriched to 10:1 when the nitrogen is acetylated with gentle heating due to the thermodynamic preference of the metal to stabilize carbeniums and iminiums distal to the PMe<sub>3</sub> ligand.<sup>9</sup> In addition to undermining downstream enantioenrichment efforts and selective substitution patterns, failing to enrich the c.d.r. undermines the core reason for seeking an alternative to the acetyl group, which is to ease spectroscopic analysis. Secondly, the protecting group needs to be compatible with a wide a range of reaction conditions. An alternate protecting group needs to be resistant to both strong acids and strong bases for incorporating nucleophiles/electrophiles and retain the chemical robustness of its acetyl predecessor. Lastly, the protecting group must be suitably activating for subsequent nucleophilic additions for which, like with enriching the c.d.r., an electron-withdrawing group is ideally suited.

A number of nitrogen protecting groups have already been screened for compatibility with this system, including -CH<sub>3</sub> (Me), -(CH<sub>2</sub>)<sub>2</sub>COMe (MVK), -SO<sub>2</sub>CF<sub>3</sub> (Tf), -CO<sub>2</sub>tBu (boc), -COPh (Bz), -CO<sub>2</sub>Bn (Cbz), and -COCF<sub>3</sub> (TFA) (Figure 2.2A).<sup>6,8</sup> While some were unsuitable due to a poor degree of c.d.r. enrichment (Me, boc, and MVK), others could not be isolated cleanly on a large scale (Tf, TFA), and others still were poorly suited to subsequent nucleophilic additions (Cbz). These results indicated a sulfonyl protecting group could be a suitable replacement for acetyl in **4D** (Figure 2.2B). Consequently, 2-nitrobenzenesulfonyl (Ns) was investigated due to its ease of addition and removal *via* thiophenol.<sup>10</sup> When **3** was stirred with NsCl in the presence of a lutidine (triethylamine (TEA) and 2,6-ditertbutylpyridine (DTBP) were unsuccessful), <sup>31</sup>P NMR and crude <sup>1</sup>H NMR spectra indicated successfully formed [W]-*N*-nosyl-pyridinium; however,

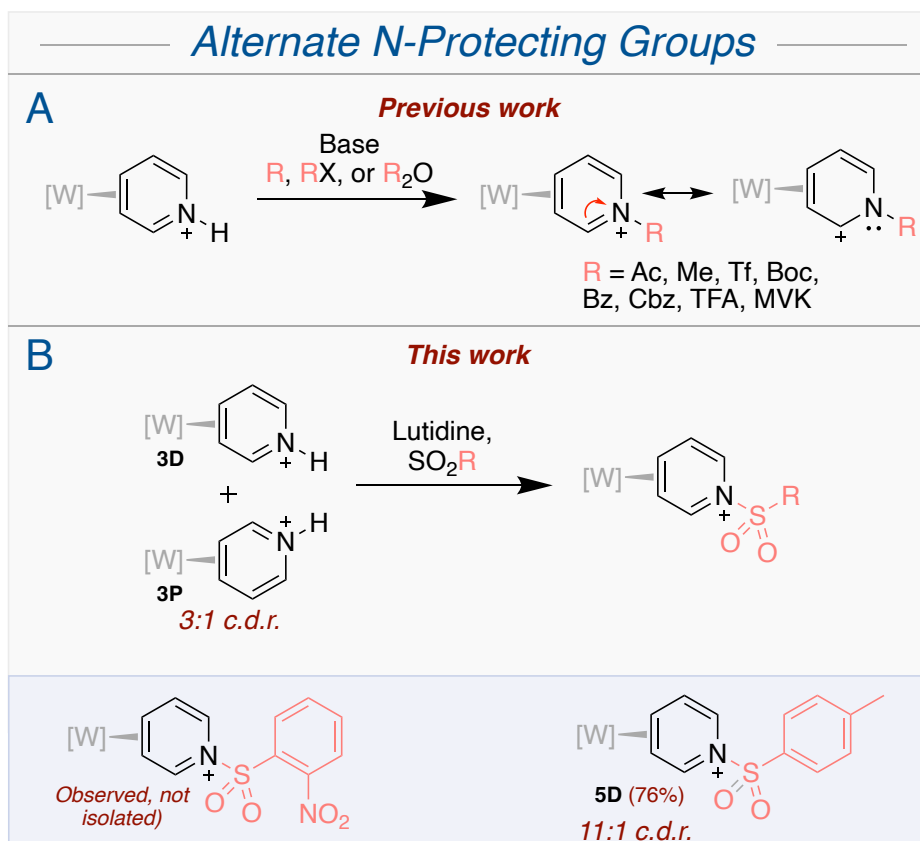


**Figure 2.2:** (A) Previous explorations of *N*-protecting groups prompted an examination of sulfonyl structures. (B) Tosyl was found to be suitably protecting of the nitrogen and activating of the adjacent iminium carbon. Additionally, the withdrawing nature of sulfonyls allowed for an improved c.d.r. enrichment.

attempting an aqueous workup, which is necessary to remove the complex away from residual lutidinium, resulted in an intractable decomposition mixture.

Next, *p*-toluenesulfonyl (tosyl or Ts) was investigated as an acetyl replacement. In a procedure analogous to the synthesis of the *N*-acetylated complex, Ts<sub>2</sub>O was stirred in the presence of **3** and lutidine. Upon addition of lutidine, a color change was immediately observed, and a change in the  $J_{WP}$  observed *via* <sup>31</sup>P NMR from ~294 Hz (consistent with **3D**) to 279 & 286 Hz suggested that tosylation occurred rapidly.<sup>11</sup> After 10 minutes at room temperature, the c.d.r. had changed from 3:1 to ~6:1 (by <sup>31</sup>P NMR). This was subsequently improved to ~11:1 upon heating and would even reach as high as 20:1 (by <sup>1</sup>H NMR) after undergoing the aqueous workup and precipitation. Like with **4D**, the distal tosylated complex (**5D**) is the favored coordination-

diastereomer due to its placement of the iminium, and the carbenium by resonance, in the thermodynamically favored position distal to the  $\text{PMe}_3$  ligand. A cyclic voltammogram showed that this complex has an  $E_{pa}$  of +1.18 V in DMA, indicating a strong resistance to oxidation given the strong  $\pi$ -accepting ability of the tosyl-pyridinium ligand. This structural assignment was supported with 2D NMR and high-resolution mass spectrometry (HRMS) and had yields as high as 89% for multigram (10 g) scale preps. Of note, the  $^1\text{H}$  and  $^{13}\text{C}$  NMRs indicated that the counteranion was a mixture of triflate ( $-\text{OTf}$ ) and tosylate ( $-\text{OTs}$ ).

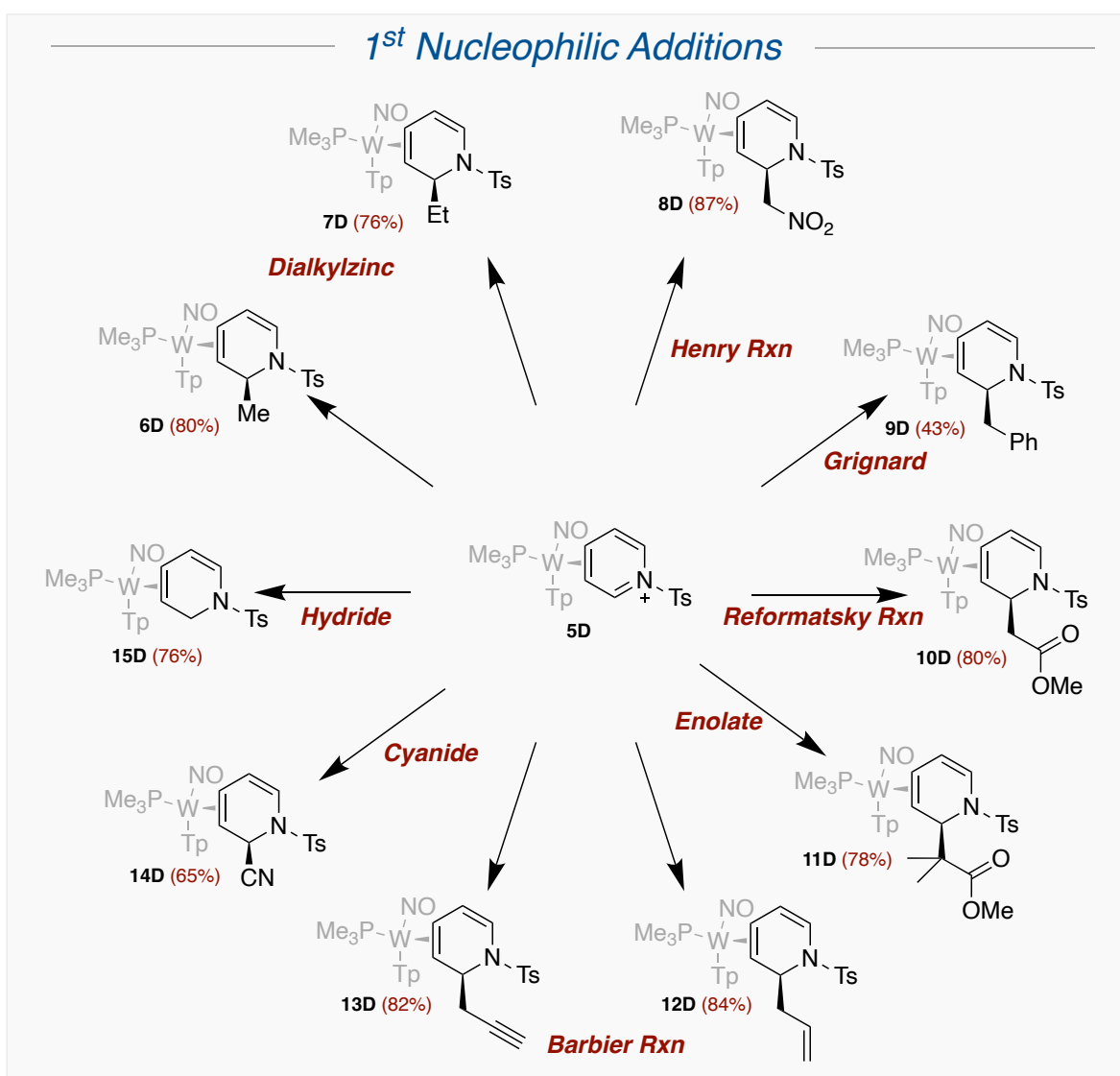


**Figure 2.3:** Nucleophiles were regio- and stereoselectively incorporated at the iminium carbon, resulting in an array of DHP complexes **6D-15D**.

### 2.3. Nucleophilic Additions to [W] $\eta^2$ *N*-Tosyl Pyridinium

The protection of  $\eta^2$ -bound pyridine with a tosyl group activates the iminium carbon for a wide range of nucleophilic additions. Nucleophilic additions to an  $\eta^2$ -arenium complex are well established; however, a distinct advantage for nucleophilic additions to pyridinium complexes over the analogous benzene systems is the lack of a competing elimination pathway. Although preventing elimination generally requires colder temperatures, iminium additions can be conducted at ambient temperatures, allowing for a wider scope of compatible nucleophiles.

The nucleophiles were selected for incorporation to reflect a wide range of compatibility, survive a subsequent protonation with strong acid in converting the  $\eta^2$ -DHP to an  $\eta^3$ -allyl, and avoid a  $\pi$ -donor mediated Zincke reaction ring opening. Yields of DHP complexes **6D-15D** range from 43–87%, and these compounds were synthesized as a mixture of metal racemates under an inert  $N_2$  atmosphere (Figure 2.3). The other incorporated nucleophiles generated carbon-carbon bonds with a handful promoted by zinc. Adding dimethylzinc and diethylzinc to a THF solution of **5D** results in **6D** and **7D** respectively. The structure of **7D** was confirmed *via* SC-XRD (Figure 2.4). A Henry reaction was conducted by stirring **5D** in a DCM solution of nitromethane and triethylamine (TEA), thus forming **8D**. Next, at  $-50\text{ }^\circ\text{C}$ , addition of benzyl magnesium chloride

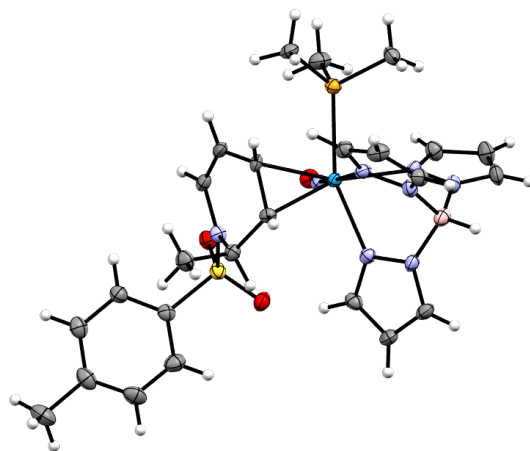


**Figure 2.4:** ORTEP/ellipsoid diagram of **7P** acquired *via* SC-XRD.

(BnMgCl) to a DME solution of **5D** yielded **9D**. An earlier attempt at a Grignard addition used methylmagnesium bromide and resulted in  $\kappa\text{N}$  product with no signs of successful addition. This strong nucleophile likely detosylated the pyridine nitrogen, causing the pyridine to isomerize from  $\eta^2$  to  $\kappa\text{N}$  to reestablish aromaticity. Similarly, a Reformatsky reaction was demonstrated with the incorporation of a methyl ester moiety from reacting a THF solution of **5D** with methyl bromoacetate (MBA) and zinc powder to produce **10D**.

Other incorporated nucleophiles include ketene acetals as methyl trimethylsilyl dimethylketene acetal (MTDA) successfully added in the presence of base to form **11D**. The presence of base quenches a highly acidic TMS intermediate, and removing this base from the reaction resulted in an allyl complex **23**. Barbier reactions were conducted in the syntheses of **12D** and **13D**, which were synthesized through allyl bromide and propargyl bromide respectively were added to a THF solution of **5D** along with zinc powder. Next, cyanide was incorporated by adding NaCN to a methanol solution of **5D** resulting in **14D**. Lastly, a carbon-hydrogen bond was formed at C2 by the addition of sodium borohydride to a solution of **5D** to synthesize **15D**.

Nucleophilic additions to *N*-activated pyridinium salts are well-established in the chemical literature.<sup>12</sup> A wide range of functional groups and nucleophile classes are incorporated via this

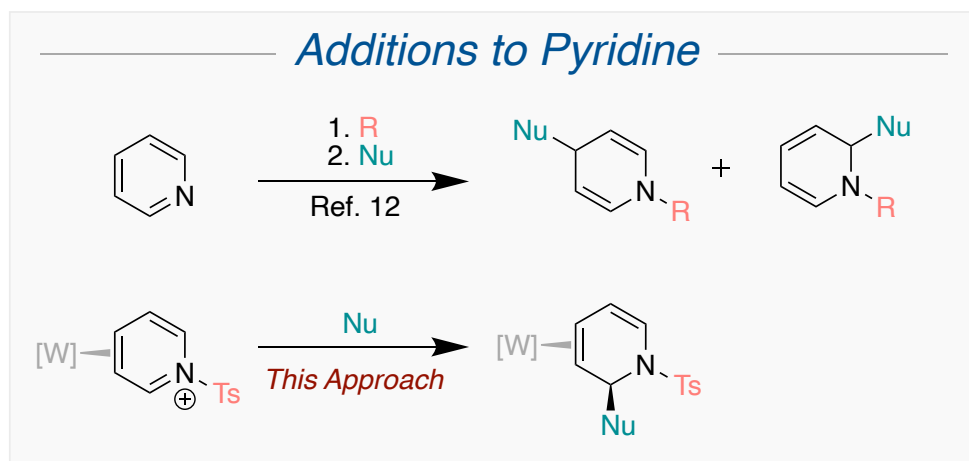


**Figure 2.5:** Additions to an *N*-activated pyridinium, while well established, is improved upon with the pyridinium  $\eta^2$ -coordinated to [W].



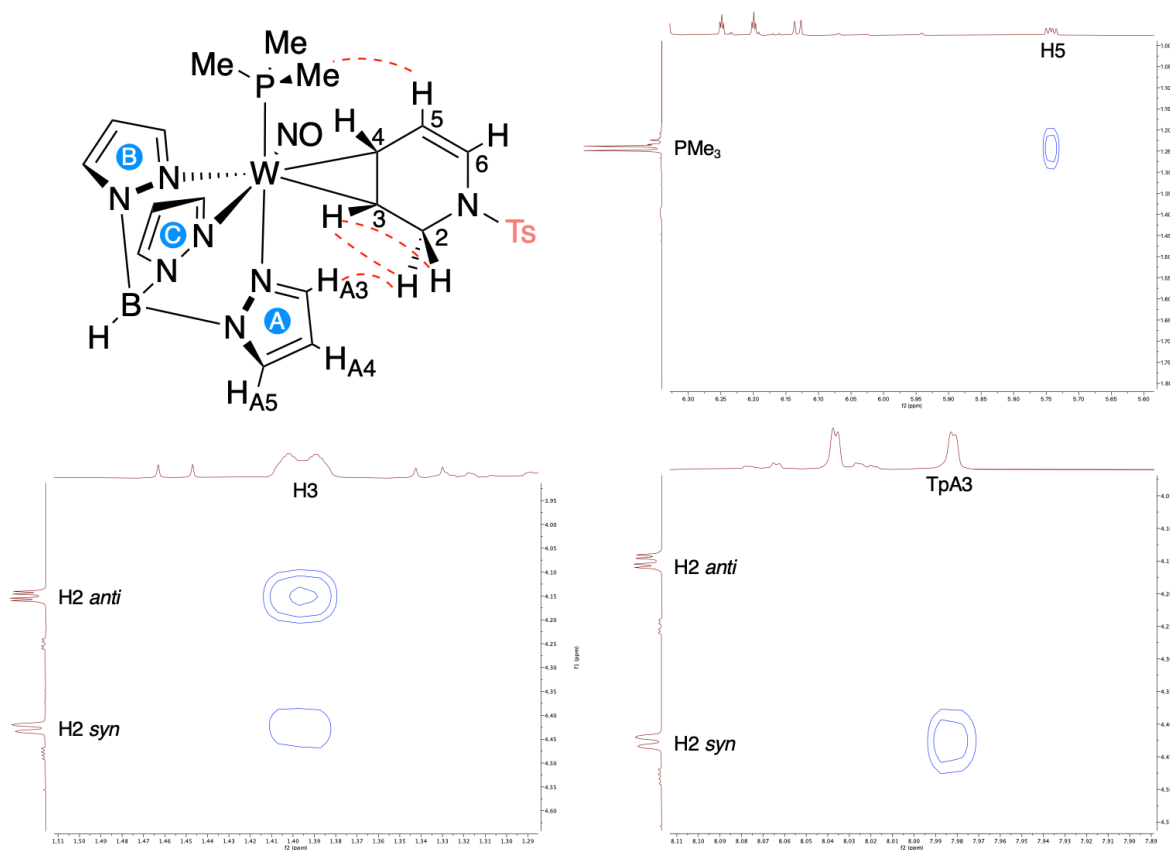


**Figure 2.6:** The H2 geminal protons on **15D** demonstrate the *anti* stereochemical assignment proposed. While the *syn* proton has a strong NOE to the TpA3 proton, the *anti* proton does not. The presence of this interaction in functionalized DHPs supports an *anti* stereochemical assignment of the incorporated functionality.

method, yet these syntheses can be fraught with regio- and enantioselectivity issues when lacking a chiral directing group (Figure 2.5). In the case of  $[W] \eta^2$ -bound pyridinium, while the asymmetric activation of the pyridinium solely activate the iminium carbon for nucleophilic additions, the bulky nature of the tungsten fragment exclusively directs these nucleophiles *anti* to  $[W]$ .<sup>6</sup> These assignments are supported by a variety of distinct NMR features. The free alkene protons consist of a doublet and doublet-of-doublets, the latter which has a Nuclear Overhauser Effect (NOE) interaction with the  $PMe_3$  ligand, supporting the depicted orientation of **15D**. The stereochemical assignments were also supported by a NOE interaction between the C2 *syn* hydrogen and the TpA3 hydrogen (Figure 2.6). NOEs to the C2 geminal set of **15D** support this argument by showing a

NOE from TpA3 to the *syn* proton, which was assigned due its weaker NOE interaction with H3, while lacking an NOE from TpA3 to the *anti* proton. The *syn* H2/TpA3 NOE interaction was present for all DHPs that underwent 2D NMR analysis, supporting the exclusive *anti* stereochemical assignment in each complex.

#### 2.4. DHP Ring Opening

Initial attempts to synthesize **8D** used identical conditions reported by Harrison *et al.* for the analogous acetyl-pyridinium system.<sup>6</sup> Excess nitromethane and TEA were combined in a DCM solution of **5D**, which was stirred for 40 minutes. <sup>1</sup>H NMR revealed the presence of a lone diamagnetic complex characterized by several unique and unexpected peaks, including a downfield doublet at 8.60 ppm and two doublet-of-doublets at 7.29 and 6.27 ppm. Puzzled by this outcome, the equivalencies of nitromethane and TEA were lowered to 1.1 each and the reaction time was shortened to ~1 minute after which a color change from maroon to dark brown occurred. These alterations resulted in the formation of **8D** with 16% of the mystery product present. Following a workup and isolation of **8D** we observed that the mystery product could be generated when **8D** was dissolved in fresh d<sub>3</sub>-MeCN and heated at 50 °C. 2D NMR analysis suggested that **18D** was the identity of this compound. Other DHPs were subjected to heating, and **6D**, **7D**, **9D**, and **10D** also formed analogous terminally substituted  $\alpha,\gamma$  dienyl tosylimines characterized by the same downfield peaks as **18D** with slightly altered chemical shifts and differing upfield peaks (Figure 2.7A). A crystal of **17D** spontaneously formed out of MeCN and confirmed the structural assignment upon successful diffraction (Figure 2.8).

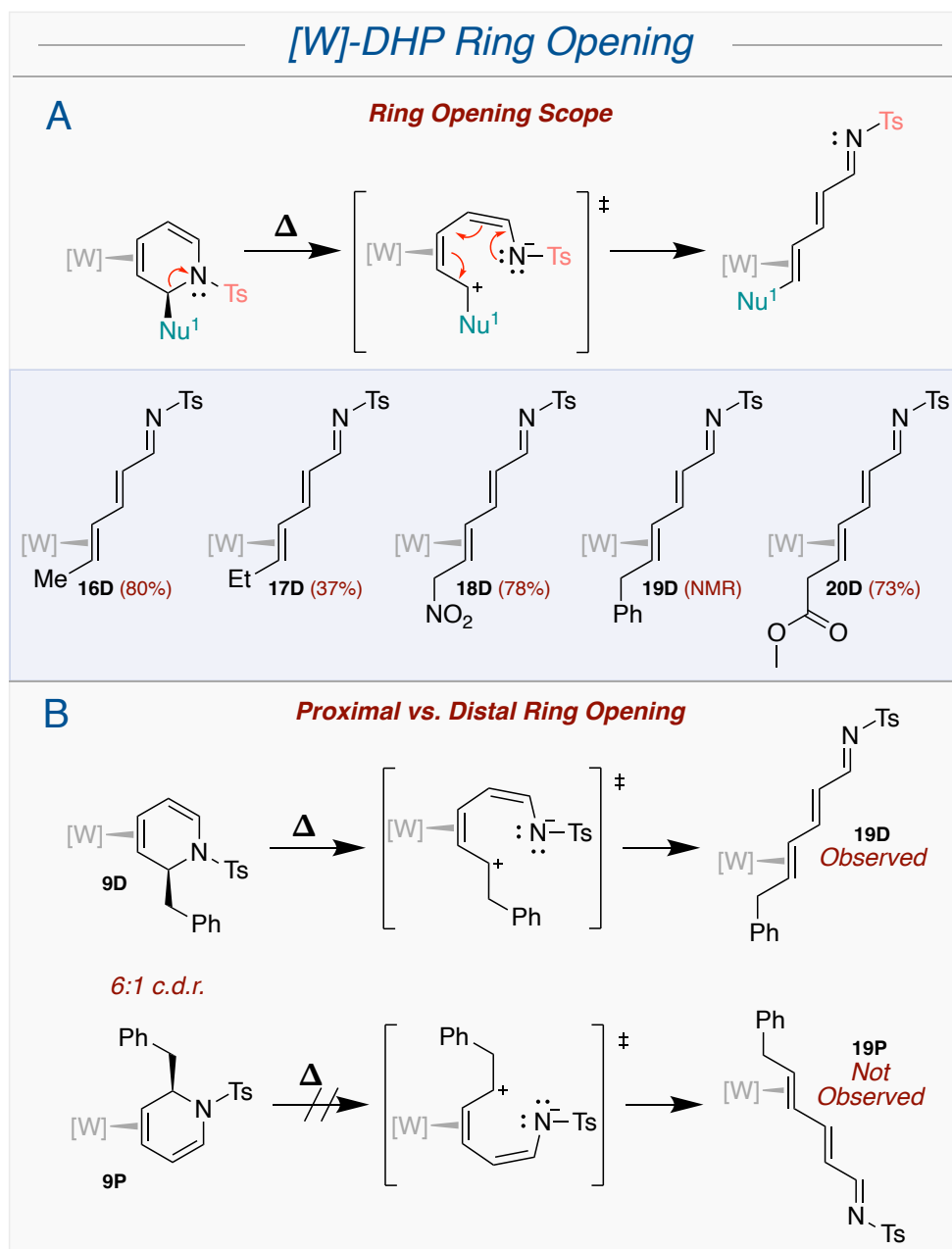


**Figure 2.7:** (A) Ring opening readily occurs with DHPs **16D-20D**. (B) Only the distal form of the DHP precursor undergoes ring-opening while the proximal form does not.

The driving force behind this reaction is the generation of the  $\alpha,\gamma$ -dienyl imines, which are excellent  $\pi$ -acceptor ligands that readily stabilize the metal. Interestingly, when a 6:1 c.d.r. mixture of **9D** to **9P** was gently heated overnight, a crude  $^1\text{H}$  NMR clearly showed that *only the major distal form* ring opened while the minor proximal form remained unreacted DHP (Figure 2.7B). Previous studies demonstrated increased metal-donated electron density on the allylic position

distal to the  $\text{PMe}_3$  ligand, which accounts for the thermodynamic preference to orient carbeniums in this position.<sup>9</sup> This experiment suggests that a similar effect stabilizes the transition state carbenium to promote ring opening of only the distal DHPs but not the proximal DHPs. Further evidence that lowering the energy of the transition state is critical is that **14D** and **15D** do not ring open even after prolonged periods (~3 days) of stronger heating, which only produced decomposition. The inductively withdrawing nitrile group would raise the energy of the transition state while **15D** would induce a transient primary carbocation.

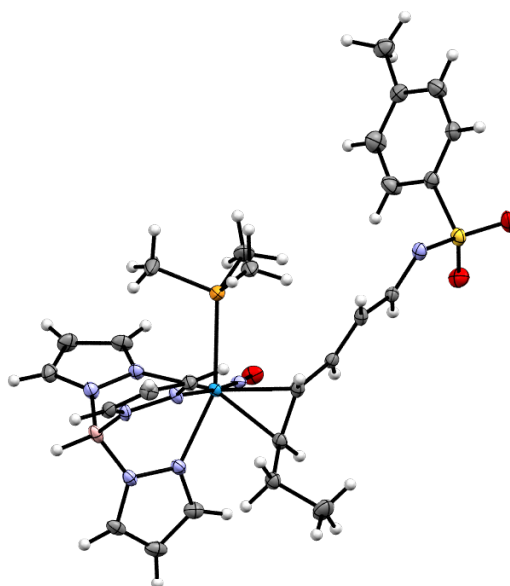


**Figure 2.8:** ORTEP/ellipsoid diagram of **17D** determined *via* SC-XRD. It reveals the ring-opened nature of the compound as well as its trans alkene stereochemistry.

Similar reactions have been previously documented in the chemical literature. DHP ring openings were first reported by Zincke, who accomplished this when adding heteroatomic nucleophiles to a pyridinium salt (Figure 2.9).<sup>13,14</sup> More germane to this study, Chapter 1 described the ring opening of carbon-substituted DHPs  $\eta^2$ -coordinated to  $\{\text{MoTp}(\text{NO})(\text{DMAP})\}$  ( $[\text{Mo}]$ ).<sup>15</sup> However, in this instance, the cumulative effects of the electron-withdrawing  $\text{CF}_3$  group, the electron-donating *N*-methyl group, and the decreased  $\pi$ -backbonding from the  $[\text{Mo}]$  fragment resulted in DHP protonation occurring at the heterocycle nitrogen instead of the carbon to form an

allyl. Nitrogen protonation initiates the observed ring-opening cascade. DHP ring-opening is also preceded when  $\eta^2$ -bound to [W]; however, unlike in this work, where the driving force is to form a good  $\pi$ -accepting  $\alpha,\gamma$ -dienyl imine and the role of the added nucleophile is to stabilize the transition state, DHP ring-opening is only observed when select nucleophiles are utilized containing numerous  $\pi$ -bonds.<sup>5</sup> In this instance, a strong  $\pi$ -acceptor ligand is also formed, but only when the added nucleophile (pyrroles, indole, malononitrile, etc.) can then act as a  $\pi$  donor to stabilize the ring-opening. It is speculated that the tosyl group is more electron-withdrawing than the acetyl, which provides further stabilization to the transition state and thus explaining why  $\alpha,\gamma$ -dienyl imine products are not observed with the acetyl system.

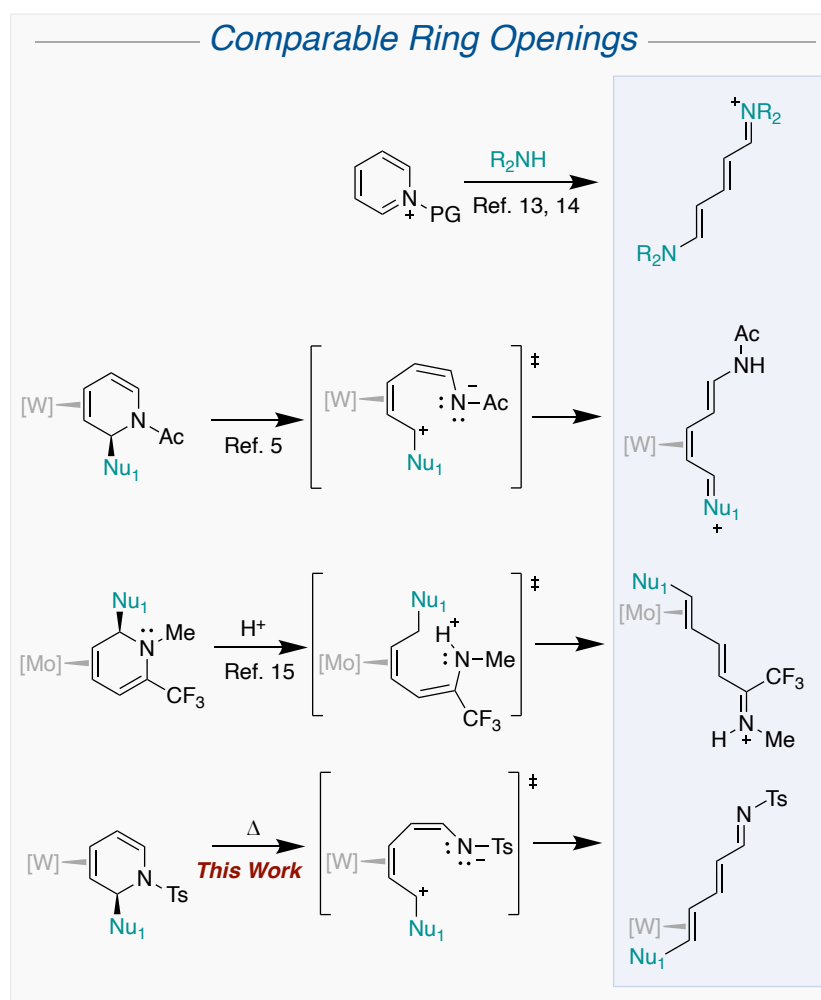


**Figure 2.9:** Other reported instances of DHP ring opening cascades.

## 2.5. Protonation to Allyl Complex

Despite the tendency of these DHPs to ring open, protonations were investigated to see if rotamers were present. Classic enamines accumulate electron density at the  $\beta$ -position as shown by resonance contributors, but the  $\eta^2$  coordination of 1,2-DHPs to a  $\pi$ -basic transition metal fragment induces an umpolung in reactivity (Figure 2.10A). The backbonding from the metal concentrates electron density on the  $\alpha$  carbon.  $\beta$ -position protonation is further disfavored due to the presence of sulfonyl group, which disfavors the charge-separated enamine resonance form due to an electron-deficient nitrogen. This reversal of polarity is consistent with the analogous acetyl system and demonstrated by DHP protonation occurring at C6. Protonation occurs readily when a DHP complex is dissolved in MeCN or DCM and protonated with triflic acid (TfOH) (1.1 eq.).

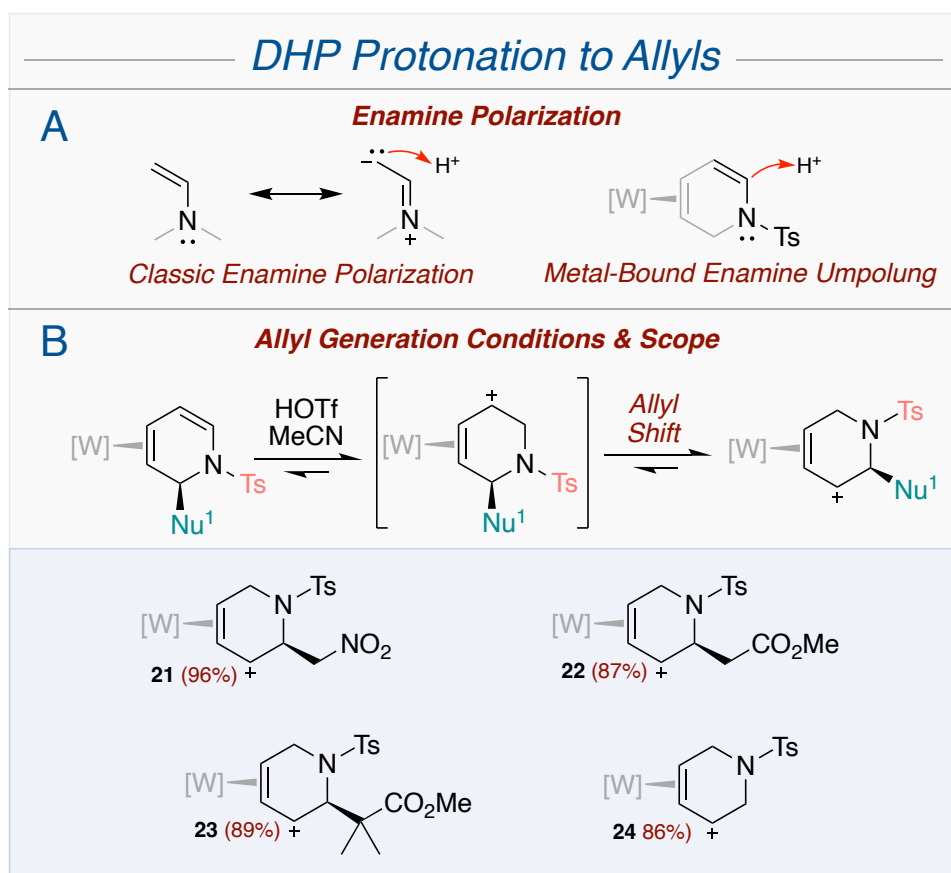


**Figure 2.10:** (A) Classic enamines promote  $\beta$ -position electrophilic additions while tungsten-bound  $\eta^2$ -DHP enamines promote  $\alpha$ -position electrophilic additions. (B) The scope of DHPs successfully protonated.

After stirring for 10 minutes, the allyls were then isolated by precipitation in stirring diethyl ether. Compounds **21-24** were obtained via this approach, and upon isolation, these allyl complexes were then each subjected to a second nucleophilic addition. It was noticed that unlike their acetyl analogues, these tosylated allyls did not have rotamers observable by NMR.

## 2.6. Nucleophilic Additions to Allyls

After isolating the allyl complexes **21-24**, a few demonstrative nucleophiles were incorporated to form highly functionalized THP complexes. Morpholine and imidazole were both incorporated into **24** at cold temperatures to form **25** and **26** respectively (Figure 2.11). Consistent with what was observed for the acetyl system, addition of the second nucleophile occurs distal to the  $\text{PMe}_3$  ligand (C3) when the first nucleophile is a hydride and proximal to the  $\text{PMe}_3$  ligand (C5) when the first nucleophile contains steric bulk profile larger than a hydride.<sup>2</sup> Because the first nucleophile for **26** was a simple hydride, imidazole addition occurred at C3 as opposed to C5. This was supported by a strong NOE interaction between the imidazole methine and a Tp pyrazole ring, which is identified as PzA3 from this interaction, as well as the lack of NOE between this same methine and the  $\text{PMe}_3$  ligand. Because this follows the general reaction pattern previously

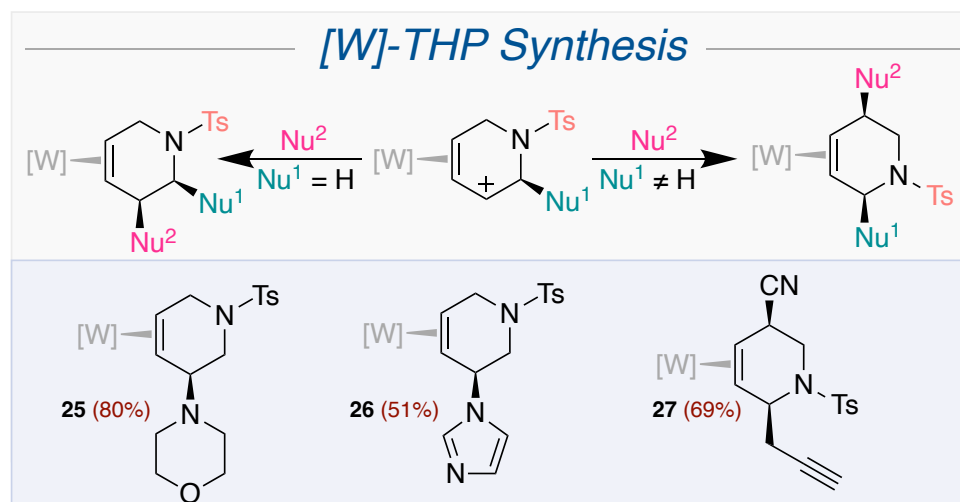


**Figure 2.11:** [W]-THP complexes formed by amine/nitrile additions to allyls.

established by the *N*-acetyl system, it is presumed that **25** also follows this convention despite lacking 2D NMR characterization.<sup>2,3</sup> In addition to adding nucleophiles to isolated allyl complexes, it was also demonstrated that they could be incorporated via tandem protonation/nucleophilic additions to a DHP complex. Cyanide ion, after adding as a first nucleophile to form **14D**, was also added to a propargyl allyl generated *in situ* from **13D** at cold temperatures to form **27**. Again, despite lacking 2D NMR data, the conventional reaction pattern suggests that nitrile addition occurs at C5 due to the bulky nature of the propargyl first nucleophile. These THP complexes were synthesized in yields ranging from 51-80% and, like the allyl complexes, did not have spectroscopically visible rotamers.

## 2.7. Oxidative Liberations

Lastly, organics were obtained by oxidizing the [W] fragment. The  $\eta^2$  bond is formed by strong backbonding from the [W] metal center; therefore, oxidizing this fragment drastically reduces its backbonding capability, allowing for free release of the organic. DDQ was found to be suitably oxidizing for organic W(0) to W(1) of these THP compounds. Free organic **28** was cleanly obtained after a DDQ-mediated oxidation and subsequent chromatography with no observed minor products; however, **29** was formed in a 1.6:1 ratio of the expected THP organic to an unknown organic. 2D NMR analysis suggests that this unknown compound is from the alkene isomerizing to carbons 4 & 5, which puts it in conjugation with the nitrile. This was speculated to occur due to the presence of excess DDQ facilitating a hydride shift, a well-established reaction for quinones. Tandem protonation/nucleophilic additions were expanded to include an added oxidation step via DDQ. This method was utilized in the synthesis of **30-32**, which incorporated cyanide, hydride, and dimethyl malonate into **10D**, **12D**, and **8D** respectively. These organics were cleanly acquired



via various chromatography methods and structurally confirmed with 2D NMR. Yields for these reactions range from 33-49% for a cumulative 3 transformations.

## 2.8. Conclusions

Herein describes a second generation [W]  $\eta^2$ -pyridine system protected by a tosyl group as opposed to an acetyl group. For this to be a suitable replacement for **4D**, the c.d.r. was enriched from 3:1 to >10:1 and the conditions for synthesizing **5D** were optimized for a multigram scale. Furthermore, this system retained previously established chemistry in its ability to regio- and stereoselectively synthesize highly functionalized THP compounds. Most critically, these were all accomplished in addition to eliminating the observed amide rotamers, which

considerably hampered spectroscopic analysis. However, we also observed an undesired Zincke-like DHP ring opening pathway that hinders the wider utility of this system.

## 2.9. References:

(1) Harrison, D. P.; Sabat, M.; Myers, W. H.; Harman, W. D. Polarization of the pyridine ring:

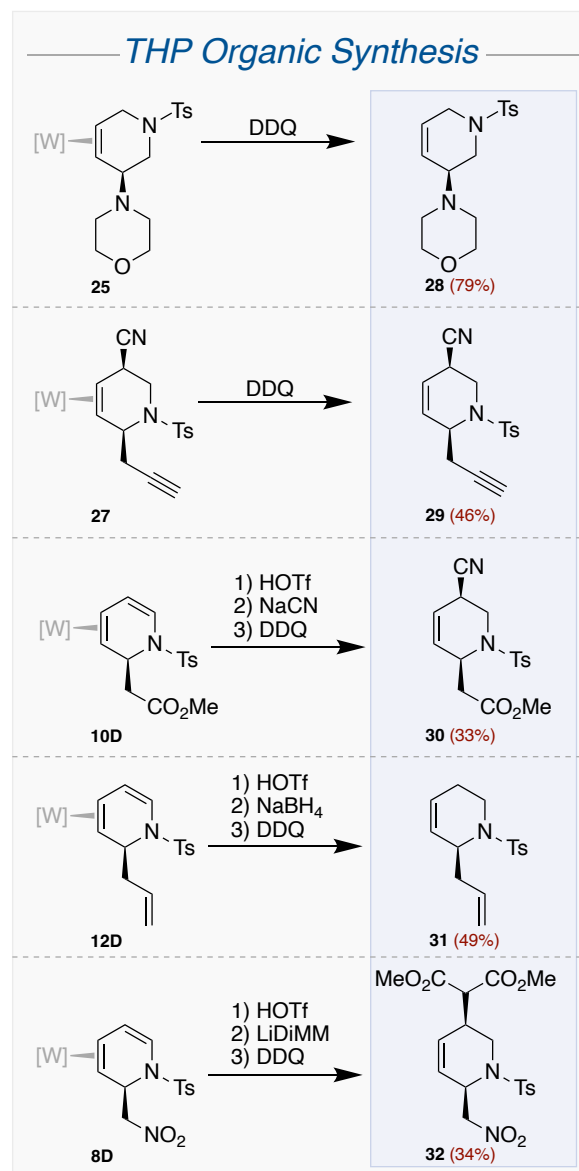


**Figure 2.12:** Liberated organics synthesized by direct THP oxidation or *in situ* tandem oxidations.

- highly functionalized piperidines from tungsten-pyridine complex. *J. Am. Chem. Soc.* **2010**, *132* (48), 17282-17295.
- (2) Kosturko, G. W.; Harrison D. P.; Sabat M.; Myers W. H.; Harman W. D. Selectfluor-mediated dialkoxylation of tungsten  $\eta^2$ -pyridinium complexes. *Organometallics* **2009**, *28* (2), 387-389.
  - (3) Wilde, J. H.; Dickie, D. A.; Harman, W. D. A Highly Divergent Synthesis of 3-Aminotetrahydropyridines. *J. Org. Chem.* **2020**, *85* (12), 8245-8252.
  - (4) Harrison, D. P.; Iovan, D. A.; Myers, W. H.; Sabat, M.; Wang, S.; Zottig, V. E.; Harman, W. D. [4 + 2] Cyclocondensation reactions of tungsten-dihydropyridine complexes and the generation of tri- and tetrasubstituted piperidines. *J. Am. Chem. Soc.* **2011**, *133* (45), 18378-18387.
  - (5) Harrison, D. P.; Kosturko, G. W.; Ramdeen, V. M.; Nielander, A. C.; Payne, S. J.; Sabat, M.; Myers, W. H.; Harman, W. D. Tungsten-Promoted Pyridine Ring Scission: The Selective Formation of  $\eta^2$ -Cyanine and  $\eta^2$ -Merocyanine Complexes and Their Derivatives. *Organometallics* **2010**, *29* (8), 1909-1915.
  - (6) Harrison, D. P.; Zottig, V. E.; Kosturko, G. W.; Welch, K. D.; Sabat, M.; Myers, W. H.; Harman, W. D. Stereo- and Regioselective Nucleophilic Addition to Dihapto-Coordinated Pyridine Complexes. *Organometallics* **2009**, *28* (19), 5682-5690.
  - (7) Clark, A. J.; Curran, D. P.; Fox, D. J.; Ghelfi, F.; Guy, C. S.; Hay, B.; James, N.; Phillips, J. M.; Roncaglia, F.; Sellars, P. B.; Wilson, P.; Zhang, H. Axially Chiral Enamides: Substituent Effects, Rotation Barriers, and Implications for their Cyclization Reactions. *J. Org. Chem.* **2016**, *81* (13), 5547-5565.
  - (8) Harrison, D. P.; Welch, K. D.; Nielander, A. C.; Sabat, M.; Myers, W. H.; Harman, W. D. Efficient synthesis of an  $\eta^2$ -pyridine complex and a preliminary investigation of the bound heterocycle's reactivity. *J. Am. Chem. Soc.* **2008**, *130* (50), 16844-16845.
  - (9) Harrison, D. P.; Nichols-Nielander, A. C.; Zottig, V. E.; Strausberg, L.; Salomon, R. J.; Trindle, C. O.; Sabat, M.; Gunnoe, T. B.; Iovan, D. A.; Myers, W. H.; Harman, W. D. Hyperdistorted Tungsten Allyl Complexes and Their Stereoselective Deprotonation to Form Dihapto-Coordinated Dienes. *Organometallics* **2011**, *30* (9), 2587-2597.
  - (10) Kan, T.; Fukuyama, T. New strategies: a highly versatile synthetic method for amines. *Chem. Commun. (Camb.)* **2004**, (4), 353-359.
  - (11) Delafuente, D. A.; Kosturko, G. W.; Graham, P. M.; Harman, W. H.; Myers, W. H.; Surendranath, Y.; Klet, R. C.; Welch, K. D.; Trindle, C. O.; Sabat, M.; Harman, W. D. Isomerization dynamics and control of the  $\eta^2$ /N equilibrium for pyridine complexes. *J. Am. Chem. Soc.* **2007**, *129* (2), 406-416.
  - (12) Bull, J. A.; Mousseau, J. J.; Pelletier, G.; Charette, A. B. Synthesis of pyridine and dihydropyridine derivatives by regio- and stereoselective addition to *N*-activated pyridines. *Am. Chem. Soc.* **2012**, *112*, 2642-2713.
  - (13) Zincke, T.; Heuser, G.; Möller, W. I. Ueber Dinitrophenylpyridiniumchlorid und dessen Umwandlungsproducte. *Justus Liebig's Annalen der Chemie* **1904**, *333* (2-3), 296-345.
  - (14) Zincke, T.; Würker, W. Ueber Dinitrophenylpyridiniumchlorid und dessen Umwandlungsproducte (2. Mittheilung.). Ueber Dinitrophenylpyridiniumchlorid und dessen Umwandlungsproducte. *Justus Liebig's Annalen der Chemie* **1904**, *338* (1), 107-141.
  - (15) Wilde, J. H.; Myers, J. T.; Dickie, D. A.; Harman, W. D. Molybdenum-Promoted Dearomatization of Pyridines. *Organometallics* **2020**, *39* (8), 1288-1298.

## Chapter 3

### The Tungsten-Promoted Synthesis of Piperidyl-Modified *erythro*- Methylphenidate Derivatives

### 3.1. Introduction

The Center for Disease Control reported over 100,000 deaths in the United States to overdoses in 2021, about a quarter of which were attributed to cocaine.<sup>1</sup> Small-molecule therapeutics have proven to be effective treatments for various drug addictions. Heroin addiction, for example, is a disorder commonly treated with methadone, which prevents drug withdrawal symptoms while being less addictive than the original drug.<sup>2,3</sup> While pharmacotherapies exist for heroin and other opioids, effective therapeutics are lacking for cocaine addiction.<sup>4</sup> Methylphenidate (MPH), commercially known as Ritalin<sup>®</sup> and prescribed extensively for treating

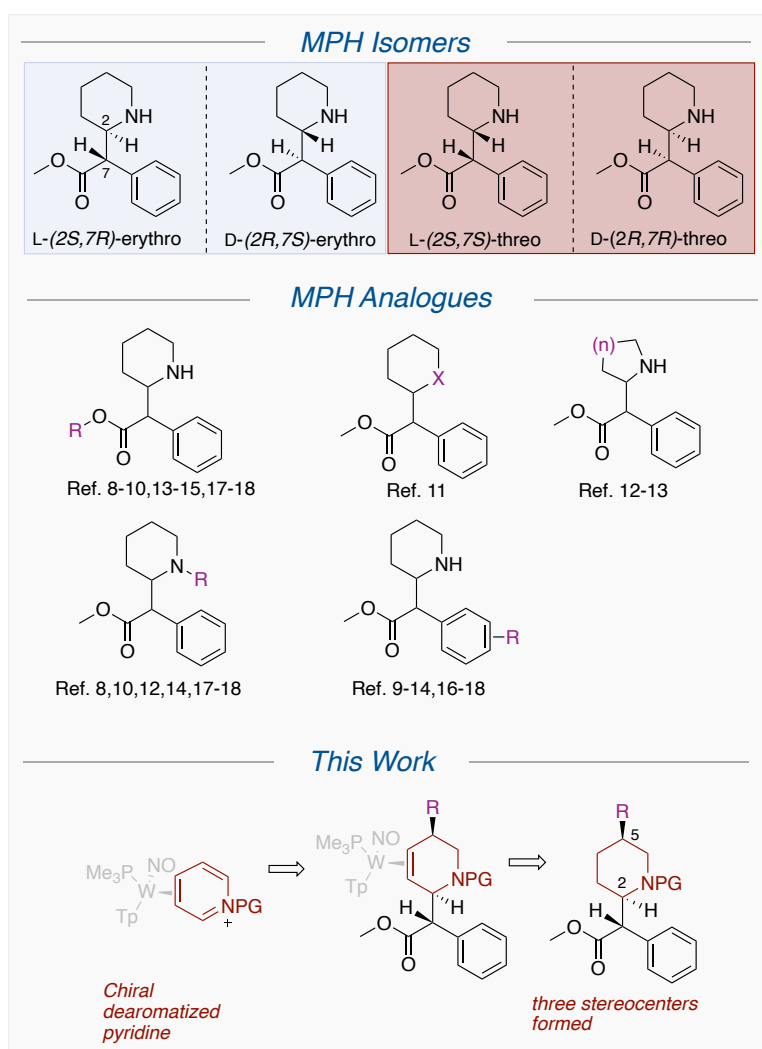


**Figure 3.1:** The two pairs of MPH diastereomers, previously reported analogues of MPH, and a proposed dearomatization approach to C5-substituted MPH analogs.

attention deficit hyperactivity disorder (ADHD), behaves as a cocaine agonist.<sup>5,6</sup> It is typically administered as a mixture of isomers, which consists of two diastereomers and their respective enantiomers (Figure 3.1). Numerous research groups have explored MPH analogues in hopes of identifying a compound that prevents cocaine from binding to the dopamine transporter (DAT) while allowing for the re-uptake of dopamine.<sup>7</sup> Most of these studies confine the areas of structural diversity on the MPH scaffold to the ester, phenyl ring, piperidine nitrogen, or the heterocycle ring-size (Figure 3.1).<sup>8-18</sup> However, there appear to be no studies that incorporate functionality on the piperidine ring, largely owing to the lack of established general synthetic methods for such compounds. Herein we demonstrate an organometallic-based approach for synthesizing *erythro*-MPH analogues in which functionalized piperidyl variants are stereoselectively prepared from a chiral,  $\eta^2$ -pyridine complex (Figure 3.1).

Previous work in our laboratory has demonstrated that highly functionalized tetrahydropyridines (THPs) can be synthesized stereoselectively from pyridine borane through its dihapto-coordination to  $\{W Tp(NO)(PMe_3)\}$  ( $[W]$ ), (Figure 2; Tp = hydrotris-(pyrazolyl)borate).<sup>19,20</sup> The tungsten binds to C3 and C4 of the pyridine on either face of the ring, resulting in two coordination diastereomers (**2D**, **2P**). Their equilibrium ratio (c.d.r.) is 3:1 favoring **2D**, with the nitrogen distal to the  $PMe_3$ . This complex can be converted to the pyridinium ( $pyH^+$ ) analogue via acetone and acid, then deprotonated in the presence of a protecting group (typically in the form of an anhydride), through which an array of protecting groups ( $PG^+$ ) can be added to the nitrogen (Figure 3.2). From this point, a range of different nucleophiles ( $Nu^1$ ) can be added to C2 to generate dihydropyridine (DHP) complexes, which in turn can be protonated at C6 of the MPH core and then treated with a second nucleophile ( $Nu^2$ ) at C5 to form  $[W]-\eta^2$  5-substituted MPH THP complexes, which can then be oxidatively liberated from the tungsten

fragment and isolated via conventional chromatographic methods. The two THP coordination diastereomers lead to the same organic product under racemic conditions; however, if a single configuration of the tungsten complex were to be used, the downstream products of the two coordination diastereomers are enantiomers. Therefore, a high c.d.r. of the pyridinium complex is essential if enantioenriched organic products are desired. Electron-withdrawing PGs have been shown to improve the c.d.r. owing to a thermodynamic preference of the complex to orient electron-deficient allylic carbons distal to the  $\text{PMe}_3$  ligand.<sup>21</sup> They also render the C2 carbon more electrophilic, providing a broader range of possible nucleophiles. Our proposed strategy in preparing MPH derivatives was to install the methyl phenylacetate portion at C2 of a distal  $\eta^2$ -pyridine complex via an aza-Reformatsky reaction, followed by elaboration of the resulting DHP to a *cis*-disubstituted THP or piperidine.

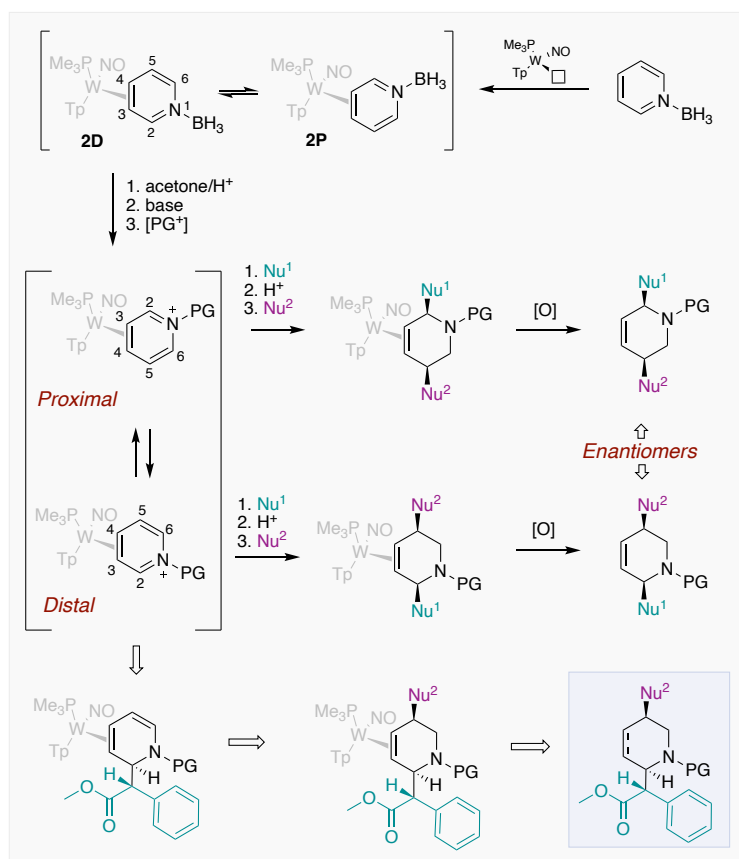


**Figure 3.2:** Tungsten-promoted dearomatization of pyridines and proposed MPH analogue pathway.

### 3.2. Generation of Highly Enriched Mesylated Pyridinium Complex

Previous studies exploring the tungsten-promoted dearomatization of pyridine utilized an acetyl protecting group (PG = Ac; Figure 3.2), where the corresponding pyridinium complex could be prepared in up to a 10:1 c.d.r. mixture.<sup>22-24</sup> The hitherto reported *N*-acetyl-2-ethylacetate-1,2-DHP [W] complex was synthesized via an aza-Reformatsky reaction between the corresponding pyridinium complex (**4D**), ethyl bromoacetate, and zinc.<sup>25</sup> Owing to the position of the metal, the addition cleanly occurs at C2, with no sign of competing C4 addition.<sup>26</sup>

It was postulated that a similar strategy could be utilized to install the methyl phenylacetate moiety to the pyridinium core. However, the acetyl protecting group resulted in rotational isomers (~1:1) for all downstream complexes for this system due to hindered acetyl rotation,<sup>27</sup> and the aza-Reformatsky reaction was not stereoselective (*erythro/threo* ratio: 1:1). Because comprehensive NMR analysis of these ~1:1:1:1 isomeric mixtures proved challenging, an alternative protecting group was sought. Given the broad use of sulfonamides in drug design,<sup>28</sup> we settled on a methanesulfonyl (mesyl or Ms) group to protect and activate the nitrogen. The reaction of mesyl anhydride in the presence of **3** and lutidine forms the new pyridinium complexes **33D** and **33P**, and stirring the solution in an oil bath at 60 °C enriches the **D/P** c.d.r. from 3:1 to 10:1 as tracked by <sup>31</sup>P NMR. After subjecting the mixture to aqueous washes, this 10:1 c.d.r. mixture of **33D** and **33P** was precipitated in stirring diethyl ether. To our delight, triturating this powder mixture in ethyl acetate further enriched the c.d.r. to >20:1 (Figure 3.3). Furthermore, any decomposition impurities are removed during this trituration, resulting in consistently clean and highly enriched material on a multigram (5 g) scale.

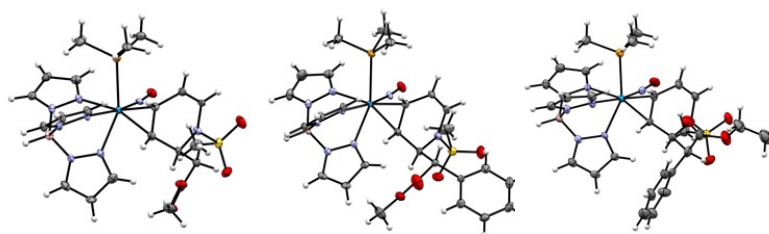
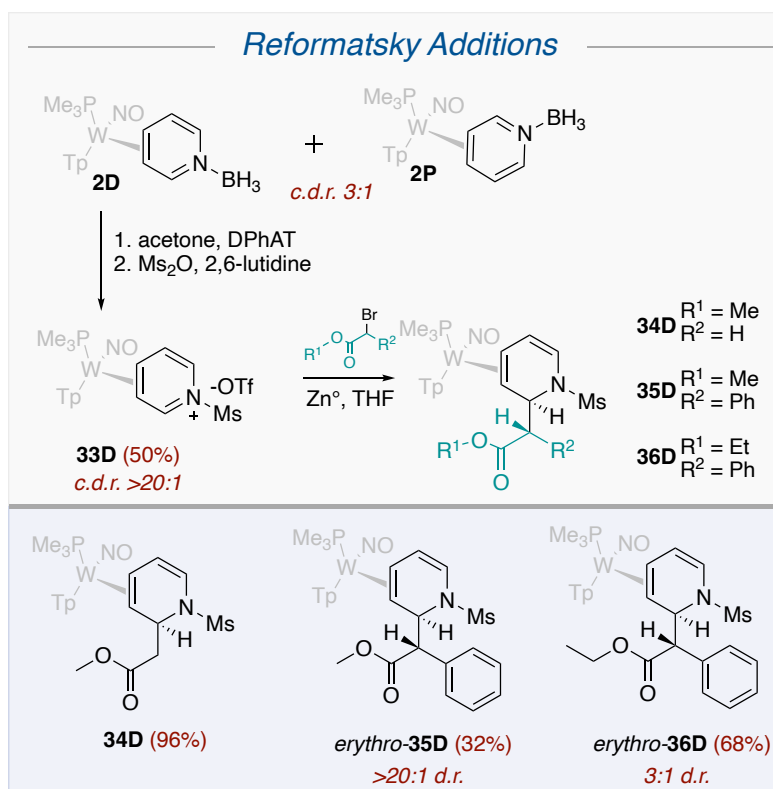


**Figure 3.3:** Various aza-Reformatsky additions to **33D**.

### 3.3. aza-Reformatsky Ester Installation

To ensure that **33D** behaved in a manner similar to the acetyl derivative,<sup>25</sup> an aza-Reformatsky reaction with methyl bromoacetate (MBA) was performed on **33D** resulting in the DHP complex **34D** (Figure 3.3). The structure was confirmed by 2D NMR analysis and single crystal X-ray diffraction (SC-XRD). Like with the acetyl analogue, nucleophile incorporation was solely observed at the iminium carbon anti relative to the metal position.



Conventionally, stereocenters are enantioselectively installed in aza-Reformatsky reactions by the addition of  $\alpha$ -bromoesters in the presence of zinc to chiral *N*-sulfinyl imines.<sup>29</sup> While this chemistry is well-established, additions to *N*-sulfonyl imines are underexplored. Synthesizing a tungsten coordinated DHP bearing an  $\alpha$ -phenyl ester (**35D**) requires selectively generating two stereocenters. Although the exclusive stereoselectivity at C2 for **34D** is attributed to the steric bulk of the tungsten, we postulated that the nitrogen protecting group could influence the stereochemistry at the  $\beta$  carbon analogous to the chiral *N*-sulfinyl protecting groups. Similar to the synthesis of **34D**, **35D** is readily synthesized by an aza-Reformatsky addition with methyl  $\alpha$ -phenyl bromoacetate (MAPBA). Again, incorporation of the methyl phenyl ester moiety occurs exclusively *anti* to the metal at C2 of the pyridine ring. However, a 3:1 mixture of  $\beta$ -carbon diastereomers is formed. While not highly enriched, this stands in contrast to the 1:1 d.r. observed with the previously reported *N*-acetyl analogue, supporting the influence of the sulfonyl group.

While varying solvent, temperature, reaction time, and various zinc ligand additives failed to enrich the d.r. of **35D**, we found that consecutive triturations in methanol and dimethoxyethane (DME) respectively once again enriches the d.r. from 3:1 to >20:1. Whereas the methanol trituration removes decomposition impurities, the isomeric enrichment occurs during the DME trituration. To probe the influence of the ester functional group on the final d.r., an ethyl version was incorporated to **33D** and similarly resulted in a 3:1 *erythro/threo* mixture of **36D**; however, this sample failed to enrich further via triturations.

#### 3.4. Chiral Determination of **35D**

SC-XRD data was obtained for the *erythro* diastereomer (*erythro*-**35D**; Figure 3.4); however, to confirm the chiral identity of the bulk material, Nuclear Overhauser Effect (NOE) data

was considered along with a DFT analysis. Calculations were performed using the M06 functional alongside a split basis set with LANL2DZ applied to tungsten and 6-31G(d,p) on all main group atoms for optimizations to the lowest energy conformations of the two diastereomers.

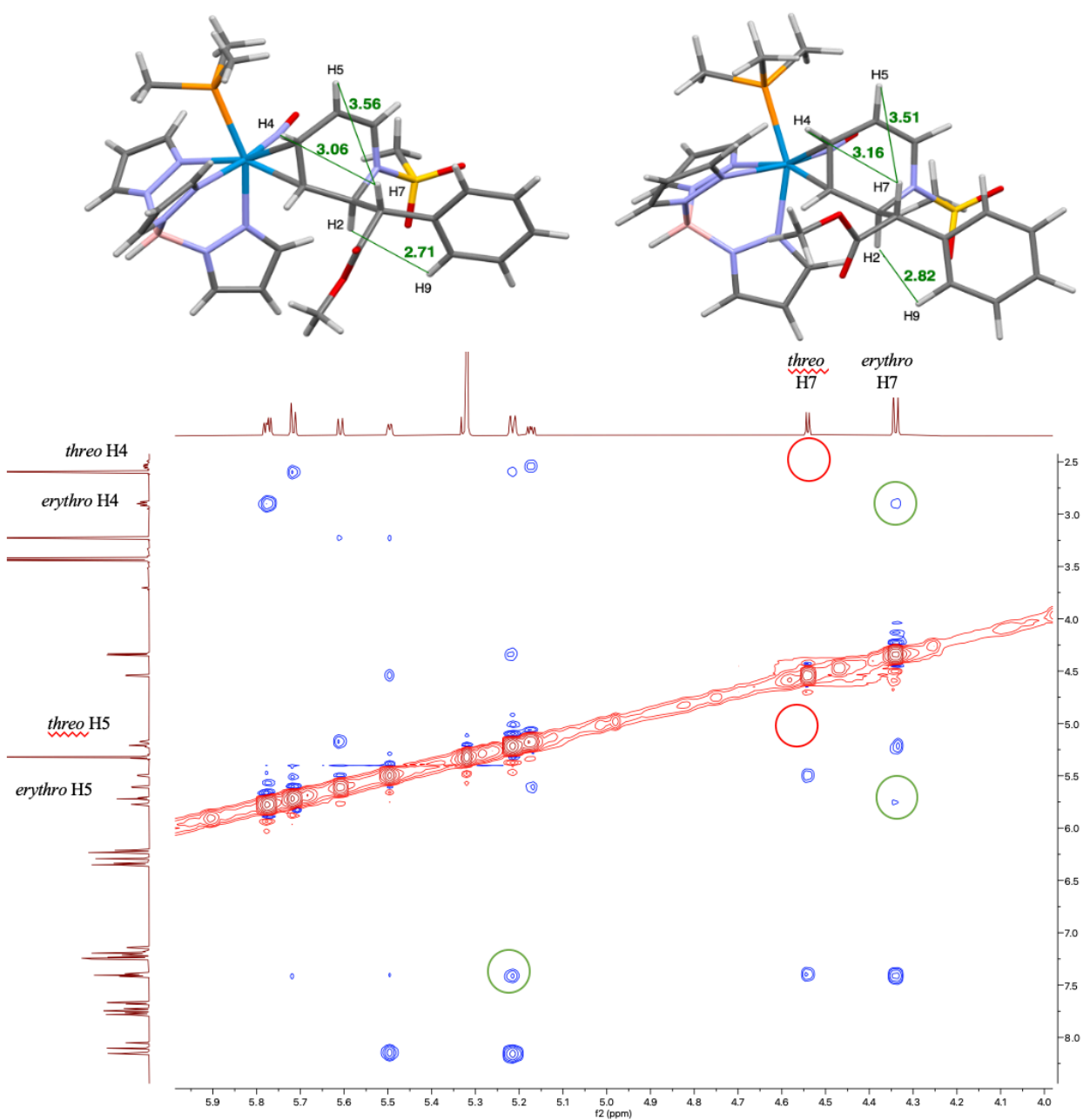


**Figure 3.4:** Comparison of computationally expected and experimentally determined NOE interactions between *threo*- and *erythro*-35D from SC-XRD (top left) and DFT calculation (top right).

Hydrogen-Hydrogen distances were determined and compared to experimental Nuclear Overhauser Effect Spectroscopy (NOESY) data of a 3:1 d.r. sample, and several unique interactions were identified. The distance between H2 and H9 was 2.82 Å in the *erythro* diastereomer and 4.34 Å in the *threo* complex. Additionally, the distances between H7 and H4/H5 were 3.16 Å /3.51 Å in the *erythro* isomer, and 4.10 Å/5.34 for *threo*. NOESY spatial interactions were present between H7/H4, and H7/H5 in the major complex but absent in the minor complex while an NOE is observed in both for H2/H9 but with an interaction that is far stronger in the *erythro* form.

Collectively, these observations support the hypothesis that the *erythro* diastereomer (*erythro-35D*) is the major complex while the *threo* (*threo-35D*) diastereomer is the minor. The addition of the methyl phenyl ester moiety can be performed on a multigram scale (overall yield of 22% from **33D**; 2-3 g), resulting in pure *erythro* methyl phenyl ester DHP complex (*erythro-35D*; d.r. >20:1) without chromatography. We note that while the *threo* isomer of MPH is most biologically active,<sup>5,6</sup> this is not necessarily the case for its derivatives,<sup>8-18</sup> so we continued our study with the high purity *erythro* isomer **35D**.

### 3.5. Protonation of **35D**

*Erythro-35D* undergoes protonation at C6 by triflic acid in propionitrile to form a single isomer of an  $\eta^3$  allyl complex (**37**; Figure 3.5). We note here that tungsten backbonding directs the proton to C6, rather than C5, the expected site of protonation for an organic enamine.<sup>30</sup> Precipitation was then induced by adding the solution to stirring ether to form a readily isolable powder. Previous studies have demonstrated how  $\pi$ -allyl complexes of [W] are hyperdistorted.<sup>21</sup> They are described herein as dihapto-coordinated with the central allylic carbon and one terminal

carbon tightly bound to the tungsten and the other terminally bound carbon loosely coordinated (the carbenium-like carbon). DFT calculations indicate that for  $[\text{W}]-\eta^2\text{-allyl}$  complexes,<sup>21</sup> there is a significant thermodynamic preference for placing the carbenium carbon distal to the  $\text{PMe}_3$  ligand. Accordingly, NOESY shows a prominent interaction between the C6 methylene protons and  $\text{PMe}_3$  ligand, indicating that **37D** is the thermodynamically favored allyl conformer. This is further supported by SC-XRD, which revealed that **37D** is the conformation present in the solid state (Figure 3.5). Yet nucleophilic attack is observed to occur at C5 (*vide infra*), indicating an allyl conformational shift to **37P** prior to nucleophilic addition.

### 3.6. Nucleophilic Additions to **37P**

With the goal of demonstrating modular diversity that would be amenable to forming combinatorial libraries, we explored the reactivity of allyl complex **37P** with various nucleophiles. *cis*-5-substituted -2-(methyl phenylester)-1,2,5,6-tetrahydropyridine (THP) complexes (Figure 3.6) were formed in solution then precipitated in stirring chilled hexanes or pentanes. The nucleophiles in Figure 3.6 were chosen to exemplify the broad compatibility of the metal complex with various classes of nucleophile, and to demonstrate the potential of this methodology to

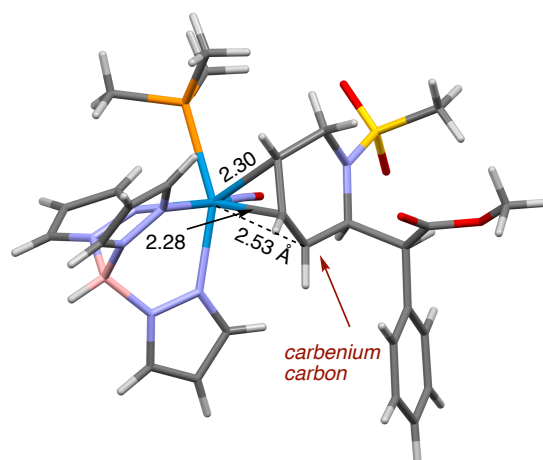


**Figure 3.5:** Molecular structure determination for the  $\eta^3\text{-allyl}$  complex **37D** showing carbenium carbon distal to the  $\text{PMe}_3$ .

directly access a wide range of functional groups. These nucleophiles, which include hydride, cyanide, enolates, Grignard reagents, amines, amides, imides, and thiols, can be added to the isolated allyl complex **37P** or added in a one-pot reaction following the protonation of *erythro*-**35D**. Despite the preference of the carbenium to be distal to the  $\text{PMe}_3$ , all of these nucleophiles add to C5 exclusively, via the minor conformer of the allyl species (**9P**). In all cases, there is a high stereochemical preference for addition *anti* to the metal, as is indicated by SC-XRD and/or NOESY data.

While the parent THP complex (**38**) was synthesized via the addition of sodium cyanoborohydride at  $-50\text{ }^\circ\text{C}$ , the addition of **37** to a lithium dimethyl malonate solution provided

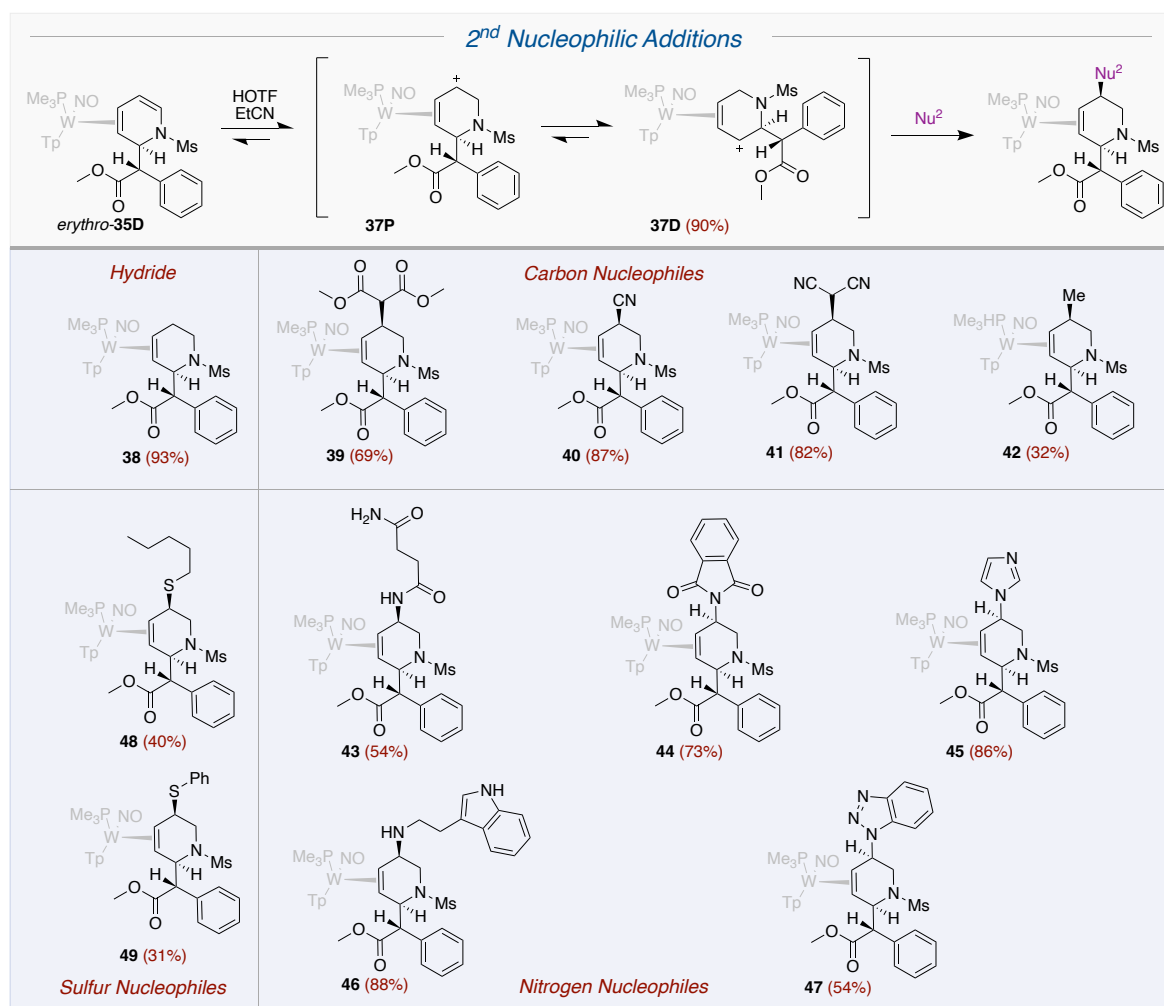


**Figure 3.6:** THP precursors to MPH analogs with C5 functionalization of the piperidine ring.

**39.** Similarly, a solution of allyl **37** was added to a cooled methanol solution (-50 °C) containing sodium cyanide to form **40**. Malononitrile was also added successfully (**41**) by combining cooled solutions of the allyl **37** and deprotonated malononitrile. Grignard reagents are also compatible nucleophiles: Successful addition of MeMgBr occurs after reacting chilled reactants at -60 °C for 60 hours to form **42**. Both aliphatic amines and amides can be incorporated, as well as *N*-heterocycles: Tryptamine addition (addition at primary amine) was achieved by combining it with potassium tert-butoxide and a solution of **37** to form **46**. Similarly, **43** was prepared by adding a solution of **37** to a solution of succinamide and base. Benzotriazole was treated with potassium *t*-butoxide and cooled before the addition of the allyl complex **37**, to form **47**. Phthalimide (**44**) and imidazole (**45**) followed a similar reaction course. Finally, thiol additions were accomplished using pentanethiol (**48**) or thiophenol (**49**) and base. Despite the presence of strong acid and base in these reactions, the diastereomeric enrichment of these compounds is retained throughout the syntheses, resulting in THP complexes with diastereomeric ratios of >20:1. THP complexes are produced in yields ranging from 31-88% and were characterized by multiple spectroscopic techniques including <sup>1</sup>H-NMR, <sup>13</sup>C-NMR, 2D-NMR and IR, as well as being characterized by SC-XRD, HRMS, and cyclic voltammetry.

### 3.7. Oxidative Demetallation of Organics

The functionalized THPs can be liberated by the oxidation of the metal center. As an example, **38** undergoes chemical oxidation with four equivalents of DDQ in acetone, and subsequent chromatography results in purified THP organic (**50-Ms**). Incomplete oxidation was observed via <sup>1</sup>H NMR when less than four equivalents were used. We attribute this to metal decomposition products undergoing multiple oxidation events, thus necessitating a greater amount

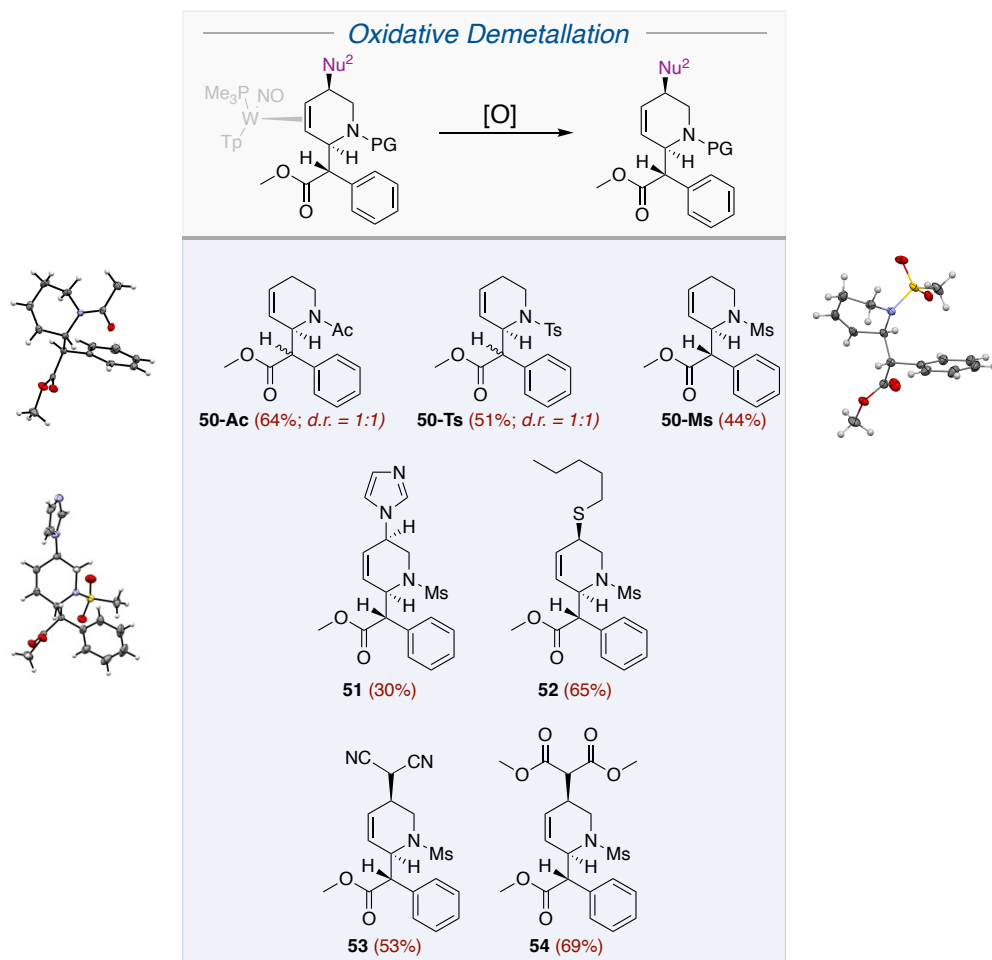


**Figure 3.7:** Oxidative decomplexation of THP compounds **50-54**.

of oxidant. Similarly, **51-54** were also oxidatively liberated via DDQ. All organics (Figure 3.7) were recovered through extraction or purified via chromatography. Similar procedures to those described above provided routes to both *N*-tosylated and *N*-acetylated variations of THP MPH derivatives. As with the mesylated analogs, the aza-Reformatsky reaction occurred with low stereoselectivity. Two examples of the parent methyl phenyl acetate THP (**50-Ac** and **50-Ts**) were prepared and are included in Figure 3.7 for comparison.<sup>26</sup>

### 3.8. MPH THP Hydrogenation

As a demonstration of the ability to generate the corresponding piperidines from THPs such as those reported in Figure 3.7, THP **50-Ms** was reduced to its saturated analogue (**55**) through

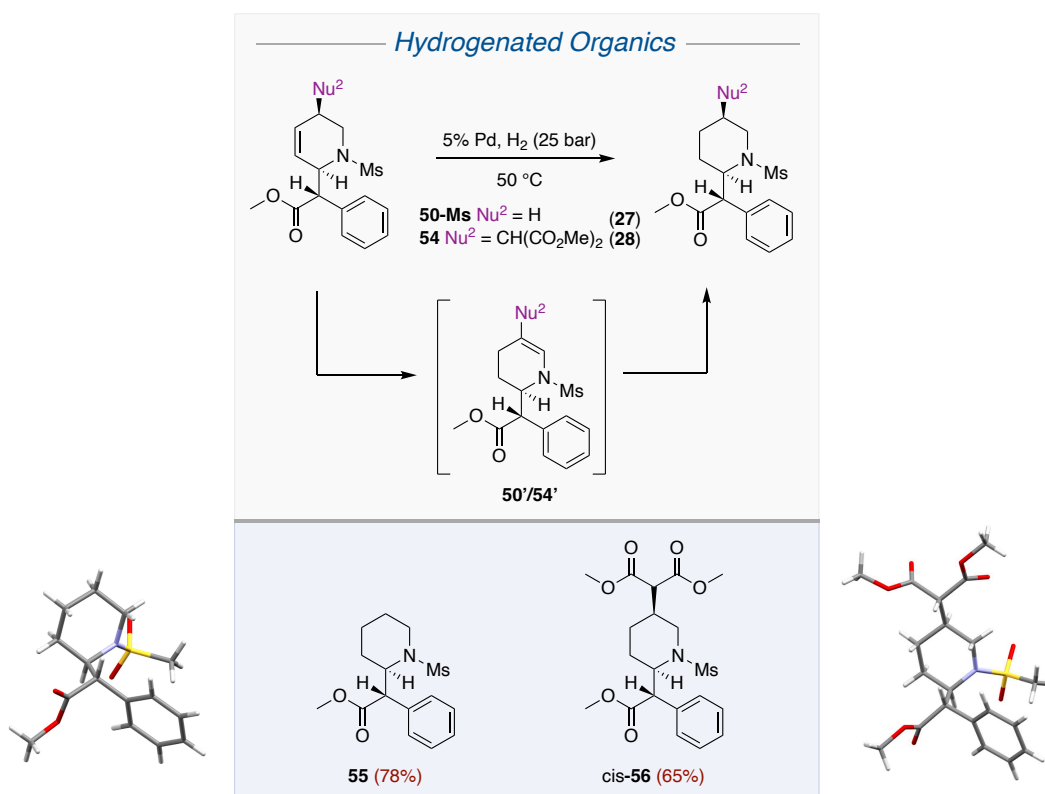


**Figure 3.8:** Hydrogenations of MPH THP organics were performed to form the corresponding *erythro* MPH analogue. The presence of the *trans* isomer is attributed to an observed enamine intermediate formed from a Pd-promoted alkene isomerization.

hydrogenation. Using a 5% Pd on activated carbon catalyst, the hydrogenation of **50-Ms** was carried out at 50 °C under 25 bars (~360 psi) of H<sub>2</sub> (Figure 3.8). Complete conversion to the reduced form (**55**) occurred after 5 hours. However, prematurely arresting the reaction revealed the presence of an intermediate (**50'**). 2D NMR analysis indicated that this compound was likely a constitutional isomer of THP **50-Ms** in which the alkene has migrated to form the “enamine **50'**”. Similar palladium-catalyzed isomerizations have been reported for other THPs and for a 3-pyrrolene, in which an enamine (2-pyrrolene) was formed.<sup>31-33</sup> As anticipated, further reduction of the mixture of **55** and **50'** resulted in complete conversion to the piperidine **55**. The structure of **55** was confirmed via SC-XRD. Compound **54** was also hydrogenated to **56** under identical conditions as confirmed by SC-XRD. Of note, Ellman *et al.* have shown the value of 3,4-THPs as precursors



to highly functionalized, oxygenated for removal of mesyl group from secondary amines, but we have not explored this aspect in any detail.<sup>34-36</sup>

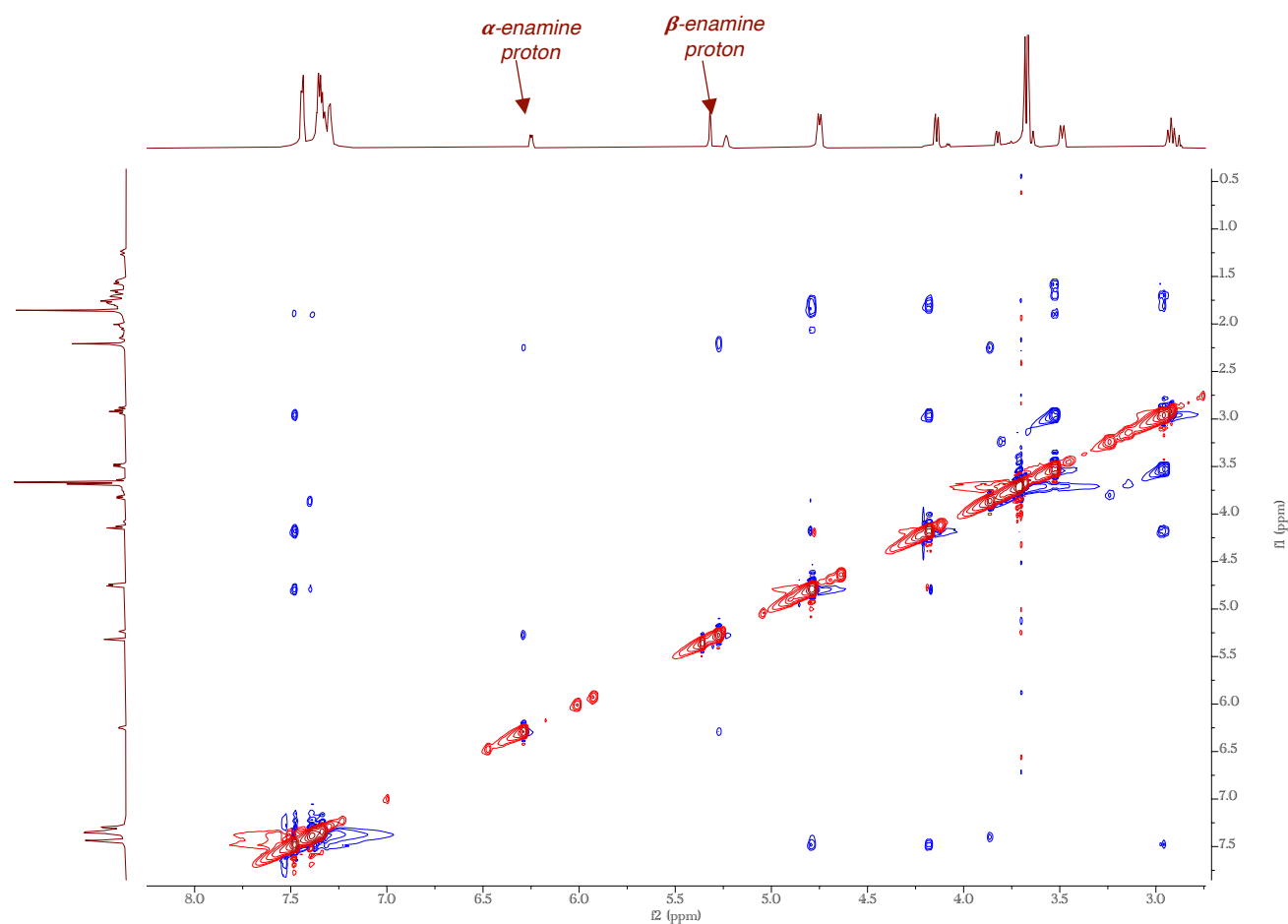
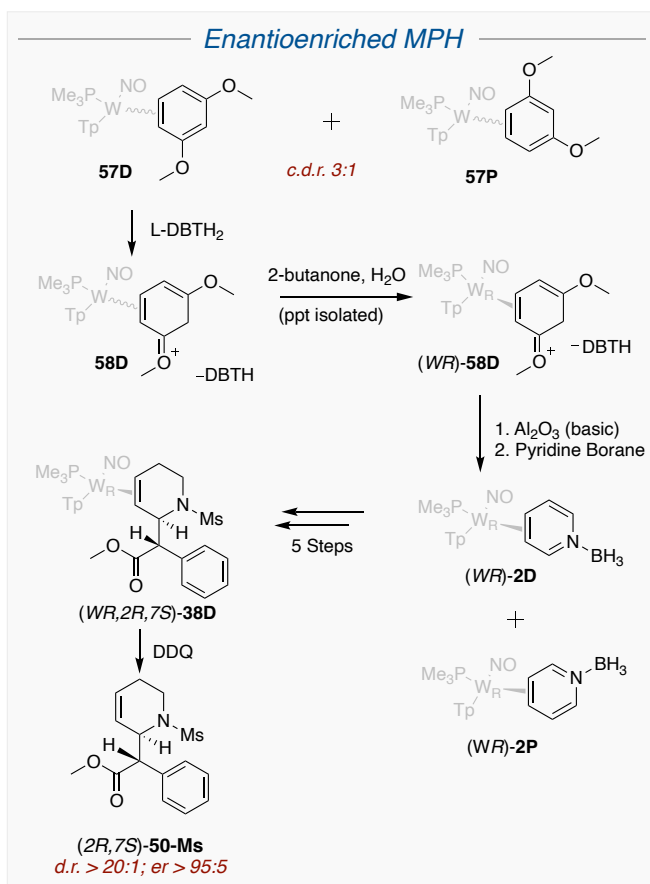


**Figure 3.9:** NOESY spectrum of mixture containing **50'-Ms** and **55'-Ms**.

### 3.9. Enantioenrichment and Chiral Resolution

We next explored the possibility of using the methodology outlined above to obtain enantioenriched compounds. Previously, Lankenau *et al.* developed a general procedure for the resolution of  $\text{WTP}(\text{NO})(\text{PMe}_3)(\eta^2\text{-1,3-dimethoxybenzene})$  enantiomers,<sup>37</sup> and this process has since been modified and optimized.<sup>38,39</sup> The procedure resolves the *S* and *R* hands of the metal by



protonating the corresponding racemic dimethoxybenzene complex mixture (**57D/P**) with L-dibenzoyl tartaric acid (L-DBTH<sub>2</sub>), then physically separating the resulting diastereomer salts based on solubility differences. This robust approach allows for enriched samples of either hand on a gram scale, with e.e.'s from 80-95+%, and the dimethoxybenzene ligand can be replaced with other aromatic molecules (e.g., benzene, anisole) with complete retention of the metal stereocenter. Applying this technique to pyridines introduced several challenges. Synthesizing enantioenriched **2** required the deprotonation of [(*WR*)-[W]-η<sup>2</sup>-dimethoxybenzenium](L-DBTH) (**58D**; d.r. ~10:1) to generate an enantioenriched exchange-labile precursor (**57**; Figure 3.10).

Deprotonation was conducted with basic alumina (owing to its ease of separation) in THF, and (*WR*)-[W]-η<sup>2</sup>-dimethoxybenzene (*WR*)-**57** was then precipitated in stirring hexanes. This

compound was then combined with pyridine borane (30 eq.) and TEA (1.5 eq.) for 36 hrs. The workup for this reaction was identical to the previously published version. This enantioenriched (*WR*)-**2** was then subjected to deprotection, mesylation, and an aza-Reformatsky addition (*vide supra*). However, the tandem methanol/DME triturations failed to clean and enrich the d.r. of (*WR,2R,7S*)-**35D**, which, as in the racemic preparation, was present as a 3:1 mixture of isomers. This apparent difference in diastereomer solubilities was attributed to the enantioenriched **35D** crystalizing in a different space group than does racemic **35D**. The racemic material crystalizes from dimethoxyethane in the spacegroup P -1, which, being centrosymmetric, requires both hands of the complex to be present in equal amount. We found that purifying (*WR,2R,7S*)-**35D** via a basic alumina column and triturating the precipitated complex in ethanol improves the d.r. to >20:1. Clean (*WR,2R,7S*)-**35D** was then protonated under conditions identical to the conditions used for the racemic mixture to form (*WR,2R,7S*)-**37**. This compound was then converted to (*WR,2R,7S*)-**38** and the desired organic (*2R,7S*)-**50-Ms** was then oxidatively liberated from the metal with DDQ. The e.r. of the free organic was determined by chiral HPLC to be >95:5. Notably, this compound has the configuration at C2 (*R*) that matches the desired D enantiomer of *threo*-MPH, and procedures have been developed by Novartis to convert (*2R,7S*)-*erythro*-MPH to the desired (*2R,7R*)-MPH (*D-threo*) in alkaline solution.<sup>40</sup> Of the numerous derivatives of MPH that have appeared in the academic and patent literature,<sup>8-18</sup> remarkably few have a substituent on a saturated piperidine ring. Of those few examples that have been reported, most are prepared from piperidines or piperidones via the C-H activation and addition of the phenylacetate group adjacent to the ring nitrogen by a rhodium catalyst.<sup>41</sup> Although there do not appear to be examples of C5-substituted MPH analogs prepared from this method, such an approach may be viable, but controlling stereochemistry would be challenging. It seems that the most general method for preparing such

analogs would be from the hydrogenation of pyridine precursors. While hydrogenations of pyridines and pyridinium salts are well established<sup>42-44</sup> and have been used to prepare the parent MPH,<sup>45</sup> such an approach has not been applied to MPH analogs in which the piperidine was functionalized.

### 3.10. Conclusions

This study describes a methodology capable of accessing piperidine-functionalized *N*-mesyl *erythro* methylphenidate analogues with high degrees of regioselectivity, stereoselectivity, and functional group tolerance. An aza-Reformatsky reaction involving a [W]- $\eta^2$ -bound *N*-mesyl pyridinium complex and MAPBA yields an *erythro* methylphenidate DHP complex, which is enriched to a d.r. of >20:1 through triturations. After the formation of an allyl complex, the successful incorporation of nucleophiles to form tetrahydropyridine complexes with high diastereoselectivity includes cyanide, malononitrile, dimethylmalonate, Grignard reagents, amines, amides, imides, and thiols. This strategy provides access to a wide range of MPH analogues functionalized at the C5-position on the piperidine ring that would be difficult to access via conventional methods. Furthermore, the ubiquity of the piperidine scaffold within small-molecule drugs underscores the potential utility of this system, which rapidly incorporates a broad range of functional groups and nucleophile types into piperidine cores. Efforts continue on developing a fully stereoselective aza-Reformatsky reaction with an  $\eta^2$  pyridinium system that would directly lead to the *threo* diastereomer family of C5-substituted MPHs which, at least for the parent, is the most biologically potent.<sup>46</sup>

### 3.11. References

(1) U.S. Overdose Deaths In 2021 Increased Half as Much as in 2020 – But Are Still Up 15%.

*Center of Disease Control, 2021.*

- (2) Ferri, M.; Minozzi, S.; Bo, A.; Amato, L. Slow-release oral morphine as maintenance therapy for opioid dependence. *Cochrane Database Syst. Rev.* **2013**, 2013 (6), CD009879.
- (3) Whelan, P. J.; Remski, K. Buprenorphine vs methadone treatment: A review of evidence in both developed and developing worlds. *J. Neurosci. Rural Pract.* **2012**, 3 (1), 45-50.
- (4) Sherman, M. M.; Ungureanu, S.; Rey, J. A. Naltrexone/Bupropion ER (Contrave): Newly Approved Treatment Option for Chronic Weight Management in Obese Adults. *P. T.* **2016**, 41 (3), 164-172.
- (5) Negus, S. S.; Henningfield, J. Agonist Medications for the Treatment of Cocaine Use Disorder. *Neuropsychopharmacology* **2015**, 40 (8), 1815-1825.
- (6) Ritz, M. C.; Lamb, R. J.; Goldberg, S. R.; Kuhar, M. J. Cocaine receptors on dopamine transporters are related to self-administration of cocaine. *Science* **1987**, 237 (4819), 1219-1223.
- (7) Deutsch, H. M.; Shi, Q.; Gruszecka-Kowalik, E.; Schweri, M. M. Synthesis and pharmacology of potential cocaine antagonists. 2. Structure-activity relationship studies of aromatic ring-substituted methylphenidate analogs. *J. Med. Chem.* **1996**, 39 (6), 1201-1209.
- (8) Kim, D. I.; Deutsch, H. M.; Ye, X.; Schweri, M. M. Synthesis and pharmacology of site-specific cocaine abuse treatment agents: restricted rotation analogues of methylphenidate. *J. Med. Chem.* **2007**, 50 (11), 2718-2731.
- (9) Froimowitz, M.; Gu, Y.; Dakin, L. A.; Kelley, C. J.; Parrish, D.; Deschamps, J. R. Vinylogous amide analogs of methylphenidate. *Bioorg. Med. Chem. Lett.* **2005**, 15 (12), 3044-3047.
- (10) Froimowitz, M.; Gu, Y.; Dakin, L. A.; Nagafuji, P. M.; Kelley, C. J.; Parrish, D.; Deschamps, J. R.; Janowsky, A. Slow-onset, long-duration, alkyl analogues of methylphenidate with enhanced selectivity for the dopamine transporter. *J. Med. Chem.* **2007**, 50 (2), 219-232.
- (11) Davies, H. M.; Hopper, D. W.; Hansen, T.; Liu, Q.; Childers, S. R. Synthesis of methylphenidate analogues and their binding affinities at dopamine and serotonin transport sites. *Bioorg. Med. Chem. Lett.* **2004**, 14 (7), 1799-1802.
- (12) Axten, J. M.; Krim, L.; Kung, H. F.; Winkler, J. D. A stereoselective synthesis of dl-threo-methylphenidate: Preparation and biological evaluation of novel analogues. *J. Org. Chem.* **1998**, 63 (26), 9628-9629.
- (13) Meltzer, P. C.; Wang, P.; Blundell, P.; Madras, B. K. Synthesis and evaluation of dopamine and serotonin transporter inhibition by oxacyclic and carbacyclic analogues of methylphenidate. *J. Med. Chem.* **2003**, 46 (8), 1538-1545.
- (14) Schweri, M. M.; Deutsch, H. M.; Massey, A. T.; Holtzman, S. G. Biochemical and behavioral characterization of novel methylphenidate analogs. *J. Pharmacol. Exp. Ther.* **2002**, 301 (2), 527-535.
- (15) Casiraghi, A.; Longhena, F.; Straniero, V.; Faustini, G.; Newman, A. H.; Bellucci, A.; Valoti, E. Design and Synthesis of Fluorescent Methylphenidate Analogues for a FRET-Based Assay of Synapsin III Binding. *ChemMedChem* **2020**, 15 (14), 1330-1337.
- (16) Liu, W.; Babl, T.; Rother, A.; Reiser, O.; Davies, H. M. L. Functionalization of Piperidine Derivatives for the Site-Selective and Stereoselective Synthesis of Positional Analogues of Methylphenidate. *Chemistry* **2020**, 26 (19), 4236-4241.
- (17) Wayment, H. K.; Deutsch H.; Schweri M. M.; Schenk J. O. Effects of methylphenidate

- analogues on phenethylamine substrates for the striatal dopamine transporter: Potential as amphetamine antagonists? *J. Neurochem.* **1999**, *72* (3), 1266-1274
- (18) Carroll, F. I.; Howell, L. L.; Kuhar, M. J. Pharmacotherapies for treatment of cocaine abuse: preclinical aspects. *J. Med. Chem.* **1999**, *42* (15), 2721-2736.
- (19) Harrison, D. P.; Welch, K. D.; Nielander, A. C.; Sabat, M.; Myers, W. H.; Harman, W. D. Efficient synthesis of an  $\eta^2$ -pyridine complex and a preliminary investigation of the bound heterocycle's reactivity. *J. Am. Chem. Soc.* **2008**, *130* (50), 16844-16845.
- (20) Welch, K. D.; Harrison, D. P.; Lis, E. C.; Liu, W. J.; Salomon, R. J.; Harman, W. D.; Myers, W. H. Large-scale syntheses of several synthons to the dearomatization agent {TpW(NO)(PMe<sub>3</sub>)} and convenient spectroscopic tools for product analysis. *Organometallics* **2007**, *26* (10), 2791-2794.
- (21) Harrison, D. P.; Nichols-Nielander, A. C.; Zottig, V. E.; Strausberg, L.; Salomon, R. J.; Trindle, C. O.; Sabat, M.; Gunnoe, T. B.; Iovan, D. A.; Myers, W. H.; Harman, W. D. Hyperdistorted Tungsten Allyl Complexes and Their Stereoselective Deprotonation to Form Dihapto-Coordinated Dienes. *Organometallics* **2011**, *30* (9), 2587-2597.
- (22) Harrison, D. P.; Sabat, M.; Myers, W. H.; Harman, W. D. Polarization of the pyridine ring: highly functionalized piperidines from tungsten-pyridine complex. *J. Am. Chem. Soc.* **2010**, *132* (48), 17282-17295.
- (23) Harrison, D. P.; Kosturko, G. W.; Ramdeen, V. M.; Nielander, A. C.; Payne, S. J.; Sabat, M.; Myers, W. H.; Harman, W. D. Tungsten-Promoted Pyridine Ring Scission: The Selective Formation of  $\eta^2$ -Cyanine and  $\eta^2$ -Merocyanine Complexes and Their Derivatives. *Organometallics* **2010**, *29* (8), 1909-1915.
- (24) Kosturko, G. W.; Harrison, D. P.; Sabat, M.; Myers, W. H.; Harman, W. D. Selectfluor-mediated dialkoxylation of tungsten  $\eta^2$ -pyridinium complexes. *Organometallics* **2009**, *28* (2), 387-389.
- (25) Harrison, D. P.; Zottig, V. E.; Kosturko, G. W.; Welch, K. D.; Sabat, M.; Myers, W. H.; Harman, W. D. Stereo- and Regioselective Nucleophilic Addition to Dihapto-Coordinated Pyridine Complexes. *Organometallics* **2009**, *28* (19), 5682-5690.
- (26) Wilde, J. H. Synthetic Applications of Molybdenum and Tungsten Dearomatization Agents. University of Virginia, 2020.
- (27) Wilde, J. H.; Dickie, D. A.; Harman, W. D. A Highly Divergent Synthesis of 3-Aminotetrahydropyridines. *J. Org. Chem.* **2020**, *85* (12), 8245-8252.
- (28) Zhao, C.; Rakesh, K. P.; Ravidar, L.; Fang, W. Y.; Qin, H.-L. Pharmaceutical and medicinal significance of sulfur (S<sup>VI</sup>)-Containing motifs for drug discovery: A critical review. *Eur. J. Med. Chem.* **2018**, *162*, 679 - 734.
- (29) Pellissier, H. Recent developments in the asymmetric Reformatsky-type reaction. *Beilstein J. Org. Chem.* **2018**, *14*, 325-344.
- (30) Harrison, D. P.; Sabat, M.; Myers, W. H.; Harman, W. D. Polarization of the Pyridine Ring: Highly Functionalized Piperidines from Tungsten-Pyridine Complex. *J. Am. Chem. Soc.* **2010**, *132* (48), 17282-17295.
- (31) Wanner, K.; Kärtner, A. Isomerization of N-Acyl-1,2,5,6-Tetrahydropyridines to N-Acyl-Enamines by Palladium on Carbon. *Heterocycles* **1987**, *26*, 917-919.
- (32) Kim, S. Y.; Kim, K. H.; Moon, H. R.; Kim, J. N. Synthesis of Tetrahydropyridines from Morita-Baylis-Hillman Acetates of  $\alpha,\beta$ -Unsaturated Aldehydes Via an Intramolecular 1,6-Conjugate Addition. *Bull. Korean Chem. Soc.* **2016**, *37* (1), 95-98.
- (33) Sonesson, C.; Larhed, M.; Nyqvist, C.; Hallberg, A. Regiochemical Control and

- Suppression of Double Bond Isomerization in the Heck Arylation of 1-(Methoxycarbonyl)-2,5-dihydropyrrole. *J. Org. Chem.* **1996**, *61* (14), 4756-4763.
- (34) Naito, H.; Hata, T.; Urabe, H. Selective Deprotection of Methanesulfonamides to Amines. *Org. Lett.* **2010**, *12* (6), 1228-1230.
- (35) Sabitha, G.; Reddy, B. V. S.; Abraham, S.; Yadav, J. S. Deprotection of sulfonamides using iodotrimethylsilane. *Tetrahedron Lett.* **1999**, *40* (8), 1569-1570.
- (36) Javorskis, T.; Orentas, E. Chemoselective Deprotection of Sulfonamides Under Acidic Conditions: Scope, Sulfonyl Group Migration, and Synthetic Applications. *J. Org. Chem.* **2017**, *82* (24), 13423-13439.
- (37) Lanckenau, A. W.; Iovan, D. A.; Pienkos, J. A.; Salomon, R. J.; Wang, S.; Harrison, D. P.; Myers, W. H.; Harman, W. D. Enantioenrichment of a tungsten dearomatization agent utilizing chiral acids. *J. Am. Chem. Soc.* **2015**, *137* (10), 3649-3655.
- (38) Wilson, K. B.; Smith, J. A.; Nedzbala, H. S.; Pert, E. K.; Dakermanji, S. J.; Dickie, D. A.; Harman, W. D. Highly Functionalized Cyclohexenes Derived from Benzene: Sequential Tandem Addition Reactions Promoted by Tungsten. *J. Org. Chem.* **2019**, *84* (10), 6094-6116.
- (39) Simpson, S. R.; Siano P.; Siela D. J.; Diment L. A.; Song B. C.; Westendorff K. S.; Ericson M. N.; Welch K. D.; Dickie D. A.; Harman W. D. Phenyl Sulfones: A Route to a Diverse Family of Trisubstituted Cyclohexenes from three Independent Nucleophilic Additions. *J. Am. Chem. Soc.* **2022**, *144* (21), 9489-9499.
- (40) Prashad, M. Approaches to the Preparation of Enantiomerically Pure (2R,2'R)-(+)-threo-Methylphenidate Hydrochloride. *Adv. Synth. & Catal.* **2001**, *343*, 379-392.
- (41) Davies, H. M.; Venkataramani, C.; Hansen, T.; Hopper, D. W. New strategic reactions for organic synthesis: catalytic asymmetric C-H activation  $\alpha$  to nitrogen as a surrogate for the mannich reaction. *J. Am. Chem. Soc.* **2003**, *125* (21), 6462-6468.
- (42) Chang, M.; Huang, Y.; Liu, S.; Chen, Y.; Krska, S. W.; Davies, I. W.; Zhang, X. Asymmetric hydrogenation of pyridinium salts with an iridium phosphole catalyst. *Angew. Chem. Int. Ed. Engl.* **2014**, *53* (47), 12761-12764.
- (43) Huang, W. X.; Yu, C. B.; Ji, Y.; Liu, L. J.; Zhou, Y. G. Iridium-Catalyzed Asymmetric Hydrogenation of Heteroaromatics Bearing a Hydroxyl Group, 3-Hydroxypyridinium Salts. *ACS Catal.* **2016**, *6* (4), 2368-2371.
- (44) Wang, D. S.; Chen, Q. A.; Lu, S. M.; Zhou, Y. G. Asymmetric hydrogenation of heteroarenes and arenes. *Chem. Rev.* **2012**, *112* (4), 2557-2590.
- (45) Patrick, K. S.; Kilts, C. D.; Breese, G. R. Synthesis and pharmacology of hydroxylated metabolites of methylphenidate. *J. Med. Chem.* **1981**, *24* (10), 1237-1240.
- (46) Heal, D. J.; Pierce, D. M. Methylphenidate and its isomers: their role in the treatment of attention-deficit hyperactivity disorder using a transdermal delivery system. *CNS Drugs* **2006**, *20* (9), 713-738.

## Chapter 4

### Syntheses and Quantitative Analyses of Selectively Deuterated Tetrahydropyridine Isotopologues and Isotopomers



## 4.1. Introduction

Despite the years of collective research and exorbitant financial capital invested, 90% of drug candidates entering clinical trials fail, with much higher percentages never advancing to this phase.<sup>1</sup> One strategy for improving upon these figures is bioisosterism, the process of replacing a drug component with another that improves the drug pharmacokinetic profile while retaining the bioactivity of the original fragment.<sup>2</sup> Pirali argues that replacing hydrogen with deuterium, while arguably the smallest chemical change, can significantly alter drug properties.<sup>3</sup>

Deuterated organic compounds have long been used as solvents, as analytical standards, and in the elucidation of reaction mechanisms and biochemical metabolic pathways. Yet the emergence of readily available deuterated "building blocks" and new methods of deuterium-hydrogen exchange have led to renewed efforts to incorporate deuterium into the Active Pharmaceutical Ingredient (API) of medicines.<sup>4</sup> The recent FDA approval of deutetrabenazine (Austedo<sup>®</sup>), a treatment for Huntington's disease, was made possible by the improved pharmacokinetic profile and mitigated side-effects.<sup>5</sup> More germane to this study, Zhu *et al.* demonstrated that replacing hydrogen with deuterium in the piperidine ring of the prodrug clopidogrel (Plavix<sup>®</sup>) resulted in a substantial increase in the active metabolite generated due to a reduction in enzymatic piperidine ring attrition.<sup>6</sup> Their study emphasizes the value of developing a general method for selectively synthesizing a wide range of isotopologues and isotopomers for piperidine, which is the most commonly occurring *N*-heterocycle in FDA-approved small-molecule drugs.<sup>7</sup>

While various catalytic<sup>8-12</sup> and metal-free<sup>13-15</sup> methods for incorporating deuterium into pyridine rings have been developed, methods for *selective* preparation of deuterated piperidines and tetrahydropyridines (THP) are lacking. In the aforementioned Zhu study, deuterium was

incorporated into the piperidine core of clopidogrel by assembling the piperidine ring via a Mannich condensation ring closure that used deuterated formaldehyde. This procedure was adapted and modified by Hesk and coworkers in the synthesis of a tetradeuterated analog of NPY<sub>5</sub> receptor SCH 430765.<sup>16,17</sup> Methods have also been developed for H/D exchange at C2 of a pyridine or piperidine ring (Figure 4.1A).<sup>8,18,19</sup> Deuterated piperidines and THPs have also been prepared via the reduction of pyridines. Incorporation of deuterium can be accomplished diastereoselectivity through the reduction of functionalized pyridines with deuterium gas (D<sub>2</sub>) (Figure 4.1A).<sup>20,21</sup> Pyridine reduction has also been accomplished with deuterated ammonium formate,<sup>22</sup> and various deuterated borohydride sources.<sup>23-27</sup> But all these approaches suffer from poor regiochemistry, stereoselectivity or over deuteration.

We envisioned an organometallic approach to the synthesis of THPs, and by extension to piperidines, comprising a series of selective deuterium additions to a tungsten-coordinated pyridine. This approach was inspired by our recent experiences with the stepwise reduction of benzene to cyclohexene. Smith *et al.* demonstrated that sequential additions of D<sup>+</sup>, D<sup>-</sup>, D<sup>+</sup>, and D<sup>-</sup> to benzene,  $\eta^2$ -bound to a {W Tp(NO)(PMe)} ([W]) fragment, enabled the highly modular

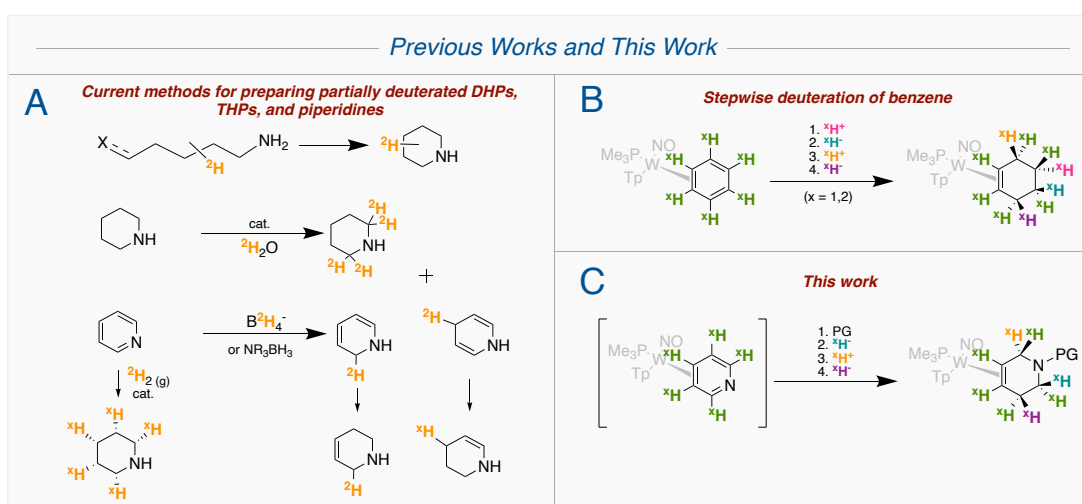


**Figure 4.1:** (A) Methods for deuterium-incorporated piperidines from pyridine are largely not chemo- or stereoselective. (B) Cyclohexene isotopologues/-mers were formed by hydrogen/deuterium additions to [W]- $\eta^2$ -bound benzene. (C) The proposed regio- and stereoselective deuterium incorporation to pyridine complex.

preparation of a small library of cyclohexene isotopomers (Figure 4.1B).<sup>28</sup> We anticipated that a similar process could be carried out on the previously reported [W]-( $\eta^2$ -(*N*-mesyl)pyridinium) (OTf) complex (**33D**) (Figure 4.1C).<sup>29</sup> As with deuterated cyclohexenes, we reasoned that molecular rotational resonance (MRR), a burgeoning analytical tool that analyzes compounds on their unique moment of inertia, would be an ideal method for precisely determining the isotopic purity of each stereoisotopomer prepared.

## 4.2. Synthesis of [W] $\eta^2$ -Dihydropyridine Complexes

The pyridine borane complex **2** was previously synthesized by exchanging pyridine borane onto a [W]-( $\eta^2$ -anisole) precursor **59**, thereby forming a mixture of coordination diastereomers, **2D** and **2P** (Figure 4.2A). This mixture can then be converted to the pyridinium complexes **3D** and **3P** via diphenylammonium triflate (DPhAT) in acetone, then mesylated via methanesulfonic anhydride in the presence of lutidine to form the  $\eta^2$ -pyridinium complex **33D**. The ratio of the distal and proximal coordination diastereomers is enriched to >20:1 upon mesylation because the electron-withdrawing sulfonyl group induces a more electron-deficient iminium, which the metal orients distal to the  $\text{PMe}_3$  upon gentle heating.<sup>30</sup> This system provides good scalability (5 g), consistent purity, and selective incorporation of nucleophiles at its iminium carbon C2 (r.r. > 99:1), making it an ideal precursor for this work. Additionally, and unlike its *N*-acetyl predecessor (**4D**),<sup>31</sup> **33D** does not form downstream mixtures of rotational isomers.

With a suitable precursor in hand, our attention turned to incorporating hydrogen and deuterium in the ring. Compound **33D** was reduced via  $\text{NaBH}_4$  at  $-30\text{ }^\circ\text{C}$  to form the DHP complex **60D** (Figure 4.2B). The reduction of the pyridinium ligand is reflected in  $^1\text{H}$  NMR spectra, which show diastereotopic methylene hydrogens adjacent to the nitrogen. Nuclear Overhauser Effect

(NOE) interactions observed between the H5 proton and the  $\text{PMe}_3$  ligand and the H2 methylene protons and the Tp pyrazole ring proton PzA3 support the proposed orientation of the DHP ligand. This structure was ultimately confirmed by single crystal X-ray diffraction (SC-XRD – Figure 4.3). We observed that this complex was insoluble in methanol, and this property could be utilized to remove impurities through trituration, thereby avoiding chromatography. In contrast to Knaus *et al.*, who reduced sulfonyl pyridinium via  $\text{NaBH}_4$  to a mixture of 1,2 & 1,4 DHP products,<sup>23</sup> the sulfonyl pyridinium is reduced exclusively to form a  $[\text{W}]-(\eta^2\text{-}1,2\text{-DHP})$  complex. This pyridinium reduction to a DHP via  $\text{NaBH}_4$  was consistent with that observed for the *N*-acetyl derivative.<sup>31</sup>

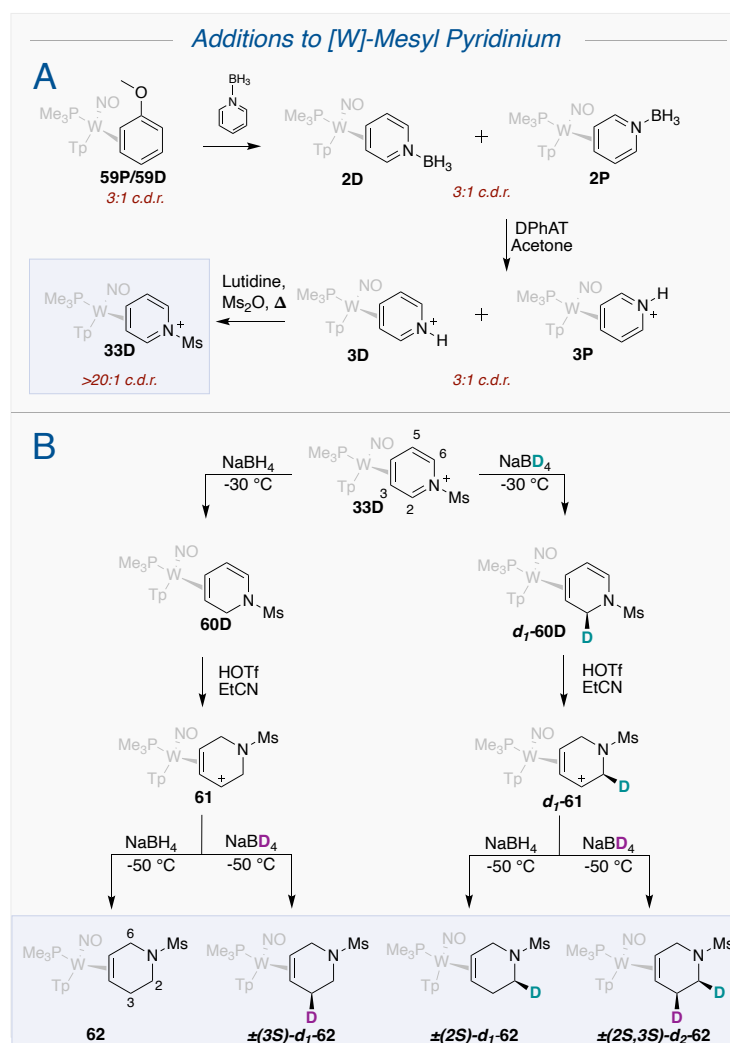


**Figure 4.2:** (A) The synthesis of a mesylated pyridinium complex. (B) The synthesis of  $d_0$ ,  $d_1$ , and  $d_2$  THP isotopologues from **33D**.

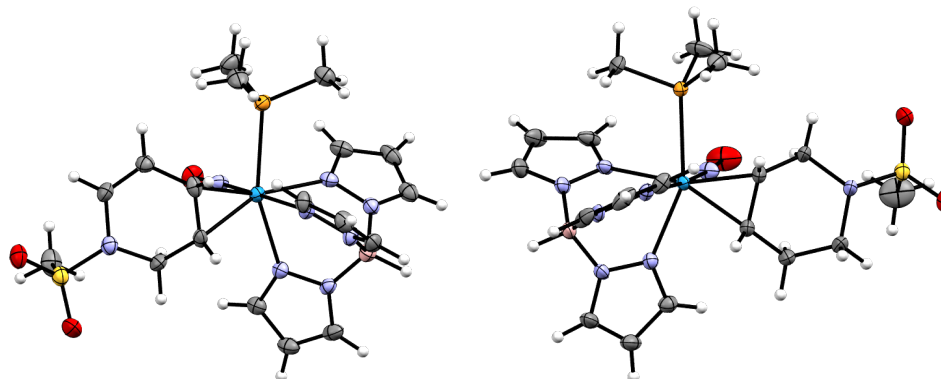


**Figure 4.3:** SC-XRD ORTEP/ellipsoid diagrams of **60D** (left) and **62** (right).

### 4.3. Synthesis of [W] $\eta^2$ -Tetrahydropyridine Complexes

Alternatively, deuterium can be incorporated into the pyridine ring at this stage to form  $d_1$ -**60D** by reducing **33D** with NaBD<sub>4</sub> (Figure 4.2B). **60D** and  $d_1$ -**60D** mirror each other spectroscopically in most features. However, an <sup>1</sup>H NMR spectrum of  $d_1$ -**60D** shows a broadened singlet that integrates to approximately one proton where the roofing doublets appear in **60D**, indicating deuterium incorporation at the C2 carbon. Unfortunately, the diastereotopic methylene resonances in **60D** are too similar to determine the configuration of C2 via NOE interactions, thus necessitating an alternate analytical method for doing so (*vide infra*).

When dissolved in propionitrile and subjected to triflic acid, the DHP complexes (**60D** or  $d_1$ -**60D**) undergo facile protonation to form  $\eta^2$ -allyl complexes. *N*-sulfonyl enamines are ambiphilic species capable of undergoing both electrophilic and nucleophilic additions at the  $\beta$  position.<sup>32</sup> However, in this case protonation is observed exclusively at the  $\alpha$  position (C6), owing to the activation from the metal complex.<sup>29</sup> The resulting compounds, **61** and  $d_1$ -**61** are two rapidly interconverting  $\eta^2$ -allyl conformers **61P** and **61D** of which there is a thermodynamic preference for the distal form, **61D** (Figure 4.2B).<sup>30</sup> This assignment is supported via NOE interactions between the C6 methylene protons and the PMe<sub>3</sub> ligand and has previously been observed with

similar systems.<sup>29,31,33</sup> A  $\eta^2$ -1,2,3,6-THP complex (**62**) is formed when NaBH<sub>4</sub> is added to C3 of **61** or *d*<sub>1</sub>-**61**. The structure of **62** was confirmed via SC-XRD (Figure 4.3). Solution <sup>1</sup>H NMR spectra indicate that this material is formed free of its purported  $\eta^2$ -1,2,5,6-THP isomer, that would have resulted from the hydride addition occurring at C5 of the allyl complex (**61P**). We note that in previous work, when the C2 carbon contains a substituent other than hydrogen, C5 additions occur preferentially to form  $\eta^2$ -1,2,5,6-THP complexes.<sup>29</sup> Repeating this reaction sequence with *d*<sub>1</sub>-**61** results in  $\pm(2S)$ -*d*<sub>1</sub>-**62**. Deuterium was also incorporated using NaBD<sub>4</sub> for the second hydride addition, resulting in the THP isotopologues  $\pm(4S)$ -*d*<sub>1</sub>-**62** and  $\pm(2S,3S)$ -*d*<sub>2</sub>-**62**.

#### 4.4. Acid-Promoted Ring-Opening of THP Complexes

Initially, the preparation of the THP complex **62** was attempted directly from the DHP complex **60D** as a one-pot reaction, combining protonation and hydride addition steps. However, this procedure resulted in varying amounts of an unknown impurity. The extent of the impurity

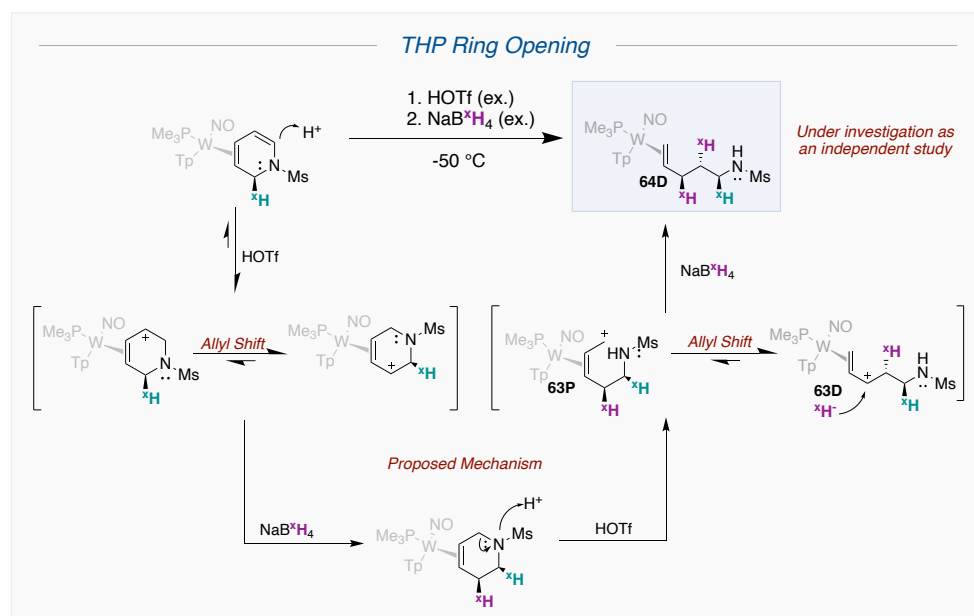


**Figure 4.4:** **64**, when formed *in situ* and in the presence of excess acid and borohydride, ring opens and forms an allyl chain that undergoes a subsequent hydride/deuteride addition.

generated directly correlated with the amount of *excess* triflic acid used. The impurity was eventually isolated and determined to be a  $\eta^2$ -(pent-4-ene-1-amine) derivative (**64**) (Figure 4.4). We postulated that **64** forms as a result of the targeted THP complex **7** undergoing nitrogen protonation, which induces a ring-opening to form the allyl complex **63**. The distal conformer of **63** (**63D**), then purportedly undergoes addition of a hydride from the excess NaBH<sub>4</sub> present. This side reaction was suppressed by isolating the allyl complexes (**61**) prior to the 2<sup>nd</sup> hydride/deuteride addition. The clean isolation of **63** by protonating **62** with DPhAT further supports this mechanism.

#### 4.5. Synthesis of High-Deuterium THP Complexes (*d*<sub>5</sub>-*d*<sub>8</sub>)

An additional opportunity to introduce deuterium would be through D<sup>+</sup> addition. Efforts to stereoselectively deuterate *d*<sub>1</sub>-**60D** to form a *d*<sub>2</sub>-**61** isotopologue were largely unsuccessful. Using DOTf in EtCN resulted in roughly 20% deuterium incorporation at the *6-syn*- position. Attempts to carry out the deuteration in CD<sub>3</sub>OD and DOTf gave similar results. This suggested that, like the  $\eta^2$ -cyclohexadiene analog, an unusually large deuterium kinetic isotope effect (DKIE;  $k_H/k_D$ ) may be responsible for trace amounts of fortuitous H<sup>+</sup> successfully competing against the large excess of D<sup>+</sup>.<sup>28</sup> However, we reasoned that it might be possible to probe the protonation at C6 by starting with a fully deuterated pyridine ring in **2** (*vide infra*).

Our next endeavor was to synthesize the complex *d*<sub>5</sub>-**2** from *d*<sub>5</sub>-pyridine borane, the latter being synthesized from *d*<sub>5</sub>-pyridine, NaBH<sub>4</sub>, and sodium bicarbonate (Figure 4.5A).<sup>34</sup> This optimized synthesis was a modified literature procedure by Ramachandran *et al.* and was scaled up to a 50 g scale. Like the procedure used to prepare **2**, *d*<sub>5</sub>-pyridine borane was exchanged with the anisole ligand of **59**, resulting in a 3:1 isolable mixture of *d*<sub>5</sub>-**2P** and *d*<sub>5</sub>-**2D**. The <sup>1</sup>H NMR of *d*<sub>5</sub>-**2** showed each pyridine ring position maintained  $\geq 95\%$  deuterium incorporation. The borane

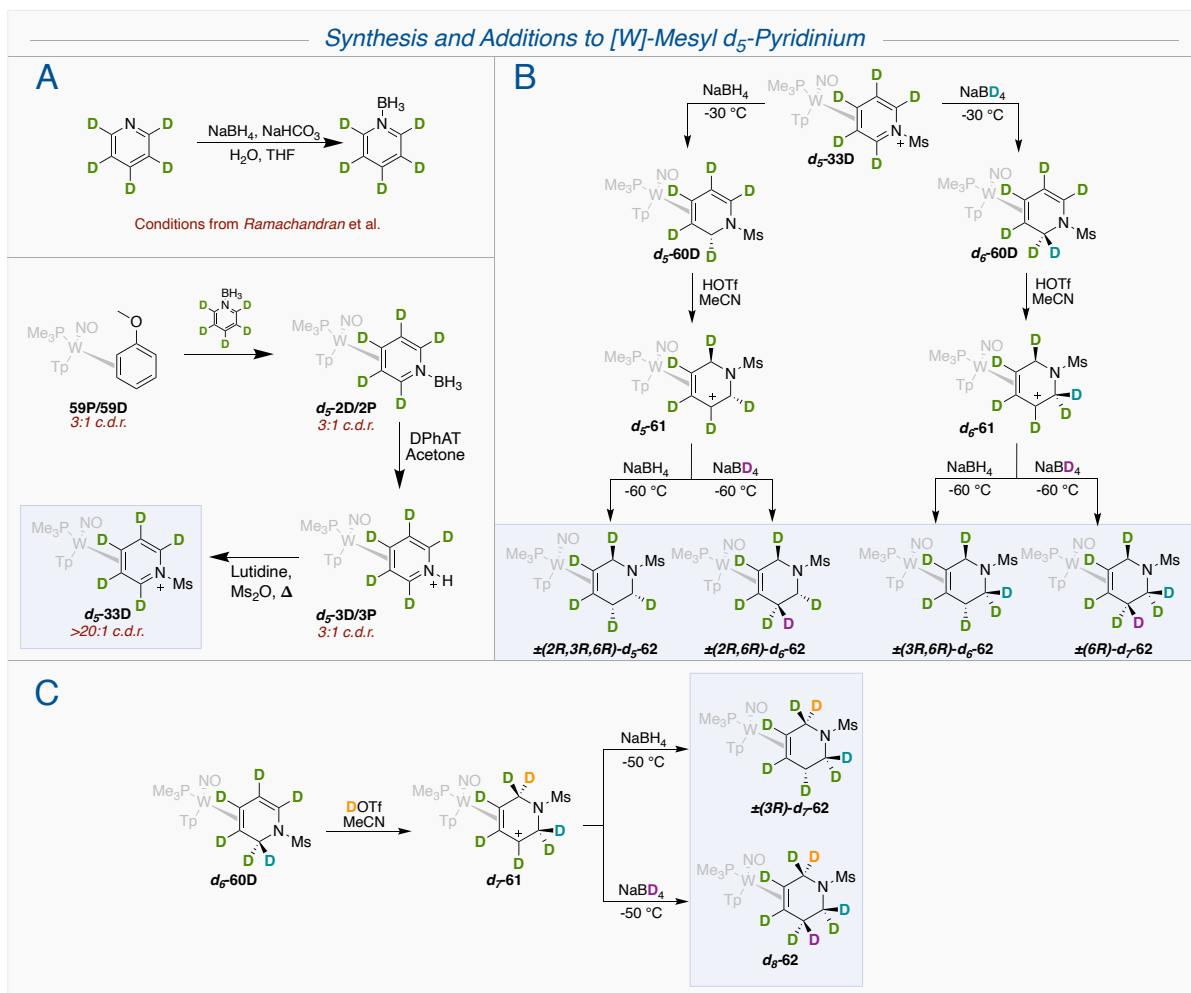


**Figure 4.5:** (A) Preparation of the  $d_5$ -**33D** precursor. (B) Synthesis of  $d_5$ -**62** through  $d_8$ -**62** complexes from  $d_5$ -**33D**. (C) The  $d_6$ -**60D** complex is deuterated to form  $d_7$ -**61**.

group was then removed as before to form a mixture of  $d_5$ -**3D/P**, which was then mesylated to  $d_5$ -**33D**. Similar to that observed for the pyridinium complex **33D**, the deuterated analog  $d_5$ -**33D** readily incorporates both hydride and deuteride to form the DHP complex isotopologues  $d_5$ -**60D** and  $d_6$ -**60D** (Figure 4.5B).

To our delight, when the  $d_6$ -**60D** was protonated using the same conditions as **60D** (triflic acid (1 eq.) in propionitrile), protium incorporation in the target allyl complex  $d_6$ -**61** was observed solely at C6 (>95%; >5% at other carbons). However, the ratio of *syn/anti* protonation ratio was only 7:3 according to  $^1\text{H}$  NMR peak integrations. The *syn* and *anti* protons of the C6 diastereotopic



methylene group were distinguished for the  $d_0$ -**60D** isotopologue via a strong NOE between the  $\text{PMe}_3$  ligand and the *syn* proton, while the *anti* proton lacks this interaction. A variety of conditions were examined to improve the stereochemical purity for this step. Temperature had no noticeable effect, and weaker acid sources resulted in poorer diastereoselectivity, potentially due to the presence of a stronger conjugate base that could epimerize C6 via deprotonation. Increasing the equivalents of acid used resulted in increased protium incorporation at both *syn* and *anti* positions on C6, and at C2. Screening various solvents revealed that acetonitrile was the optimal solvent choice as it had a *syn/anti* ratio as high as 9:1. In analogous fashion,  $d_5$ -**61** could be prepared from  $d_5$ -**60D** with a d.r. of 9:1. Incorporating  $\text{H}^+$  *syn* relative to [W] has precedent with the protonation of the  $\eta^2$ - $d_6$ -benzene complex.<sup>28</sup> In that study, computations indicated that ring protonation may be occurring via the nitrosyl ligand. Even so, Harrison *et al.* report that the analogous  $\eta^2$ -(1-acetyl-2-ethyl-1,2-dihydropyridine) complex undergoes  $\text{D}^+$  addition *anti* to the metal, and this observation suggests that the nitrogen protecting group may influence the stereochemistry of C6 protonation as well as the tungsten complex.<sup>31</sup>

Following the synthesis of a  $d_5$ -**61** and  $d_6$ -**61**,  $\text{NaBH}_4$  or  $\text{NaBD}_4$  was added to each of the allyl complexes to render  $d_5$ -,  $d_6$ -, and  $d_7$ -**62** isotopologues (Figure 4.5B), where the  $d_6$  isotopologue was prepared as two different isotopomers  $\pm(2R,6R)$ - $d_6$ -**62** and  $\pm(3R,6R)$ - $d_6$ -**62**. Similar to the previous reactions, the hydride (deuteride) additions occurs distal to the  $\text{PMe}_3$  ligand at C3, exclusively *anti* to the metal. In order to access a fully deuterated  $d_8$ -**62** complex, we sought to synthesize a  $d_7$ -**61** allyl complex  $d_7$ -**61** by incorporating  $\text{D}^+$  into  $d_6$ -**60D** (DOTf in acetonitrile; Figure 4.5C). While we were unsuccessful in this endeavor with **60D** and  $d_1$ -**60D** (*vide supra*), ~80% deuterium incorporation was achieved for the  $d_6$ -**60D** reaction with ~10:1 *syn:anti*

stereoselectivity. Deuteride was subsequently added to *d*<sub>7</sub>-**61** resulting in *d*<sub>8</sub>-**62**. Alternatively, the addition of hydride to *d*<sub>7</sub>-**61** resulted in a second *d*<sub>7</sub> isotopomer:  $\pm(3R)$ -*d*<sub>7</sub>-**62**.

#### 4.6. Synthesis of Methylphenidate Isotopologues/-mers

After synthesizing a library of THP isotopologues and isotopomers, we then endeavored to demonstrate the utility of this method by synthesizing a library of biologically relevant THP derivatives. Previous studies from our group have demonstrated that *N*-mesyl analogues of *erythro* methylphenidate (MPH; Ritalin<sup>®</sup>) are accessible by subjecting **33D** to a Reformatsky reaction.<sup>29,35</sup> Thus, **33D** in the presence of methyl  $\alpha$ -phenyl bromoacetate (MAPBA), Zn<sup>0</sup>, and THF will incorporate the methyl phenylacetate moiety at C2 (**35D**; Figure 4.6A). *d*<sub>5</sub>-**35D** was synthesized using *d*<sub>5</sub>-**33D** and identical reaction conditions to **33D**, and the <sup>1</sup>H NMR signals between **35D** and *d*<sub>5</sub>-**35D** were identical except for the absence of signals in *d*<sub>5</sub>-**35D** corresponding to the five ring deuterons (Figure 4.6B).

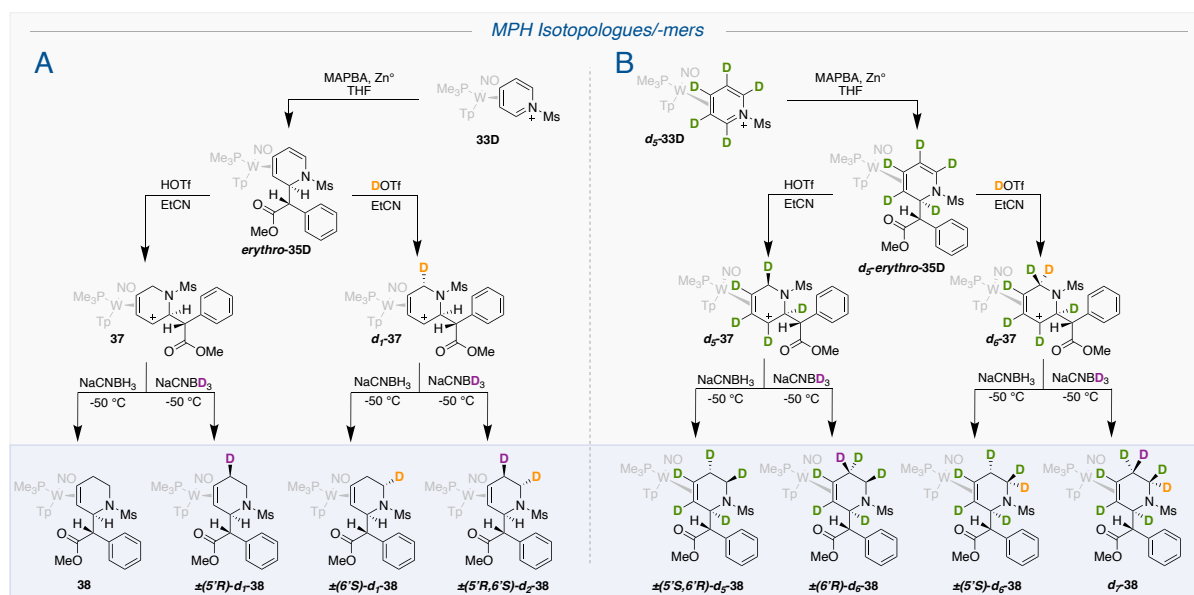


**Figure 4.6:** Eight different MPH THP isotopologues/-mers were synthesized from *erythro*-**35D** (A) and *d*<sub>5</sub>-*erythro*-**35D** (B).

As previously reported, **35D** is readily protonated by triflic acid in propionitrile to form an  $\eta^2$ -allyl complex (**37**) similar to **61** with the carbenium orientation favored distal to the  $\text{PMe}_3$  ligand. Interestingly, unlike **61**, when the reaction conditions used to prepare **61** were applied to  $d_5$ -**35D**, protium incorporation was observed almost exclusively *syn* to the metal at C6 (~20:1 d.r. by  $^1\text{H}$  NMR) to form the allyl complex  $d_5$ -**37**. Emboldened by the selectivity demonstrated with  $\text{H}^+$  additions, we attempted  $\text{D}^+$  addition to C6. Given the difficulties we had selectively adding  $\text{D}^+$  to **60D** (*vide supra*), a large deuterium reservoir was prepared by using  $d_4$ -methanol. To offset the acid-leveling of the  $d_4$ -methanol, 6 eq of DOTf was used.  $d_6$ -**37** was successfully synthesized with deuterium incorporation >93% at the *syn* C6 position by  $^1\text{H}$  NMR. When these same conditions were applied to the proteated analog **35D**, 90% deuterium was incorporated *syn* relative to the metal at C6 ( $d_1$ -**37**), however, 65% overdeuteration was observed *anti* to the metal at C6 (*i.e.*, 6,6- $d_2$ -**37**). A compromise was ultimately reached by replacing  $d_4$ -methanol with acetonitrile, but still using six equivalents of DOTf. This process yielded  $d_1$ -**37** with ~80% deuterium incorporation *syn* at C6 and no observable overdeuteration.

Adding a hydride to **37** was previously conducted with  $\text{NaCNBH}_3$  at  $-60\text{ }^\circ\text{C}$  to form an  $\eta^2$ -1,2,5,6-THP complex (**38**). Unlike the synthesis of **62**, addition of a subsequent nucleophile occurs at C5 instead of C3, resulting in 1,2,5,6-THPs instead of 1,2,3,6-THPs. This putatively occurs due to the presence of the bulky methyl phenylacetate group raising the kinetic barrier for addition at C3. A range of 1,2,5,6-THP isotopologues ( $d_1$ -,  $d_2$ -,  $d_5$ -,  $d_6$ -,  $d_7$ -**38**) and isotopomers  $\pm(5'R)$ - $d_1$ -**38**,  $\pm(6'S)$ - $d_1$ -**38**;  $\pm(6'R)$ - $d_6$ -**38**,  $\pm(5'S)$ - $d_6$ -**38**) were thus synthesized by performing hydride or deuteride additions to the appropriate isotopologue of **37** (Figure 4.6A/B).

## 4.7. THP Oxidative Demetallations

Liberation of 1,2,3,6-THP and 1,2,5,6-THP organic ligands readily occurs when the corresponding complex is exposed to a chemical oxidant. The oxidation of tungsten to W(I) or W(II) greatly diminishes its backbonding capability, thus weakening the THP-W bond and allowing the dissociation of the organic. 2,3-dichloro-5,6-dicyano-1,4-benzoquinone (DDQ) dissolved in acetone was suitably oxidizing to effect liberation of the THP. To ensure complete decomplexation, an excess of DDQ (4 equivalents) was used. After four hours of stirring, (*N*-mesyl)-1,2,3,6-tetrahydropyridine (**65**) was then cleanly eluted off a basic alumina column with

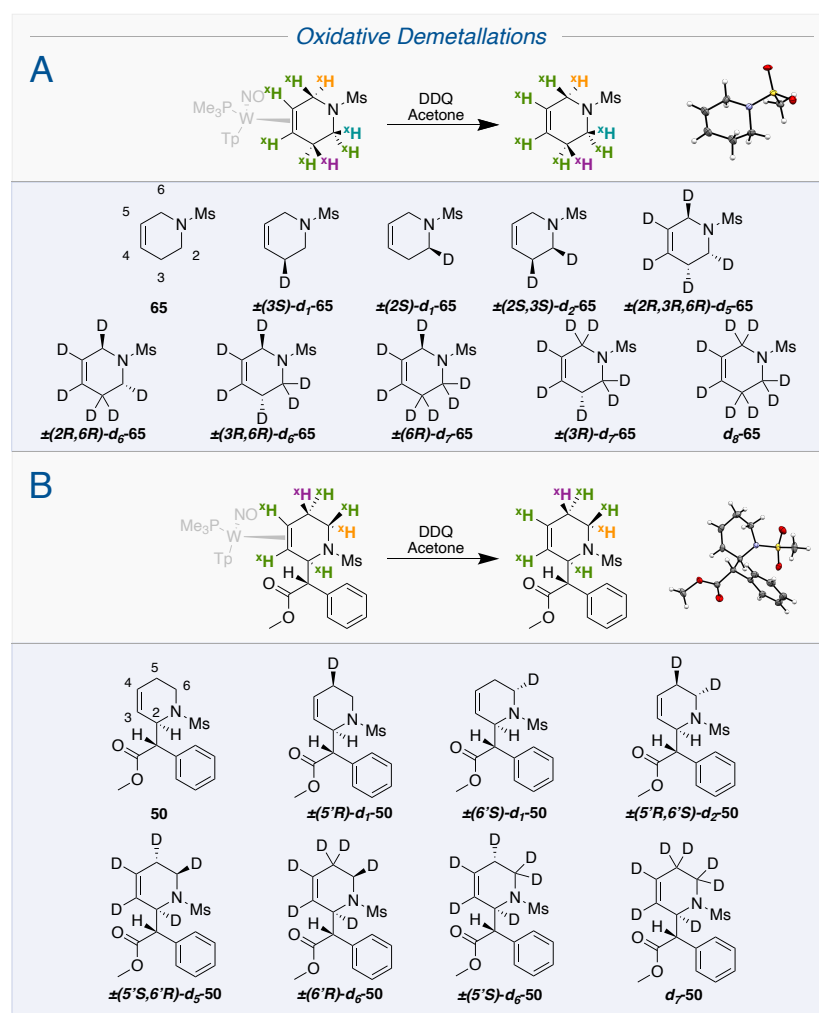


**Figure 4.7:** Scope of THP organics isolated from the DHP tungsten complexes **62** (A) and **38** (B).

40% ethyl acetate in hexanes (Figure 4.7A). This process was generalized for the isolation of all isotopologues of **65**, as well as the MPH isotopologues of **50** (Figure 4.7B).

#### 4.8. MRR Analysis of THPs

While NMR can be a useful analysis tool for determining the site and amount of deuterium incorporation, simply measuring the decline in peak integration to determine the extent of deuterium incorporation becomes a substantial challenge when peaks overlap. This problem is further accentuated when deuterium is incorporated into molecules rich in  $sp^3$ -hybridized carbons as these protons tend to accumulate in the upfield region, and the introduction of stereogenic centers renders all methylene groups diastereotopic. While mass spectrometry is also useful for determining the number of isotopologues present, it cannot determine the location of deuterium incorporation. Molecular Rotational Resonance (MRR) spectroscopy is a method of small-molecule analysis capable of distinguishing compounds based on their unique moments of inertia. This highly sensitive technique determines the presence of isotopic impurities present down to 0.3% relative to the major species. Each isotopologue of **65** was analyzed via MRR to confirm the regio- and stereochemistry of the target compound as well as identify the and quantify any impurities present (Table 4.1) and these results were compared to NMR analysis. For each sample of **65**, the mixture was comprised of at least 60% of the target and as high as 94%. Because enantiomers have the same moment of inertia, they cannot be distinguished by conventional MRR, although MRR analysis of absolute stereochemistry has been reported.<sup>36</sup>

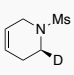
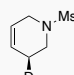
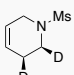
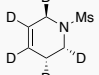
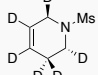
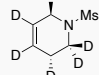
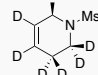
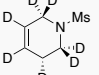
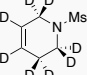
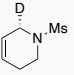
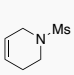
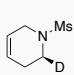
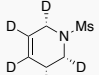
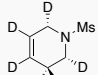
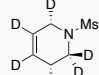
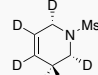
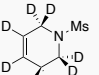
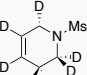
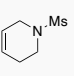
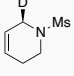
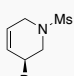
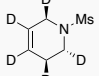
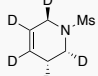
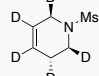
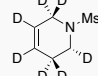
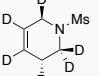
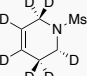
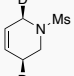
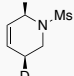
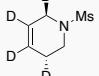
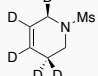
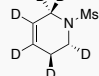
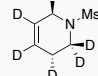
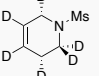
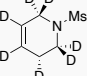
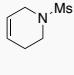
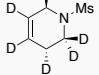
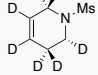
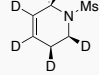
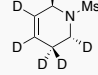
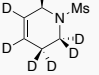
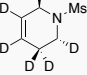
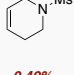
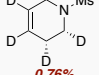
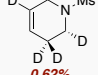
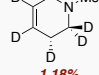
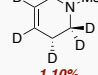
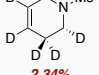
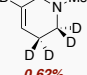
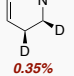
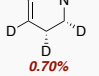
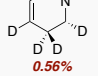
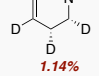
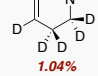
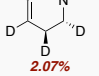
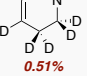
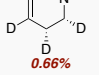
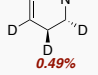
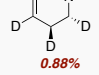
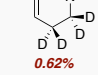
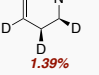
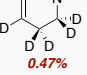
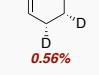
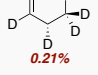
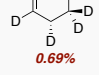
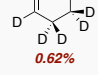
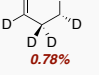
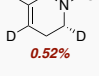
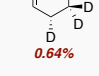
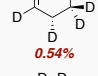
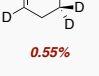
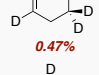
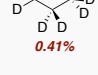
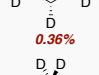
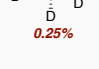
MRR sample analysis revealed several general recurring impurity pathways (Figure 4.8A). Underdeuteration impurities ( $d_{n-1}$ -**65**) were observed at each deuterium incorporation step (1<sup>st</sup> deuteride, deuterium, 2<sup>nd</sup> deuteride – Pathways A, E, and B respectively). These were attributed to

residual impurities in the system sourced from the reagents themselves or proton-exchanging sources (i.e. water) either in the solvent or on the glassware. While rigorous drying of solvents and glassware proved capable of minimizing these pathways, they could not be removed altogether. It is likely that a large DKIE exists for protonation at C6 of the DHP complexes **60D** and **35D**, analogous to that previously observed for H<sup>+</sup>/D<sup>+</sup> addition to tungsten η<sup>2</sup>-diene complexes (DKIE ≈ 37 at -30 °C).<sup>28</sup> An alternate mechanism of underdeuteration stems from the *d*<sub>5</sub>-pyridine borane ligand. This is synthesized from 99% isotopically enriched *d*<sub>5</sub>-pyridine (Cambridge Isotope); however, proteo *d*<sub>4</sub>-pyridine impurities in complex **33D** would enhance the relevance of impurity pathways H-L (Figure 4.7B). Some compounds produced through these routes are unique while others are identical to impurities accessed through different mechanisms.

Alternatively, misdeuterations can occur when hydride/deuteride addition occurs at C5 (proximal) instead of C3 (distal) on the η<sup>2</sup>-allyl complex *d*<sub>x</sub>-**61** (Pathway A).<sup>29,30</sup> While 2D NMR analyses of the resulting *d*<sub>x</sub>-**62** compounds indicate that addition is heavily favored at C3, C5 addition accounts for a minor impurities detected via MRR (except with symmetrical allyl complexes, like **61** or *d*<sub>7</sub>-**61**, which would yield identical organic THPs (as racemic mixtures) upon either C3 or C5 hydride addition and subsequent decomplexation). The ratio of C3 to C5 addition products is found to be approximately 19:1 across various species (see analyses of: ±(2*S*,3*S*)-*d*<sub>2</sub>-**65**, ±(2*R*,3*R*,6*R*)-*d*<sub>5</sub>-**65**, ±(3*R*,6*R*)-*d*<sub>6</sub>-**65**, ±(6*R*)-*d*<sub>7</sub>-**65**). A brief study conducted to determine the temperature dependence of the regioselectivity resulted in no improvement at colder temperatures and increased formation of **64** at temperatures of -30 °C and above. Furthermore, misdeuteration can occur during the synthesis of *d*<sub>5</sub>-*d*<sub>7</sub> THPs due to protonation at C6 *anti* to the [W] fragment (Pathway E). Consistent with <sup>1</sup>H NMR observations, *syn* addition was favored ~9:1 over *anti* addition, and this is reinforced by MRR data.

**Table 4.1:** Detailed composition of each sample mixture as determined by MRR. Detection limit is >0.2%.

9

 91.13% Target	 94.28% Target	 75.34% Target	 82.36% Target	 85.26% Target	 72.50% Target	 81.89% Target	 60.84% Target	 72.09% Target
 5.36%	 4.022%	 14.37%	 7.95%	 7.87%	 13.39%	 4.21%	 10.57%	 18.78%
 3.49%	 1.04%	 6.23%	 3.68%	 2.39%	 4.37%	 4.18%	 9.77%	 4.32%
	 0.64%	 1.72%	 1.57%	 1.80%	 2.67%	 3.55%	 7.25%	 2.34%
		 1.47%	 1.18%	 0.76%	 1.39%	 1.75%	 4.39%	 0.85%
		 0.49%	 0.76%	 0.62%	 1.18%	 1.10%	 2.34%	 0.62%
		 0.35%	 0.70%	 0.56%	 1.14%	 1.04%	 2.07%	 0.51%
			 0.66%	 0.49%	 0.88%	 0.62%	 1.39%	 0.47%
			 0.56%	 0.21%	 0.69%	 0.62%	 0.78%	
			 0.52%		 0.64%	 0.54%	 0.55%	
					 0.47%	 0.41%		
					 0.36%			
					 0.25%			

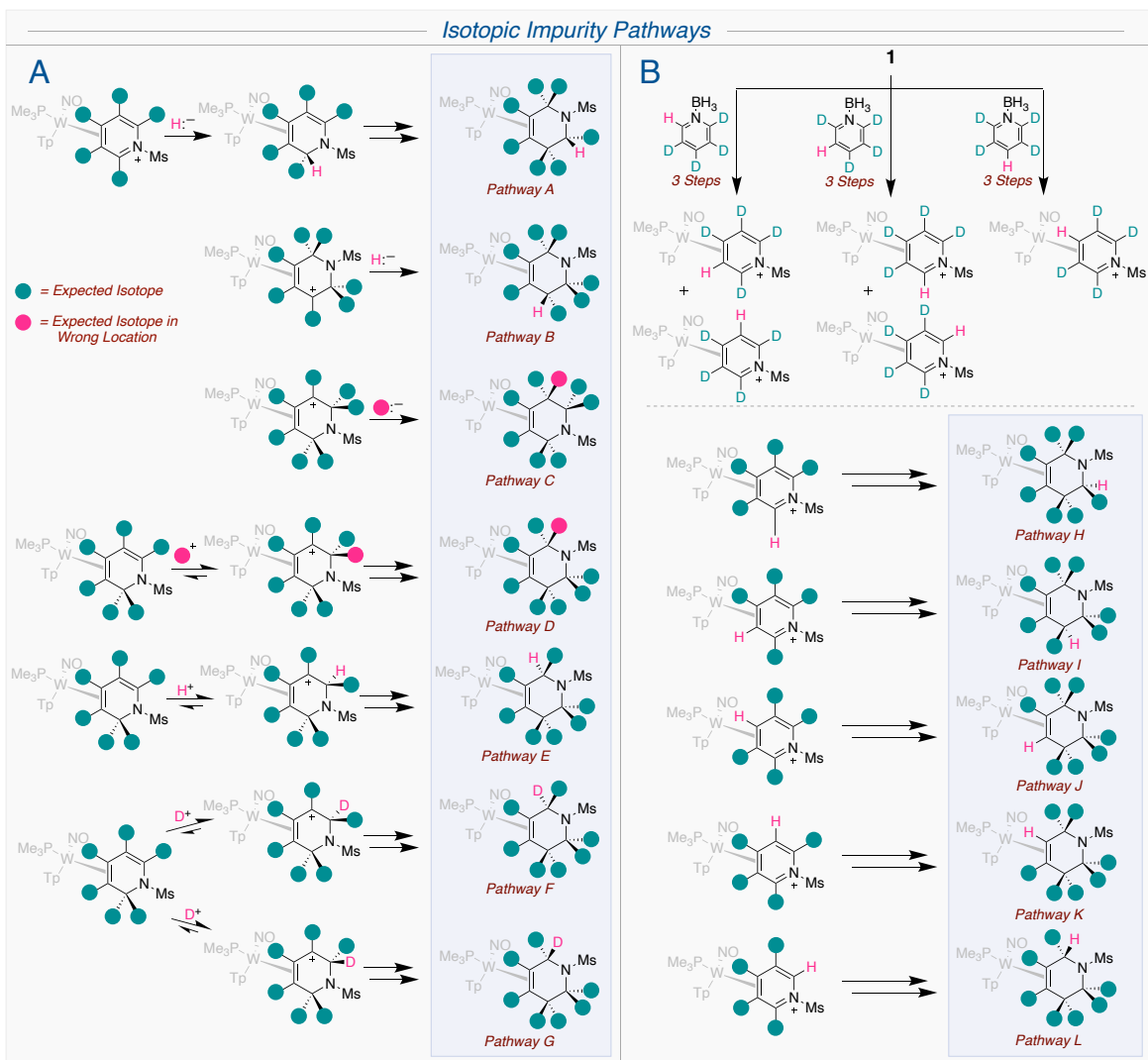


**Figure 4.8:** (A) Mechanisms for impurities originating from  $d_5$ -**33D**. (B) Mechanisms for impurities generated from underdeuterated  $d_4$ -pyridine coordination to **59**.

speculated that deuterated methanol is a deuteron source for these impurity pathways. Deuterated ( $d_4$ ) methanol, which is used to triturate  $d_5$ - and  $d_6$ -**60D** away from paramagnetic impurities, can facilitate an H/D isotope exchange with the triflic acid utilized in DHP protonations, thus incorporating an extra deuterium into C6 as opposed to protium (Pathways G). A more thorough breakdown of the impurity composition and the proposed mechanisms for generating them can be found in Appendix D.



In addition to providing highly detailed analyses of THP mixtures, MRR proved useful in optimizing sample syntheses.  $\pm(2S,3S)$ - $d_2$ -**65** was originally synthesized with the final step using  $d_4$ -methanol as the solvent. MRR determined that this sample was a mixture of compounds including 79% of the target, 4% misdeuteration (C5 addition), a combined 4% underdeuteration, and a combined 13% over-deuteration. The overdeuteration impurities were the most troubling. These impurities purportedly develop from the transient deprotonation of the allyl  $d_1$ -**61** back to  $d_1$ -**60P** followed by a deuteration at C6 to form a mixture of  $d_2$ -**61** allyl complexes. These impurities then undergo deuteride addition to form the over-deuterated  $d_3$ -**65** isotopologue impurities.

$d_4$ -Methanol was believed to facilitate both the deprotonation and deuteration steps; therefore, a modified procedure replaced  $d_4$ -methanol with dry tetrahydrofuran, which resulted in a mixture of products that featured less of the target (75%) but a drastic reduction of over-deuteration. This came at the price of increasing the underdeuteration products from 4% to 22%. Despite the large increase in underdeuteration, improvements in water-free techniques reduced underdeuteration impurities in future samples that also used THF as a cosolvent.

The results of MRR were then compared directly to  $^1\text{H}$  NMRs of the [W] complexed and free organic THPs. The integrations of the protons on C2, C3, and C6, the sites of additions, were analyzed in the  $^1\text{H}$  NMR spectra of the highly deuterated ( $d_5$ - $d_8$ ) samples and were then compared to expected integrations calculated based on the weighted accumulation of each MRR-identified compound present (Table 4.2). Most NMR peaks either matched or over-integrated relative to the MRR-determined integrations, which was reasonable given the likelihood of residual metal and solvent impurities in the baseline contributing to the area of the integrated peaks. The  $\pm(3R)$ - $d_7$ -**65**

**Table 4.2:** Comparison of observed <sup>1</sup>H NMR integrations and MRR data for protons on C2, C3, and C6 for **62** and **65**.

	$\pm(2R,3R,6R)-d_5-65$	$\pm(3R,6R)-d_6-65$	$\pm(2R,6R)-d_6-65$	$\pm(6R)-d_7-65$	$\pm(3R)-d_7-65$	$d_8-65$
7: NMR H2- <i>syn</i>	0.06	0.05	0.05	0.08	0.02	0.03
7: NMR H2- <i>anti</i>	1.01	0.07	1.01	0.03	0.06	0.10
<b>7: NMR H2 sum</b>	<b>1.07</b>	<b>0.12</b>	<b>1.06</b>	<b>0.11</b>	<b>0.08</b>	<b>0.13</b>
14: NMR H2	1.03	0.10	1.01	0.10	0.07	0.05
14: MRR H2	1.02	0.11	1.02	0.10	0.07	0.05
<b>7: NMR H3 sum</b>	<b>1.09</b>	<b>0.98</b>	<b>0.09</b>	<b>0.10</b>	<b>1.02</b>	<b>0.10</b>
14: NMR H3	1.02	0.92	0.04	0.05	0.94	0.05
14: NMR H3	0.99	1.01	0.03	0.05	0.82	0.02
7: NMR H6- <i>syn</i>	0.94	0.90	0.93	0.91	0.14	0.12
7: NMR H6- <i>anti</i>	0.09	0.15	0.08	0.16	0.08	0.07
<b>7: NMR H6 sum</b>	<b>1.03</b>	<b>1.05</b>	<b>1.01</b>	<b>1.07</b>	<b>0.22</b>	<b>0.19</b>
7: NMR H6	1.00	0.97	1.00	0.97	0.21	0.17
7: MRR H6	1.00	0.97	0.99	0.96	0.24	0.21

and  $\pm(3R,6R)-d_6-65$  samples notably differed from the expected values, but even these were within 8% and 9% of the expected respectively.

The rest of the samples all fell within a 5% range, demonstrating a general agreement between these two analysis methods on the overall composition of each sample. This also underscores that the chiral [W] fragment aids significantly in the optimization and analysis of various isotopomers, especially when analyzing diastereotopic methylene groups rendered asymmetric solely by deuterium. Significantly, the data provided by MRR provided the means to test reaction mechanisms and optimize reaction conditions in situations where NMR data was either ambiguous or indeterminant.

#### 4.9. Analysis of MPH THPs

After establishing a general agreement between MRR and  $^1\text{H}$  NMR analysis, the extent of deuterium incorporation for the corresponding MPH organics (**50**) was analyzed via  $^1\text{H}$  NMR (Table 4.3). While deuterium incorporation remained an issue for both deuteride and deuteron additions, the protonation/deuteration of C6 (**35D**  $\rightarrow$  **37**; Figure 4.6A) proved more stereoselective than the simple THP analogs. The integrity of the  $d_5$ -pyridine borane also was demonstrated by the high levels of signal knockout at H2, H3, H4, H5', and H6 for the highly deuterated species.

**Table 4.3:** Deuterium incorporation at each position of **50** samples measured by  $^1\text{H}$  NMR integrations.

	H2 (%D)	H3 (%D)	H4 (%D)	H5 <sub>syn</sub> (%D)	H5 <sub>anti</sub> (%D)	H6 <sub>syn</sub> (%D)	H6 <sub>anti</sub> (%D)
<b>50</b>	0	0	0	0	0	0	0
$\pm(5R)\text{-}d_1\text{-}50$	0	0	0	89	0	0	0
$\pm(6S)\text{-}d_1\text{-}50$	0	0	0	0	0	79	0
$\pm(5R,6S)\text{-}d_2\text{-}50$	0	0	0	91	0	76	0
$\pm(5S,6R)\text{-}d_5\text{-}50$	99	99	99	0	99	1	97
$\pm(6R)\text{-}d_6\text{-}50$	99	99	99	93	99	0	97
$\pm(5S)\text{-}d_6\text{-}50$	99	99	99	2	99	94	98
$d_7\text{-}50$	99	99	99	98	98	94	98

#### 4.10. Catalytic Hydrogenation of THPs

Lastly, **65** and **50** were reduced to fully saturated piperidines via a catalytic hydrogenation (Figure 4.9). The conditions for the reduction of **50** to **55** were previously reported<sup>26</sup> and similar conditions were utilized in the synthesis of **66**. Using 5% Pd on carbon with 25 bars of  $\text{H}_2$  at 50  $^\circ\text{C}$ , an enamine intermediate was observed that gave way to piperidine **66** over the course of 4 h. When these conditions were repeated in the reduction of  $(6'R)\text{-}d_6\text{-}65$  (*i.e.*,  $(6'R)\text{-}2',3',4',5',5',6'\text{-}d_6\text{-}65$ ) ~40% H/D scrambling was observed for all positions on C3', C4', and C5', thus underscoring the difficulty in selectively generating deuterium-containing scaffolds via Pd

catalyzed hydrogenations/deuterations. Mesyl deprotection, while preceded with piperidines,<sup>37</sup> has not been explored with this system.

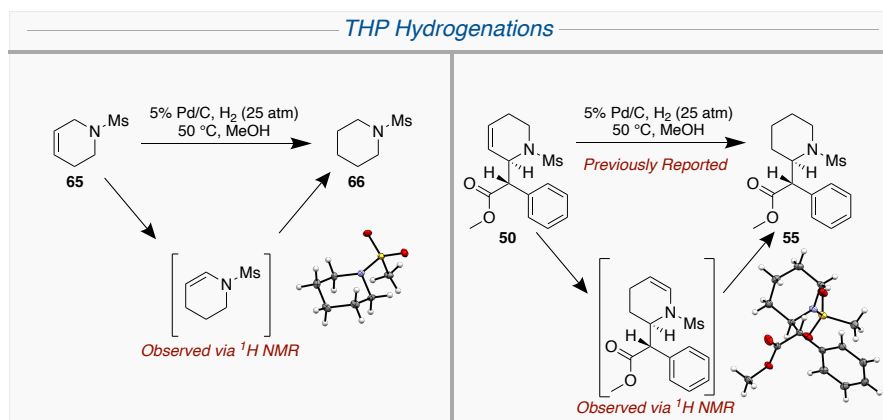


**Figure 4.9:** THPs **65** and **50** were hydrogenated to piperidines **66** and **55** respectively.

#### 4.11. Asymmetric Synthesis

Previous work describes a process for enantioenriching the [W] fragment via the  $\eta^2$  coordination of dimethoxybenzene (**57**), protonation to an  $\eta^2$ -dimethoxybenzenium complex (**58**) via a chiral acid, and then a trituration in a butanone/water mixture for the chiral resolution (Figure 4.10). After obtaining the *R* hand of **58**, deprotonation back to an  $\eta^2$ -dimethoxybenzenium complex and exchange with pyridine borane yielded enantiopure **2**. The enantioenriched material demonstrated identical downstream reactivity in the synthesis of (*WR*)-*d*<sub>1</sub>-**60D**. One that a 20:1 c.d.r. enriched solution of (*WR*)-**33D** resulted in (*WR*)-*d*<sub>1</sub>-**60D** with a c.d.r. of 10:1. This lower c.d.r. enrichment is tenuously attributed to differences in solubility of the enantioenriched material in hexanes, which was used to precipitate the material. (*WR*)-*d*<sub>1</sub>-**60D**, after being protonated to (*WR*)-*d*<sub>1</sub>-**61**, underwent hydride and deuteride additions respectively, which resulted in *2S*-*d*<sub>1</sub>-**65** and *2S,3S*-*d*<sub>2</sub>-**65** enantioenriched organics upon oxidative demetallation.

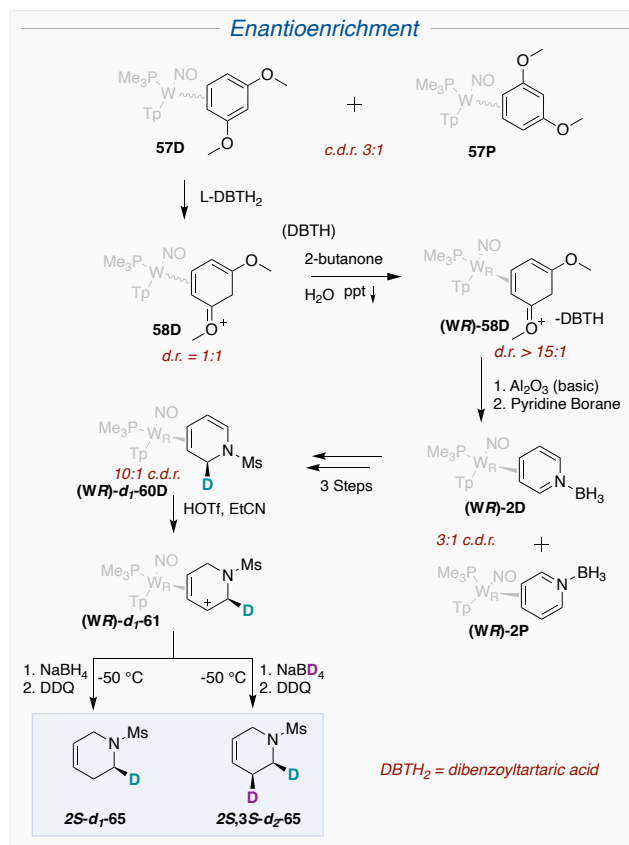


**Figure 4.10:** Asymmetric synthesis of (2*S*)-*d*<sub>1</sub>-65 and (2*S*,3*S*)-*d*<sub>1</sub>-65 via the chiral protonation of 57.

## 4.12. Conclusions

The resurgence in the interest of deuterated compounds in pharma compels the development of robust methods of deuterium incorporation into druglike small molecules. Herein we report a highly modular methodology for synthesizing a library of piperidine isotopologues and isotopomers *via* regio- and stereoselective tandem additions of deuterides and deuterons to an  $\eta^2$ -pyridinium complex. While conventional wisdom argues against the use of stoichiometric metal reagents, the continual presence of the [W] fragment throughout the syntheses efficiently promotes 4 electrophilic/nucleophilic additions while imparting a high degree of regio- and stereocontrol. Owing to the tungsten's stability under a wide range of reaction conditions and its ease of removability, this complex effectively performs as a bulky protecting group that can be cleaved

under mildly oxidizing conditions. Although the THP/piperidine isotopic substitution patterns generated *via* the  $d_0$  and  $d_5$ -pyridine borane systems are not exhaustive, we postulate that this system would also be compatible with alternative pyridine isotopologues/-mers generated *via* other methods<sup>12,14,38-42</sup> used in the formation of the pyridinium complex **33D** (Figure 4.11) Therefore, the cooperation between stepwise additions to **33D** with conventional pyridine deuteration methods would exponentially increase the amount of accessible deuterated THPs. Furthermore, the tungsten can also be utilized for functionalizing sites  $\alpha$  and  $\beta$ <sup>29</sup> to the nitrogen without sacrificing the selectivity of the deuterium incorporations. The demonstrated compatibility of this system, even the rare highly deuterated system, with increased functionalization of the pyridine ligand drastically expands the scope of accessible deuterated functionalized THPs and, by extension, piperidines.

In addition to reporting a synthetic approach for accessing piperidine isotopologues/-mers *via* this tungsten complex, we also have demonstrated the unique ability of MRR as a tool for analyzing the composition, purity, and reaction mechanisms for these compounds. While techniques such as mass spectrometry convey the extent of overall deuteration, but with no regard

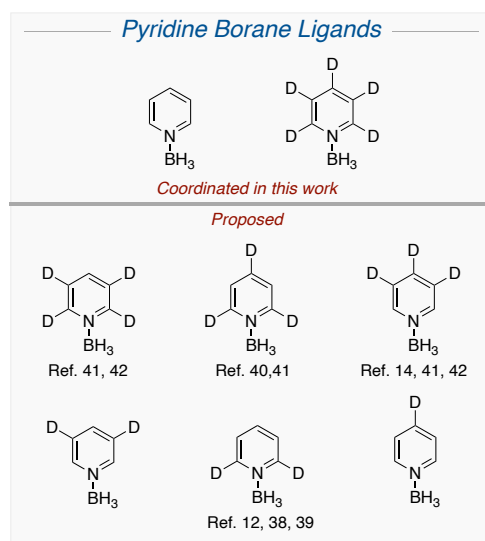


**Figure 4.11:** Various pyridine isotopes are compatible with this system, leading to a large array of possible THP isotopologue substitution patterns.

to position, and  $^1\text{H}$  NMR provides often incomplete information of the site and extent of deuterium incorporation, MRR's analysis provides a highly quantitative measure of both, thus paving the way for an optimized synthesis of these target compounds. The combination of the organometallic chemistry of tungsten combined with MRR analysis enables a modular method for selectively generating highly deuterated unfunctionalized and functionalized piperidines.

#### 4.13. References

- (1) Hinkson, I. V.; Madej, B.; Stahlberg, E. A., Accelerating Therapeutics for Opportunities in Medicine: A Paradigm Shift in Drug Discovery. *Front. Pharmacol.* **2020**, *11*, 770-777.
- (2) Patani, G. A.; LaVoie, E. J., Bioisosterism: A Rational Approach in Drug Design. *Chem. Rev.* **1996**, *96* (8), 3147-3176.
- (3) Di Martino, R. M. C.; Maxwell, B. D.; Pirali, T., Deuterium in drug discovery: progress, opportunities and challenges. *Nat. Rev. Drug Discov.* **2023**, *22* (7), 562-584.
- (4) Gant, T. G., Using deuterium in drug discovery: leaving the label in the drug. *J. Med. Chem.* **2014**, *57* (9), 3595-611.
- (5) Dean, M.; Sung, V. W., Review of deutetrabenazine: a novel treatment for chorea associated with Huntington's disease. *Drug Des. Devel. Ther.* **2018**, *12*, 313-319.
- (6) Zhu, Y. Q.; Zhou, J.; Jiao, B., Deuterated Clopidogrel Analogues as a New Generation of Antiplatelet Agents. *ACS Med. Chem. Lett.* **2013**, *4* (3), 349-352.
- (7) Vitaku, E.; Smith, D. T.; Njardarson, J. T., Analysis of the structural diversity, substitution patterns, and frequency of nitrogen heterocycles among U.S. FDA approved pharmaceuticals. *J. Med. Chem.* **2014**, *57* (24), 10257-74.
- (8) Li, W.; Rabeah, J.; Bourriquen, F.; Yang, D.; Kreyenschulte, C.; Rockstroh, N.; Lund, H.; Bartling, S.; Surkus, A.-E.; Junge, K.; Brückner, A.; Lei, A.; Beller, M., Scalable and selective deuteration of (hetero)arenes. *Nat. Chem.* **2022**, *14* (3), 334-341.
- (9) Yu, R. P.; Hesk, D.; Rivera, N.; Pelczer, I.; Chirik, P. J., Iron-catalysed tritiation of pharmaceuticals. *Nature* **2016**, *529* (7585), 195-9.
- (10) Ellames, G. J.; Gibson, J. S.; Herbert, J. M.; McNeill, A. H., The scope and limitations of deuteration mediated by Crabtree's catalyst. *Tetrahedron* **2001**, *57* (46), 9487-9497.
- (11) Eguillor, B.; Esteruelas, M. A.; García-Raboso, J.; Oliván, M.; Oñate, E., Stoichiometric and Catalytic Deuteration of Pyridine and Methylpyridines by H/D Exchange with Benzene- $d_6$  Promoted by an Unsaturated Osmium Tetrahydride Species. *Organometallics* **2009**, *28* (13), 3700-3709.
- (12) Rubottom, G. M.; Evain, E. J., Deuteration of pyridine derivatives: A very mild procedure. *Tetrahedron* **1990**, *46* (15), 5055-5064.
- (13) Grainger, R.; Nikmal, A.; Cornella, J.; Larrosa, I., Selective deuteration of (hetero)aromatic compounds *via* deuterio-decarboxylation of carboxylic acids. *Org. Biomol. Chem.* **2012**, *10* (16), 3172-4.
- (14) Li, Y.; Zheng, C.; Jiang, Z. J.; Tang, J.; Tang, B.; Gao, Z., Potassium tert-butoxide promoted

- regioselective deuteration of pyridines. *Chem. Commun. (Camb.)* **2022**, 58 (21), 3497-3500.
- (15) Koniarczyk, J. L.; Hesk, D.; Overgard, A.; Davies, I. W.; McNally, A., A General Strategy for Site-Selective Incorporation of Deuterium and Tritium into Pyridines, Diazines, and Pharmaceuticals. *J. Am. Chem. Soc.* **2018**, 140 (6), 1990-1993.
- (16) Hesk, D.; Koharski, D.; McNamara, P.; Royster, P.; Saluja, S.; Truong, V.; Voronin, K., Synthesis of  $^3\text{H}$ ,  $^{13}\text{C}_2$ ,  $^2\text{H}_4$   $^{14}\text{C}$ -SCH 430765 and  $^{35}\text{S}$ -SCH 500946, potent and selective inhibitors of the NPY<sub>5</sub> receptor. *J. Labelled Comp. Radiopharm.* **2018**, 61 (7), 533-539.
- (17) Lambert, J. B.; Keske, R. G., The Conformational Preference of the Nonbonding Electron Pair in Piperidine. *J. Am. Chem. Soc.* **1966**, 88 (3), 620-622.
- (18) Chatterjee, B.; Krishnakumar, V.; Gunanathan, C., Selective  $\alpha$ -Deuteration of Amines and Amino Acids Using D<sub>2</sub>O. *Org. Lett.* **2016**, 18 (22), 5892-5895.
- (19) Pieters, G.; Taglang, C.; Bonnefille, E.; Gutmann, T.; Puente, C. Berthet, J.-C.; Dugave, C.; Chaudret, B.; Rousseau, B., Regioselective and Stereospecific Deuteration of Bioactive Aza Compounds by the Use of Ruthenium Nanoparticles. *Angew. Chem. Int. Ed.* **2014**, 53 (1), 230-234.
- (20) Wagener, T.; Luckemeier, L.; Daniliuc, C. G.; Glorius, F., Interrupted Pyridine Hydrogenation: Asymmetric Synthesis of delta-Lactams. *Angew. Chem. Int. Ed. Engl.* **2021**, 60 (12), 6425-6429.
- (21) Nairoukh, Z.; Wollenburg, M.; Schlepfforst, C.; Bergander, K.; Glorius, F., The formation of all-*cis*-(multi)fluorinated piperidines by a dearomatization–hydrogenation process. *Nat. Chem.* **2019**, 11 (3), 264-270.
- (22) Derdau, V., Deuterated ammonium formate as deuterium source in a mild catalytic deuterium transfer reaction of pyridines, pyrazines and isoquinolines. *Tetrahedron Lett.* **2004**, 45 (48), 8889-8893.
- (23) Knaus, E. E.; Redda, K., The sodium borohydride reduction of N-sulfonylpyridinium salts. Synthesis of N-sulfonyl-1,4-(1,2-) dihydropyridines. *Can. J. Chem.* **1977**, 55 (10), 1788-1791.
- (24) Lyle, R. E.; Boyce, C. B., Sodium-Borohydride Reduction of Sterically Hindered Pyridinium Salts. *J. Org. Chem.* **1974**, 39 (25), 3708-3711.
- (25) Liberatore, F.; Casini, A.; Carelli, V.; Arnone, A.; Mondelli, R., Borohydride reduction of pyridinium salts. V. Thermal dimerization of 1,6-dihydro-1-methylpyridine-2-carbonitrile. *J. Org. Chem.* **2002**, 40 (5), 559-563.
- (26) Heusler, A.; Fliege, J.; Wagener, T.; Glorius, F., Substituted Dihydropyridine Synthesis by Dearomatization of Pyridines. *Angew. Chem. Int. Ed. Engl.* **2021**, 60 (25), 13793-13797.
- (27) Yang, H.; Zhang, L.; Zhou, F.-Y.; Jiao, L., An umpolung approach to the hydroboration of pyridines: a novel and efficient synthesis of N-H 1,4-dihydropyridines. *Chem. Sci.* **2020**, 11 (3), 742-747.
- (28) Smith, J. A.; Wilson, K. B.; Sonstrom, R. E.; Kelleher, P. J.; Welch, K. D.; Pert, E. K.; Westendorff, K. S.; Dickie, D. A.; Wang, X.; Pate, B. H.; Harman, W. D., Preparation of cyclohexene isotopologues and stereoisotopomers from benzene. *Nature* **2020**, 581 (7808), 288-293.
- (29) Dabbs, J. D.; Ericson, M. N.; Wilde, J. H.; Lombardo, R. F.; Ashcraft, E. C.; Dickie, D. A.; Harman, W. D., The Tungsten-Promoted Synthesis of Piperidyl-Modified *erythro*-Methylphenidate Derivatives. *ACS Cent. Sci.* **2023**, 9 (9), 1775-1783.
- (30) Harrison, D. P.; Nichols-Nieler, A. C.; Zottig, V. E.; Strausberg, L.; Salomon, R. J.;



- Trindle, C. O.; Sabat, M.; Gunnoe, T. B.; Iovan, D. A.; Myers, W. H.; Harman, W. D., Hyperdistorted Tungsten Allyl Complexes and Their Stereoselective Deprotonation to Form Dihapto-Coordinated Dienes. *Organometallics* **2011**, *30* (9), 2587-2597.
- (31) Harrison, D. P.; Sabat, M.; Myers, W. H.; Harman, W. D., Polarization of the Pyridine Ring: Highly Functionalized Piperidines from Tungsten–Pyridine Complex. *J. Am. Chem. Soc.* **2010**, *132* (48), 17282-17295.
- (32) Hegedus, L. S.; Holden, M. S., The chemistry of N-sulfonyl enamines. *J. Org. Chem.* **1986**, *51* (8), 1171-1174.
- (33) Wilde, J. H.; Dickie, D. A.; Harman, W. D., A Highly Divergent Synthesis of 3-Aminotetrahydropyridines. *J. Org. Chem.* **2020**, *85* (12), 8245-8252.
- (34) Ramachandran, P. V.; Kulkarni, A. S.; Zhao, Y.; Mei, J., Amine-boranes bearing borane-incompatible functionalities: application to selective amine protection and surface functionalization. *Chem. Commun. (Camb.)* **2016**, *52* (80), 11885-11888.
- (35) Harrison, D. P.; Sabat, M.; Myers, W. H.; Harman, W. D., Polarization of the pyridine ring: highly functionalized piperidines from tungsten-pyridine complex. *J. Am. Chem. Soc.* **2010**, *132* (48), 17282-95.
- (36) Sonstrom, R. E.; Vang, Z. P.; Scolati, H. N.; Neill, J. L.; Pate, B. H.; Clark, J. R., Rapid Enantiomeric Excess Measurements of Enantioisotopomers by Molecular Rotational Resonance Spectroscopy. *Org. Process Res. Dev.* **2023**, *27* (7), 1185-1197.
- (37) Carballo, R. M.; Valdomir, G.; Purino, M.; Martin, V. S.; Padron, J. I., Broadening the Synthetic Scope of the Iron(III)-Catalyzed Aza-Prins Cyclization. *Eur. J. Org. Chem.* **2010**, *2010* (12), 2304-2313.
- (38) Groll, B.; Schnurch, M.; Mihovilovic, M. D., Selective Ru(0)-catalyzed deuteration of electron-rich and electron-poor nitrogen-containing heterocycles. *J. Org. Chem.* **2012**, *77* (9), 4432-7.
- (39) Yang, H. F.; Zarate, C.; Palmer, W. N.; Rivera, N.; Hesk, D.; Chirik, P. J., Site-Selective Nickel-Catalyzed Hydrogen Isotope Exchange in N-Heterocycles and Its Application to the Tritiation of Pharmaceuticals. *ACS Catal.* **2018**, *8* (11), 10210-10218.
- (40) Zarate, C.; Yang, H.; Bezdek, M. J.; Hesk, D.; Chirik, P. J., Ni(I)-X Complexes Bearing a Bulky  $\alpha$ -Diimine Ligand: Synthesis, Structure, and Superior Catalytic Performance in the Hydrogen Isotope Exchange in Pharmaceuticals. *J. Am. Chem. Soc.* **2019**, *141* (12), 5034-5044.
- (41) Norcott, P.; Burns, M. J.; Rayner, P. J.; Mewis, R. E.; Duckett, S. B., Using  $^2\text{H}$  labelling to improve the NMR detectability of pyridine and its derivatives by SABRE. *Magn. Reson. Chem.* **2018**, *56* (7), 663-671.
- (42) Pavlik, J. W.; Laohhasurayotin, S., Synthesis and spectroscopic properties of isomeric trideuterio- and tetradeuterio pyridines. *J. Heterocycl. Chem.* **2007**, *44* (6), 1485-1492.

## Chapter 5

Pyridine Nitrogen Transplant *via* a Tungsten-Promoted Zincke-like  
Ring Opening/Ring Closing Cascade of 2-Aminodihydropyridines

## 5.1. Introduction: Accessing *N*-Alkyl Piperidines

While chapter 1 already established the ubiquity of the piperidine scaffold in small-molecule drugs (*vide supra*),<sup>1</sup> specific attention should be appropriated to the prevalence of the *N*-alkylated piperidine scaffolds in drugs. While some piperidine containing drugs bear withdrawing groups, the vast majority have an unfunctionalized or alkylated nitrogen.<sup>2</sup> These include commonly used drugs such as donepezil, ketotifen, and mepivacaine.

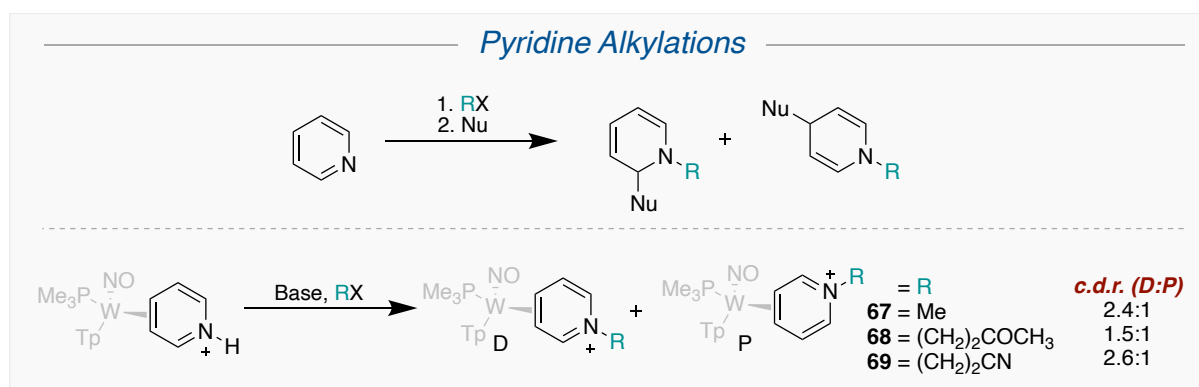


**Figure 5.1:** Conventional *N*-alkylations of free and [W]-bound pyridines.

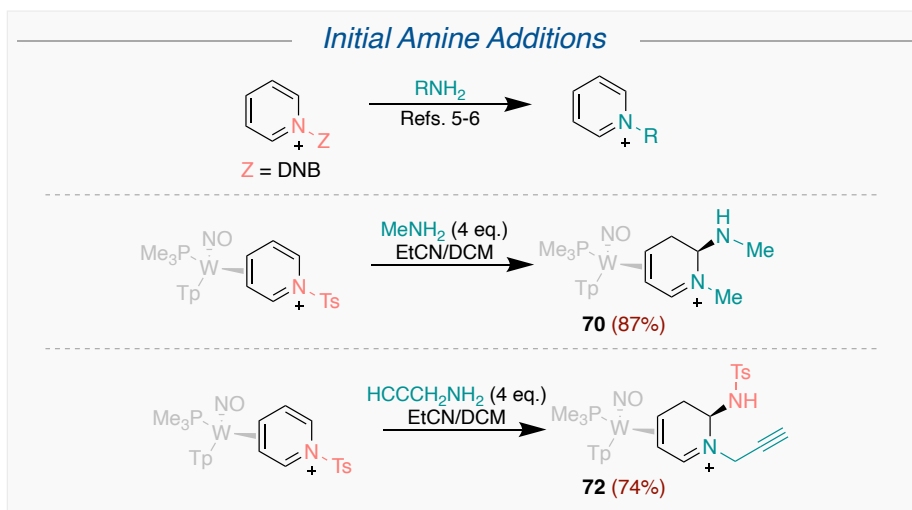
The prevalence of these *N*-alkylated piperidines in drugs necessitates methods of selectively generating drug candidate libraries that feature them. Uncoordinated pyridines readily undergo *N*-alkylations to and undergo subsequent nucleophilic additions to form functionalized DHPs (*vide supra*; Figure 5.1); however, this methodology is often plagued with regio- and enantioselectivity issues, DHP rearomatization, and difficulty in functionalizing the remaining alkenes.<sup>3</sup> While *N*-H pyridinium  $\eta^2$ -bound to {WTP(NO)(PMe<sub>3</sub>)} ([W]) (compound **3**) can undergo alkylation *via* MeOTf, MVK, and acrylonitrile to form **67**, **68**, and **69** respectively.<sup>4</sup> However, each of these [W]-pyridinium complexes are hindered from selective downstream reactivity due poor *c.d.r.* enrichment. It stands to reason that these compounds demonstrate the chemical ability to incorporate alkyl groups at the [W]-bound pyridine nitrogen, but the lack of withdrawing group generally precludes a high degree of *c.d.r.* enrichment. Therefore, an

advancement that selectively generates [W]-bound *N*-alkylated pyridiniums bound would further unlock druglike chemical space accessible *via* tungsten dearomatization, which could then in turn be utilized as a tool for rapidly generating piperidyl modified analogues of *N*-alkyl drugs.

## 5.2. Zincke Ring Opening/Ring Closing Cascade

In chapter 2, **5D** demonstrated a Zincke-like ring-opening mechanism wherein [W]-DHPs bearing carbon substituents at the C2 position undergo a ring-opening cascade to form terminally substituted  $\alpha,\gamma$ -dienylimine complexes (**16-20**) (*vide supra*). This was particularly novel due to the Zincke reaction classically proceeding in the presence of  $\pi$ -donor nucleophiles.<sup>5-6</sup> However, the analogous ring-opening reported by Zincke occurred with secondary amines adding as nucleophiles. On the other hand, primary amines added to the same pyridinium salt resulted in a pyridinium salts containing an R group on the heterocycle nitrogen equivalent to the primary amine substituent (Figure 5.2). These pyridiniums were purportedly generated *via* a ring-opening/ring-closing cascade that transplanted the heterocyclic nitrogen with that of the primary amine. To probe how if a similar ring-opening would occur in the presence of  $\pi$ -donor nucleophiles, amines were added to **5D**. It was previously observed that these imines readily would hydrolyze to the aldehyde in the presence of water; therefore, it was postulated an amine addition to C2 could promote an intramolecular cyclization, although the exact nature of this was difficult to predict.

When **5D** was stirred with methylamine (4 eq.) at room temperature, it readily precipitated in stirring ether and was determined to cleanly generate a single complex. This compound was characterized in the <sup>1</sup>H NMR by a downfield iminium doublet, what appeared to be geminal protons, two methyl singlets, and a lack of tosyl peaks. This indicated that somehow, the tosyl group disappeared, methylamine added *twice*, a protonation likely occurred to form the methylene



group, and the iminium remained intact. 2D NMR experiments determined the identity of this compound to be a  $[W]-\eta^2-(N\text{-methyl-6-methylamino-5,6-dihydropyridin-1-ium})$  complex (**70**) (Figure 5.2). This complex assignment was further supported by HRMS data. Critically, **70** was generated in the absence of a detectable amount of its coordination diastereomer; however, it was observed that after 4 hours, a solution of **70** decomposed to a 2:1 solution of **67D** and **67P**. Ultimately, this reaction indicated that **5D** undergoes a nitrogen transplant as the pyridinium was somehow opened and the nitrogen within the heterocycle bearing the tosyl group was replaced by the alkylated nitrogen, and tosylamine was eventually expelled for the incorporation of another equivalent of methylamine.

After generating **70**, the generality of this reaction was probed by investigating another primary amine. Propargylamine, however, when introduced to **5D** resulted in **72** where the DHPium nitrogen within the ring bore the propargyl group, but the tosyl group was still attached at C6, indicating a monoamination occurred (Figure 5.2). Why this specific case did not undergo diamination like methylamine is likely due to time as this reaction only stirred for less than a minute whereas **72** stirred for ten minutes. This indicated that mono- and deaminated products

could be obtained after reaction optimization and also suggested that C6 amination process is not crucial in closing the DHPium ring.

Since a methylamine addition resulted in an *N*-methyl dihydropyridinium (DHPium), it was postulated that secondary amines would undergo ring-opening, but not undergo recyclization, which could impart mechanistic insight into this reaction. To this end, **5D** was stirred at -20 °C in the presence of morpholine (ambient temperatures resulted in the formation of numerous products). A mixture of two products with twinned <sup>1</sup>H NMR features resulted; and a combination of 2D NMR spectroscopy and HRMS suggest a ring-opened dienylyl imine with morpholinium on one terminus distal to the PMe<sub>3</sub> ligand and an allylic terminal tosylamine moiety (**71** - Figure 5.3A). Given the similarity between the peaks in the <sup>1</sup>H NMR between the major and the minor

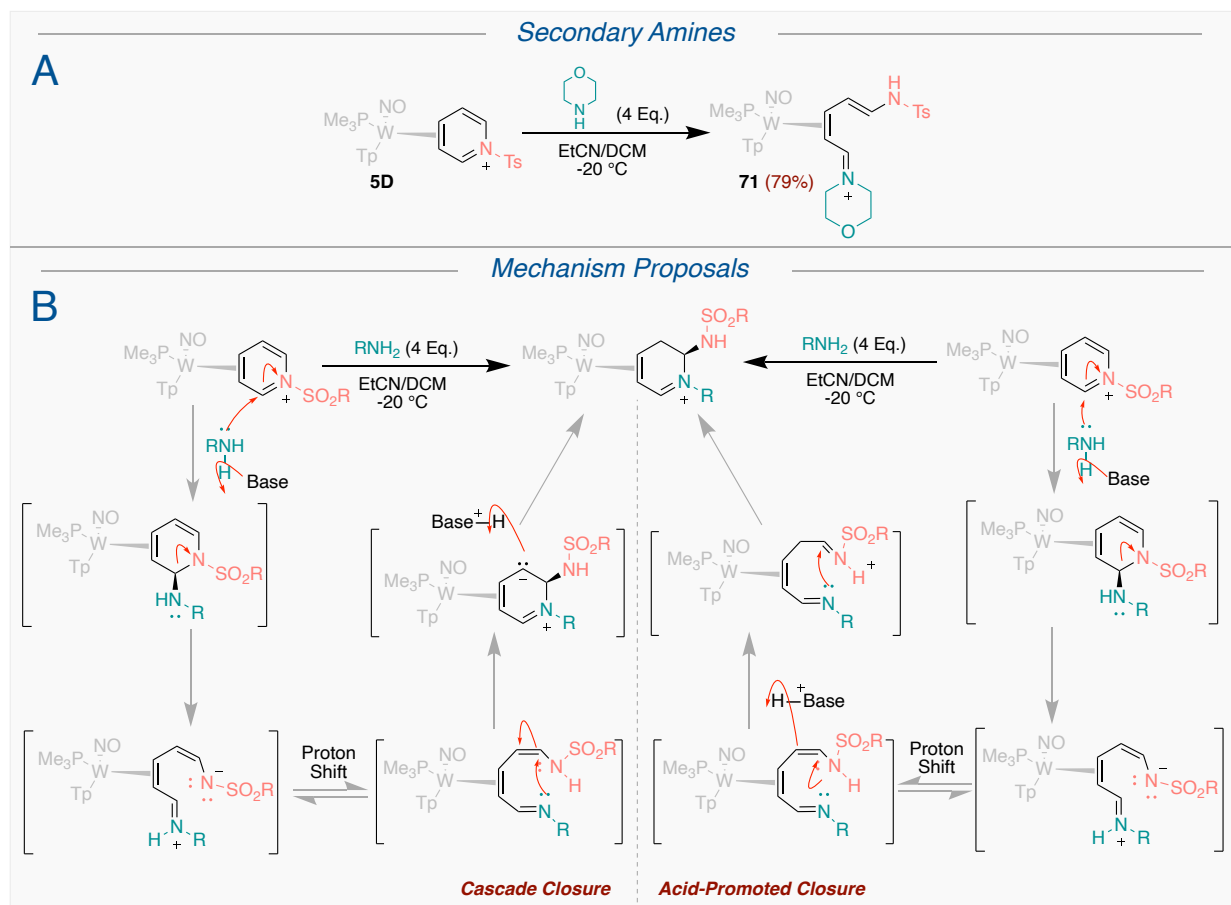


**Figure 5.3:** (A) Addition of morpholine failed to reclose the ring. (B) Mechanism proposals for the ring opening/ring closing observed with primary amines.

compounds, it is postulated that these are simply E/Z isomers of each other, albeit with uncertainty about specifically which alkene this could be.

Mechanistically, it was postulated that primary amines attack **5D** at C2 like previous nucleophiles and initiate a ring opening; however, this ring opening appears to resemble the pathway observed with **4D** in the presence of  $\pi$ -donor nucleophiles that results in [W] establishing conjugation with the added nucleophile instead of with a sulfonyl-imine observed in chapter 2 (Figure 5.3B).<sup>7</sup> At this point, two possible ring-closure pathways can be rationalized. The first pathway is the imine distal to the  $\text{PMe}_3$  initiates a ring closure to reestablish a [W]-conjugated iminium, which, upon closing, promotes protonation at C5 by a weak acid due to an accumulation of electron-density. The second is where residual acid first protonates the alkene at C5, thus briefly generating a sulfoniminium that undergoes a cyclization with the distal imine. While neither can be conclusively ruled out, it is unlikely that the residually generated acid in the reaction would be strong enough to protonate C5 without a large accumulation of electron density.

### 5.3. Nitrogen Substitutions

Next, while seeking to establish a wider scope of compatible primary amines for this reaction, we also wished to probe if **33D** would undergo this reaction as well. To this end, allylamine, benzylamine, furfurylamine, piperonylamine, and tryptamine were all reacted with **33D** to form a scope of *N*-alkylated 6-mesyl DHPium complexes (**72-77**) (Figure 5.4). Each of these reactions were conducted with 4 equivalents of amine in a DCM/propionitrile solvent mixture and at temperatures ranging from ambient temperatures to  $-40\text{ }^\circ\text{C}$ . Several examples, such as piperonylamine and tryptamine, were isolated as mono- and deamination mixtures at ambient temperatures and required cold temperatures to cleanly generate the monoamination products. It

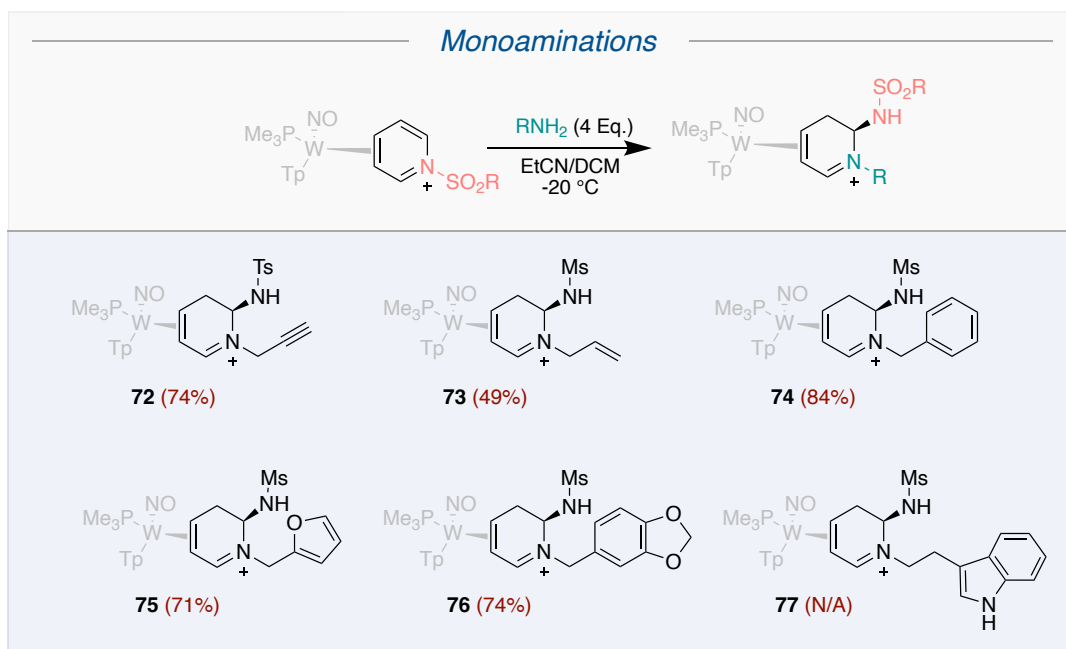


**Figure 5.4:** Scope of monoaminations products generated.

is postulated that simply allowing longer reactions times in these cases would have rendered cleaner diamination products. Although secondary aliphatic amines and hydrazines both proved incapable of undergoing this reaction scheme, efforts are currently ongoing to determine if aryl amines and amides are compatible with this ring-opening ring-closing process.

#### 5.4. Bicyclics

Next, terminal diaminoalkanes were investigated given the success other [W] projects have had in generating polycyclic compounds by closing both amino termini on the dearomatized ligand. Ethylenediamine, the first diamine investigated, was stirred with **5D** and resulted in a single complex generated *via*  $^1\text{H}$  NMR. Other notable features in the  $^1\text{H}$  NMR included a lack of tosyl peaks (indicating it had left), enough protons for only 1 equivalent of diamine addition, and the presence of the downfield iminium proton. These features indicated that in addition to undergoing the established pyridine nitrogen transplant, the other amine terminus then closed on the adjacent



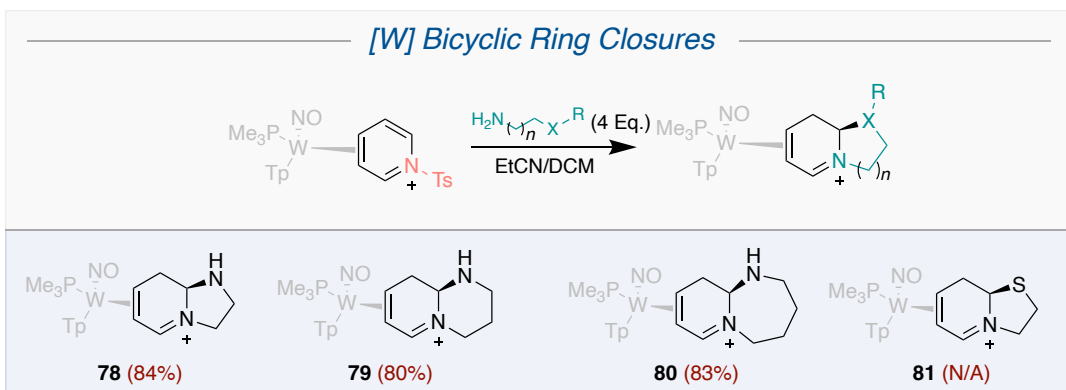


**Figure 5.5:** Scope of bicyclic DHPium complexes generated.

C6, forming a 6/5 bicyclic complex (**78** - Figure 5.5). This hypothesis was then confirmed *via* SC-XRD (Figure 5.6). A range of terminal diamines including diaminopropane and diaminobutane were then added to **5D** and subsequently closed to form **79** and **80** respectively, the structure of **79** which was also confirmed *via* SC-XRD (Figure 5.6). It is worth noting that the upper limit of the ring size fused to the DHPium ring has not been established. Lastly, cysteamine, after stirring with **5D** in the presence of methanol and basic alumina, also successfully formed a bicyclic complex **81**, which indicates heteroatoms other than nitrogen can also close at C6 and represents a huge potential point of future scope expansion.

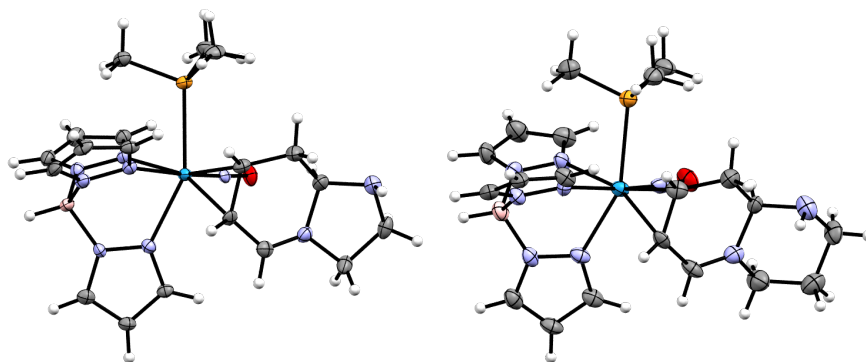


**Figure 5.6:** SC-XRD determined structures of **78** (left) and **79** (right).

## 5.5. Iminium Functionalizations

A very brief study was conducted on **78** to functionalize the iminium, which would theoretically generate substituted bicyclic aminal complexes. NMR scale experiments conducted in  $d_4$ -MeOH showed that **78** is unreactive with NaCN and simply remains as starting material. On

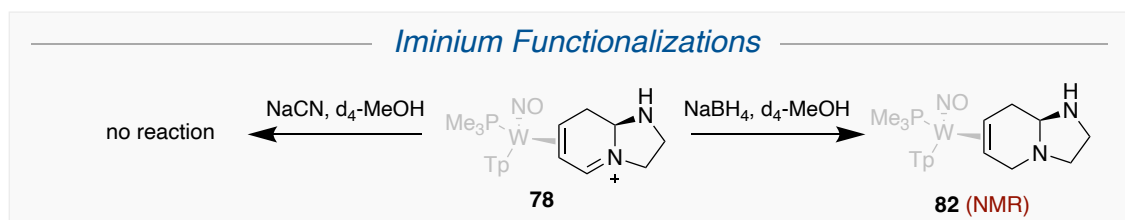


**Figure 5.7:** NMR scale attempts to functionalization the iminium of **78**.

the other hand, NaBH<sub>4</sub> appears to reduce the iminium, which is noted by a complete disappearance of the downfield iminium doublet and general shift upfield of the Tp and bicyclic proton residues, thus indicating that the complex is no longer charged. However, conclusive 2D NMR and/or microanalysis to support claim are forthcoming. Iminium functionalizations remain a highly-underdeveloped part of this project.

## 5.6. Discussion

While this fledgling study still requires a great deal future work to round-out the full potential of this system (see chapter 6 for future directions of this work), the nature of the compounds isolated thus far underscore the high degree of potential of this system. Developing a highly modular protocol for selectively accessing *N*-alkylated DHP complexes unlocks a vast amount of previously inaccessible piperidine-containing chemical space. In addition to expanding the established druglike chemical space accessible by [W]-mediated dearomatization, the highly alkaloid-like bicyclic compounds represent hitherto unexplored chemical space in general. Alkaloids, which contain nitrogen and are often heterocycles, are one of the largest classes of natural products and include common treatments such as atropine, quinidine, and taxol.<sup>8</sup> Accessing

novel alkaloid cores represents a significant advancement for the discovery process of drug development.

## 5.7. References

- (1) Vitaku, E.; Smith, D. T.; Njardarson, J. T. Analysis of the structural diversity, substitution patterns, and frequency of nitrogen heterocycles among U.S. FDA approved pharmaceuticals. *J. Med. Chem.* **2014**, *57* (24), 10257-10274.
- (2) Schnider, P.; Dolente, C.; Stalder, H.; Martin, R. E.; Reinmüller, V.; Marty, R.; Gramberg, C. W.; Wagner, B.; Fischer, H.; Alker, A. M.; Müller, K. Modulation of Pharmacologically Relevant Properties of Piperidine Derivatives by Functional Groups in an Equatorial or Axial  $\beta$ -position to the Amino Group. *ChemBioChem* **2019**, *21* (1-2), 212-234.
- (3) Bull, J. A.; Mousseau, J. J.; Pelletier, G.; Charette, A. B. Synthesis of pyridine and dihydropyridine derivatives by regio- and stereoselective addition to N-activated pyridines. *American Chemical Society* **2012**, *112*, 2642-2713.
- (4) Harrison, D. P.; Zottig, V. E.; Kosturko, G. W.; Welch, K. D.; Sabat, M.; Myers, W. H.; Harman, W. D. Stereo- and Regioselective Nucleophilic Addition to Dihapto-Coordinated Pyridine Complexes. *Organometallics* **2009**, *28* (19), 5682-5690.
- (5) Zincke, T.; Heuser, G.; Möller, W. I. Ueber Dinitrophenylpyridiniumchlorid und dessen Umwandlungsproducte. *Justus Liebig's Annalen der Chemie* **1904**, *333* (2-3), 296-345.
- (6) Zincke, T.; Würker, W. Ueber Dinitrophenylpyridiniumchlorid und dessen Umwandlungsproducte (2. Mittheilung.). Ueber Dinitrophenylpyridiniumchlorid und dessen Umwandlungsproducte. *Justus Liebig's Annalen der Chemie* **1904**, *338* (1), 107-141.
- (7) Harrison, D. P.; Kosturko, G. W.; Ramdeen, V. M.; Nielander, A. C.; Payne, S. J.; Sabat, M.; Myers, W. H.; Harman, W. D. Tungsten-Promoted Pyridine Ring Scission: The Selective Formation of  $\eta^2$ -Cyanine and  $\eta^2$ -Merocyanine Complexes and Their Derivatives. *Organometallics* **2010**, *29* (8), 1909-1915.
- (8) Heinrich, M.; Mah, J.; Amirkia, V. Alkaloids Used as Medicines: Structural Phytochemistry Meets Biodiversity—An Update and Forward Look. *Molecules* **2021**, *26* (7), 1836-1854.

# Chapter 6

## Concluding Remarks

## 6.1. General Comments

The prevalence of highly functionalized alkaloids in medicinal chemistry accentuates the need for robust syntheses capable of accessing them reliably. The chemistry demonstrated by [W]- $\eta^2$ -(*N*-acetyl) pyridinium (**4D**) for synthesizing highly functionalized tetrahydropyridines<sup>1-3</sup> and isoquinuclidines<sup>4</sup> is a powerful tool for accessing novel druglike chemical space. The goal of this work was to develop a second generation [W]-pyridinium system that both prevented observable rotational isomers and retained the chemistry of the first-generation system **4D** and explore its novel synthetic capability. These goals were accomplished by the work described in Chapters 2-5 (Figure 6.1).

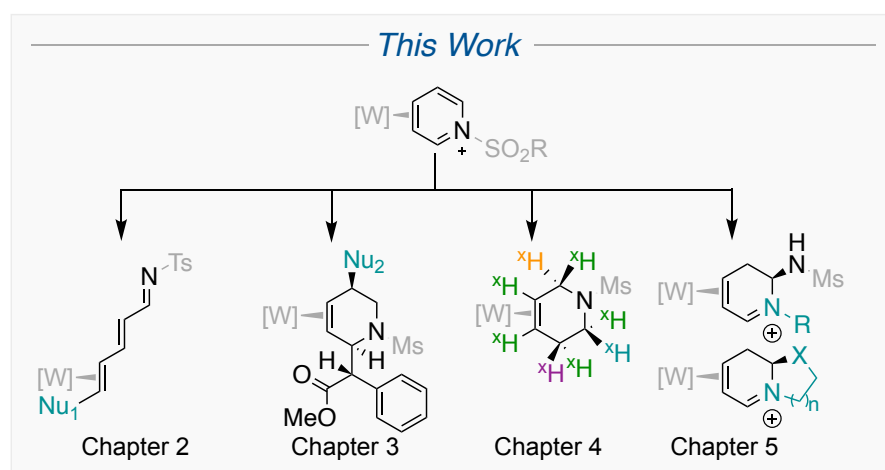


**Figure 6.1:** Summary of the research conducted in this work.

## 6.2. Summary of Chapter 2

The work of chapter 2 established the foundation for the future work contained herein. It demonstrated that [W]- $\eta^2$ -pyridine can undergo nitrogen protecting with sulfonyl protecting groups. The conjugate acid form can then undergo a sequence of nucleophile-electrophile-nucleophile additions to form [W]-TTHPs free of rotational isomers that were present with the corresponding amide system. These principles were the foundation of work contained in chapters

3 & 4. Furthermore, a novel reactivity pathway was determined that showed a Zincke-like ring-opening with carbon-nucleophiles to  $[W]-\eta^2$ -DHP complexes.

### 6.3. Novel Piperidine-Containing Drug Analogues

Chapter 3 describes the application of  $[W]$ -pyridine dearomatization in the synthesis of piperidine-substituted analogues of methylphenidate. The novelty stemming from this work rests upon the widening of the scope of second nucleophiles compatible with pyridine (now including amides, imides, phthalimides, thiols, and Grignards) as well as the novel application of  $[W]$ -promoted dearomatization of pyridine for accessing drug scaffolds. The ubiquity of piperidine in drugs suggests more drug libraries with THP substituted analogs could be assembled. One such drug would be troxipide, which could be accessed by adding an appropriate amide as a second nucleophile  $\beta$  to the pyridine nitrogen (Figure 6.2). A wide range of nucleophiles were incorporated at the iminium in chapter 2, including cyanide, allyl, propargyl, benzyl, and esters. The wider the nucleophile range, the larger the library of troxipide analogues can be assembled. While troxipide represents a promising scaffold to pursue, furthermore developments, such  $\gamma$ -amination, would drastically increase the amount of current accessible drugs to derivatize.

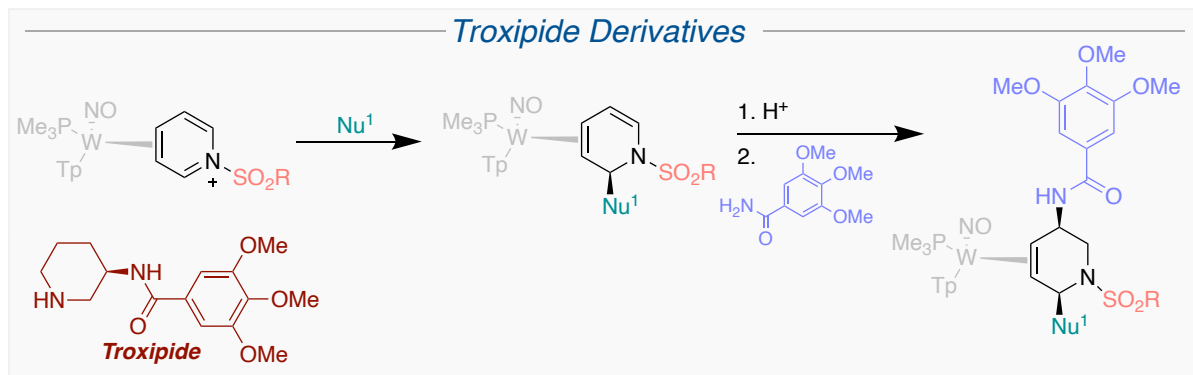


**Figure 6.2:** Adding range of nucleophiles to the iminium established in Chapter 2 and following them up with an amide addition  $\beta$  to the pyridine nitrogen results in  $\alpha$ -substituted troxified derivatives.

## 6.4. Novel Deuterated THPs

A variety of deuterated THPs and MPH THPs were assembled in Chapter 4. As was mentioned in the chapter, a large variety of novel isotope substitution patterns can be accessed by coordinating alternate isotopologues/-mers of pyridine borane that can be accessed *via* alternate pyridine deuteration methods (Figure 6.3A). Additionally, [W]-DHP protonations/deuterations

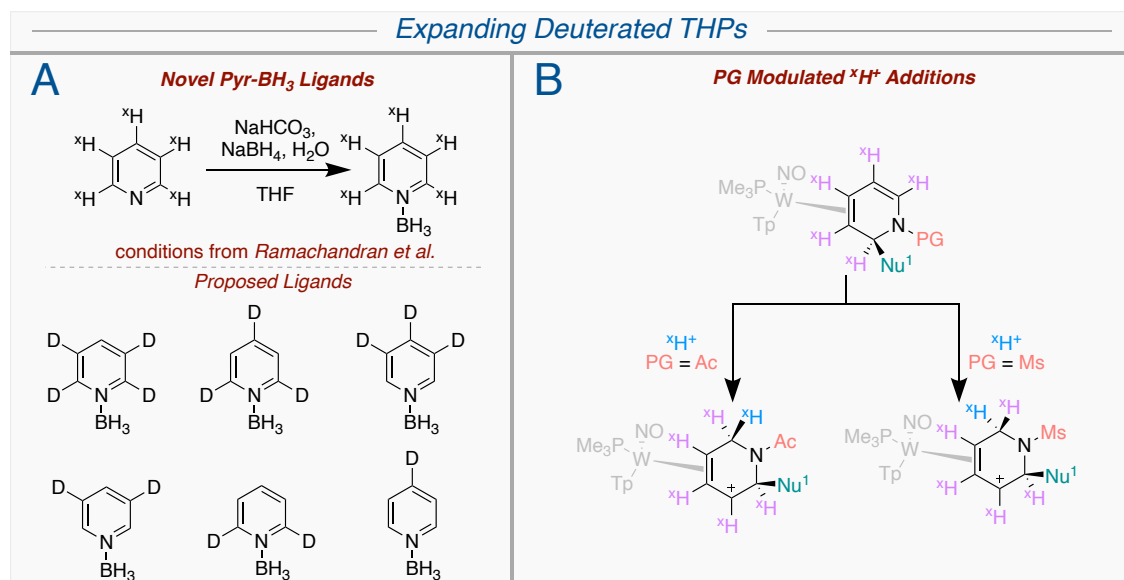


**Figure 6.3:** (A) Alternate isotopologues/-mers of pyridine, after undergoing the Ramachandran BH<sub>3</sub> addition, could be coordinated to [W] to access novel deuterated THPs. (B) <sup>x</sup>H<sup>+</sup> additions occur at C6 *syn* to the metal with a mesyl nitrogen protecting group, but they occur *anti* with an acetyl protecting group. Deducing the precise cause of this stereodivergence could access even more deuterated THP substitution patterns.

added at C6 *syn* to the metal for the study conducted; however, a previous work observed D<sup>+</sup> addition *anti* to the metal (Figure 6.3B).<sup>1</sup> Although the precise nature of this stereodivergence is unknown, it suggests that the stereochemistry of this addition can be modulated depending on the protecting group. Uncovering this could allow for the selective synthesis of even more deuterated THP substitution patterns.

## 6.5. Functionalized Linear Amines

This study also uncovered an unprecedented ring-opening of the [W]-bound THP, thus forming a [W]-η<sup>2</sup>-linear amine complex. Although a brief study was conducted to cleanly generate

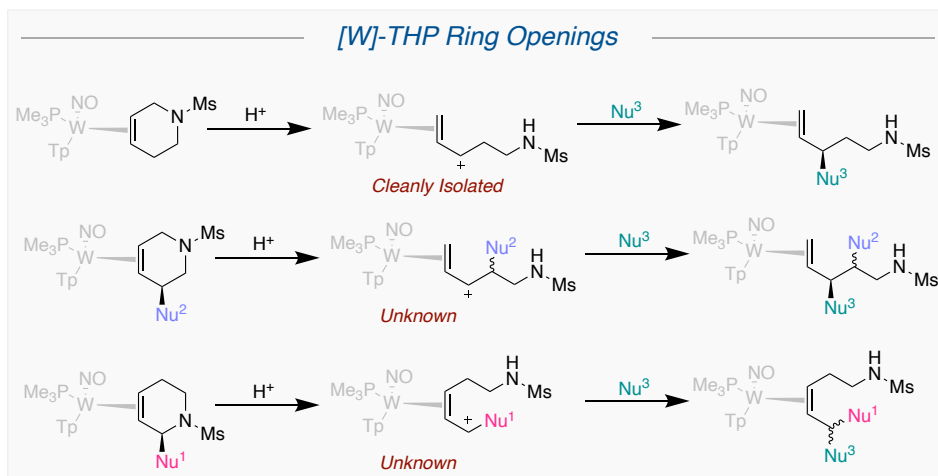


**Figure 6.4:** The previously isolated ring opened allyl is an optimal precursor to generating functionalized linear amine compounds.

functionalized linear amines, a more in-depth study is warranted as clean isolation of the ring-opened allyl complex would allow for modular syntheses of functionalized linear amines. While hydride has cleanly been incorporated into this ring-opened allyl, a deeper study could discover the scope of compatible nucleophile additions, determine if  $\alpha$ - and  $\beta$ -substituted THPs undergo a similar ring opening, and oxidatively liberate generated organics from the metal (Figure 6.4).

## 6.6. Expanding the Ring Opening/Closing Chemistry

Lastly, large opportunities for future innovation remain for the work described in chapter 5, which concentrates on the Zincke-like ring-opening/closing cascade for hydroaminating [W]-bound *N*-alkyl pyridiniums. Although currently limited to primary aliphatic amines, efforts to expand this to include aryl amines and chiral amino acids could drastically expand the scope of druglike compounds generated *via* this method. Furthermore, the scope of multicyclic alkaloids generated would sharply increase by expanding the scope of primary amine pendant functional groups closing on the  $\alpha$ -DHP carbon. Demonstrating ring closures with pendant thiols, alcohols,



and amides of varying ring sizes would multiply the number drug-like multicyclic compounds accessible *via* this approach.

Although hydride has successfully added to these electron-rich iminiums, further developing out this methodology would incorporate another stereocenter into the demetallated organics (Figure 6.5A). Triethylenetetramine, if successfully cyclized with one equivalent of **5D**, could be reacted with another equivalent of **5D** to form a bicyclic dimer (Figure 6.5B). Furthermore, the electronic similarity alkylated DHPs share with an  $\eta^2$ -*N,N*-dimethylanilinium complex suggests that the DHP, like the anilinium, can undergo a Friedel-Crafts arylation *via* a [W]-supported dication generated *via* a strong acid. In this case, strong acid could promote leaving of the sulfonamide leaving group, thus generating the [W]-stabilized dicationic intermediate capable of arylation (Figure 6.5C). While established in this work, the scope of diaminations can be greatly expanded, and amide ring closures can be explored (Figure 6.5D). Lastly, successful

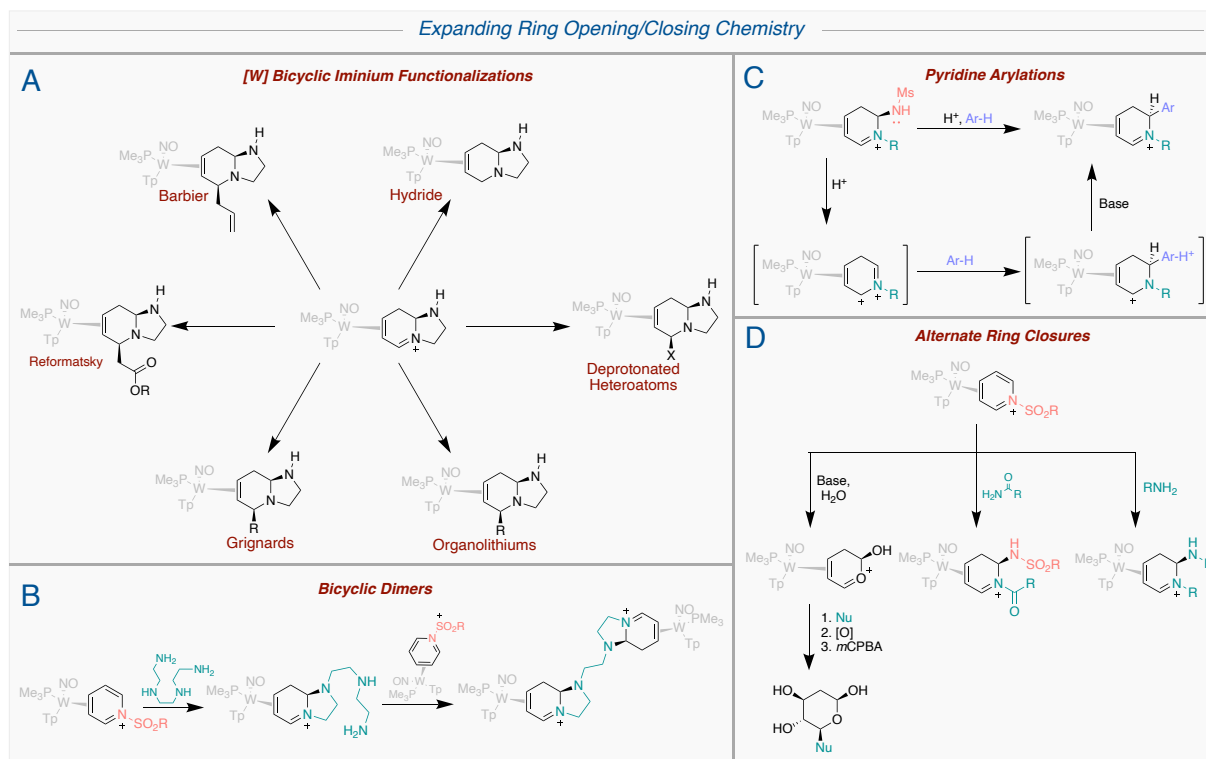


**Figure 6.5:** (A) Increase scope of iminium additions. (B) Access bicyclic dimers *via* tetradentate amines. (C) Attempt acid-promoted pyridine arylations. (D) Attempt ring closures with oxygen, amides, and diaminations.

heteroatom transmutation could access a pyrylium-like complex for generating functionalized sugars (Figure 6.5D).

This comprehensive work stands on the shoulders of many previous works and is only a small thread in the tapestry of research stemming from [W]-mediated dearomatization. Nevertheless, it successfully broadens the scope of chemical structures accessible via this method and applies the technique to several medicinally useful methods. Even still, there remains much fertile ground for discovery with tungsten-promoted dearomatization of pyridines, discoveries which could greatly contribute to the ceaseless efforts of drug development.

## 6.7. References

- (1) Harrison, D. P.; Sabat, M.; Myers, W. H.; Harman, W. D. Polarization of the pyridine ring: highly functionalized piperidines from tungsten-pyridine complex. *J. Am. Chem. Soc.* **2010**, *132* (48), 17282-17295.
- (2) Kosturko, G. W.; Harrison, D. P.; Sabat, M.; Myers, W. H.; Harman, W. D. Selectfluor-mediated dialkoxylation of tungsten  $\eta^2$ -pyridinium complexes. *Organometallics* **2009**, *28* (2), 387-389.
- (3) Wilde, J. H.; Dickie, D. A.; Harman, W. D. A Highly Divergent Synthesis of 3-Aminotetrahydropyridines. *J. Org. Chem.* **2020**, *85* (12), 8245-8252.
- (4) Harrison, D. P.; Iovan, D. A.; Myers, W. H.; Sabat, M.; Wang, S.; Zottig, V. E.; Harman, W. D. [4 + 2] Cyclocondensation reactions of tungsten-dihydropyridine complexes and the generation of tri- and tetrasubstituted piperidines. *J. Am. Chem. Soc.* **2011**, *133* (45), 18378-18387.

# Appendix A

## General Parameters

## General Methods:

Unless specified otherwise, all syntheses were conducted inside of a glovebox under an inert N<sub>2</sub> atmosphere. Unless otherwise specified, all cationic complexes are triflate salts. NMR spectra were obtained on an 800 MHz spectrometer. Chemical shifts are referenced to tetramethylsilane (TMS) utilizing residual <sup>1</sup>H or <sup>13</sup>C signals of the deuterated solvents as internal standards. Chemical shifts are reported in ppm, and coupling constants (*J*) are reported in hertz (Hz). Infrared Spectra (IR) were recorded on a spectrometer as a glaze on a diamond anvil ATR assembly, with peaks reported in cm<sup>-1</sup>. Electrochemical experiments were performed under a nitrogen atmosphere. Most cyclic voltammetric (CV) data were recorded at ambient temperature at 100 mV/s, unless otherwise noted, with a standard three-electrode cell from +1.25 V to -1.25 V with a platinum working electrode, *N,N*-dimethylacetamide (DMA) or acetonitrile solvent, and tetrabutylammonium hexafluorophosphate (TBAH) electrolyte (~1.0 M). All potentials are reported versus the normal hydrogen electrode (NHE) using cobaltocenium hexafluorophosphate ( $E_{1/2} = -0.78$  V,  $-1.75$  V) or ferrocene ( $E_{1/2} = 0.55$  V) as an internal standard. The peak separation of all reversible couples was less than 100 mV. All synthetic reactions were performed in a glovebox under a dry nitrogen atmosphere unless otherwise noted. All solvents were purged with nitrogen prior to use. Deuterated solvents were used as received from Cambridge Isotopes. NMR assignments of all compounds were determined using 2D NMR methods, including NOESY, COSY, HMBC, and HSQC. When possible, pyrazole (Pz) protons of the (trispyrazolyl) borate (Tp) ligand were uniquely assigned (e.g., “PzB3”) using two-dimensional NMR data (see Figure S1). If unambiguous assignments were not possible, Tp protons were labeled as “Pz3/5 or Pz4”. All *J* values for Pz protons are 2 (±0.4) Hz. BH peaks (around 4-5 ppm) in the <sup>1</sup>H NMR spectra are not assigned due to their quadrupole broadening. High-resolution electrospray ionization mass

spectrometry (ESI-MS analyses were taken on an Agilent 6545B Q-TOF LC/MS using purine and hexakis(1H, 1H, 3H-tetrafluoropropoxy)phosphazine as internal standards. Samples were dissolved in MeCN and eluted with a MeCN/H<sub>2</sub>O solution containing 0.1% formic acid.

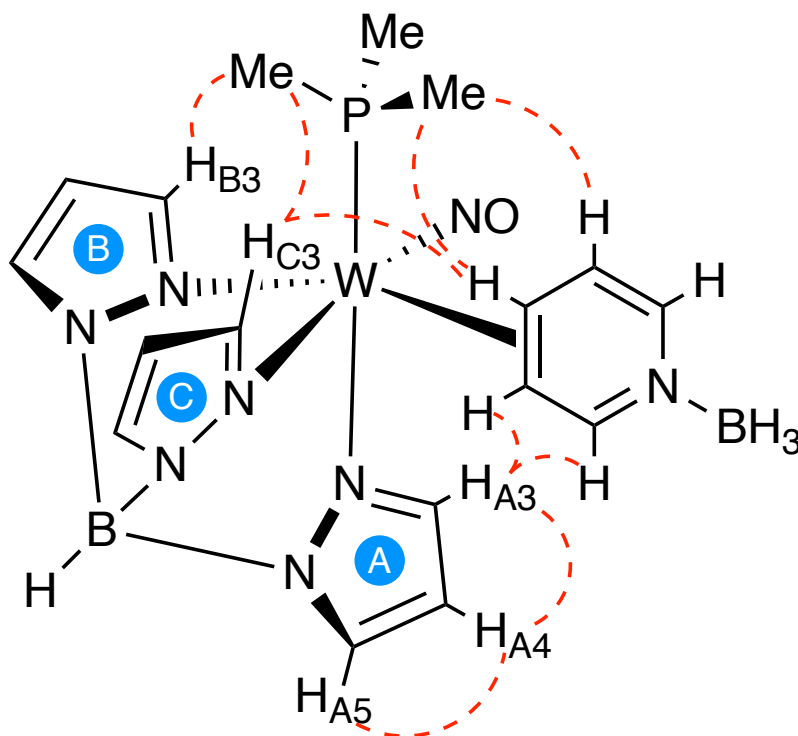


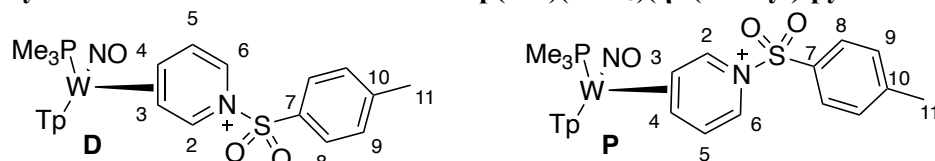
**Figure above:** The red lines indicate observable NOE interactions between protons observed for most complexes.

# Appendix B

## Chapter 2 Data

## Compound Synthetic Methodologies and Characterizations

### Synthesis and characterization of $W\text{Tp}(\text{NO})(\text{PMe}_3)(\eta^2\text{-}(N\text{-tosyl})\text{-pyridinium}) (\text{OTf})$ (**5**)



Methanesulfonic anhydride (10.51 g, 32.20 mmol), **3** (8.34 g, 11.39 mmol), and DCE (100 mL) were charged to a flame-dried 250 mL round-bottom flask with a 1-inch stir bar. Lutidine (2.31 g, 21.56 mmol) was added to initiate the reaction, and the flask was submerged in a pre-heated oil bath set to 55 °C. After stirring the solution for ~2 hours, the solution was diluted with 150 mL of DCM and added to a separatory funnel. This solution was washed 3x with 200 mL of saturated aqueous  $\text{NaHCO}_3$ . The organic layer was isolated and set aside. The combined aqueous layers were combined and back extracted with 50 mL of DCM to prevent product loss. The organic layers were combined in a single flask and dried with anhydrous  $\text{MgSO}_4$ . This powder was then filtered off into a 60 mL coarse porosity fritted funnel and washed with DCM. The dried organic layers were then reduced *in vacuo* down to dryness. The residue in the flask was redissolved in minimal DCM (approximately 10 mL). The solution was then slowly added to 500mL of stirring  $\text{Et}_2\text{O}$ . An orange precipitate formed immediately and was allowed to stir for ~10 minutes to ensure total precipitation. This powder was collected on a 60 mL medium porosity frit and washed 2x with 30 mL of ether. This powder was dried in a desiccator under vacuum for ~30 minutes. (7.74 g, 76% yield)

$^1\text{H}$  NMR ( $\text{CD}_2\text{Cl}_2$ ,  $\delta$ , 25 °C):

**D**: 9.05 (d,  $J = 6.0$  Hz, 1H, H2), 7.97 (d,  $J = 8.5$  Hz, 2H, H8), 7.94 (d,  $J = 2.2$ , 2H (2 overlapping doublets), Tp3/5), 7.93 (d,  $J = 2.0$  Hz, 1H, Tp3/5), 7.91 (d,  $J = 2.4$  Hz, 1H, Tp3/5), 7.76 (d,  $J = 2.5$  Hz, 1H, Tp3/5), 7.66 (d,  $J = 2.5$  Hz, 1H, Tp3/5), 7.49 (d,  $J = 8.3$  Hz, 1H, H9), 6.54 (ddd,  $J = 1.8, 5.5, 7.6$ , 1H, H5), 6.46 (t,  $J = 2.3$  Hz, 1H, Tp4), 6.43 (dd,  $J = 1.6, 7.6$ , 1H, H6), 6.42 (t,  $J = 2.3$  Hz, 1H, Tp4), 6.40 (t,  $J = 2.4$  Hz, 1H, Tp4), 4.13 (dt,  $J = 6.1, 12.4$  Hz, 1H, H4), 3.00 (td,  $J = 1.8, 6.4$  Hz, 1H, H3), 2.49 (s, 3H, H11), 1.23 (d,  $J_{\text{PH}} = 9.2$  Hz, 9H,  $\text{PMe}_3$ ).

**P**: 9.57 (d,  $J = 5.4$  Hz, 1H, H2), [Tp doublets and triplets buried] 6.72 (t,  $J = 6.8$  Hz, 1H, H5), 6.21 (dd,  $J = 1.2, 7.4$ , 1H, H6), 4.36 (q,  $J = 6.5$  Hz, 1H, H3), 2.76 (t,  $J = 6.5$  Hz, 1H, H4), 2.50 (s, 3H, H11), 1.23 (d,  $J_{\text{PH}} = 8.8$  Hz, 9H,  $\text{PMe}_3$ ).

$^{13}\text{C}$  NMR ( $\text{CD}_2\text{Cl}_2$ ,  $\delta$ , 25 °C):

**D**: 167.2 (C2), 148.5 (C7), 146.4 (Tp3/5), 145.9 (Tp3/5), 138.6 (Tp3/5), 138.4 (Tp3/5), 137.6 (Tp3/5), 133.1 (C10), 131.5 (C9), 129.0 (C8), 126.6 (Tp3/5), 124.1 (d,  $J_{\text{PC}} = 2.9$  Hz, C5), 114.8 (C6), 108.2 (Tp4), 108.2 (Tp4), 107.8 (Tp4), 67.1 (d,  $J_{\text{PC}} = 13.9$  Hz, C4), 66.6 (C3), 22.0 (C11), 13.2 (d,  $J_{\text{PC}} = 31.1$  Hz, 3C,  $\text{PMe}_3$ ).

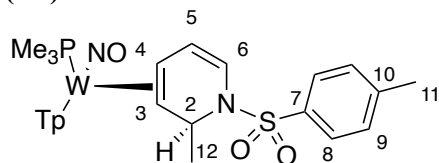
**P**: signals too weak to assign.

IR:  $\nu(\text{NO}) = 1607 \text{ cm}^{-1}$

CV (DMA; 100 mV/s):  $E_{\text{p,a}} = +1.18 \text{ V}$  (NHE)

HRMS (ESI)  $m/z$ :  $[\text{M}]^+$  Calcd for  $\text{C}_{24}\text{H}_{31}\text{BN}_8\text{O}_3\text{PSW}^+$  737.1574; Found 737.1575

**Synthesis and characterization of WTp(NO)(PMe<sub>3</sub>)(η<sup>2</sup>-(*N*-tosyl)-2-(methyl)-1,2-dihydropyridine) (6D)**



An oven dried 4-dram vial and stir pea were set up on a stir plate and charged with **5D** (4 g, 4.46 mmol). This was then diluted with dry THF (20 mL), and 1.2 M ZnMe<sub>2</sub> (in THF) was added to the solution (14.8 mL, 17.8 mmol). This solution was then stirred for 15 minutes and then quenched with a few drops of saturated aqueous NaHCO<sub>3</sub>. The solution was diluted with 150 mL of DCM and added to a separatory funnel. This solution was washed 3x with 200 mL of sat. aq. NaHCO<sub>3</sub>. The organic layer was isolated and set aside. The combined aqueous layers were combined and back extracted with 50 mL of DCM to prevent product loss. The organic layers were combined in a single flask and dried with anhydrous MgSO<sub>4</sub>. This powder was then filtered off into a 60 mL coarse porosity fritted funnel and washed with DCM. The dried organic layers were then reduced *in vacuo* to dryness. The residue in the flask was redissolved in minimal DCM (approximately 5 mL). The solution was then slowly added to 200mL of stirring pentane. A tan precipitate formed immediately and was allowed to stir for ~10 minutes to ensure total precipitation. This powder was collected on a 60 mL medium porosity frit and washed 2x with 30 mL of pentane. This powder was dried in a desiccator under vacuum for ~30 minutes (2.70 g, 80% yield).

<sup>1</sup>H NMR (CD<sub>3</sub>CN, δ, 25 °C): 8.03 (d, *J* = 1.80 Hz, 1H, PzA3), 8.02 (d, *J* = 2.0 Hz, 1H, PzB3), 7.84 (d, *J* = 2.4 Hz, 1H, PzB5), 7.81 (d, *J* = 8.3 Hz, 2H, H8), 7.81 (d, *J* = 2.2 Hz, 1H, PzC5), 7.75 (d, *J* = 2.4 Hz, 1H, PzA5), 7.35 (d, *J* = 8.7 Hz, 2H, H9), 7.32 (d, *J* = 2.2 Hz, 1H, PzC3), 6.36 (t, *J* = 2.2 Hz, 1H, PzB4), 6.25 (t, *J* = 2.2 Hz, 1H, PzA5), 6.24 (t, *J* = 2.2 Hz, 1H, PzC4), 5.91 (d, *J* = 7.9 Hz, 1H, H6), 5.75 (dd, *J* = 5.1, 7.9 Hz, 1H, H5), 4.57 (q, *J* = 6.1, 12.2 Hz, 1H, H2), 2.77 (ddd, *J* = 5.1, 10.5, 13.7 Hz, H4), 2.39 (s, 3H, H11), 1.23 (d, *J* = 10.5 Hz, 1H, H3), 1.21 (d, *J*<sub>PH</sub> = 8.5 Hz, 9H, PMe<sub>3</sub>), 0.96 (d, *J* = 6.1 Hz, 3H, H12).

<sup>13</sup>C NMR (CD<sub>3</sub>CN, δ, 25 °C): 144.3 (C7), 144.2 (d, *J*<sub>PC</sub> = 2.2 Hz, PzB3), 144.1 (PzA3), 141.5 (PzC3), 140.1 (C10), 137.7 (PzC5), 137.3 (PzB5), 136.9 (PzA5), 130.6 (2C, C9), 128.4 (2C, C8), 115.7 (C6), 114.3 (d, *J*<sub>PC</sub> = 2.7 Hz, C5), 107.4 (PzB4), 107.2 (PzC4), 107.0 (PzA4), 67.5 (C3), 51.4 (C2), 43.7 (d, *J*<sub>PC</sub> = 10.3 Hz, C4), 22.3 (C12), 21.5 (C11), 13.6 (d, *J*<sub>PC</sub> = 28.4 Hz, 3C, PMe<sub>3</sub>).

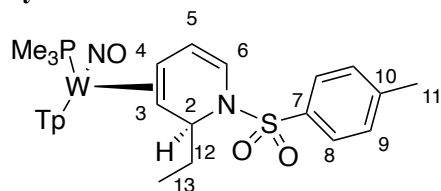
IR: ν(NO) = 2492 cm<sup>-1</sup>

CV (DMA; 100 mV/s): *E*<sub>p,a</sub> = +0.44 V (NHE)

SC-XRD data on page 191



## Synthesis and characterization of $\text{WTP}(\text{NO})(\text{PMe}_3)(\eta^2\text{-}(N\text{-tosyl})\text{-}2\text{-}(ethyl)\text{-}1,2\text{-dihydropyridine})$ (**7D**)



An oven dried 4-dram vial and stir pea were set up on a stir plate and charged with **5D** (970 mg, 1.08 mmol). This was then diluted with dry THF (12 mmol), and  $\text{ZnEt}_2$  was added to the solution (703 mg, 5.69 mmol). This solution was then stirred for 20 minutes and then quenched with a few drops of saturated aqueous  $\text{NaHCO}_3$ . The solution was diluted with 150 mL of DCM and added to a separatory funnel. This solution was washed 3x with 200 mL of sat. aq.  $\text{NaHCO}_3$ . The organic layer was isolated and set aside. The combined aqueous layers were combined and back extracted with 50 mL of DCM to prevent product loss. The organic layers were combined in a single flask and dried with anhydrous  $\text{MgSO}_4$ . This powder was then filtered off into a 60 mL coarse porosity fritted funnel and washed with DCM. The dried organic layers were then reduced *in vacuo* to dryness. The residue in the flask was redissolved in minimal DCM (approximately 5 mL). The solution was then slowly added to 100 mL of stirring pentane. A tan precipitate formed immediately and was allowed to stir for ~10 minutes to ensure total precipitation. This powder was collected on a 60 mL medium porosity frit and washed 2x with 30 mL of pentane. This powder was dried in a desiccator under vacuum for ~30 minutes (630 mg, 76% yield).

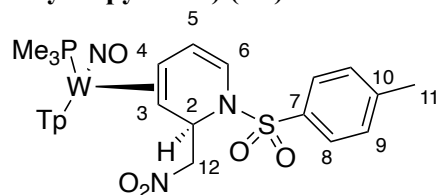
$^1\text{H}$  NMR ( $\text{CD}_2\text{Cl}_2$ ,  $\delta$ , 25 °C): 8.14 (d,  $J = 1.9$  Hz, 1H, PzA3), 8.05 (d,  $J = 1.9$  Hz, 1H, PzB3), 7.81 (d,  $J = 8.3$  Hz, 2H, H8), 7.75 (d,  $J = 2.4$  Hz, 1H, PzB5), 7.73 (d,  $J = 2.2$  Hz, 1H, PzC5), 7.65 (d,  $J = 2.4$  Hz, 1H, PzA5), 7.30 (d,  $J = 8.6$  Hz, 2H, H9), 7.25 (d,  $J = 2.2$  Hz, 1H, PzC3), 6.32 (t,  $J = 2.2$  Hz, 1H, PzB4), 6.23 (t,  $J = 2.2$  Hz, 1H, PzA4), 6.21 (t,  $J = 2.2$  Hz, 1H, PzC4), 6.01 (d,  $J = 7.9$  Hz, 1H, H6), 5.65 (dd,  $J = 5.0$ , 7.9 Hz, 1H, H5), 4.42 (d,  $J = 9.3$  Hz, 1H, H2), 2.73 (ddd,  $J = 5.0$ , 10.6, 13.6 Hz, 1H, H4), 2.41 (s, 3H, H11), 1.69 (ddd,  $J = 7.5$ , 9.3, 13.0 Hz, 1H, H12), 1.61 (d,  $J = 10.7$ , 1H, H3), 1.29 (m, 1H H12'), 1.21 (d,  $J_{\text{PH}} = 8.3$  Hz, 9H,  $\text{PMe}_3$ ), 0.63 (t,  $J = 7.5$  Hz, 3H, H13).

$^{13}\text{C}$  NMR ( $\text{CD}_2\text{Cl}_2$ ,  $\delta$ , 25 °C): 143.7 (PzA3), 143.5 (d,  $J_{\text{PC}} = 1.7$  Hz, PzB3), 143.2 (C7), 140.2 (PzC3), 139.8 (C10), 136.8 (PzB5), 136.3 (PzC5), 135.8 (PzA5), 129.8 (2C, C9), 127.7 (2C, C8), 116.6 (C6), 113.3 ( $J_{\text{PC}} = 2.8$  Hz, C5), 106.6 (PzB4), 106.2 (PzC4), 106.2 (PzA4), 61.9 ( $J_{\text{WC}} = 1.9$ , 16.5 Hz, C3), 56.7 (C2), 44.1 (C4), 29.6 (C12), 21.6 (C11), 13.5 (d,  $J_{\text{PC}} = 27.8$  Hz, 3C,  $\text{PMe}_3$ ), 10.8 (C13).

IR:  $\nu(\text{NO}) = 1560 \text{ cm}^{-1}$

CV (DMA; 100 mV/s):  $E_{\text{p,a}} = +0.44 \text{ V}$  (NHE)

### Synthesis and characterization of $\text{WTP}(\text{NO})(\text{PMe}_3)(\eta^2\text{-}(N\text{-tosyl)-2-(nitromethyl)-1,2\text{-dihydropyridine)})$ (**8D**)



An oven dried 4-dram vial and stir pea were set up on a stir plate and charged with **5D** (970 mg, 1.08 mmol). This was then diluted with DCM (7 mL), and nitromethane (105 mg, 1.72 mmol) and TEA (115 mg, 1.13 mmol) were added to the solution. This solution was stirred for 5 minutes. The solution was diluted with 150 mL of DCM and added to a separatory funnel. This solution was washed 3x with 200 mL of saturated aqueous  $\text{NaHCO}_3$ . The organic layer was isolated and set aside. The combined aqueous layers were combined and back extracted with 50 mL of DCM to prevent product loss. The organic layers were combined in a single flask and dried with anhydrous  $\text{MgSO}_4$ . This powder was then filtered off into a 60 mL coarse porosity fritted funnel and washed with DCM. The dried organic layers were then reduced *in vacuo* to dryness. The residue in the flask was redissolved in minimal DCM (approximately 5 mL). The solution was then slowly added to 200mL of stirring pentane. A tan precipitate formed immediately and was allowed to stir for ~10 minutes to ensure total precipitation. This powder was collected on a 60 mL medium porosity frit and washed 2x with 30 mL of pentane. This powder was dried in a desiccator under vacuum for ~30 minutes (755 mg, 87% yield).

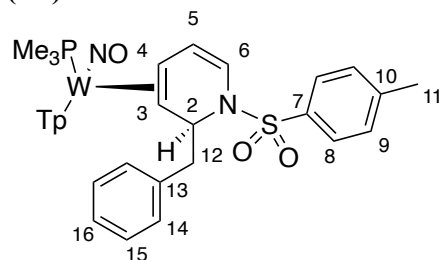
$^1\text{H}$  NMR ( $\text{CD}_2\text{Cl}_2$ ,  $\delta$ , 25 °C): 8.05 (d,  $J = 1.9$  Hz, 1H, Tp3/5), 7.93 (d,  $J = 8.2$  Hz, 2H, H8), 7.76 (d,  $J = 2.4$  Hz, 1H, Tp3/5), 7.71 (d,  $J = 2.2$  Hz, 1H, Tp3/5), 7.61 (d,  $J = 2.4$  Hz, 1H, Tp3/5), 7.60 (d,  $J = 1.9$  Hz, 1H, T3/5p), 7.36 (d,  $J = 8.6$  Hz, 2H, H9), 7.20 (d,  $J = 2.2$  Hz, 1H, Tp3/5), 6.34 (t,  $J = 2.2$  Hz, 1H, Tp4), 6.20 (t,  $J = 2.2$  Hz, 1H, Tp4), 6.16 (t,  $J = 2.2$  Hz, 1H, Tp4), 6.05 (d,  $J = 7.8$  Hz, 1H, H6), 5.75 (ddd,  $J = 0.8$ , 5.1, 7.8 Hz, 1H, H5), 5.04 (m, 1H, H2), 4.57 (dd,  $J = 9.1$ , 11.1 Hz, 1H, H12), 4.35 (dd,  $J = 3.6$ , 11.1 Hz, 1H, H12'), 2.74 (ddd,  $J = 5.1$ , 10.4, 13.2 Hz, 1H, H4), 2.42 (s, 3H, H11), 1.40 (d,  $J = 10.4$  Hz, 1H, H3), 1.19 (d,  $J_{\text{PH}} = 8.5$  Hz, 9H,  $\text{PMe}_3$ ).

IR:  $\nu(\text{NO}) = 1559 \text{ cm}^{-1}$

CV (DMA; 100 mV/s):  $E_{p,a} = +0.60 \text{ V}$  (NHE)

SC-XRD data of **8P** on page 192

## Synthesis and characterization of $\text{WTP}(\text{NO})(\text{PMe}_3)(\eta^2\text{-}(N\text{-tosyl})\text{-}2\text{-}(\text{benzyl})\text{-}1,2\text{-dihydropyridine})$ (**9D**)

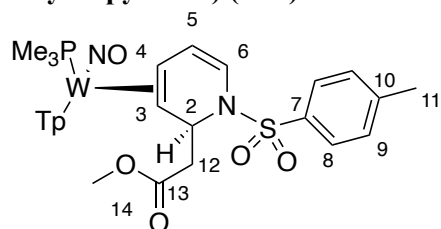


An oven dried 4-dram vial and stir pea were set up on a stir plate and charged with **5D** (198 mg, 0.22 mmol). This was then diluted with dry DME (3 mL), and  $\text{BnMgCl}$  (1.0 M in THF) was added to the solution (0.24 mL, 0.24 mmol). This solution was then stirred for 5 minutes and quenched with sat. aq.  $\text{NaHCO}_3$ . The solution was diluted with 150 mL of DCM and added to a separatory funnel. This solution was washed 3x with 200 mL of saturated aqueous  $\text{NaHCO}_3$ . The organic layer was isolated and set aside. The combined aqueous layers were combined and back extracted with 50 mL of DCM to prevent product loss. The organic layers were combined in a single flask and dried with anhydrous  $\text{MgSO}_4$ . This powder was then filtered off into a 60 mL coarse porosity fritted funnel and washed with DCM. The dried organic layers were then reduced *in vacuo* to dryness. The residue in the flask was redissolved in minimal DCM (approximately 5 mL). The solution was then slowly added to 100 mL of stirring pentane. A tan precipitate formed immediately and was allowed to stir for ~10 minutes to ensure total precipitation. This powder was collected on a 60 mL medium porosity frit and washed 2x with 30 mL of pentane. This powder was dried in a desiccator under vacuum for ~30 minutes (78 mg, 43% yield).

$^1\text{H}$  NMR ( $\text{CD}_2\text{Cl}_2$ ,  $\delta$ , 25 °C): 8.06 (d,  $J = 1.8$  Hz, 1H, PzA3), 8.04 (d,  $J = 1.9$  Hz, 1H, PzB3), 7.92 (d,  $J = 8.3$  Hz, 2H, H8), 7.71 (d,  $J = 2.3$  Hz, 1H, PzB5), 7.63 (d,  $J = 2.2$  Hz, 1H, PzC5), 7.53 (d,  $J = 2.4$  Hz, 1H, PzA5), 7.34 (d,  $J = 8.3$  Hz, 2H, H9), 7.14 (d,  $J = 2.0$  Hz, 1H, PzC3), 7.03 (t,  $J = 7.5$  Hz, 2H, H15), 6.94-6.98 (m, 13H, H14/16), 6.31 (t,  $J = 2.2$  Hz, 1H, PzB4), 6.14 (t,  $J = 2.2$  Hz, 1H, PzA4), 6.13 (t,  $J = 2.2$  Hz, 1H, PzC4), 6.06 (d,  $J = 7.8$  Hz, 1H, H6), 5.76 (dd,  $J = 5.1, 7.8$  Hz, 1H, H5), 4.68 (d,  $J = 10.3$  Hz, 1H, H2), 2.87 (dd,  $J = 10.3, 12.6$  Hz, 1H, H12'), 2.74 (ddd,  $J = 4.9, 10.6, 13.5$  Hz, 1H, H4), 2.61 (dd,  $J = 3.0, 12.6$  Hz, 1H, H12), 2.39 (s, 3H, H11), 1.45 (d,  $J = 10.3$  Hz, 1H, H3), 1.20 (d,  $J_{\text{PH}} = 8.3$  Hz, 1H,  $\text{PMe}_3$ ).

$^{13}\text{C}$  NMR ( $\text{CD}_2\text{Cl}_2$ ,  $\delta$ , 25 °C): 143.6 (C7), 143.5 (PzA3), 143.4 (d,  $J_{\text{PC}} = 1.7$  Hz, PzB3), 140.1 (C13), 139.9 (PzC3), 139.5 (C10), 136.7 (PzC5), 136.2 (PzB5), 135.7 (PzA5), 130.0 (2C, C9), 129.8 (2C, C14), 128.2 (2C, C15), 127.9 (2C, C8), 125.8 (C16), 115.9 (C6), 114.1 (d,  $J_{\text{PC}} = 3.2$  Hz, C5), 106.6 (PzB4), 106.1 (PzA4/C4), 106.0 (PzA4/C4), 62.4 (d,  $J_{\text{PC}} = 1.6$  Hz, C3), 56.7 (C2), 43.8 (d,  $J_{\text{PC}} = 10.3$  Hz, C4), 41.7 (C12), 21.6 (C11), 13.6 (d,  $J_{\text{PC}} = 27.9$  Hz, 3C,  $\text{PMe}_3$ ).

### Synthesis and characterization of WTP(NO)(PMe<sub>3</sub>)(η<sup>2</sup>-(*N*-tosyl)-2-(methylacetate)-1,2-dihydropyridine) (10D)



Methyl bromoacetate (224 mg, 1.46 mmol), **5D** (956 mg, 1.07 mmol), and THF (12 mL) were charged to a flame-dried 50 mL round-bottom flask with a 1-inch stir bar. Zinc powder (281 mg, 4.30 mmol) was added to initiate the reaction, and the heterogenous solution was stirred for 1 hour. The zinc was removed by filtering the solution through a celite plug set up in a 60 mL coarse porosity frit with 1 inch of celite, which was then washed with residual DCM to prevent loss of product. The solution was diluted with 150 mL of DCM and added to a separatory funnel. This solution was washed 3x with 200 mL of saturated aqueous NaHCO<sub>3</sub>. The organic layer was isolated and set aside. The combined aqueous layers were combined and back extracted with 50 mL of DCM to prevent product loss. The organic layers were combined in a single flask and dried with anhydrous MgSO<sub>4</sub>. This powder was then filtered off into a 60 mL coarse porosity fritted funnel and washed with DCM. The dried organic layers were then reduced *in vacuo* to dryness. The residue in the flask was redissolved in minimal DCM (approximately 5 mL). The solution was then slowly added to 200mL of stirring pentane. A tan precipitate formed immediately and was allowed to stir for ~10 minutes to ensure total precipitation. This powder was collected on a 60 mL medium porosity frit and washed 2x with 30 mL of pentane. This powder was dried in a desiccator under vacuum for ~30 minutes (690 mg, 80% yield).

<sup>1</sup>H NMR (CD<sub>2</sub>Cl<sub>2</sub>, δ, 25 °C): 8.05 (d, *J* = 1.9 Hz, 1H, PzB3), 7.90 (d, *J* = 1.6 Hz, 1H, PzA3), 7.86 (d, *J* = 8.3 Hz, 2H, H8), 7.75 (d, *J* = 2.4 Hz, 1H, PzB5), 7.72 (d, *J* = 2.4 Hz, 1H, PzC5), 7.63 (d, *J* = 2.4 Hz, 1H, PzA5), 7.32 (d, *J* = 8.2 Hz, 2H, H9), 7.21 (d, *J* = 1.9 Hz, 1H, PzC3), 6.33 (t, *J* = 2.2 Hz, 1H, PzB4), 6.20 (t, *J* = 2.2 Hz, 1H, PzA4), 6.19 (t, *J* = 2.1 Hz, 1H, PzC4), 6.01 (d, *J* = 7.8 Hz, 1H, H6), 5.72 (dd, *J* = 5.1, 7.8 Hz, 1H, H5), 4.90 (d, *J* = 9.8 Hz, 1H, H2), 3.38 (s, 3H, H14), 2.70 (m, 2H, H4 & H12), 2.40 (s, 3H, H11), 2.36 (dd, *J* = 8.4, 15.1 Hz, 1H, H12'), 1.46 (d, *J* = 10.7 Hz, 1H, H3), 1.20 (d, *J*<sub>PH</sub> = 8.4 Hz, 9H, PMe<sub>3</sub>).

<sup>13</sup>C NMR (CD<sub>2</sub>Cl<sub>2</sub>, δ, 25 °C): 172.5 (C13), 143.8 (C7), 143.7 (PzA3), 143.5 (d, *J*<sub>PC</sub> = 2.2 Hz, PzB3), 140.2 (PzC3), 138.4 (C10), 136.9 (PzC5), 136.4 (PzB5), 135.8 (PzA5), 130.0 (2C, C9), 128.2 (2C, C8), 115.4 (C6), 113.7 (d, *J*<sub>PC</sub> = 3.0 Hz, C5), 106.6 (PzB4), 106.3 (PzC4), 106.0 (PzA4), 64.3 (d, *J*<sub>PC</sub> = 2.2 Hz, *J*<sub>WC</sub> = 33.0 Hz, C3), 52.1 (C2), 51.4 (C14), 43.5 (d, *J*<sub>PC</sub> = 10.7 Hz, C4), 41.3 (C12), 21.7 (C11), 13.4 (d, *J*<sub>PC</sub> = 27.8 Hz, 3C, PMe<sub>3</sub>).

IR: ν(NO) = 1570 cm<sup>-1</sup>

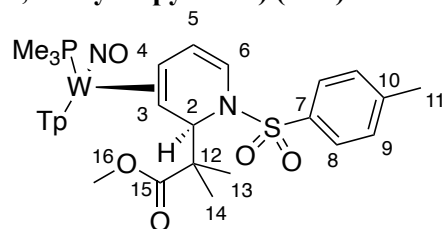
CV (DMA; 100 mV/s): *E*<sub>p,a</sub> = +0.50 V (NHE)

EA for C<sub>27</sub>H<sub>36</sub>BN<sub>8</sub>O<sub>5</sub>PSW:

Calcd: (%C, 40.02), (%H, 4.48), (%N, 14.05)

Found: (%C, 39.95), (%H, 4.40), (%N, 14.20)

### Synthesis and characterization of $\text{WTP}(\text{NO})(\text{PMe}_3)(\eta^2\text{-}(N\text{-tosyl})\text{-}2\text{-}(\alpha, \alpha\text{-dimethyl-methylacetate})\text{-}1,2\text{-dihydropyridine})$ (**11D**)



An oven dried 4-dram vial and stir pea were set up on a stir plate and charged with **5D** (1.004 g, 1.13 mmol). This was then diluted with DCM (11 mL), and MTDA (412 mg, 2.36 mmol) was added to the solution. This solution was stirred for 2 hours and quenched with minutes and the solution was quenched with TEA (311 mg, 3.07 mmol). The reaction was diluted with 150 mL of DCM and added to a separatory funnel. This solution was washed 3x with 200 mL of saturated aqueous  $\text{NaHCO}_3$ . The organic layer was isolated and set aside. The combined aqueous layers were combined and back extracted with 50 mL of DCM to prevent product loss. The organic layers were combined in a single flask and dried with anhydrous  $\text{MgSO}_4$ . This powder was then filtered off into a 60 mL coarse porosity fritted funnel and washed with DCM. The dried organic layers were then reduced *in vacuo* to dryness. The residue in the flask was redissolved in minimal DCM (approximately 5 mL). The solution was then slowly added to 200mL of stirring pentane. A tan precipitate formed immediately and was allowed to stir for ~10 minutes to ensure total precipitation. This powder was collected on a 60 mL medium porosity frit and washed 2x with 30 mL of pentane. This powder was dried in a desiccator under vacuum for ~30 minutes (740 mg, 78% yield).

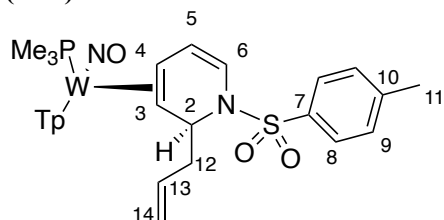
$^1\text{H}$  NMR ( $\text{CD}_2\text{Cl}_2$ ,  $\delta$ , 25 °C): 8.41 (d,  $J = 1.9$  Hz, 1H, PzA3), 8.05 (d,  $J = 1.9$  Hz, 1H, PzB3), 7.80 (d,  $J = 8.3$  Hz, 2H, H8), 7.75 (d,  $J = 2.4$  Hz, 1H, PzB5), 7.72 (d,  $J = 2.3$  Hz, 1H, PzC5), 7.66 (d,  $J = 2.4$  Hz, 1H, PzA5), 7.26 (d,  $J = 8.2$  Hz, 2H, H9), 7.24 (d,  $J = 1.8$  Hz, 1H, PzC3), 6.33 (t,  $J = 2.4$  Hz, 1H, PzA4), 6.32 (t,  $J = 2.3$  Hz, 1H, PzB4), 6.22 (t,  $J = 2.2$  Hz, 1H, PzC4), 6.04 (d,  $J = 7.8$  Hz, 1H, H6), 5.67 (dd,  $J = 5.0, 7.8$  Hz, 1H, H5), 5.34 (s, 1H, H2), 2.87 (s, 3H, H16), 2.81 (ddd,  $J = 5.0, 10.8, 14.1$  Hz, 1H, H4), 2.39 (s, 3H, H11), 1.25 (s, 3H, H14), 1.19 (d,  $J_{\text{PH}} = 8.3$  Hz, 9H,  $\text{PMe}_3$ ), 1.00 (d,  $J = 10.8$  Hz, 1H, H3), 0.89 (s, 3H, H13)

$^{13}\text{C}$  NMR ( $\text{CD}_2\text{Cl}_2$ ,  $\delta$ , 25 °C): 177.4 (C15), 144.3 (PzA3), 143.2 (d,  $J_{\text{PC}} = 1.7$  Hz, PzB3), 143.1 (C7), 140.7 (C10), 140.0 (PzC3), 136.7 (PzC5), 136.4 (PzB5), 135.8 (PzA5), 129.6 (2C, C9), 127.9 (2C, C8), 119.1 (C6), 115. (d,  $J_{\text{PC}} = 2.7$  Hz, C5), 106.6 (PzA4/B4), 106.4 (PzC4), 106.1 (PzA4/B4), 59.9 (2C, C2 and C3), 54.7 (C12), 51.0 (C16), 44.7 (d,  $J_{\text{PC}} = 10.6$  Hz, C4), 25.9 (C13), 21.6 (C11), 19.8 (C14), 13.4 (d,  $J_{\text{PC}} = 27.9$  Hz, 3C,  $\text{PMe}_3$ ).

IR:  $\nu(\text{NO}) = 1577 \text{ cm}^{-1}$

CV (DMA; 100 mV/s):  $E_{p,a} = +0.46 \text{ V}$  (NHE)

**Synthesis and characterization of WTp(NO)(PMe<sub>3</sub>)(η<sup>2</sup>-(*N*-tosyl)-2-(allyl)-1,2-dihydropyridine) (12D)**



Allyl bromide (350 mg, 2.89 mmol), **5D** (999 mg, 1.11 mmol), and THF (8 mL) were charged to a flame-dried 50 mL round-bottom flask with a 1-inch stir bar. Zinc powder (323 mg, 4.93 mmol) was added to initiate the reaction, and the heterogeneous solution was stirred for 1 hour. The zinc was removed by filtering the solution through a celite plug set up in a 60 mL coarse porosity frit with 1 inch of celite, which was then washed with residual DCM to prevent loss of product. The solution was diluted with 150 mL of DCM and added to a separatory funnel. This solution was washed 3x with 200 mL of saturated aqueous NaHCO<sub>3</sub>. The organic layer was isolated and set aside. The combined aqueous layers were combined and back extracted with 50 mL of DCM to prevent product loss. The organic layers were combined in a single flask and dried with anhydrous MgSO<sub>4</sub>. This powder was then filtered off into a 60 mL coarse porosity fritted funnel and washed with DCM. The dried organic layers were then reduced *in vacuo* to dryness. The residue in the flask was redissolved in minimal DCM (approximately 5 mL). The solution was then slowly added to 200 mL of stirring pentane. A tan precipitate formed immediately and was allowed to stir for ~10 minutes to ensure total precipitation. This powder was collected on a 60 mL medium porosity frit and washed 2x with 30 mL of pentane. This powder was dried in a desiccator under vacuum for ~30 minutes (730 mg, 84% yield).

<sup>1</sup>H NMR (CD<sub>2</sub>Cl<sub>2</sub>, δ, 25 °C): 8.14 (d, *J* = 1.9 Hz, 1H, PzA3), 8.05 (d, *J* = 1.9 Hz, 1H, PzB3), 7.83 (d, *J* = 8.3 Hz, 2H, H8), 7.75 (d, *J* = 2.4 Hz, 1H, PzB5), 7.73 (d, *J* = 2.2 Hz, 1H, PzC5), 7.64 (d, *J* = 2.4 Hz, 1H, PzA5), 7.32 (d, *J* = 8.3 Hz, 2H, H9), 7.22 (d, *J* = 2.2 Hz, 1H, PzC3), 6.32 (t, *J* = 2.2 Hz, 1H, PzB4), 6.23 (t, *J* = 2.2 Hz, 1H, PzA4), 6.20 (t, *J* = 2.2 Hz, 1H, PzC4), 6.01 (d, *J* = 7.8 Hz, 1H, H6), 5.68 (dd, *J* = 5.0, 7.8 Hz, 1H, H5), 5.60 (m, 1H, H13), 4.72 (d, *J* = 10.2 Hz, 1H, H14), 4.70 (d, *J* = 17.9 Hz, 1H, H14'), 4.53 (d, *J* = 9.5 Hz, 1H, H2), 2.73 (ddd, *J* = 5.0, 10.6, 13.5 Hz, 1H, H4), 2.41 (s, 3H, H11), 2.41 (m, 1H, H12), 1.99 (m, 1H, H12'), 1.61 (d, *J* = 10.6 Hz, 1H, H3), 1.21 (d, *J*<sub>PH</sub> = 8.3 Hz, 9H, PMe<sub>3</sub>.)

<sup>13</sup>C NMR (CD<sub>2</sub>Cl<sub>2</sub>, δ, 25 °C): 143.7 (PzA3), 143.5 (d, *J*<sub>PC</sub> = 1.5 Hz, PzB3), 143.5 (C7), 140.2 (PzC3), 139.6 (C10), 136.8 (PzB5), 136.6 (C13), 136.3 (PzC5), 135.8 (PzA5), 129.9 (2C, C9), 127.8 (2C, C8), 116.3 (C14), 116.2 (C6), 113.7 (d, *J*<sub>PC</sub> = 3.0 Hz, C5), 106.6 (PzB4), 106.3 (PzC4), 106.2 (PzA4), 62.8 (td, *J*<sub>WP</sub> = 1.5, 16.6 Hz, C3), 55.2 (C2), 43.7 (d, *J*<sub>PC</sub> = 10.4 Hz, C4), 41.0 (C12), 21.6 (C11), 13.6 (d, *J*<sub>PC</sub> = 27.9 Hz, 3C, PMe<sub>3</sub>).

IR: ν(NO) = 1561 cm<sup>-1</sup>

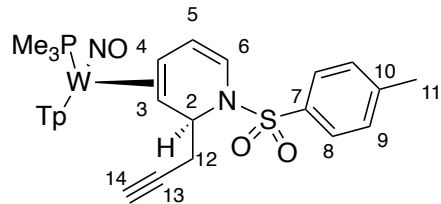
CV (DMA; 100 mV/s): *E*<sub>p,a</sub> = +0.46 V (NHE)

EA for C<sub>27</sub>H<sub>36</sub>BN<sub>8</sub>O<sub>3</sub>PSW:

Calcd: (%C, 41.67), (%H, 4.66), (%N, 14.40)

Found: (%C, 41.97), (%H, 4.81), (%N, 14.24)

**Synthesis and characterization of WTp(NO)(PMe<sub>3</sub>)(η<sup>2</sup>-(*N*-tosyl)-2-(propargyl)-1,2-dihydropyridine) (13D)**



Propargyl bromide (220 mg, 1.85 mmol), **5D** (935 mg, 1.04 mmol), and THF (10 mL) were charged to a flame-dried 50 mL round-bottom flask with a 1-inch stir bar. Zinc powder (391 mg, 5.98 mmol) was added to initiate the reaction, and the heterogenous solution was stirred for 1 hour. The zinc was removed by filtering the solution through a celite plug set up in a 60 mL coarse porosity frit with 1 inch of celite, which was then washed with residual DCM to prevent loss of product. The solution was diluted with 150 mL of DCM and added to a separatory funnel. This solution was washed 3x with 200 mL of saturated aqueous NaHCO<sub>3</sub>. The organic layer was isolated and set aside. The combined aqueous layers were combined and back extracted with 50 mL of DCM to prevent product loss. The organic layers were combined in a single flask and dried with anhydrous MgSO<sub>4</sub>. This powder was then filtered off into a 60 mL coarse porosity fritted funnel and washed with DCM. The dried organic layers were then reduced *in vacuo* to dryness. The residue in the flask was redissolved in minimal DCM (approximately 5 mL). The solution was then slowly added to 200mL of stirring pentane. A tan precipitate formed immediately and was allowed to stir for ~10 minutes to ensure total precipitation. This powder was collected on a 60 mL medium porosity frit and washed 2x with 30 mL of pentane. This powder was dried in a desiccator under vacuum for ~30 minutes (666 mg, 82% yield).

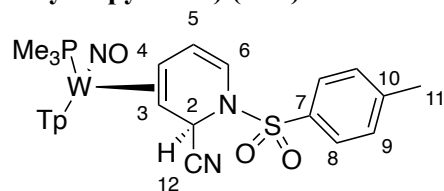
<sup>1</sup>H NMR (CD<sub>2</sub>Cl<sub>2</sub>, δ, 25 °C): 8.06 (d, *J* = 1.7 Hz, 1H, PzB3), 8.00 (d, *J* = 1.6 Hz, 1H, PzA3), 7.84 (d, *J* = 8.3 Hz, 2H, H8), 7.76 (d, *J* = 2.3 Hz, 1H, PzB5), 7.74 (d, *J* = 2.1 Hz, 1H, PzC5), 7.65 (d, *J* = 2.3 Hz, 1H, PzA5), 7.33 (d, *J* = 8.0 Hz, 2H, H9), 7.25 (d, *J* = 1.9 Hz, 1H, PzC3), 6.33 (t, *J* = 2.2 Hz, 1H, PzB4), 6.22 (t, *J* = 2.2 Hz, 2H, PzA4 & PzC4), 5.96 (d, *J* = 7.7 Hz, 1H, H6), 5.73 (dd, *J* = 5.1, 7.7 Hz, 1H, H5), 4.60 (d, *J* = 9.5 Hz, 1H, H2), 2.74 (ddd, *J* = 5.1, 10.7, 13.5 Hz, 1H, H4), 2.56 (ddd, *J* = 2.7, 10.0, 16.1 Hz, 1H, H12), 2.42 (s, 3H, H11), 2.15 (dt, *J* = 2.7, 16.1 Hz, 1H, H12'), 1.96 (d, *J* = 10.7 Hz, 1H, H3), 1.71 (t, *J* = 2.7 Hz, 1H, H14), 1.20 (d, *J*<sub>PH</sub> = 8.3 Hz, 1H, PMe<sub>3</sub>).

<sup>13</sup>C NMR (CD<sub>2</sub>Cl<sub>2</sub>, δ, 25 °C): 143.8 (C7), 143.7 (PzA3), 143.5 (PzB3), 140.3 (PzC3), 138.8 (C10), 136.9 (PzC5), 136.4 (PzB5), 135.9 (PzA5), 130.1 (2C, C9), 127.9 (2C, C8), 115.1 (C6), 114.2 (C5), 106.6 (PzB4), 106.3 (PzC4), 106.2 (PzA4), 83.1 (C13), 69.8 (C14), 62.7 (*J*<sub>WC</sub> = 33.9 Hz, C3), 54.6 (C2), 43.6 (d, *J*<sub>PC</sub> = 10.6 Hz, C4), 25.5 (C12), 21.7 (C11), 13.5 (d, *J*<sub>PC</sub> = 28.0 Hz, 3C, PMe<sub>3</sub>).

IR: ν(NO) = 1607 cm<sup>-1</sup>

CV (DMA; 100 mV/s): *E*<sub>p,a</sub> = +1.18 V (NHE)

### Synthesis and characterization of WTP(NO)(PMe<sub>3</sub>)(η<sup>2</sup>-(*N*-tosyl)-2-(carbonitrile)-1,2-dihydropyridine) (14D)



An oven dried 4-dram vial and stir pea were set up on a stir plate and charged with **5D** (963 mg, 1.07 mmol). This was then diluted with MeOH (12 mL), and NaCN was added to the solution (189 mg, 3.86 mmol). This solution was then stirred for 2.5 hours. The solution was diluted with 150 mL of DCM and added to a separatory funnel. This solution was washed 3x with 200 mL of saturated aqueous NaHCO<sub>3</sub>. The organic layer was isolated and set aside. The combined aqueous layers were combined and back extracted with 50 mL of DCM to prevent product loss. The organic layers were combined in a single flask and dried with anhydrous MgSO<sub>4</sub>. This powder was then filtered off into a 60 mL coarse porosity fritted funnel and washed with DCM. The dried organic layers were then reduced *in vacuo* to dryness. The residue in the flask was redissolved in minimal DCM (approximately 5 mL). The solution was then slowly added to 200mL of stirring pentane. A tan precipitate formed immediately and was allowed to stir for ~10 minutes to ensure total precipitation. This powder was collected on a 60 mL medium porosity frit and washed 2x with 30 mL of pentane. This powder was dried in a desiccator under vacuum for ~30 minutes (534 mg, 65% yield).

<sup>1</sup>H NMR (CD<sub>2</sub>Cl<sub>2</sub>, δ, 25 °C): 8.04 (d, *J* = 1.9, 1H, PzB3), 8.03 (d, *J* = 1.9 Hz, 1H, PzA3), 7.83 (d, *J* = 8.4 Hz, 2H, H8), 7.77 (d, *J* = 2.4 Hz, 1H, PzB5), 7.76 (d, *J* = 2.2 Hz, 1H, PzC5), 7.69 (d, *J* = 2.4 Hz, 1H, PzA5), 7.38 (d, *J* = 8.2 Hz, 2H, H9), 7.26 (d, *J* = 2.2 Hz, 1H, PzC3), 6.35 (t, *J* = 1.9 Hz, 1H, PzB4), 6.30 (t, *J* = 2.2 Hz, 1H, PzA4), 6.24 (t, *J* = 2.4 Hz, 1H, PzC4), 6.05 (d, *J* = 7.8 Hz, 1H, H6), 5.95 (dd, *J* = 5.3, 7.8 Hz, 1H, H5), 5.26 (m, 1H, H2), 2.77 (ddd, *J* = 5.3, 10.3, 12.9 Hz, 1H, H4), 2.44 (s, 3H, H11), 1.77 (d, *J* = 10.3, 1H, H3), 1.25 (d, *J*<sub>PH</sub> = 8.5 Hz, 9H, PMe<sub>3</sub>).

<sup>13</sup>C NMR (CD<sub>2</sub>Cl<sub>2</sub>, δ, 25 °C): 144.7 (C7), 143.8 (d, *J*<sub>PC</sub> = 1.9 Hz, PzB3), 143.0 (PzA3), 140.5 (PzC3), 137.1 (PzC5), 136.8 (PzB5), 136.2 (PzA5), 135.8 (C10), 130.1 (2C, C9), 128.1 (2C, C8), 121.3 (C12), 115.5 (d, *J*<sub>PC</sub> = 2.7 Hz, C6), 115.3 (C5), 106.8 (PzB4), 106.7 (PzA4), 106.6 (PzC4), 62.4 (d, *J*<sub>PC</sub> = 3.0 Hz, *J*<sub>WC</sub> = 33.8 Hz, C3), 47.1 (C2), 42.8 (d, *J*<sub>PC</sub> = 11.2 Hz, C4), 21.7 (C11), 13.7 (d, *J*<sub>PC</sub> = 28.6 Hz, 3C, PMe<sub>3</sub>).

IR: ν(NO) = 1577 cm<sup>-1</sup>

CV (DMA; 100 mV/s): *E*<sub>p,a</sub> = +0.66 V (NHE)

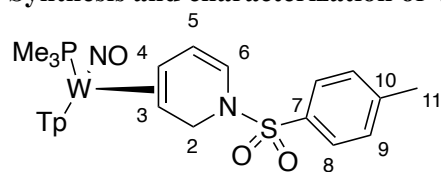
EA for C<sub>25</sub>H<sub>31</sub>BN<sub>9</sub>O<sub>3</sub>PSW:

Calcd: (%C, 39.34), (%H, 4.09), (%N, 16.52)

Found: (%C, 39.27), (%H, 4.02), (%N, 16.41)



## Synthesis and characterization of $\text{Wtp}(\text{NO})(\text{PMe}_3)(\eta^2\text{-}(N\text{-tosyl})\text{-}1,2\text{-dihydropyridine})$ (**15D**)



Two separate solutions were prepared in two 30 mL glass screw-cap test tubes. Tube A was comprised of **5D** (1.052 g, 1.17 mmol) dissolved in MeOH and Tube B was a heterogeneous slurry of NaBH<sub>4</sub> (125 mg, 3.30 mmol) in dry THF (10 mL). The tube B slurry was added to tube A, and the tube sat for 10 minutes (bubbling occurred). The solution was diluted with 150 mL of DCM and added to a separatory funnel. This solution was washed 3x with 200 mL of saturated aqueous NaHCO<sub>3</sub>. The organic layer was isolated and set aside. The combined aqueous layers were combined and back-extracted with 50 mL of DCM to prevent loss of product. The organic layers were combined in a single flask and dried with anhydrous MgSO<sub>4</sub>. This powder was then filtered off into a 60 mL coarse porosity fritted funnel and washed with DCM. The dried organic layers were then reduced *in vacuo* to dryness. The residue in the flask was redissolved in minimal DCM (approximately 5 mL). The solution was then slowly added to a stirring 100mL solution of pentane. A tan precipitate formed immediately and was allowed to stir for ~10 minutes to ensure total precipitation. This powder was collected on a 60 mL medium porosity frit and washed 2x with 30 mL of pentane. This powder was dried in a desiccator under vacuum overnight. (663 mg mg, 76% yield)

<sup>1</sup>H NMR (CD<sub>2</sub>Cl<sub>2</sub>, δ, 25 °C): 8.04 (d, *J* = 1.8 Hz, 1H, PzB3), 7.98 (d, *J* = 1.6 Hz, 1H, PzA3), 7.75 (d, *J* = 2.2 Hz, 1H, PzB5), 7.74 (d, *J* = 8.2 Hz, 2H, H8), 7.73 (d, *J* = 2.2 Hz, 1H, PzC5), 7.66 (d, *J* = 2.3 Hz, 1H, PzA5), 7.32 (d, *J* = 8.1 Hz, 2H, H9), 7.23 (d, *J* = 1.8 Hz, 1H, PzC3), 6.33 (t, *J* = 2.2 Hz, 1H, PzB4), 6.25 (t, *J* = 2.1 Hz, 1H, PzB4), 6.20 (t, *J* = 2.2 Hz, 1H, PzC4), 6.10 (d, *J* = 7.9 Hz, 1H, H6), 5.75 (dd, *J* = 4.6, 7.9 Hz, 1H, H5), 4.42 (d, *J* = 11.2 Hz, 1H, H2), 4.10 (dd, *J* = 3.9, 11.2 Hz, 1H, H2'), 2.63 (ddd, *J* = 4.6, 10.3, 12.7 Hz, 1H, H4), 2.41 (s, 3H, H11), 1.39 (d, *J* = 10.3 Hz, 1H, H3), 1.23 (d, *J*<sub>PH</sub> = 8.4 Hz, 9H, PMe<sub>3</sub>).

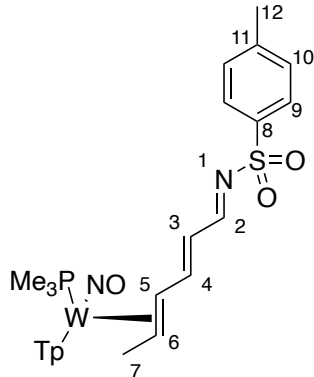
<sup>13</sup>C NMR (CD<sub>2</sub>Cl<sub>2</sub>, δ, 25 °C): 143.9 (d, *J*<sub>PC</sub> = 1.9 Hz, PzB3), 143.6 (C7), 143.4 (PzA3), 140.5 (PzC3), 136.9 (PzC5), 136.5 (PzB5), 136.4 (C10), 135.9 (PzA5), 129.9 (2C, C9), 127.9 (2C, C8), 119.3 (C6), 115.3 (d, *J*<sub>PC</sub> = 2.9 Hz, C5), 106.7 (PzB4), 106.4 (PzA4), 106.3 (PzC4), (C3 obscured behind CD<sub>2</sub>Cl<sub>2</sub>), 47.3 (C2), 46.0 (d, *J*<sub>PC</sub> = 10.7 Hz, C4), 21.7 (C11), 14.0 (d, *J*<sub>PC</sub> = 27.9 Hz, 3C PMe<sub>3</sub>).

IR:  $\nu(\text{NO}) = 1560 \text{ cm}^{-1}$

CV (DMA; 100 mV/s):  $E_{p,a} = +0.47 \text{ V (NHE)}$

SC-XRD data of **15P** on page 193

**Synthesis and characterization of WTp(NO)(PMe<sub>3</sub>)( $\eta^2$ -(*NE,3E,5E*)-(N-tosyl)-3,5-hexadien-1-ylidene) (16D)**



A 10 mL screw cap test tube was tared and charged with **6D** (76 mg, 0.09 mmol) and MeCN (3 mL). This tube was then added to a 55 °C mineral oil bath heated for 18 hours. The reaction solution was then precipitated in 80 mL of stirring Et<sub>2</sub>O, and the yellow precipitate was collected on a 15 mL F frit. The frit was then dried in the desiccator overnight. (61 mg, 80%)

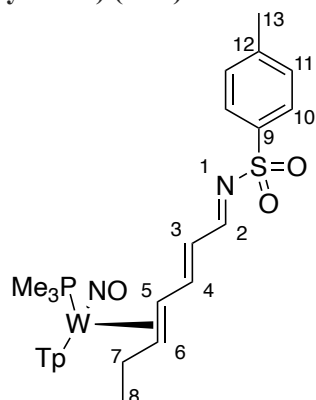
<sup>1</sup>H NMR (CDCl<sub>3</sub>,  $\delta$ , 25 °C): 8.60 (d,  $J$  = 10.1 Hz, 1H, H2), 8.02 (d,  $J$  = 1.8 Hz, 1H, PzB3), 7.99 (d,  $J$  = 1.8 Hz, 1H, PzA3), 7.81 (d,  $J$  = 8.2 Hz, 1H, H9), 7.74 (d,  $J$  = 2.2 Hz, 2H, PzB5/C5), 7.61 (d,  $J$  = 2.3 Hz, 1H, PzA5), 7.43 (d,  $J$  = 1.9 Hz, 1H, PzC3), 7.28 (d,  $J$  = 8.2 Hz, 1H, H10), 7.24 (dd,  $J$  = 11.5, 14.6 Hz, 1H, H4), 6.32 (t,  $J$  = 2.2 Hz, 1H, PzB4), 6.27 (t,  $J$  = 2.1 Hz, 1H, PzA4), 6.23 (t,  $J$  = 2.2 Hz, 1H, PzC4), 6.24 (dd,  $J$  = 10.1, 14.6 Hz, 1H, H3), 3.26 (dt,  $J$  = 7.8, 11.5 Hz, 1H, H5), 3.19 (m, 1H, H6), 2.40 (s, 3H, H12), 1.15 (d,  $J_{PH}$  = 8.3 Hz, 9H, PMe<sub>3</sub>), 1.11 (d,  $J$  = 6.6 Hz, 3H, H7).

<sup>13</sup>C NMR (CDCl<sub>3</sub>,  $\delta$ , 25 °C): 177.9 (C4), 171.1 (C2), 144.0 (PzA3), 143.7 (d,  $J_{PC}$  = 1.4 Hz, PzB3), 143.2 (C8), 141.9 (PzC3), 137.8 (C11), 136.8 (PzB5/PzC5), 136.3 (PzB5/PzC5), 135.4 (PzA4), 129.6 (C10), 127.5 (C9), 118.2 (C3), 106.9 (PzB4), 106.7 (PzA4), 106.0 (PzC4), 69.0 (d,  $J_{PC}$  = 6.3 Hz, C5), 65.7 (C6), 21.7 (C12), 17.2 (C7), 12.7 (d,  $J_{PC}$  = 27.9 Hz, PMe<sub>3</sub>).

IR:  $\nu(\text{NO})$  = 1541 cm<sup>-1</sup>

HRMS (ESI)  $m/z$ : [M]<sup>+</sup> Calcd for C<sub>25</sub>H<sub>35</sub>BN<sub>8</sub>O<sub>3</sub>PSW<sup>+</sup> 753.1887; Found 753.1887

**Synthesis and characterization of  $\text{Wtp}(\text{NO})(\text{PMe}_3)(\eta^2\text{-(NE,3E,5E)-(N-tosyl)-3,5-heptadien-1-ylidene})$  (**17D**)**

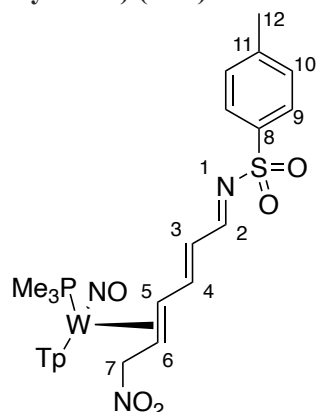


A 10 mL screw cap test tube was tared and charged with **7D** (41 mg, 0.05 mmol) and MeCN (3 mL). This tube was then added to a 55 °C mineral oil bath heated for 18 hours. The reaction solution was then precipitated in 80 mL of stirring Et<sub>2</sub>O, and the yellow precipitate was collected on a 15 mL F frit. The frit was then dried in the desiccator overnight. (15 mg, 37%)

<sup>1</sup>H NMR (CD<sub>3</sub>CN, δ, 25 °C): 8.47 (d, *J*=10.2 Hz, 1H, H2), 8.04 (d, *J*= 2.0 Hz, 1H, Tp3/5), 7.99 (d, *J*= 1.8 Hz, 1H, Tp3/5), 7.89 (d, *J*= 2.4 Hz, 1H, Tp3/5), 7.86 (d, *J*= 2.3 Hz, 1H, Tp3/5), 7.75 (d, *J*= 2.3 Hz, 1H, Tp3/5), 7.72 (d, *J*= 8.4 Hz, 2H, H10), 7.60 (d, *J*= 2.2 Hz, 1H, Tp3/5), 7.43 (dd, *J*= 11.2, 13.4 Hz, 1H, H4), 7.36 (d, *J*= 8.4 Hz, 2H, H11), 6.38 (t, *J*= 2.2 Hz, 1H, Tp4), 6.33 (t, *J*= 2.2 Hz, 1H, Tp4), 6.29 (t, *J*= 2.3 Hz, 1H, Tp4), 6.14 (dd, *J*= 10.2, 14.5 Hz, 1H, H3), 3.43 (m, 1H, H5/6), 3.10 (m, 1H, H5/6), 2.41 (s, 3H, H13), 1.12 (d, *J*= 8.6 Hz, 9H, PMe<sub>3</sub>), 0.87 (t, *J*= 5.0 Hz, 3H, H8), 0.83 (m, 1H, H7'), 0.66 (m, 1H, H7).

SC-XRD data on page 194

**Synthesis and characterization of  $WTP(NO)(PMe_3)(\eta^2-(NE,3E,5E)-(N\text{-tosyl})-(7\text{-nitro})-3,5\text{-hexadien-1-ylidene})$  (**18D**)**

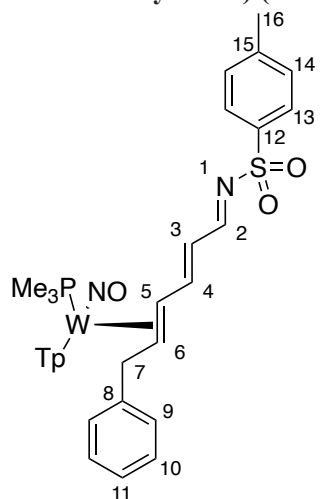


A 10 mL screw cap test tube was tared and charged with **8D** (102 mg, 0.13 mmol) and MeCN (3 mL). This tube was then added to a 55 °C mineral oil bath heated for 18 hours. The reaction solution was then precipitated in 80 mL of stirring Et<sub>2</sub>O, and the yellow precipitate was collected on a 15 mL F frit. The frit was then dried in the desiccator overnight. (80 mg, 78%)

<sup>1</sup>H NMR (CD<sub>2</sub>Cl<sub>2</sub>, δ, 25 °C): 8.58 (d, *J* = 9.9 Hz, 1H, H2), 8.05 (d, *J* = 1.9 Hz, 1H, Tp3/5), 8.04 (d, *J* = 1.9 Hz, 1H, Tp3/5), 7.83 (d, *J* = 2.3 Hz, 1H, Tp3/5), 7.82 (d, *J* = 2.4 Hz, 1H, Tp3/5), 7.76 (d, *J* = 8.3 Hz, 2H, H9), 7.70 (d, *J* = 2.4 Hz, 1H, Tp3/5), 7.53 (d, *J* = 2.1 Hz, 1H, Tp3/5), 7.33 (d, *J* = 8.3 Hz, 2H, H10), 7.27 (dd, *J* = 10.6, 14.8 Hz, 1H, H4), 6.40 (t, *J* = 2.3 Hz, 1H, Tp4), 6.36 (t, *J* = 2.3 Hz, 1H, Tp4), 6.35 (t, *J* = 2.3 Hz, 1H, Tp4), 6.27 (dd, *J* = 9.9, 14.8 Hz, 1H, H3), 3.74 (ddd, *J* = 1.4, 3.8, 12.8 Hz, 1H, H7'), 3.48 (t, *J* = 12.3, 1H, H7'), 3.40 (m, 1H, H5), 3.35 (m, 1H, H6), 2.43 (s, 3H, H12), 1.16 (d, *J*<sub>PH</sub> = 8.7 Hz, 9H, PMe<sub>3</sub>).

<sup>13</sup>C NMR (CD<sub>2</sub>Cl<sub>2</sub>, δ, 25 °C): 174.3 (C4), 171.3 (C2), 144.3 (Tp3/5), 144.2 (d, *J*<sub>PC</sub> = 1.8 Hz, Tp3/5), 144.1 (C8), 142.1 (Tp3/5), 138.0 (Tp3/5), 137.6 (C11), 137.2 (Tp3/5), 136.5 (Tp3/5), 130.0 (2C, C10), 127.7 (2C, C9), 120.2 (C3), 107.6 (Tp4), 107.5 (Tp4), 107.1 (Tp4), 82.1 (C7), 64.5 (d, *J*<sub>PC</sub> = 2.0 Hz, H5), 60.5 (d, *J*<sub>PC</sub> = 2.0 Hz, H6), 21.7 (C12), 12.7 (d, *J*<sub>PC</sub> = 28.9 Hz, 3C, PMe<sub>3</sub>).

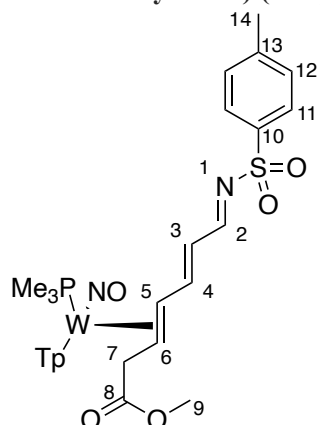
**Synthesis and characterization of  $W\text{Tp}(\text{NO})(\text{PMe}_3)(\eta^2\text{-(NE,3E,5E)-(N-tosyl)-(7-phenyl)-3,5-hexadien-1-ylidene})$  (**19D**)**



A 10 mL screw cap test tube was tared and charged with **9D** (15 mg, 0.02 mmol) and MeCN (3 mL). This tube was then added to a 55 °C mineral oil bath heated for 18 hours. The reaction solution was then precipitated in 80 mL of stirring Et<sub>2</sub>O, and the yellow precipitate was collected on a 15 mL F frit. The frit was then dried in the desiccator overnight. (NMR)

<sup>1</sup>H NMR (CD<sub>2</sub>Cl<sub>2</sub>, δ, 25 °C): 8.51 (d, *J* = 10.1 Hz, 1H, H2), 8.04-8.05 (m, 2H, Tp3/5), 7.81-7.83 (m, 2H, Tp3/5), 7.72-7.75 (m, 3H, H13 & Tp3/5), 7.31 (d, *J* = 7.9 Hz, 2H, H14), 7.27 (dd, *J* = 11.6, 14.6 Hz, 1H, H4), 7.17 (t, *J* = 7.4 Hz, 2H, H10), 7.06 (t, *J* = 7.4 Hz, 1H, H11), 6.99 (d, *J* = 7.4 Hz, 2H, H9), 6.38 (t, *J* = 2.1 Hz, 1H, Tp4), 6.37 (t, *J* = 2.2 Hz, 1H, Tp4), 6.30 (t, *J* = 2.2 Hz, 1H, Tp4), 6.20 (dd, *J* = 10.1, 14.6 Hz, 1H, H3), 3.39-3.43 (m, 1H, H5), 3.27-3.31 (m, 1H, H6), 2.42 (s, 3H, H11), 2.12 (d, *J* = 14.8 Hz, 1H, H7), 1.93 (dd, *J* = 11.2, 14.8 Hz, 1H, H7), 1.18 (d, *J*<sub>PH</sub> = 8.5 Hz, 9H, PMe<sub>3</sub>). (15% **9P** is present)

**Synthesis and characterization of WTp(NO)(PMe<sub>3</sub>)( $\eta^2$ -(*NE,3E,5E*)-(N-tosyl)-(7-methylester)-3,5-hexadien-1-ylidene) (20D)**



A 10 mL screw cap test tube was tared and charged with **10D** (30 mg, 0.10 mmol) and MeCN (3 mL). This tube was then added to a 55 °C mineral oil bath heated for 18 hours. The reaction solution was then precipitated in 80 mL of stirring Et<sub>2</sub>O, and the yellow precipitate was collected on a 15 mL F frit. The frit was then dried in the desiccator overnight. (22 mg, 73%)

<sup>1</sup>H NMR (CD<sub>3</sub>CN,  $\delta$ , 25 °C): 8.50 (d,  $J$  = 10.1 Hz, 1H, H2), 8.05 (d,  $J$  = 2.0 Hz, 1H, PzB3), 8.00 (d,  $J$  = 2.0 Hz, 1H, PzA3), 7.90 (d,  $J$  = 2.4 Hz, 1H, PzA5), 7.89 (d,  $J$  = 2.4 Hz, 1H, PzC5), 7.77 (d,  $J$  = 2.3 Hz, 1H, PzB5), 7.73 (d,  $J$  = 8.2 Hz, 2H, H11), 7.63 (d,  $J$  = 2.2 Hz, 1H, PzC3), 7.43 (dd,  $J$  = 10.6, 14.6 Hz, 1H, H4), 7.37 (d,  $J$  = 8.2 Hz, 2H, H12), 6.40 (t,  $J$  = 2.2 Hz, 1H, PzB4), 6.34 (t,  $J$  = 2.3 Hz, 1H, PzA4), 6.32 (t,  $J$  = 2.2 Hz, 1H, PzC4), 6.14 (dd,  $J$  = 10.1, 14.6 Hz, 1H, H3), 3.47 (s, 3H, H9), 3.41 (m, 1H, H5), 3.22 (m, 1H, H6), 2.41 (s, 3H, H14), 1.68 (dd,  $J$  = 3.5, 15.6 Hz, 1H, H7'), 1.59 (dd,  $J$  = 11.1, 15.6 Hz, 1H, H7), 1.12 (d,  $J_{PH}$  = 8.7 Hz, 9H, PMe<sub>3</sub>).

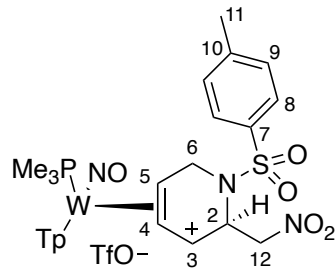
<sup>13</sup>C NMR (CD<sub>3</sub>CN,  $\delta$ , 25 °C): 177.8 (C8), 177.5 (C4), 172.0 (C2), 144.9 (d,  $J_{PC}$  = 1.9 Hz, PzB3), 144.7 (PzA3), 144.6 (C10), 143.6 (PzC3), 139.0 (C13), 138.4 (PzC5), 137.8 (PzA5), 137.1 (PzB5), 130.7 (2C, C12), 127.9 (2C, C11), 117.7 (C3), 108.0 (PzA4), 107.9 (PzB4), 107.3 (PzC4), 67.0 (d,  $J_{PC}$  = 6.2 Hz, C5), 63.9 (C6), 51.8 (C9), 37.9 (C7), 21.6 (C14), 12.8 (d,  $J_{PC}$  = 29.0 Hz, 3C, PMe<sub>3</sub>).

IR:  $\nu(\text{NO}) = 1531 \text{ cm}^{-1}$

CV (DMA; 100 mV/s):  $E_{p,a} = +0.85 \text{ V (NHE)}$

HRMS (ESI)  $m/z$ : [M]<sup>+</sup> Calcd for C<sub>27</sub>H<sub>37</sub>BN<sub>8</sub>O<sub>5</sub>PSW<sup>+</sup> 811.1942; Found 811.1947

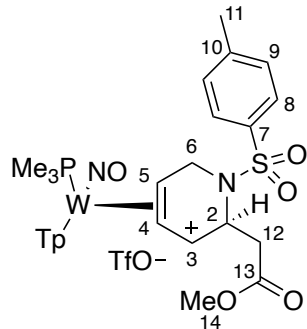
### Synthesis and characterization of $W Tp(NO)(PMe_3)(\eta^3\text{-}(N\text{-tosyl)-2-(nitromethyl)-1,2,3,6-tetrahydropyridinium (OTf) (21)$



An oven-dried 4-dram vial containing a stir pea was tared, and **8D** (742 mg, 0.93 mmol) was massed out and diluted with DCM (5 mL). To a separate 4-dram vial was added DCM (1 mL) and TfOH (131 mg, 0.87 mmol). The acid/DCM solution was slowly added to the **8D**/DCM solution and stirred for 2 minutes. The reaction was then slowly added to 100 mL of stirring Et<sub>2</sub>O, which immediately formed a tan precipitate. This powder was triturated for 5 minutes and then collected on a 30 mL medium porosity frit. The collected powder was then washed 2x with 20 mL of Et<sub>2</sub>O and dried overnight in a desiccator. (842 mg, 96% yield)

<sup>1</sup>H NMR (CD<sub>3</sub>CN,  $\delta$ , 25 °C): 8.45 (d,  $J$  = 2.2 Hz, 1H, Tp3/5), 8.13 (d,  $J$  = 2.3 Hz, 1H, Tp3/5), 8.03 (d,  $J$  = 2.4 Hz, 1H, Tp3/5), 7.97 (d,  $J$  = 2.3 Hz, 1H, Tp3/5), 7.95 (d,  $J$  = 2.2 Hz, 1H, Tp3/5), 7.82 (d,  $J$  = 2.4 Hz, 1H, Tp3/5), 7.80 (d,  $J$  = 8.3 Hz, 2H, H8), 7.43 (d,  $J$  = 8.3 Hz, 2H, H9), 6.54 (m, 2H, Tp4), 6.35 (t,  $J$  = 2.3 Hz, 1H, Tp4), 5.84 (d,  $J$  = 7.4 Hz, 1H, H3), 5.61 (s, 1H, H2), 5.26 (t,  $J$  = 7.7 Hz, 1H, H4), 4.99-4.93 (m, 2H, H12), 4.50-4.55 (m, 2H, HH5 & H6), 4.20 (d,  $J$  = 11.9 Hz, 1H, H6), 2.44 (s, 3H, H11), 1.22 (d,  $J_{PH}$  = 10.0 Hz, 9H, PMe<sub>3</sub>).

**Synthesis and characterization of WTp(NO)(PMe<sub>3</sub>)( $\eta^3$ -(*N*-tosyl)-2-(methylacetate)-1,2,3,6-tetrahydropyridinium (OTf) (22)**

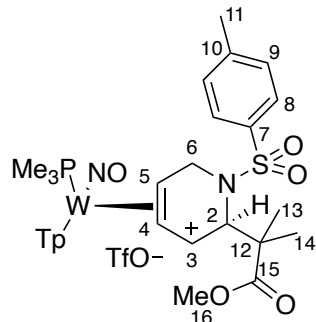


An oven-dried 4-dram vial containing a stir pea was tared, and **10D** (486 mg, 0.60 mmol) was massed out and diluted with dried MeCN (2 mL). To a separate 4-dram vial was added dried MeCN (1 mL) and TfOH (112 mg, 0.75 mmol). The acid/MeCN solution was slowly added to the **10D**/MeCN solution and stirred for 2 minutes. The reaction was then slowly added to 100 mL of stirring Et<sub>2</sub>O, which immediately formed a tan precipitate. This powder was triturated for 5 minutes and then collected on a 30 mL medium porosity frit. The collected powder was then washed 2x with 20 mL of Et<sub>2</sub>O and dried overnight in a desiccator. (499 mg, 87% yield)

<sup>1</sup>H NMR (CD<sub>2</sub>Cl<sub>2</sub>,  $\delta$ , 25 °C): 8.40 (d,  $J$  = 2.1 Hz, 1H, Tp3/5), 8.14 (d,  $J$  = 2.2 Hz, 2H, Tp3/5), 7.92 (d,  $J$  = 2.2 Hz, 1H, Tp3/5), 7.86 (d,  $J$  = 2.4 Hz, 1H, Tp3/5), 7.69-7.72 (m, 3H, Tp3/5 & H8), 7.38 (d,  $J$  = 8.2 Hz, 2H, H9), 6.57 (t,  $J$  = 2.3 Hz, 1H, Tp4), 6.53 (t,  $J$  = 2.4 Hz, 1H, Tp4), 6.35 (t,  $J$  = 2.3 Hz, 1H, Tp4), 6.18 (dt,  $J$  = 3.1, 7.8 Hz, 1H, H3), 5.53 (dt,  $J$  = 3.1, 10.0 Hz, 1H, H2), 5.07 (t,  $J$  = 7.8 Hz, 1H, H4), 4.60 (dd,  $J$  = 1.9, 12.8 Hz, 1H, H6), 4.57 (m, 1H, H5), 4.14 (dd,  $J$  = 1.9, 12.8 Hz, 1H, H6'), 3.61 (s, 3H, H14), 3.11 (dd,  $J$  = 3.1, 16.9 Hz, 1H, H12), 2.62 (dd,  $J$  = 10.0, 16.9 Hz, 1H, H12'), 2.45 (s, 3H, H11), 1.28 (d,  $J_{PH}$  = 9.7 Hz, 9H, PMe<sub>3</sub>).



**Synthesis and characterization of WTp(NO)(PMe<sub>3</sub>)( $\eta^3$ -(*N*-tosyl)-2-( $\alpha,\alpha$ -dimethyl-methylacetate)-1,2,3,6-tetrahydropyridinium (OTf) (23)**



An oven-dried 4-dram vial containing a stir pea was tared, and **11D** (502 mg, 0.60 mmol) was massed out and diluted with dried DCM (8 mL). To a separate 4-dram vial was added DCM (2 mL) and TfOH (109 mg, 0.72 mmol). The acid/DCM solution was slowly added to the **11D**/DCM solution and stirred for 2 minutes. The reaction was then slowly added to 100 mL of stirring Et<sub>2</sub>O, which immediately formed a tan precipitate. This powder was triturated for 5 minutes and then collected on a 30 mL medium porosity frit. The collected powder was then washed 2x with 20 mL of Et<sub>2</sub>O and dried overnight in a desiccator. (533 mg, 89% yield)

<sup>1</sup>H NMR (CD<sub>3</sub>CN,  $\delta$ , 25 °C): 8.48 (d,  $J$  = 2.2 Hz, 1H, PzC3), 8.04 (d,  $J$  = 2.3 Hz, 1H, PzB5), 8.01 (d,  $J$  = 2.2 Hz, 1H, PzA3), 7.99 (d,  $J$  = 2.3 Hz, 1H, PzB3), 7.96 (d,  $J$  = 2.5 Hz, 1H, PzC5), 7.82 (d,  $J$  = 2.4 Hz, 1H, PzA5), 7.75 (d,  $J$  = 8.3 Hz, 2H, H8), 7.39 (d,  $J$  = 8.3 Hz, 2H, H9), 6.56 (t,  $J$  = 2.3 Hz, 1H, PzC4), 6.53 (t,  $J$  = 2.4 Hz, 1H, PzB4), 6.37 (t,  $J$  = 2.4 Hz, 1H, PzA4), 5.83 (m,  $J$  = 8.0 Hz, 1H, H3), 5.79 (m,  $J$  = 2.6 Hz, 1H, H2), 5.24 (t,  $J$  = 8.0 Hz, 1H, H4), 4.80 (dd,  $J$  = 2.2, 13.7 Hz, 1H, H6), 4.48 (d,  $J$  = 13.7, 1H, H6), 4.30 (m, 1H, H5), 3.70 (s, 3H, H16), 2.43 (s, 3H, H11), 1.23 (m, 12H, PMe<sub>3</sub>/H14), 1.05 (s, 3H, H14).

<sup>13</sup>C NMR (CD<sub>3</sub>CN,  $\delta$ , 25 °C): 176.7 (C15), 148.0 (PzA3), 145.4 (d,  $J_{PC}$  = 2.2 Hz, PzC3), 144.6 (C7), 143.0 (PzB3), 140.5 (C10), 139.9 (PzA/B/C5), 139.8 (PzA/B/C5), 139.6 (PzA/B/C5), 130.6 (2C, C9), 127.7 (2C, C8), 121.0 (C3), 109.4 (PzC4), 109.2 (PzB4), 108.5 (PzA4), 98.4 (C4), 66.7 (d,  $J_{PC}$  = 14.2 Hz, C5), 60.4 (C2), 53.1 (C16), 52.1 (C12), 45.7 (d,  $J_{PC}$  = 2.2 Hz, C6), 26.2 (C13), 21.5 (C11), 21.0 (C14), 13.4 (d,  $J_{PC}$  = 33.1, 3C, PMe<sub>3</sub>).

IR:  $\nu$ (NO) = 1661 cm<sup>-1</sup>

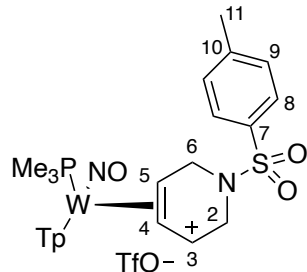
CV (MeCN; 100 mV/s):  $E_{p,c}$  = -0.72 V (NHE)

HRMS (ESI)  $m/z$  [M]<sup>+</sup> for C<sub>29</sub>H<sub>41</sub>BN<sub>8</sub>O<sub>5</sub>PSW<sup>+</sup>

Calcd: 839.2255

Found: 839.2250

**Synthesis and characterization of WTp(NO)(PMe<sub>3</sub>)(η<sup>3</sup>-(*N*-tosyl)-1,2,3,6-tetrahydropyridinium (OTf) (24)**



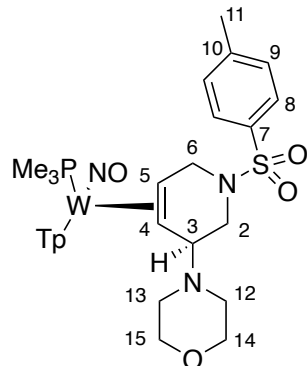
An oven-dried 4-dram vial containing a stir pea was tared, and **15D** (215 mg, 0.29 mmol) was massed out and diluted with dried MeCN (3 mL). To a separate 4-dram vial was added dried MeCN (1 mL) and TfOH (100 mg, 0.67 mmol). The acid/MeCN solution was slowly added to the **15D**/MeCN solution and stirred for 2 minutes. The reaction was then slowly added to 100 mL of stirring Et<sub>2</sub>O, which immediately formed a tan precipitate. This powder was triturated for 5 minutes and then collected on a 30 mL medium porosity frit. The collected powder was then washed 2x with 20 mL of Et<sub>2</sub>O and dried overnight in a desiccator. (222 mg, 86% yield)

<sup>1</sup>H NMR (CD<sub>2</sub>Cl<sub>2</sub>, δ, 25 °C): 8.38 (d, J = 2.1 Hz, 1H, PzB3), 8.10 (d, J = 2.2 Hz, 1H, PzC3), 7.96 (d, J = 2.2 Hz, 1H, PzA3), 7.93 (d, J = 2.3 Hz, 1H, PzC5), 7.86 (d, J = 2.4 Hz, 1H, PzB5), 7.69 (m, 3H, PzA5 & H8), 7.40 (d, J = 7.9 Hz, 2H, H9), 6.56 (t, J = 2.3 Hz, 1H, PzC4), 6.52 (t, J = 2.4 Hz, 1H, PzB4), 6.33 (m, 1H, H3), 6.31 (t, J = 2.4 Hz, 1H, PzA4), 4.95 (d, J = 7.9 Hz, 1H, H4), 4.93 (m, 1H, H2), 4.33 (m, 1H, H5), 4.31 (m, 1H, H6), 4.10 (d, J = 18.0 Hz, 1H, H2), 4.00 (dd, J = 2.2, 12.2 Hz, 1H, H6), 2.45 (s, 3H, H11), 1.30 (d, J = 9.6 Hz, 9H, PMe<sub>3</sub>).

<sup>13</sup>C NMR (CD<sub>2</sub>Cl<sub>2</sub>, δ, 25 °C): 147.8 (PzA3), 144.9(C7), 144.8 (d, J<sub>PC</sub> = 2.3 Hz, PzB3), 142.8 (PzC3), 139.0 (PzA5), 138.8 (PzC5), 138.6 (PzB5), 133.2 (C10), 130.4 (2C, C9), 127.8 (2C, C8), 126.9 (C3), 108.9 (2C, PzB4 & PzC4), 107.7 (PzA4), 94.9 (d, J<sub>PC</sub> = 2.8 Hz, C4), 65.7 (d, J<sub>PC</sub> = 15.3 Hz, C5), 44.8 (C2), 44.1 (d, J<sub>PC</sub> = 2.9 Hz, C6), 21.7 (C11), 13.5 (d, J<sub>PC</sub> = 32.7 Hz, 3C, PMe<sub>3</sub>).

IR: ν(NO) = 1651 cm<sup>-1</sup>

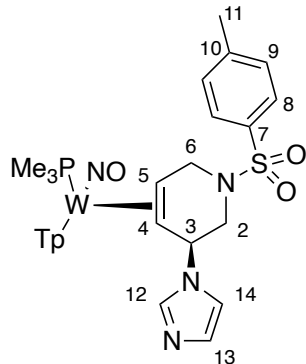
## Synthesis and characterization of $W\text{Tp}(\text{NO})(\text{PMe}_3)(\eta^2\text{-}(N\text{-tosyl})\text{-}(3\text{-morpholino})\text{-}1,2,3,6\text{-tetrahydropyridine (25)}$



A 10 mL screw cap test tube was charged with **24** (361 mg, 0.49 mmol) and MeCN (3 mL). A separate 10 mL screw cap test tube was charged with morpholine (408 mg, 4.68 mmol) and MeCN (1 mL). After chilling both tubes in a  $-40\text{ }^{\circ}\text{C}$  toluene bath for 15 minutes, the morpholine/MeCN solution was added to the **24**/MeCN solution, and the combined solution was chilled in the bath for 16 hours. A 2.0 M THF solution of NaOtBu (0.55 mL, 1.1 mmol) was then added to the solution to quench the reaction. The solution was diluted with 150 mL of DCM and added to a separatory funnel. This solution was washed 3x with 200 mL of saturated aqueous  $\text{Na}_2\text{CO}_3$ . The organic layer was isolated and set aside. The combined aqueous layers were combined and back extracted with 50 mL of DCM to prevent product loss. The organic layers were combined in a single flask and dried with anhydrous  $\text{MgSO}_4$ . This powder was then filtered off into a 60 mL coarse porosity fritted funnel and washed with DCM. The dried organic layers were then reduced *in vacuo* to dryness. The residue in the flask was redissolved in minimal DCM (approximately 5 mL). The solution was then slowly added to 100 mL of stirring pentane. A tan precipitate formed immediately and was allowed to stir for  $\sim 10$  minutes to ensure total precipitation. This powder was collected on a 60 mL medium porosity frit and washed 2x with 30 mL of pentane. This powder was dried in a desiccator under vacuum for  $\sim 30$  minutes (322 mg, 80% yield).

$^1\text{H}$  NMR ( $\text{CD}_3\text{CN}$ ,  $\delta$ ,  $25\text{ }^{\circ}\text{C}$ ): 8.24 (d,  $J = 2.1$  Hz, 1H, Tp3/5), 7.96 (d,  $J = 2.1$  Hz, 1H, Tp3/5), 7.84 (d,  $J = 2.4$  Hz, 1H, Tp3/5), 7.81 (d,  $J = 2.3$  Hz, 1H, Tp3/5), 7.74 (d,  $J = 2.4$  Hz, 1H, Tp3/5), 7.69 (d,  $J = 8.3$  Hz, 2H, H8), 7.38 (d,  $J = 8.3$  Hz, 2H, H9), 7.36 (d,  $J = 2.2$  Hz, 1H, Tp3/5), 6.34 (t,  $J = 2.3$  Hz, 1H, Tp4), 6.26 (t,  $J = 2.3$  Hz, 1H, Tp4), 6.23 (t,  $J = 2.3$  Hz, 1H, Tp4), 4.45 (ddd,  $J = 1.9, 8.9, 11.4$  Hz, 1H, H6), 3.94 (s, 1H, H3), 3.72 (d,  $J = 11.9$  Hz, 2H, H14), H15s obscured under solvent, 3.32 (dd,  $J = 6.0, 11.4$  Hz, 1H, H6), 2.98 (m, 1H, H5), 2.90 (ddd,  $J = 2.7, 6.3, 11.7$  Hz, 2H, H12), H2 and H13s obscured under solvent, 2.64 (dd,  $J = 4.4, 11.7$  Hz, 1H, H2), 2.40 (s, 3H, H11), 1.08 (d,  $J_{\text{PH}} = 8.4$  Hz, 9H,  $\text{PMe}_3$ ), 0.97 (d,  $J = 11.5$  Hz, 1H, H4).

## Synthesis and characterization of WTp(NO)(PMe<sub>3</sub>)(η<sup>2</sup>-(*N*-tosyl)-(3-imidazolyl)-1,2,3,6-tetrahydropyridine (26)



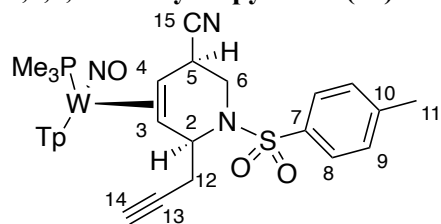
A 10 mL screw cap test tube was charged with **24** (135 mg, 0.15 mmol) and MeCN (3 mL). A separate 10 mL screw cap test tube was charged with imidazole (95 mg, 1.40 mmol) and MeCN (1 mL). After chilling both tubes in a -30 °C toluene bath for 15 minutes, the imidazole/MeCN solution was added to the **24**/MeCN solution, and the combined solution was chilled in the bath for 16 hours. A 2.0 M THF solution of NaOtBu (0.1 mL, 0.2 mmol) was then added to the solution to quench the reaction. The solution was diluted with 150 mL of DCM and added to a separatory funnel. This solution was washed 3x with 200 mL of saturated aqueous Na<sub>2</sub>CO<sub>3</sub>. The organic layer was isolated and set aside. The combined aqueous layers were combined and back extracted with 50 mL of DCM to prevent product loss. The organic layers were combined in a single flask and dried with anhydrous MgSO<sub>4</sub>. This powder was then filtered off into a 60 mL coarse porosity fritted funnel and washed with DCM. The dried organic layers were then reduced *in vacuo* to dryness. The residue in the flask was redissolved in minimal DCM (approximately 5 mL). The solution was then slowly added to 100 mL of stirring pentane. A tan precipitate formed immediately and was allowed to stir for ~10 minutes to ensure total precipitation. This powder was collected on a 60 mL medium porosity frit and washed 2x with 30 mL of pentane. This powder was dried in a desiccator under vacuum for ~30 minutes (63 mg, 51% yield).

<sup>1</sup>H NMR (CD<sub>2</sub>Cl<sub>2</sub>, δ, 25 °C): 7.96 (s, 1H, Tp3/5), 7.88 (s, 1H, Tp3/5), 7.79 (s, 1H, H12), 7.76 (d, *J* = 2.1 Hz, 1H, Tp3/5), 7.70 (d, *J* = 1.9 Hz, 1H, Tp3/5), 7.66 (d, *J* = 2.0 Hz, 1H, Tp3/5), 7.63 (d, *J* = 7.9 Hz, 2H, H8), 7.32-7.34 (m, 3H, H9 & H14), 7.25 (s, 1H, Tp3/5), 6.98 (s, 1H, H13), 6.33 (s, 1H, Tp4), 6.23 (s, 1H, Tp4), 6.20 (s, 1H, Tp4), 5.36 (s, 1H, H3), 4.72 (t, *J* = 10.6 Hz, 1H, H6), 3.62-3.66 (m, 2H, H2 & H6), 3.20 (dd, *J* = 2.9, 12.1 Hz, 1H, H2), 3.00-3.06 (m, 1H, H5), 2.42 (s, 3H, H11), 1.18 (d, *J* = 11.3 Hz, 1H, H4), 1.13 (d, *J*<sub>PH</sub> = 8.3 Hz, 9H, PMe<sub>3</sub>).

<sup>13</sup>C NMR (CD<sub>2</sub>Cl<sub>2</sub>, δ, 25 °C): 143.9 (C7), 143.7 (Tp3/5), 142.3 (Tp3/5), 140.6 (Tp3/5), 137.2 (Tp3/5), 136.8 (Tp3/5), 136.7 (Tp3/5), 136.5 (C12), 135.5 (C10), 129.9 (2C, C9), 128.5 (C13), 128.0 (2C, C8), 118.8 (C14), 107.0 (Tp4), 106.6 (Tp4), 106.4 (Tp4), 58.4 (C3), 52.9 (C4), 50.6 (C2), 49.5 (d, *J*<sub>PC</sub> = 3.2 Hz, C6), 46.7 (d, *J*<sub>PC</sub> = 12.8 Hz, C5), 21.7 (C11), 14.06 (d, *J*<sub>PC</sub> = 27.9 Hz, 3C, PMe<sub>3</sub>).

IR: ν(NO) = 1545 cm<sup>-1</sup>  
 CV (DMA; 100 mV/s): *E*<sub>p,a</sub> = +0.79 V (NHE)

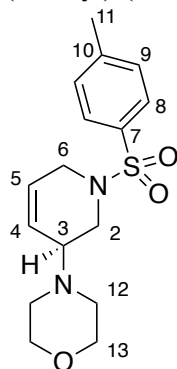
**Synthesis and characterization of WTp(NO)(PMe<sub>3</sub>)( $\eta^2$ -(*N*-tosyl)-(2-propargyl)-(5-carbonitrile)-1,2,5,6-tetrahydropyridine (27)**



A 10 mL screw cap test tube was charged with **13D** (350 mg, 0.45 mmol) and MeCN (3 mL). A separate 10 mL screw cap test tube was charged with MeCN (1 mL) and HOTf (101 mg, 0.67 mmol). The acidic solution was added to the **13D**/MeCN solution, and the combined solution was swirled and added to a -40 °C toluene bath. A separate 10 mL screw cap test tube was charged with NaCN (160 mg, 3.26 mmol) and MeOH (1 mL). After chilling both tubes in a -40 °C toluene bath for 15 minutes, the NaCN/MeOH solution was added to the [W]/MeCN solution, and the combined solution was chilled in the bath for 3 hours. The solution was diluted with 150 mL of DCM and added to a separatory funnel. This solution was washed 3x with 200 mL of saturated aqueous NaHCO<sub>3</sub>. The organic layer was isolated and set aside. The combined aqueous layers were combined and back extracted with 50 mL of DCM to prevent product loss. The organic layers were combined in a single flask and dried with anhydrous MgSO<sub>4</sub>. This powder was then filtered off into a 60 mL coarse porosity fritted funnel and washed with DCM. The dried organic layers were then reduced *in vacuo* to dryness. The residue in the flask was redissolved in minimal DCM (approximately 5 mL). The solution was then slowly added to 100 mL of stirring pentane. A tan precipitate formed immediately and was allowed to stir for ~10 minutes to ensure total precipitation. This powder was collected on a 60 mL medium porosity frit and washed 2x with 30 mL of pentane. This powder was dried in a desiccator under vacuum for ~30 minutes (250 mg, 69% yield).

<sup>1</sup>H NMR (CD<sub>3</sub>CN,  $\delta$ , 25 °C): 8.02 (d,  $J$  = 2.0 Hz, 1H, Tp3/5), 7.86 (d,  $J$  = 2.4 Hz, 1H, Tp3/5), 7.84 (d,  $J$  = 2.3 Hz, 1H, Tp3/5), 7.82 (d,  $J$  = 8.4 Hz, 2H, H8), 7.76 (d,  $J$  = 2.4 Hz, 1H, Tp3/5), 7.68 (d,  $J$  = 1.9 Hz, 1H, Tp3/5), 7.38 (d,  $J$  = 8.0 Hz, 2H, H9), 7.37 (d,  $J$  = 2.2 Hz, 1H, Tp3/5), 6.37 (t,  $J$  = 2.1 Hz, 1H, Tp4), 6.28 (t,  $J$  = 2.3 Hz, 1H, Tp4), 6.26 (t,  $J$  = 2.3 Hz, 1H, Tp4), 4.72 (d,  $J$  = 8.8 Hz, 1H, C2), 3.84-3.89 (m, 2H, H5 & H6), 2.80 (ddd,  $J$  = 3.4, 11.6, 12.7 Hz, 1H, H6), 2.66 (ddd,  $J$  = 2.8, 9.0, 16.3 Hz, 1H, H12), 2.53 (dt,  $J$  = 2.8, 16.3 Hz, 1H, H12), 2.40-2.42 (m, 1H, H4), 2.40 (s, 3H, H11), 1.80 (t,  $J$  = 2.8 Hz, 1H, H14), 1.20 (d,  $J_{PH}$  = 8.5 Hz, 9H, PMe<sub>3</sub>), 1.09 (d,  $J$  = 11.7 Hz, 1H, H3)

**(*N*-tosyl)-(3-morpholino)-1,2,3,6-tetrahydropyridine (28)**

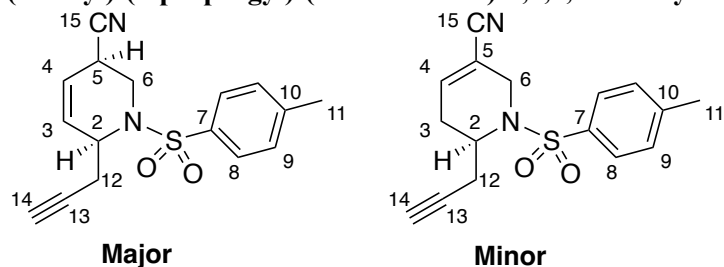


A 4-dram vial was charged with **24** (322 mg, 0.39 mmol), acetone (3 mL), and a stir pea. DDQ was then added (92 mg, 0.41 mmol), and the solution was stirred for 2 hours. The solution was diluted with 50 mL of DCM and added to a separatory funnel. This solution was washed 3x with 200 mL of saturated aqueous NaHCO<sub>3</sub>. The organic layer was isolated and set aside. The combined aqueous layers were combined and back extracted with 30 mL of DCM to prevent product loss. The organic layers were combined in a single flask and dried with anhydrous MgSO<sub>4</sub>. This powder was then filtered off into a 60 mL coarse porosity fritted funnel and washed with DCM. The dried organic layers were then reduced *in vacuo* to dryness. The solution was then slowly added to a 4:1 100 mL solution of stirring pentane/Et<sub>2</sub>O. A tan precipitate formed immediately and was allowed to stir for ~10 minutes to ensure total precipitation. This powder was collected on a 60 mL medium porosity frit and washed 2x with 30 mL of Et<sub>2</sub>O before being set aside. The filtrate was reduced in vacuum with silica powder and loaded onto a Combiflash powder cartridge. The obtained organic was eluted through a 12 g silica column with 60% ethyl acetate in hexanes. The combined fractions were then reduced to a pale yellow oil. (99 mg, 79% yield).

<sup>1</sup>H NMR (CDCl<sub>3</sub>, δ, 25 °C): 7.66 (d, *J* = 8.2 Hz, 2H, H8), 7.32, (d, *J* = 8.2 Hz, 2H, H9), 5.83 (dq, *J* = 3.2, 5.2, 8.5, 10.2 Hz, 1H, H5), 5.77 (dq, *J* = 2.2, 5.1, 7.3, 10.2 Hz, 1H, H4), 3.67 (m, 4H, H13), 3.50 (q, *J* = 2.5, 5.2, 7.9 Hz, 2H, H6), 3.29 (m, 1H, H3), 3.18 (ddd, *J* = 5.1, 11.7, 28.3 Hz, 2H, H2), 2.63 (m, 4H, H12), 2.42 (s, 3H, H11).

<sup>13</sup>C NMR (CDCl<sub>3</sub>, δ, 25 °C): 143.8 (C7), 133.0 (C10), 129.8 (C9), 127.8 (C8), 126.5 (C4), 125.9 (C5), 67.5 (C13), 58.5 (C3), 49.6 (C12), 44.9 (C6), 43.5 (C2), 21.6 (C11).

**(*N*-tosyl)-(2-propargyl)-(5-carbonitrile)-1,2,5,6-tetrahydropyridine (29)**



A 4-dram vial was charged with **27** (250 mg, 0.31 mmol), MeCN (3 mL), and a stir pea. DDQ was then added (80 mg, 0.35 mmol), and the solution was stirred for 2 hours. The solution was diluted with 50 mL of DCM and added to a separatory funnel. This solution was washed 3x with 200 mL of saturated aqueous NaHCO<sub>3</sub>. The organic layer was isolated and set aside. The combined aqueous layers were combined and back extracted with 30 mL of DCM to prevent product loss. The organic layers were combined in a single flask and dried with anhydrous MgSO<sub>4</sub>. This powder was then filtered off into a 60 mL coarse porosity fritted funnel and washed with DCM. The dried organic layers were then reduced *in vacuo* to dryness. The solution was then slowly added to a 4:1 100 mL solution of stirring pentane/Et<sub>2</sub>O. A tan precipitate formed immediately and was allowed to stir for ~10 minutes to ensure total precipitation. This powder was collected on a 60 mL medium porosity frit and washed 2x with 30 mL of Et<sub>2</sub>O before being set aside. The filtrate was reduced in vacuum with basic alumina powder and loaded onto a Combiflash powder cartridge. The obtained organic was eluted through an 8 g basic alumina column with 70% ethyl acetate in hexanes. The combined fractions were then reduced to a pale yellow oil. (43 mg, 46% yield).

<sup>1</sup>H NMR (CDCl<sub>3</sub>, δ, 25 °C):

**Major:** 7.70 (d, *J* = 8.2 Hz, 2H, H8), 7.32 (d, *J* = 8.2 Hz, 2H, H9), 6.05 (ddd, *J* = 3.1, 3.7, 10.3, 1H, H3), 5.80 (dq, *J* = 1.7, 10.2 Hz, 1H, H4), 4.54 (m, 1H, H2), 4.11 (dd, *J* = 5.7, 14.3 Hz, 1H, H6), 3.42 (dd, *J* = 10.9, 14.2 Hz, 1H, H6'), 3.10 (m, 1H, H5), 2.55 (m, 2H, H12), 2.44 (s, 3H, H11), 2.07 (t, *J* = 2.7 Hz, 1H, H14).

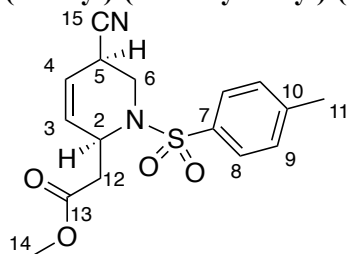
**Minor:** 7.70 (d, *J* = 8.4 Hz, 2H, H8), 7.32 (d, *J* = 8.1 Hz, 2H, H9), 6.58-6.60 (m, 1H, H4), 4.35 (dt, *J* = 5.9, 9.4 Hz, 1H, H2), 4.32 (d, *J* = 18.1 Hz, 1H, H3), 3.65 (d, *J* = 17.9 Hz, 1H, H3), 2.44 (s, 3H, H11), 2.41-2.43 (m, 1H, H6), 2.33-2.39 (m, 1H, H6), 2.29 (ddd, *J* = 2.7, 9.5, 16.6 Hz, 1H, H12), 2.25 (ddd, *J* = 2.7, 5.7, 16.6 Hz, 1H, H12), 2.00 (t, *J* = 2.7 Hz, 1H, H14).

<sup>13</sup>C NMR (CDCl<sub>3</sub>, δ, 25 °C):

**Major:** 144.5 (C7), 137.1 (C10), 130.3 (C9), 129.8 (C3), 127.1 (C8), 121.9 (C4), 117.9 (C15), 79.5 (C13), 72.3 (C14), 51.1 (C2), 41.0 (C6), 25.4 (C5), 25.0 (C12), 21.5 (C11).

**Minor:** 144.4 (C7), 141.5 (C4), 136.4 (C10), 130.2 (2C, C9), 127.2 (2C, C8), 116.5 (C5), 109.5 (C15), 79.4 (C13), 71.8 (C14), 48.5 (C2), 40.5 (C3), 27.8 (C11), 21.5 (C12).

**(*N*-tosyl)-(2-methylacetyl)-(5-carbonitrile)-1,2,5,6-tetrahydropyridine (30)**



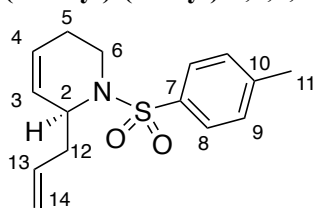
A 10 mL screw cap test tube was charged with **10D** (225 mg, 0.28 mmol) and MeCN (3 mL). A separate 10 mL screw cap test tube was charged with MeCN (1 mL) and HOTf (51 mg, 0.34 mmol). The acidic solution was added to the **10D**/MeCN solution, and the combined solution was swirled and added to a -40 °C toluene bath. A separate 10 mL screw cap test tube was charged with NaCN (51 mg, 1.04 mmol) and MeOH (1 mL). After chilling both tubes in a -40 °C toluene bath for 15 minutes, the NaCN/MeOH solution was added to the [W]/MeCN solution, and the combined solution was chilled in the bath for 3 hours. The solution was diluted with 150 mL of DCM and added to a separatory funnel. This solution was washed 3x with 200 mL of saturated aqueous NaHCO<sub>3</sub>. The organic layer was isolated and set aside. The combined aqueous layers were combined and back extracted with 50 mL of DCM to prevent product loss. The organic layers were combined in a single flask and dried with anhydrous MgSO<sub>4</sub>. This powder was then filtered off into a 60 mL coarse porosity fritted funnel and washed with DCM. The dried organic layers were then reduced *in vacuo* to dryness. The residue in the flask was redissolved in minimal acetone (approximately 5 mL) and added to a 4-dram vial w/stir pea. This vial was removed from the glovebox, DDQ was then added (100 mg, 0.44 mmol), and the solution was stirred for 2 hours. The solution was diluted with 50 mL of DCM and added to a separatory funnel. This solution was washed 3x with 200 mL of saturated aqueous NaHCO<sub>3</sub>. The organic layer was isolated and set aside. The combined aqueous layers were combined and back extracted with 30 mL of DCM to prevent product loss. The organic layers were combined in a single flask and dried with anhydrous MgSO<sub>4</sub>. This powder was then filtered off into a 60 mL coarse porosity fritted funnel and washed with DCM. The dried organic layers were then reduced *in vacuo* to dryness. The solution was then slowly added to a 4:1 100 mL solution of stirring pentane/Et<sub>2</sub>O. A tan precipitate formed immediately and was allowed to stir for ~10 minutes to ensure total precipitation. This powder was collected on a 60 mL medium porosity frit and washed 2x with 30 mL of Et<sub>2</sub>O before being set aside. The filtrate was reduced in vacuum with silica powder and loaded onto a Combiflash powder cartridge. The obtained organic was eluted through a 12 g silica column with 60% ethyl acetate in hexanes. The combined fractions were then reduced to a pale yellow oil. (31 mg, 33% yield).

<sup>1</sup>H NMR (CDCl<sub>3</sub>, δ, 25 °C): 7.69 (d, J = 8.3 Hz, 2H, H8), 7.31 (d, J = 8.2 Hz, 2H, H9), 5.99 (ddd, J = 2.9, 4.0, 10.3 Hz, 1H, H3), 5.70 (dq, J = 1.7, 10.3 Hz, 1H, H4), 4.82 (m, 1H, H2), 4.14 (dd, J = 5.4, 14.4 Hz, 1H, H6), 3.68 (s, 3H, H14), 3.23 (dd, J = 10.9, 14.3 Hz, 1H, H6'), 3.15 (m, 1H, H5), 2.69 (dd, J = 6.3, 15.4 Hz, 1H, H12), 2.62 (dd, J = 8.1, 15.4 Hz, 1H, H12'), 2.44 (s, 3H, H11).

<sup>13</sup>C NMR (CDCl<sub>3</sub>, δ, 25 °C): 170.4 (C13), 144.5 (C7), 137.0 (C10), 130.4 (C3), 130.3 (C9), 127.1 (C8), 121.3 (C4), 117.9 (C15), 52.2 (C14), 49.6 (C2), 40.6 (C6), 39.2 (C12), 25.4 (C5), 21.7 (C11).



**(*N*-tosyl)-(2-allyl)-1,2,5,6-tetrahydropyridine (31)**

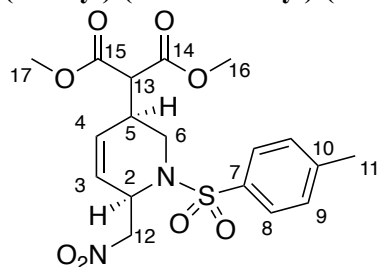


A 10 mL screw cap test tube was charged with **12D** (251 mg, 0.32 mmol) and MeCN (3 mL). A separate 10 mL screw cap test tube was charged with MeCN (1 mL) and HOTf (55 mg, 0.37 mmol). The acidic solution was added to the **12D**/MeCN solution, and the combined solution was swirled and added to a -40 °C toluene bath. A separate 10 mL screw cap test tube was charged with NaBH<sub>4</sub> (35 mg, 0.93 mmol) and MeOH (1 mL). After chilling both tubes in a -40 °C toluene bath for 15 minutes, the NaBH<sub>4</sub>/MeOH solution was added to the [W]/MeCN solution, and the combined solution was chilled in the bath for 3 hours. The solution was diluted with 150 mL of DCM and added to a separatory funnel. This solution was washed 3x with 200 mL of saturated aqueous NaHCO<sub>3</sub>. The organic layer was isolated and set aside. The combined aqueous layers were combined and back extracted with 50 mL of DCM to prevent product loss. The organic layers were combined in a single flask and dried with anhydrous MgSO<sub>4</sub>. This powder was then filtered off into a 60 mL coarse porosity fritted funnel and washed with DCM. The dried organic layers were then reduced *in vacuo* to dryness. The residue in the flask was redissolved in minimal acetone (approximately 5 mL) and added to a 4-dram vial w/stir pea. This vial was removed from the glovebox, DDQ was then added (35 mg, 0.15 mmol), and the solution was stirred for 2 hours. The solution was diluted with 50 mL of DCM and added to a separatory funnel. This solution was washed 3x with 200 mL of saturated aqueous NaHCO<sub>3</sub>. The organic layer was isolated and set aside. The combined aqueous layers were combined and back extracted with 30 mL of DCM to prevent product loss. The organic layers were combined in a single flask and dried with anhydrous MgSO<sub>4</sub>. This powder was then filtered off into a 60 mL coarse porosity fritted funnel and washed with DCM. The dried organic layers were then reduced *in vacuo* to dryness. The solution was then slowly added to a 4:1 100 mL solution of stirring pentane/Et<sub>2</sub>O. A tan precipitate formed immediately and was allowed to stir for ~10 minutes to ensure total precipitation. This powder was collected on a 60 mL medium porosity frit and washed 2x with 30 mL of Et<sub>2</sub>O before being set aside. The filtrate was reduced in vacuum with silica powder and loaded onto a Combiflash powder cartridge. The obtained organic was eluted through a 12 g silica column with 40% ethyl acetate in hexanes. The combined fractions were then reduced to a pale yellow oil. (44 mg, 49% yield).

<sup>1</sup>H NMR (CDCl<sub>3</sub>, δ, 25 °C): 7.70 (d, *J* = 8.2 Hz, 2H, H8), 7.24 (d, *J* = 8.2 Hz, 2H, H9), 5.83 (m, 1H, H13), 5.67 (dd, *J* = 5.4, 10.4 Hz, 1H, H4), 5.64 (dt, *J* = 3.0, 10.4 Hz, 1H, H3), 5.08 (d, *J* = 7.9 Hz, 1H, H14), 5.07 (d, *J* = 10.1 Hz, 1H, H14'), 4.36 (s, 1H, H2), 3.83 (dd, *J* = 6.0, 14.4 Hz, 1H, H6), 3.14 (ddd, *J* = 4.4, 11.7, 14.5 Hz, 1H, H6'), 2.40 (s, 3H, H11), 2.39 (m - obscured, 2H, H12), 1.81 (m, 1H, H5), 1.75 (dt, *J* = 1.8, 16.6 Hz, 1H, H5').

<sup>13</sup>C NMR (CDCl<sub>3</sub>, δ, 25 °C): 143.1 (C7), 138.7 (C10), 134.4 (C13), 129.7 (C9), 127.5 (C3), 127.1 (C8), 125.5 (C4), 117.8 (C14), 53.4 (C2), 40.0 (C12), 38.7 (C6), 23.2 (C5), 21.6 (C11).

**(*N*-tosyl)-(2-nitromethyl)-(5-dimethylmalonyl)-1,2,5,6-tetrahydropyridine (32)**



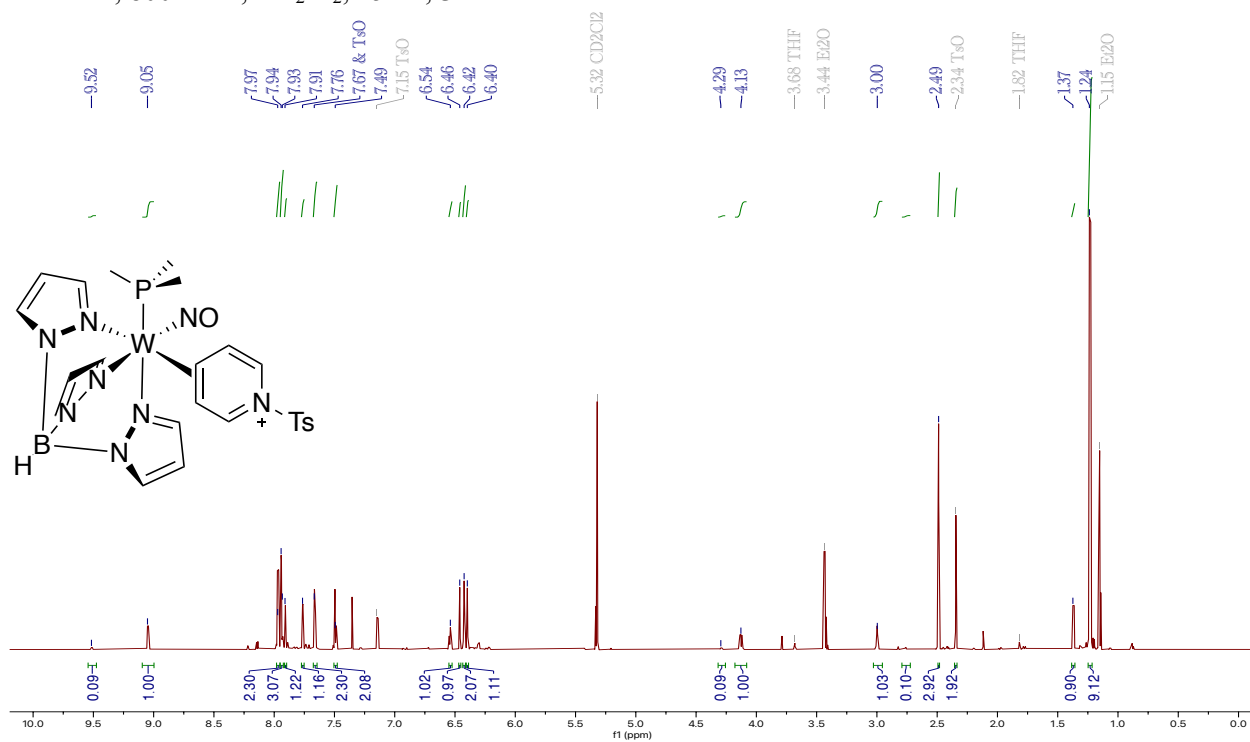
A 10 mL screw cap test tube was charged with **8D** (190 mg, 0.24 mmol) and MeCN (3 mL). A separate 10 mL screw cap test tube was charged with MeCN (1 mL) and HOTf (40 mg, 0.27 mmol). The acidic solution was added to the **8D**/MeCN solution, and the combined solution was swirled and added to a -40 °C toluene bath. A separate 10 mL screw cap test tube was charged with LiDiMM (85 mg, 0.62 mmol) and MeCN (1 mL). After chilling both tubes in a -40 °C toluene bath for 15 minutes, the LiDiMM/MeCN solution was added to the [W]/MeCN solution, and the combined solution was chilled in the bath for 3 hours. The solution was diluted with 150 mL of DCM and added to a separatory funnel. This solution was washed 3x with 200 mL of saturated aqueous NaHCO<sub>3</sub>. The organic layer was isolated and set aside. The combined aqueous layers were combined and back extracted with 50 mL of DCM to prevent product loss. The organic layers were combined in a single flask and dried with anhydrous MgSO<sub>4</sub>. This powder was then filtered off into a 60 mL coarse porosity fritted funnel and washed with DCM. The dried organic layers were then reduced *in vacuo* to dryness. The residue in the flask was redissolved in minimal acetone (approximately 5 mL) and added to a 4-dram vial w/stir pea. This vial was removed from the glovebox, DDQ was then added (30 mg, 0.13 mmol), and the solution was stirred for 2 hours. The solution was diluted with 50 mL of DCM and added to a separatory funnel. This solution was washed 3x with 200 mL of saturated aqueous NaHCO<sub>3</sub>. The organic layer was isolated and set aside. The combined aqueous layers were combined and back extracted with 30 mL of DCM to prevent product loss. The organic layers were combined in a single flask and dried with anhydrous MgSO<sub>4</sub>. This powder was then filtered off into a 60 mL coarse porosity fritted funnel and washed with DCM. The dried organic layers were then reduced *in vacuo* to dryness. The solution was then slowly added to a 4:1 100 mL solution of stirring pentane/Et<sub>2</sub>O. A tan precipitate formed immediately and was allowed to stir for ~10 minutes to ensure total precipitation. This powder was collected on a 60 mL medium porosity frit and washed 2x with 30 mL of Et<sub>2</sub>O before being set aside. The filtrate was reduced in vacuum with silica powder and loaded onto a Combiflash powder cartridge. The obtained organic was eluted through a 12 g silica column with 45% ethyl acetate in hexanes. The combined fractions were then reduced to a pale yellow oil. (35 mg, 34% yield).

<sup>1</sup>H NMR (CDCl<sub>3</sub>, δ, 25 °C): 7.72 (d, *J* = 8.2 Hz, 2H, H8), 7.31 (d, *J* = 8.2 Hz, 2H, H9), 5.81 (d, *J* = 10.4 Hz, 1H, H4), 5.73 (ddd, *J* = 2.6, 3.9, 10.4 Hz, 1H, H3), 4.98 (m, 1H, H2), 4.63 (dd, *J* = 6.8, 12.1 Hz, 1H, H12), 4.48 (dd, *J* = 6.3, 12.1 Hz, 1H, H12'), 3.94 (dd, *J* = 5.6, 14.4 Hz, 1H, H6), 3.75 (s, 3H, H16/17), 3.74 (s, 3H, H16/17), 3.30 (d, *J* = 7.0 Hz, 1H, H13), 3.06 (dd, *J* = 10.7, 14.4 Hz, 1H, H6'), 2.78 (m, 1H, H5), 2.43 (s, 3H, H11).

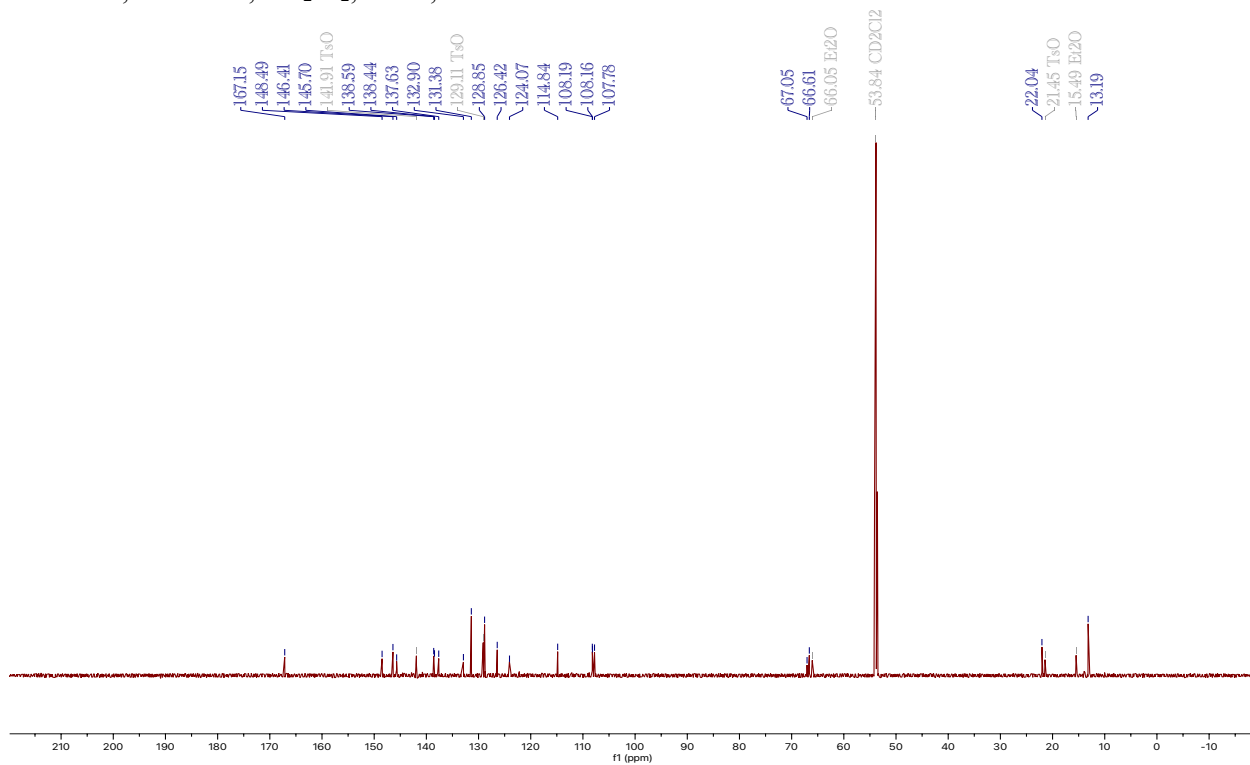
<sup>13</sup>C NMR (CDCl<sub>3</sub>, δ, 25 °C): 167.9 (C14/15), 167.7 (C14/15), 144.4 (C7), 136.6 (C10), 130.6 (C4), 130.1 (C9), 127.4 (C8), 124.2 (C3), 77.7 (C12), 53.0 (C13), 52.9 (2C, C16/17), 50.9 (C2), 41.7 (C6), 32.8 (C5), 21.8 (C11).

### NMR Spectroscopy:

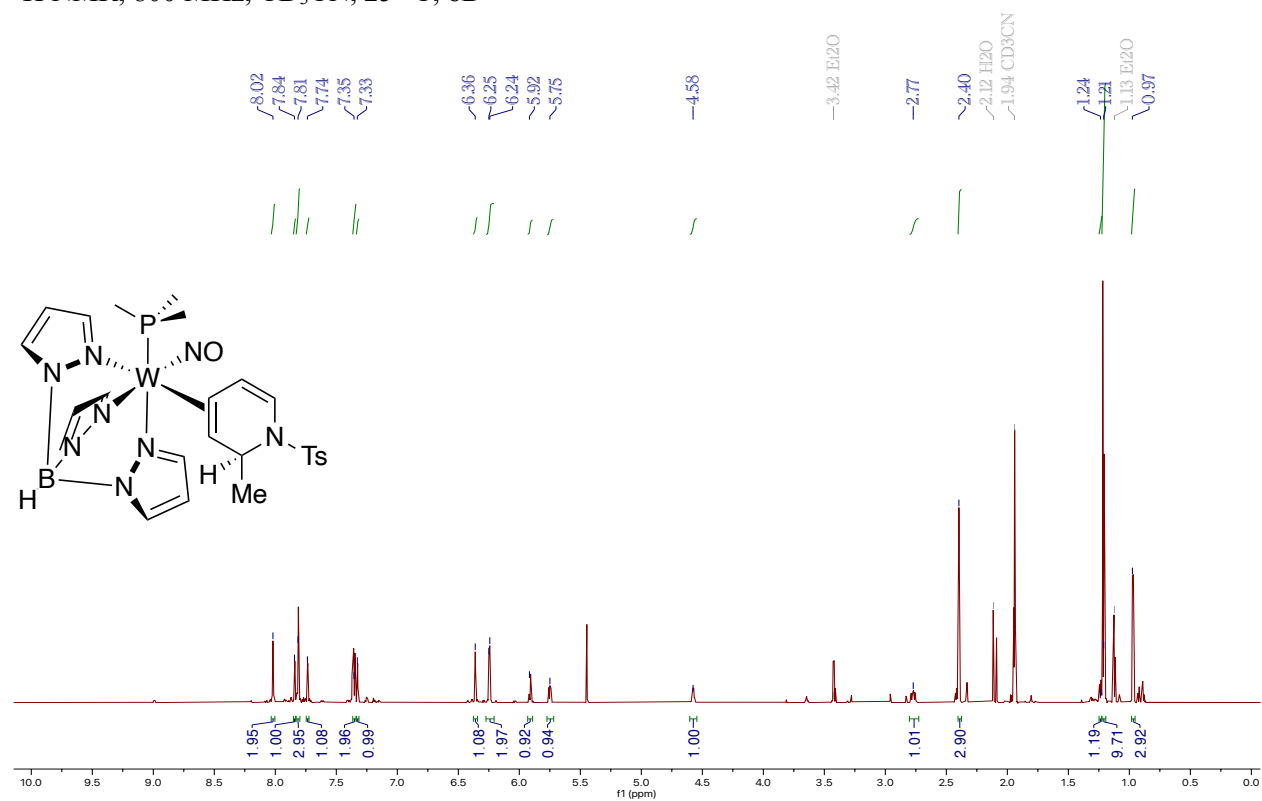
<sup>1</sup>H NMR, 800 MHz, CD<sub>2</sub>Cl<sub>2</sub>, 25 °C, **5D**



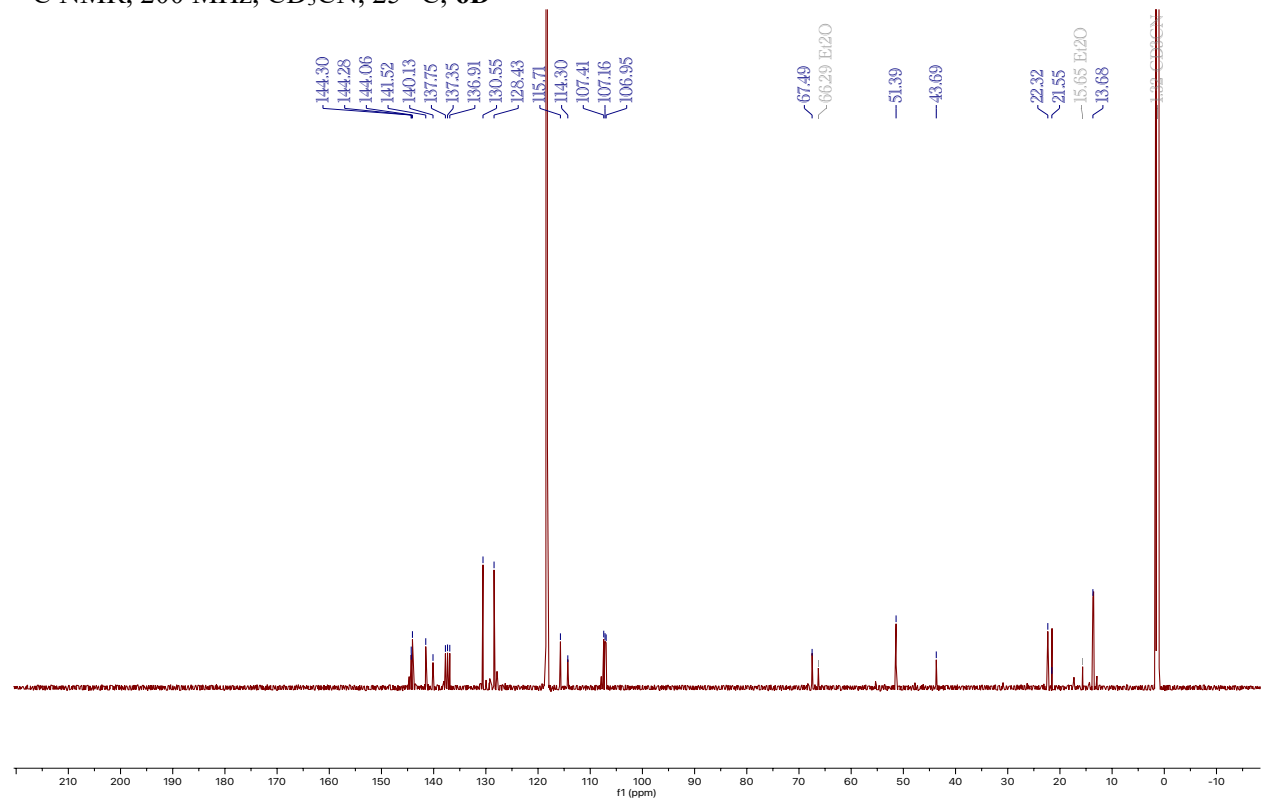
<sup>13</sup>C NMR, 200 MHz, CD<sub>2</sub>Cl<sub>2</sub>, 25 °C, **5D**



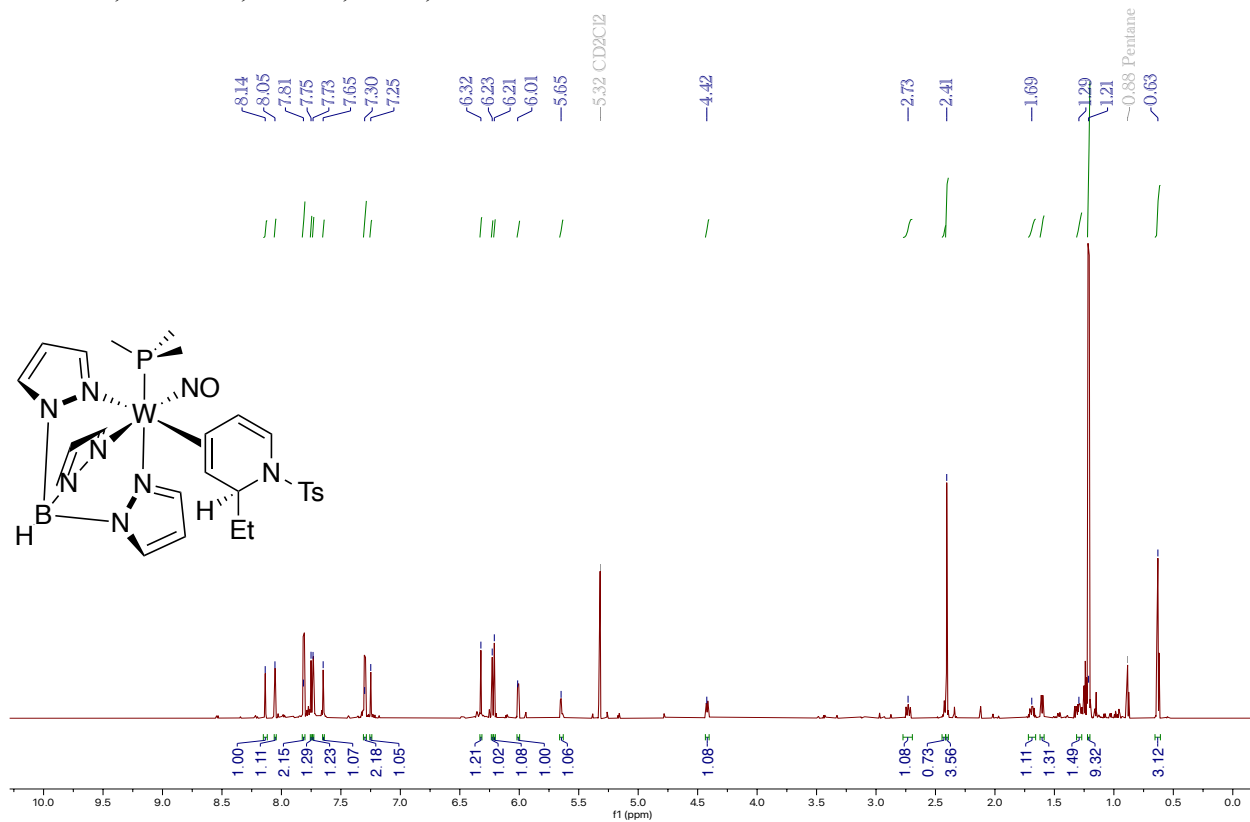
$^1\text{H}$  NMR, 800 MHz,  $\text{CD}_3\text{CN}$ , 25 °C, **6D**



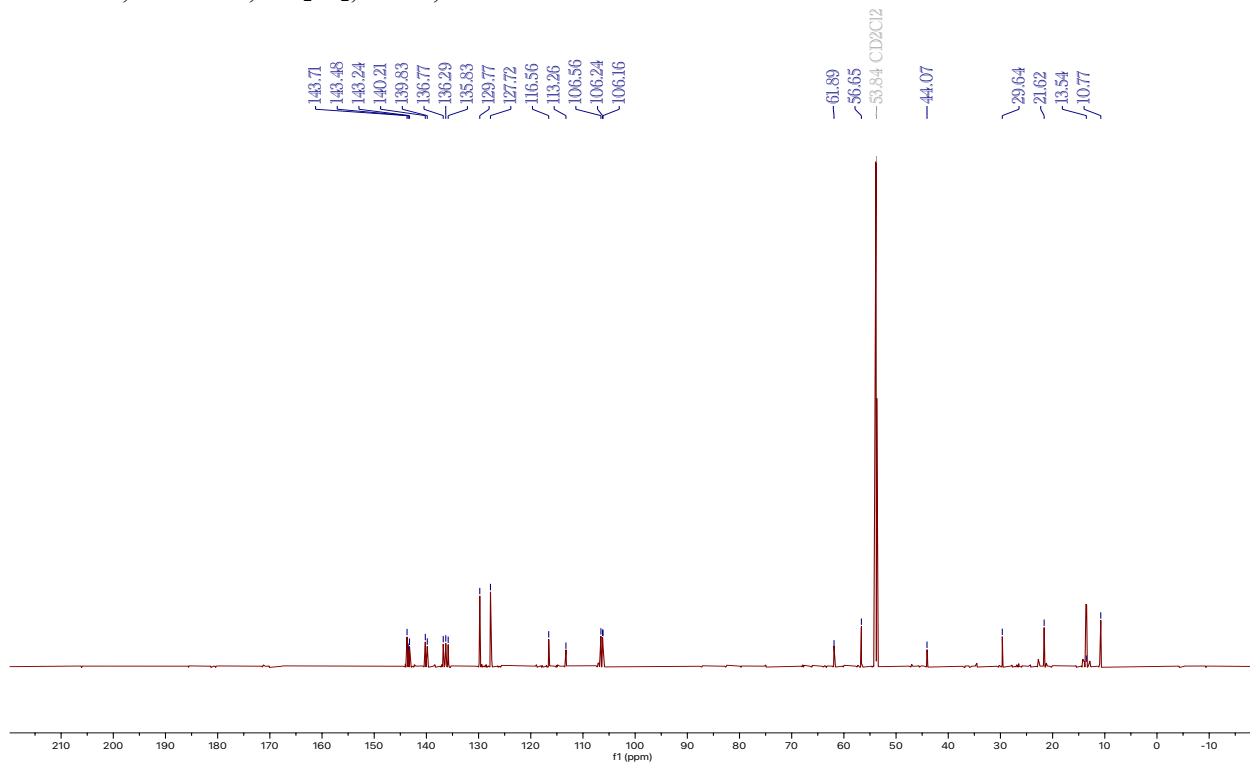
$^{13}\text{C}$  NMR, 200 MHz,  $\text{CD}_3\text{CN}$ , 25 °C, **6D**



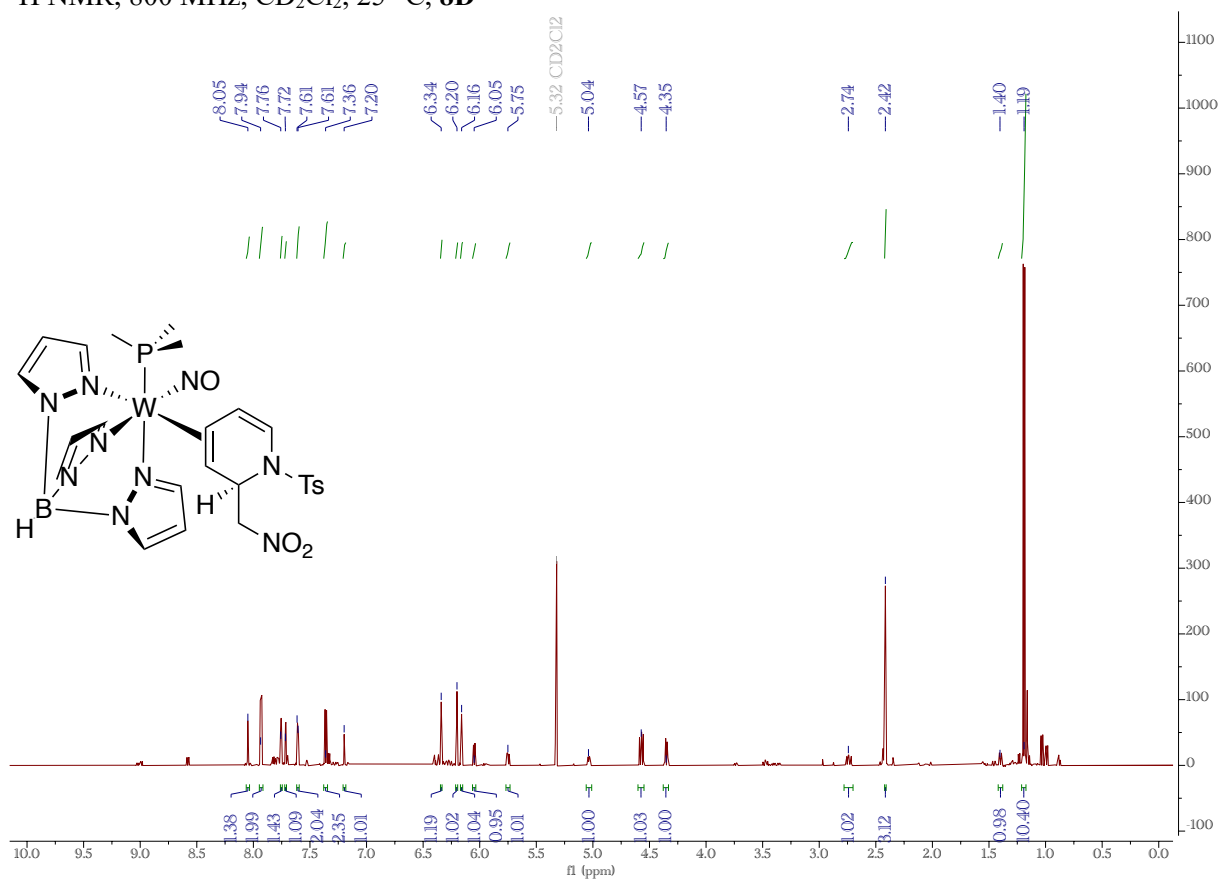
$^1\text{H}$  NMR, 800 MHz,  $\text{CD}_2\text{Cl}_2$ , 25  $^\circ\text{C}$ , **7D**



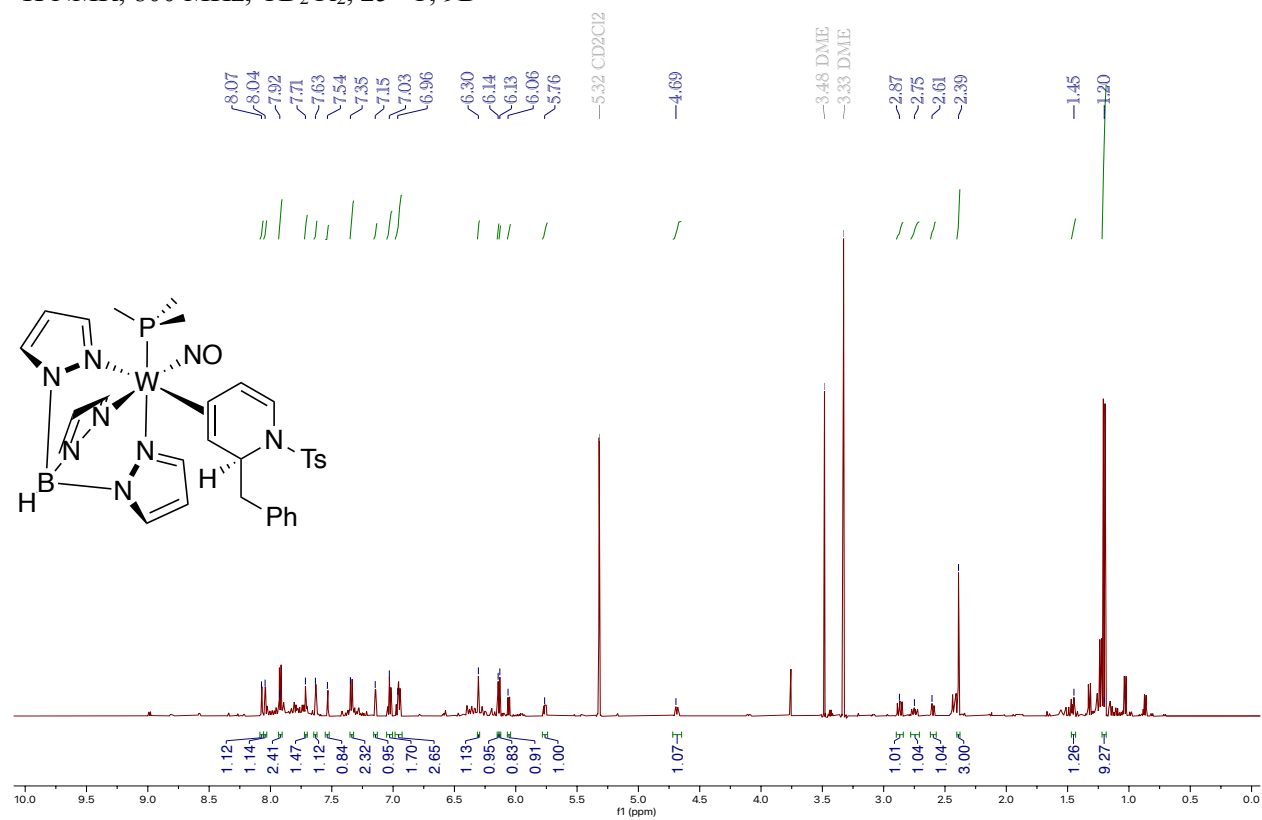
$^{13}\text{C}$  NMR, 200 MHz,  $\text{CD}_2\text{Cl}_2$ , 25  $^\circ\text{C}$ , **7D**



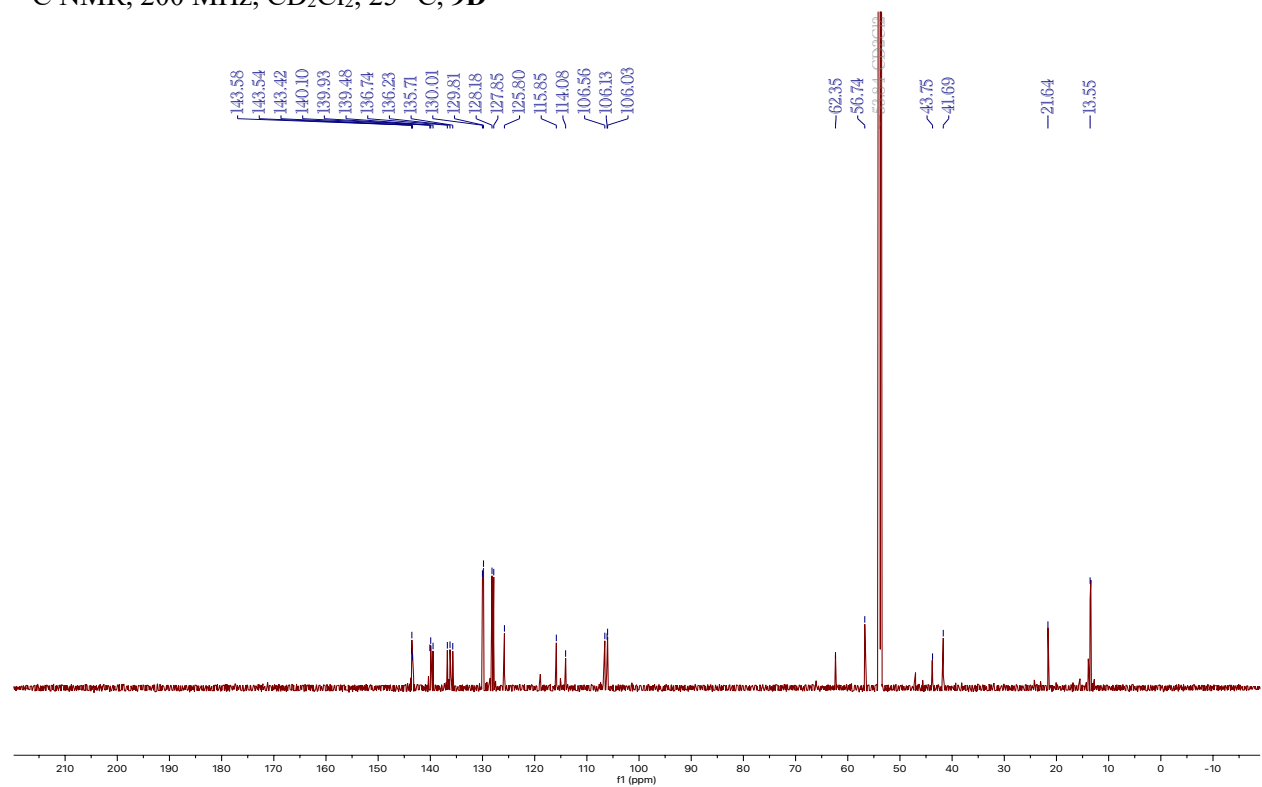
$^1\text{H}$  NMR, 800 MHz,  $\text{CD}_2\text{Cl}_2$ , 25  $^\circ\text{C}$ , **8D**



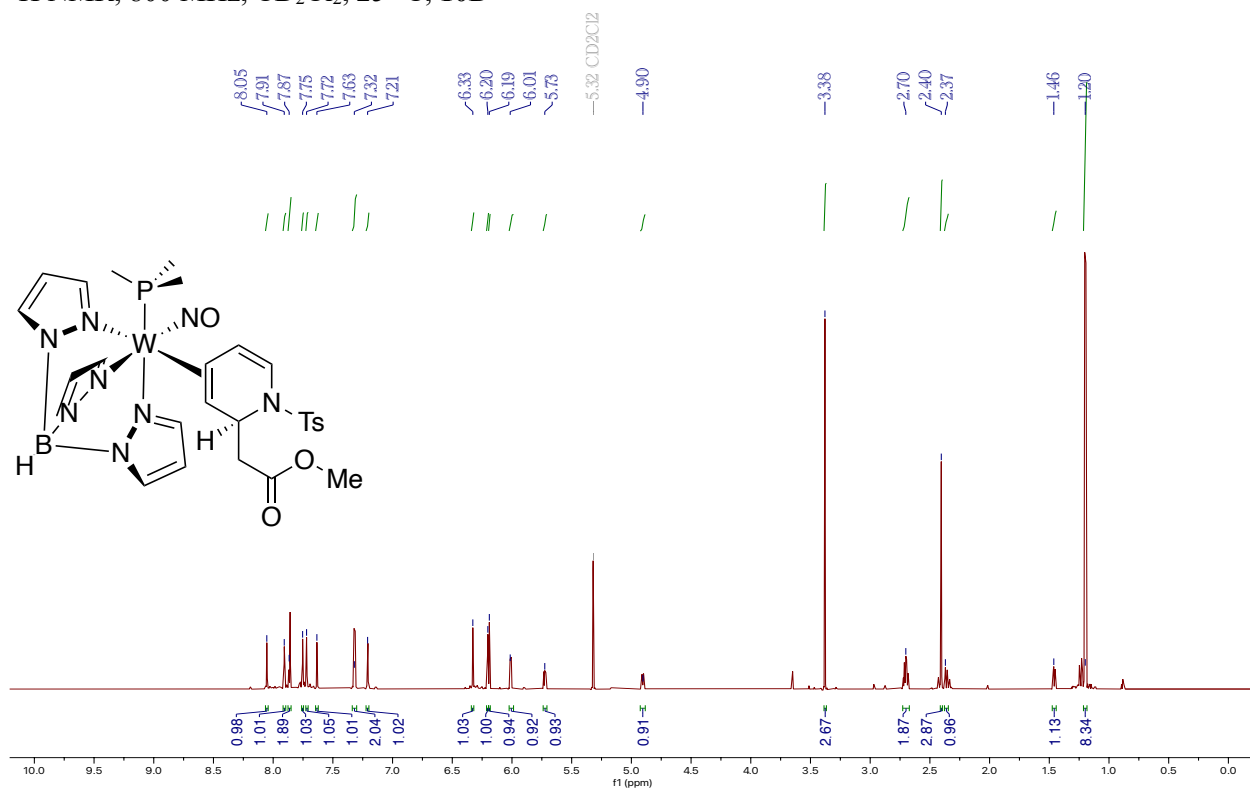
$^1\text{H}$  NMR, 800 MHz,  $\text{CD}_2\text{Cl}_2$ , 25 °C, **9D**



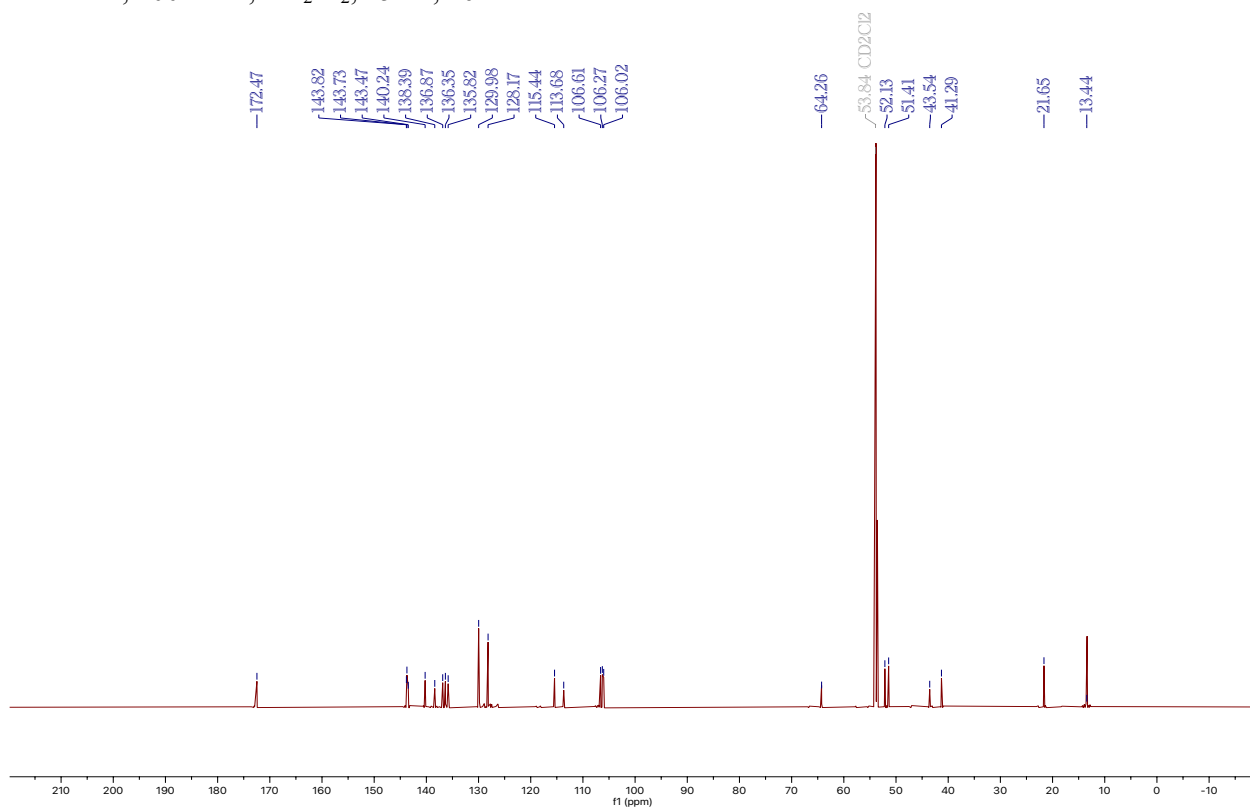
$^{13}\text{C}$  NMR, 200 MHz,  $\text{CD}_2\text{Cl}_2$ , 25 °C, **9D**



$^1\text{H}$  NMR, 800 MHz,  $\text{CD}_2\text{Cl}_2$ , 25 °C, **10D**

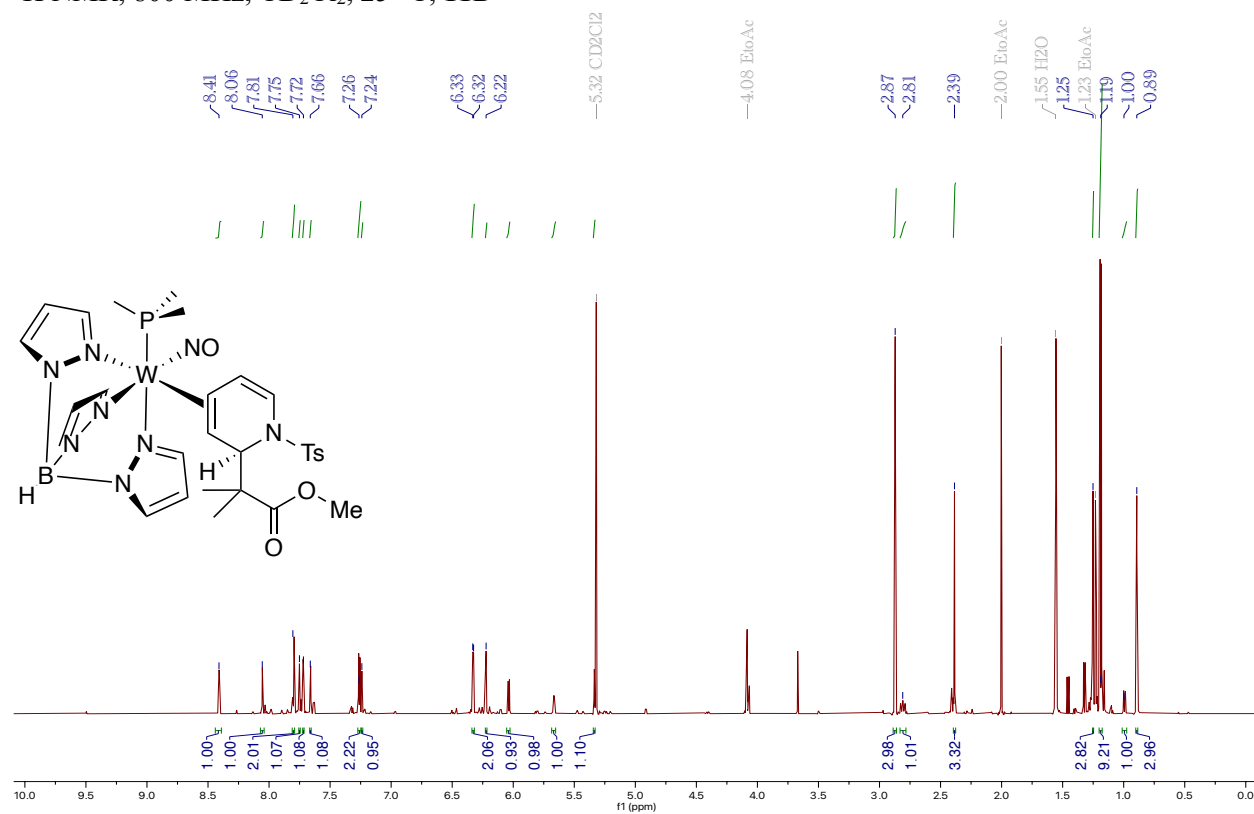


$^{13}\text{C}$  NMR, 200 MHz,  $\text{CD}_2\text{Cl}_2$ , 25 °C, **10D**

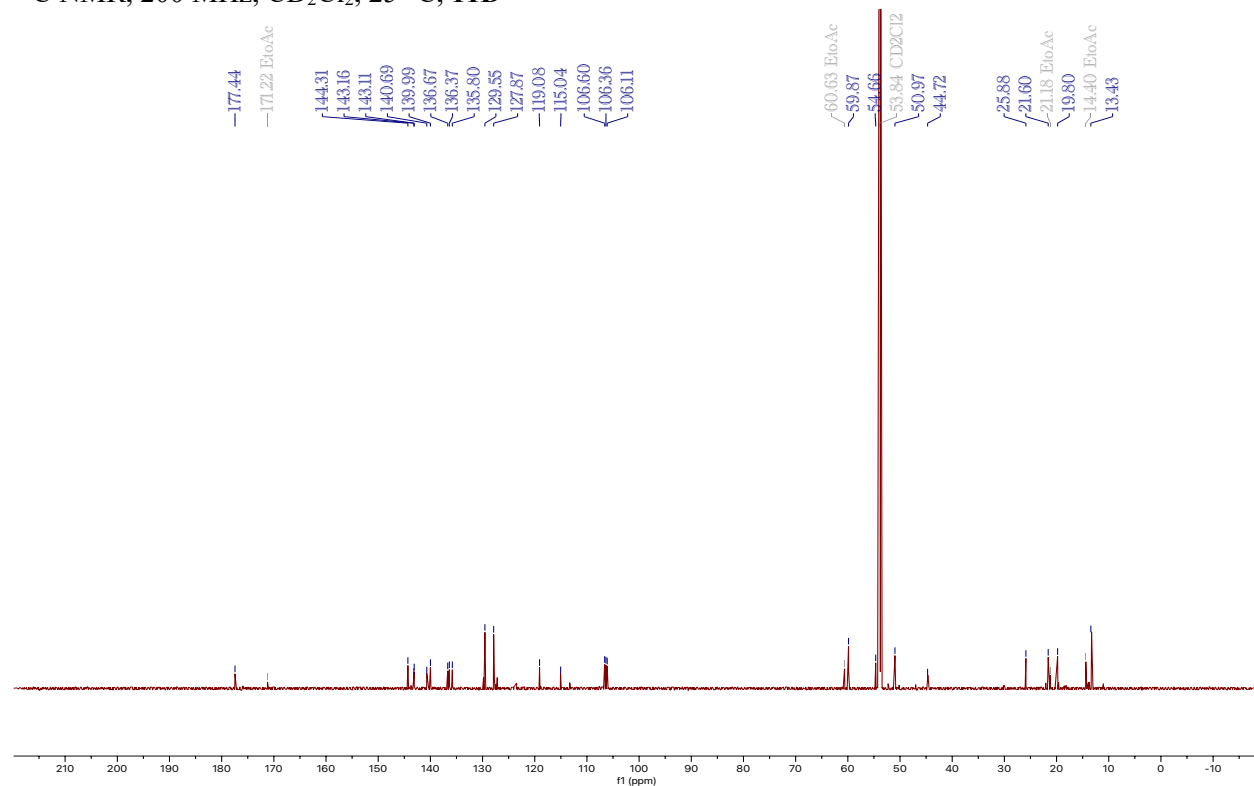




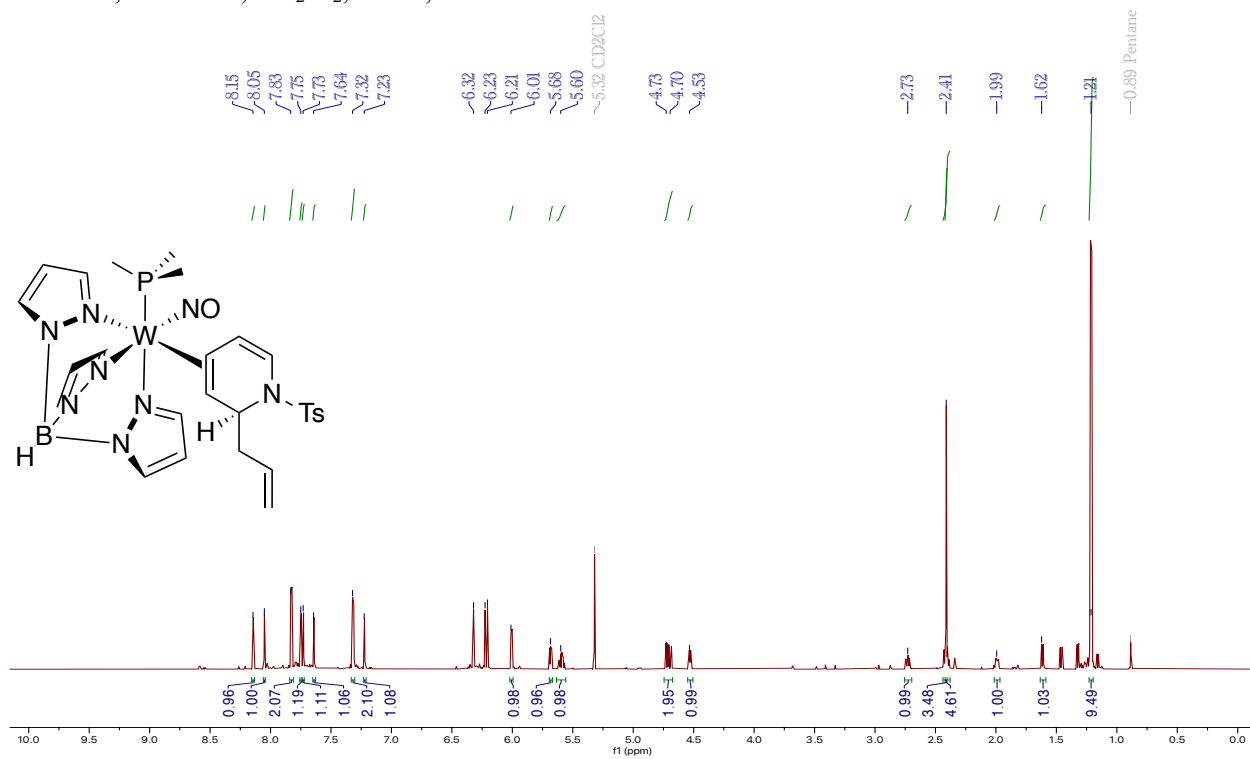
$^1\text{H}$  NMR, 800 MHz,  $\text{CD}_2\text{Cl}_2$ , 25 °C, **11D**



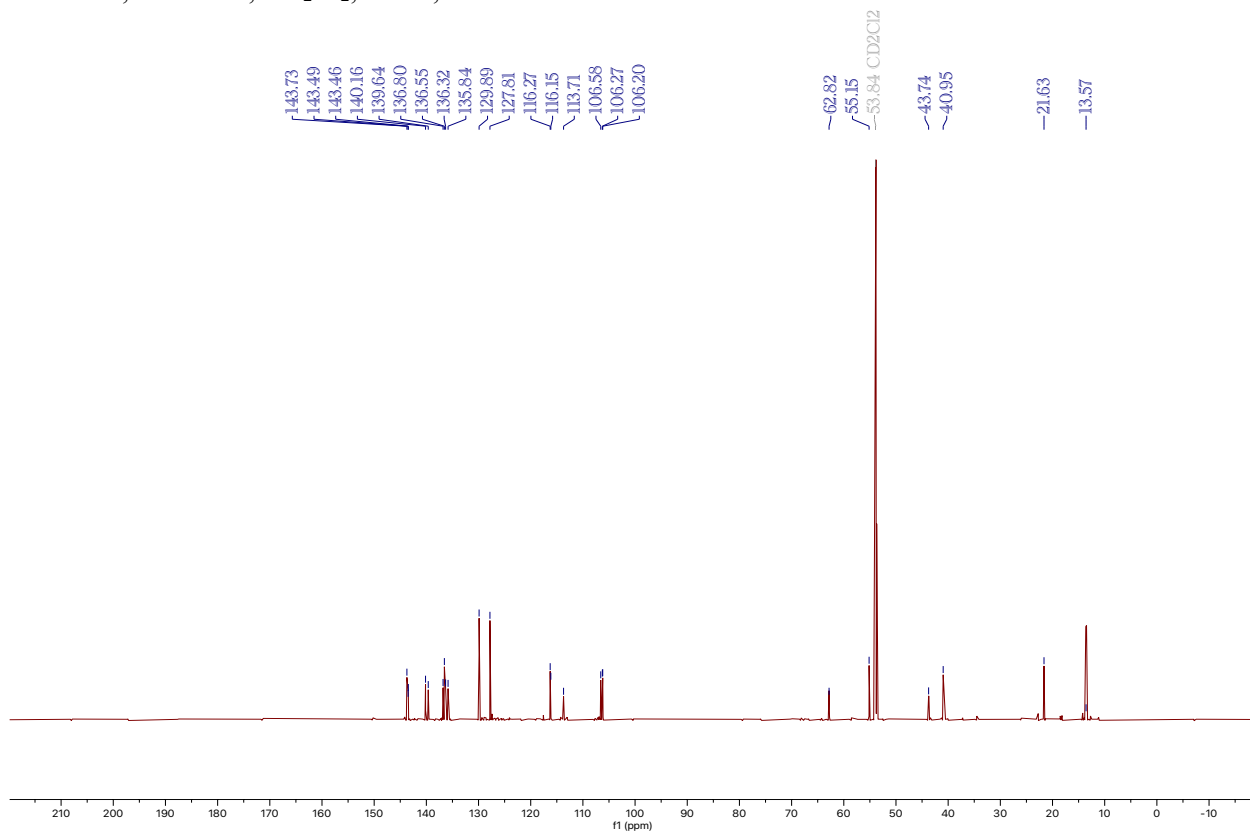
$^{13}\text{C}$  NMR, 200 MHz,  $\text{CD}_2\text{Cl}_2$ , 25 °C, **11D**



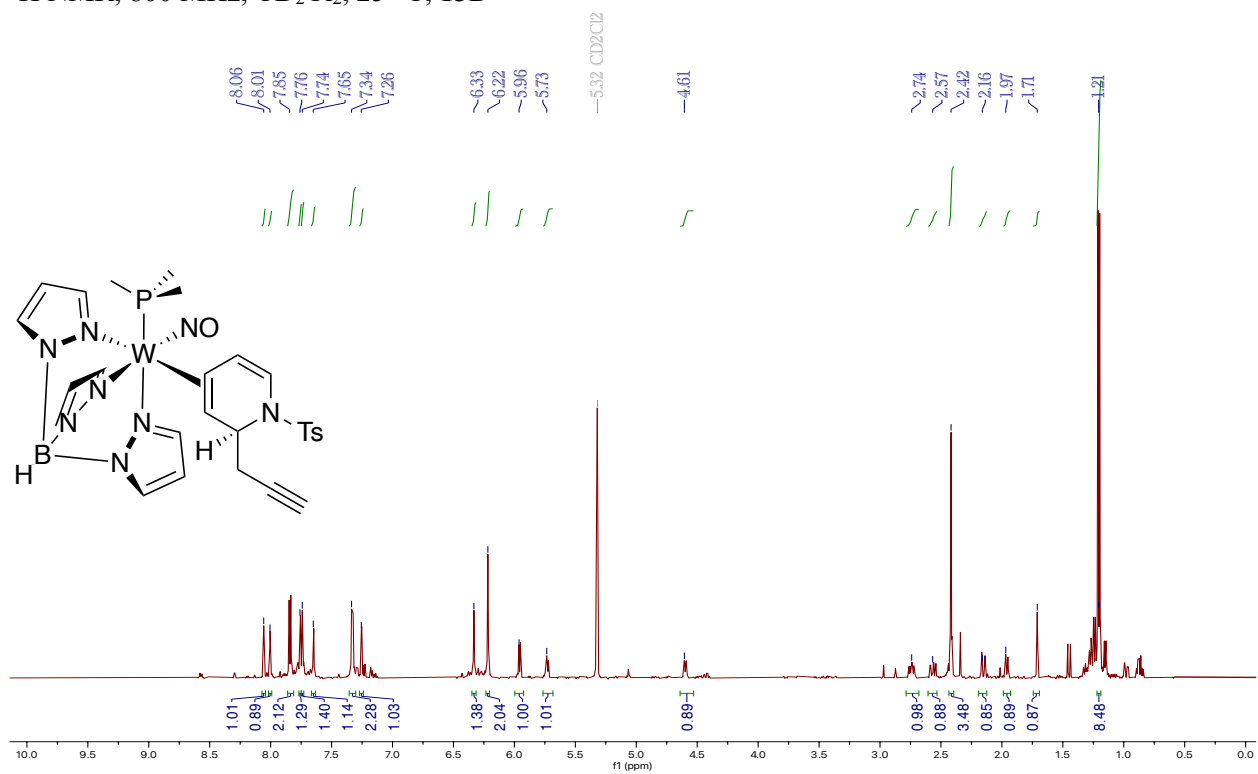
$^1\text{H}$  NMR, 800 MHz,  $\text{CD}_2\text{Cl}_2$ , 25 °C, **12D**



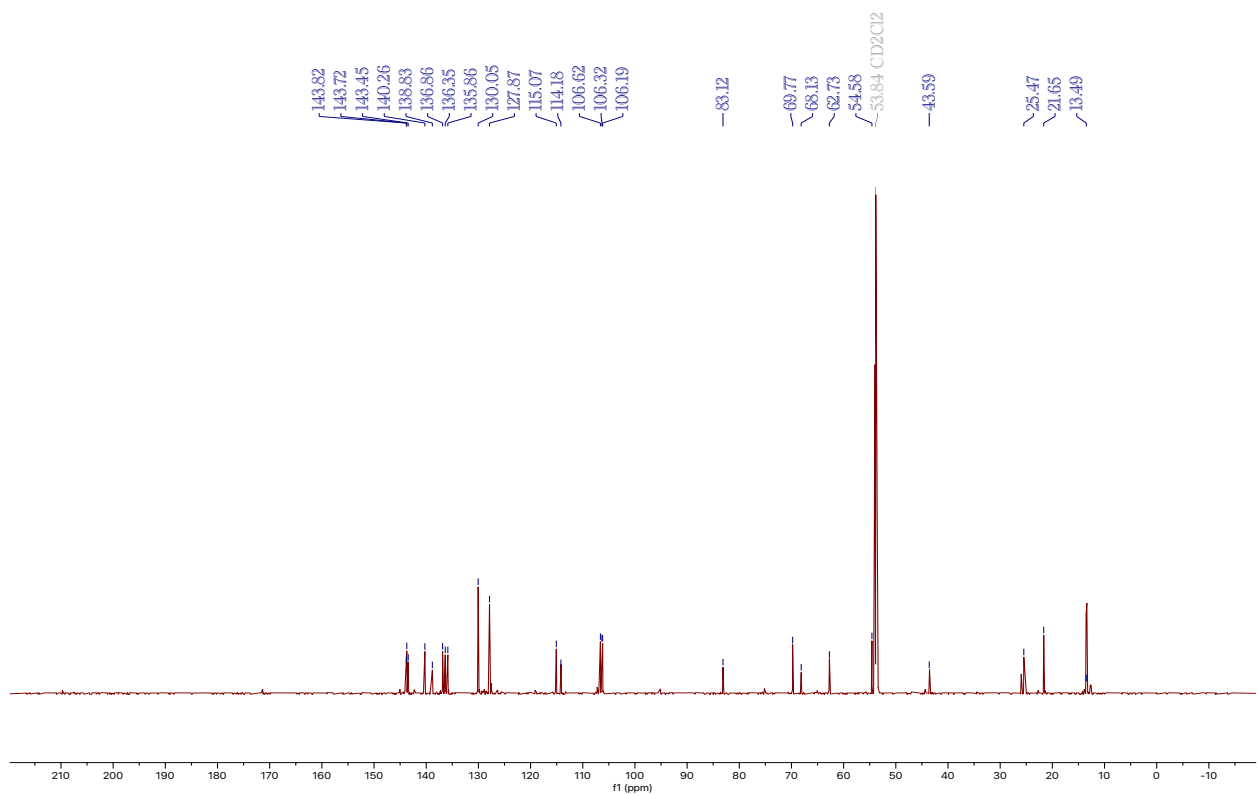
$^{13}\text{C}$  NMR, 200 MHz,  $\text{CD}_2\text{Cl}_2$ , 25 °C, **12D**



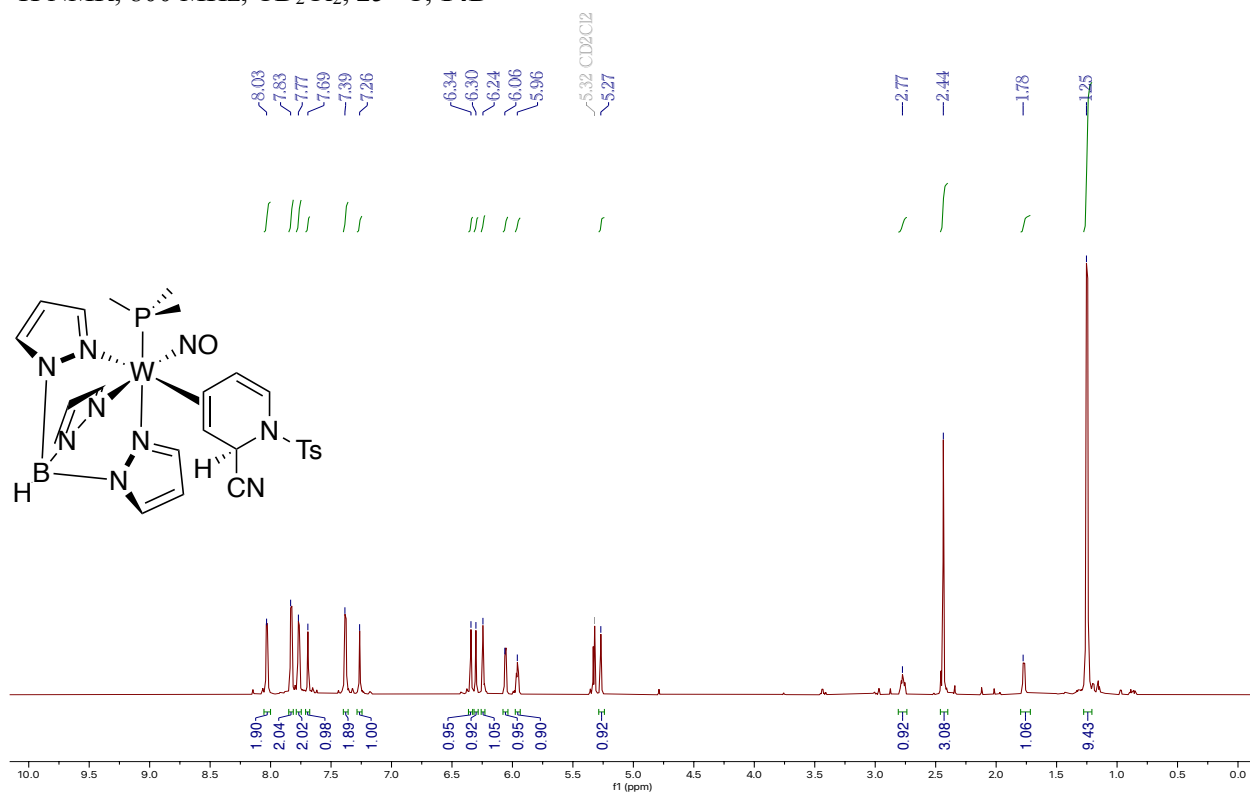
$^1\text{H}$  NMR, 800 MHz,  $\text{CD}_2\text{Cl}_2$ , 25 °C, **13D**



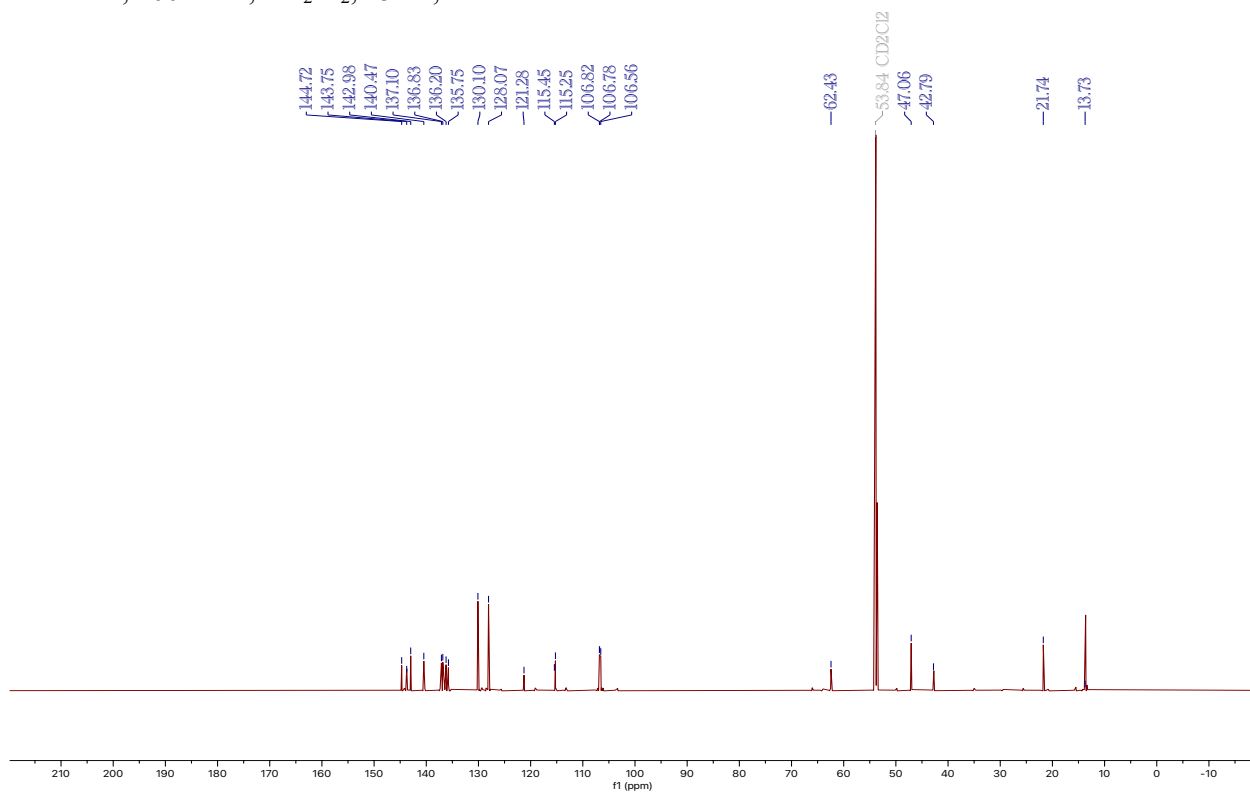
$^{13}\text{C}$  NMR, 200 MHz,  $\text{CD}_2\text{Cl}_2$ , 25 °C, **13D**



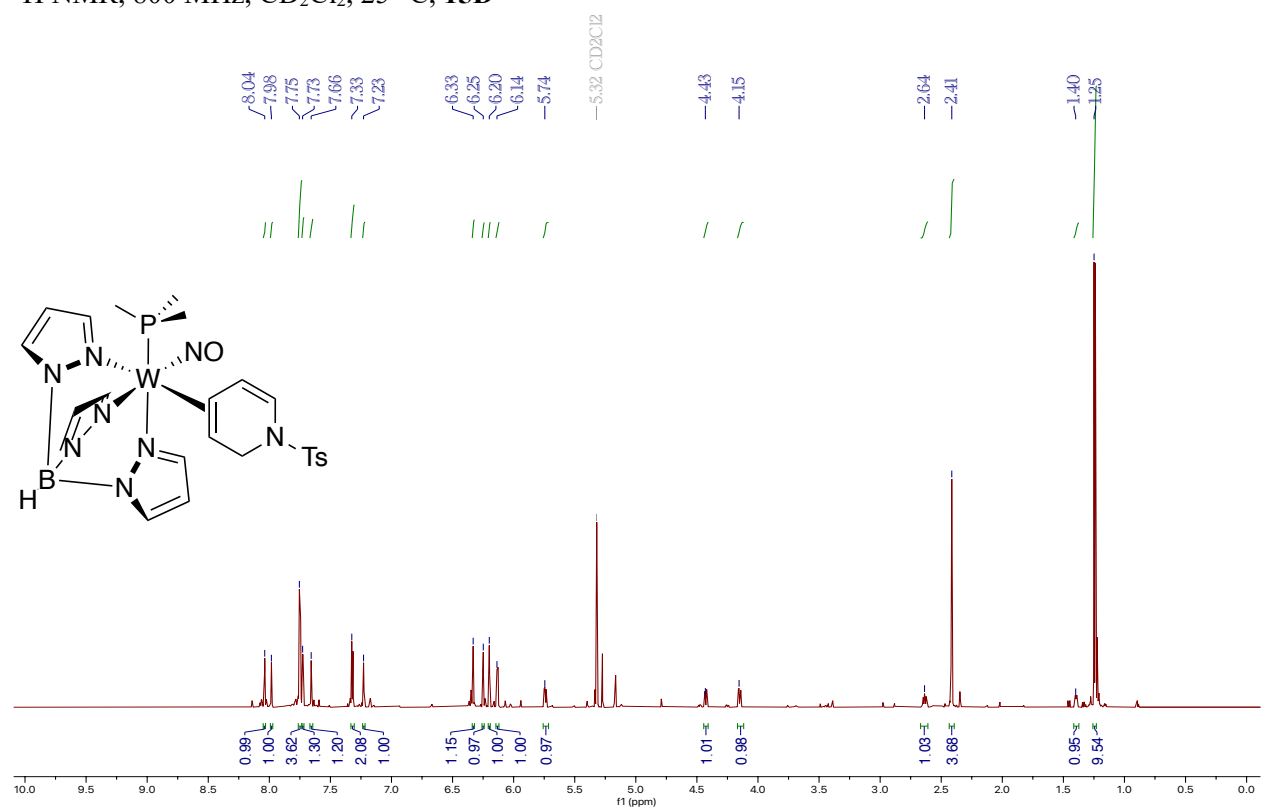
$^1\text{H}$  NMR, 800 MHz,  $\text{CD}_2\text{Cl}_2$ , 25 °C, **14D**



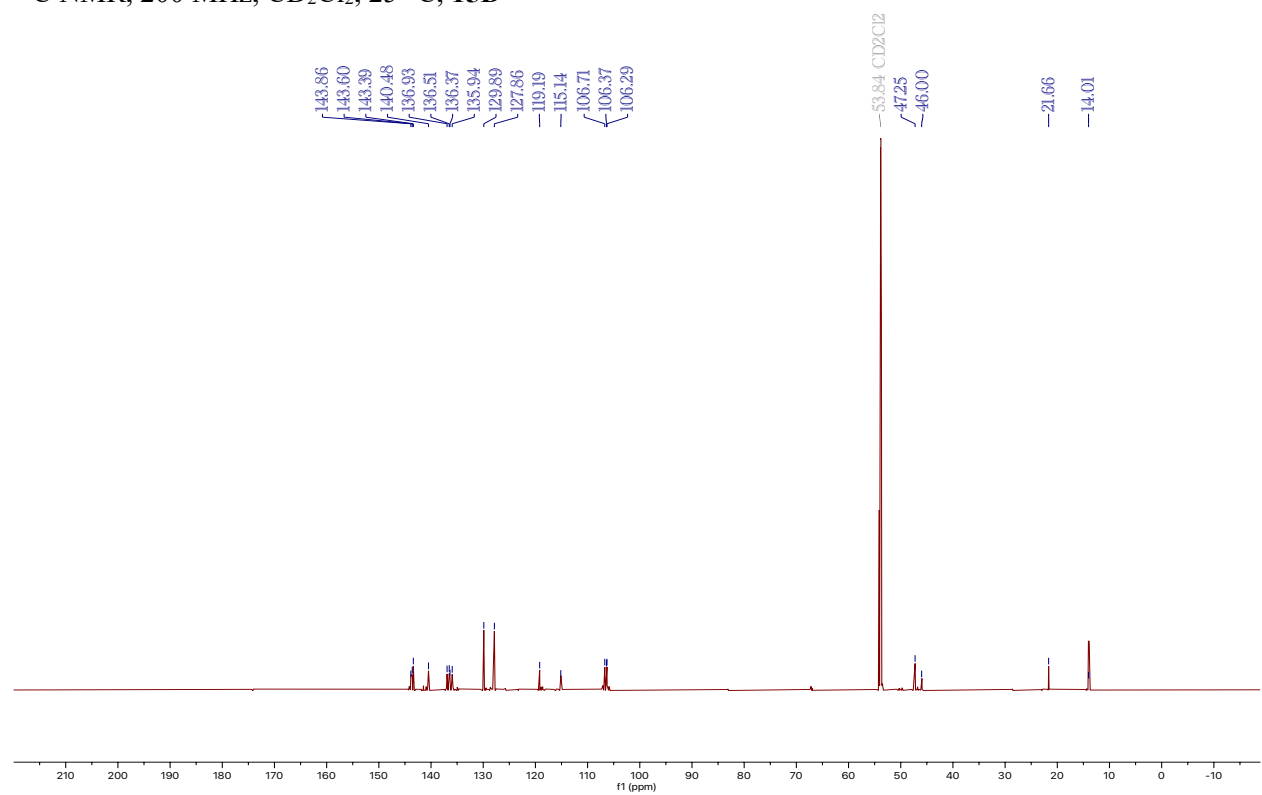
$^{13}\text{C}$  NMR, 200 MHz,  $\text{CD}_2\text{Cl}_2$ , 25 °C, **14D**



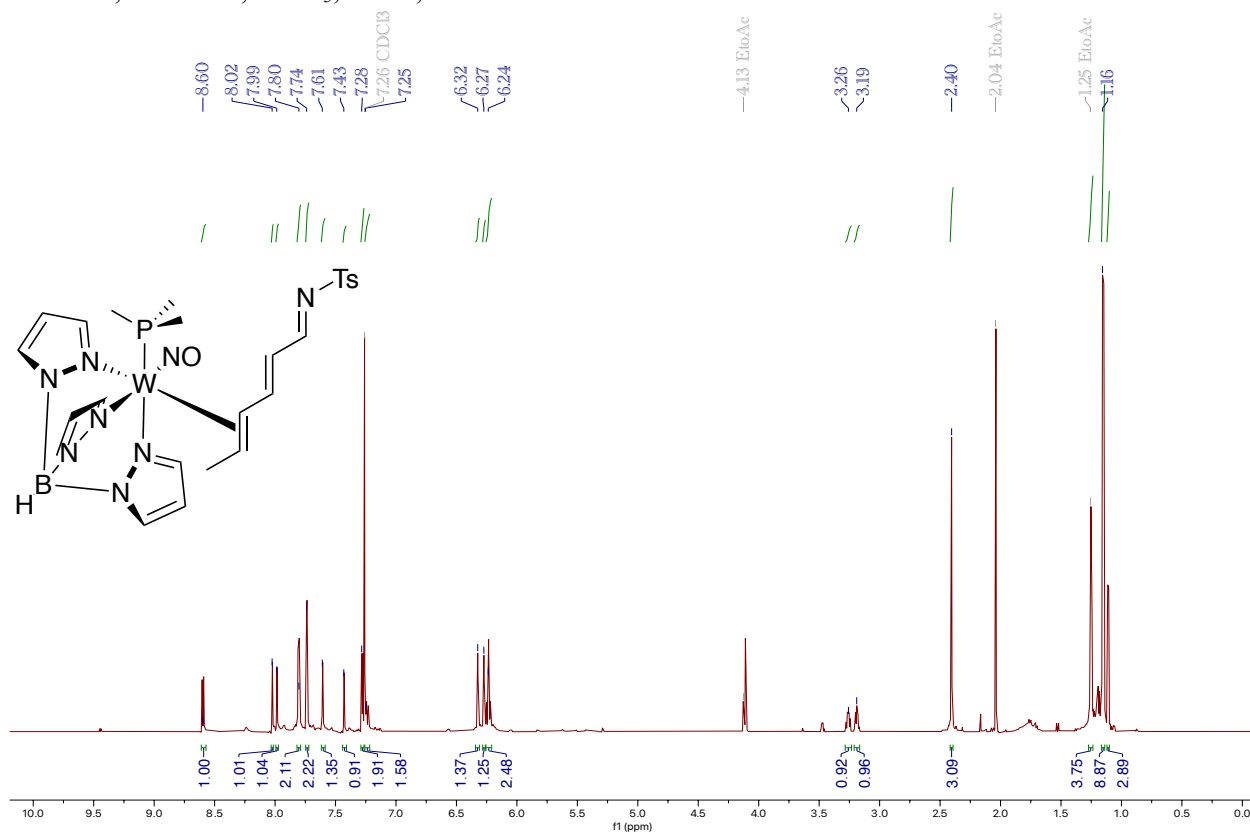
$^1\text{H}$  NMR, 800 MHz,  $\text{CD}_2\text{Cl}_2$ , 25 °C, **15D**



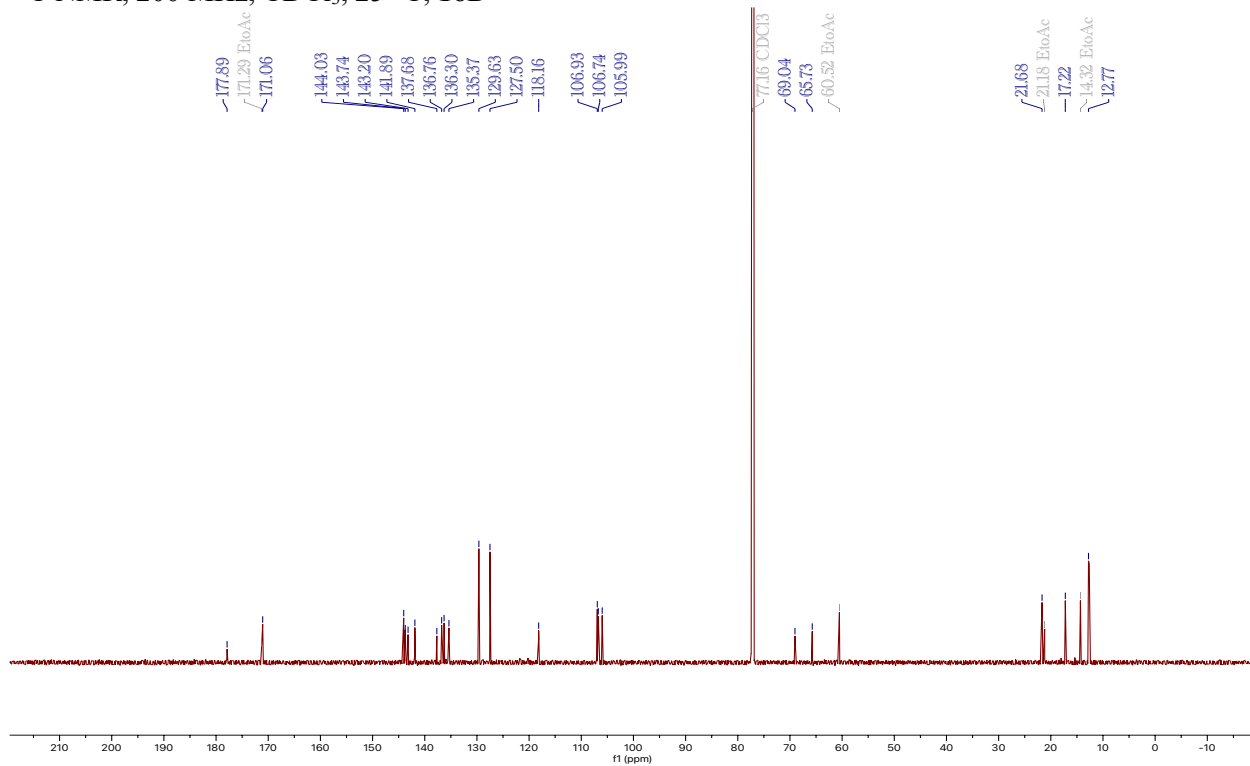
$^{13}\text{C}$  NMR, 200 MHz,  $\text{CD}_2\text{Cl}_2$ , 25 °C, **15D**



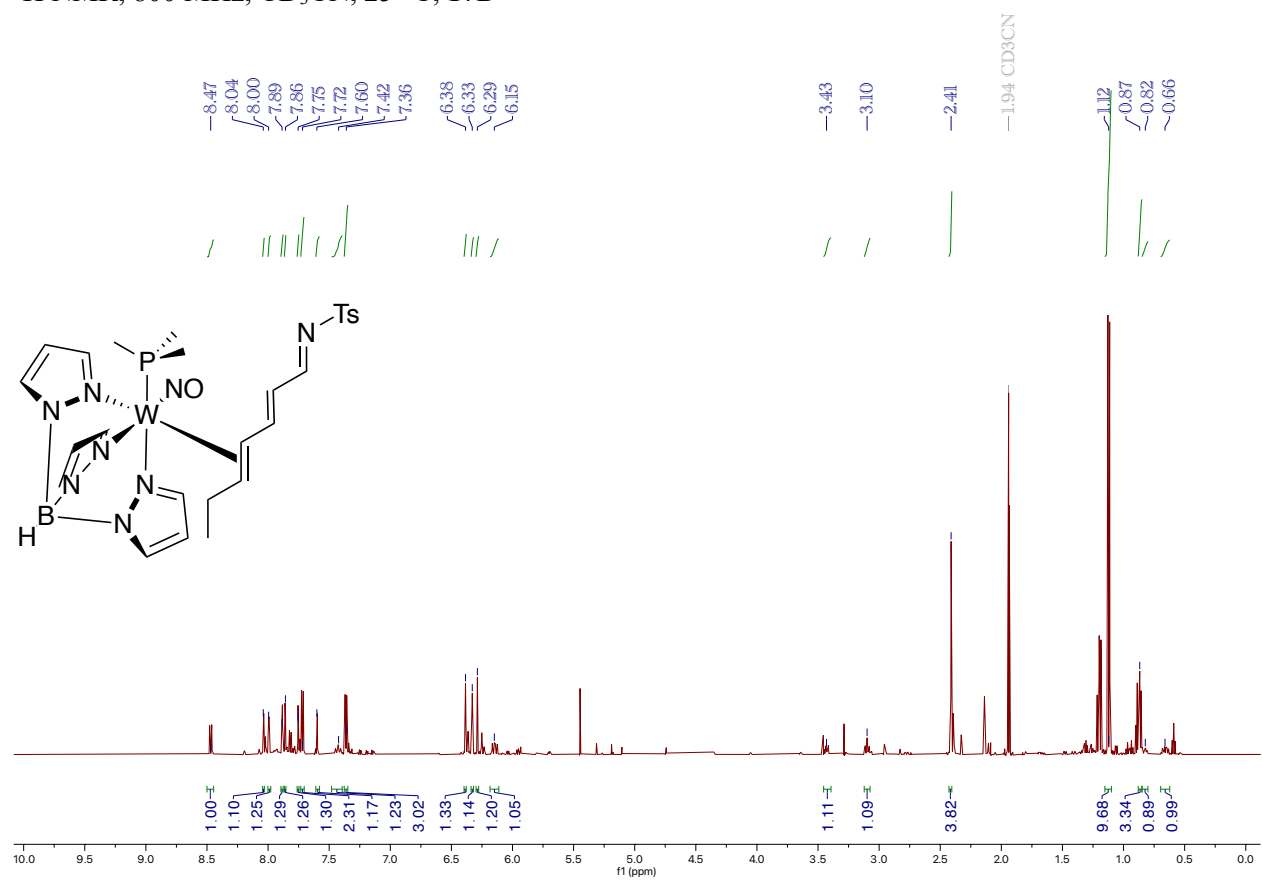
$^1\text{H}$  NMR, 800 MHz,  $\text{CDCl}_3$ , 25 °C, **16D**



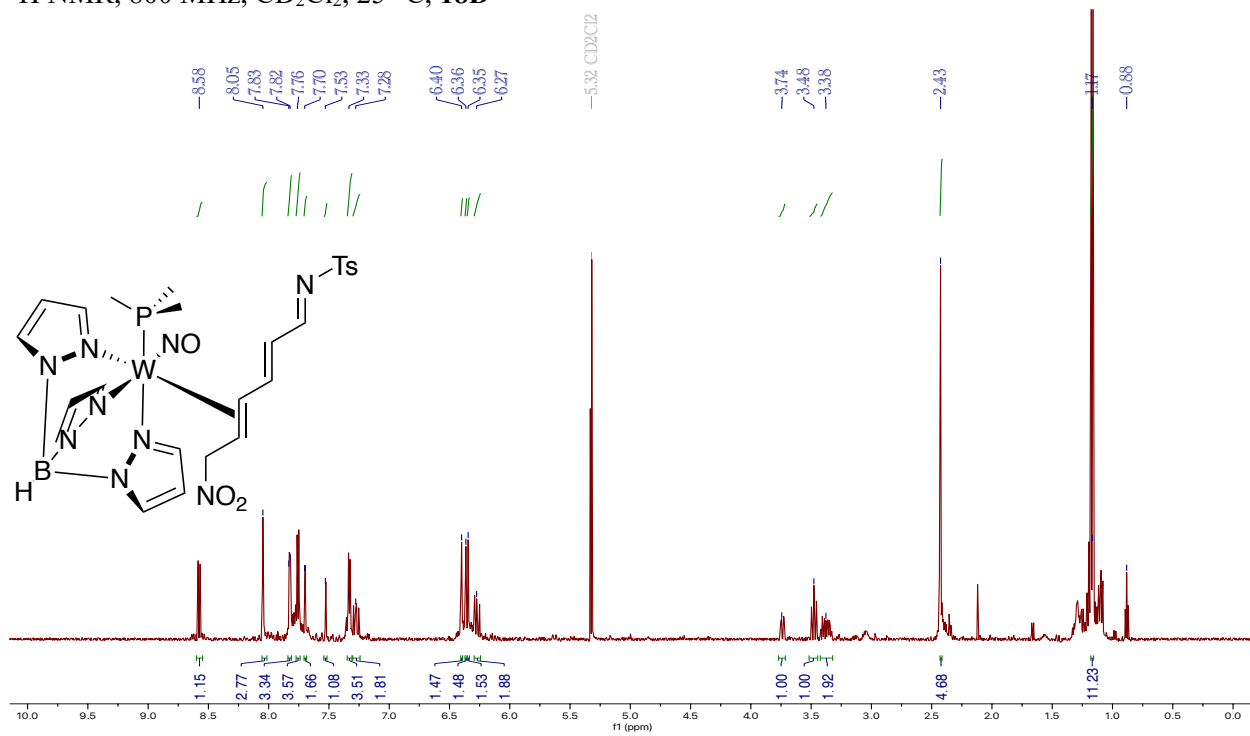
$^{13}\text{C}$  NMR, 200 MHz,  $\text{CDCl}_3$ , 25 °C, **16D**



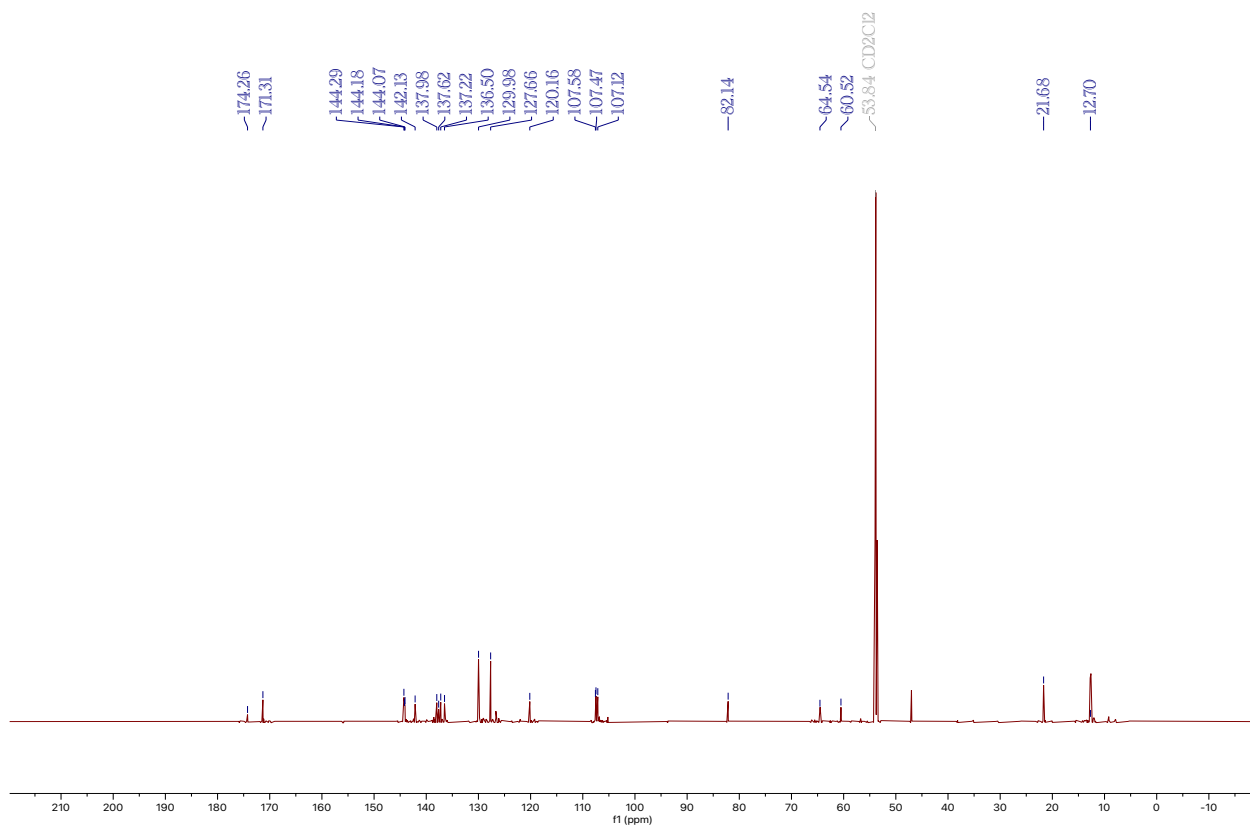
$^1\text{H}$  NMR, 800 MHz,  $\text{CD}_3\text{CN}$ , 25 °C, **17D**



$^1\text{H}$  NMR, 800 MHz,  $\text{CD}_2\text{Cl}_2$ , 25 °C, **18D**

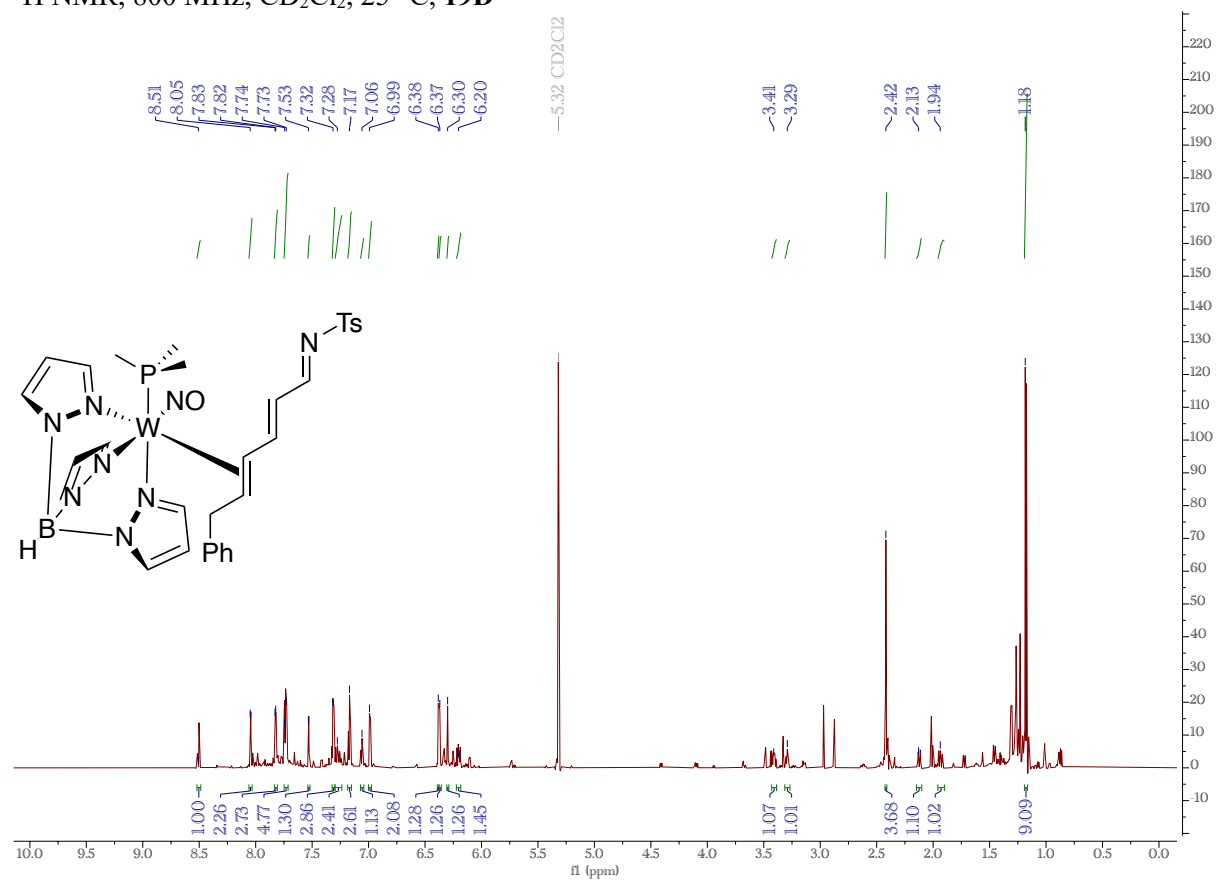


$^{13}\text{C}$  NMR, 200 MHz,  $\text{CD}_2\text{Cl}_2$ , 25 °C, **18D**

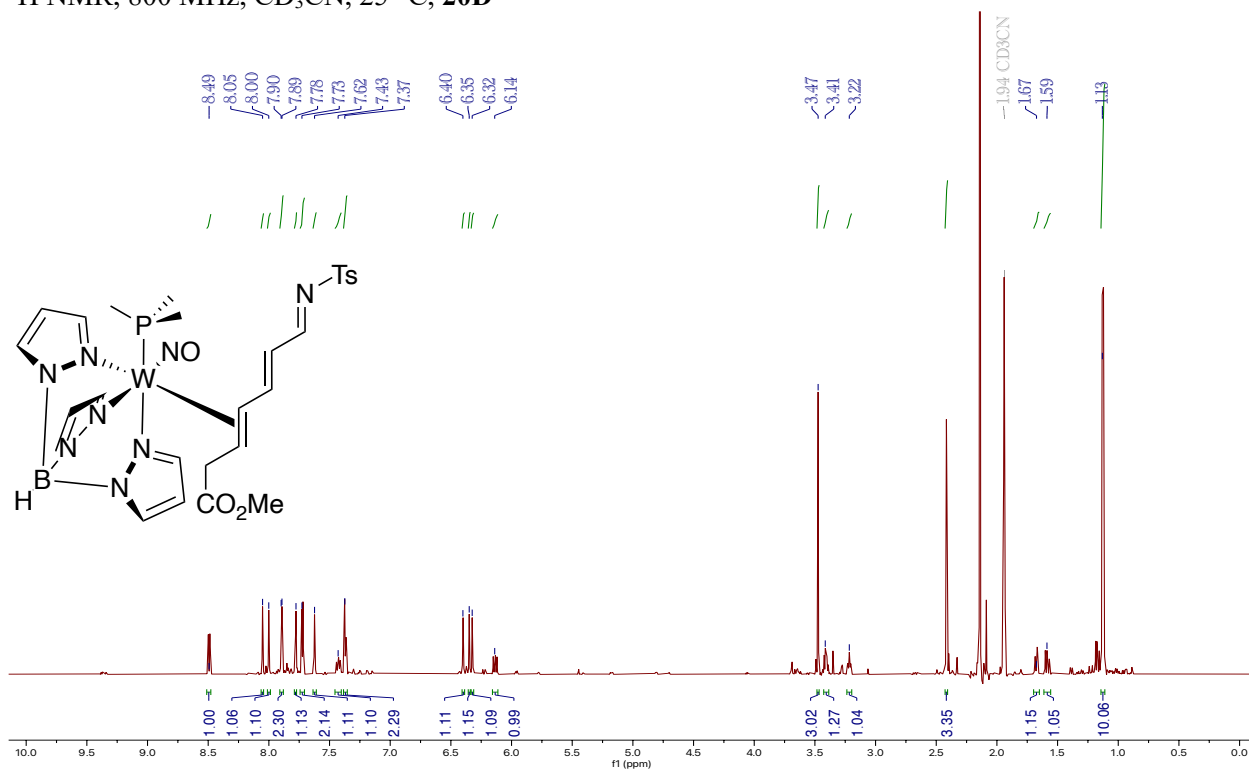




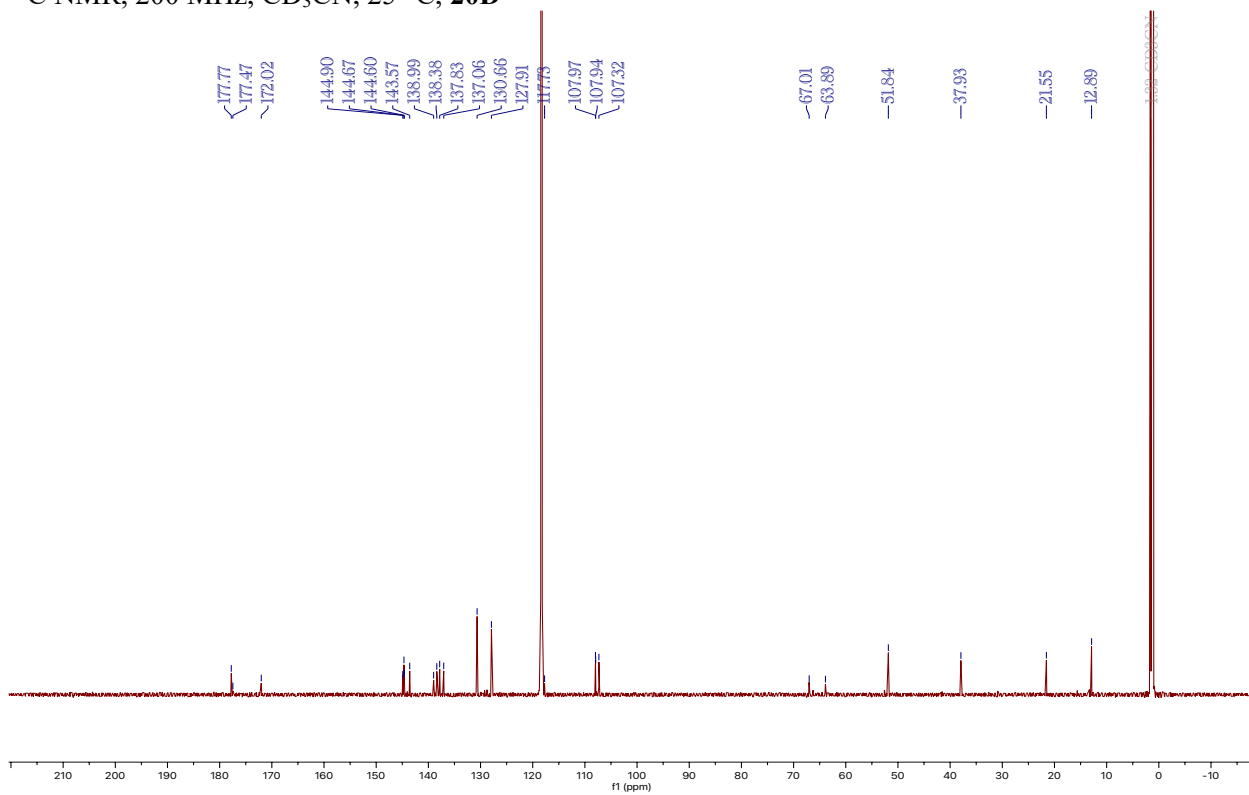
$^1\text{H}$  NMR, 800 MHz,  $\text{CD}_2\text{Cl}_2$ , 25  $^\circ\text{C}$ , **19D**



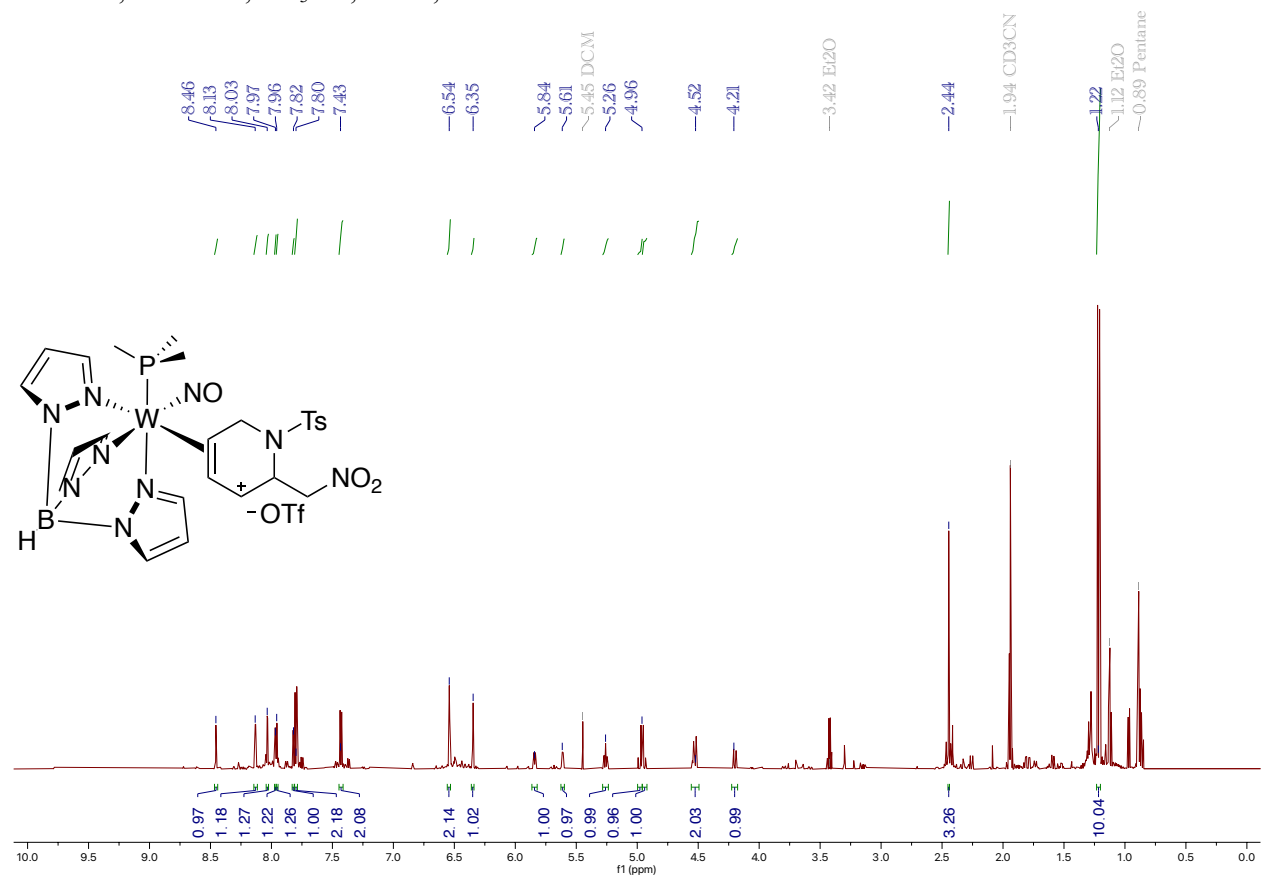
$^1\text{H}$  NMR, 800 MHz,  $\text{CD}_3\text{CN}$ , 25 °C, **20D**



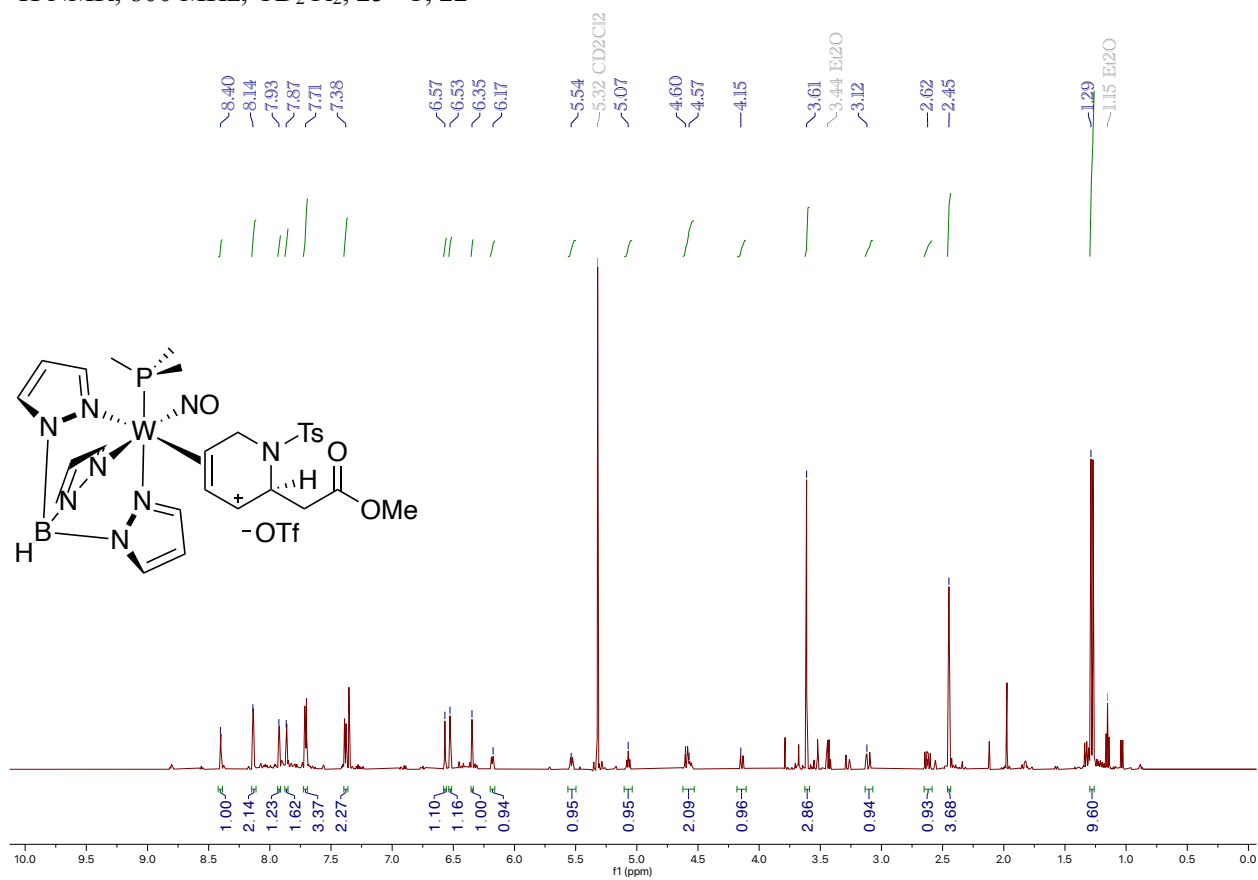
$^{13}\text{C}$  NMR, 200 MHz,  $\text{CD}_3\text{CN}$ , 25 °C, **20D**



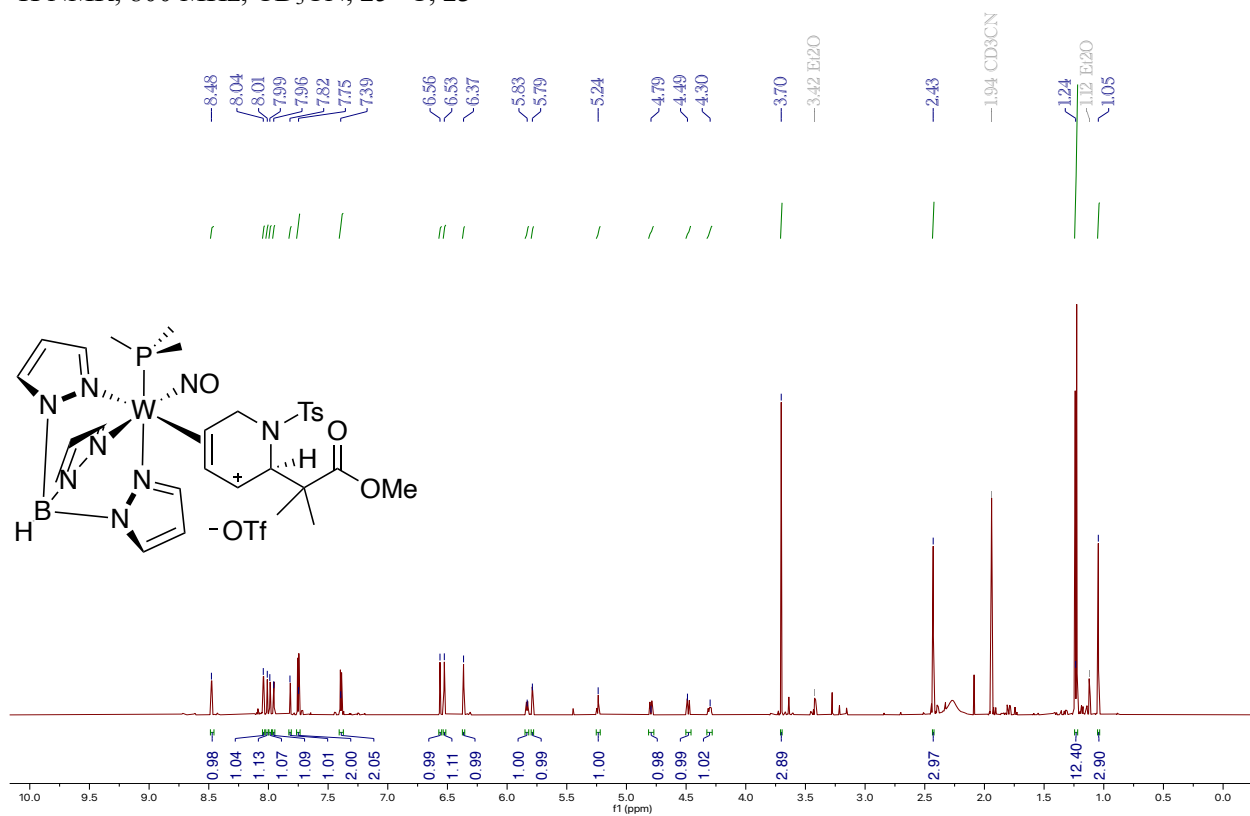
$^1\text{H}$  NMR, 800 MHz,  $\text{CD}_3\text{CN}$ , 25 °C, **21**



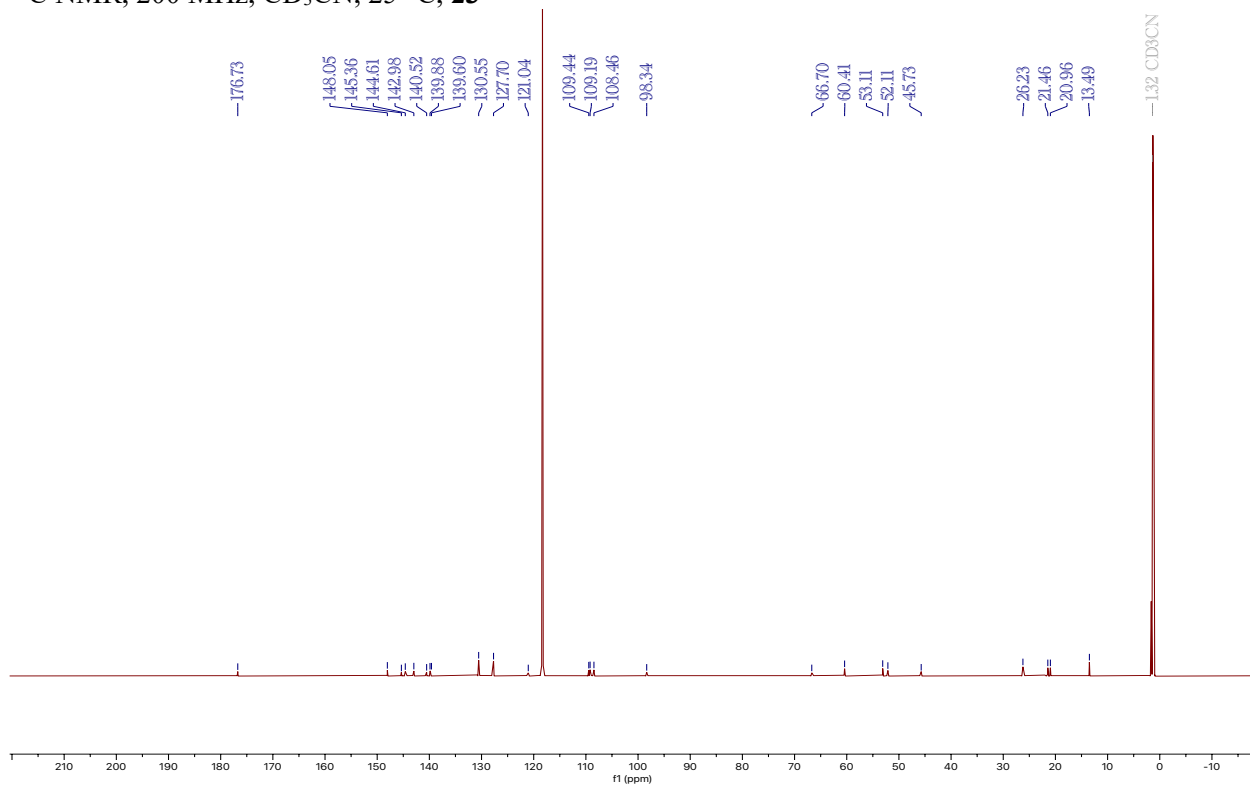
$^1\text{H}$  NMR, 800 MHz,  $\text{CD}_2\text{Cl}_2$ , 25  $^\circ\text{C}$ , **22**



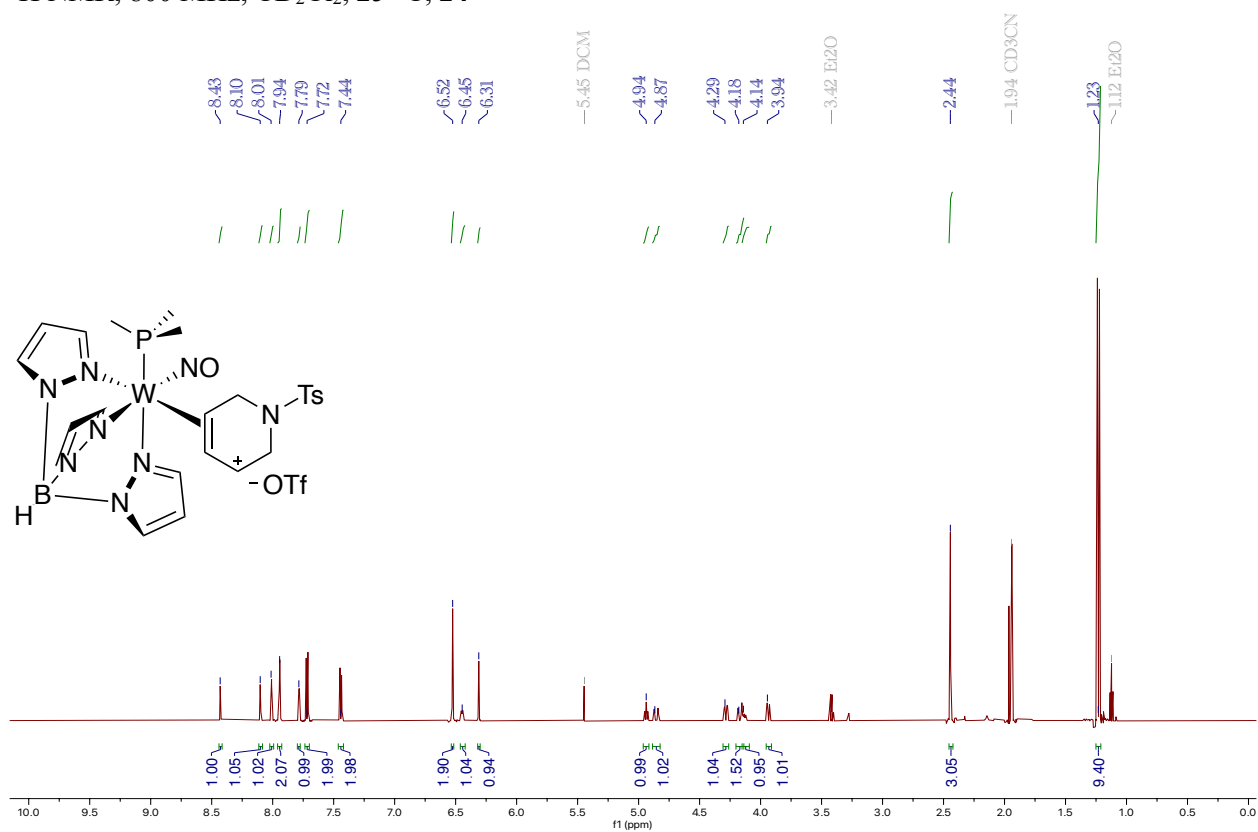
$^1\text{H}$  NMR, 800 MHz,  $\text{CD}_3\text{CN}$ , 25 °C, **23**



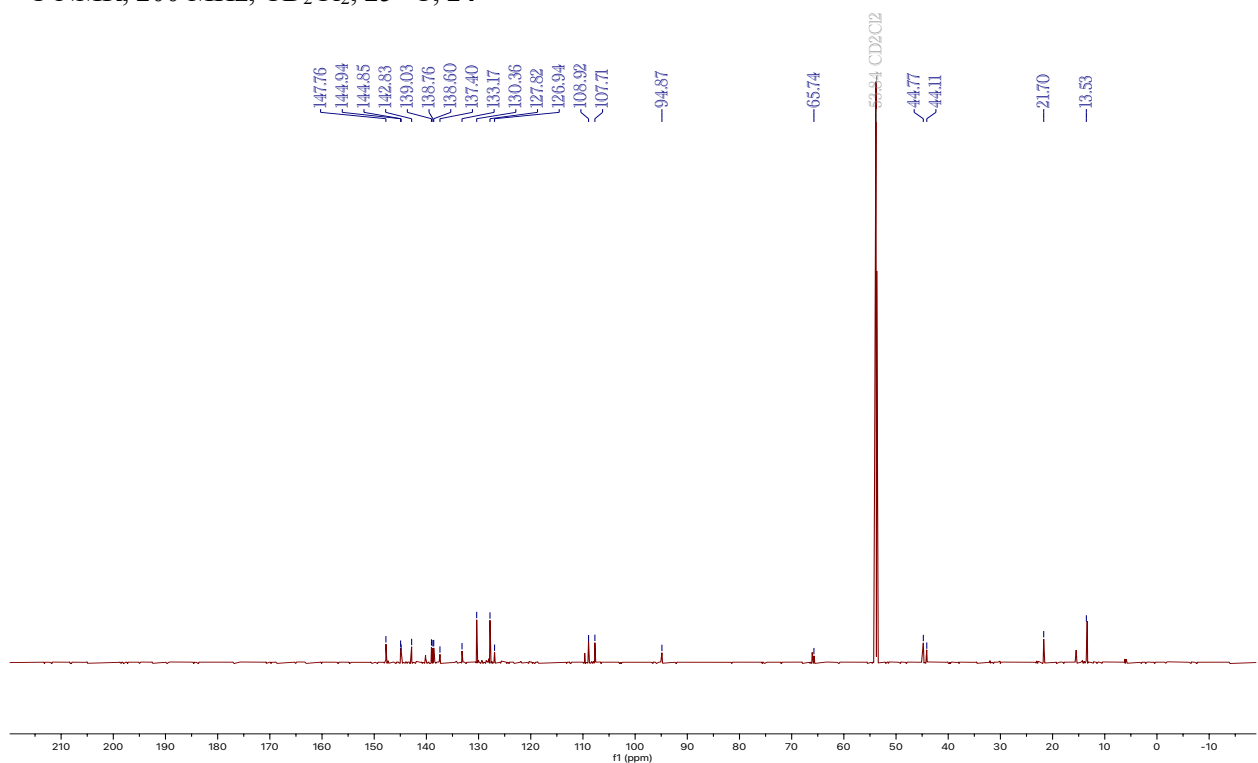
$^{13}\text{C}$  NMR, 200 MHz,  $\text{CD}_3\text{CN}$ , 25 °C, **23**



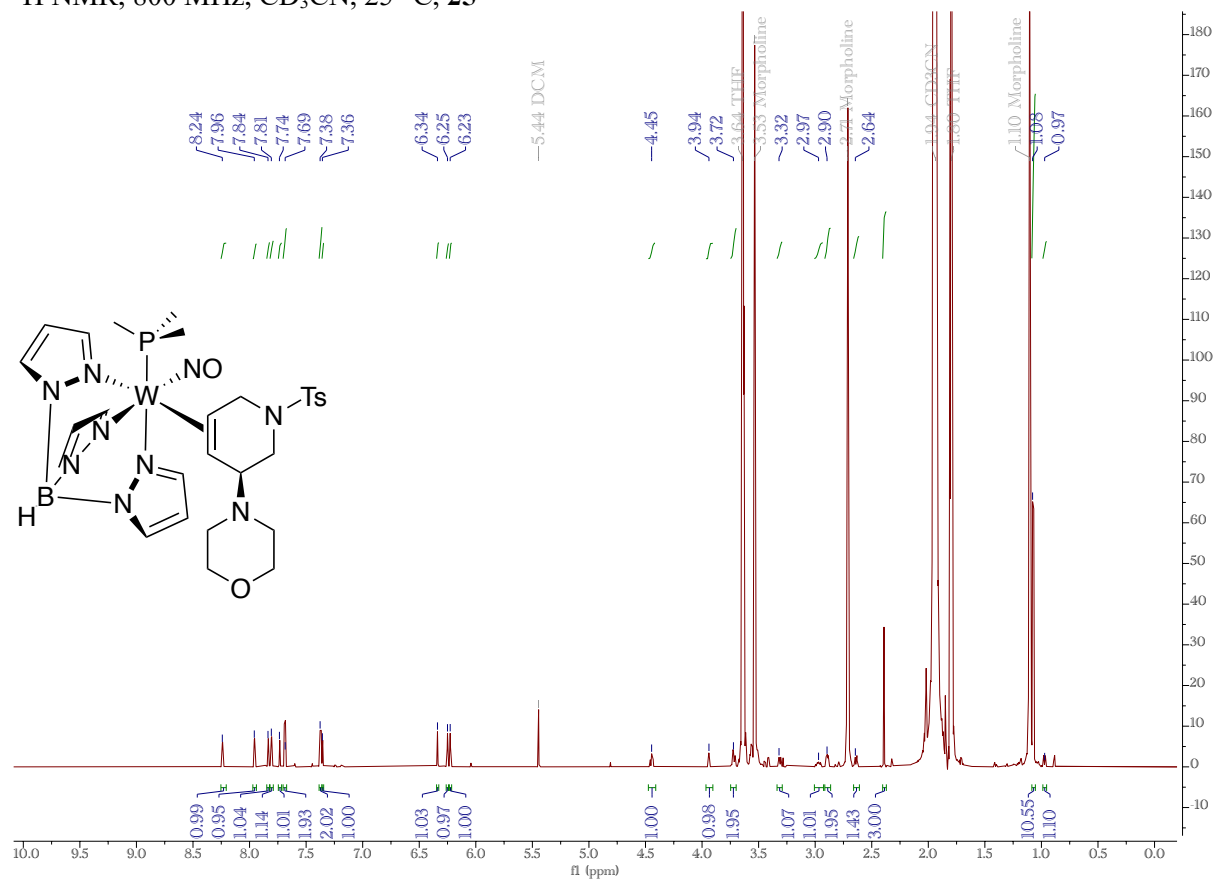
$^1\text{H}$  NMR, 800 MHz,  $\text{CD}_2\text{Cl}_2$ , 25 °C, **24**



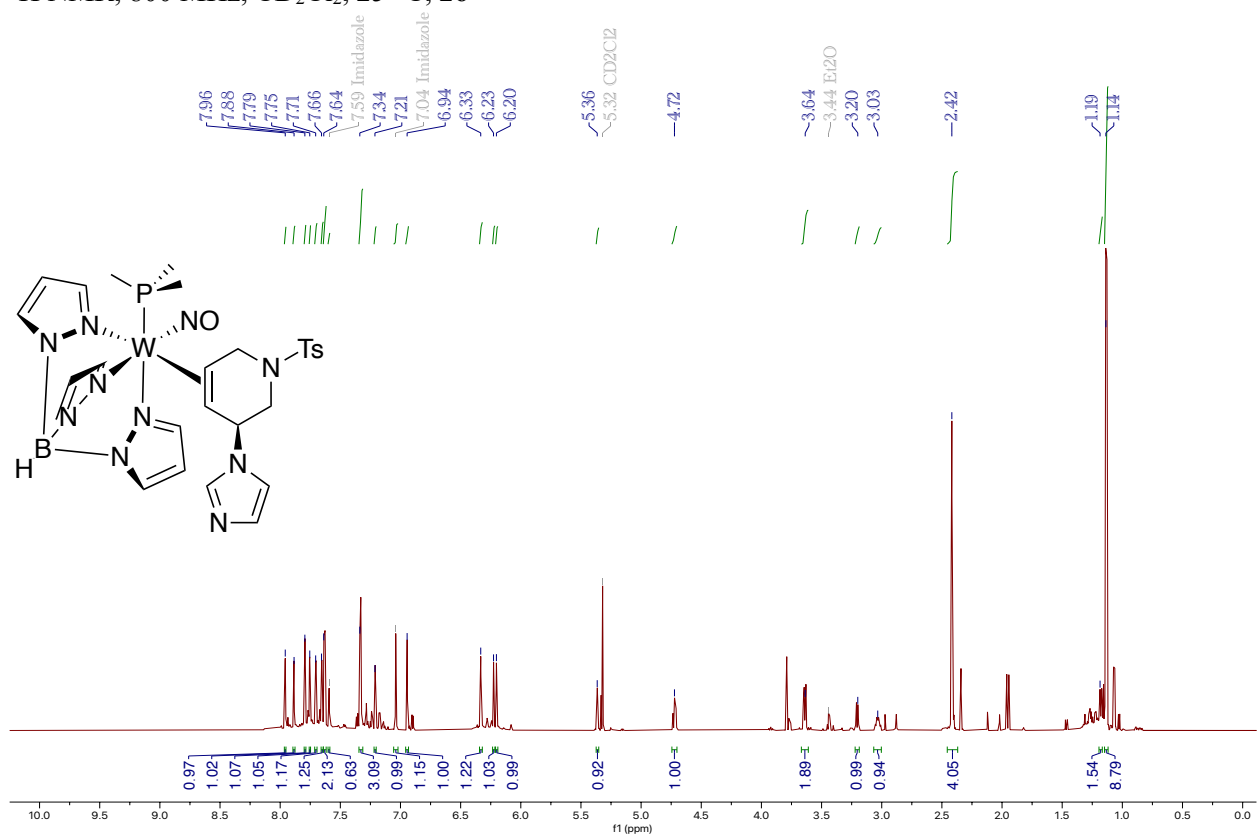
$^{13}\text{C}$  NMR, 200 MHz,  $\text{CD}_2\text{Cl}_2$ , 25 °C, **24**



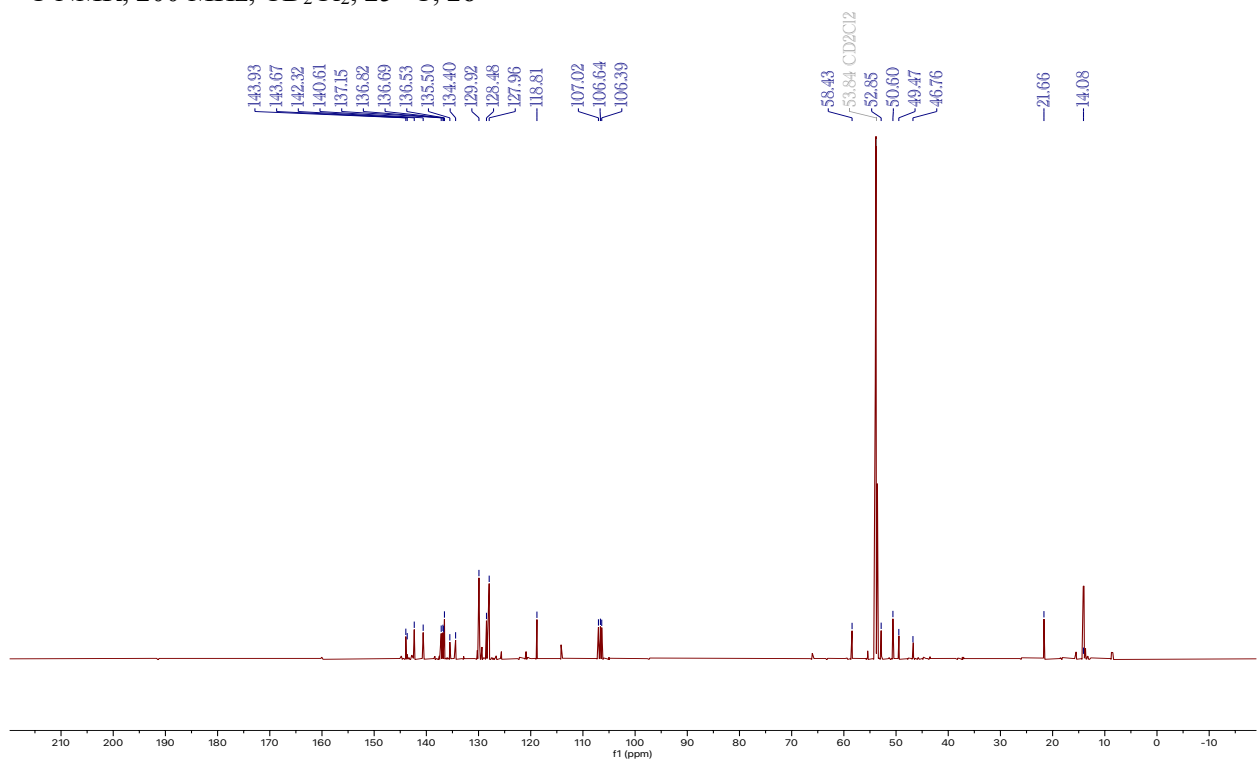
$^1\text{H}$  NMR, 800 MHz,  $\text{CD}_3\text{CN}$ , 25  $^\circ\text{C}$ , **25**



$^1\text{H}$  NMR, 800 MHz,  $\text{CD}_2\text{Cl}_2$ , 25  $^\circ\text{C}$ , **26**

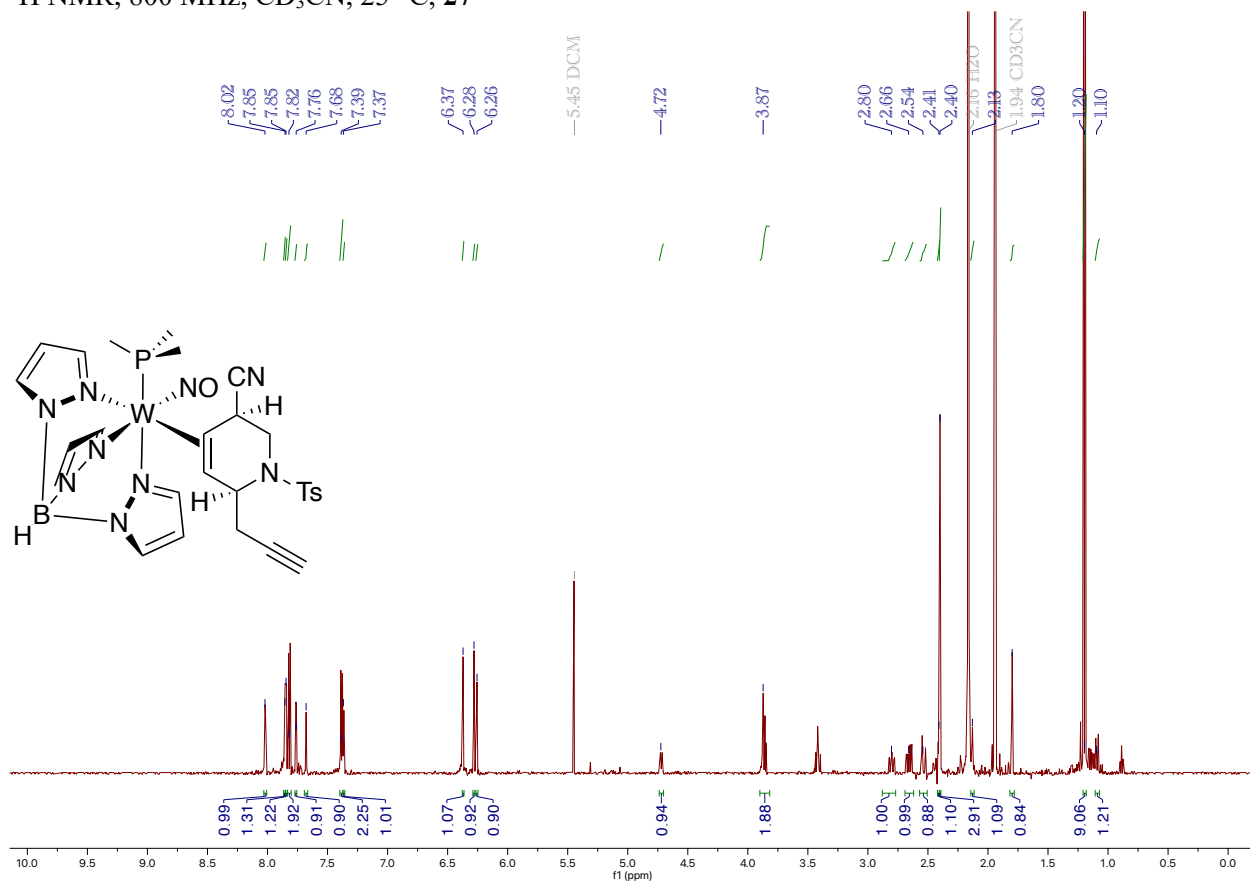


$^{13}\text{C}$  NMR, 200 MHz,  $\text{CD}_2\text{Cl}_2$ , 25  $^\circ\text{C}$ , **26**

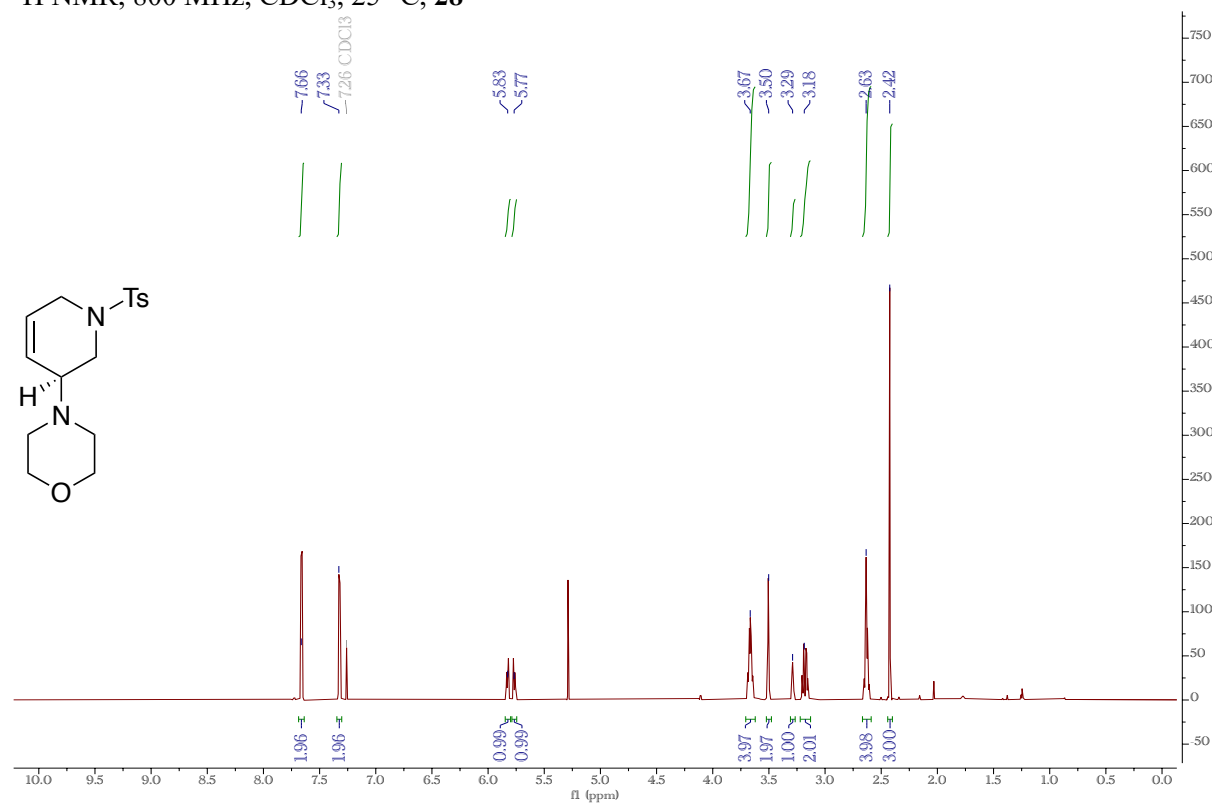




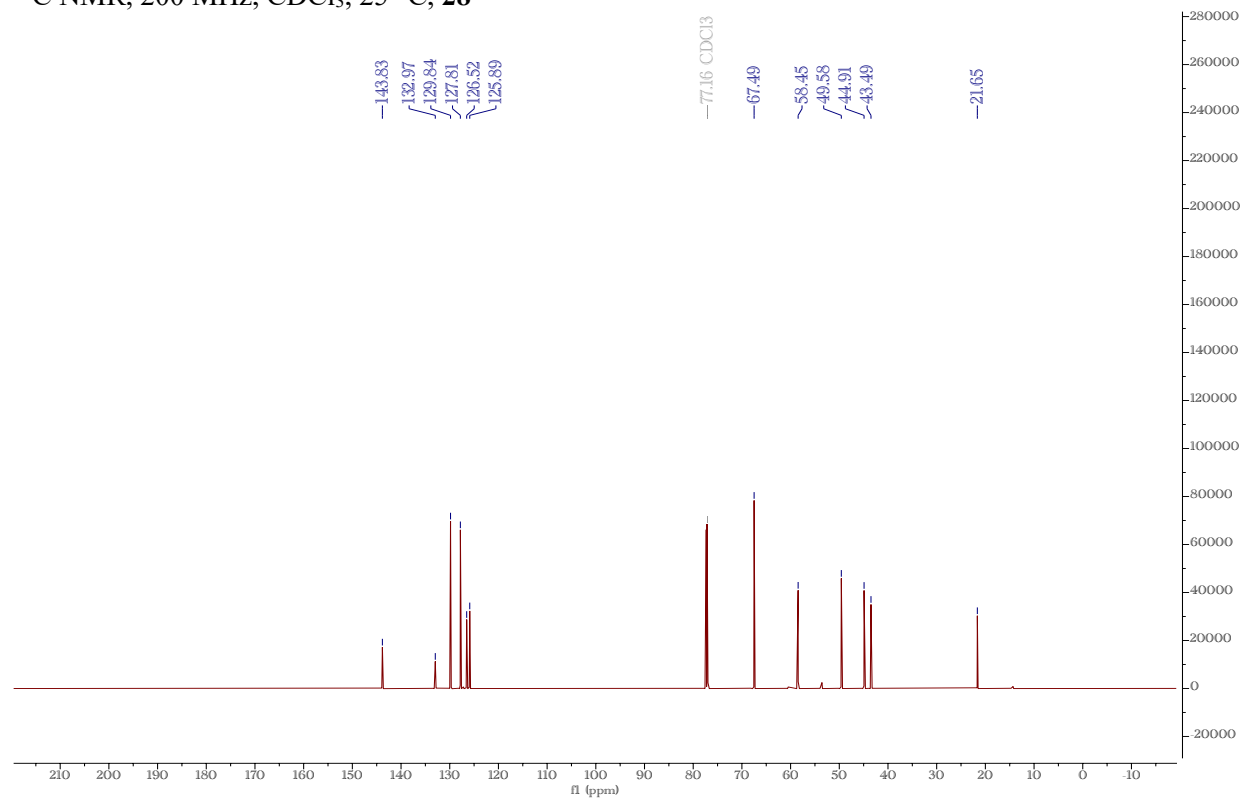
$^1\text{H}$  NMR, 800 MHz,  $\text{CD}_3\text{CN}$ , 25  $^\circ\text{C}$ , **27**



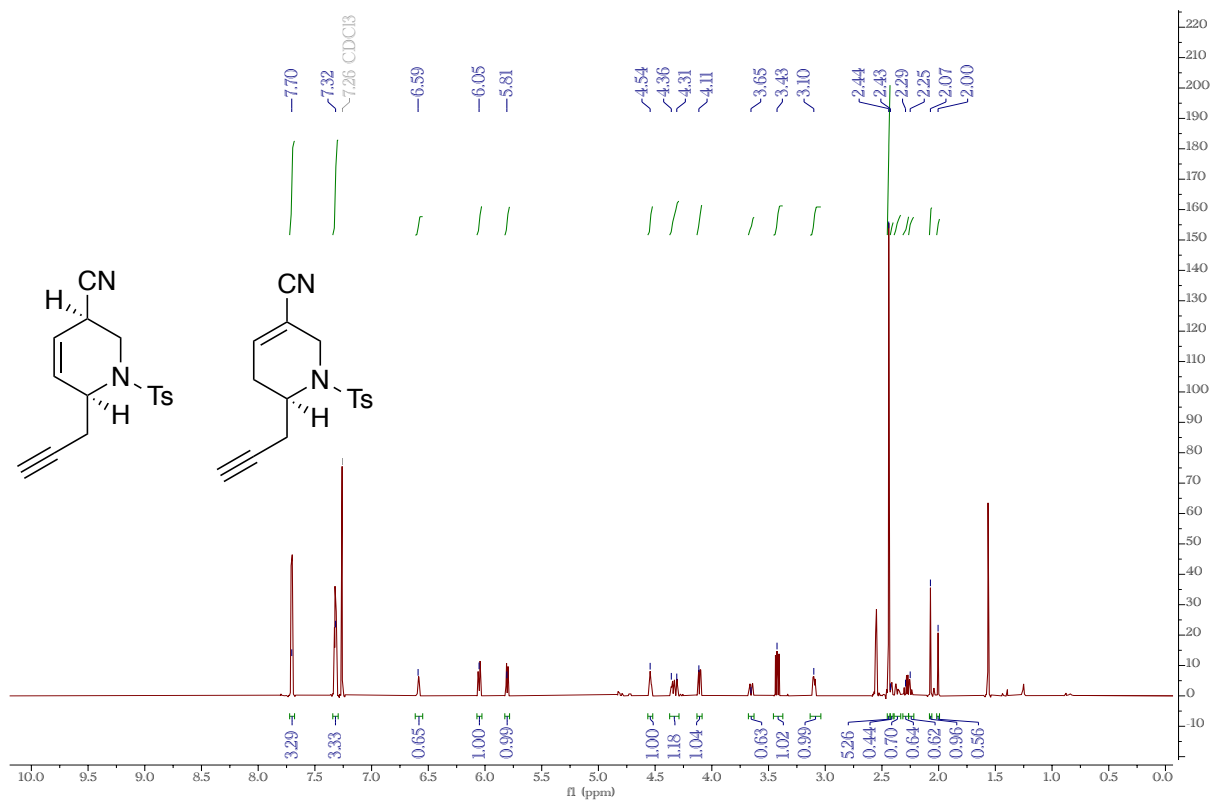
$^1\text{H}$  NMR, 800 MHz,  $\text{CDCl}_3$ , 25 °C, **28**



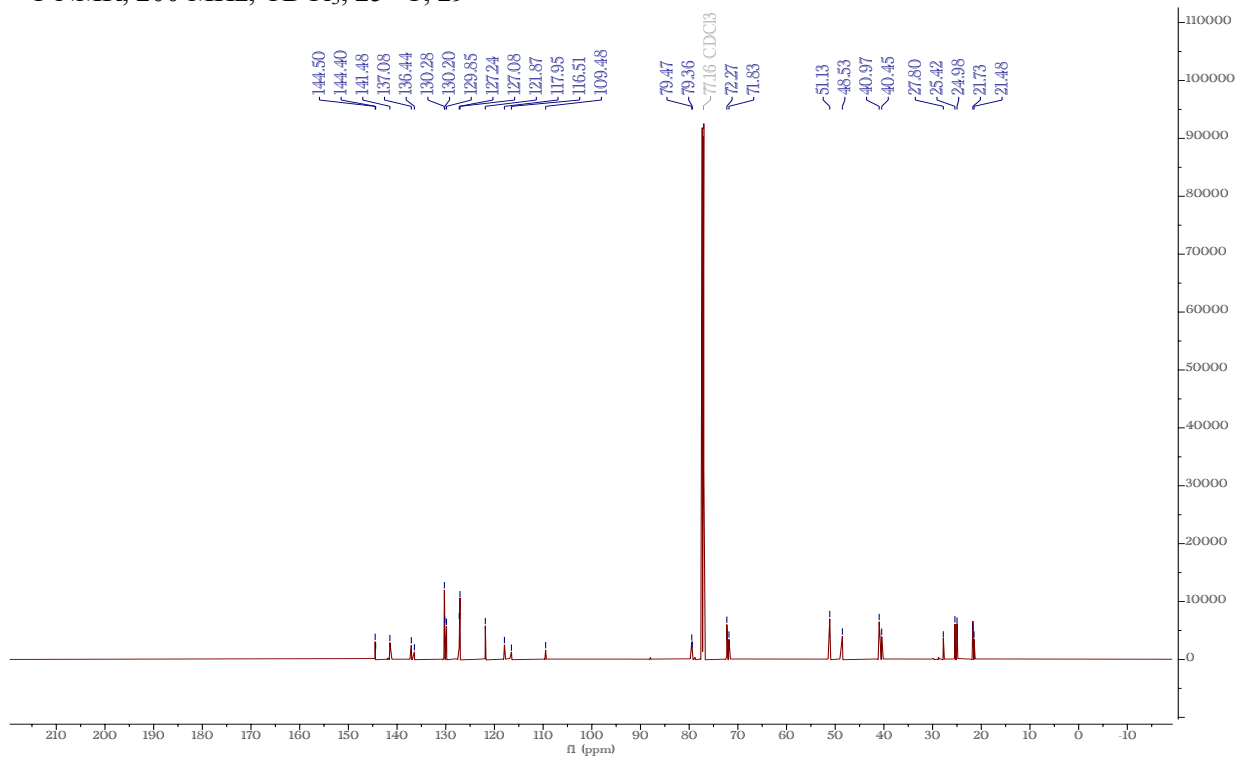
$^{13}\text{C}$  NMR, 200 MHz,  $\text{CDCl}_3$ , 25 °C, **28**



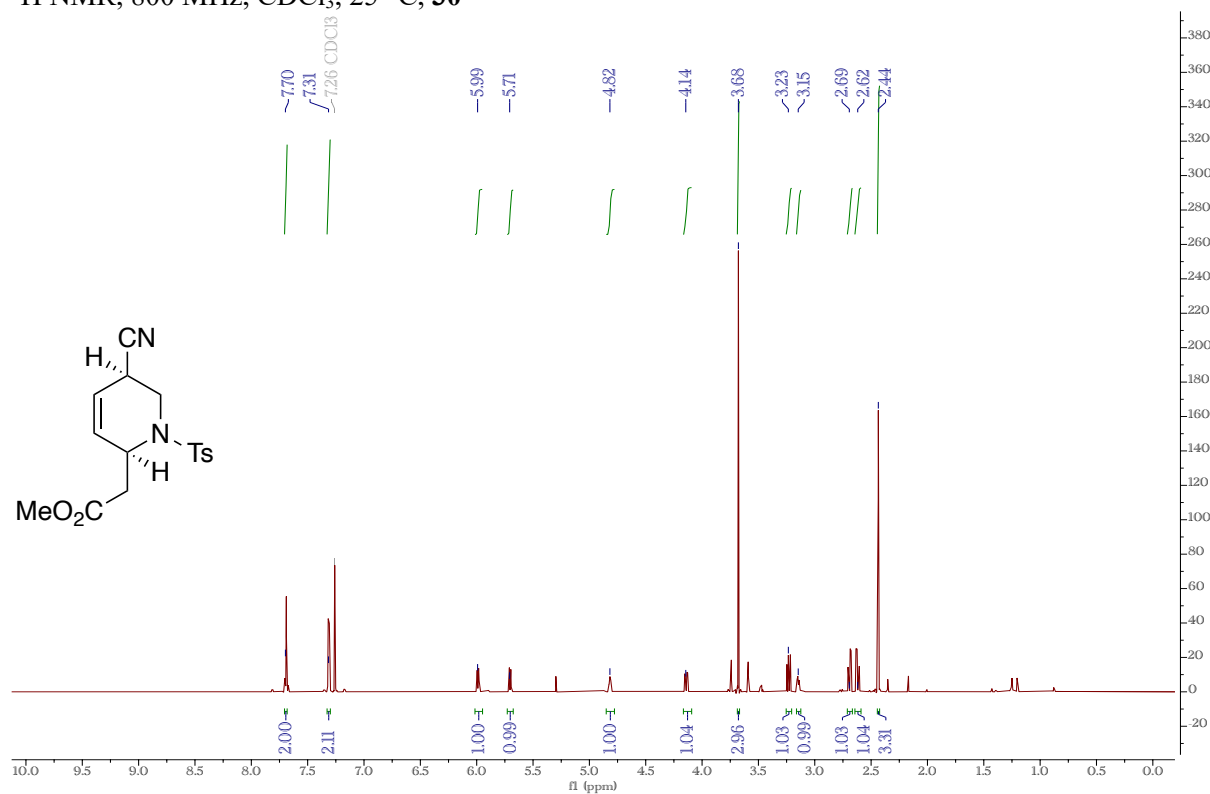
$^1\text{H}$  NMR, 800 MHz,  $\text{CDCl}_3$ , 25 °C, **29**



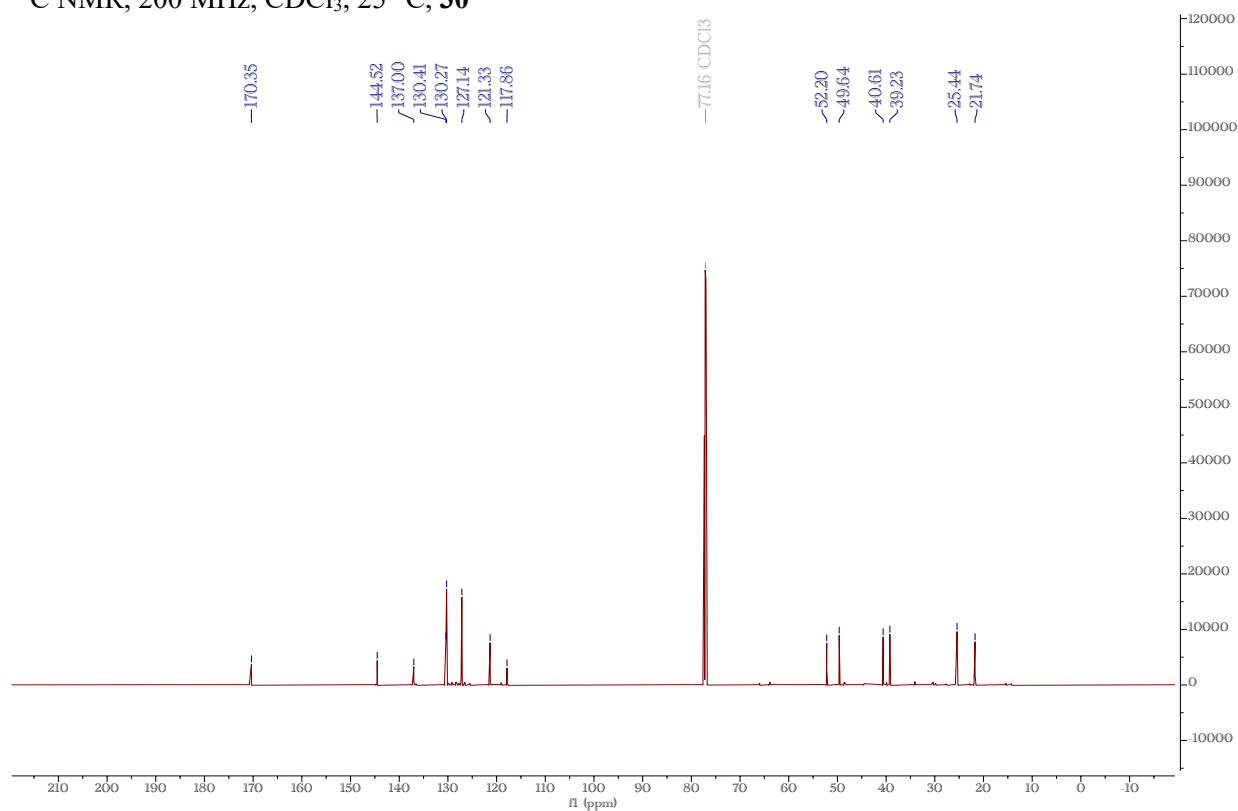
$^{13}\text{C}$  NMR, 200 MHz,  $\text{CDCl}_3$ , 25 °C, **29**



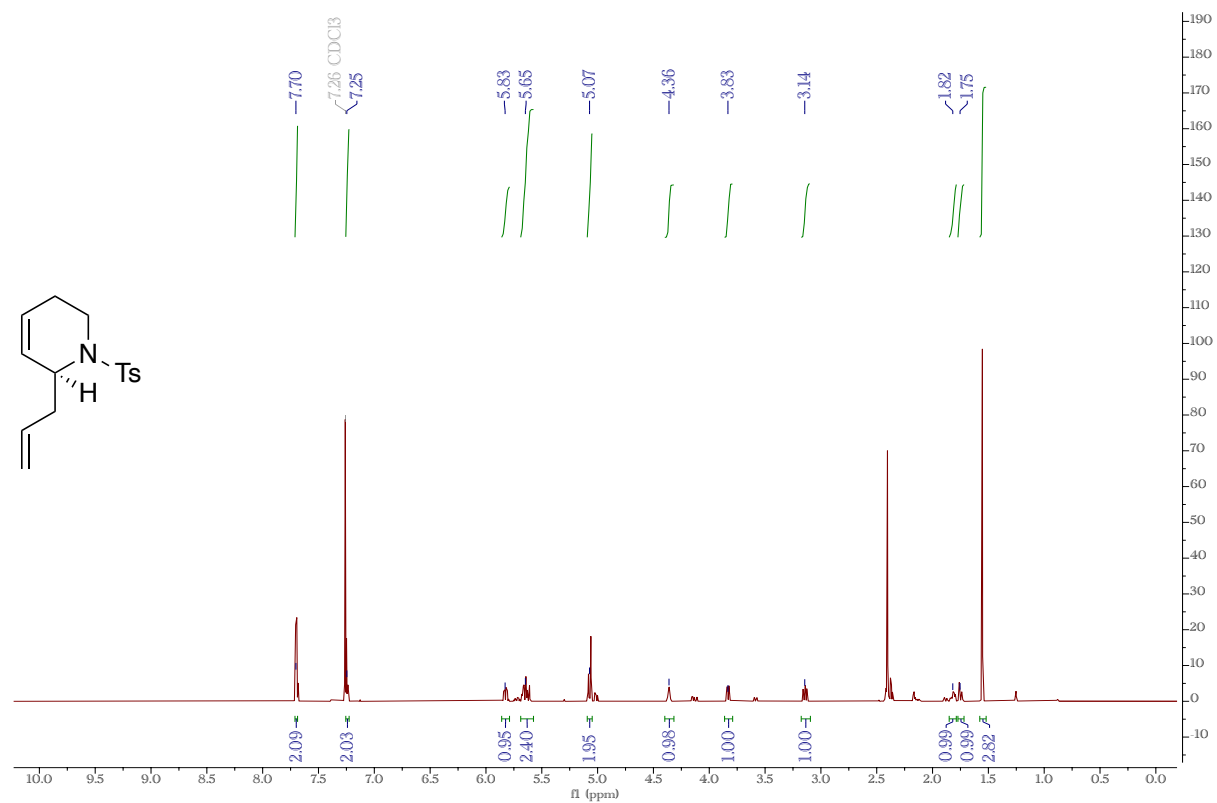
<sup>1</sup>H NMR, 800 MHz, CDCl<sub>3</sub>, 25 °C, **30**



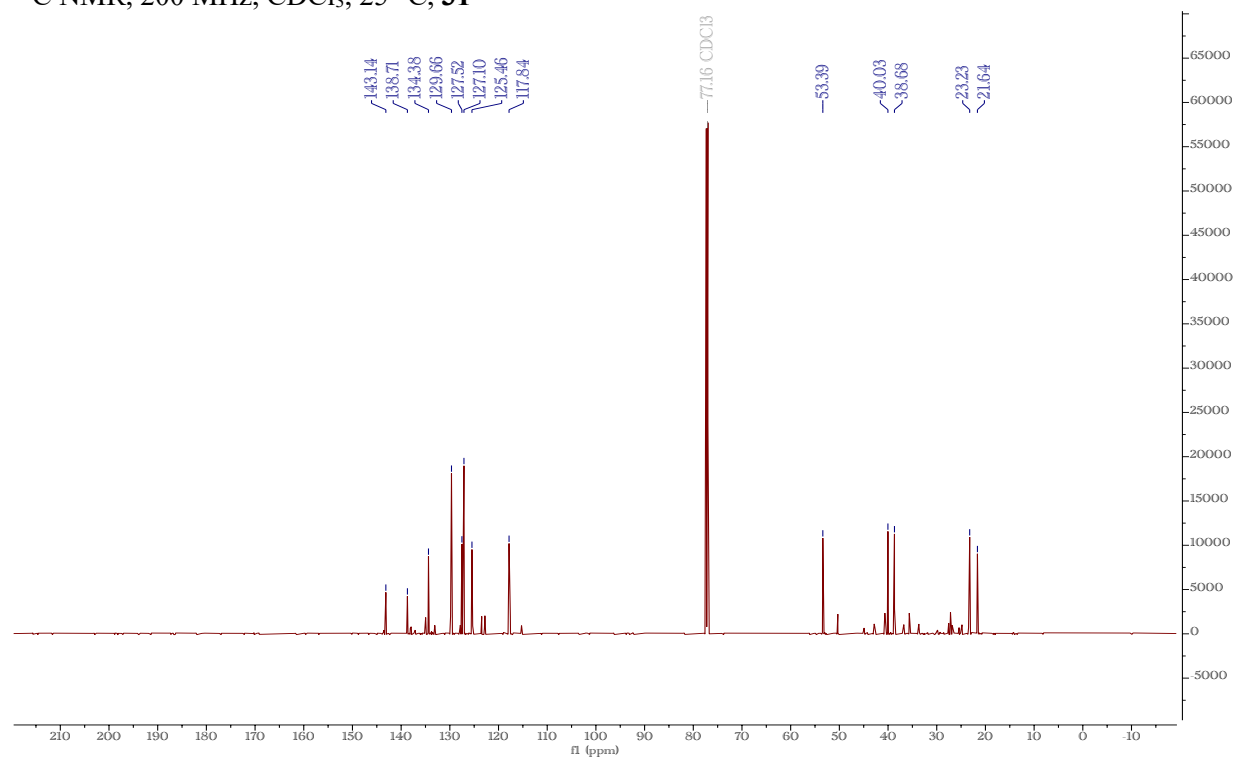
<sup>13</sup>C NMR, 200 MHz, CDCl<sub>3</sub>, 25 °C, **30**



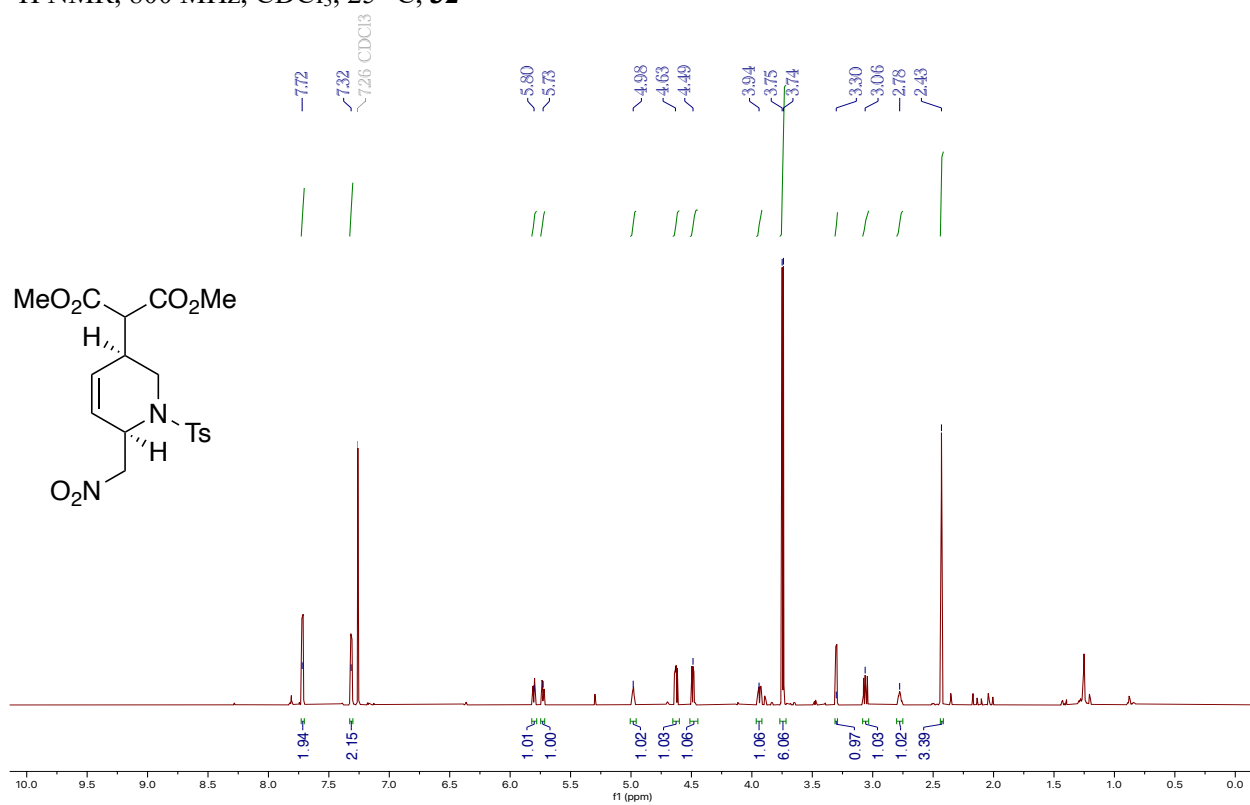
$^1\text{H}$  NMR, 800 MHz,  $\text{CDCl}_3$ , 25 °C, **31**



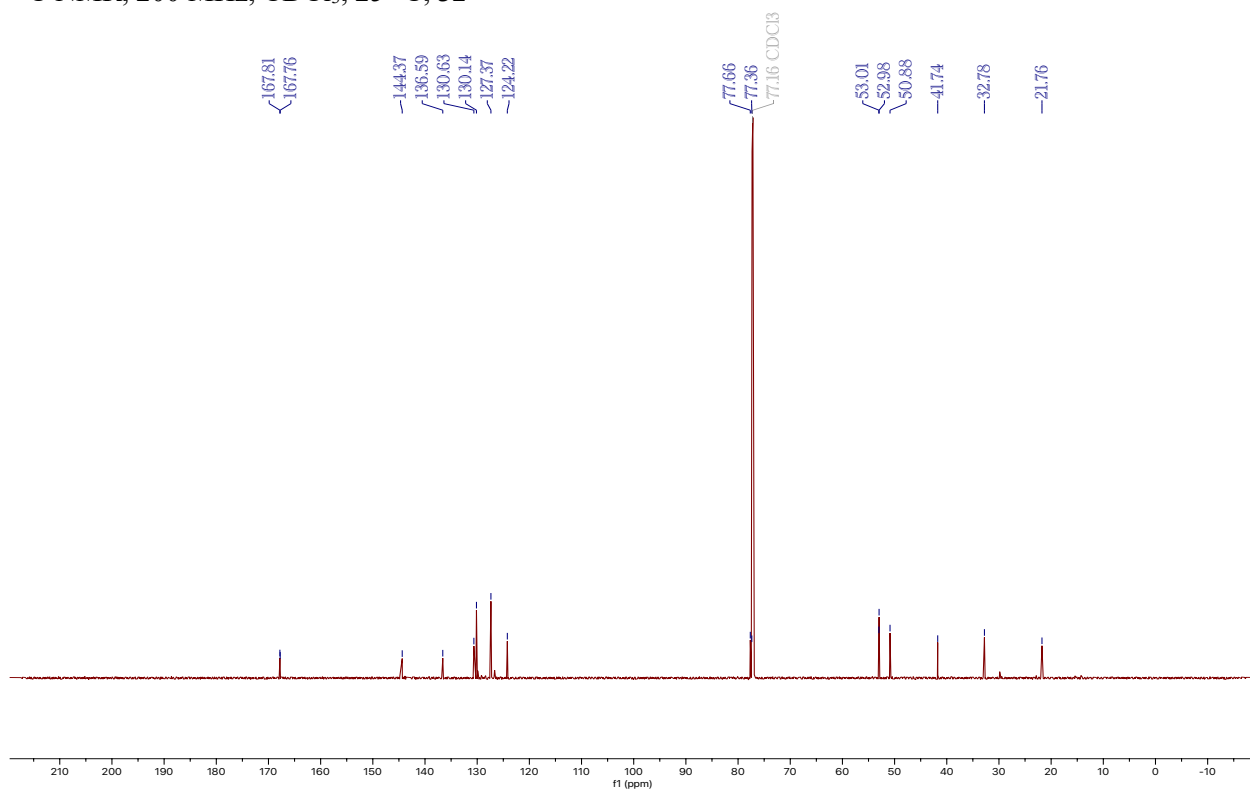
$^{13}\text{C}$  NMR, 200 MHz,  $\text{CDCl}_3$ , 25 °C, **31**



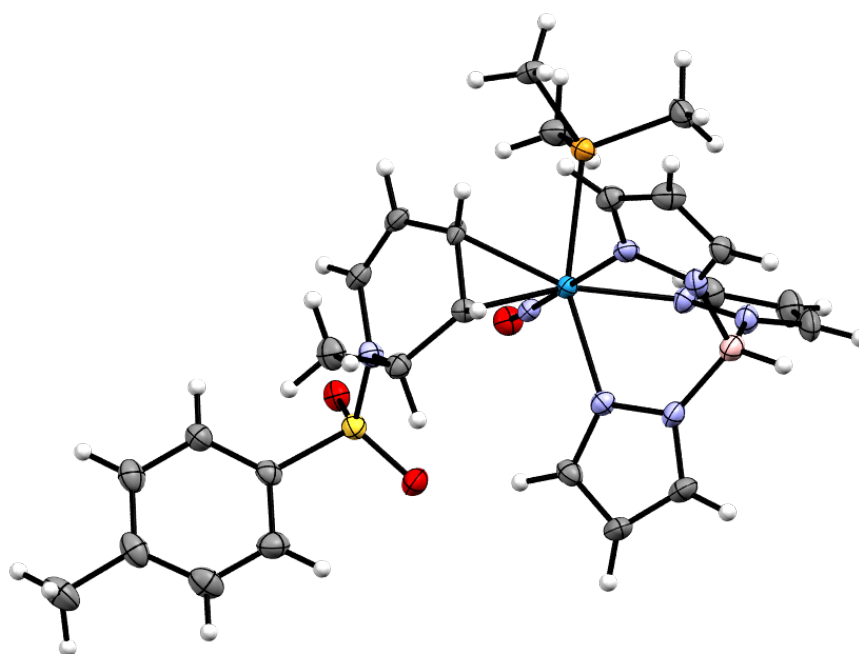
$^1\text{H}$  NMR, 800 MHz,  $\text{CDCl}_3$ , 25 °C, **32**



$^{13}\text{C}$  NMR, 200 MHz,  $\text{CDCl}_3$ , 25 °C, **32**



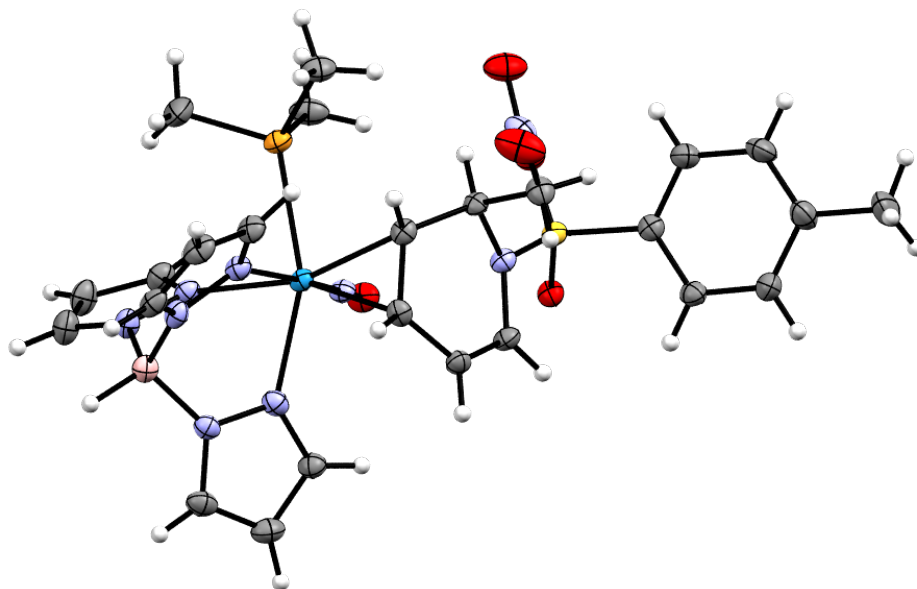
SC-XRD Data:



ORTEP/ellipsoid diagram of **6D**.

SC-XRD data for **6D**.

CCDC N/A	Chemical Formula $C_{25}H_{34}BN_8O_3PSW$	FW (g/mol) 752.29
T (K) 100(2)	$\lambda$ (Å) 0.71073	Crystal size (mm) 0.025 x 0.032 x 0.615
Crystal habit Colorless needle	Crystal system monoclinic	Space group P 2 <sub>1</sub> /c
a (Å) 13.9628(4)	b (Å) 12.4970(4)	c (Å) 16.9468(5)
$\alpha$ (°) 90	$\beta$ (°) 91.0580(10)	$\gamma$ (°) 90
V (Å <sup>3</sup> ) 2956.60(15)	Z 4	$\rho_{calc}$ (g/cm <sup>3</sup> ) 1.690
$\mu$ (mm <sup>-1</sup> ) 4.074	F(000) 1496	$\theta$ range (°) 2.40 to 27.50
Index ranges -18 ≤ h ≤ 18 -16 ≤ k ≤ 16 -22 ≤ l ≤ 18	Data/restraints/parameters 6780 / 0 / 369	Goodness-of-fit on F <sup>2</sup> 0.999
R <sub>1</sub> [I > 2σ(I)] 0.0374	wR <sub>2</sub> [all data] 0.0863	

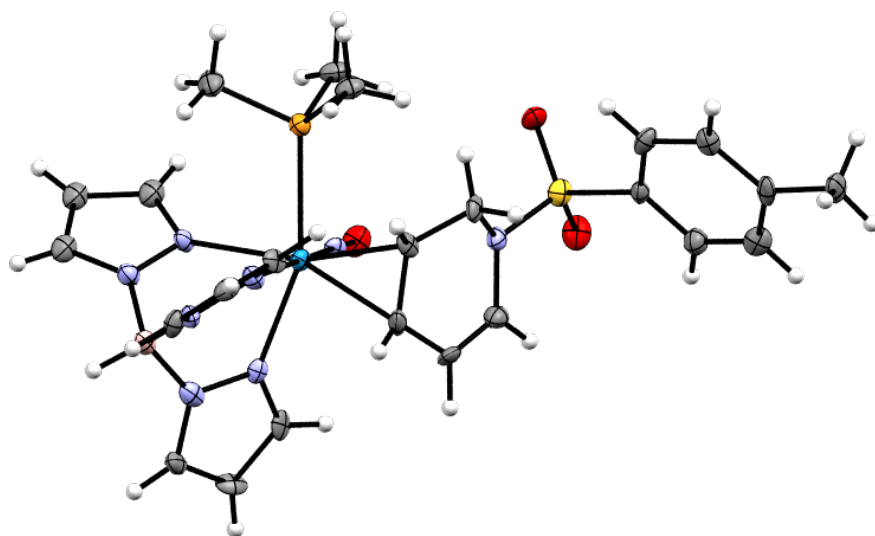


ORTEP/ellipsoid diagram of **8P**.

SC-XRD data for **8P**.

CCDC N/A	Chemical Formula $C_{28}H_{40}BN_9O_5PSW$	FW (g/mol) 840.38
T (K) 100(2)	$\lambda$ (Å) 0.71073	Crystal size (mm) 0.054 x 0.074 x 0.123
Crystal habit Colorless block	Crystal system Triclinic	Space group P -1
a (Å) 11.7763(7)	b (Å) 12.4329(6)	c (Å) 12.8307(7)
$\alpha$ (°) 110.553(2)	$\beta$ (°) 99.703(2)	$\gamma$ (°) 94.396(2)
V (Å <sup>3</sup> ) 1714.97(16)	Z 2	$\rho_{calc}$ (g/cm <sup>3</sup> ) 1.627
$\mu$ (mm <sup>-1</sup> ) 3.526	F(000) 842	$\theta$ range (°) 2.21 to 31.58
Index ranges -17 ≤ h ≤ 17 -18 ≤ k ≤ 16 -17 ≤ l ≤ 18	Data/restraints/parameters 11429 / 0 / 432	Goodness-of-fit on F <sup>2</sup> 1.029
R <sub>1</sub> [I > 2σ(I)] 0.0398	wR <sub>2</sub> [all data] 0.0970	

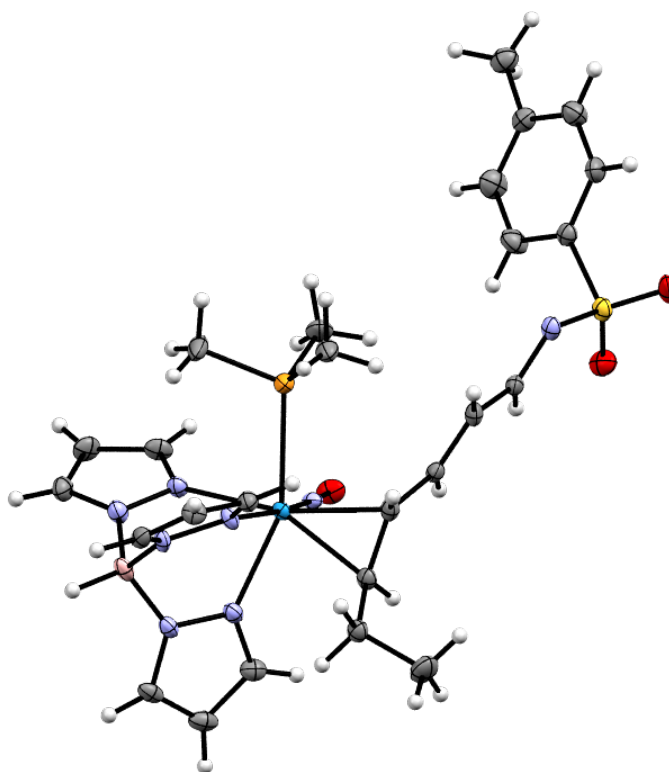




ORTEP/ellipsoid diagram of **15P**.

SC-XRD data for **15P**.

CCDC	Chemical Formula	FW (g/mol)
N/A	$C_{24}H_{32}BN_8O_3PSW$	738.26
T (K)	$\lambda$ (Å)	Crystal size (mm)
100(2)	0.71073	0.034 x 0.055 x 0.258
Crystal habit	Crystal system	Space group
Yellow rod	Triclinic	P -1
a (Å)	b (Å)	c (Å)
8.7191(10)	12.0085(15)	13.9368(16)
$\alpha$ (°)	$\beta$ (°)	$\gamma$ (°)
96.925(4)	90.003(3)	103.280(4)
V (Å <sup>3</sup> )	Z	$\rho_{calc}$ (g/cm <sup>3</sup> )
1409.3(3)	2	1.740
$\mu$ (mm <sup>-1</sup> )	F(000)	$\theta$ range (°)
4.272	732	1.47 to 25.83
Index ranges	Data/restraints/parameters	Goodness-of-fit on F <sup>2</sup>
-10 ≤ h ≤ 10 -14 ≤ k ≤ 14 -17 ≤ l ≤ 17	5384 / 0 / 355	1.005
R <sub>1</sub> [I > 2σ(I)]	wR <sub>2</sub> [all data]	
0.0432	0.0761	



ORTEP/ellipsoid diagram of **17D**.

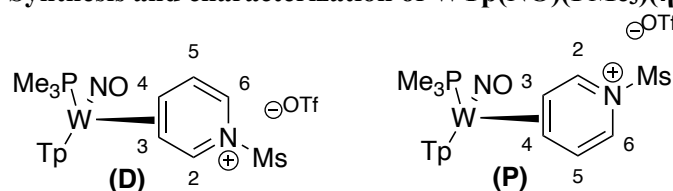
SC-XRD data for **17D**.

CCDC	Chemical Formula	FW (g/mol)
N/A	$C_{26}H_{36}BN_8O_3PSW$	766.32
T (K)	$\lambda$ (Å)	Crystal size (mm)
100(2)	0.71073	0.058 x 0.071 x 0.149
Crystal habit	Crystal system	Space group
Orange plate	Monoclinic	$P 2_1/n$
a (Å)	b (Å)	c (Å)
10.0944(5)	21.6966(10)	14.0302(8)
$\alpha$ (°)	$\beta$ (°)	$\gamma$ (°)
90	92.636(2)	90
V (Å <sup>3</sup> )	Z	$\rho_{calc}$ (g/cm <sup>3</sup> )
3069.6(3)	4	1.658
$\mu$ (mm <sup>-1</sup> )	F(000)	$\theta$ range (°)
3.926	1528	1.73 to 29.63
Index ranges	Data/restraints/parameters	Goodness-of-fit on $F^2$
-13 $\leq h \leq$ 14	8622 / 0 / 379	0.997
-28 $\leq k \leq$ 30		
-19 $\leq l \leq$ 19		
$R_1$ [ $I > 2\sigma(I)$ ]	$wR_2$ [all data]	
0.0327	0.0604	

# Appendix C

## Chapter 3 Data

## Synthesis and characterization of $\text{WTP}(\text{NO})(\text{PMe}_3)(\eta^2\text{-}(N\text{-mesyl})\text{pyridinium}) (\text{OTf})$ (**33D**)



**D:P > 20:1**

Methanesulfonic anhydride (5.87 g, 33.70 mmol), **3** (9.87 g, 13.48 mmol), and EtCN (40 mL) were charged to a flame-dried 100 mL round-bottom flask with a 1-inch stir bar. Lutidine (3.69 g, 34.43 mmol) was added to initiate the reaction, and the flask was submerged in a pre-heated oil bath set to 55 °C. After stirring the solution for ~2 hours, the solution was diluted with 150 mL of DCM and added to a separatory funnel. This solution was washed 3x with 200 mL of saturated aqueous  $\text{NaHCO}_3$ . The organic layer was isolated and set aside. The combined aqueous layers were combined and back-extracted with 50 mL of DCM to prevent product loss. The organic layers were combined in a single flask and dried with anhydrous  $\text{MgSO}_4$ . This powder was then filtered off into a 60 mL coarse porosity fritted funnel and washed with DCM. The dried organic layers were then reduced *in vacuo* down to dryness. The residue in the flask was redissolved in minimal DCM (approximately 10 mL). The solution was then slowly added to 500mL of stirring diethyl ether. An orange precipitate formed immediately and was allowed to stir for ~10 minutes to ensure total precipitation. This powder was collected on a 60 mL medium porosity frit and washed 2x with 30 mL of ether. This powder was dried in a desiccator under vacuum for ~30 minutes. The dried powder was gently added to a stirring solution of 150 mL of HPLC grade ethyl acetate and triturated overnight. The final orange precipitate was collected on the F frit, washed 2x with 30 mL of ethyl acetate and 2x with 30 mL of diethyl ether, and dried in the desiccator overnight under vacuum (5.5 g, 50% yield).

$^1\text{H}$  NMR ( $\text{CD}_2\text{Cl}_2$ ,  $\delta$ , 25 °C): (**D**): 9.14 (d,  $J = 5.9$  Hz, 1H, H2), 7.97 (d,  $J = 2.1$  Hz, 1H, PzB3), 7.96 (d,  $J = 2.3$  Hz, 1H, PzC5), 7.93 (d,  $J = 2.4$  Hz, 1H, PzB5), 7.90 (d,  $J = 2.1$  Hz, 1H, PzA3), 7.76 (d,  $J = 2.4$  Hz, 1H, PzA5), 7.65 (d,  $J = 2.1$  Hz, 1H, PzC3), 6.64 (ddd,  $J = 1.8, 5.6, 7.8$  Hz, 1H, H5), 6.48 (t,  $J = 2.3$  Hz, 1H, PzC4), 6.45 (dd,  $J = 1.6, 7.8$  Hz, 1H, H6), 6.44 (t,  $J = 2.2$  Hz, 1H, PzB4), 6.39 (t,  $J = 2.3$  Hz, 1H, PzA4), 4.16 (dt,  $J = 6.2, 12.4$  Hz, 1H, H4), 3.61 (s, 3H, Ms), 3.08 (td,  $J = 1.8, 6.2$  Hz, 1H, H3), 1.26 (d,  $J_{\text{PH}} = 9.2$  Hz, 9H,  $\text{PMe}_3$ ). (**P**): 9.43 (d,  $J = 5.1$  Hz, 1H, H2), (2 other Pz3/5 signals buried) 7.93 (d,  $J = 2.3$  Hz, 1H, Pz3/5), 7.91 (d,  $J = 2.4$  Hz, 1H, Pz3/5), 7.78 (d,  $J = 2.4$  Hz, 1H, Pz3/5), 7.58 (d,  $J = 2.1$  Hz, 1H, Pz3/5), 6.81 (dd,  $J = 1.0, 6.7$  Hz, 1H, H5), 6.42 (t,  $J = 2.3$  Hz, 1H, Pz4), 6.41 (t,  $J = 2.3$  Hz, 1H, Pz4), 6.32 (t,  $J = 2.2$  Hz, 1H, Pz4), 6.31 (dd,  $J = 1.4, 7.3$  Hz, 1H, H6), 4.21 (q,  $J = 6.2$  Hz, 1H, H4), 3.71 (s, 3H, Ms), 2.86 (t,  $J = 6.7$  Hz, 1H, H3), 1.33 (d,  $J_{\text{PH}} = 8.80$  Hz, 9H,  $\text{PMe}_3$ ).

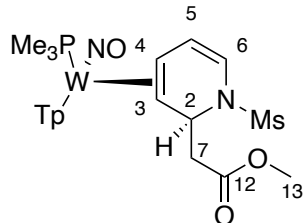
$^{13}\text{C}$  NMR ( $\text{CD}_2\text{Cl}_2$ ,  $\delta$ , 25 °C): (**D**): 167.9 (C2), 146.8 (PzA3), 145.8 (d,  $J_{\text{PC}} = 2.0$  Hz, PzB3), 141.9 (PzC3), 138.9 (PzC5), 138.7 (PzB5), 137.8 (PzA5), 124.1 (d,  $J_{\text{PC}} = 3.0$  Hz, C5), 121.5 (q,  $J_{\text{FC}} = 320.5$  Hz, TfO<sup>-</sup>), 115.2 (C6), 108.4 (PzC4), 108.3 (PzB4), 108.0 (PzA4), 67.1 (d,  $J_{\text{PC}} = 13.9$  Hz, C4), 66.1 (C3), 44.2 (Ms), 13.2 (d,  $J_{\text{PC}} = 31.3$  Hz, 3C,  $\text{PMe}_3$ ). (**P**): 163.0 (C2), 144.7 (Pz3/5), 142.4 (Pz3/5), 141.1 (Pz3/5), 138.6 (Pz3/5), 138.1 (Pz3/5), 137.1 (Pz3/5), 127.3 (C5), 112.6 (C6), 108.1 (Pz4), 108.0 (Pz4), 106.9 (Pz4), 68.1 (C4), 65.1 (C3), 43.4 (Ms), 13.8 (d,  $J_{\text{PC}} = 30.3$  Hz, 3C,  $\text{PMe}_3$ ).

IR  $\nu(\text{NO}) = 1617 \text{ cm}^{-1}$ ,  $\nu(\text{BH}) = 2519 \text{ cm}^{-1}$ .

CV (DMA; 100 mV/s)  $E_{\text{p,a}} = +1.18 \text{ V}$  (NHE),  $E_{\text{p,c}} = -0.96 \text{ V}$  (NHE).

HRMS (ESI)  $m/z$ :  $[\text{M}]^+$  Calcd for  $\text{C}_{18}\text{H}_{27}\text{BN}_8\text{O}_3\text{PSW}^+$  661.1261; Found 661.1261

### Synthesis and characterization of $\text{WTp}(\text{NO})(\text{PMe}_3)(\eta^2\text{-}(N\text{-mesyl})\text{-}2\text{-}(\text{methylacetate})\text{-}1,2\text{-dihydropyridine})$ (**34D**)



Methyl bromoacetate (107 mg, 0.70 mmol), (**33D**) (204 mg, 0.25 mmol), and THF (3.0 mL) were charged to a flame-dried 50 mL round-bottom flask with a 1-inch stir bar. Zinc powder (67 mg, 1.02 mmol) was added to initiate the reaction, and the heterogenous solution was stirred for 1 hour. The zinc was removed by filtering the solution through a celite plug set up in a 60 mL coarse porosity frit with 1 inch of celite, which was then washed with residual DCM to prevent loss of product. The solution was diluted with 150 mL of DCM and added to a separatory funnel. This solution was washed 3x with 200 mL of saturated aqueous  $\text{NaHCO}_3$ . The organic layer was isolated and set aside. The combined aqueous layers were combined and back-extracted with 50 mL of DCM to prevent product loss. The organic layers were combined in a single flask and dried with anhydrous  $\text{MgSO}_4$ . This powder was then filtered off into a 60 mL coarse porosity fritted funnel and washed with DCM. The dried organic layers were then reduced *in vacuo* to dryness. The residue in the flask was redissolved in minimal DCM (approximately 10 mL). The solution was then slowly added to 200mL of stirring pentane. A tan precipitate formed immediately and was allowed to stir for ~10 minutes to ensure total precipitation. This powder was collected on a 60 mL medium porosity frit and washed 2x with 30 mL of pentane. This powder was dried in a desiccator under vacuum for ~30 minutes (178 mg, 96% yield).

$^1\text{H}$  NMR ( $\text{CD}_2\text{Cl}_2$ ,  $\delta$ , 25 °C): 8.12 (d,  $J = 1.9$  Hz, 1H, PzA3), 8.08 (d,  $J = 1.9$  Hz, 1H, PzB3), 7.78 (d,  $J = 2.3$  Hz, 1H, PzB5), 7.75 (d,  $J = 2.3$  Hz, 1H, PzC5), 7.69 (d,  $J = 2.3$  Hz, 1H, PzA5), 7.28 (d,  $J = 2.1$  Hz, 1H, PzC3), 6.36 (t,  $J = 2.2$  Hz, 1H, PzB4), 6.32 (t,  $J = 2.3$  Hz, 1H, PzA4), 6.23 (t,  $J = 2.3$  Hz, 1H, PzC4), 5.86 (d,  $J = 7.8$  Hz, 1H, H6), 5.66 (ddd,  $J = 0.7, 5.1, 7.8$  Hz, 1H, H5), 5.06 (m, 1H, H2), 3.47 (s, 3H, H9), 3.19 (s, 3H, Ms), 3.09 (dd,  $J = 3.8, 14.7$  Hz, 1H, H7), 3.00 (dd,  $J = 9.0, 14.7$  Hz, 1H, H7'), 2.79 (ddd,  $J = 5.1, 10.6, 13.1$  Hz, 1H, H4), 1.55 (d,  $J = 10.6$  Hz, 1H, H3), 1.17 (d,  $J_{\text{PH}} = 8.5$  Hz, 9H,  $\text{PMe}_3$ ).

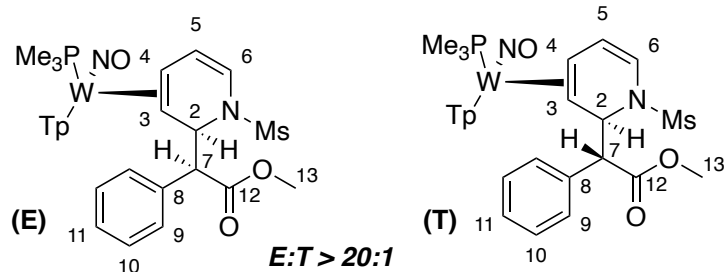
$^{13}\text{C}$  NMR ( $\text{CD}_2\text{Cl}_2$ ,  $\delta$ , 25 °C): 172.5 (C8), 143.5 (PzA3), 143.3 (d,  $J_{\text{PC}} = 1.7$  Hz, PzB3), 140.7 (PzC3), 137.3 (PzC5), 136.6 (PzB5), 136.4 (PzA5), 115.3 (C6), 112.6 (d,  $J_{\text{PC}} = 3.0$  Hz, C5), 107.1 (PzB4), 106.6 (PzC4), 106.4 (PzA4), 62.2 (d,  $J_{\text{PC}} = 1.4$  Hz, C3), 53.2 (C2), 51.7 (C10), 44.9 (C7), 44.5 (d,  $J_{\text{PC}} = 10.5$  Hz, C4), 42.4 (Ms), 13.3 (d,  $J_{\text{PC}} = 28.6$  Hz, 3C,  $\text{PMe}_3$ ).

IR  $\nu(\text{NO}) = 1537 \text{ cm}^{-1}$ ,  $\nu(\text{BH}) = 2483 \text{ cm}^{-1}$ ,  $\nu(\text{C=O}) = 1725 \text{ cm}^{-1}$

CV (DMA; 50 mV/s)  $E_{\text{p,a}} = +0.53 \text{ V}$  (NHE)

SC-XRD data on page 257

### Synthesis and characterization of WTp(NO)(PMe<sub>3</sub>)( $\eta^2$ -(*N*-mesyl)-2-(methyl- $\alpha$ -phenylacetate)-1,2-dihydropyridine) (**35D**)



Methyl  $\alpha$ -phenylbromoacetate (1.69 g, 7.38 mmol), (**33D**) (1.75 g, 2.16 mmol), and THF (10 mL) were charged to a flame-dried 50 mL round-bottom flask with a 1-inch stir bar. Zinc powder (490 mg, 7.49 mmol) was added to initiate the reaction, and the heterogenous solution was stirred for 1 hour. The zinc was removed by filtering the solution through a celite plug set up in a 60 mL coarse porosity frit with 1 inch of celite, which was then washed with residual DCM to prevent loss of product. The solution was diluted with 150 mL of DCM and added to a separatory funnel. This solution was washed 3x with 200 mL of saturated aqueous NaHCO<sub>3</sub>. The organic layer was isolated and set aside. The combined aqueous layers were combined and back-extracted with 50 mL of DCM to prevent product loss. The organic layers were combined in a single flask and dried with anhydrous MgSO<sub>4</sub>. This powder was then filtered off into a 60 mL coarse porosity fritted funnel and washed with DCM. The dried organic layers were then reduced *in vacuo* to dryness. The residue in the flask was redissolved in minimal DCM (approximately 10 mL). The solution was then slowly added to 200mL of stirring pentane. A tan precipitate formed immediately and was allowed to stir for ~10 minutes to ensure total precipitation. This powder was collected on a 60 mL medium porosity frit and washed 2x with 30 mL of pentane. This powder was dried in a desiccator under vacuum for ~30 minutes. The dried powder was gently added to a 4-dram vial containing a stir pea, filled with 10 mL of stirring MeOH, and triturated overnight. This trituration is performed to remove residual paramagnetic tungsten impurities; however, eluting the product off a basic alumina plug with ethyl acetate and subsequently precipitating the reduced solution in pentane will suffice to replace this step. The tan precipitate was collected on a 15 mL fine porosity frit and washed 2x with 10 mL of MeOH. After drying in a desiccator for 2 hours, the highly pure tan precipitate was added to a 4-dram vial and stir pea filled with 10 mL of DME and triturated overnight. This step is where enrichment occurs, but is only successful when the material has no tungsten impurities by <sup>1</sup>H NMR or CV. Both diastereomers are partially soluble in DME, so having a batch that is slightly enriched (>3:1 c.d.r.) is crucial. A 1:1 c.d.r. batch will not enrich via this approach. After stirring overnight, the highly enriched tan powder was collected on a 15 mL fine porosity frit and washed 1x with 10 mL of DME and 2x with 10 mL of diethyl ether. This powder was then dried in the desiccator (32% yield).

<sup>1</sup>H NMR (CD<sub>2</sub>Cl<sub>2</sub>,  $\delta$ , 25 °C): (**E**): 8.15 (d,  $J$  = 1.8 Hz, 1H, PzA3), 8.10 (d,  $J$  = 1.9 Hz, 1H, PzB3), 7.78 (d,  $J$  = 2.4 Hz, 1H, PzB5), 7.75 (d,  $J$  = 2.3 Hz, 1H, PzC5), 7.67 (d,  $J$  = 2.4 Hz, 1H, PzA5), 7.41 (m, 2H, H9), 7.25 (m, 1H, PzC3), 7.24 (m, 2H, H10), 7.20 (m, 1H, H11), 6.35 (t,  $J$  = 2.2 Hz, 1H, PzB4), 6.29 (t,  $J$  = 2.2 Hz, 1H, PzA4), 6.23 (t,  $J$  = 2.2 Hz, 1H, PzC4), 5.78 (ddd,  $J$  = 0.7, 5.0, 7.7 Hz, 1H, H5), 5.72 (d,  $J$  = 7.7 Hz, 1H, H6), 5.22 (dd,  $J$  = 1.1, 8.3 Hz, 1H, H2), 4.34 (d,  $J$  = 8.3 Hz, 1H, H7), 3.42 (s, 3H, H13), 2.90 (ddd,  $J$  = 4.9, 10.7, 14.5 Hz, 1H, H4), 2.60 (s, 3H, Ms), 1.64 (dd,  $J$  = 1.1, 10.7 Hz, 1H, H3), 1.20 (d,  $J_{PH}$  = 8.5 Hz, 9H, PMe<sub>3</sub>). (**T**): 8.14 (d,  $J$  = 1.8 Hz, 1H, Pz3/5), 8.05 (d,  $J$  = 1.9 Hz, 1H, Pz3/5), 7.77 (d,  $J$  = 2.4 Hz, 1H, Pz3/5), 7.73 (d,  $J$  = 2.2 Hz, 1H, Pz3/5), 7.68 (d,  $J$  = 2.3 Hz, 1H, Pz3/5), (H9, 10, and 11 are buried), 6.34 (t,  $J$  = 2.2 Hz, 1H, Pz4), 6.33 (t,  $J$  = 2.2 Hz, 1H, Pz4), 6.21 (t,  $J$  = 2.2 Hz, 1H, Pz4), 5.61 (d,  $J$  = 7.8 Hz, 1H, H6), 5.50 (dd,  $J$  = 0.9, 5.4 Hz, 1H, H2), 5.17 (dd,  $J$  = 4.9, 7.8 Hz, 1H, H5), 4.54 (d,  $J$  = 5.4 Hz, 1H, H7), 3.44 (s, 3H, H13), 3.23 (s, 3H, Ms), 2.54 (ddd,  $J$  = 4.9, 10.7, 13.6 Hz, 1H, H4), 1.42 (dd,  $J$  = 0.9, 10.7 Hz, 1H, H3), 1.08 (d,  $J_{PH}$  = 8.5 Hz, 9H, PMe<sub>3</sub>).

<sup>13</sup>C NMR (CD<sub>2</sub>Cl<sub>2</sub>,  $\delta$ , 25 °C): (**E**): 173.70 (C12), 144.17 (PzA3), 143.10 (d,  $J_{PC}$  = 1.6 Hz, 1C, PzB3), 140.16 (PzC3), 137.83 (C8), 137.22 (PzC5), 136.61 (PzB5), 136.11 (PzA5), 130.29 (2C, C9), 128.51 (2C, C10), 127.90 (C11), 116.02 (C6), 114.92 (d,  $J_{PC}$  = 2.6 Hz, 1C, C5), 107.01 (PzB4), 106.61 (PzC4), 106.40 (PzA4), 64.11 (d,  $J_{PC}$  = 1.6 Hz, 1C,

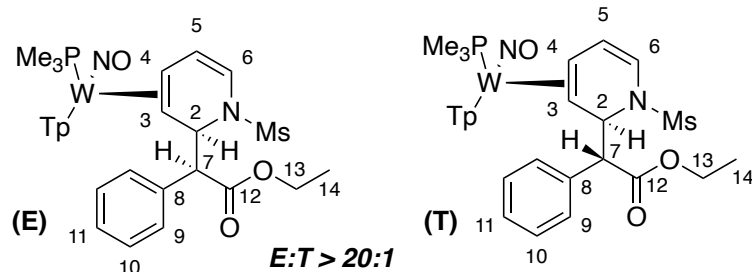
C3), 60.19 (C7), 59.36 (C2), 52.02 (C13), 44.57 (d,  $J_{PC} = 10.4$  Hz, 1C, C4), 42.15 (Ms), 13.25 (d,  $J_{PC} = 28.0$  Hz, 3C, PMe<sub>3</sub>). (**T**): 173.11 (C12), 143.65 (Pz3/5), 143.18 (d,  $J_{PC} = 2.2$  Hz, 1C, Pz3/5), 140.36 (Pz3/5), 137.26 (Pz3/5), 136.81 (Pz3/5), 136.41 (Pz3/5), (C8 obscured), 131.52 (2C, C9/C10), 127.73 (2C, C9/C10), 127.22 (C11), 115.94 (C6), 112.22 ((d,  $J_{PC} = 3.0$  Hz, 1C, C5), 107.07 (Pz4), 106.61 (Pz4), 106.26 (Pz4), 60.98 (C7), 58.25 (C2), 57.85 (d,  $J_{PC} = 1.4$  Hz, 1C, C3), 52.00 (C13), 46.16 (d,  $J_{PC} = 10.6$  Hz, 1C, C4), 42.37 (Ms), 13.10 (d,  $J_{PC} = 28.0$  Hz, 3C, PMe<sub>3</sub>).

IR:  $\nu(\text{NO}) = 1557 \text{ cm}^{-1}$ ,  $\nu(\text{BH}) = 2489 \text{ cm}^{-1}$ ,  $\nu(\text{CO}) = 1732 \text{ cm}^{-1}$ .

CV (DMA; 100 mV/s):  $E_{p,a} = +0.52 \text{ V}$  (NHE).

SC-XRD data on page 258

### Synthesis and characterization of WTP(NO)(PMe<sub>3</sub>)(η<sup>2</sup>-(*N*-mesyl)-2-(ethyl- $\alpha$ -phenylacetate)-1,2-dihydropyridine) (**36D**)



Ethyl  $\alpha$ -phenylbromoacetate (310 mg, 1.28 mmol), (**33D**) (498 mg, 0.61 mmol), and THF (6 mL) were charged to a flame-dried 4-dram vial with a 1-inch stir bar. Zinc powder (160 mg, 2.45 mmol) was added to initiate the reaction, and the heterogenous solution was stirred for 1 hour. The zinc was removed by filtering the solution through a celite plug set up in a 30 mL coarse porosity frit with 1 inch of celite, which was then washed with residual DCM to prevent loss of product. The solution was diluted with 50 mL of DCM and added to a separatory funnel. This solution was washed 3x with 50 mL of saturated aqueous NaHCO<sub>3</sub>. The organic layer was isolated and set aside. The combined aqueous layers were combined and back-extracted with 30 mL of DCM to prevent product loss. The organic layers were combined in a single flask and dried with anhydrous MgSO<sub>4</sub>. This powder was then filtered off into a 30 mL coarse porosity fritted funnel and washed with DCM. The dried organic layers were then reduced *in vacuo* to dryness. The residue in the flask was redissolved in minimal DCM (approximately 10 mL). The solution was then slowly added to 100 mL of stirring pentane. A tan precipitate formed immediately and was allowed to stir for ~10 minutes to ensure total precipitation. This powder was collected on a 60 mL medium porosity frit and washed 2x with 30 mL of pentane. This powder was dried in a desiccator under vacuum for ~30 minutes (67% yield).

<sup>1</sup>H NMR (CD<sub>2</sub>Cl<sub>2</sub>,  $\delta$ , 25 °C): (**E**): 8.22 (d,  $J$  = 1.9 Hz, 1H, PzA3), 8.11 (d,  $J$  = 1.9 Hz, 1H, PzB3), 7.79 (d,  $J$  = 2.4 Hz, 1H, PzB5), 7.74 (d,  $J$  = 2.2 Hz, 1H, PzC5), 7.67 (d,  $J$  = 2.3 Hz, 1H, PzA5), 7.42-7.44 (m, 2H, H9), 7.26 (t,  $J$  = 7.2 Hz, 2H, H10), 7.25 (d,  $J$  = 2.0 Hz, 1H, PzC3), 7.19-7.23 (m, 1H, H11), 6.35 (t,  $J$  = 2.2 Hz, 1H, PzB4), 6.32 (t,  $J$  = 2.2 Hz, 1H, PzA4), 6.23 (t,  $J$  = 2.1 Hz, 1H, PzC4), 5.81 (ddd,  $J$  = 0.6, 5.0, 7.6 Hz, 1H, H5), 5.71 (d,  $J$  = 7.7 Hz, 1H, H6), 5.24 (dd,  $J$  = 1.2, 9.0 Hz, 1H, H2), 4.26 (d,  $J$  = 8.9 Hz, 1H, H7), 3.90 (dq,  $J$  = 7.1, 10.8 Hz, 1H, H13), 3.79 (dq,  $J$  = 7.1, 10.8 Hz, 1H, H13), 2.92 (ddd,  $J$  = 4.9, 10.7, 15.5 Hz, 1H, H4), 2.52 (s, 3H, Ms), 1.67 (dd,  $J$  = 1.2, 10.7 Hz, 1H, H3), 1.22 (d,  $J_{PH}$  = 8.5 Hz, 9H, PMe<sub>3</sub>), 0.72 (t,  $J$  = 7.1 Hz, 3H, H14). (**T**): 8.13 (d,  $J$  = 1.9 Hz, 1H, PzA3), 8.05 (d,  $J$  = 1.9 Hz, 1H, PzB3), 7.77 (d,  $J$  = 2.4 Hz, 1H, PzB5), 7.73 (d,  $J$  = 2.2 Hz, 1H, PzC5), 7.69 (d,  $J$  = 2.4 Hz, 1H, PzA5), 7.42-7.44 (m, 2H, H9), 7.19-7.22 (m, 3H, H10&H11), 7.17 (d,  $J$  = 2.0 Hz, 1H, PzC3), 6.34 (t,  $J$  = 2.2 Hz, 1H, PzB4), 6.33 (t,  $J$  = 2.2 Hz, 1H, PzA4), 6.23 (t,  $J$  = 2.2 Hz, 1H, PzC4), 5.56 (d,  $J$  = 7.8 Hz, 1H, H6), 5.50 (dd,  $J$  = 1.0, 5.3 Hz, 1H, H2), 5.12 (dd,  $J$  = 4.9, 7.8 Hz, 1H, H5), 4.53 (d,  $J$  = 5.3 Hz, 1H, H7), 3.94 (dq,  $J$  = 7.1, 10.7 Hz, 1H, H13), 3.83 (dq,  $J$  = 7.1, 10.7 Hz, 1H, H13), 3.23 (s, 3H, Ms), 2.58 (ddd,  $J$  = 5.0, 10.7, 15.5 Hz, 1H, H4), 1.47 (dd,  $J$  = 1.0, 10.7 Hz, 1H, H3), 1.09 (d,  $J_{PH}$  = 8.5 Hz, 9H, PMe<sub>3</sub>), 0.82 (t,  $J$  = 7.1 Hz, 3H, H14).

<sup>13</sup>C NMR (CD<sub>2</sub>Cl<sub>2</sub>,  $\delta$ , 25 °C): (**E**): 172.6 (C12), 144.2 (PzA3), 143.0 (d,  $J_{PC}$  = 2.0 Hz, PzB3), 140.0 (PzC3), 137.8 (C8), 136.9 (PzC5), 136.5 (PzB5), 135.8 (PzA5), 130.2 (2C, C9), 128.4 (2C, C10), 127.5 (C11), 115.8 (C6), 115.1 (d,  $J_{PC}$  = 2.9 Hz, C5), 106.8 (Pz4), 106.4 (Pz4), 106.3 (Pz4), 64.4 (d,  $J_{PC}$  = 1.5 Hz,  $J_{WC}$  = 32.9, C3), 60.6 (C13), 60.5 (C7), 58.7 (C2), 44.2 (d,  $J_{PC}$  = 10.5 Hz,  $J_{WC}$  = 26.4 Hz, C4), 41.9 (Ms), 13.7 (C14), 13.2 (d,  $J_{PC}$  = 28.4 Hz, 9H, PMe<sub>3</sub>). (**T**): 172.4 (C12), 143.5 (PzA3), 143.1 (d,  $J_{PC}$  = 1.8 Hz, PzB3), 140.1 (PzC3), 137.1 (Pz5), 136.7 (C8), 136.5 (Pz5), 136.2 (Pz5), 131.6 (2C, C9), 127.8 (C10), 127.0 (C8), 115.8 (C6), 111.9 (d,  $J_{PC}$  = 3.0 Hz, C5), 106.9 (Pz4), 106.5 (Pz4), 106.2 (Pz4), 61.1 (C7), 60.7 (C13), 57.8 (C2), 57.4 (d,  $J_{PC}$  = 1.3 Hz,  $J_{WC}$  = 32.4 Hz, C3), 46.0 (d,  $J_{PC}$  = 10.4,  $J_{WC}$  = 26.4 Hz, C4), 42.2 (Ms), 13.8 (C14), 12.6 (d,  $J_{PC}$  = 28.2 Hz, 9H, PMe<sub>3</sub>).

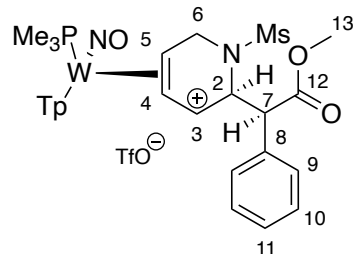
IR:  $\nu(\text{NO}) = 1553 \text{ cm}^{-1}$ ,  $\nu(\text{C=O}) = 1729 \text{ cm}^{-1}$

CV (DMA; 50 mV/s):  $E_{p,a} = +0.52 \text{ V}$

SC-XRD data on page 259



**Synthesis and characterization of WTp(NO)(PMe<sub>3</sub>)(η<sup>3</sup>-(*N*-mesyl)-2-(methyl- $\alpha$ -phenylacetate)-1,2,3,6-tetrahydropyridinium (OTf) (37)**



**Erythro-35D** (97 mg, 0.12 mmol) was added to a 4-dram vial containing a stir pea and diluted with propionitrile (3 mL). To a separate 4-dram vial, propionitrile (1 mL) and TfOH (24 mg, 0.16 mmol) were added. The acid/propionitrile solution was slowly added to the **erythro-35D**/propionitrile solution and stirred for 5 minutes. The reaction was then slowly added to 100 mL of stirring diethyl ether, which immediately formed a tan precipitate. This powder was triturated in the ether solution for 10 minutes and then collected on a 30 mL medium porosity frit. The collected powder was then washed 2x with 20 mL of diethyl ether and dried in a desiccator (104 mg, 90% yield).

<sup>1</sup>H NMR (CD<sub>2</sub>Cl<sub>2</sub>,  $\delta$ , 25 °C): 8.31 (d,  $J$  = 2.2 Hz, 1H, PzB3), 8.14 (d,  $J$  = 2.3 Hz, 1H, PzC3), 7.90 (d,  $J$  = 2.3 Hz, 1H, PzC5), 7.81 (d,  $J$  = 2.3 Hz, 1H, PzB5), 7.60 (d,  $J$  = 2.4 Hz, 1H, PzA5), 7.54 (d,  $J$  = 7.4 Hz, 2H, H9), 7.46 (t,  $J$  = 7.4 Hz, 2H, H10), 7.42 (t,  $J$  = 7.4 Hz, 1H, H11), 6.86 (d,  $J$  = 2.2 Hz, 1H, PzA4), 6.58 (t,  $J$  = 2.3 Hz, 1H, PzC4), 6.47 (t,  $J$  = 2.4 Hz, 1H, PzB4), 5.98 (t,  $J$  = 2.4 Hz, 1H, PzA4), 5.89 (d,  $J$  = 7.9 Hz, 1H, H3), 5.46-5.48 (m, 1H, H2), 5.23 (t, 7.8 Hz, 1H, H4), 4.81 (dd,  $J$  = 2.3, 12.7 Hz, 1H, H6), 4.78 (d,  $J$  = 5.3 Hz, 1H, H7), 4.53-4.58 (m, 1H, H5), 4.12 (d,  $J$  = 12.7 Hz, 1H, H6'), 3.84 (s, 3H, H13), 2.95 (s, 3H, Ms), 1.27 (d,  $J_{PH}$  = 9.7 Hz, 9H, PMe<sub>3</sub>).

<sup>13</sup>C NMR (CD<sub>2</sub>Cl<sub>2</sub>,  $\delta$ , 25 °C): 171.3 (C12), 146.4 (PzA3), 144.4 (d,  $J_{PC}$  = 2.2 Hz, PzB3), 142.7 (PzC3), 138.9 (PzC5), 138.7 (PzA5/B5), 138.6 (PzA5/B5), 134.6 (C8), 129.7 (2C, C10), 129.0 (2C, C9), 128.8 (C11), 121.4 (q,  $J_{FC}$  = 320.4 Hz, TfO<sup>-</sup>), 120.0 (C3), 109.1 (PzB4/C4), 108.9 (PzB4/C4), 107.3 (PzA4), 98.3 (d,  $J_{PC}$  = 3.0 Hz, C4), 65.3 (d,  $J_{PC}$  = 14.5 Hz, C5), 58.7 (C2), 55.9 (C7), 53.0 (C13), 42.9 (d,  $J_{PC}$  = 2.5 Hz, C6), 41.1 (Ms), 13.5 (d,  $J_{PC}$  = 33.0 Hz, 3C, PMe<sub>3</sub>).

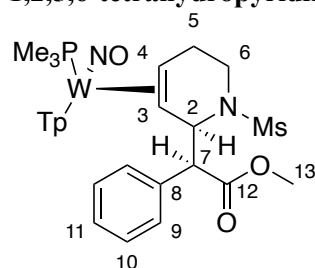
IR:  $\nu$ (NO) = 1661 cm<sup>-1</sup>,  $\nu$ (BH) = 2511 cm<sup>-1</sup>,  $\nu$ (CO) = 1733 cm<sup>-1</sup>.

CV (MeCN; 100 mV/s):  $E_{p,c}$  = -0.74 V (NHE).

HRMS (ESI) m/z: [M]<sup>+</sup> Calcd for C<sub>27</sub>H<sub>37</sub>BN<sub>8</sub>O<sub>5</sub>PSW<sup>+</sup> 811.1942; Found 811.1945

SC-XRD data on page 260

**Synthesis and characterization of WTP(NO)(PMe<sub>3</sub>)(η<sup>2</sup>-(*N*-mesyl)-2-(methyl-α-phenylacetate)-1,2,5,6-tetrahydropyridine) (38)**



Cyanoborohydride (136 mg, 2.16 mmol) and methanol (2.0 mL) were added to a screw-cap test tube and placed in a cold bath at -50 °C. To another tube, **erythro-35D** (185 mg, 0.228 mmol) and propionitrile (3.0 mL) were added. Triflic acid (41 mg, 0.273 mmol) was then added to the **erythro-35D** solution, which was swirled until dissolution and then also added to the cold bath. Both tubes were chilled for approximately 15 minutes before the cyanoborohydride/methanol solution was added to the solution of **37**, which sat in the cold bath for 16 hours. This solution was diluted with 50 mL of DCM and was washed 3x with 50 mL of saturated aqueous NaHCO<sub>3</sub>. The organic layer was isolated and set aside. The combined aqueous layers were combined and back-extracted with 50 mL of DCM to prevent product loss. The organic layers were combined in a single flask and dried with anhydrous MgSO<sub>4</sub>. This powder was then filtered off into a 60 mL coarse porosity fritted funnel and washed with DCM. The dried organic layers were then reduced *in vacuo* down to dryness. The residue in the flask was redissolved in minimal DCM (approximately 10 mL). The solution was then slowly added to 100 mL of stirring pentane. A tan precipitate formed immediately and was allowed to stir for ~10 minutes to ensure total precipitation. This powder was collected on a 15 mL fine porosity frit and washed 2x with 10 mL of pentane to yield **38**. This powder was dried in a desiccator under vacuum overnight (172 mg, 93% yield).

<sup>1</sup>H NMR ((CD<sub>3</sub>)<sub>2</sub>CO, δ, 25 °C): 8.27 (d, *J* = 1.8 Hz, 1H, PzA3), 8.10 (d, *J* = 1.8 Hz, 1H, PzB3), 7.92 (d, *J* = 2.3 Hz, 1H, PzC5), 7.91 (d, *J* = 2.4 Hz, 1H, PzB5), 7.78 (d, *J* = 2.3 Hz, 1H, PzA5), 7.43 (d, *J* = 2.0 Hz, 1H, PzC3), 7.35-7.38 (m, 2H, H9), 7.15-7.17 (m, 3H, H10/11), 6.38 (t, *J* = 2.2 Hz, 1H, PzB4), 6.32 (t, *J* = 2.2 Hz, 1H, PzC4), 6.26 (t, *J* = 2.2 Hz, 1H, PzA4), 5.57 (dd, *J* = 1.5, 6.8 Hz, 1H, H2), 4.13 (d, *J* = 6.8 Hz, 1H, H7), 3.41 (dt, *J* = 4.3, 13.0 Hz, H6'), 3.22 (s, 3H, H13), 2.98 (ddd, *J* = 3.8, 10.9, 14.6 Hz, 1H, H6), 2.86-2.92 (m, 1H, H4), 2.64-2.70 (m, 1H, H5'), 2.58-2.62 (m, 1H, H5), 2.49 (s, 3H, Ms), 1.26 (d, *J*<sub>PH</sub> = 8.4 Hz, 9H, PMe<sub>3</sub>), 0.94 (d, *J* = 11.7 Hz, 1H, H3).

<sup>13</sup>C NMR: ((CD<sub>3</sub>)<sub>2</sub>CO, δ, 25 °C): 172.8 (C12), 144.0 (PzA3), 143.9 (d, *J*<sub>PC</sub> = 1.5 Hz, PzB3), 141.2 (PzC3), 138.1 (C8), 137.4 (PzB5/C5), 137.0 (PzB5/C5), 136.6 (PzA5), 130.8 (2C, C9), 128.6 (2C, C10), 127.9 (C11), 107.0 (PzB4), 106.9 (PzC4), 106.6 (PzA4), 63.3 (C7), 60.7 (C2), 53.8 (t, *J*<sub>WC</sub> = 32.3 Hz, C3), 51.4 (C13), 47.3 (d, *J*<sub>PC</sub> = 12.5 Hz, C4), 42.0 (C6), 40.5 (Ms), 28.8 (d, *J*<sub>PC</sub> = 2.2 Hz, C5), 13.5 (d, *J*<sub>PC</sub> = 27.9 Hz, 3C, PMe<sub>3</sub>).

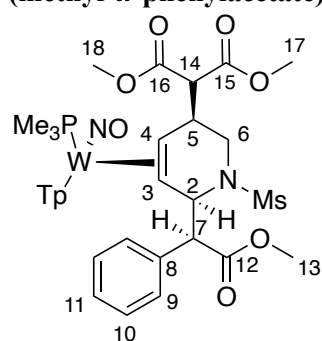
IR: ν(NO) = 1538 cm<sup>-1</sup>, ν(BH) = 2486 cm<sup>-1</sup>, ν(CO) = 1729 cm<sup>-1</sup>

CV (DMA; 100 mV/s): *E*<sub>p,a</sub> = +0.44 V (NHS)

HRMS (ESI) *m/z*: [M]<sup>+</sup> Calcd for C<sub>27</sub>H<sub>37</sub>BN<sub>8</sub>O<sub>5</sub>PSW<sup>+</sup> 811.1942; Found 811.1945

SC-XRD data on page 261

**Synthesis and characterization of WTp(NO)(PMe<sub>3</sub>)(η<sup>2</sup>-(*N*-mesyl)-5-dimethylpropanedioate-2-(methyl-α-phenylacetate)-1,2,5,6-tetrahydropyridine (39)**



**Erythro-35D** (200 mg, 0.247 mmol) was dissolved in 1 mL acetonitrile in a test tube with a stir pea. HOTf (38 mg, 0.253 mmol) was added to the test tube, and the mixture was stirred at room temperature for 5 minutes. The dark brown solution was cooled at -10 °C for 15 minutes. Lithium dimethylmalonate (227 mg, 1.64 mmol) was dissolved in 1 mL acetonitrile in a test tube with a stir pea. The solution was then cooled to -10 °C for 15 minutes. The allyl solution was added to the lithium dimethylmalonate solution and reacted for 30 minutes at 0 °C. The solution was stirred at room temperature for an additional 30 minutes. The solution was diluted with DCM (10mL), washed with H<sub>2</sub>O (3 x 5 mL), and the aqueous solution was back extracted with DCM (3 x 2mL). The solution was dried with MgSO<sub>4</sub>, removed on a 15 mL medium porosity frit, washed with DCM (3 x 2 mL), and the resulting filtrate was evaporated to dryness. The product was dissolved in minimal DCM and added to a stirring solution of hexanes (75 mL), yielding a precipitate. This precipitate was isolated on a 15 mL fine porosity frit, washed with hexanes (10 mL), and desiccated to yield **39** (160 mg, 69% yield).

<sup>1</sup>H NMR (CD<sub>2</sub>Cl<sub>2</sub>, δ, 25 °C): 8.42 (d, *J* = 1.0 Hz, 1H, PzA3), 8.08 (d, *J* = 1.8 Hz, 1H, PzB3), 7.77 (d, *J* = 2.2 Hz, 1H, PzC5), 7.76 (d, *J* = 2.5 Hz, 1H, PzB5), 7.70 (d, *J* = 2.3 Hz, 1H, PzA5), 7.42 (d, *J* = 7.2 Hz, 2H, H9), 7.30 (t, *J* = 7.3 Hz, 2H, H10), 7.25 (t, *J* = 7.3, 1H, H11), 7.07 (d, *J* = 2.0 Hz, 1H, PzC3), 6.34 (t, *J* = 2.5 Hz, 1H, PzA4), 6.31 (t, *J* = 2.2 Hz, 1H, PzB4), 6.26 (t, *J* = 2.2 Hz, 1H, PzC4), 5.54 (d, *J* = 9.4 Hz, 1H, H2), 4.13 (d, *J* = 9.6 Hz, 1H, H7), 3.95 (bs, 4H, H14/17/18) 3.77 (s, 3H, H17/18), 3.49 (m, 2H, H6/H5), 3.38 (m, 1H, H6), 2.97 (s, 3H, H13), 2.57 (ddd, *J* = 3.4, 13.7, 15.1 Hz, 1H, H4), 1.88 (s, 3H, Ms), 1.23 (d, *J*<sub>PH</sub> = 8.0 Hz, 9H, PMe<sub>3</sub>), 0.72 (d, *J* = 6.6 Hz, 1H, H3).

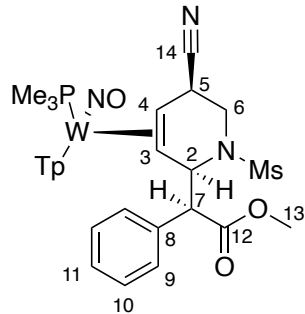
<sup>13</sup>C NMR (CD<sub>2</sub>Cl<sub>2</sub>, δ, 25 °C): 172.3 (C12), 169.5/169.3 (2C, C15/16), 144.6 (PzA3), 143.8 (PzB3), 140.4 (PzC3), 137.6 (C8), 137.1 (PzC5), 136.9 (PzB5), 136.5 (PzA5), 129.9 (2C, C9), 129.0 (2C, C10), 128.4 (C11), 106.4 (PzA4), 106.7 (PzB4), 106.6 (PzC4), 61.8 (C7), 58.7 (C2), 56.8 (C3), 56.3 (C14), 53.0/53.1 (2C, C17/18), 51.5 (C13), 46.6 (d, *J*<sub>PC</sub> = 12.0 Hz, C4), 40.4 (C6), 39.5 (C5), 37.1 (Ms), 14.5 (d, *J*<sub>PC</sub> = 27.6 Hz, 3C, PMe<sub>3</sub>).

IR: ν(NO) = 1543 cm<sup>-1</sup>, ν(CO) = 1728 cm<sup>-1</sup>

CV (DMA; 100 mV/s): *E*<sub>p,a</sub> = +0.61 V (NHE)

HRMS (APCI) *m/z*: [M]<sup>+</sup> Calcd for C<sub>32</sub>H<sub>46</sub>BN<sub>8</sub>O<sub>9</sub>PSW<sup>+</sup> 943.2365; Found 943.2368

**Synthesis and characterization of WTp(NO)(PMe<sub>3</sub>)(η<sup>2</sup>-(*N*-mesyl)-5-cyano-2-(methyl- $\alpha$ -phenylacetate)-1,2,5,6-tetrahydropyridine (40)**



**Erythro-35D** (469 mg, 0.578 mmol) was dissolved in 3 mL propionitrile in a test tube with a stir pea. HOTf (375 mg, 2.50 mmol) was added to the test tube, and the mixture was allowed to stir at room temperature for 5 minutes. The dark brown solution was cooled at  $-40\text{ }^{\circ}\text{C}$  for 15 minutes. Sodium cyanide (235 mg, 4.79 mmol) was dissolved in 3 mL methanol in a test tube with a stir pea. The solution was then cooled to  $-40\text{ }^{\circ}\text{C}$  for 15 minutes. The allyl solution was added to the sodium cyanide solution and reacted for 12 hours at  $-40\text{ }^{\circ}\text{C}$ . The solution was warmed to room temperature. The solution was diluted with DCM (10 mL), washed with Na<sub>2</sub>CO<sub>3</sub> (3 x 5 mL), and the aqueous solution was back extracted with DCM (3 x 2 mL). The solution was dried with MgSO<sub>4</sub>, removed on a 15 mL medium porosity frit, washed with DCM (3 x 2 mL), and the resulting filtrate was evaporated to dryness. The product was dissolved in minimal DCM and added to a stirring solution of hexanes (75 mL), yielding a precipitate. This precipitate was isolated on a 15 mL fine porosity frit, washed with hexanes (10 mL), and desiccated to yield **40** (421 mg, 87% yield).

<sup>1</sup>H NMR (CD<sub>2</sub>Cl<sub>2</sub>,  $\delta$ , 25  $^{\circ}\text{C}$ ): 8.44 (d,  $J$  = 1.3 Hz, 1H, PzB3), 8.05 (d,  $J$  = 1.7 Hz, 1H, PzA5), 7.77 (d,  $J$  = 2.2 Hz, 1H, PzA3), 7.76 (d,  $J$  = 2.2 Hz, 1H, PzC5), 7.72 (d,  $J$  = 2.6 Hz, 1H, PzB5), 7.41 (d,  $J$  = 7.3 Hz, 2H, H9), 7.32 (t,  $J$  = 7.3 Hz, 2H, H10), 7.27 (t,  $J$  = 7.7 Hz, 1H, H11), 7.13 (d,  $J$  = 1.7 Hz, 1H, PzC3), 6.39 (t,  $J$  = 2.2 Hz, 1H, PzB4), 6.34 (t,  $J$  = 2.2 Hz, 1H, PzA4), 6.27 (t,  $J$  = 2.2 Hz, 1H, PzC4), 5.53 (dd,  $J$  = 1.4, 10.4 Hz, 1H, H2), 4.03 (d,  $J$  = 10.3 Hz, 1H, H7), 3.82 (ddd,  $J$  = 5.1, 5.8, 11.3 Hz, 1H, H5), 3.67 (dd,  $J$  = 4.8, 13.2 Hz, 1H, H6), 3.18 (dd,  $J$  = 11.3, 13.2 Hz, 1H, H6), 2.92 (ddd,  $J$  = 6.0, 11.4, 14.1 Hz, 1H, H4), 2.83 (s, 3H, H13), 1.73 (s, 3H, Ms), 1.30 (d,  $J_{PH}$  = 8.0 Hz, 9H, PMe<sub>3</sub>), 0.46 (d,  $J$  = 11.9 Hz, 1H, H3).

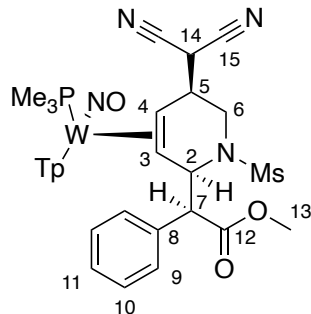
<sup>13</sup>C NMR (CD<sub>2</sub>Cl<sub>2</sub>,  $\delta$ , 25  $^{\circ}\text{C}$ ): 171.9 (C12), 144.7 (PzB3), 143.6 (PzA5), 140.0 (PzC3), 137.8 (C13), 136.9 (PzA3), 136.8 (PzC5), 136.4 (PzB5), 129.6 (2C, C9), 129.2 (2C, C10), 128.5 (C11), 123.6 (C14), 106.8 (PzA4), 106.6 (PzB4), 106.6 (PzC4), 61.9 (C7), 58.4 (C2), 52.9 (C3), 51.4 (13), 43.4 (d,  $J_{PC}$  = 13.6 Hz, C4), 42.7 (C6), 40.7 (Ms), 29.6 (C5), 14.2 (d,  $J_{PC}$  = 29.0 Hz, 3C, PMe<sub>3</sub>).

IR:  $\nu(\text{NO})$  = 1556 cm<sup>-1</sup>,  $\nu(\text{CO})$  = 1732 cm<sup>-1</sup>,  $\nu(\text{CN})$  = 2225 cm<sup>-1</sup>

CV (DMA; 100 mV/s):  $E_{p,a}$  = +0.68 V (NHE)

HRMS (ESI)  $m/z$ : [M]<sup>+</sup> Calcd for C<sub>30</sub>H<sub>38</sub>BN<sub>6</sub>O<sub>5</sub>PSW<sup>+</sup> 838.2051; Found 838.2055

**Synthesis and characterization of WTp(NO)(PMe<sub>3</sub>)(η<sup>2</sup>-(*N*-mesyl)-5-dicyanomethyl-2-(methyl- $\alpha$ -phenylacetate)-1,2,5,6-tetrahydropyridine (41)**



**Erythro-35D** (200 mg, 0.247 mmol) was dissolved in ~0.5 mL propionitrile in a test tube with a stir pea. HOTf (44 mg, 0.293 mmol) was added to the test tube, and the mixture was allowed to stir at room temperature for 5 minutes. The dark brown solution was cooled to 0 °C for 15 minutes. Malononitrile (162 mg, 2.45 mmol) was dissolved in ~0.5 mL THF in a test tube with a stir pea. tBuOK (20% wt., 692 mg, 1.23 mmol) was added. The solution was then cooled to 0 °C for 15 minutes. The allyl solution was added to the deprotonated malononitrile solution and reacted for 4 hours at 0 °C. The solution was warmed to room temperature, diluted with DCM (10 mL), washed with Na<sub>2</sub>CO<sub>3</sub> (3 x 5 mL), and the aqueous solution was back extracted with DCM (3 x 2 mL). The solution was dried with Na<sub>2</sub>SO<sub>4</sub>, removed on a 15 mL medium porosity frit, washed with DCM (3 x 2 mL), and the resulting filtrate was evaporated to dryness. The product was dissolved in minimal DCM and added to a stirring solution of cold pentanes (75 mL), yielding a precipitate. This precipitate was isolated on a 15 mL fine porosity frit, washed with pentanes (5 mL), and desiccated to yield **41** (177 mg, 82% yield).

<sup>1</sup>H NMR (CD<sub>2</sub>Cl<sub>2</sub>, δ, 25 °C): 8.28 (bs, 1H, PzA3), 8.17 (d, *J* = 1.7 Hz, 1H, PzB3), 8.01 (d, *J* = 2.2 Hz, 1H, PzC5), 7.97 (d, *J* = 2.4 Hz, 1H, PzB5), 7.82 (d, *J* = 2.0 Hz, 1H, PzA5), 7.49 (d, *J* = 2.0, 1H, PzC3), 7.35 (d, *J* = 7.0 Hz, 1H, H9), 7.26 (t, *J* = 7.3 Hz, 1H, H11), 7.23 (t, *J* = 6.2 Hz, 2H, H10), 6.45 (t, *J* = 2.0 Hz, 1H, PzC4), 6.43 (t, *J* = 2.4 Hz, 1H, PzB4), 6.24 (t, *J* = 2.1 Hz, 1H, PzA4), 5.72 (bs, 1H, H2), 4.39 (bs, 1H, H7), 3.74 (dd, *J* = 3.2, 13.1 Hz, 1H, H6), 3.58 (dd, *J* = 4.4, 13.1 Hz, 1H, H6), 3.54 (s, 3H, H13), 3.44 (bs, 1H, H5), 3.32 (bs, 1H, H14), 2.91 (s, 3H, Ms), 2.63 (t, *J* = 11.3 Hz, 1H, H4), 1.38 (dd, *J* = 11.6 Hz, 1H, H3), 1.25 (d, *J*<sub>PH</sub> = 8.5 Hz, 9H, PMe<sub>3</sub>).

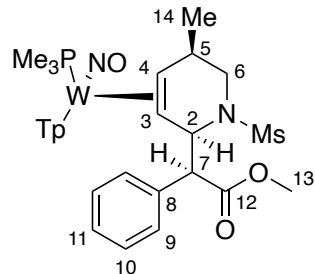
<sup>13</sup>C NMR (CD<sub>2</sub>Cl<sub>2</sub>, δ, 25 °C): 173.1 (C12), 144.3 (PzB3), 143.5 (PzA3), 141.6 (PzC3), 138.3 (PzC5), 137.6 (PzA5), 137.5 (PzB5), 137.0 (C8), 132.0 (2C, C9), 129.1 (2C, C10), 128.1 (C11), 114.2/113.1 (2C, C15), 107.6 (2C, PzC4/PzB4), 107.1 (PzA4), 63.3 (C7), 61.3 (C2), 52.5 (C3), 52.0 (C13), 50.0 (d, *J*<sub>PC</sub> = 12.7 Hz, C4), 44.2 (C6), 41.3 (C5), 36.0 (Ms), 23.4 (C14), 13.3 (d, *J*<sub>PC</sub> = 28.4 Hz, 3C, PMe<sub>3</sub>).

IR:  $\nu(\text{NO}) = 1538 \text{ cm}^{-1}$ ,  $\nu(\text{CO}) = 1725 \text{ cm}^{-1}$ ,  $\nu(\text{CN}) = 2221 \text{ cm}^{-1}$

CV (MeCN; 100 mV/s):  $E_{p,a} = +0.83 \text{ V}$  (NHE)

HRMS (ESI) *m/z*: [M]<sup>+</sup> Calcd for C<sub>30</sub>H<sub>39</sub>BN<sub>10</sub>O<sub>5</sub>PSW<sup>+</sup> 877.2160; Found 877.2150.

**Synthesis and characterization of  $\text{WTp}(\text{NO})(\text{PMe}_3)(\eta^2\text{-}(N\text{-mesyl})\text{-5-methyl-2-(methyl-}\alpha\text{-phenylacetate)-1,2,5,6-tetrahydropyridine (42)}$**



**37** (100 mg, 0.104 mmol) was dissolved in ~0.5 mL propionitrile in a test tube with a stir pea. The solution was cooled to  $-60\text{ }^\circ\text{C}$  for 2 hours.  $\text{MeMgBr}$  (3M, 0.173 mL, 5.20 mmol) was added to 0.5 mL THF and chilled to  $-60\text{ }^\circ\text{C}$  for 2 hours. The allyl solution was added to the Grignard solution and allowed to react for 60 hours. The solution was warmed to room temperature, diluted with DCM (10 mL), washed with  $\text{Na}_2\text{CO}_3$  (3 x 5 mL), and the aqueous solution was back extracted with DCM (3 x 2 mL). The solution was dried with  $\text{Na}_2\text{SO}_4$ , removed on a 15 mL medium porosity frit, washed with DCM (3 x 2 mL), and the resulting filtrate was evaporated to dryness. The product was dissolved in minimal DCM and added to a stirring solution of cold hexanes (75 mL), yielding a precipitate. This precipitate was isolated on a 15 mL fine porosity frit, washed with hexanes (5 mL), and desiccated to yield **42** (32 mg, 37% yield).

$^1\text{H NMR}$  ( $\text{CD}_3\text{CN}$ ,  $\delta$ ,  $25\text{ }^\circ\text{C}$ ): 8.4 (bs, 1H, PzA3), 8.0 (d,  $J = 1.5\text{ Hz}$ , 1H, PzB3), 7.8 (d,  $J = 3.0\text{ Hz}$ , 1H, PzC5), 7.83 (d,  $J = 2.4\text{ Hz}$ , 1H, PzB5), 7.79 (d,  $J = 2.5\text{ Hz}$ , 1H, PzA5), 7.37 (d,  $J = 7.3\text{ Hz}$ , 2H, H9), 7.27 (t,  $J = 7.0\text{ Hz}$ , 2H, H10), 7.23 (t,  $J = 7.0\text{ Hz}$ , 1H, H11), 7.20 (d,  $J = 1.5\text{ Hz}$ , 1H, PzC3), 6.36 (t,  $J = 2.2\text{ Hz}$ , 1H, PzA4), 6.34 (t,  $J = 2.3\text{ Hz}$ , 1H, PzB4), 6.27 (t,  $J = 2.2\text{ Hz}$ , 1H, PzC4), 5.50 (dd,  $J = 1.4, 9.6\text{ Hz}$ , 1H, H2), 4.06 (d,  $J = 9.6\text{ Hz}$ , 1H, H7), 3.20 (dd,  $J = 4.9, 13.3\text{ Hz}$ , 1H, H6), 2.83 (s, 3H, H13), 2.68 (dd,  $J = 11.4, 13.1\text{ Hz}$ , 1H, H6), 2.67 (ddd,  $J = 4.4, 11.6, 15.6\text{ Hz}$ , 1H, H4), 1.97 (s, 3H, Ms), 1.26 (d,  $J = 6.7\text{ Hz}$ , 3H, H14), 1.31 (m, 1H, H5), 1.25 (d,  $J_{\text{PH}} = 8.2\text{ Hz}$ , 9H,  $\text{PMe}_3$ ), 1.18 (d,  $J = 8.6\text{ Hz}$ , 1H, H3).

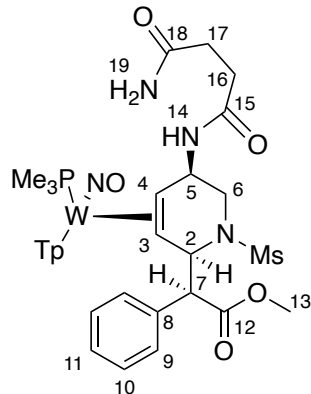
$^{13}\text{C NMR}$  ( $\text{CD}_3\text{CN}$ ,  $\delta$ ,  $25\text{ }^\circ\text{C}$ ): 173.1 (C12), 144.8 (PzA3), 144.4 (PzB3), 141.3 (PzC3), 138.7 (C8), 137.4 (PzC5), 137.3 (PzB5), 137.0 (PzA5), 130.4 (2C, C9), 129.3 (2C, C10), 128.6 (C11), 107.1 (PzC4), 107.0 (PzA4), 106.9 (PzB4), 62.6 (C7), 59.1 (C2), 57.3 (C3), 52.1 (d,  $J_{\text{PC}} = 10.7\text{ Hz}$ , C4), 51.6 (C13), 47.8 (C6), 40.7 (Ms), 23.0 (C5), 22.0 (C14), 14.4 (d,  $J_{\text{PC}} = 30.0\text{ Hz}$ , 3C,  $\text{PMe}_3$ ).

IR:  $\nu(\text{NO}) = 1537\text{ cm}^{-1}$ ,  $\nu(\text{CO}) = 1730\text{ cm}^{-1}$

CV (MeCN; 100 mV/s):  $E_{\text{p,a}} = +0.50\text{ V}$  (NHE)

SC-XRD data on page 262

**Synthesis and characterization of WTp(NO)(PMe<sub>3</sub>)( $\eta^2$ -(*N*-mesyl)-5-succinamide-2-(methyl- $\alpha$ -phenylacetate)-1,2,5,6-tetrahydropyridine (43)**



**37** (150 mg, 0.156 mmol) was dissolved in ~1 mL THF in a test tube with a stir pea. The solution was cooled to -60 °C for 15 minutes. Succinamide (155 mg, 1.56 mmol) was dissolved in 1 mL THF in a test tube with a stir pea, *n*-butyl lithium (1.5 M, 0.2 mL, 0.30 mmol) was added and allowed to react for 10 minutes. The solution was then cooled to -60 °C for 15 minutes. The allyl solution was added to the deprotonated succinimide solution and reacted for 60 hours at -60 °C. The solution was warmed to room temperature. The solution was diluted with DCM (10 mL), washed with Na<sub>2</sub>CO<sub>3</sub> (3 x 5 mL), and the aqueous solution was back extracted with DCM (3 x 2 mL). The solution was dried with Na<sub>2</sub>SO<sub>4</sub>, removed on a 15 mL medium porosity frit, washed with DCM (3 x 2 mL), and the resulting filtrate was evaporated to dryness. The product was dissolved in minimal DCM and added to a stirring solution of chilled hexanes (200 mL), yielding a precipitate. This precipitate was isolated on a 15 mL fine porosity frit, washed with hexanes (10 mL), and desiccated to yield **43** (78 mg, 54% yield).

<sup>1</sup>H NMR (CD<sub>3</sub>CN,  $\delta$ , 25 °C): 8.47 (bs, 1H, PzA3), 8.03 (d,  $J$  = 2.3 Hz, 1H, PzB3), 7.86 (d,  $J$  = 2.3 Hz, 1H, PzB5), 7.84 (d,  $J$  = 2.3 Hz, 1H, PzC5), 7.82 (d,  $J$  = 2.4 Hz, 1H, PzA5), 7.41 (d,  $J$  = 7.3 Hz, 2H, H9), 7.32 (t,  $J$  = 7.4 Hz, 2H, H10), 7.26 (t,  $J$  = 7.2 Hz, 1H, H11), 7.13 (d,  $J$  = 2.2 Hz, 1H, PzC3), 6.41 (t,  $J$  = 2.3 Hz, 1H, PzA4), 6.36 (t,  $J$  = 2.1 Hz, 1H, PzB4), 6.28 (t,  $J$  = 2.3 Hz, 1H, PzC4), 5.52 (d,  $J$  = 10.4 Hz, 1H, H2), 5.36 (m, 1H, H5), 4.42 (d,  $J$  = 10.3 Hz, 1H, H7), 3.53 (dd,  $J$  = 11.1, 12.9 Hz, 1H, H6), 3.41 (bs, 2H, H19), 3.28 (s, 1H, H14), 3.10 (dd,  $J$  = 6.5, 12.9 Hz, 1H, H6), 3.02 (ddd,  $J$  = 3.8, 12.0, 14.4 Hz, 1H, H4), 2.91 (s, 3H, 13), 2.77 (m, 4H, H16/H17), 1.85 (s, 3H, Ms), 1.05 (d,  $J_{PH}$  = 8.3 Hz, 9H, PMe<sub>3</sub>), 0.58 (d,  $J$  = 12.1 Hz, 1H, H3). Minor Complex – DHP *erythro*-**35D**.

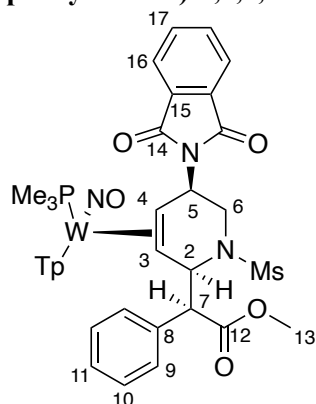
<sup>13</sup>C NMR (CD<sub>3</sub>CN,  $\delta$ , 25 °C): 178.9 (2C, C15/C18), 173.2 (C12), 145.1 (PzA3), 143.5 (PzB3), 140.7 (PzC3), 138.7 (C8), 137.5 (2C, PzB5/C5), 137.3 (PzA5), 130.3 (2C, C9), 129.6 (2C, C10), 128.9 (C11), 107.5 (PzB4), 107.3 (PzA4), 107.0 (PzC4), 62.0 (C8), 58.7 (C2), 56.6 (C3), 51.7 (C13), 50.0 (C5), 45.6 (d,  $J_{PC}$  = 12.0 Hz, C4), 40.6 (Ms), 40.1 (C6), 29.0. (2C, C16/C17), 14.0. (d,  $J_{PC}$  = 30.8 Hz, 3C, PMe<sub>3</sub>).

IR:  $\nu$ (NO) = 1553 cm<sup>-1</sup>,  $\nu$ (Ester CO) = 1735 cm<sup>-1</sup>,  $\nu$ (Amide CO) = 1695 cm<sup>-1</sup>

CV (MeCN; 100 mV/s):  $E_{p,a}$  = +0.63V (NHE)

HRMS (ESI)  $m/z$ : [M]<sup>+</sup> Calcd for C<sub>31</sub>H<sub>43</sub>BN<sub>10</sub>O<sub>6</sub>PSW<sup>+</sup> due to H<sub>2</sub>O loss from McLafferty rearrangement of amide 909.2422; Found 909.2412.

**Synthesis and characterization of WTp(NO)(PMe<sub>3</sub>)(η<sup>2</sup>-(*N*-mesyl)-5-phthalimide-2-(methyl-α-phenylacetate)-1,2,5,6-tetrahydropyridine (44)**



**Erythro-35D** (50 mg, 0.062 mmol) was dissolved in ~0.5 mL propionitrile in a test tube with a stir pea. HOTf (57 mg, 0.380 mmol) was added, and the mixture was allowed to stir at room temperature. The dark brown solution was cooled at -60 °C for 15 minutes. Phthalimide (46 mg, 0.312 mmol) was dissolved in 0.5 mL EtCN in a test tube with a stir pea, tBuOK/THF (20% wt., 70 mg, 0.125 mmol) was added and allowed to react for 10 minutes. The solution was then cooled to -60 °C for 15 minutes. The allyl solution was added to the deprotonated phthalimide solution and reacted for 12 hours at -60 °C. The solution was warmed to room temperature. The solution was diluted with DCM (10 mL), washed with Na<sub>2</sub>CO<sub>3</sub> (3 x 5 mL), and the aqueous solution was back extracted with DCM (3 x 2 mL). The solution was dried with Na<sub>2</sub>SO<sub>4</sub>, removed on a 15 mL medium porosity frit, washed with DCM (3 x 2 mL), and the resulting filtrate was evaporated to dryness. The product was dissolved in minimal DCM and added to a stirring solution of chilled hexanes (200 mL), yielding a precipitate. This precipitate was isolated on a 15 mL fine porosity frit, washed with hexanes (10mL), and desiccated to yield **44** (42 mg, 73% yield).

<sup>1</sup>H NMR (CD<sub>3</sub>CN, δ, 25 °C): 8.51 (bs, 1H, PzA3), 8.07 (d, *J* = 1.8 Hz, 1H, PzB3), 7.80-7.94 (m, 4H, H16/H17), 7.75 (d, *J* = 2.5 Hz, 1H, PzB5), 7.73 (d, *J* = 2.5, 3.1 Hz, 2H, PzC5/PzA5), 7.45 (d, *J* = 7.3 Hz, 2H, H9), 7.29 (t, *J* = 7.3 Hz, 2H, H10), 7.23 (t, *J* = 6.3 Hz, 1H, H11), 7.10 (d, *J* = 2.1 Hz, 1H, PzC3), 6.40 (t, *J* = 2.1 Hz, 1H, PzA4), 6.32 (t, *J* = 2.3 Hz, 1H, PzB4), 6.20 (t, *J* = 2.3 Hz, 1H, PzC4), 5.57 (d, *J* = 10.3 Hz, 1H, H2), 5.55 (m, 1H, H5), 4.52 (d, *J* = 10.1 Hz, 1H, H7), 3.58 (dd, *J* = 10.8, 12.7 Hz, 1H, H6), 3.25 (dd, *J* = 6.7, 12.8 Hz, 1H, H6), 3.11 (ddd, *J* = 3.8, 12.1, 14.3 Hz, 1H, H4), 2.98 (s, 3H, H13), 1.92 (bs, 3H, Ms), 1.02 (d, *J*<sub>PH</sub> = 8.4 Hz, 9H, PMe<sub>3</sub>), 0.71 (d, *J* = 11.8 Hz, 1H, H3). Minor Complex – DHP **erythro-35D**.

<sup>13</sup>C NMR (CD<sub>3</sub>CN, δ, 25 °C): 172.7 (C12), 168.7 (2C, C14), 144.9 (PzA3A), 142.8 (PzB3), 139.8 (PzC3), 138.1 (C8), 136.6 (PzA5), 136.6 (PzC5), 136.3 (PzB5), 134.7 (2C, C16), 132.3 (2C, C15), 129.9 (2C, C9), 129.0 (2C, C10), 128.3 (C11), 123.7 (2C, C17), 106.8 (PzB4), 106.5 (PzC4), 106.5 (PzC4), 61.5 (C7), 58.4 (C2), 56.1 (C3), 51.5 (C13), 49.0 (C5), 45.7 (d, *J*<sub>PC</sub> = 11.7 Hz, C4), 40.8 (C6), 40.7 (Ms), 13.9 (d, *J*<sub>PC</sub> = 28.6 Hz, PMe<sub>3</sub>).

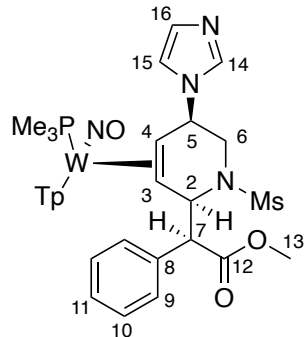
IR: ν(NO) = 1557 cm<sup>-1</sup>, ν(Ester CO) = 1732 cm<sup>-1</sup>, ν(Imide CO) = 1705 cm<sup>-1</sup>

CV (DMA; 100 mV/s): *E*<sub>p,a</sub> = +0.58V (NHE)

HRMS (APCI) *m/z*: [M]<sup>+</sup> Calcd for C<sub>35</sub>H<sub>43</sub>BN<sub>9</sub>O<sub>7</sub>PSW<sup>+</sup> 958.2262; Found 958.2270.



**Synthesis and characterization of WTp(NO)(PMe<sub>3</sub>)(η<sup>2</sup>-(*N*-mesyl)-5-imidazole-2-(methyl- $\alpha$ -phenylacetate)-1,2,5,6-tetrahydropyridine (45)**



**Erythro-35D** (250 mg, 0.308 mmol) was dissolved in 1 mL propionitrile in a test tube with a stir pea. HOTf (55.5 mg, 0.370 mmol) was added to form the allyl species, and the mixture was allowed to stir at room temperature. The dark brown solution was cooled at -30 °C for 15 minutes. Imidazole (210 mg, 3.08 mmol) was dissolved in 1.5 mL methanol in a test tube with a stir pea and cooled to -30 °C for 15 minutes. The allyl solution was added to the imidazole solution and reacted for 12 hours at -30 °C. tBuOK/THF (20% wt, 346 mg, 0.617 mmol) was added at -30 °C and allowed to react for 10 minutes. The solution was warmed to room temperature. The solution was diluted with DCM (10 mL), washed with Na<sub>2</sub>CO<sub>3</sub> (3 x 5 mL), and the aqueous solution was back extracted with DCM (3 x 2 mL). The solution was dried with Na<sub>2</sub>SO<sub>4</sub>, removed on a 15 mL medium porosity frit, washed with DCM (3 x 2 mL), and the resulting filtrate was evaporated to dryness. The product was dissolved in minimal DCM and added to a stirring solution of hexanes (200 mL), yielding a precipitate. This precipitate was isolated on a 15 mL fine porosity frit, washed with hexanes (10 mL), and desiccated to yield **45** (232 mg, 86% yield).

<sup>1</sup>H NMR (CD<sub>3</sub>CN, δ, 25 °C): 8.47 (bs, 1H, PzA3), 8.03 (d, *J* = 1.7 Hz, 1H, PzB3), 7.85 (bs, 1H, H14), 7.76 (d, *J* = 2.4 Hz, 1H, PzB5), 7.75 (d, *J* = 2.1 Hz, 1H, PzC5), 7.73 (d, *J* = 2.3 Hz, 1H, PzA5), 7.43 (bs, 1H, H15), 7.40 (d, *J* = 7.3 Hz, 2H, H9), 7.29 (t, *J* = 7.4 Hz, 2H, H10), 7.24 (t, *J* = 7.3 Hz, 1H, H11), 7.15 (bs, 1H, H16), 7.10 (d, *J* = 2.1 Hz, 1H, PzC3), 6.40 (d, *J* = 2.2 Hz, 1H, PzA4), 6.33 (t, *J* = 2.1 Hz, 1H, PzB4), 6.25 (t, *J* = 2.1 Hz, 1H, PzC4), 5.62 (dd, *J* = 1.7, 10.0 Hz, 1H, H2), 5.30 (m, 1H, H5), 4.14 (d, *J* = 10.0 Hz, 1H, H7), 3.47 (dd, *J* = 5.2, 13.1 Hz, 1H, H6), 3.05 (dd, *J* = 11.2, 13.1 Hz, 1H, H6), 2.94 (ddd, *J* = 4.6, 11.6, 14.0 Hz, 1H, H4), 2.88 (s, 3H, 13), 1.76 (s, 3H, Ms), 0.86 (d, *J*<sub>PH</sub> = 8.4 Hz, 9H, PMe<sub>3</sub>), 0.65 (d, *J* = 12.2 Hz, 1H, H3). Minor Complex – DHP **erythro-35D**.

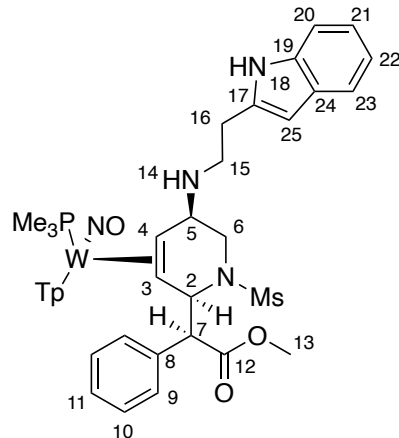
<sup>13</sup>C NMR (CD<sub>3</sub>CN, δ, 25 °C): 172.2 (C12), 144.8 (PzA3), 143.0 (PzB3), 139.7 (PzC3), 137.9 (C8), 137.1 (PzB5), 136.8 (C14), 136.7 (PzC5), 136.5 (PzA5), 130.2 (C16), 129.6 (2C, C9), 129.2 (2C, C10), 128.5 (C11), 118.2 (C15), 106.9 (PzB4), 106.6 (PzA4), 106.6 (PzC4), 62.0 (C7), 58.5 (C2), 56.2 (C5), 54.5 (C3), 51.5 (C13), 48.6 (d, *J*<sub>PC</sub> = 12.6 Hz, C4), 47.2 (C6), 40.7 (Ms), 13.6 (d, *J*<sub>PC</sub> = 28.4 Hz, 3C, PMe<sub>3</sub>).

IR: ν(NO) = 1563 cm<sup>-1</sup>, ν(Ester CO) = 1728 cm<sup>-1</sup>

CV (DMA; 100 mV/s): *E*<sub>p,a</sub> = +0.57V (NHE)

HRMS (APCI) *m/z*: [M]<sup>+</sup> Calcd for C<sub>30</sub>H<sub>41</sub>BN<sub>10</sub>O<sub>5</sub>PSW<sup>+</sup> 879.2317; Found 879.2318.

**Synthesis and characterization of WTp(NO)(PMe<sub>3</sub>)(η<sup>2</sup>-(*N*-mesyl)-5-tryptamine-2-(methyl- $\alpha$ -phenylacetate)-1,2,5,6-tetrahydropyridine (46)**



**Erythro-35D** (100 mg, 0.123 mmol) was dissolved in ~0.5 mL propionitrile in a test tube with a stir pea. HOTf (24 mg, 0.160 mmol) was added, and the mixture was allowed to stir at room temperature. The dark brown solution was cooled at -50 °C for 15 minutes. Tryptamine (85 mg, 0.531 mmol) was dissolved in 0.5 mL EtCN in a test tube with a stir pea, tBuOK/THF (20% wt., 114 mg, 0.203 mmol) was added and allowed to react for 10 minutes. The solution was then cooled to -50 °C for 15 minutes. The allyl solution was added to the deprotonated tryptamine solution and reacted for 12 hours at -50 °C. The solution was warmed to room temperature. The solution was diluted with DCM (10 mL), washed with Na<sub>2</sub>CO<sub>3</sub> (3 x 5 mL), and the aqueous solution was back extracted with DCM (3 x 2 mL). The solution was dried with MgSO<sub>4</sub>, removed on a 15 mL medium porosity frit, washed with DCM (3 x 2 mL), and the resulting filtrate was evaporated to dryness. The product was dissolved in minimal DCM and added to a stirring solution of chilled pentanes (200 mL), yielding a precipitate. This precipitate was isolated on a 15 mL fine porosity frit, washed with pentanes (10 mL), and desiccated to yield **46** (103 mg, 88% yield).

<sup>1</sup>H NMR (CD<sub>2</sub>Cl<sub>2</sub>,  $\delta$ , 25 °C): 8.52 (bs, 1H, H18), 8.38 (d,  $J$  = 1.5 Hz, 1H, PzA3), 8.01 (d,  $J$  = 1.9 Hz, 1H, PzB3), 7.73 (d,  $J$  = 2.3 Hz, 1H, PzB5), 7.71 (d,  $J$  = 2.2 Hz, 1H, PzC5), 7.68 (d,  $J$  = 2.4 Hz, 1H, PzA5), 7.64 (d,  $J$  = 7.8 Hz, 1H, H23), 7.38 (d,  $J$  = 8.0 Hz, 1H, H20), 7.36 (d,  $J$  = 7.2 Hz, 2H, H9), 7.25 (t,  $J$  = 7.2 Hz, 2H, H10), 7.21 (t,  $J$  = 7.2 Hz, 1H, H11), 7.16 (t,  $J$  = 7.9 Hz, 1H, H22), 7.11 (d,  $J$  = 7.2 Hz, PzC3), 7.09 (t,  $J$  = 8.1 Hz, 1H, H21), 7.07 (d,  $J$  = 2.2 Hz, 1H, H25), 6.32 (t,  $J$  = 2.3 Hz, 1H, PzA4), 6.28 (t,  $J$  = 2.0 Hz, 1H, PzB4), 6.20 (t,  $J$  = 2.2 Hz, 1H, PzC4), 5.50 (d,  $J$  = 9.4 Hz, 1H, H2), 4.02 (d,  $J$  = 9.5 Hz, 1H, H7), 3.56-3.83 (m, 1H, H5), 3.64 (dd,  $J$  = 4.8, 12.6 Hz, 1H, H6), 3.27 (dt,  $J$  = 6.8, 13.8 Hz, 1H, H15), 3.00 (td,  $J$  = 6.47, 13.83 Hz, 1H, H17), 2.98 (td,  $J$  = 6.87, 13.95 Hz, 1H, H17), 2.88 (dt,  $J$  = 6.7, 10.9 Hz, 1H, H15), 2.84 (s, 3H, H9), 2.47-2.42 (m, 2H, H6/H4), 1.92 (s, 3H, H7), 1.43 (bs, 1H, H14), 1.18 (d,  $J_{PH}$  = 8.7 Hz, 9H, PMe<sub>3</sub>), 0.47 (d,  $J$  = 11.7 Hz, 1H, H3).

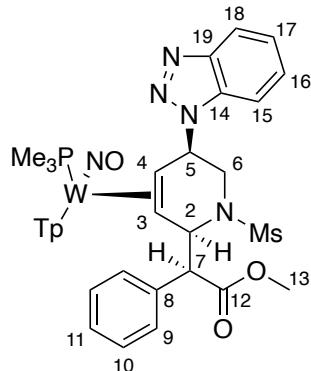
<sup>13</sup>C NMR (CD<sub>2</sub>Cl<sub>2</sub>,  $\delta$ , 25 °C): 172.5 (C12), 144.4 (PzA3), 143.6 (PzB3), 140.1 (PzC3), 138.0 (C8) 136.9 (C24), 136.5 (PzB5), 136.4 (PzC5), 136.0 (PzA5), 129.9 (2C, C9), 128.8 (2C, C10), 128.1 (C11), 128.1 (C19), 122.7 (C25), 122.0 (2C, C22), 119.3 (2C, C21), 119.2 (2C, C23), 111.6 (2C, C20), 114.4 (C17), 106.4 (PzB4), 106.3 (PzA4), 106.2 (PzC4), 62.2 (C7), 58.9 (C2), 56.5 (C5), 54.9 (C3), 51.8 (d,  $J_{PC}$  = 13.4 Hz, C4), 51.2 (C13), 47.4 (C15), 46.0 (C6), 40.5 (Ms), 27.1 (C16), 14.2 (d,  $J_{PC}$  = 28.9 Hz, 3C, PMe<sub>3</sub>).

IR:  $\nu(\text{NO}) = 1563 \text{ cm}^{-1}$ ,  $\nu(\text{Ester CO}) = 1725 \text{ cm}^{-1}$

CV (DMA; 100 mV/s):  $E_{p,a} = +0.59\text{V}$  (NHE)

HRMS (APCI) m/z: [M]<sup>+</sup> Calcd for C<sub>37</sub>H<sub>49</sub>BN<sub>10</sub>O<sub>5</sub>PSW<sup>+</sup> 971.2943; Found 971.2922.

**Synthesis and characterization of Wtp(NO)(PMe<sub>3</sub>)(η<sup>2</sup>-(*N*-mesyl)-5-benzotriazole-2-(methyl- $\alpha$ -phenylacetate)-1,2,5,6-tetrahydropyridine (47)**



**Erythro-35D** (50 mg, 0.062 mmol) was dissolved in 1ml propionitrile in a test tube with a stir pea. HOTf/MeCN (0.6 M, 260 mg, 0.093mmol) was added, and the mixture was allowed to stir at room temperature. The dark brown solution was cooled at -40 °C for 15 minutes. Benzotriazole (40 mg, 0.311 mmol) was dissolved in 0.5 mL THF in a test tube with a stir pea, tBuOK/THF (20% wt, 104 mg, 0.185 mmol) as added and allowed to react for 10 minutes. The solution was then cooled to -40 °C for 15 minutes. The allyl solution was added to the deprotonated benzotriazole solution and reacted for 12 hours at -40 °C. The solution was warmed to room temperature. The solution was diluted with DCM (10 mL), washed with Na<sub>2</sub>CO<sub>3</sub> (3 x 5 mL), and the aqueous solution was back extracted with DCM (3 x 2mL). The solution was dried with MgSO<sub>4</sub>, removed on a 15 mL medium porosity frit, washed with DCM (3 x 2 mL), and the resulting filtrate was evaporated to dryness. The product was dissolved in minimal DCM and added to a stirring solution of hexanes (75 mL), yielding a precipitate. This precipitate was isolated on a 15 mL fine porosity frit, washed with hexanes (10 mL), and desiccated to yield **47** (31 mg, 54% yield).

<sup>1</sup>H NMR (CD<sub>2</sub>Cl<sub>2</sub>,  $\delta$ , 25 °C): 8.52 (bs, 1H, PzA3), 8.07 (d,  $J$  = 1.6 Hz, 1H, PzB3), 7.96 (d, 2H, H15/H18), 7.77 (d,  $J$  = 2.3 Hz, 1H, PzB5), 7.74-7.76 (m, 2H, PzA5/C5), 7.45 (m, 4H, H9/H16/H17), 7.31 (t,  $J$  = 7.6 Hz, 2H, H10), 7.25 (t,  $J$  = 7.3 Hz, 1H, H11), 7.15 (d,  $J$  = 1.8 Hz, 1H, PzC3), 6.43 (t,  $J$  = 2.2 Hz, 1H, PzA4), 6.33 (t,  $J$  = 2.2 Hz, 1H, PzB4), 6.23 (t,  $J$  = 2.2 Hz, 1H, PzC4), 6.09 (ddd,  $J$  = 4.5, 10.2, 15.4 Hz, 1H, H5), 5.67 (d,  $J$  = 10.1 Hz, 1H, H2), 4.23 (d,  $J$  = 10.1 Hz, 1H, H7), 3.63 (dd,  $J$  = 5.1, 12.9 Hz, 1H, H6), 3.56 (ddd,  $J$  = 4.7, 11.6, 14.6 Hz, 1H, H4), 3.50 (dd,  $J$  = 11.0, 12.8 Hz, 1H, H6), 2.90 (s, 3H, H13), 1.79 (s, 3H, Ms), 0.78 (d,  $J_{PH}$  = 8.3 Hz, 9H, PMe<sub>3</sub>), 0.68 (d,  $J$  = 7.7 Hz, 1H, H3).

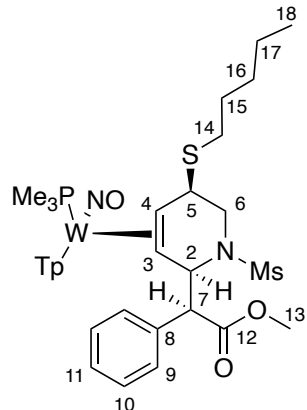
<sup>13</sup>C NMR (CD<sub>2</sub>Cl<sub>2</sub>,  $\delta$ , 25 °C): 172.1 (C12), 144.8 (4C, PzA3/C14/C19), 143.2 (PzB3), 140.1 (PzC3), 138.0 (C8), 136.7 (2C, PzA5/B5/C5), 136.4 (PzA5/B5/C5), 129.7 (2C, C9), 129.1 (2C, C10), 128.4 (C11), 126.7 (2C, C16/C17), 118.5 (2C, C15/C18), 106.8 (PzB4), 106.6 (PzA4), 106.5 (PzC4), 68.1, (C5), 65.6 (C7), 62.0 (C2), 58.9 (C3), 51.5 (C13), 47.8 (C4), 46.0 (C6), 40.7 (Ms), 13.5 (d,  $J_{PC}$  = 8.4 Hz, 3C, PMe<sub>3</sub>).

IR:  $\nu$ (NO) = 1568 cm<sup>-1</sup>,  $\nu$ (Ester CO) = 1731 cm<sup>-1</sup>

CV (DMA; 100 mV/s):  $E_{p,a}$  = +0.67 V (NHE)

HRMS (APCI)  $m/z$ : [M]<sup>+</sup> Calcd for C<sub>33</sub>H<sub>42</sub>BN<sub>11</sub>O<sub>5</sub>PSW<sup>+</sup> 930.2426; Found 930.2438.

**Synthesis and characterization of WTp(NO)(PMe<sub>3</sub>)(η<sup>2</sup>-(*N*-mesyl)-5-pentyl sulfide-2-(methyl- $\alpha$ -phenylacetate)-1,2,5,6-tetrahydropyridine (48)**



**Erythro-35D** (100 mg, 0.123 mmol) was dissolved in 1 mL propionitrile in a test tube with a stir pea. HOTf/MeCN (30 mg, 0.200 mmol) was added, and the mixture was allowed to stir at room temperature. The dark brown solution was cooled at  $-50\text{ }^{\circ}\text{C}$  for 15 minutes. Pentanethiol (90 mg, 0.864 mmol) was dissolved in 0.5 mL THF in a test tube with a stir pea, tBuOK/THF (20% wt, 208 mg, 0.371 mmol) was added and allowed to react for 10 minutes. The solution was then cooled to  $-50\text{ }^{\circ}\text{C}$  for 15 minutes. The allyl solution was added to the deprotonated pentanethiol solution and reacted for 12 hours at  $-50\text{ }^{\circ}\text{C}$ . The solution was warmed to room temperature. The solution was diluted with DCM (10 mL), washed with Na<sub>2</sub>CO<sub>3</sub> (3 x 5 mL), and the aqueous solution was back extracted with DCM (3 x 2 mL). The solution was dried with Na<sub>2</sub>SO<sub>4</sub>, removed on a 15 mL medium porosity frit, washed with DCM (3 x 2 mL), and the resulting filtrate was evaporated to dryness. The product was dissolved in minimal DCM and added to a stirring solution of chilled stirring pentanes (75 mL), yielding a precipitate. This precipitate was isolated on a 15 mL fine porosity frit, washed with pentanes (10 mL), and desiccated to yield **19D** (44 mg, 40% yield).

<sup>1</sup>H NMR ((CD<sub>3</sub>)<sub>2</sub>CO,  $\delta$ , 25  $^{\circ}\text{C}$ ): 8.45 (bs, 1H, PzA3), 8.09 (d,  $J = 1.5$  Hz, 1H, PzB3), 7.94 (d,  $J = 2.1$  Hz, 1H, PzC5), 7.92 (d,  $J = 2.4$  Hz, 1H, PzB5), 7.82 (d,  $J = 2.4$  Hz, 1H, PzA5), 7.42 (d,  $J = 7.4$  Hz, 2H, H9), 7.31 (d,  $J = 1.5$  Hz, 1H, PzC3), 7.25 (t,  $J = 7.2$  Hz, 2H, H10), 7.22 (t,  $J = 7.5$  Hz, 1H, H11), 6.37 (t,  $J = 2.2$  Hz, 1H, PzB4), 6.34 (m, 2H, PzC4/PzA4), 5.57 (dd,  $J = 1.7, 9.4$  Hz, 1H, H2), 4.1 (d,  $J = 9.6$  Hz, 1H, H7), 3.93 (ddd,  $J = 5.4, 10.3, 15.7$  Hz, 1H, H5), 3.61 (dd,  $J = 4.9, 13.4$  Hz, 1H, H6), 3.03 (dd,  $J = 10.9, 13.4$  Hz, 1H, H6), 2.87 (s, 3H, H13), 2.72 (m, 3H, H4/H14), 2.00 (s, 3H, Ms), 1.74-1.64 (m, 2H, H15), 1.48-1.41 (m, 2H, H16/H17), 1.41-1.34 (m, 2H, H16/H17), 1.38 (d,  $J_{PH} = 8.70$  Hz, 9H, PMe<sub>3</sub>), 0.92 (t,  $J = 7.3$  Hz, 3H, H18), 0.58 (d,  $J = 11.5$  Hz, 1H, H3).

<sup>13</sup>C NMR ((CD<sub>3</sub>)<sub>2</sub>CO,  $\delta$ , 25  $^{\circ}\text{C}$ ): 172.6 (C12), 145.1 (PzA3), 144.3 (PzB3), 141.4 (PzC3), 138.9 (C8), 137.4 (PzC5), 137.3 (PzB5), 137.0 (PzA5), 130.6 (2C, C9), 129.3 (2C, C10), 128.5 (C11), 107.12/107.08 (PzC4/PzA4), 62.8 (C7), 59.1 (C2), 55.8 (C3), 51.4 (C13), 48.1 (d,  $J_{PC} = 14.0$  Hz, C4), 47.3 (C6), 43.9 (C5), 41.0 (Ms), 32.2/23.1 (2C, C16/C17), 31.7 (C14), 30.6 (C15), 14.4 (C18), 14.3 (d,  $J_{PC} = 28.8$  Hz, 3C, PMe<sub>3</sub>).

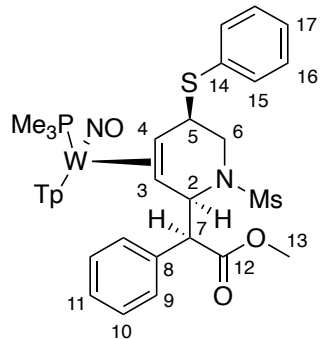
IR:  $\nu(\text{NO}) = 1567\text{ cm}^{-1}$ ,  $\nu(\text{Ester CO}) = 1732\text{ cm}^{-1}$

CV (DMA; 100 mV/s):  $E_{p,a} = +0.54\text{V}$  (NHE)

HRMS (APCI) m/z: [M]<sup>+</sup> Calcd for C<sub>32</sub>H<sub>49</sub>BN<sub>8</sub>O<sub>5</sub>PS<sub>2</sub>W<sup>+</sup> 915.2602; Found 915.2581.

SC-XRD data on page 263

**Synthesis and characterization of WTp(NO)(PMe<sub>3</sub>)(η<sup>2</sup>-(*N*-mesyl)-5-benzyl sulfide-2-(methyl- $\alpha$ -phenylacetate)-1,2,5,6-tetrahydropyridine (49)**



**Erythro-35D** (100 mg, 0.123 mmol) was dissolved in 1ml propionitrile in a test tube with a stir pea. HOTf/MeCN (30 mg, 0.200 mmol) was added, and the mixture was allowed to stir at room temperature. The dark brown solution was cooled at -40 °C for 15 minutes. Benzenethiol (100 mg, 0.908 mmol) was dissolved in 0.5 mL THF in a test tube with a stir pea, tBuOK/THF (20% wt, 208 mg, 0.371 mmol) was added and allowed to react for 10 minutes. The solution was then cooled to -40 °C for 15 minutes. The allyl solution was added to the deprotonated benzenethiol solution and reacted for 12 hours at -60 °C. The solution was warmed to room temperature. The solution was diluted with DCM (10 mL), washed with Na<sub>2</sub>CO<sub>3</sub> (3 x 5 mL), and the aqueous solution was back extracted with DCM (3 x 2 mL). The solution was dried with MgSO<sub>4</sub>, removed on a 15 mL medium porosity frit, washed with DCM (3 x 2 mL), and the resulting filtrate was evaporated to dryness. The product was dissolved in minimal DCM and added to a stirring solution of hexanes (75 mL), yielding a precipitate. This precipitate was isolated on a 15 mL fine porosity frit, washed with hexanes (10 mL), and desiccated to yield **49** (34 mg, 31% yield).

<sup>1</sup>H NMR ((CD<sub>3</sub>)<sub>2</sub>CO,  $\delta$ , 25 °C): 8.53 (d,  $J$  = 1.5 Hz, 1H, PzA3), 8.10 (d,  $J$  = 2.2 Hz, 1H, PzB3), 7.97 (d,  $J$  = 2.2 Hz, 1H, PzC5), 7.94 (d,  $J$  = 2.2 Hz, 1H, PzB5), 7.85 (d,  $J$  = 2.8 Hz, 1H, PzA5), 7.48 (d,  $J$  = 8.7 Hz, 2H, H15), 7.44 (d,  $J$  = 7.7 Hz, 2H, H9), 7.37 (d,  $J$  = 2.2 Hz, 1H, PzC3), 7.32 (t,  $J$  = 7.7 Hz, 2H, H10), 7.26 (t,  $J$  = 7.7 Hz, 2H, H16), 7.23 (t,  $J$  = 7.2 Hz, 1H, H11), 7.19 (t,  $J$  = 7.0 Hz, 1H, H17), 6.38-6.37 (m, 2H, PzA4/PzB4), 6.36 (t,  $J$  = 2.2 Hz, 1H, PzC4), 5.60 (d,  $J$  = 9.8 Hz, 1H, H2), 4.60 (m,  $J$  = 4.5, 9.9 Hz, 1H, H5), 4.14 (d,  $J$  = 9.7 Hz, 1H, H7), 3.57 (dd,  $J$  = 4.7, 13.6 Hz, 1H, H6), 3.06 (dd,  $J$  = 10.8, 13.6 Hz, 1H, H6), 2.85 (s, 3H, H13), 2.77 (m, 1H, H4), 1.83 (s, 3H, Ms), 1.36 (d,  $J_{PH}$  = 8.5 Hz, 9H, PMe<sub>3</sub>), 0.59 (d,  $J$  = 10.9 Hz, 1H, H3).

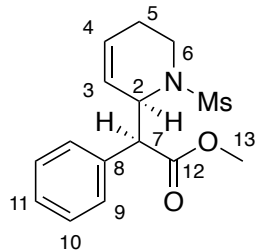
<sup>13</sup>C NMR ((CD<sub>2</sub>Cl<sub>2</sub>),  $\delta$ , 25 °C): 172.2 (C12), 144.8 (PzA3), 143.7 (PzB3), 140.3 (PzC3), 138.1/136.4 (2C, C8/C14), 136.7 (PzC5), 136.7 (PzB5), 136.3 (PzA5), 129.0 (2C, C15), 129.7 (2C, C9), 129.6 (2C, C10), 128.9 (2C, C16), 128.3 (C11), 126.2 (C17), 106.5/106.4 (2C, PzA4/PzB4), 106.4 (PzC4), 62.0 (C7), 58.8 (C2), 55.6 (C3), 51.3 (C13), 46.5 (m, 2C, C4/C6), 43.60 (C5), 40.6 (Ms), 14.5 (d,  $J_{PC}$  = 30.8 Hz, 3C, PMe<sub>3</sub>).

IR:  $\nu$ (NO) = 1559 cm<sup>-1</sup>,  $\nu$ (Ester CO) = 1732 cm<sup>-1</sup>

CV (DMA; 100 mV/s):  $E_{p,a}$  = +0.59V (NHE)

HRMS (APCI) m/z: [M]<sup>+</sup> Calcd for C<sub>33</sub>H<sub>44</sub>BN<sub>8</sub>O<sub>5</sub>PS<sub>2</sub>W<sup>+</sup> 921.2132; Found 921.2136

### Synthesis and characterization of (*N*-mesyl)-2-(methyl- $\alpha$ -phenylacetate)-1,2,5,6-tetrahydropyridine (**50-Ms**)



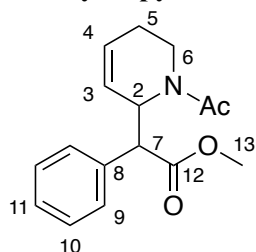
Acetone (3 mL), 2,3-dichloro-5,6-dicyano-1,4-benzoquinone (DDQ) (130 mg, 0.573 mmol), and **38** (107 mg, 0.132 mmol) were added to a 4-dram vial containing a stir pea. The reaction was stirred in a fume hood for 4 hours. The solution was flushed through a 1 cm basic alumina plug set up in a 30 mL coarse porosity frit. This solution was diluted with 30 mL of DCM and was washed 3x with 50 mL of saturated aqueous NaHCO<sub>3</sub>. The organic layer was isolated and set aside. The combined aqueous layers were combined and back-extracted with 30 mL of DCM to prevent loss of product. The organic layers were combined in a single round-bottom flask to which 5 grams of basic alumina powder were added. The solution was then reduced off *in vacuo*, bringing the eluted organic into the basic alumina powder. This powder was then dry loaded onto an 8-gram Teledyne basic alumina column, upon which clean product was eluted off of with 40% ethyl acetate in hexanes. The tubes containing organic were combined and reduced *in vacuo*, yielding a white residue (20 mg, 49% yield).

<sup>1</sup>H NMR ((CD<sub>3</sub>)<sub>2</sub>CO,  $\delta$ , 25 °C): 7.45 (d,  $J$  = 7.2 Hz, 2H, H9), 7.36 (t,  $J$  = 7.8 Hz, 2H, H10), 7.31 (tt,  $J$  = 2.0, 7.4 Hz, 1H, H11), 5.95-5.98 (m, 1H, H4), 5.85-5.88 (m, 1H, H3), 4.90 (d,  $J$  = 10.7 Hz, 1H, H2), 3.89 (d,  $J$  = 10.7 Hz, 1H, H7), 3.68 (s, 3H, H13), 3.60 (ddd,  $J$  = 0.9, 6.5, 14.6 Hz, 1H, H6), 3.26 (ddd,  $J$  = 4.4, 11.9, 14.50 Hz, 1H, H6), 2.31-2.37 (m, 1H, H5), 2.06 (s, 3H, Ms), 2.00 (dt,  $J$  = 4.9 18.1 Hz, 1H, H5).

<sup>13</sup>C NMR ((CD<sub>3</sub>)<sub>2</sub>CO,  $\delta$ , 25 °C): 172.8 (C12), 137.6 (C8), 129.8 (2C, C9), 129.4 (2C, C10), 128.7 (C11), 128.5 (C4), 127.3 (C3), 56.5 (C7), 56.1 (C2), 52.5 (C13), 39.8 (Ms), 39.0 (C6), 24.7 (C5).

SC-XRD data on page 264

### Synthesis and characterization of (*N*-acetyl)-2-(methyl- $\alpha$ -phenylacetate)-1,2,5,6-tetrahydropyridine (**50-Ac**)



**38-Ac** (90 mg, 0.12 mmol) was dissolved in MeCN (3.0 mL) in a 4 dram vial containing a stir pea. Separately, DDQ (50 mg, 0.22 mmol) was dissolved in MeCN (1.0 mL). The DDQ solution was added to the solution of **38-Ac**, and the resulting mixture was stirred for 5 min. The reaction mixture was then diluted with DCM (50 mL) and extracted with saturated aqueous NaHCO<sub>3</sub> (50 mL). The aqueous layer was back-extracted with DCM (15 mL), and the combined organic layers were dried with Na<sub>2</sub>SO<sub>4</sub>. The solids were filtered off on a 30 mL medium fritted funnel, and rinsed with DCM (10 mL). The filtrate was evaporated on a rotary evaporator. The residue was dissolved in DCM (2 mL) and added to stirring Et<sub>2</sub>O (100 mL). The precipitate was filtered off on a 30 mL medium porosity fritted funnel and rinsed with Et<sub>2</sub>O (10 mL). The filtrate was evaporated onto silica on a rotary evaporator. The desired product was purified by Combiflash flash chromatography using a 0-100% EtOAc in hexanes gradient 30 mL/min elution on a 12 g silica column. The desired product eluted at ~48% EtOAc. The fractions containing the product were combined and evaporated on a rotary evaporator. The residue was desiccated under high vacuum for 30 min to yield compound **50-Ac** as a colorless oil (22 mg, 66%).

*Erythro* isomer: A mixture of two rotamers **A**:**B** = 4:3. <sup>1</sup>H NMR (CDCl<sub>3</sub>,  $\delta$ , 25 °C): **A** 7.45-7.25 (m, 5H, H9-H11), 6.00 (m, 1H, H4), 5.88 (m, 1H, H3), 4.72 (dd,  $J$ =13.1, 6.2 Hz, 1H, H6), 4.60 (m, 1H, H2), 3.87 (d,  $J$ = 10.4 Hz, 1H, H7), 3.76 (s, 3H, H13), 2.83 (m, 1H, H6'), 2.27 (m, 1H, H5), 2.04 (dt,  $J$ = 5.0, 18.1 Hz, 1H, H5'), 1.44 (s, 3H, *N*-Ac). **B** 7.45-7.25 (m, 5H, H9-H11), 5.88 (m, 1H, H4), 5.85 (m, 1H, H3), 5.60 (m, 1H, H2), 3.89 (d,  $J$ = 9.4 Hz, 1H, H7), 3.64 (dd,  $J$ = 13.9, 5.9 Hz, 1H, H6), 3.72 (s, 3H, H13), 3.22 (ddd,  $J$ = 4.2, 12.9, 13.9 Hz, 1H, H6'), 2.27 (m, 1H, H5), 1.96 (dt,  $J$ = 5.0, 18.3 Hz, 1H, H5'), 1.90 (s, 3H, *N*-Ac).

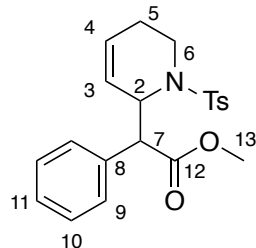
<sup>13</sup>C NMR (CDCl<sub>3</sub>,  $\delta$ ): **A** 172.0 (C12), 170.0 (*N*-Ac), 135.3 (C8), 129.1 (C9), 128.5 (C10), 127.8 (C11), 129.2 (C4), 126.2 (C3), 57.2 (C2), 55.3 (C7), 52.4 (C13), 34.8 (C6), 24.9 (C5), 20.9 (*N*-Ac). **B** 172.4 (C12), 169.1 (*N*-Ac), 134.8 (C8), 128.8 (C9), 128.4 (C10), 127.8 (C11), 126.6 (C3), 126.2 (C4), 55.3 (C7), 52.4 (C13), 51.6 (C2), 40.3 (C6), 24.5 (C5), 21.6 (*N*-Ac).

*Threo* isomer: A mixture of two rotamers **A**:**B** = 1:1. <sup>1</sup>H NMR (CDCl<sub>3</sub>,  $\delta$ ): **A** 7.45-7.25 (m, 5H, H9-H11), 5.85 (m, 1H, H4), 5.27 (m, 1H, H3), 4.79 (m, 1H, H2), 4.66 (dd,  $J$ = 6.4, 13.5 Hz, 1H, H6), 3.94 (d,  $J$ = 10.2 Hz, 1H, H7), 3.69 (s, 3H, H13), 2.82 (m, 1H, H6'), 2.32 (s, 3H, *N*-Ac), 2.22 (m, 1H, H5), 2.08 (dt,  $J$ = 4.4, 17.2 Hz, 1H, H5'). **B** 7.45-7.25 (m, 5H, H9-H11), 5.85 (m, 1H, H4), 5.69 (m, 1H, H3), 5.54 (m, 1H, H2), 4.07 (d,  $J$ = 7.8 Hz, 1H, H7), 3.67 (s, 3H, H13), 3.54 (dd,  $J$ = 5.8, 13.8 Hz, 1H, H6), 2.63 (ddd,  $J$ = 3.9, 12.7, 14.1 Hz, 1H, H6'), 2.13 (s, 3H, *N*-Ac), 2.13 (m, 1H, H5), 1.90 (buried, 1H, H5').

<sup>13</sup>C NMR (CDCl<sub>3</sub>,  $\delta$ ): **A** 172.3 (C12), 170.6 (*N*-Ac), 135.3 (C8), 129.0 (C9), 128.6 (C4), 128.4 (C10), 128.3 (C11), 125.6 (C3), 57.3 (C2), 54.5 (C7), 52.3 (C13), 35.1 (C6), 24.6 (C5), 21.7 (*N*-Ac). **B** 172.5 (C12), 169.4 (*N*-Ac), 135.3 (C8), 129.9 (C9), 128.8 (C10), 128.4 (C11), 127.3 (C4), 126.2 (C3), 56.5 (C7), 52.3 (C2), 52.2 (C13), 40.5 (C6), 25.3 (C5), 22.1 (*N*-Ac).

ESI-MS: obs'd (%), calc'd (%), ppm, (M+H)<sup>+</sup>: 274.1439 (100), 274.1438 (100), 0.4.  
SC-XRD data on page 265

### Synthesis and characterization of (*N*-tosyl)-2-(methyl- $\alpha$ -phenylacetate)-1,2,5,6-tetrahydropyridine (**50-Ts**)



**38-Ts** (70 mg, 0.0788 mmol) was dissolved in MeCN (3.0 mL) in a 4 dram vial containing a stir pea. Separately, DDQ (40 mg, 0.176 mmol) was dissolved in MeCN (1.0 mL). The DDQ solution was added to the solution of **38-Ts**, and the resulting mixture was stirred for 5 min. The reaction mixture was then diluted with DCM (50 mL) and extracted with saturated aqueous NaHCO<sub>3</sub> (50 mL). The aqueous layer was back-extracted with DCM (15 mL), and the combined organic layers were dried with Na<sub>2</sub>SO<sub>4</sub>. The solids were filtered off on a 30 mL medium fritted funnel, and rinsed with DCM (10 mL). The filtrate was evaporated on a rotary evaporator. The residue was dissolved in DCM (2 mL) and added to stirring Et<sub>2</sub>O (100 mL). The precipitate was filtered off on a 30 mL medium porosity fritted funnel and rinsed with Et<sub>2</sub>O (10 mL). The filtrate was evaporated onto silica on a rotary evaporator. The desired product was purified by Combiflash flash chromatography using a 0-100% EtOAc in hexanes gradient 30 mL/min elution on a 12 g silica column. The desired product eluted at ~48% EtOAc. The fractions containing the product were combined and evaporated on a rotary evaporator. The residue was desiccated under high vacuum for 30 min to yield compound **50-Ts** as a colorless oil which spontaneously crystallized (19 mg, 62%).

Two diastereomers **A**:**B**.

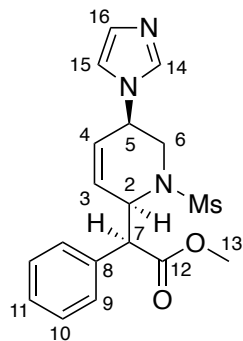
<sup>1</sup>H NMR (CDCl<sub>3</sub>,  $\delta$ , 25 °C): **A** 7.72 (d,  $J$  = 8.3 Hz, 2H, Ts), 7.36-7.28 (m, 5H, H9-H11), 7.25 (d,  $J$  = 8.3 Hz, 2H, Ts), 5.63 (m, 1H, H4), 5.54 (m, 1H, H3), 5.03 (m, 1H, H2), 4.00 (d,  $J$  = 8.2 Hz, 1H, H7), 3.68 (dd,  $J$  = 14.8, 6.4 Hz, 1H, H6), 3.66 (s, 3H, H13), 2.69 (dd,  $J$  = 14.8, 4.6 Hz, 1H, H6'), 2.40 (s, 3H, Ts), 1.71 (m, 1H, H5), 1.58 (ddd,  $J$  = 18.0, 6.4, 4.6 Hz, 1H, H5'). **B** 7.36-7.28 (m, 5H, H9-H11), 7.23 (d,  $J$  = 8.3 Hz, 2H, Ts), 7.07 (d,  $J$  = 8.3 Hz, 2H, Ts), 6.84 (m, 1H, H3), 5.79 (m, 1H, H4), 5.03 (m, 1H, H2), 3.80 (d,  $J$  = 9.8 Hz, 1H, H7), 3.69 (s, 3H, H13), 3.54 (dd,  $J$  = 14.8, 6.4 Hz, 1H, H6), 3.07 (ddd,  $J$  = 14.8, 12.0 Hz, 4.6 Hz, 1H, H6'), 2.35 (s, 3H, Ts), 2.06 (m, 1H, H5), 1.80 (ddd,  $J$  = 18.0, 6.4, 4.6 Hz, 1H, H5').

<sup>13</sup>C NMR (CDCl<sub>3</sub>,  $\delta$ ): **A** 171.9 (C12), 143.4 (Ts), 138.3 (Ts), 134.8 (C8), 129.7 (Ts), 129.7 (C09), 128.6 (C10), 128.0 (Ts), 127.2 (C11), 127.1 (C3), 125.0 (C4), 57.5 (C7), 55.3 (C2), 52.3 (C13), 38.8 (C6), 22.7 (C5), 21.6 (Ts). **B** 172.2 (C12), 143.1 (Ts), 137.4 (Ts), 135.6 (C8), 129.4 (C09), 129.0 (C10), 128.8 (Ts), 128.0 (Ts), 127.5 (C11), 127.3 (C4), 126.1 (C3), 56.7 (C7), 54.9 (C2), 52.4 (C13), 38.4 (C6), 22.9 (C5), 21.6 (Ts).

ESI-MS: obs'd (%), calc'd (%), ppm, (M+H)<sup>+</sup>: 386.1420 (100), 386.1421 (100), 0.2. (M+Na)<sup>+</sup>: 408.1242(100), 408.1240 (100), 0.5.



## Synthesis and characterization of (*N*-mesyl)-5-imidazole-2-(methyl- $\alpha$ -phenylacetate)-1,2,5,6-tetrahydropyridine (**51**)



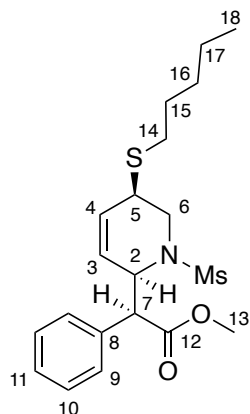
**45** (62 mg, 0.071 mmol) was dissolved in 2 mL propionitrile in a test tube with a stir pea. In a separate test tube, DDQ (16 mg, 0.070 mmol) was dissolved in 2 mL propionitrile, and HOTf (32 mg, 0.211 mmol) was added. Both test tubes were chilled to  $-40\text{ }^{\circ}\text{C}$  for 15 minutes. The DDQ/HOTf solution was added to the THP complex and allowed to stir for 1 minute. The solution was removed from the glove box and diluted with DCM (50 mL), and extracted with  $\text{Na}_2\text{CO}_3$  (2 x 20 mL). The aqueous solution was back extracted with DCM (3 x 6 mL). The organic solution was dried with  $\text{Na}_2\text{SO}_4$ , filtered on a 15 mL medium porosity frit, and rinsed with 5 mL diethyl ether. The solvent was removed, dissolved in minimal DCM, and added to stirring hexanes. The precipitate was filtered off using a 15 mL medium porosity frit and washed with 15 mL diethyl ether. The filtrate was reduced, and **51** (8 mg, 30% yield) was isolated.

$^1\text{H}$  NMR ( $(\text{CD}_3)_2\text{CO}$ ,  $\delta$ ,  $25\text{ }^{\circ}\text{C}$ ): 7.70 (bs, 1H, H14), 7.48 (d,  $J = 7.5$  Hz, 2H, H9), 7.39 (t,  $J = 7.2$  Hz, 2H, H10), 7.34 (t,  $J = 7.6$  Hz, 1H, H11), 7.20 (bs, 1H, H15), 6.98 (bs, 1H, H16), 6.2 (ddd,  $J = 2.5, 3.9, 6.4$  Hz, 1H, H3), 6.01 (dd,  $J = 1.5, 10.5$  Hz, 1H, H4), 5.1 (dd,  $J = 1.4, 10.4$  Hz, 1H, H2), 5.05 (m,  $J = 2.1, 5.6, 8.1$  Hz, 1H, H5), 4.17 (d,  $J = 10.6$  Hz, 1H, H7), 3.88 (dd,  $J = 6.1, 14.2$  Hz, 1H, H6), 3.72 (s, 3H, H13), 3.37 (dd,  $J = 10.5, 14.3$  Hz, 1H, H6), 2.08 (s, 3H, Ms).

$^{13}\text{C}$  NMR ( $(\text{CD}_3)_2\text{CO}$ ,  $\delta$ ,  $25\text{ }^{\circ}\text{C}$ ): 172.9 (C12), 137.7 (C8), 137.4 (C14), 130.9 (C3), 130.0 (C16), 129.9 (2C, C9), 129.7 (2C, C10), 129.3 (C4), 129.0 (C11), 118.5 (C15), 56.0 (C2), 55.4 (C7), 52.8 (C13), 51.3 (C5), 45.2 (C6), 39.8 (Ms).

SC-XRD data on page 266

## Synthesis and characterization of (*N*-mesyl)-5-pentyl sulfide-2-(methyl- $\alpha$ -phenylacetate)-1,2,5,6-tetrahydropyridine (**52**)



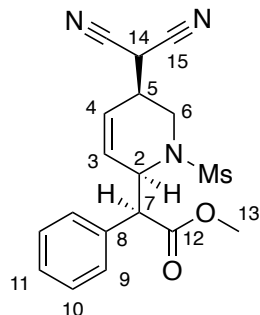
**48** (88 mg, 0.096 mmol) was dissolved in 2 mL propionitrile in a test tube with a stir pea. In a separate test tube, DDQ (24 mg, 0.106 mmol) was dissolved in 2 mL propionitrile. The DDQ solution was added to the THP complex and allowed to stir for 10 minutes. The solution was removed from the glove box and packed onto a basic alumina column, **52** was collected after reducing the eluent from a 35% EtOAc/Hexanes solution (8 mg, 65% yield).

$^1\text{H}$  NMR (( $\text{CDCl}_3$ ),  $\delta$ , 25 °C): 7.39 (d,  $J$  = 7.6 Hz, 2H, H9), 7.35 (t,  $J$  = 7.3 Hz, 2H, H10), 7.30 (t,  $J$  = 7.5 Hz, 1H, H11), 5.96 (ddd,  $J$  = 2.3, 4.1, 10.4 Hz, 1H, H3), 5.90 (ddd,  $J$  = 1.7, 3.3, 10.4 Hz, 1H, H4), 4.98 (dd,  $J$  = 1.9, 10.8 Hz, 1H, H2), 3.79 (dd,  $J$  = 6.0, 14.2 Hz, 1H, H6), 3.70 (s, 3H, H13), 3.69 (d,  $J$  = 10.8 Hz, 1H, H7), 3.54 (m, 1H, H5), 2.94 (dd,  $J$  = 11.3, 14.0 Hz, 1H, H6), 2.58 (dt,  $J$  = 2.9, 7.1 Hz, 2H, H14), 1.91 (s, 3H, Ms), 1.60 (q,  $J$  = 7.4, 14.8 Hz, 2H, H15), 1.36 (m, 2H, H16), 1.33 (m, 2H, H17), 0.90 (t,  $J$  = 7.51 Hz, 3H, H18).

$^{13}\text{C}$  NMR (( $\text{CDCl}_3$ ),  $\delta$ , 25 °C): 171.77 (C14), 136.39 (C13), 130.53 (C4), 129.06 (C11), 128.86 (C10), 128.45 (C12), 128.12 (C3), 55.76 (C8), 55.44 (C2), 52.56 (C9), 45.07 (C6), 39.85 (C7), 38.70 (C5), 31.15 (C17), 30.66 (C15), 29.86 (C16), 22.38 (C18), 14.08 (C19).

HRMS (APCI)  $m/z$ :  $[\text{M}]^+$  Calcd for  $\text{C}_{20}\text{H}_{30}\text{NO}_4\text{S}_2^+$  412.1611; Found 412.1614.

## Synthesis and characterization of (*N*-mesyl)-5-malononitrile-2-(methyl- $\alpha$ -phenylacetate)-1,2,5,6-tetrahydropyridine (**53**)



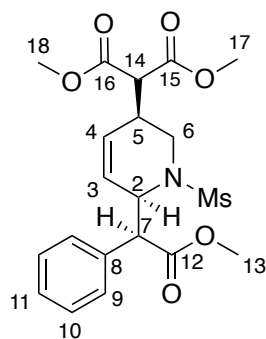
**41** (134 mg, 0.153 mmol) was dissolved in 5 mL of acetone in a vial with a stir pea. Ammonium Cerium(IV) Nitrate (CAN) (345 mg, 0.629 mmol) was added to the solution and allowed to react for 4 hours. The solution was diluted with DCM (50 mL) and extracted with H<sub>2</sub>O (3 x 300 mL). The aqueous solution was back extracted with DCM (3 x 6 mL). The organic solution was dried with Na<sub>2</sub>SO<sub>4</sub>, filtered, and rinsed with DCM. The solvent was removed and packed onto a basic alumina column rinsed with 40% EtOAc/Hexanes solution. **53** (30 mg, 53% yield) was isolated.

<sup>1</sup>H NMR ((CDCl<sub>3</sub>),  $\delta$ , 25 °C): 7.46 (d,  $J$  = 8.03 Hz, 2H, H9), 7.40 (t,  $J$  = 7.42 Hz, 2H, H10), 7.35 (t,  $J$  = 7.42 Hz, 1H, H11), 6.29 (ddd,  $J$  = 2.34, 4.16, 6.38 Hz, 1H, H3), 5.98 (dd,  $J$  = 3.28, 10.41 Hz, 1H, H4), 5.03 (d,  $J$  = 10.82 Hz, 1H, H2), 4.79 (d,  $J$  = 5.14 Hz, 1H, H14), 3.93 (dd,  $J$  = 4.93, 13.08 Hz, 1H, H6), 3.87 (d,  $J$  = 10.72 Hz, 1H, H7), 3.70 (s, 3H, H13), 3.26 (bs, 1H, H5), 3.22 (dd,  $J$  = 11.00, 13.40 Hz, 1H, H6), 2.12 (s, 3H, Ms).

<sup>13</sup>C NMR ((CDCl<sub>3</sub>),  $\delta$ , 25 °C): 172.6 (C12), 137.3 (C8), 132.7 (C3), 129.8 (4C, C9/C10), 129.1 (C11), 126.3 (C4), 113.0 (2C, C15), 56.4 (C7), 56.2 (C2), 52.8 (C13), 41.9 (C6), 40.0 (Ms), 35.8 (C5), 26.2 (C14).

HRMS (APCI)  $m/z$ : [M]<sup>+</sup> Calcd for C<sub>18</sub>H<sub>20</sub>N<sub>3</sub>O<sub>4</sub>S<sup>+</sup> 374.1169; Found 374.1166.

**Synthesis and characterization of (*N*-mesyl)-5-dimethyl malonate-2-(methyl- $\alpha$ -phenylacetate)-1,2,5,6-tetrahydropyridine (**54**)**



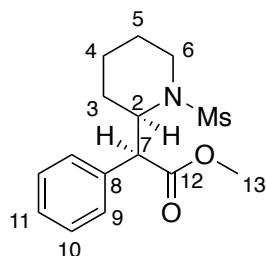
**39** (62 mg, 0.066 mmol) was dissolved in 2ml of acetone in a vial with a stir pea. DDQ (38 mg, 0.167 mmol) was added to the solution and allowed to react for 3 hours. The solution was diluted with DCM (50ml) and extracted with H<sub>2</sub>O (3 x 100 mL). The aqueous solution was back extracted with DCM (3 x 6 mL). The organic solution was dried with Na<sub>2</sub>SO<sub>4</sub>, filtered, and rinsed with DCM. The solvent was removed, redissolved in minimal DCM, and precipitated in hexanes. The precipitate was rinsed with ether, and the filtrate was reduced. **54** (20 mg, 69% yield) was isolated.

<sup>1</sup>H NMR ((CDCl<sub>3</sub>),  $\delta$ , 25 °C): 7.42 (d,  $J$  = 7.59 Hz, 2H, H9), 7.37 (t,  $J$  = 7.59 Hz, 2H, H10), 7.32 (t,  $J$  = 7.26 Hz, 1H, H11), 5.98 (ddd,  $J$  = 2.64, 4.12, 10.54 Hz, 1H, H3), 5.83 (dd,  $J$  = 1.45, 10.47 Hz, 1H, H4), 4.93 (d,  $J$  = 10.83, 1H, H2), 3.87 (d,  $J$  = 11.09, 1H, H7), 3.74-3.75 (m, 7H, H6/17/18), 3.68 (s, 3H, H13), 3.57 (d,  $J$  = 7.51 Hz, 1H, H14), 3.21 (dd,  $J$  = 11.07, 14.11 Hz, 1H, H6), 3.13 (m, 1H, H5), 2.06 (s, 3H, Ms).

<sup>13</sup>C NMR ((CDCl<sub>3</sub>),  $\delta$ , 25 °C): 172.80 (C12), 168.97/168.94 (2C, C15/16), 137.58 (C8), 129.80 (2C, C9), 129.65 (2C, C10), 129.55 (C11), 129.13 (C4), 128.93 (C3), 56.40 (C7), 56.08 (C2), 54.13 (C14), 52.99/52.97 (2C, C17/18), 52.68 (C13), 41.94 (C6), 39.92 (Ms), 34.63 (C5).

HRMS (APCI)  $m/z$ : [M]<sup>+</sup> Calcd for C<sub>20</sub>H<sub>26</sub>NO<sub>8</sub>S<sup>+</sup> 440.1374; Found 440.1380.

## Synthesis and characterization of *erythro*-(*N*-mesyl)-methylphenidate (**55**)



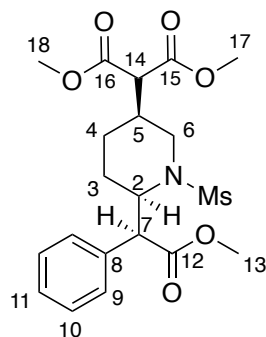
**50** (21 mg, 0.068 mmol) was dissolved in ethyl acetate (3 mL) and added to a 4-dram vial. This solution was then circulated through a ThalesNano H-Cube flow hydrogenator for 5 hours. The temperature was set to 50 °C, the H<sub>2</sub> pressure to 25 bars, and the catalyst cartridge used contained 5% Pd on carbon. After circulation, the solution was collected and reduced to dryness (17 mg 78% yield).

<sup>1</sup>H NMR ((CD<sub>3</sub>)<sub>2</sub>CO), δ, 25 °C): 7.52 (d, *J* = 7.2, 2H, H9), 7.36 (tt, *J* = 1.3, 7.2 Hz, 2H, H10), 7.31 (tt, *J* = 1.3, 7.3 Hz, 1H, H11), 4.75 (dd, *J* = 5.1, 11.8 Hz, 1H, H2), 4.32 (d, *J* = 11.8 Hz, 1H, H7), 3.66 (s, 3H, H13), 3.47 (dd, *J* = 3.3, 14.2 Hz, 1H, H6), 3.11 (ddd, *J* = 2.8, 13.0, 14.2 Hz, 1H, H6), 1.91 (s, 3H, Ms), 1.81-1.88 (m, 1H, H4), 1.73-1.78 (m, 1H, H3), 1.70-1.73 (m, 1H, H3), 1.67-1.70 (m, 1H, H4), 1.61-1.65 (m, 1H, H5), 1.48-1.55 (m, 1H, H5).

<sup>13</sup>C NMR ((CD<sub>3</sub>)<sub>2</sub>CO), δ, 25 °C): 173.2 (C12), 138.0 (C8), 129.7 (C9), 129.5 (C10), 128.7 (C11), 56.2 (C2), 52.5 (C7), 51.4 (C13), 41.3 (C6), 39.7 (Ms), 29.0 (C3), 26.0 (C5), 19.5 (C4).

SC-XRD data on page 267

## Synthesis and characterization of *erythro*-(*N*-mesyl)-methylphenidate (**56**)



**54** (27mg, 0.061 mmol) was dissolved in ethyl acetate (3 mL) and added to a 4-dram vial. This solution was then circulated through a ThalesNano H-Cube flow hydrogenator for 5 hours. The temperature was set to 50 °C, the H<sub>2</sub> pressure to 25 bars, and the catalyst cartridge used contained 5% Pd on carbon. After circulation, the solution was collected and reduced to dryness (17 mg, 65% yield)

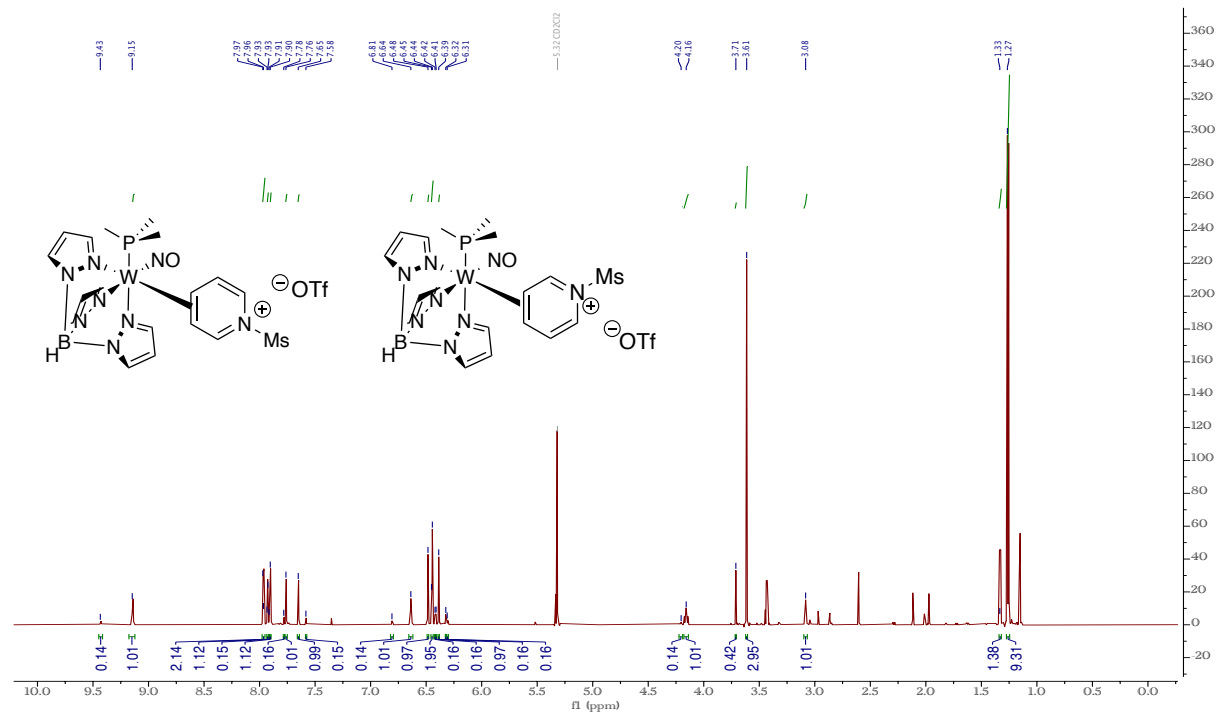
<sup>1</sup>H NMR (CD<sub>2</sub>Cl<sub>2</sub>), δ, 25 °C): 7.42 (d, *J* = 7.5 Hz, 2H, H9), 7.35 (t, *J* = 7.5 Hz, 2H, H10), 7.30 (t, *J* = 7.4 Hz, 1H, H11), 4.74 (dd, *J* = 5.0, 11.5 Hz, 1H, H2), 4.05 (d, *J* = 11.8 Hz, 1H, H7), 3.75 (s, 6H, H17/18), 3.66 (s, 3H, H13), 3.54 (dd, *J* = 3.5, 13.7 Hz, 1H, H6), 3.29 (d, *J* = 7.70 Hz, 1H, H14), 2.84 (dd, *J* = 11.8, 13.7 Hz, 1H, H6), 2.25-2.31 (m, 1H, H5), 1.92 (s, 3H, Ms), 1.84-1.90 (m, 1H, H3), 1.73-1.79 (m, 2H, H3/4), 1.67 (dq, *J* = 3.2, 12.8 Hz, 1H, H4).

<sup>13</sup>C NMR (CD<sub>2</sub>Cl<sub>2</sub>), δ, 25 °C): 172.5 (C12), 168.5 (C15/16), 136.8 (C8), 129.2 (2C, C9/10), 129.1 (2C, C9/10), 128.6 (C11), 55.3 (C2), 55.1 (C14), 52.9 (2C, C17/18), 52.7 (C13), 51.2, (C7), 43.5 (C6), 39.9 (Ms), 36.2 (C5), 28.5 (C3), 23.4 (C4).

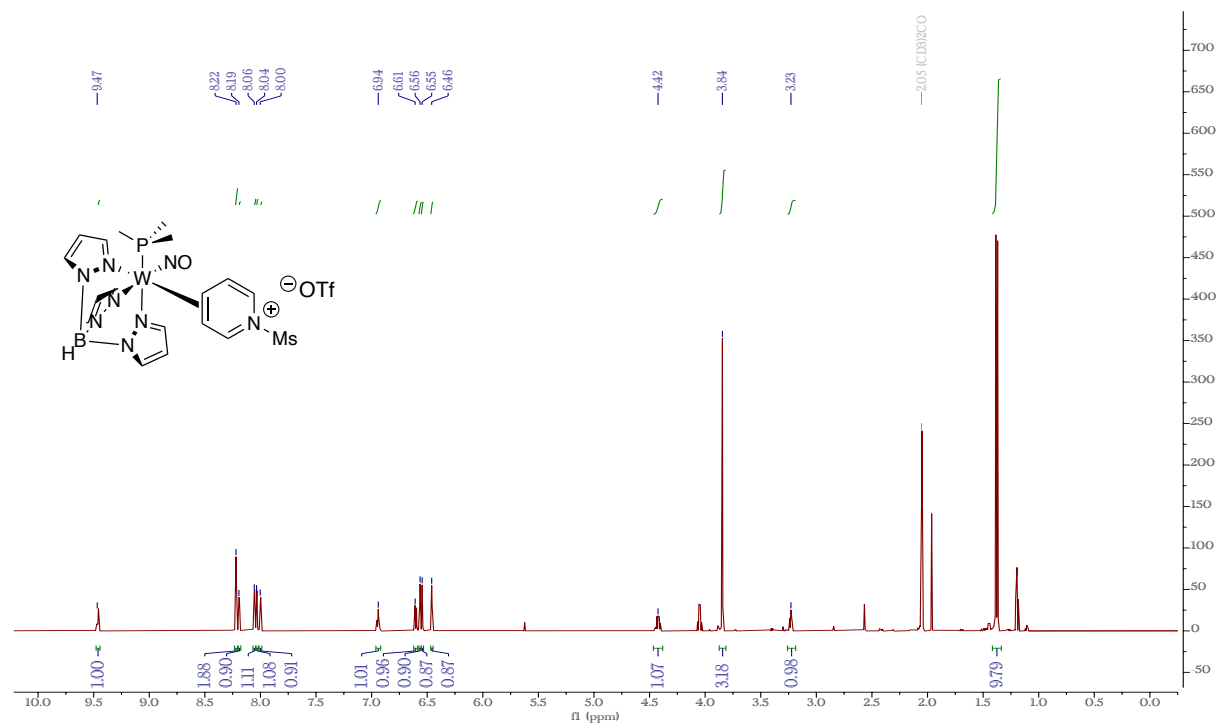
SC-XRD data on page 268

# NMR Spectroscopy:

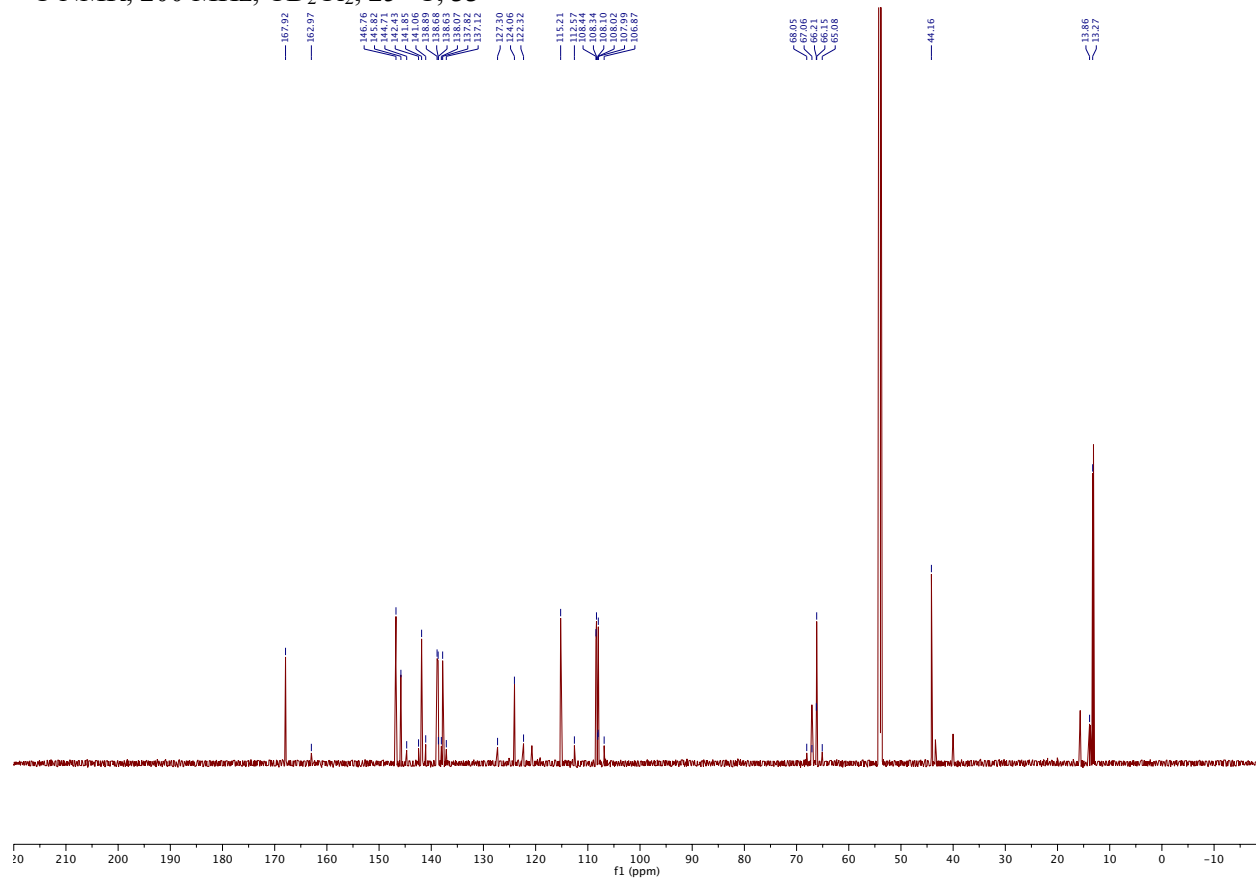
$^1\text{H}$  NMR, 800 MHz,  $\text{CD}_2\text{Cl}_2$ , 25 °C, **33**



$^1\text{H}$  NMR, 800 MHz,  $(\text{CD}_3)_2\text{CO}$ , 25 °C, **33D**

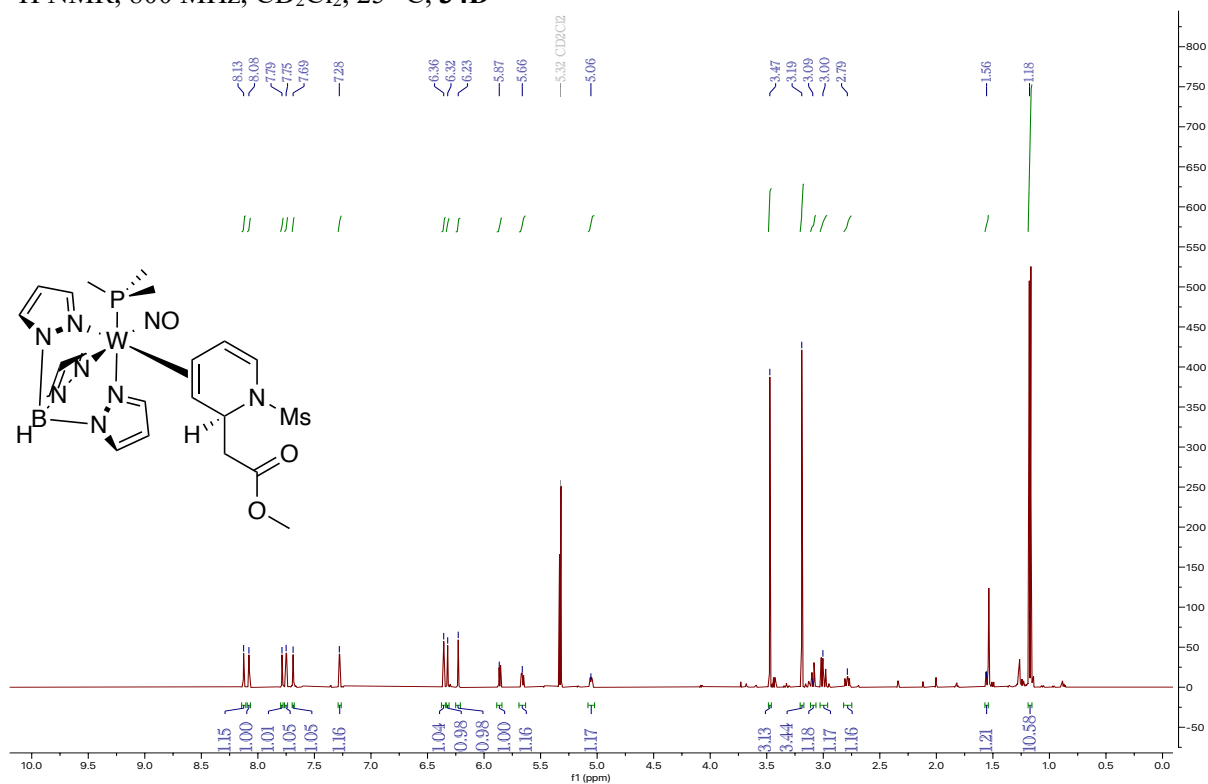


$^{13}\text{C}$  NMR, 200 MHz,  $\text{CD}_2\text{Cl}_2$ , 25 °C, **33**

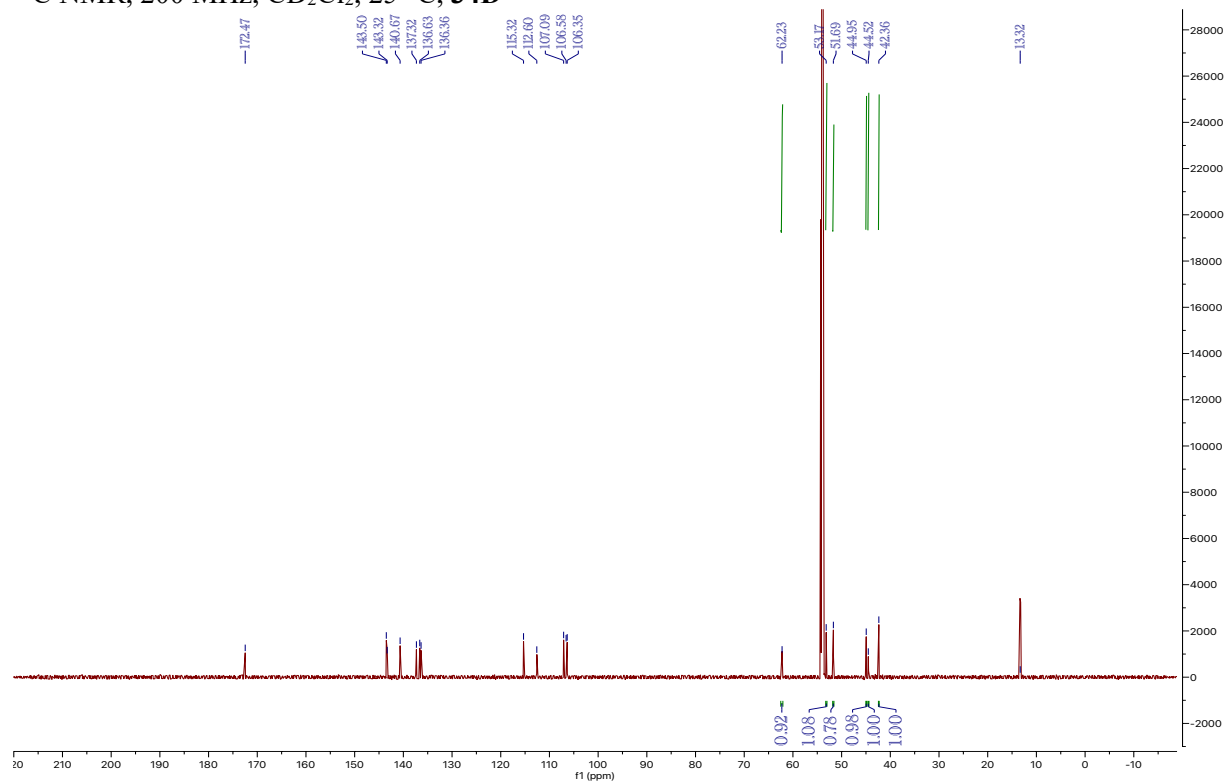




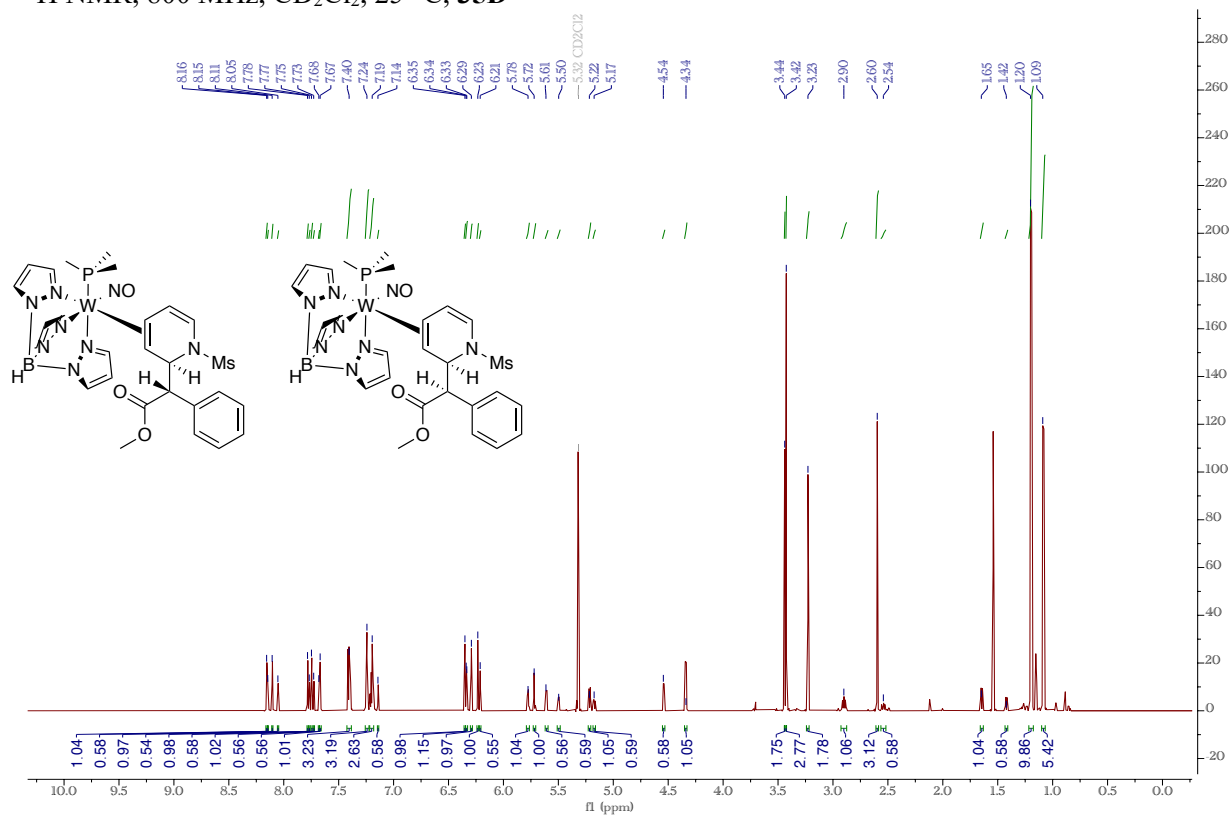
$^1\text{H}$  NMR, 800 MHz,  $\text{CD}_2\text{Cl}_2$ , 25  $^\circ\text{C}$ , **34D**



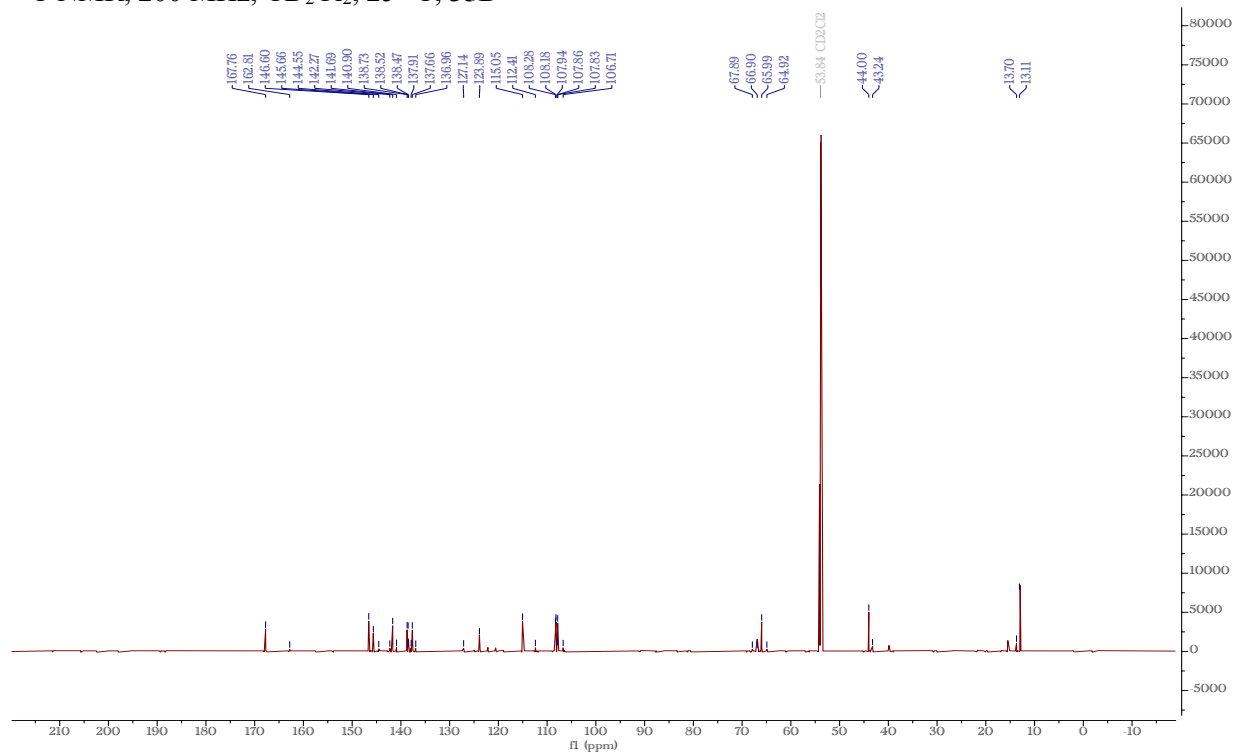
$^{13}\text{C}$  NMR, 200 MHz,  $\text{CD}_2\text{Cl}_2$ , 25  $^\circ\text{C}$ , **34D**



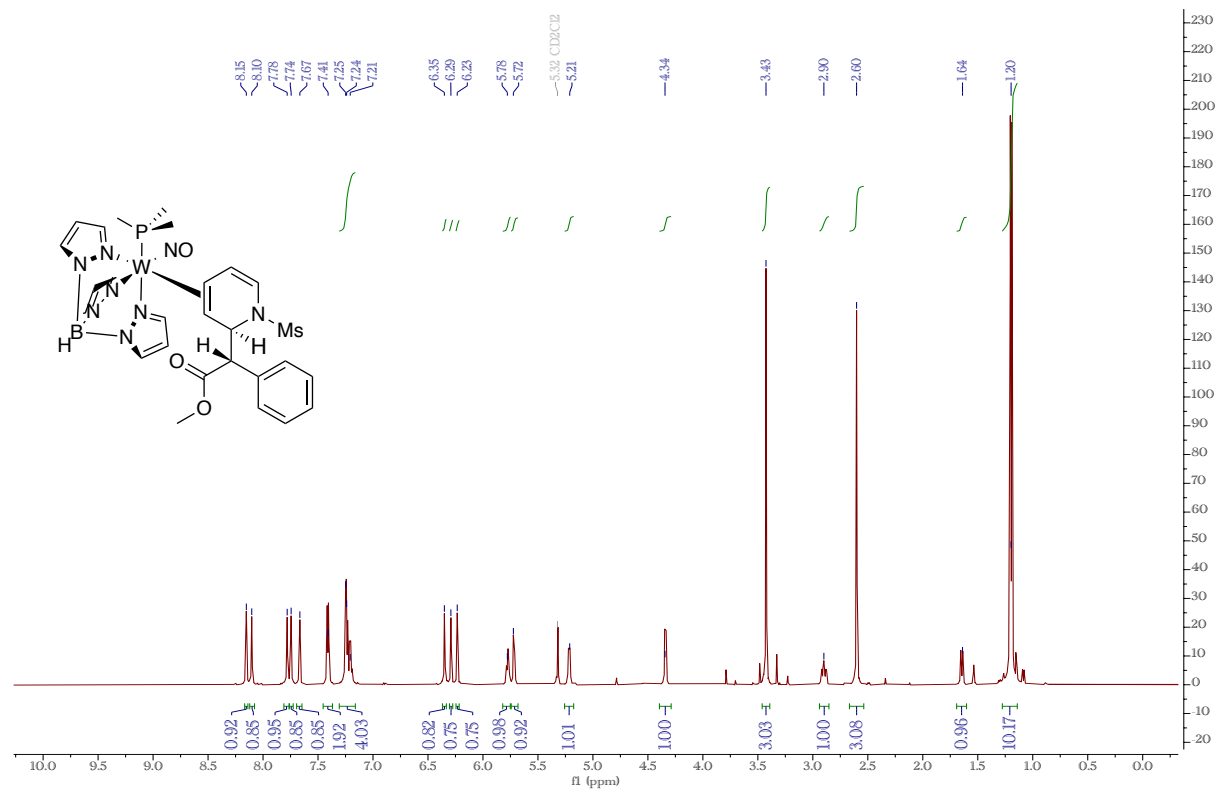
<sup>1</sup>H NMR, 800 MHz, CD<sub>2</sub>Cl<sub>2</sub>, 25 °C, **35D**



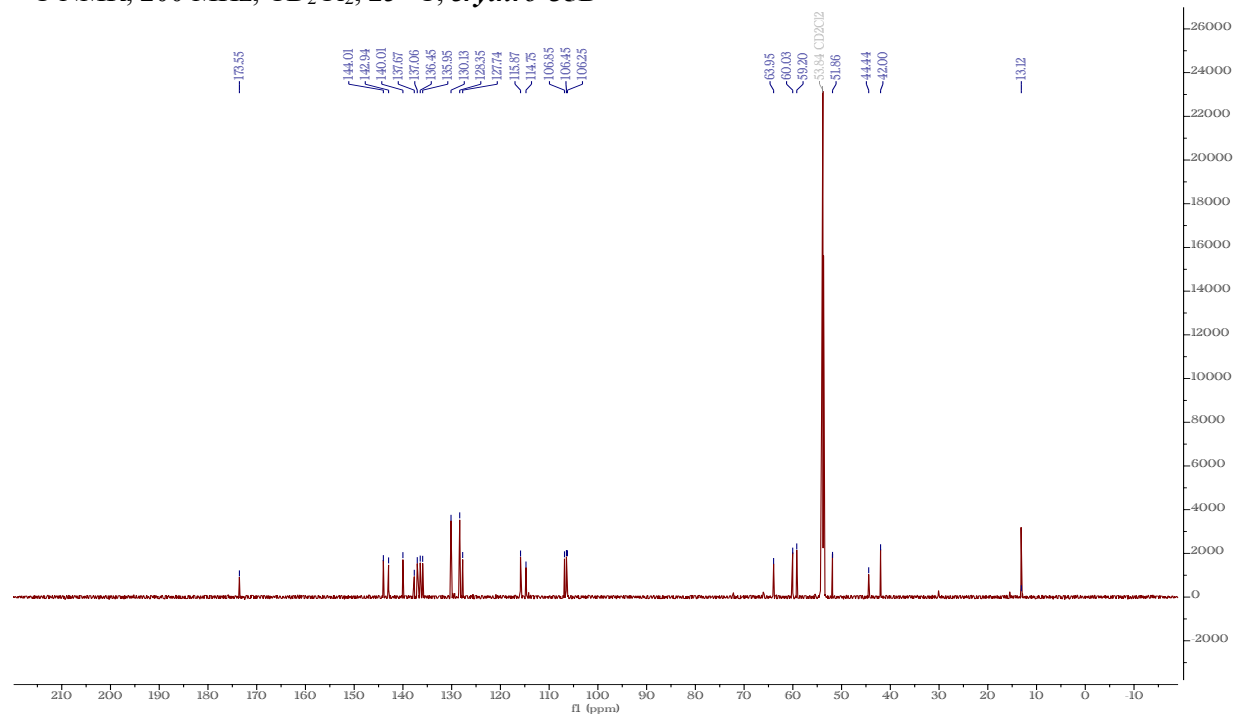
<sup>13</sup>C NMR, 200 MHz, CD<sub>2</sub>Cl<sub>2</sub>, 25 °C, **35D**



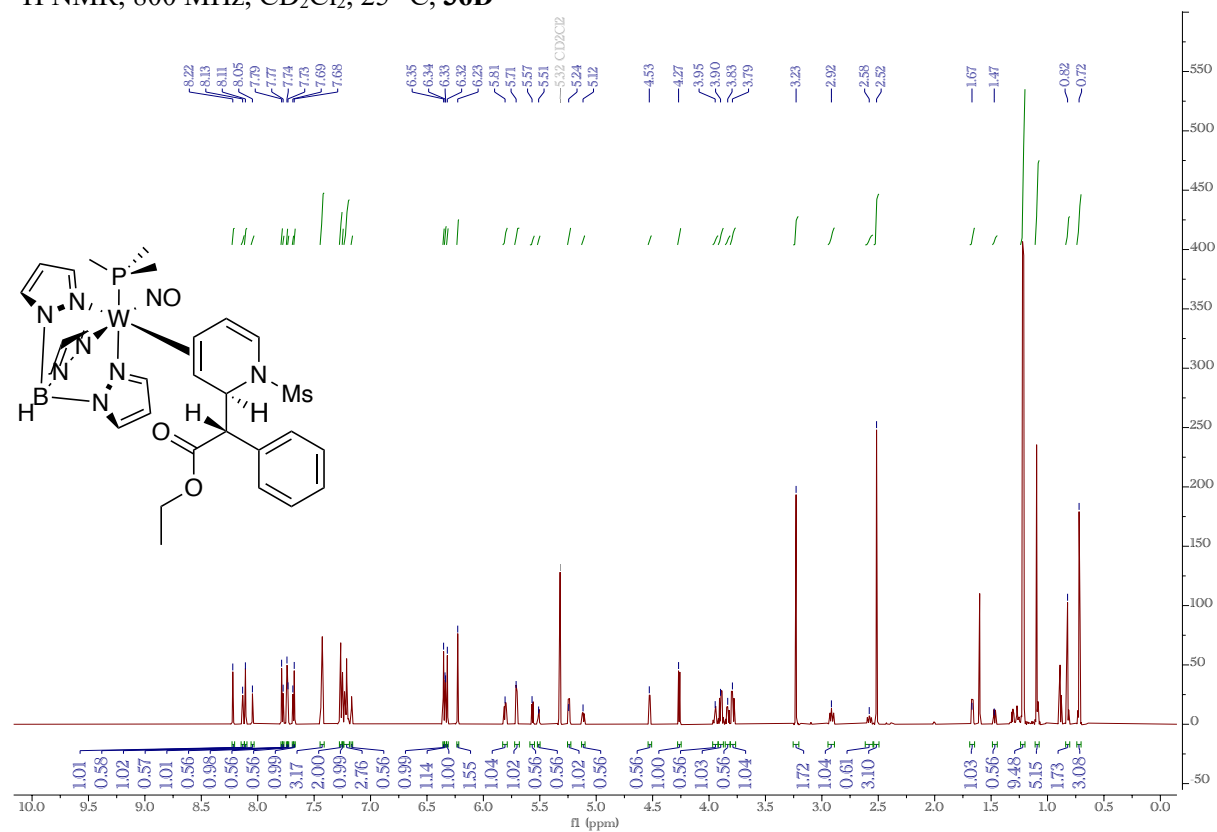
$^1\text{H}$  NMR, 800 MHz,  $\text{CD}_2\text{Cl}_2$ , 25 °C, Highly Enriched *erythro*-35D



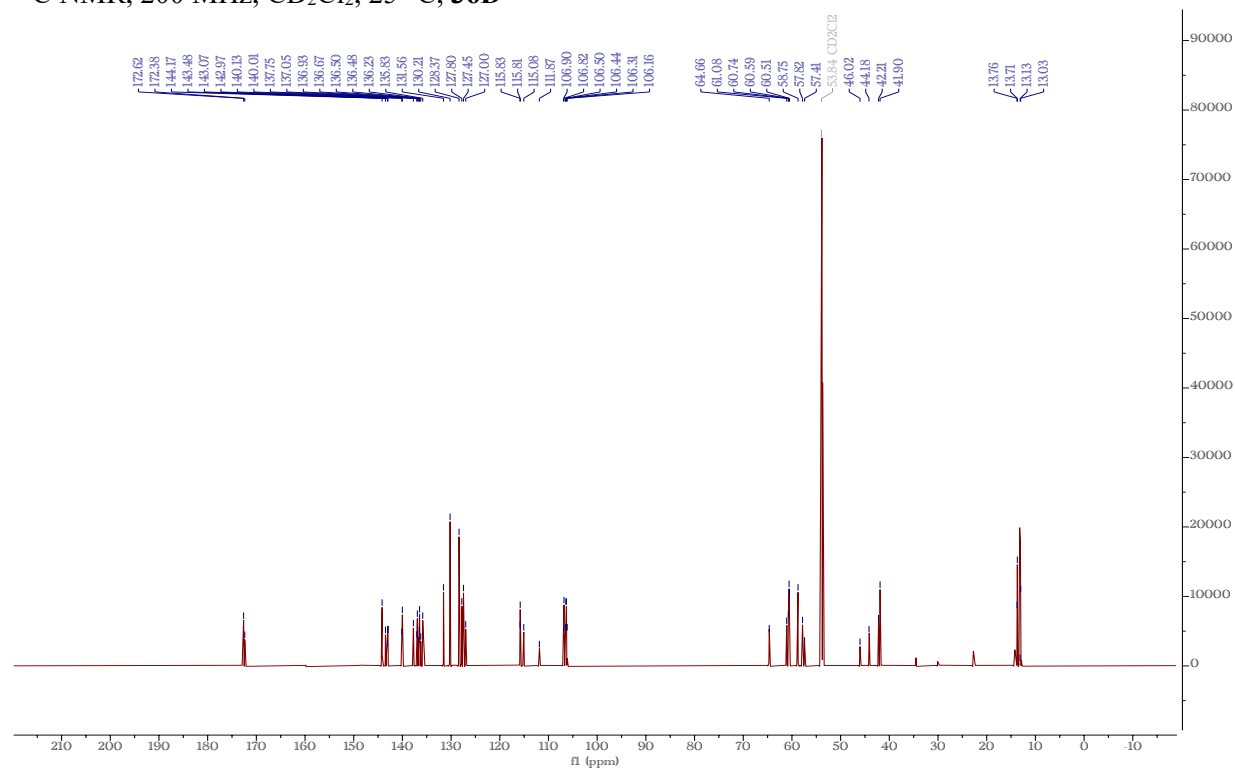
$^{13}\text{C}$  NMR, 200 MHz,  $\text{CD}_2\text{Cl}_2$ , 25 °C, *erythro*-35D



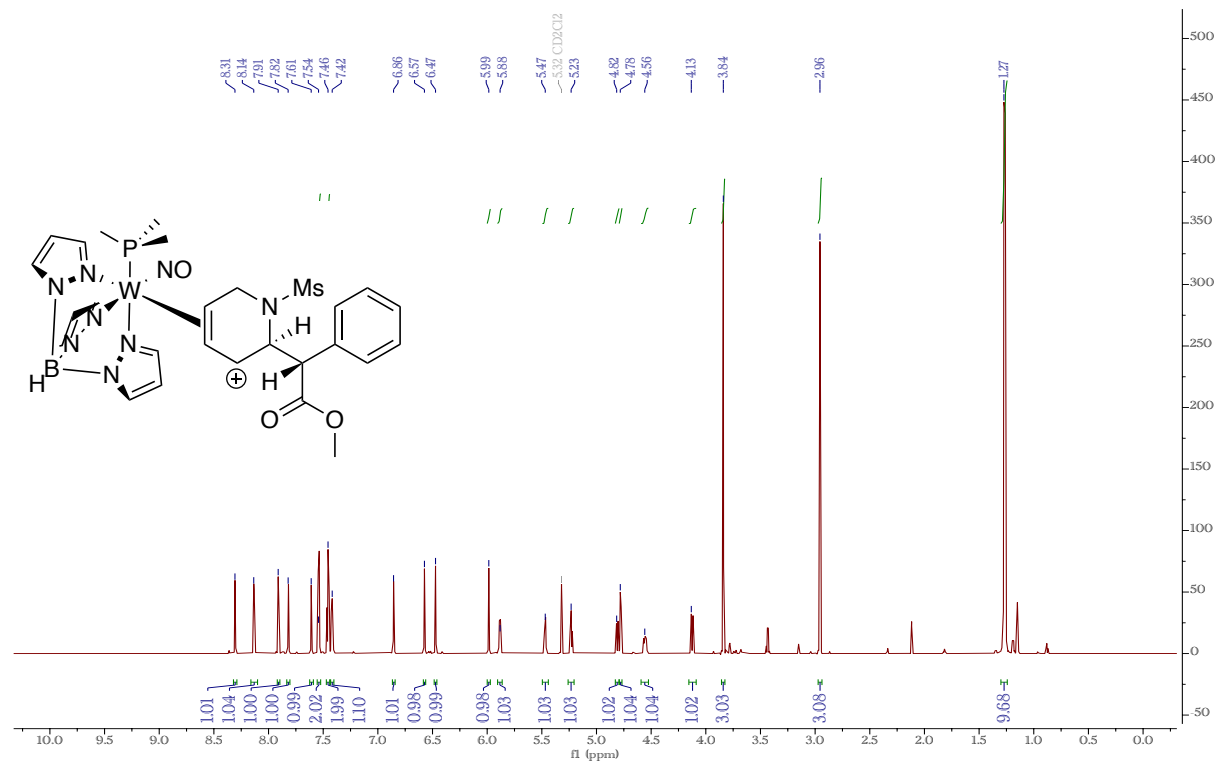
<sup>1</sup>H NMR, 800 MHz, CD<sub>2</sub>Cl<sub>2</sub>, 25 °C, **36D**



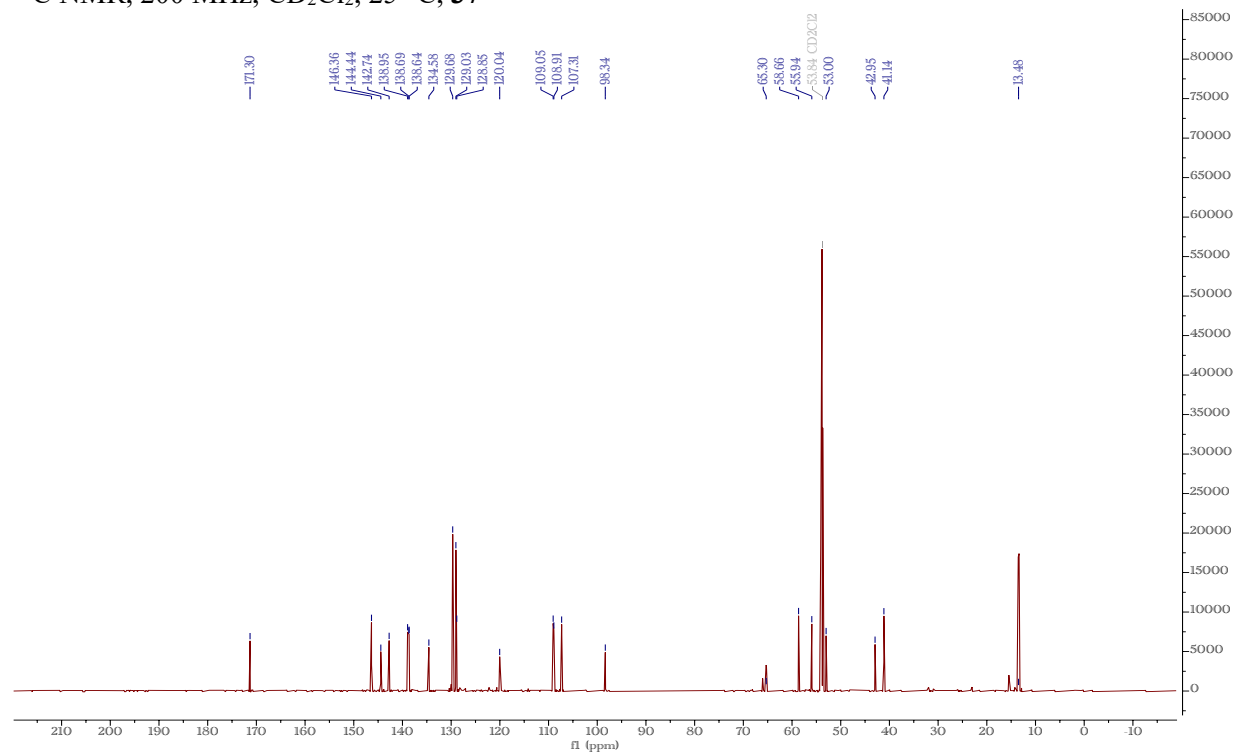
<sup>13</sup>C NMR, 200 MHz, CD<sub>2</sub>Cl<sub>2</sub>, 25 °C, **36D**



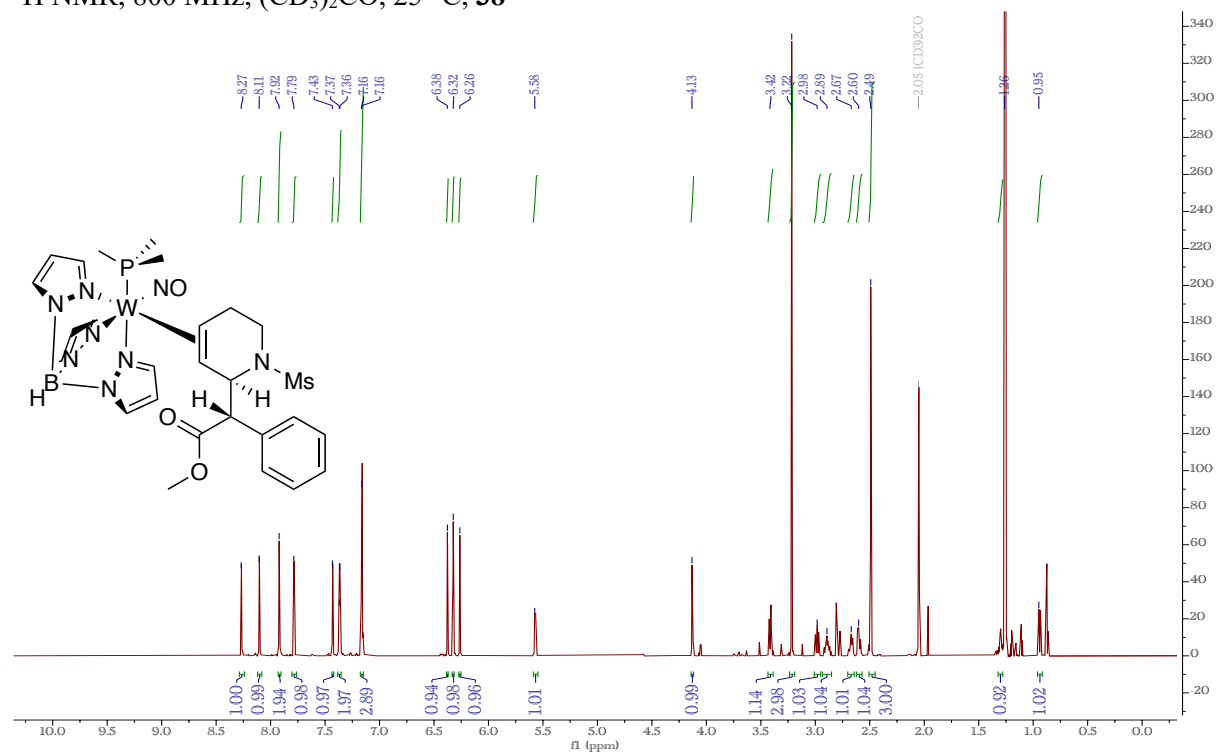
$^1\text{H}$  NMR, 800 MHz,  $\text{CD}_2\text{Cl}_2$ , 25 °C, **37**



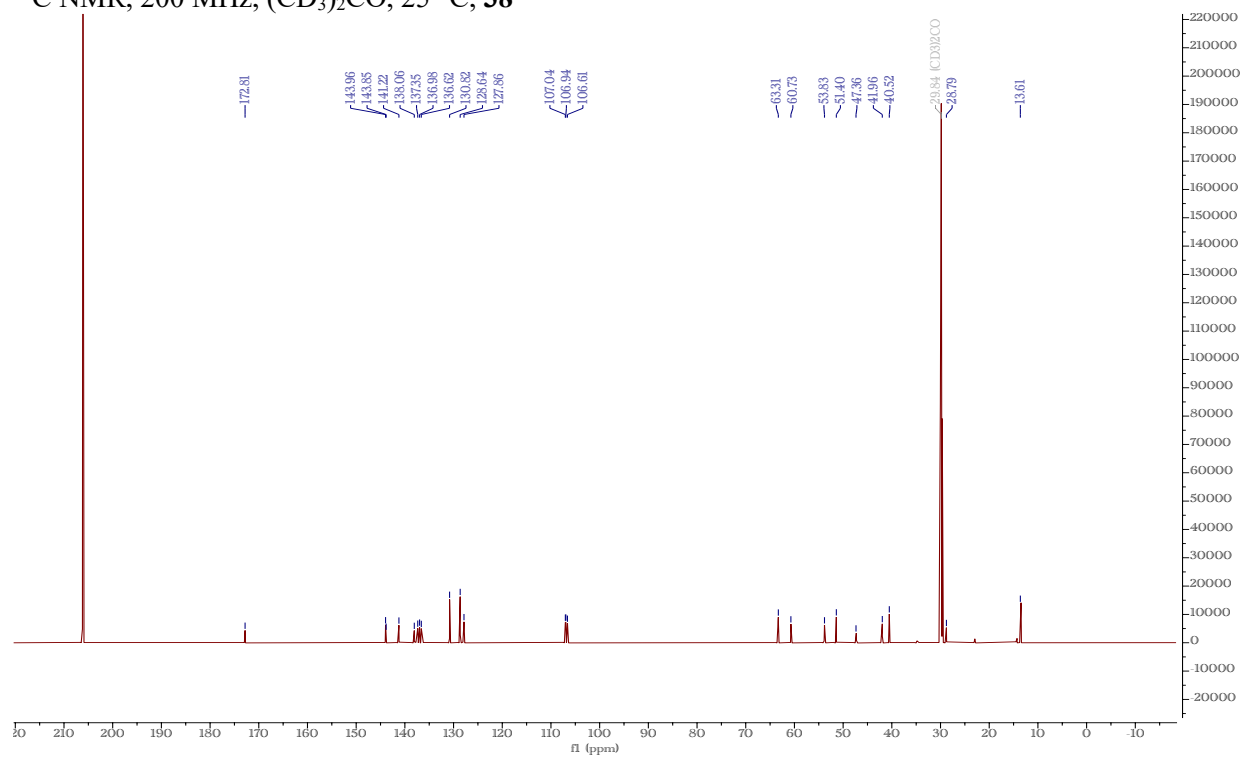
$^{13}\text{C}$  NMR, 200 MHz,  $\text{CD}_2\text{Cl}_2$ , 25 °C, **37**



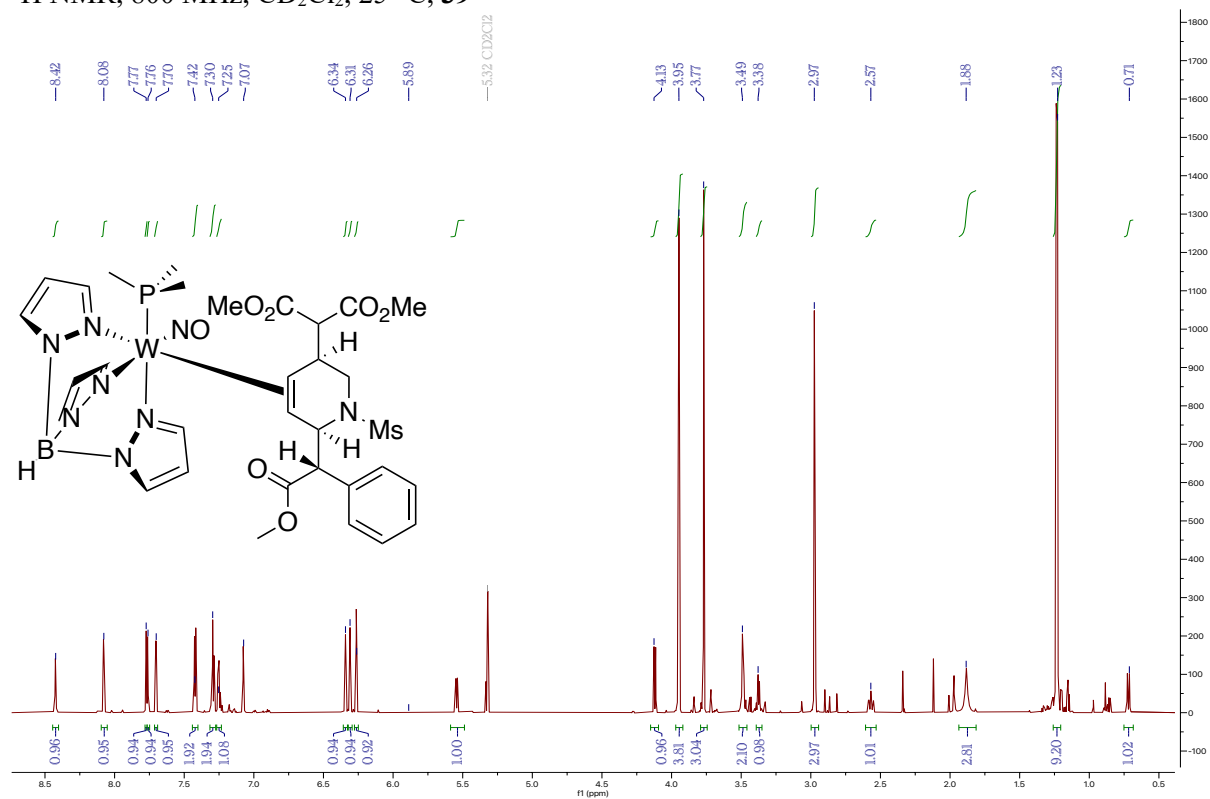
$^1\text{H}$  NMR, 800 MHz,  $(\text{CD}_3)_2\text{CO}$ , 25 °C, **38**



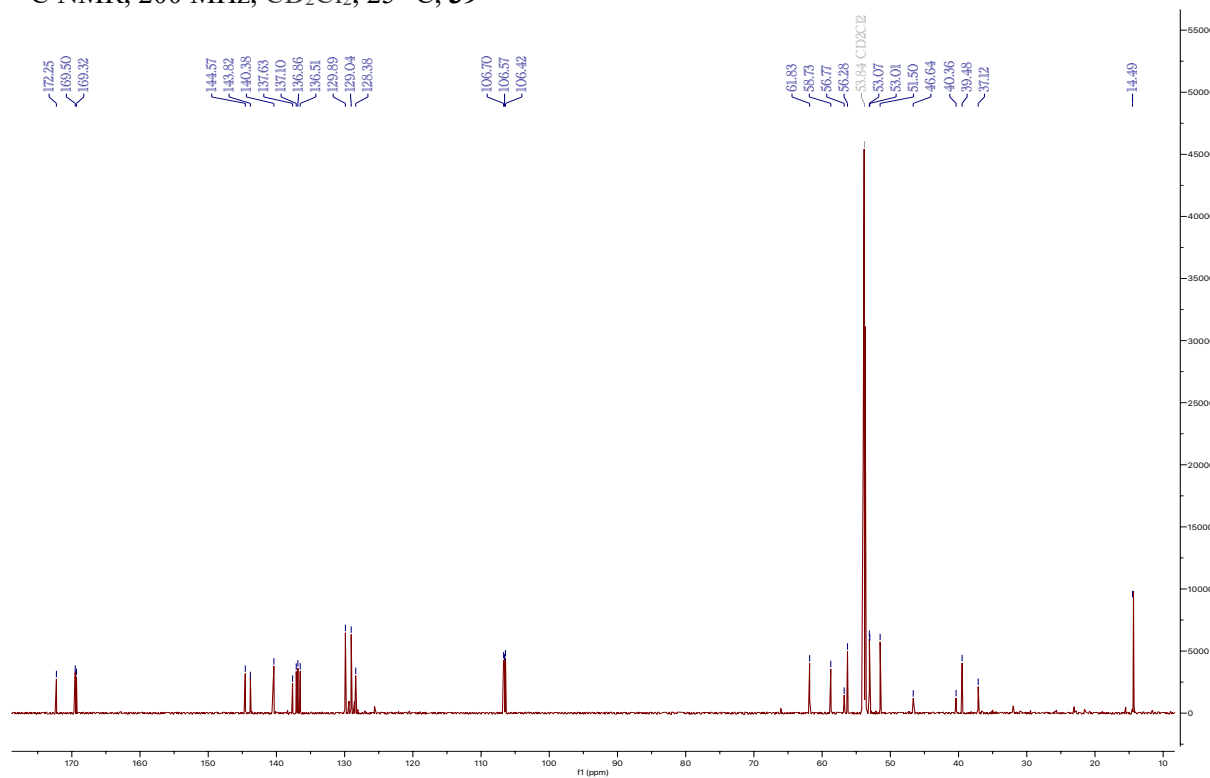
$^{13}\text{C}$  NMR, 200 MHz,  $(\text{CD}_3)_2\text{CO}$ , 25 °C, **38**



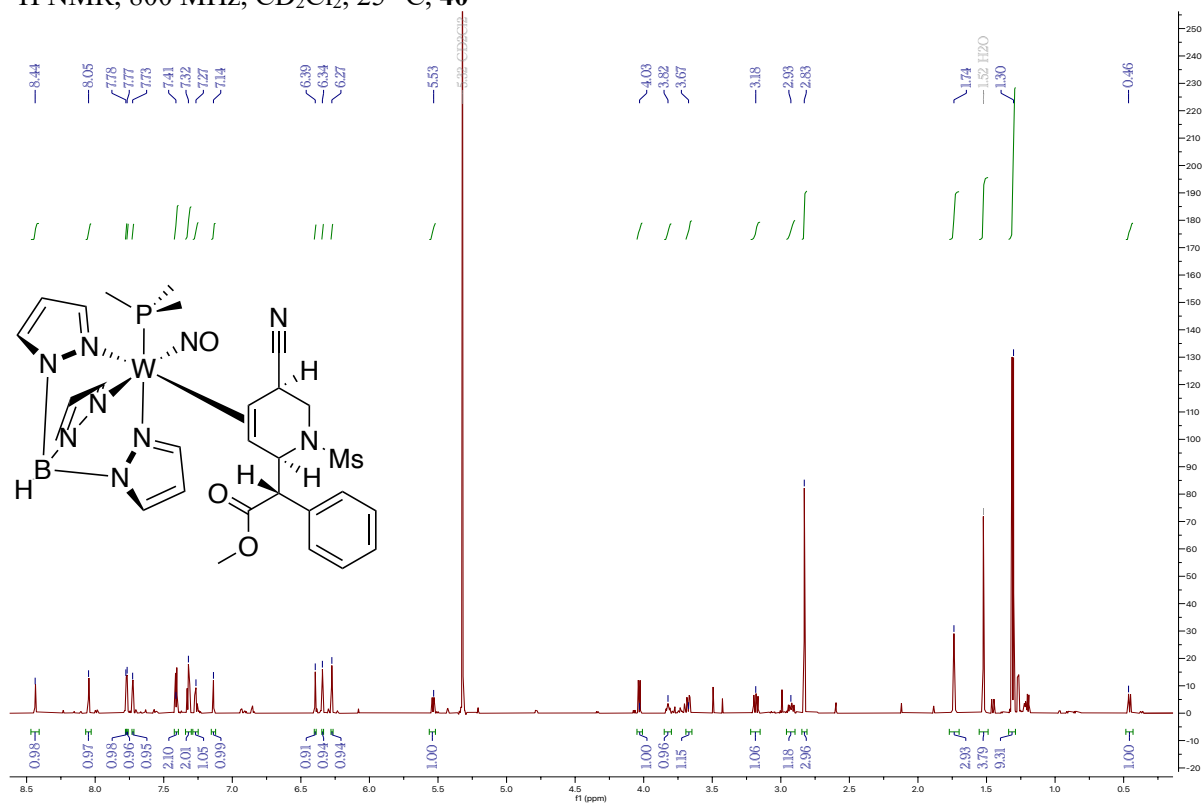
$^1\text{H}$  NMR, 800 MHz,  $\text{CD}_2\text{Cl}_2$ , 25  $^\circ\text{C}$ , **39**



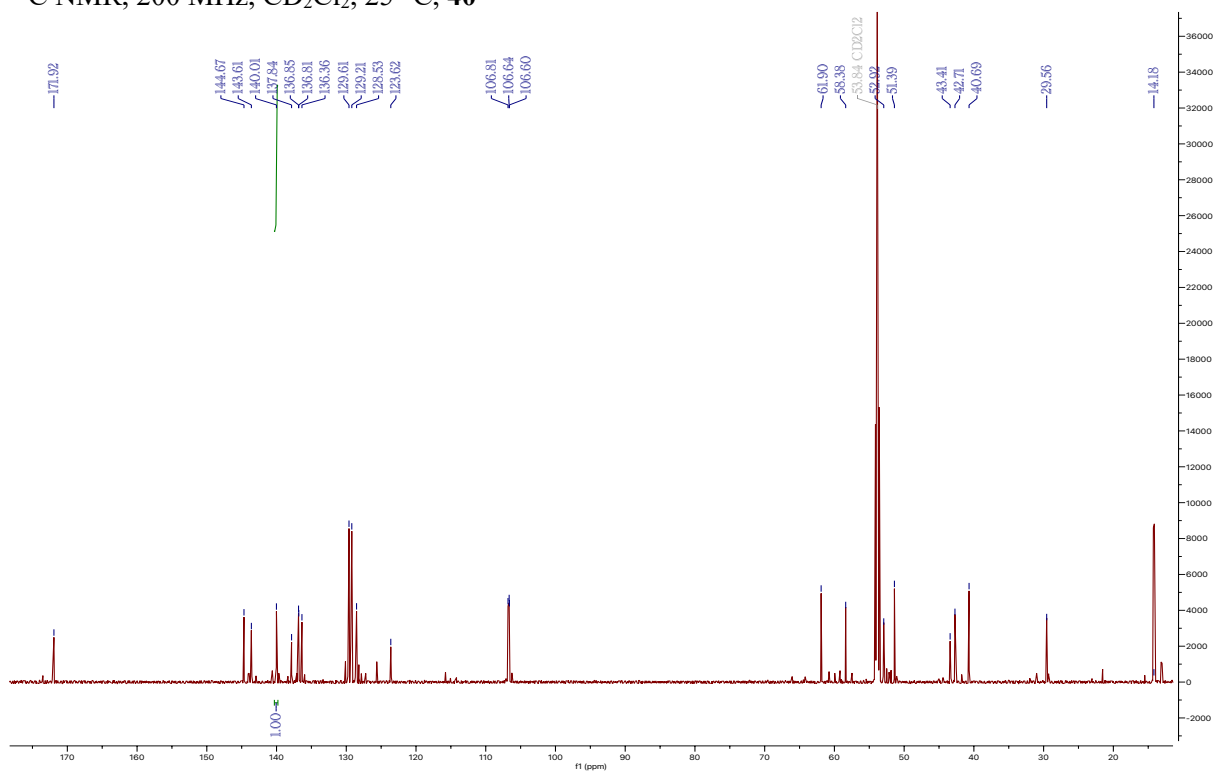
$^{13}\text{C}$  NMR, 200 MHz,  $\text{CD}_2\text{Cl}_2$ , 25  $^\circ\text{C}$ , **39**



$^1\text{H}$  NMR, 800 MHz,  $\text{CD}_2\text{Cl}_2$ , 25 °C, 40

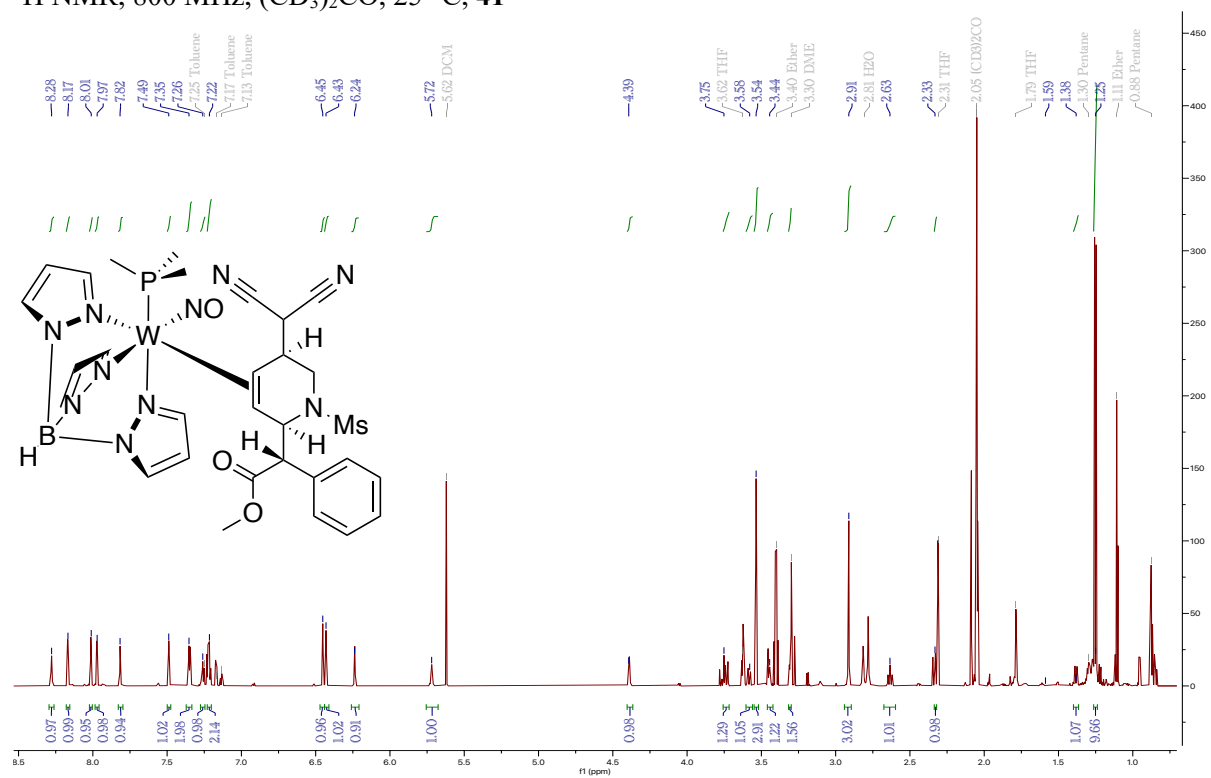


$^{13}\text{C}$  NMR, 200 MHz,  $\text{CD}_2\text{Cl}_2$ , 25 °C, 40

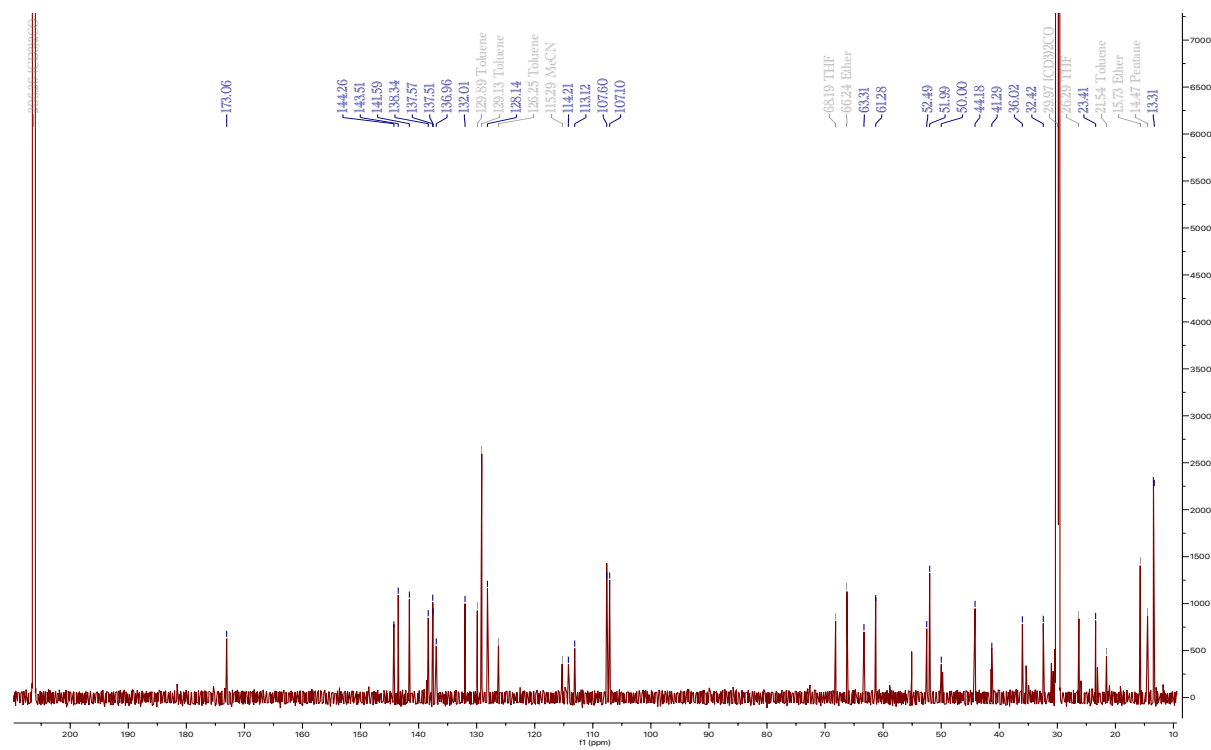




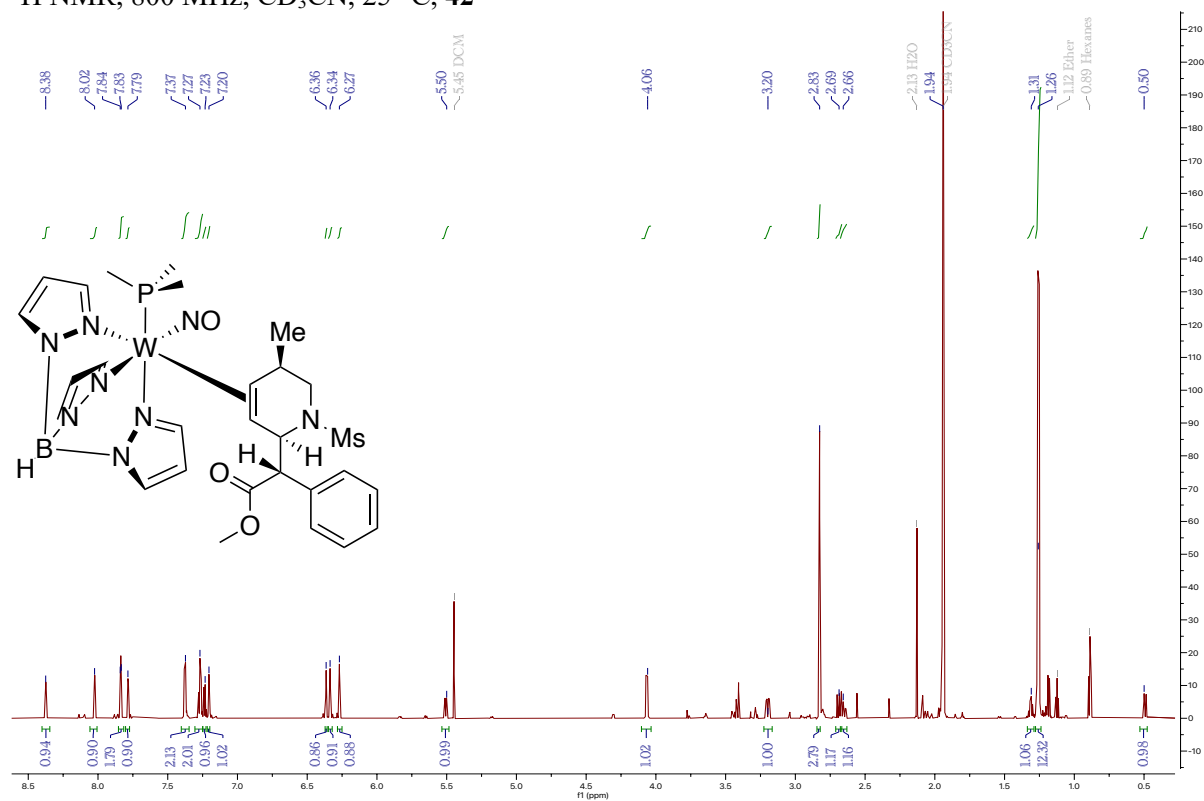
$^1\text{H}$  NMR, 800 MHz,  $(\text{CD}_3)_2\text{CO}$ , 25 °C, **41**



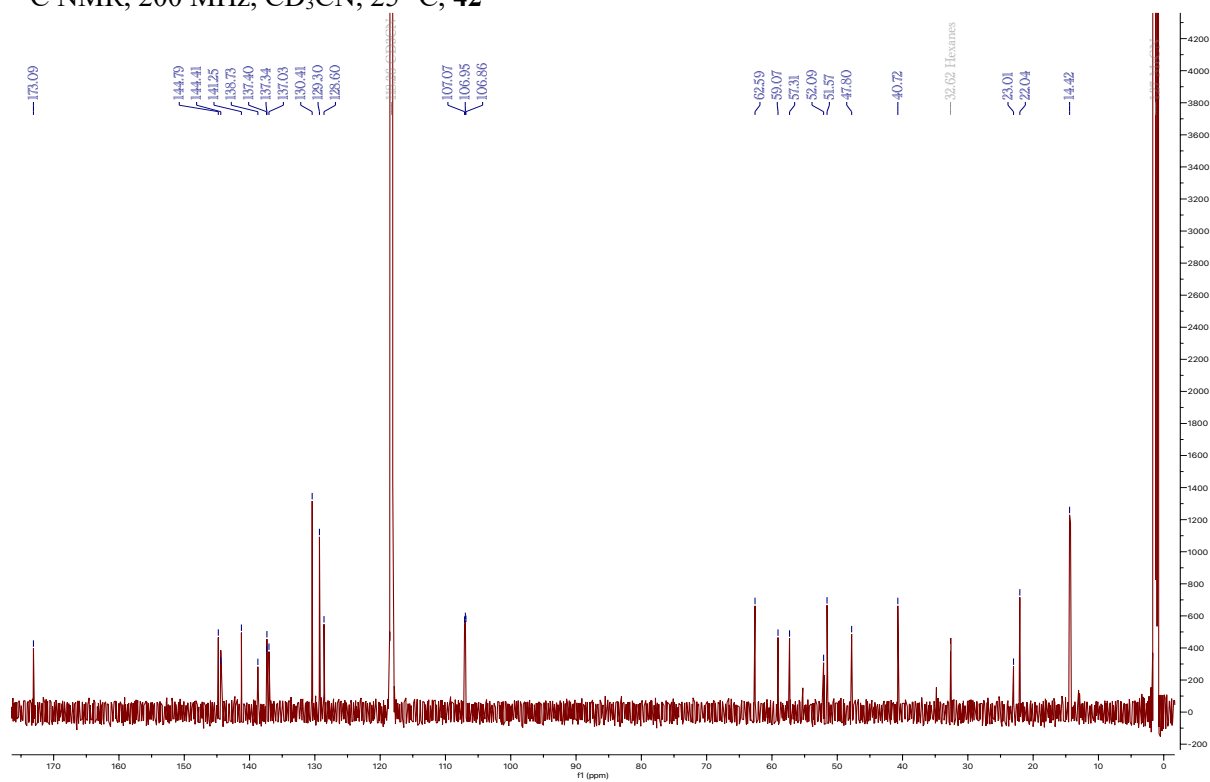
$^{13}\text{C}$  NMR, 200 MHz,  $(\text{CD}_3)_2\text{CO}$ , 25 °C, **41**



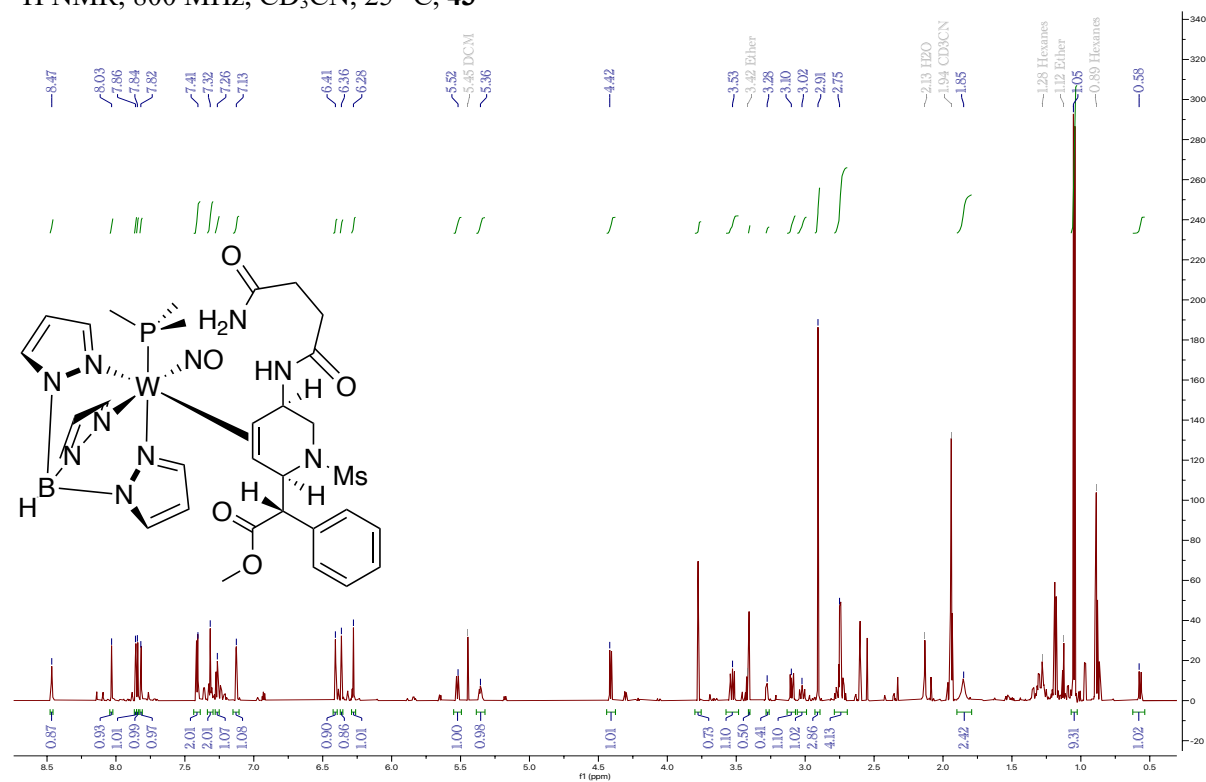
$^1\text{H}$  NMR, 800 MHz,  $\text{CD}_3\text{CN}$ , 25 °C, **42**



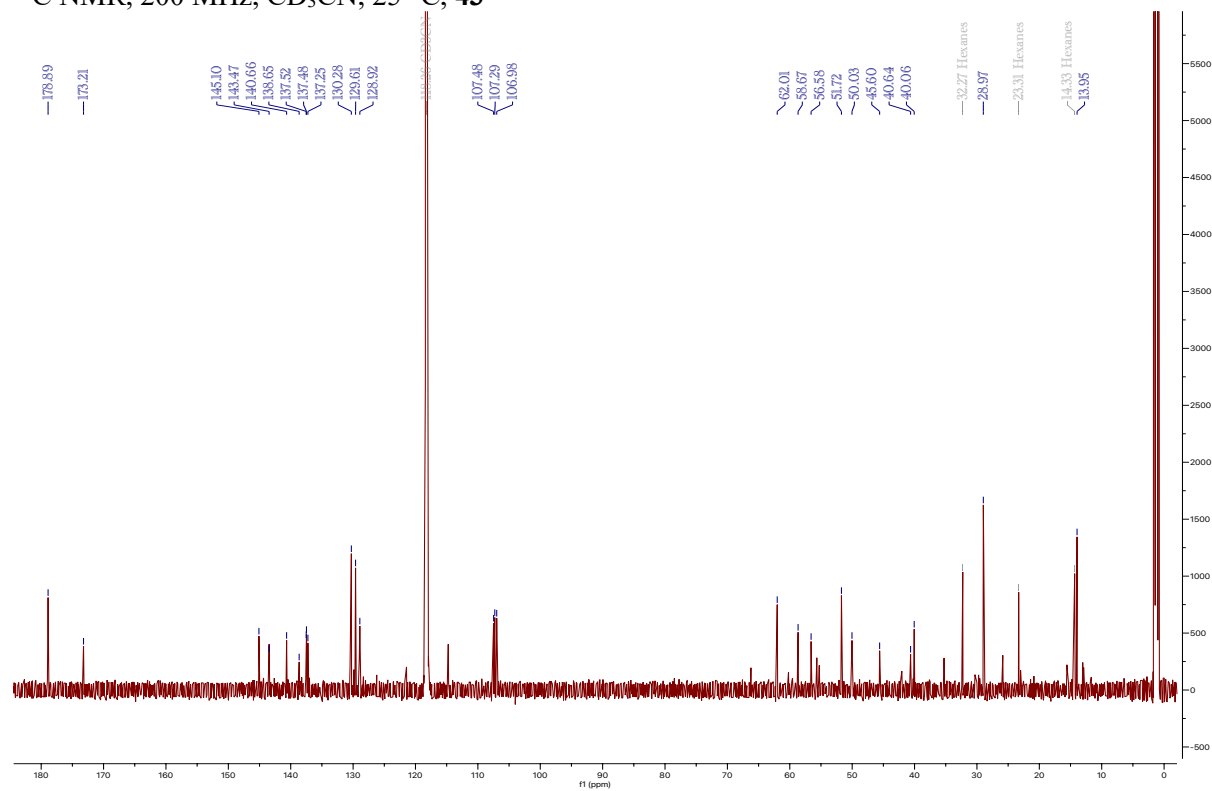
$^{13}\text{C}$  NMR, 200 MHz,  $\text{CD}_3\text{CN}$ , 25 °C, **42**



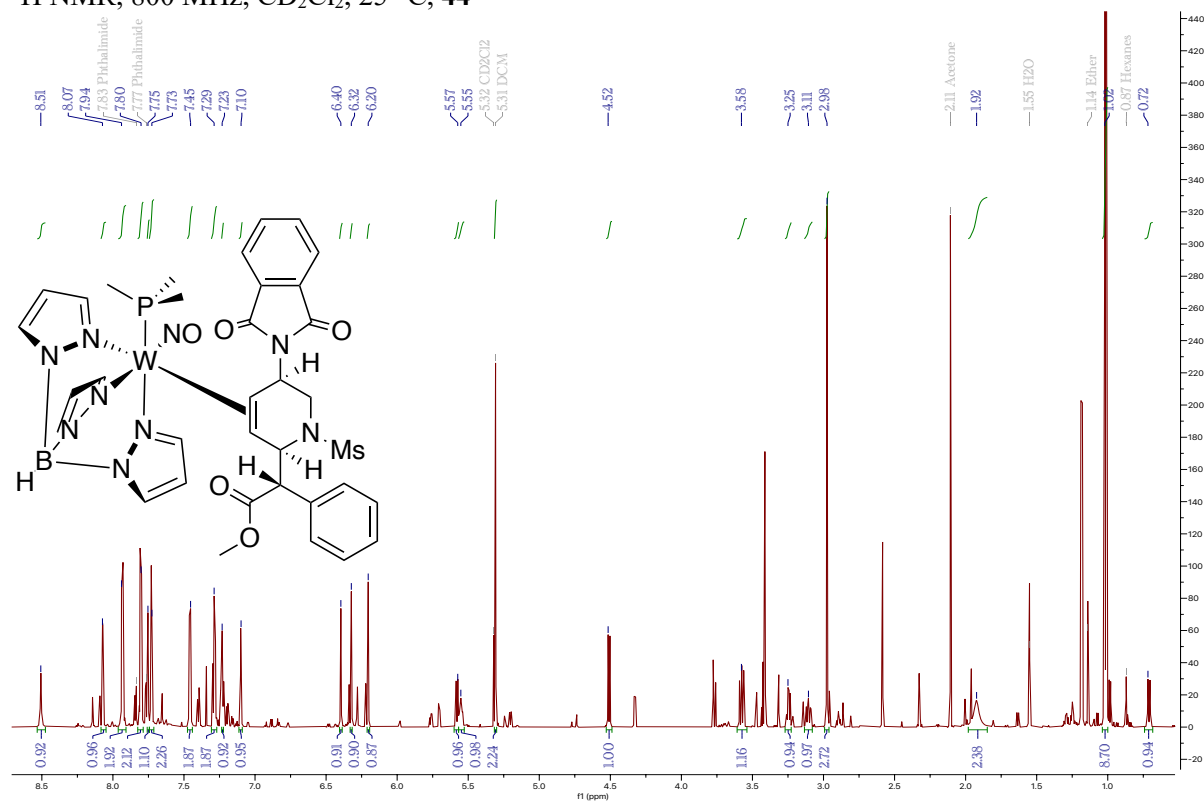
<sup>1</sup>H NMR, 800 MHz, CD<sub>3</sub>CN, 25 °C, **43**



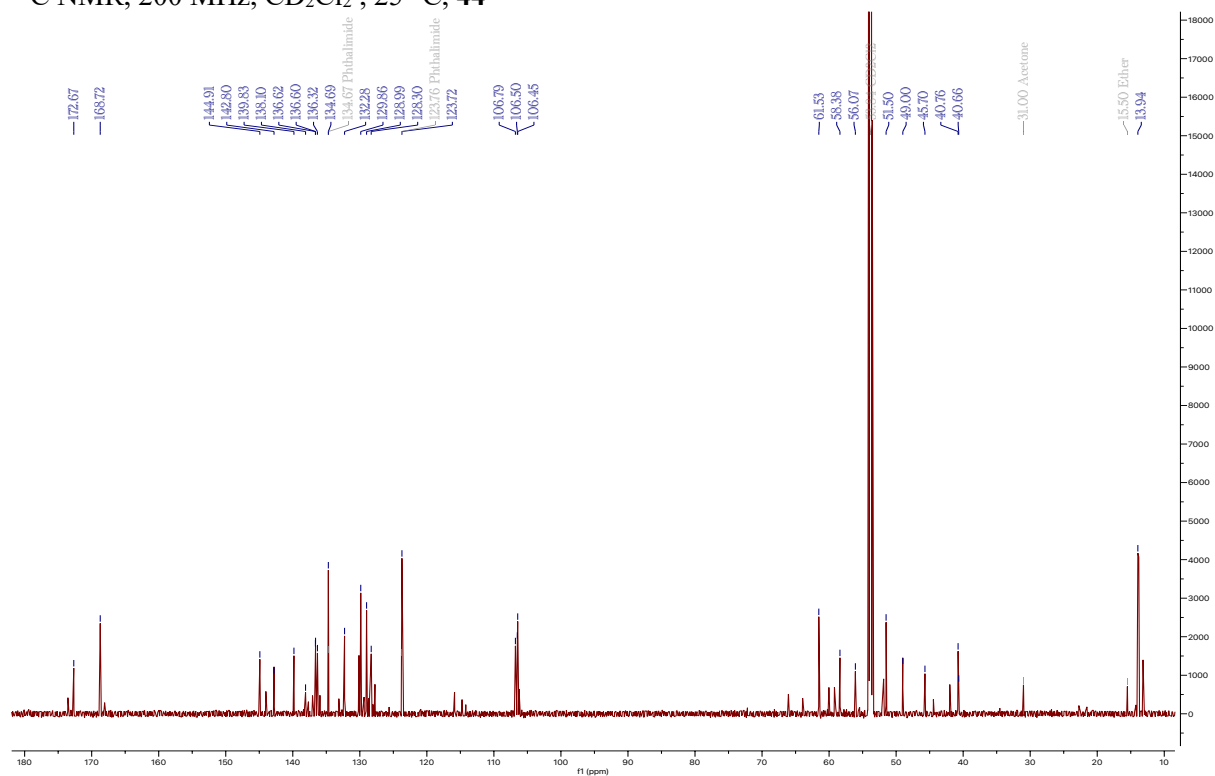
<sup>13</sup>C NMR, 200 MHz, CD<sub>3</sub>CN, 25 °C, **43**



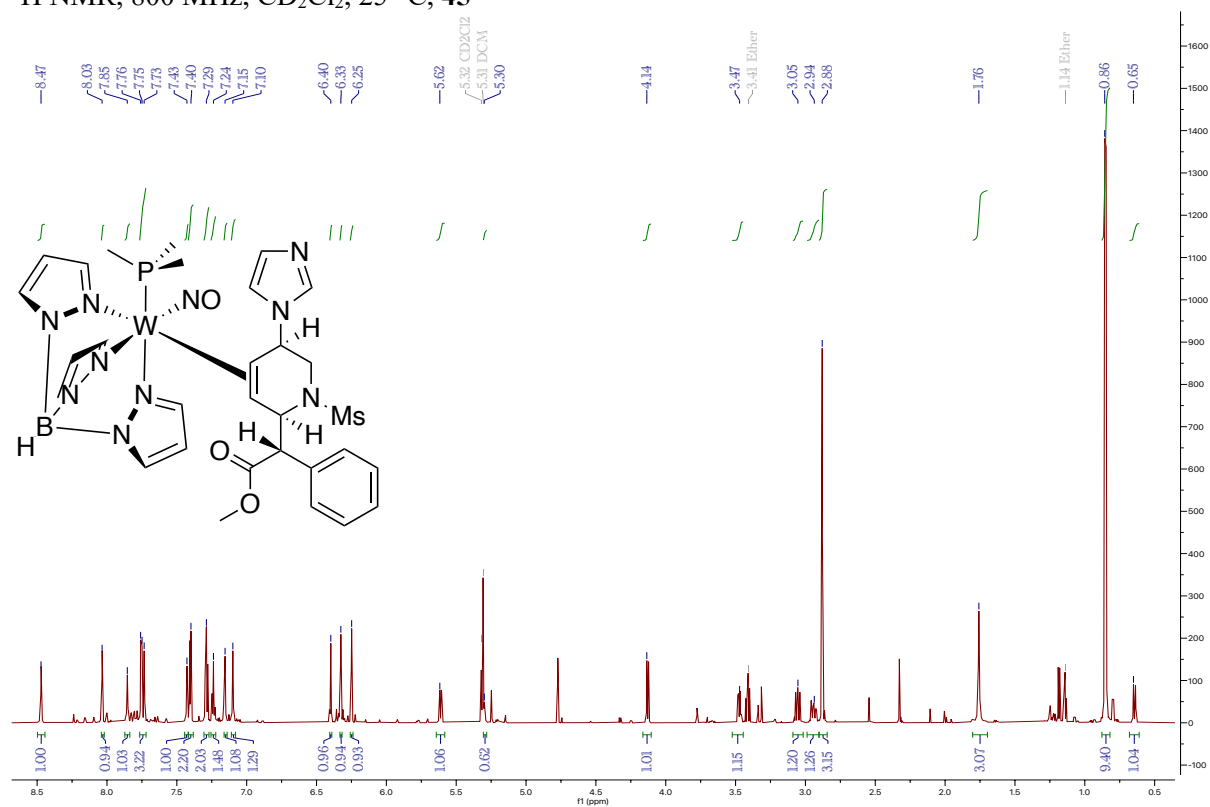
$^1\text{H}$  NMR, 800 MHz,  $\text{CD}_2\text{Cl}_2$ , 25 °C, 44



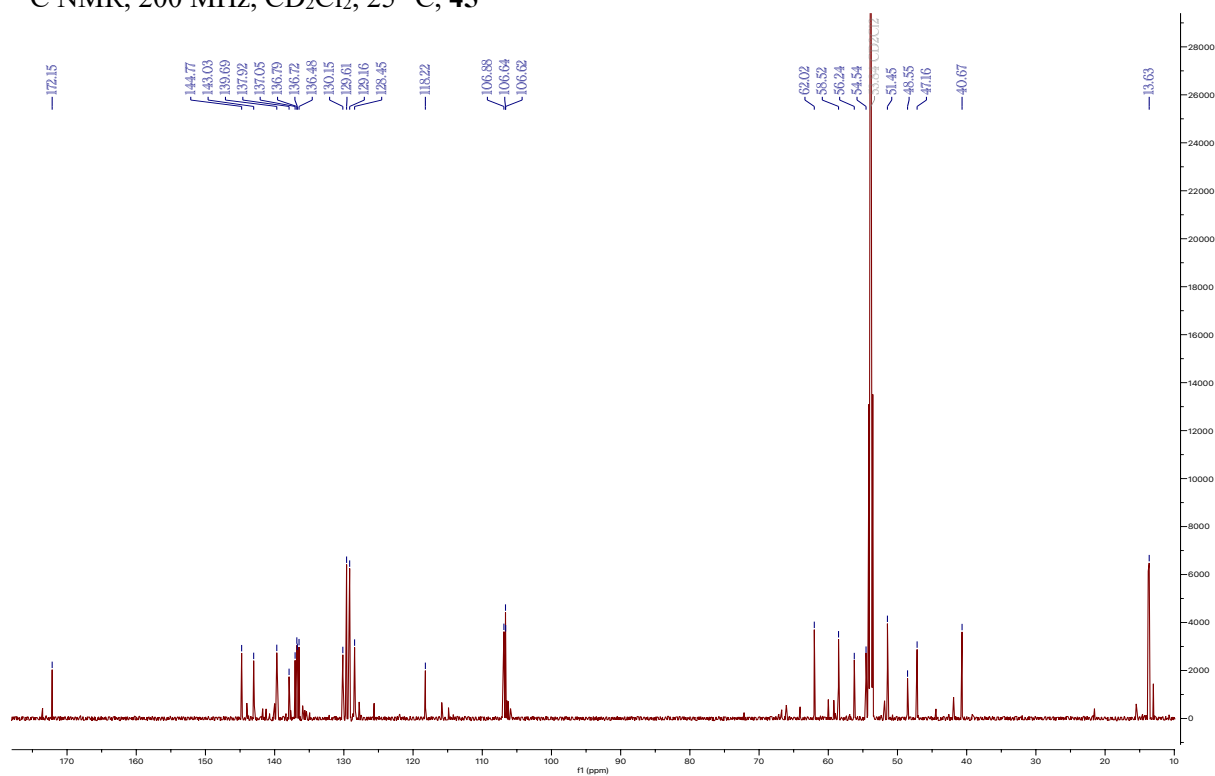
$^{13}\text{C}$  NMR, 200 MHz,  $\text{CD}_2\text{Cl}_2$ , 25 °C, 44



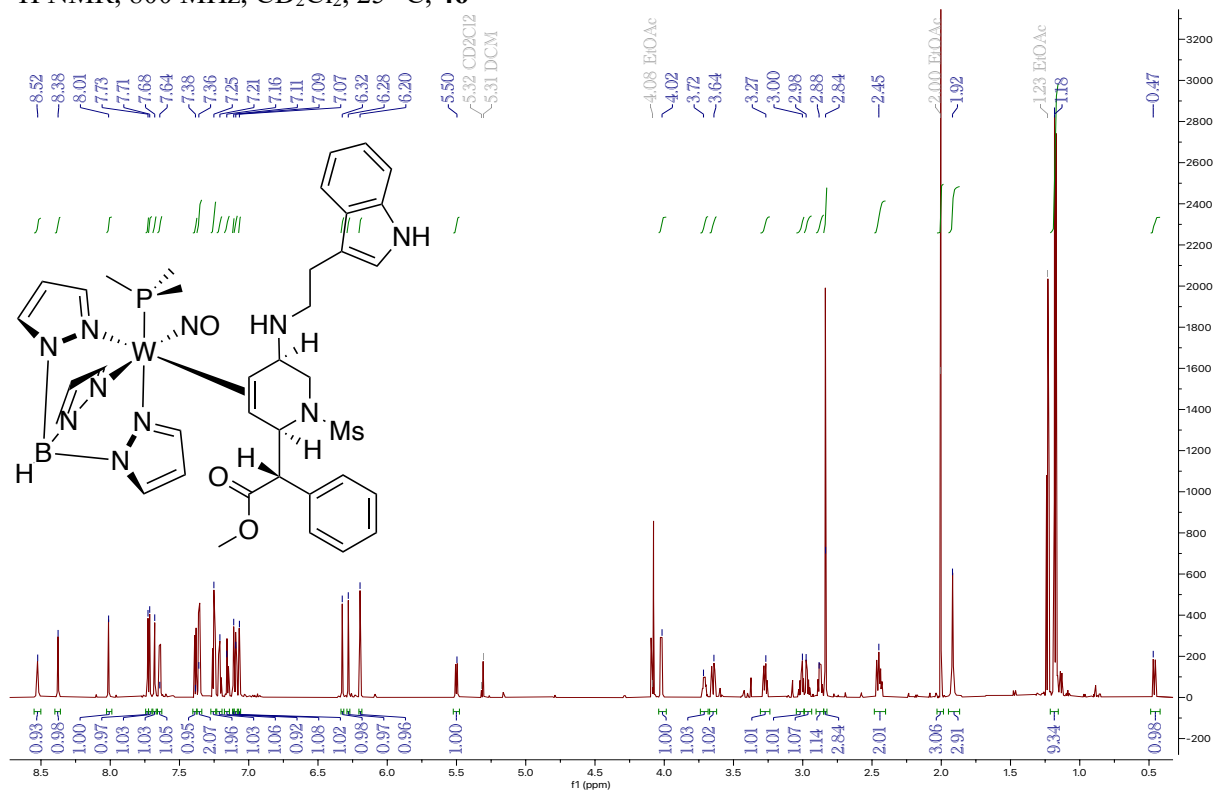
$^1\text{H}$  NMR, 800 MHz,  $\text{CD}_2\text{Cl}_2$ , 25 °C, 45



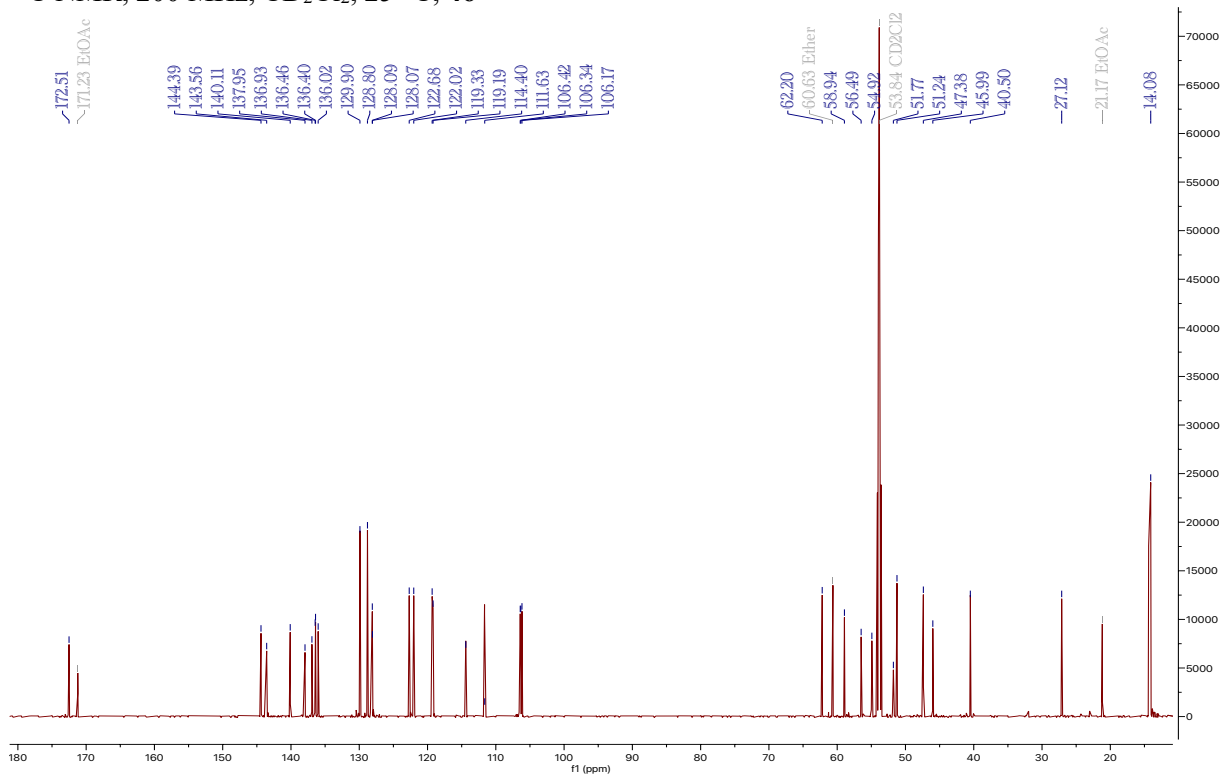
$^{13}\text{C}$  NMR, 200 MHz,  $\text{CD}_2\text{Cl}_2$ , 25 °C, 45



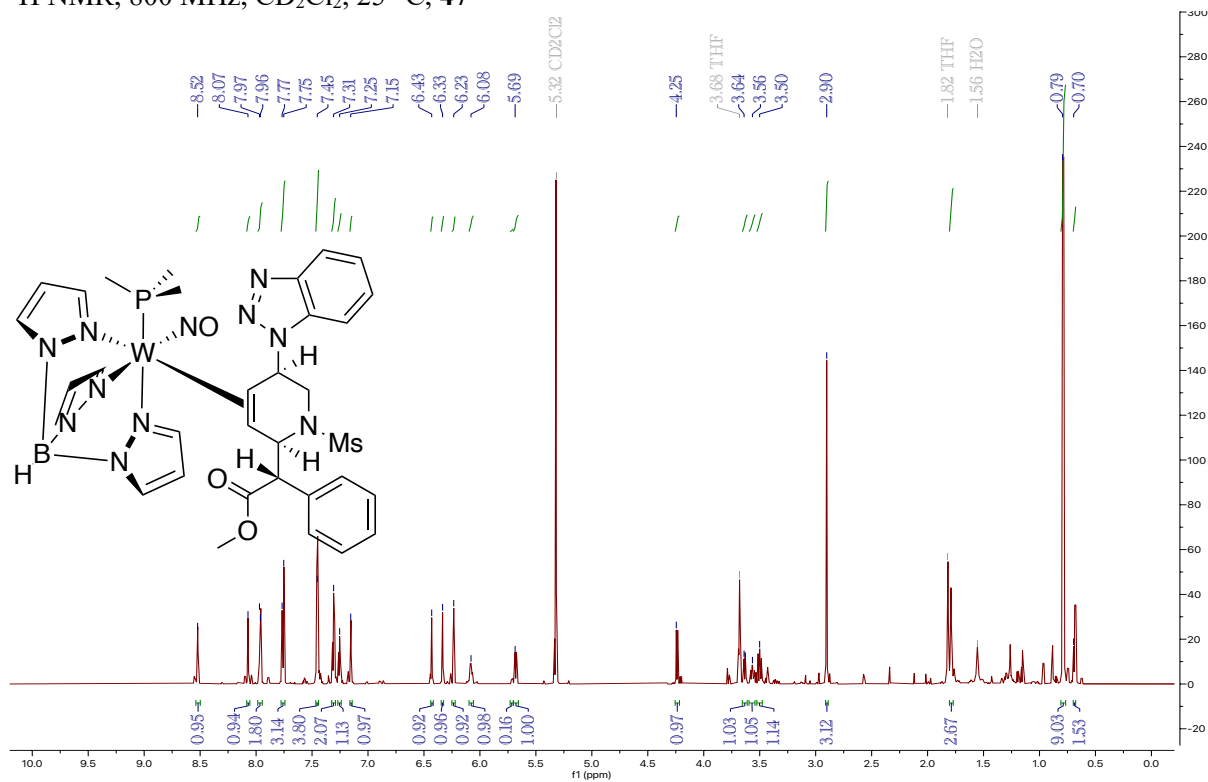
$^1\text{H}$  NMR, 800 MHz,  $\text{CD}_2\text{Cl}_2$ , 25 °C, **46**



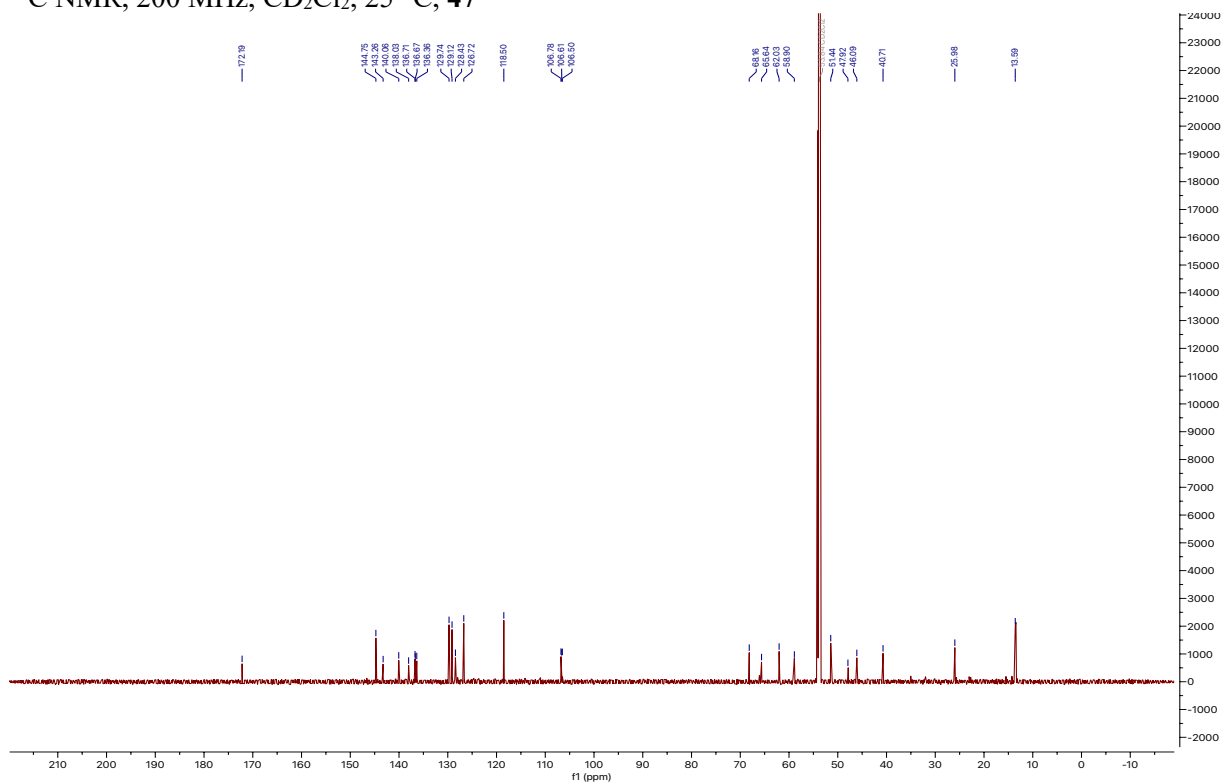
$^{13}\text{C}$  NMR, 200 MHz,  $\text{CD}_2\text{Cl}_2$ , 25 °C, **46**



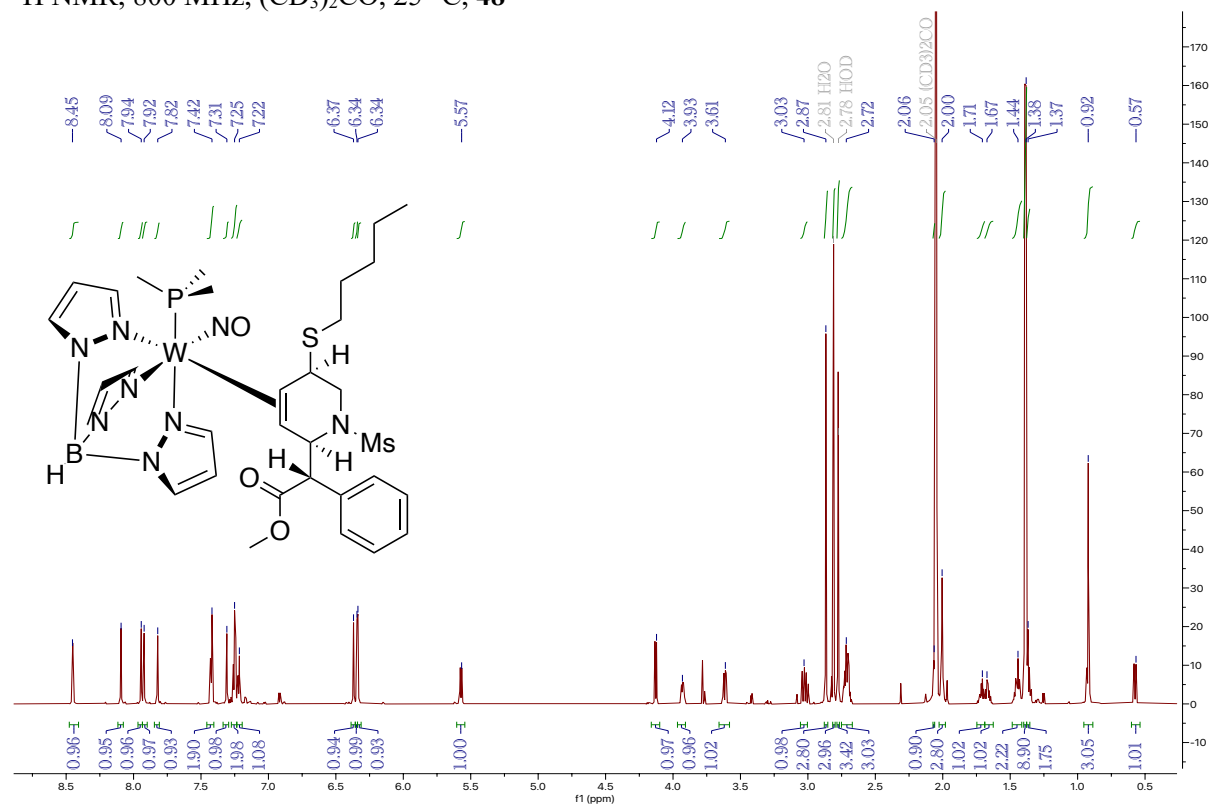
$^1\text{H}$  NMR, 800 MHz,  $\text{CD}_2\text{Cl}_2$ , 25 °C, **47**



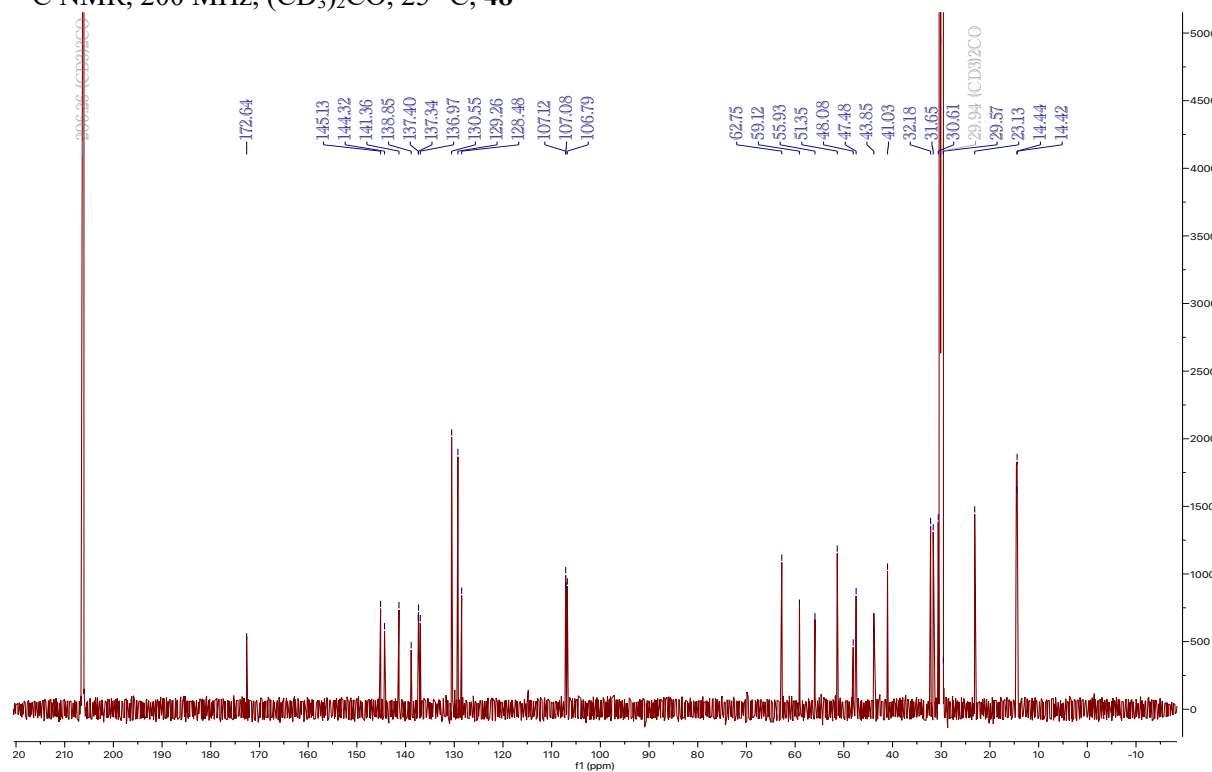
$^{13}\text{C}$  NMR, 200 MHz,  $\text{CD}_2\text{Cl}_2$ , 25 °C, **47**



$^1\text{H}$  NMR, 800 MHz,  $(\text{CD}_3)_2\text{CO}$ , 25 °C, **48**

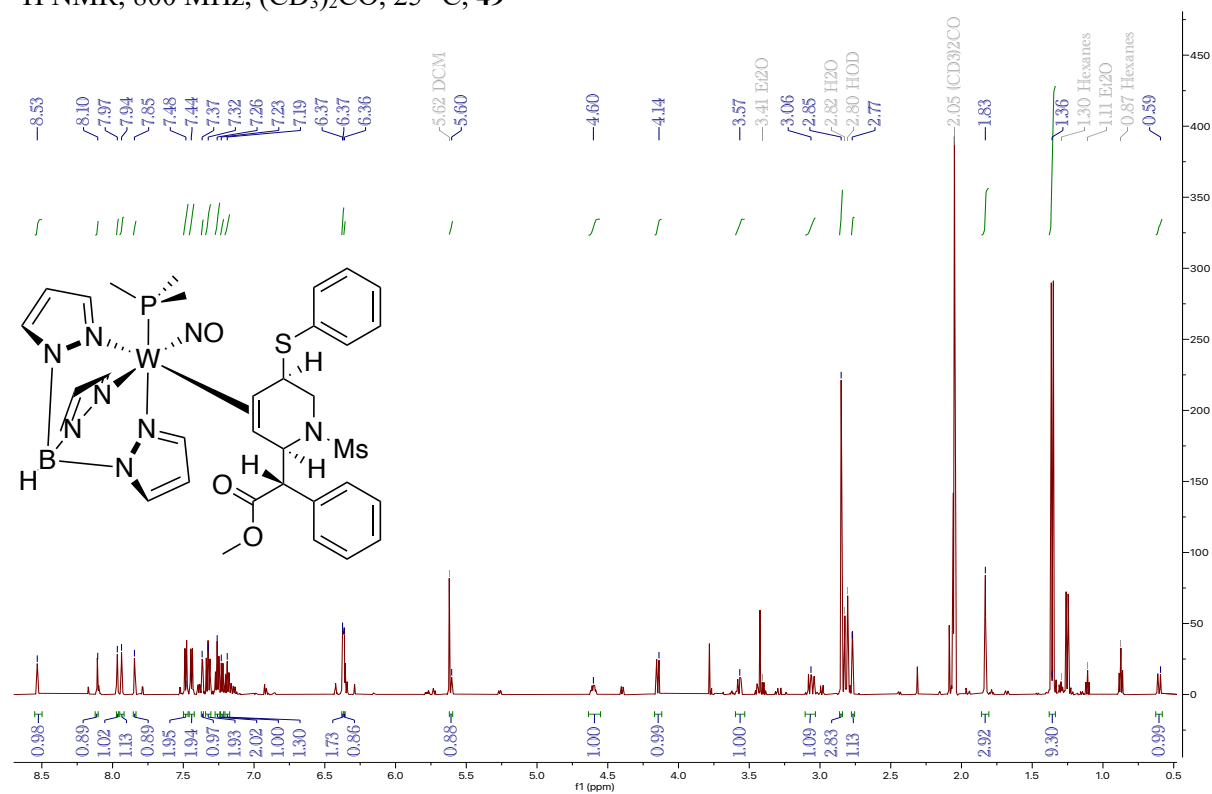


$^{13}\text{C}$  NMR, 200 MHz,  $(\text{CD}_3)_2\text{CO}$ , 25 °C, **48**

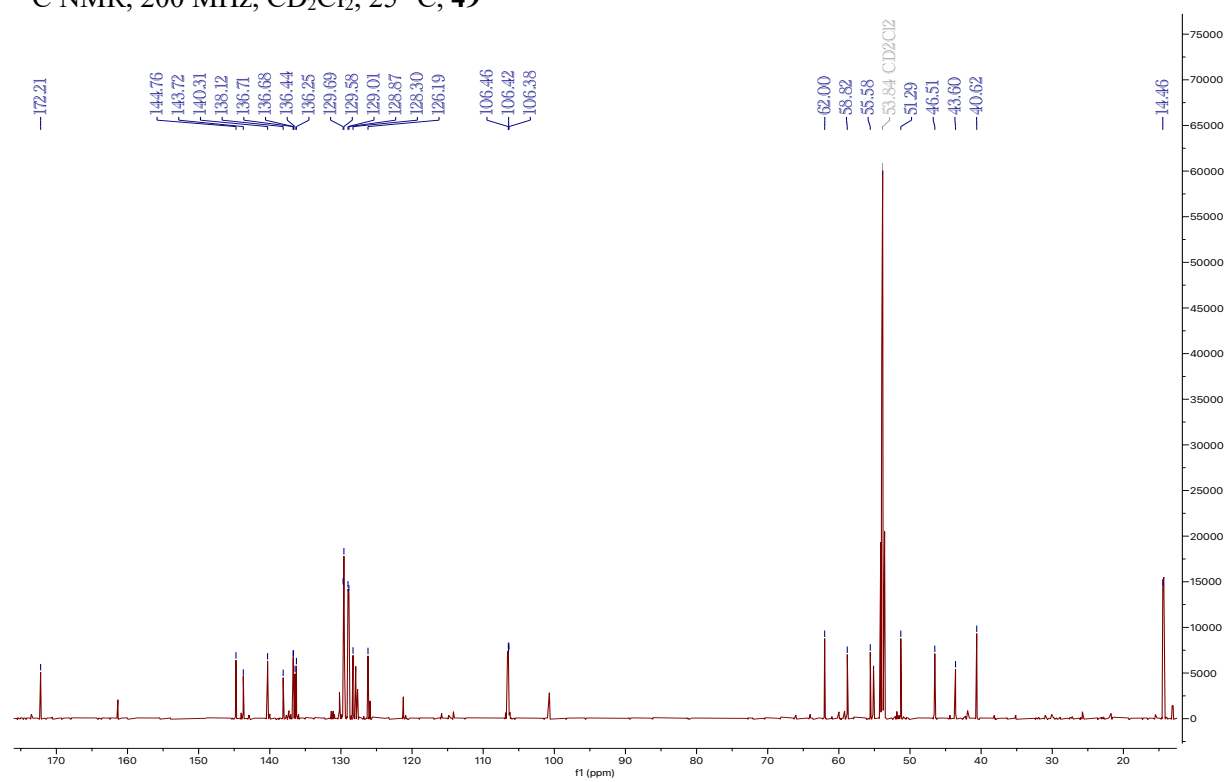




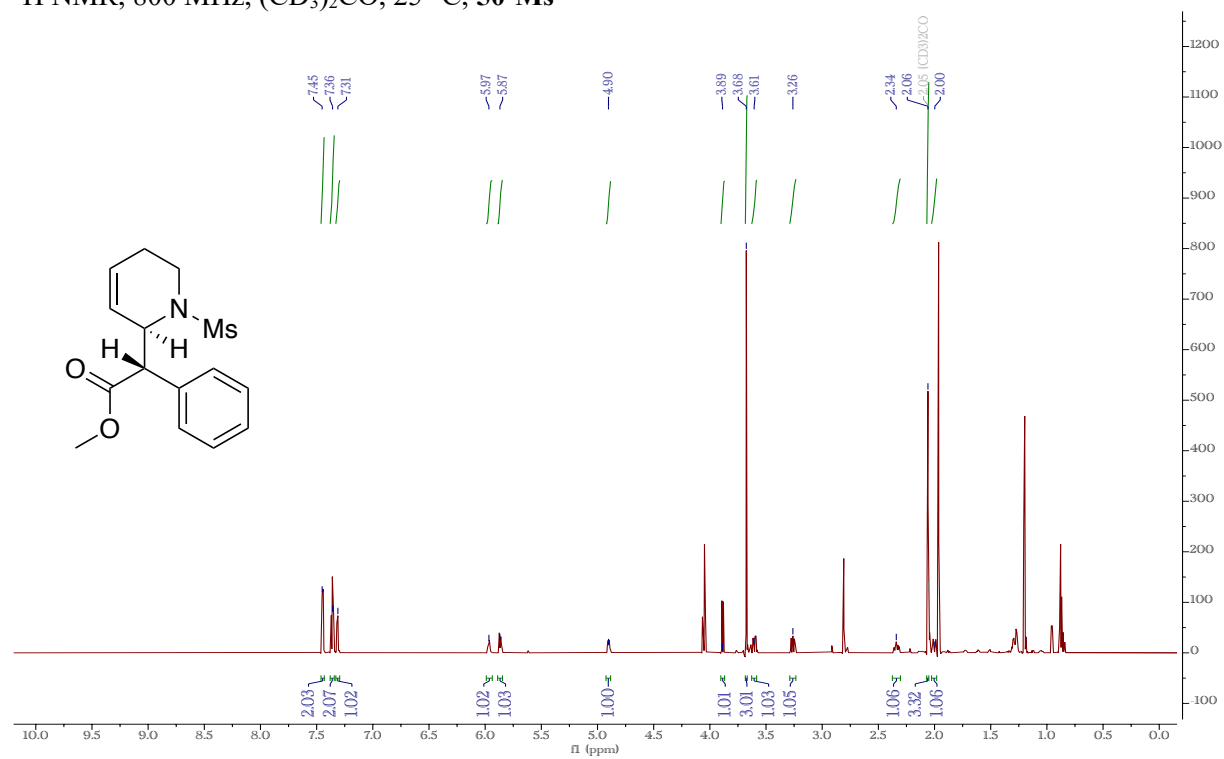
$^1\text{H}$  NMR, 800 MHz,  $(\text{CD}_3)_2\text{CO}$ , 25 °C, **49**



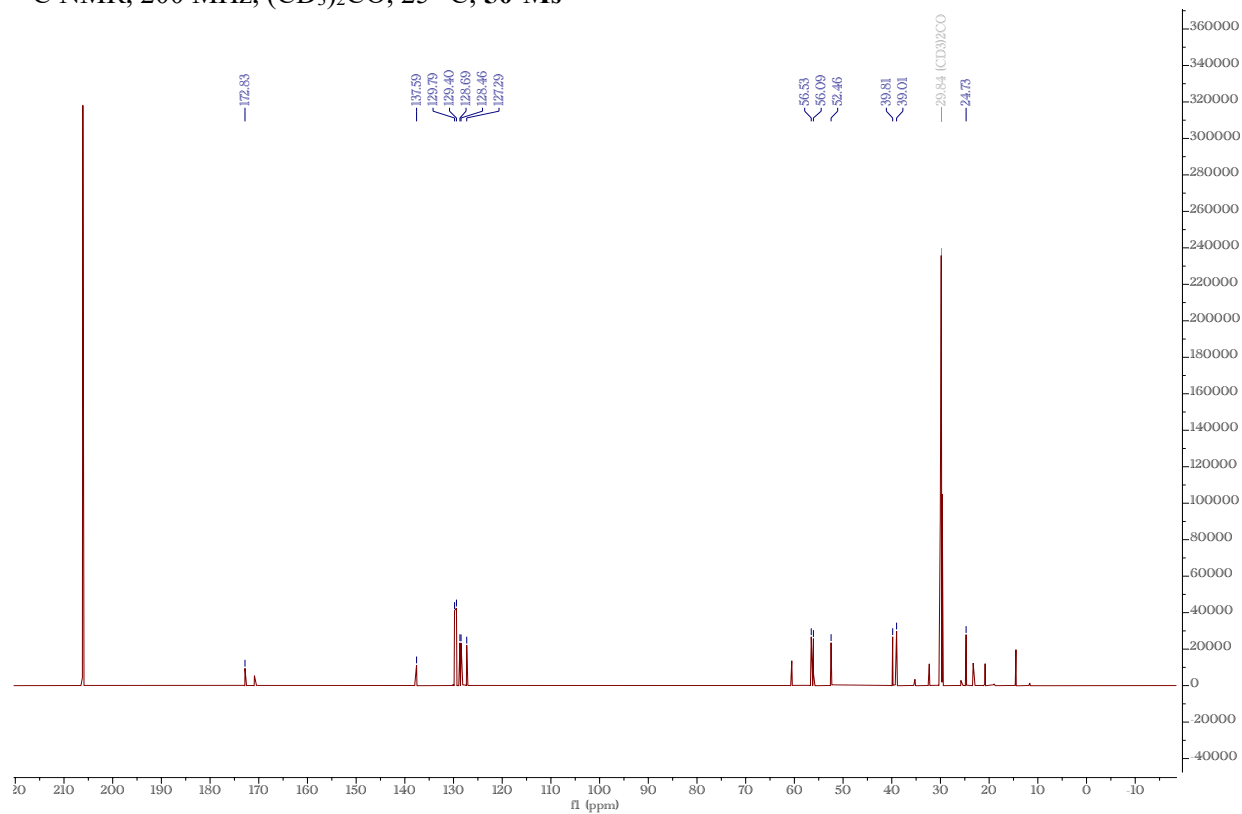
$^{13}\text{C}$  NMR, 200 MHz,  $\text{CD}_2\text{Cl}_2$ , 25 °C, **49**



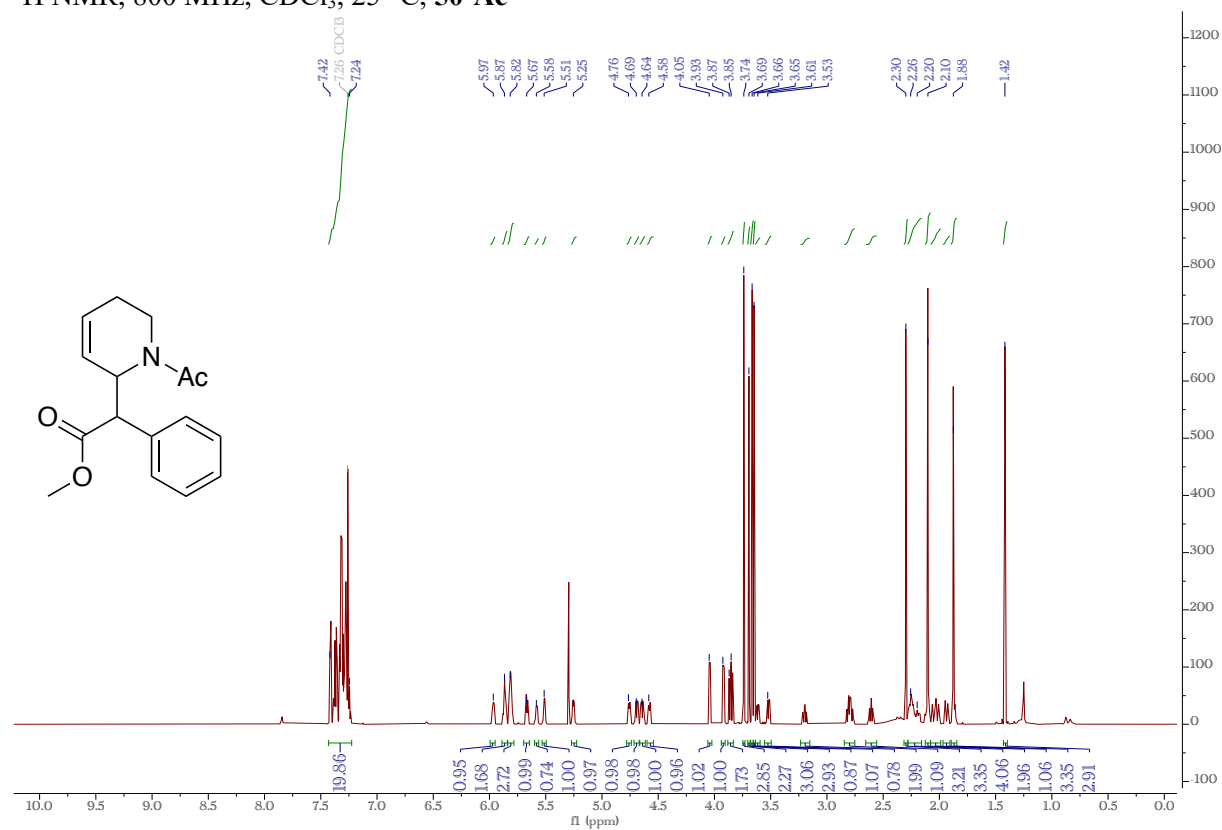
<sup>1</sup>H NMR, 800 MHz, (CD<sub>3</sub>)<sub>2</sub>CO, 25 °C, **50-Ms**



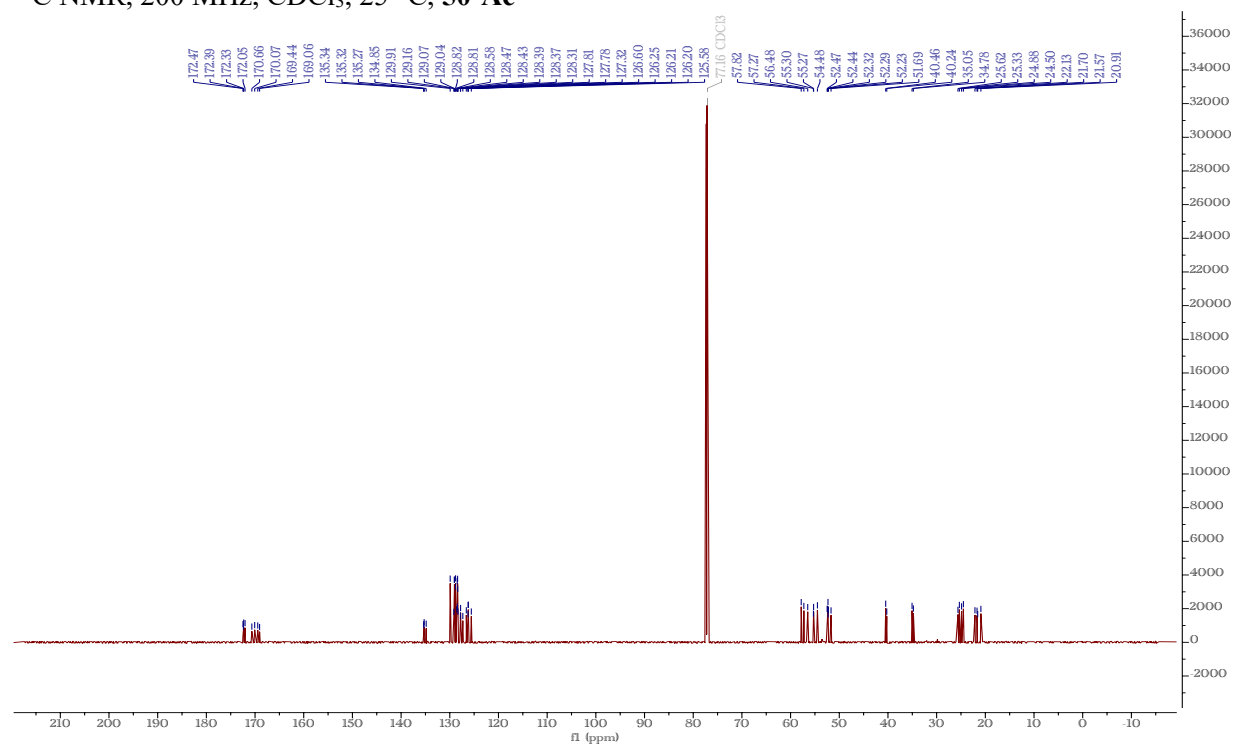
<sup>13</sup>C NMR, 200 MHz, (CD<sub>3</sub>)<sub>2</sub>CO, 25 °C, **50-Ms**



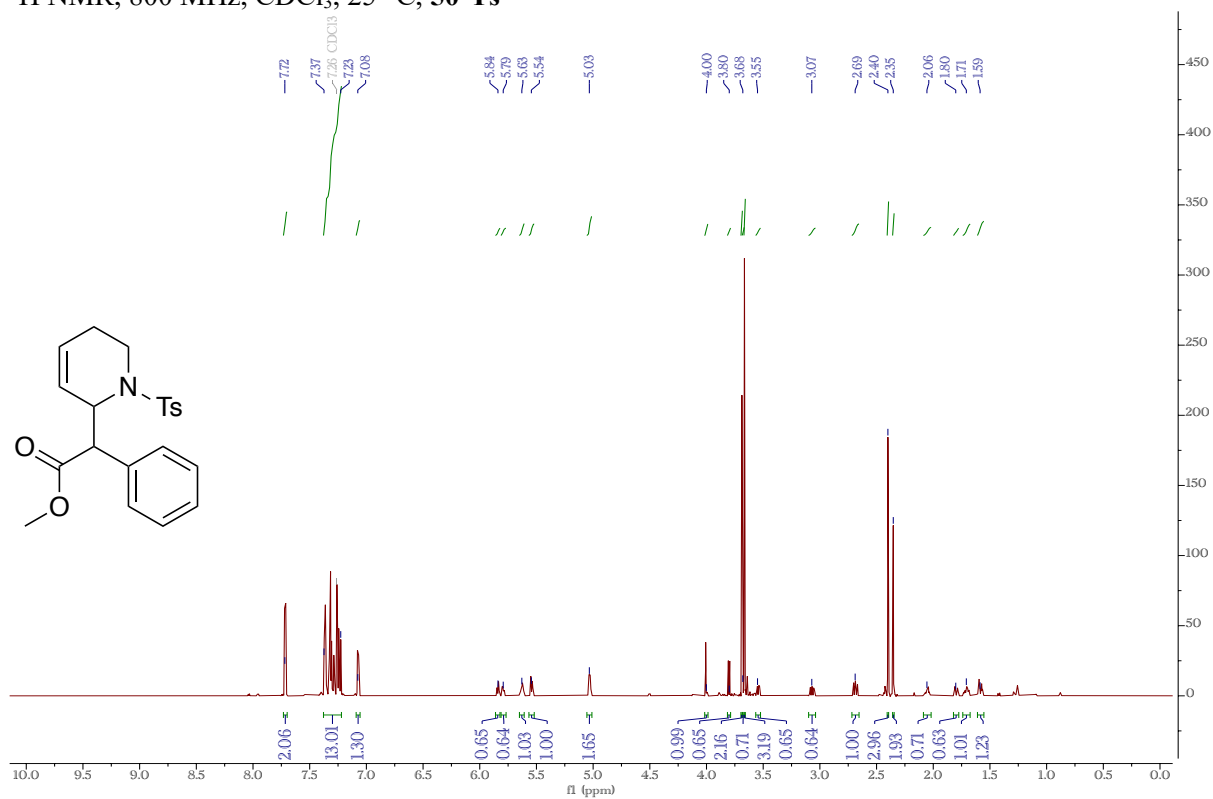
<sup>1</sup>H NMR, 800 MHz, CDCl<sub>3</sub>, 25 °C, 50-Ac



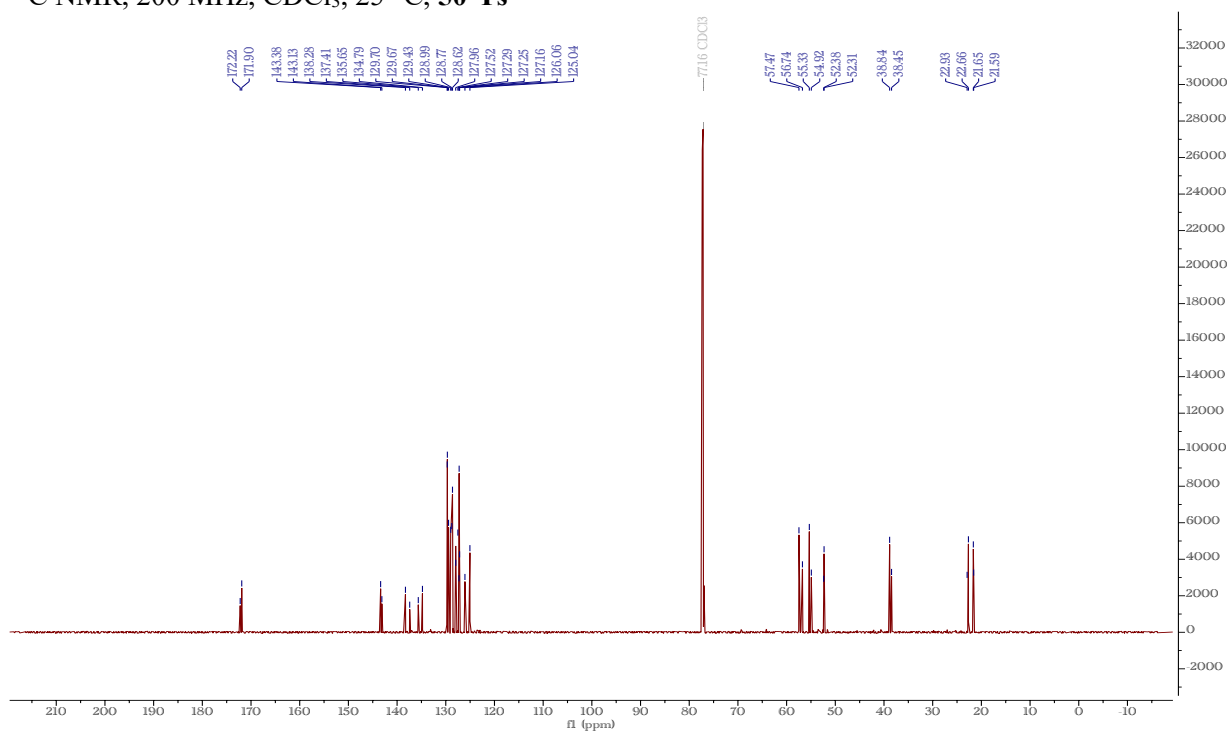
<sup>13</sup>C NMR, 200 MHz, CDCl<sub>3</sub>, 25 °C, 50-Ac



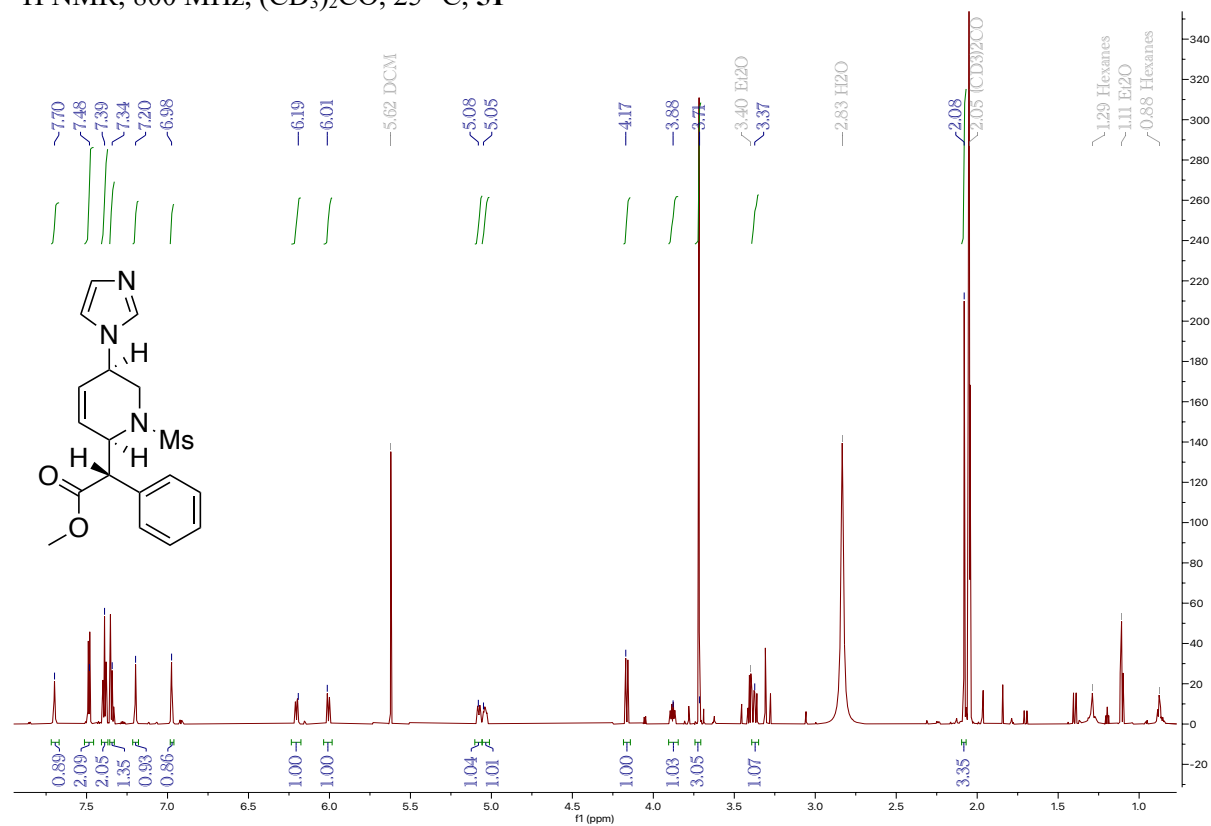
$^1\text{H}$  NMR, 800 MHz,  $\text{CDCl}_3$ , 25 °C, **50-Ts**



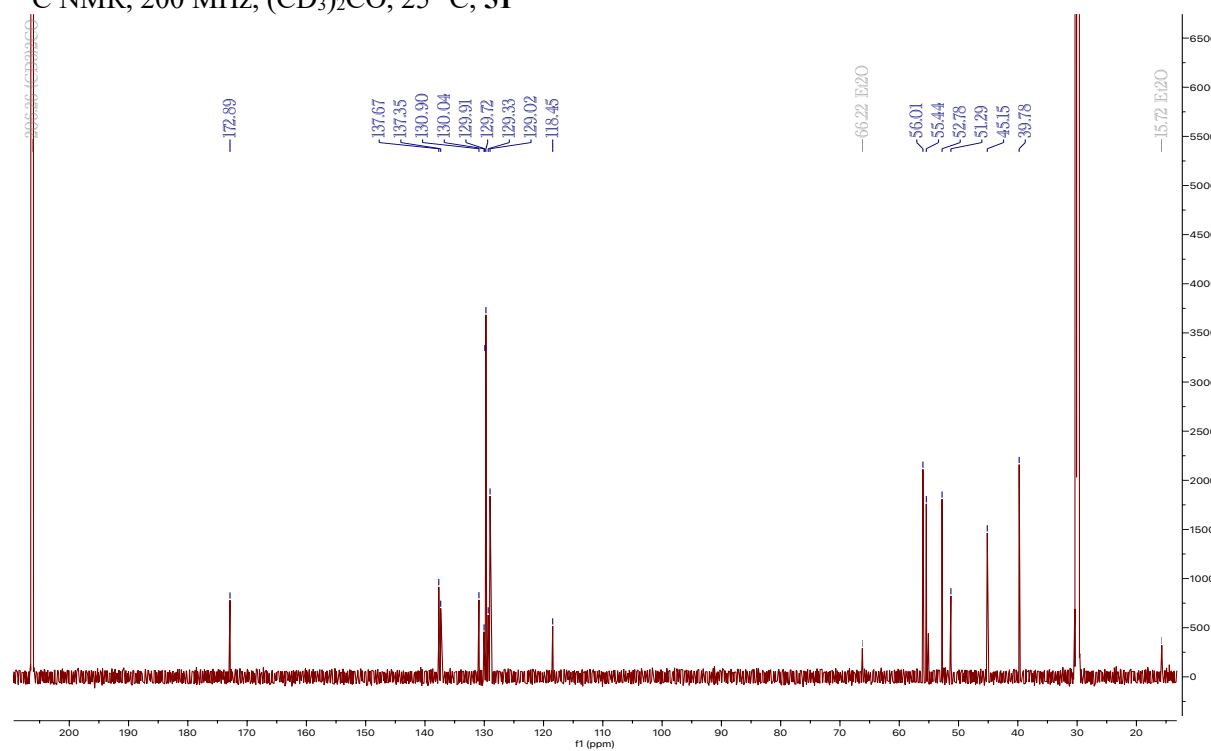
$^{13}\text{C}$  NMR, 200 MHz,  $\text{CDCl}_3$ , 25 °C, **50-Ts**



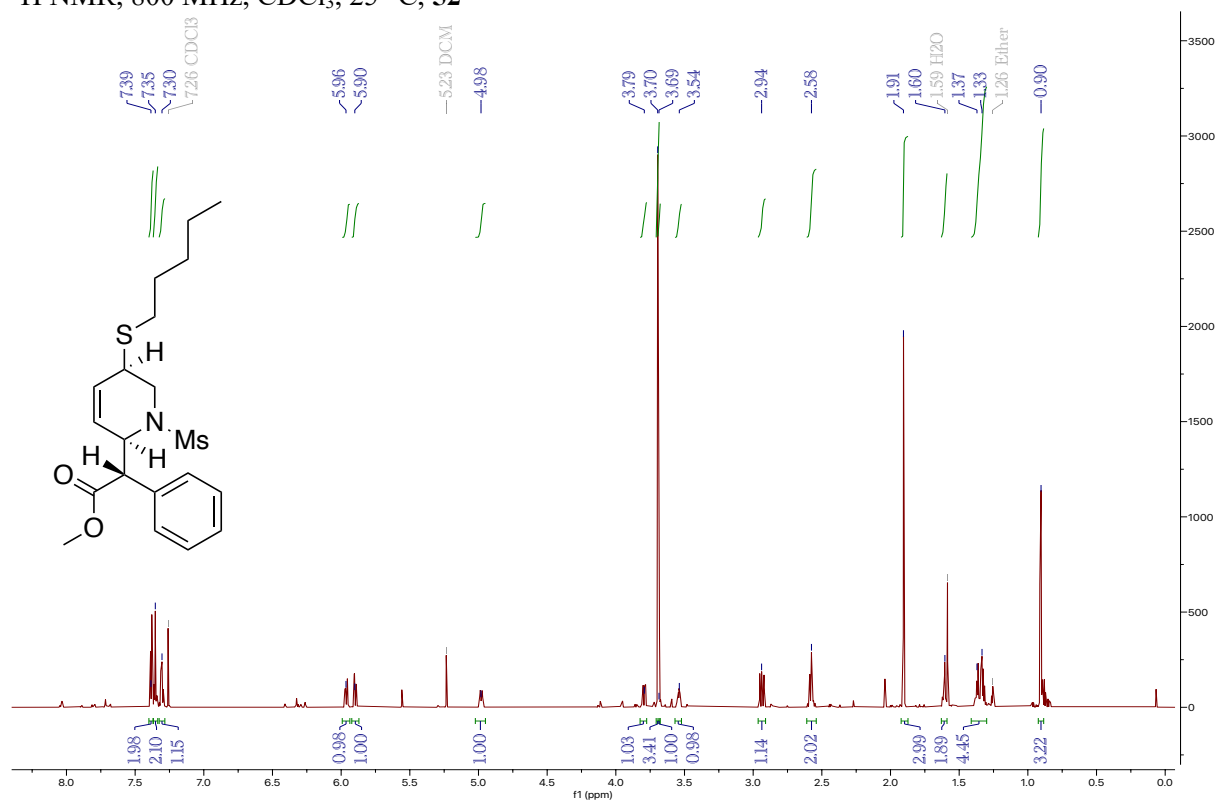
$^1\text{H}$  NMR, 800 MHz,  $(\text{CD}_3)_2\text{CO}$ , 25 °C, **51**



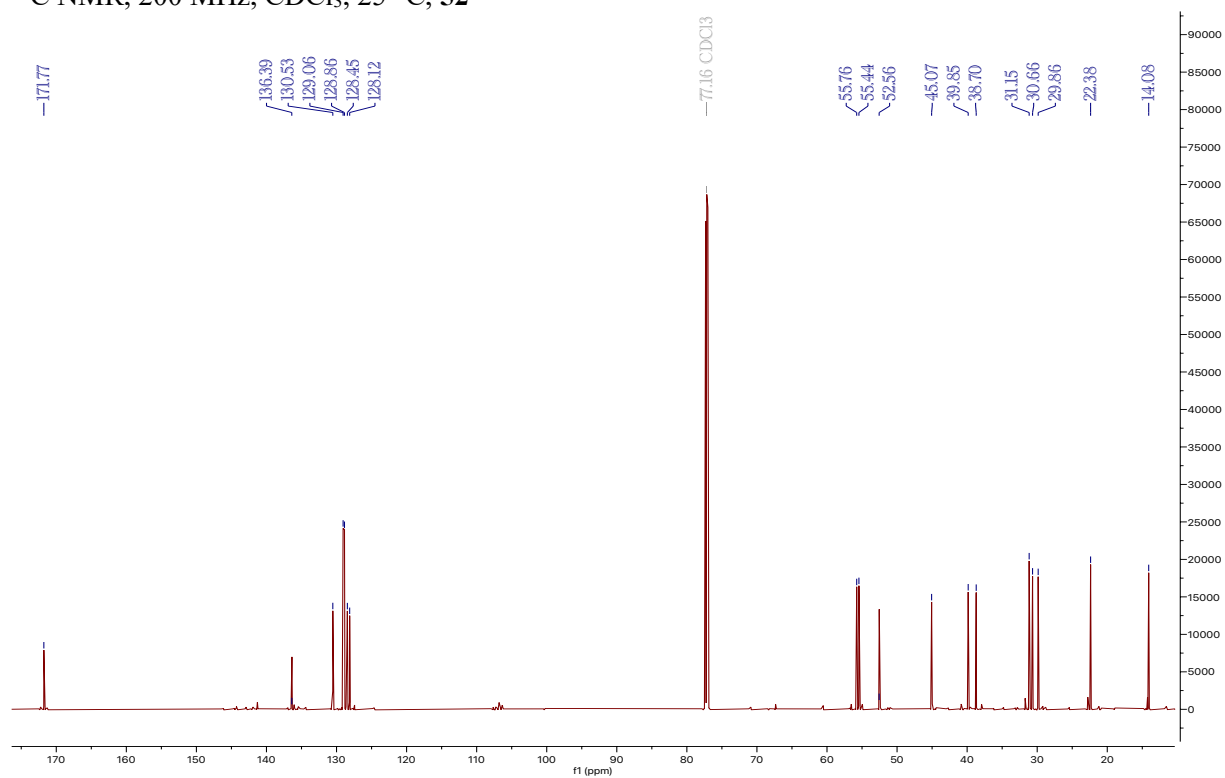
$^{13}\text{C}$  NMR, 200 MHz,  $(\text{CD}_3)_2\text{CO}$ , 25 °C, **51**



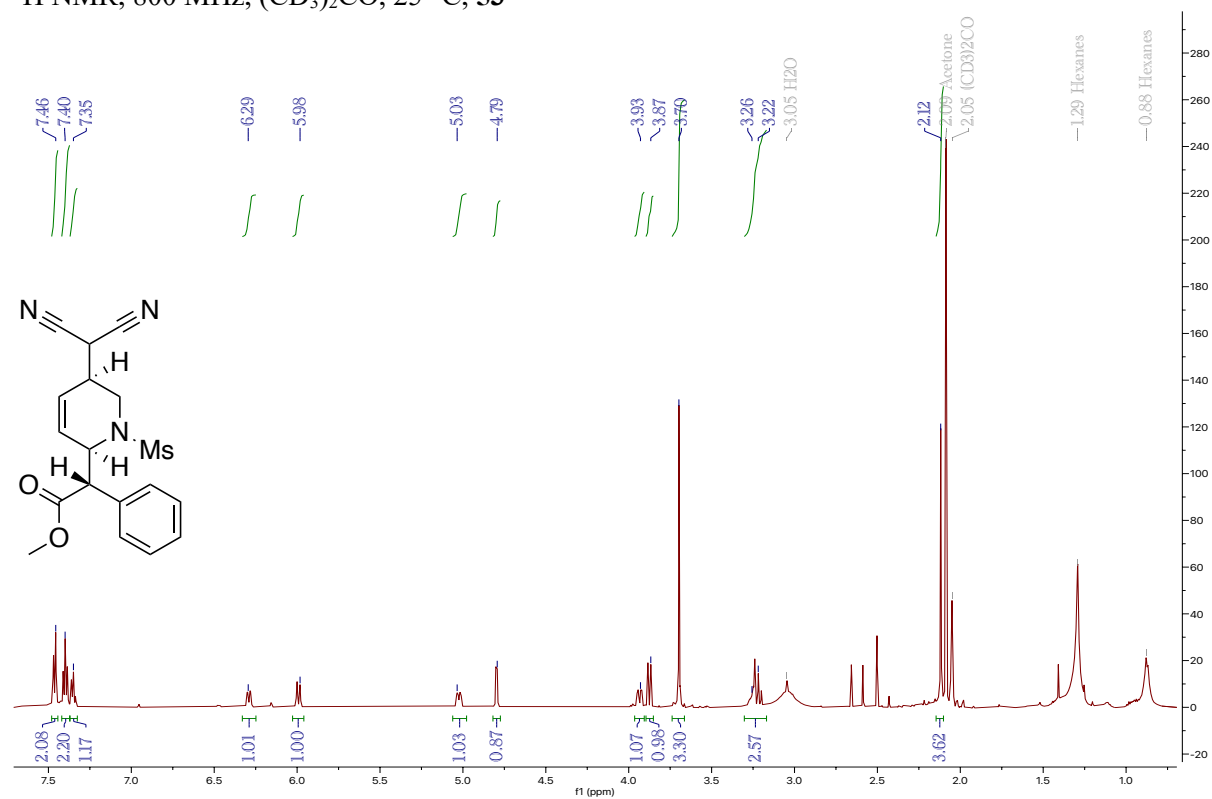
$^1\text{H}$  NMR, 800 MHz,  $\text{CDCl}_3$ , 25 °C, **52**



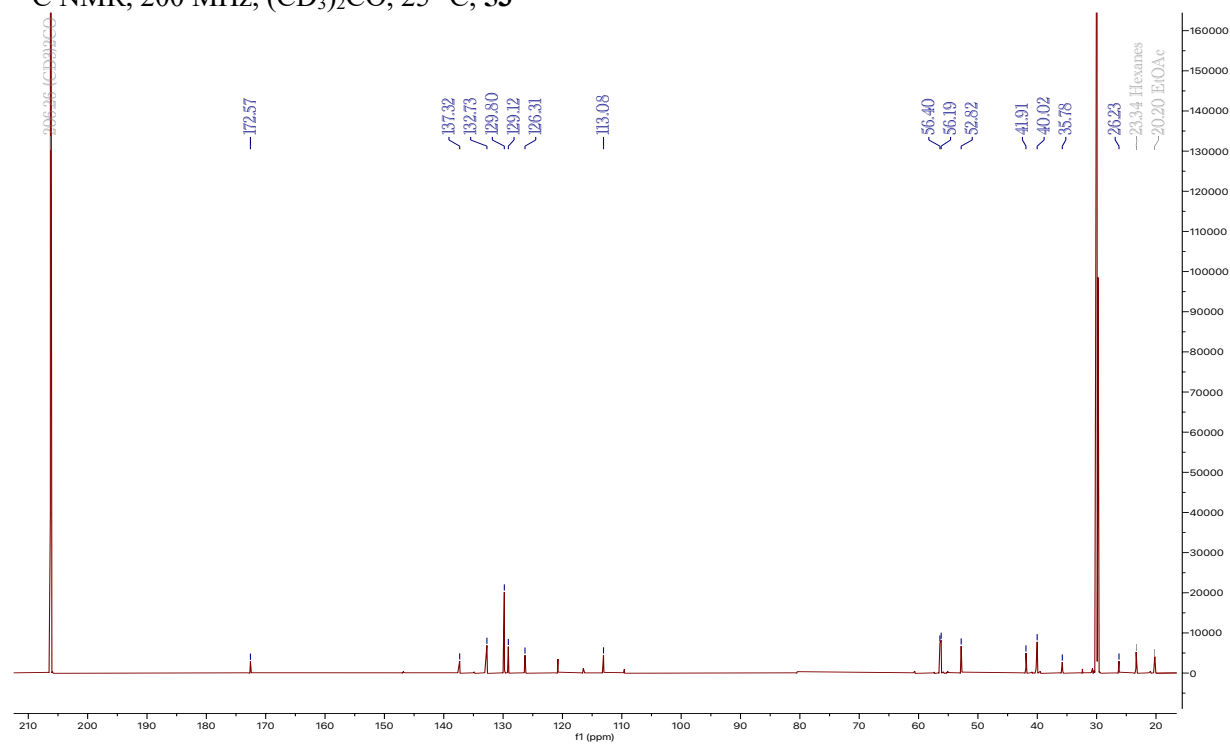
$^{13}\text{C}$  NMR, 200 MHz,  $\text{CDCl}_3$ , 25 °C, **52**



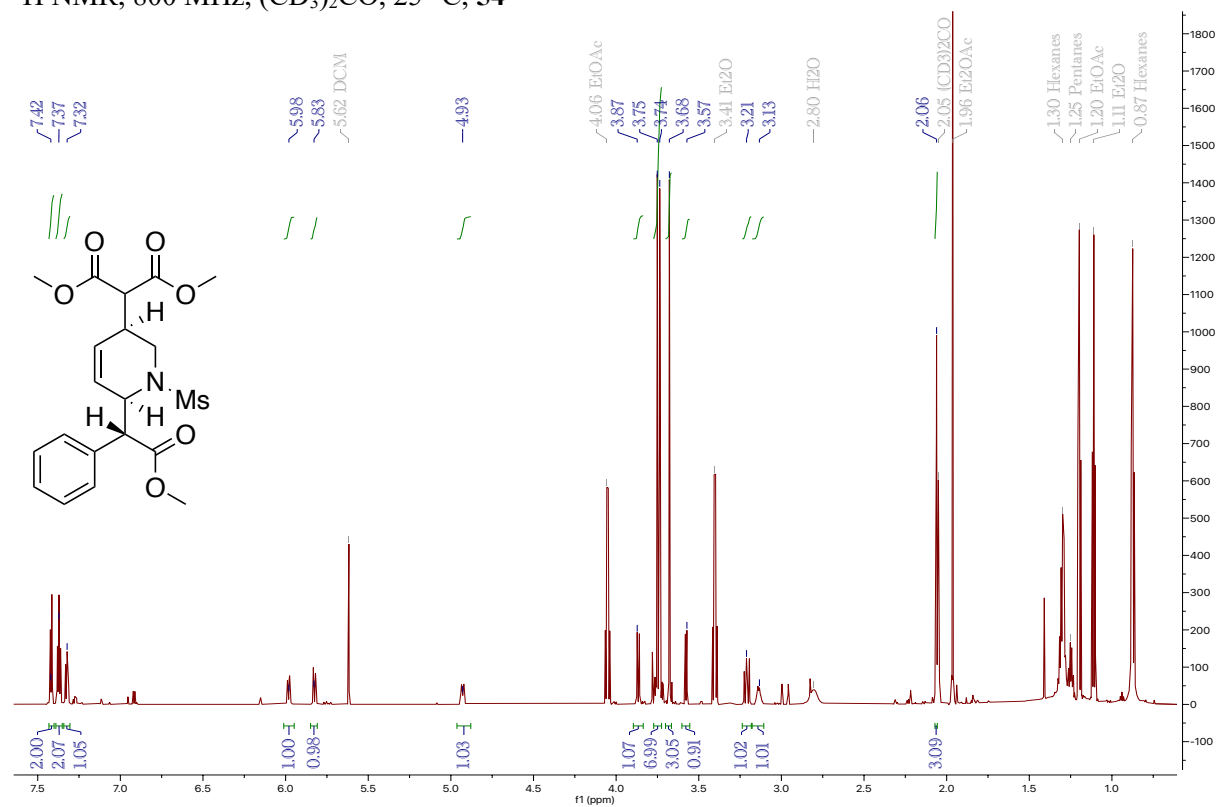
$^1\text{H}$  NMR, 800 MHz,  $(\text{CD}_3)_2\text{CO}$ , 25 °C, **53**



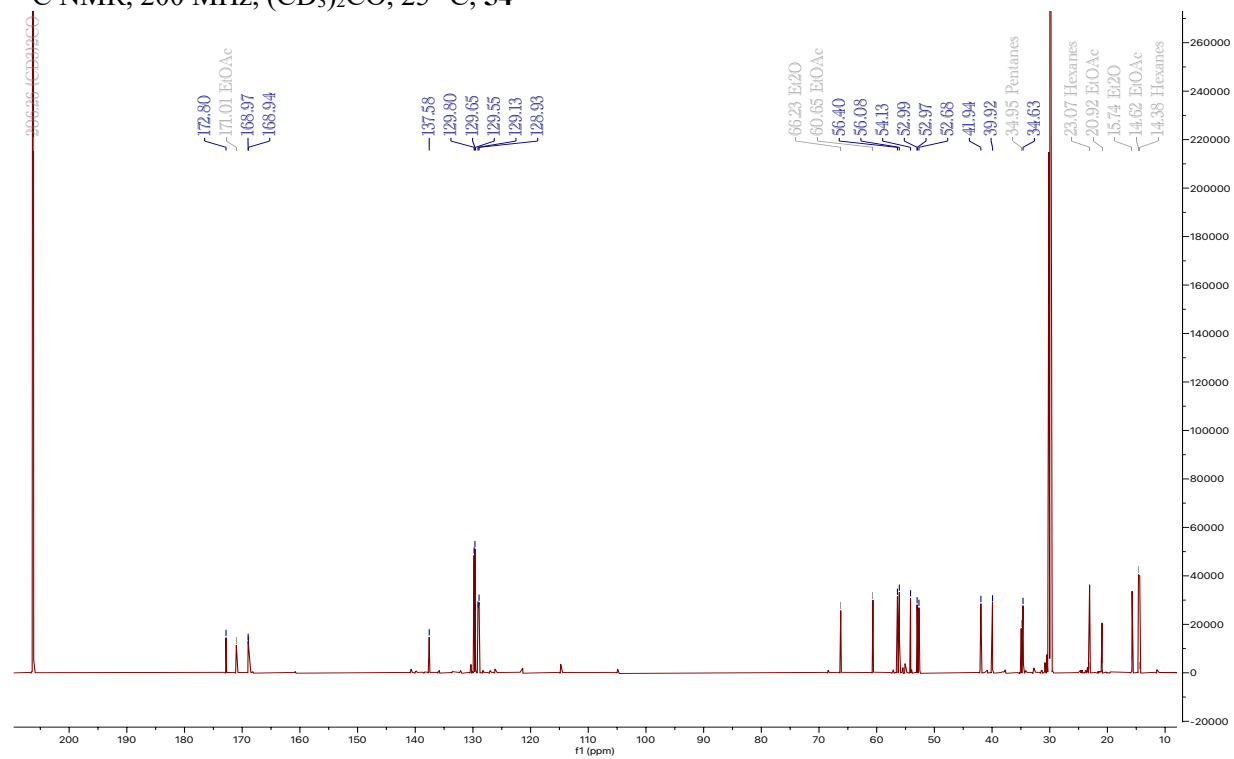
$^{13}\text{C}$  NMR, 200 MHz,  $(\text{CD}_3)_2\text{CO}$ , 25 °C, **53**



$^1\text{H}$  NMR, 800 MHz,  $(\text{CD}_3)_2\text{CO}$ , 25 °C, **54**

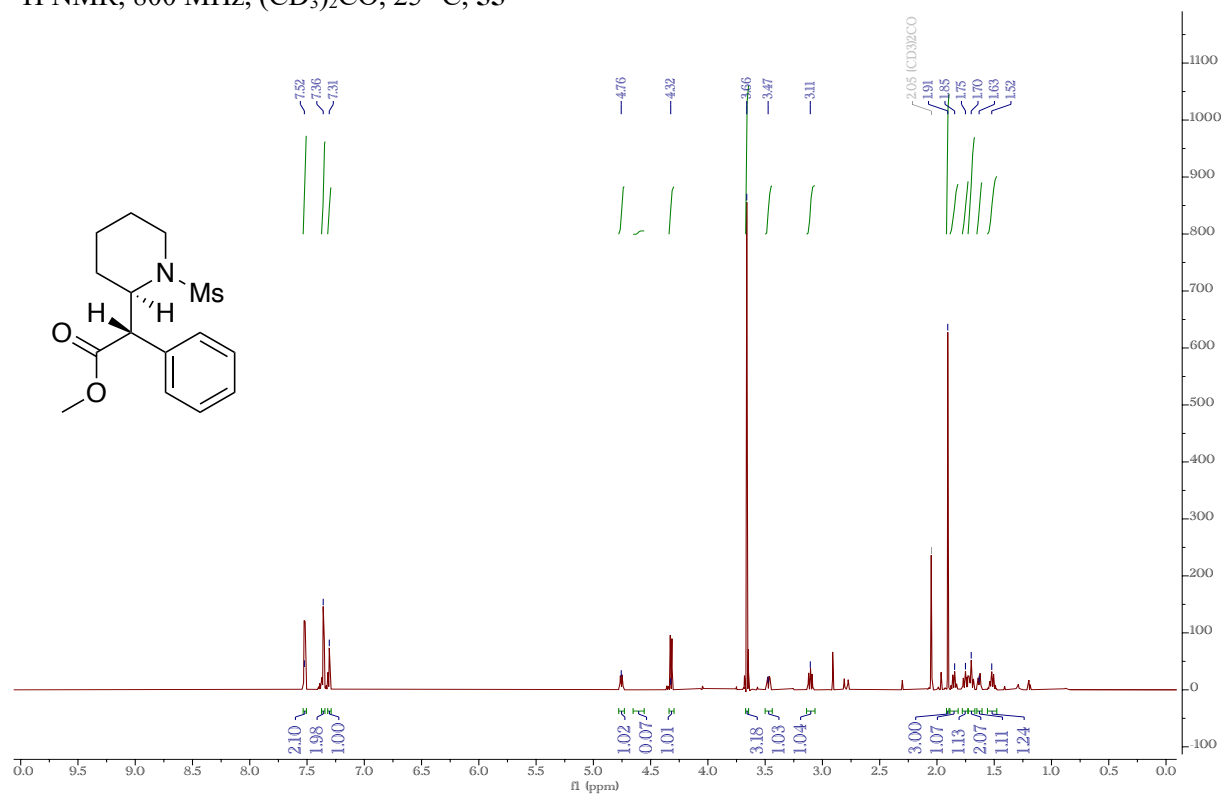


$^{13}\text{C}$  NMR, 200 MHz,  $(\text{CD}_3)_2\text{CO}$ , 25 °C, **54**

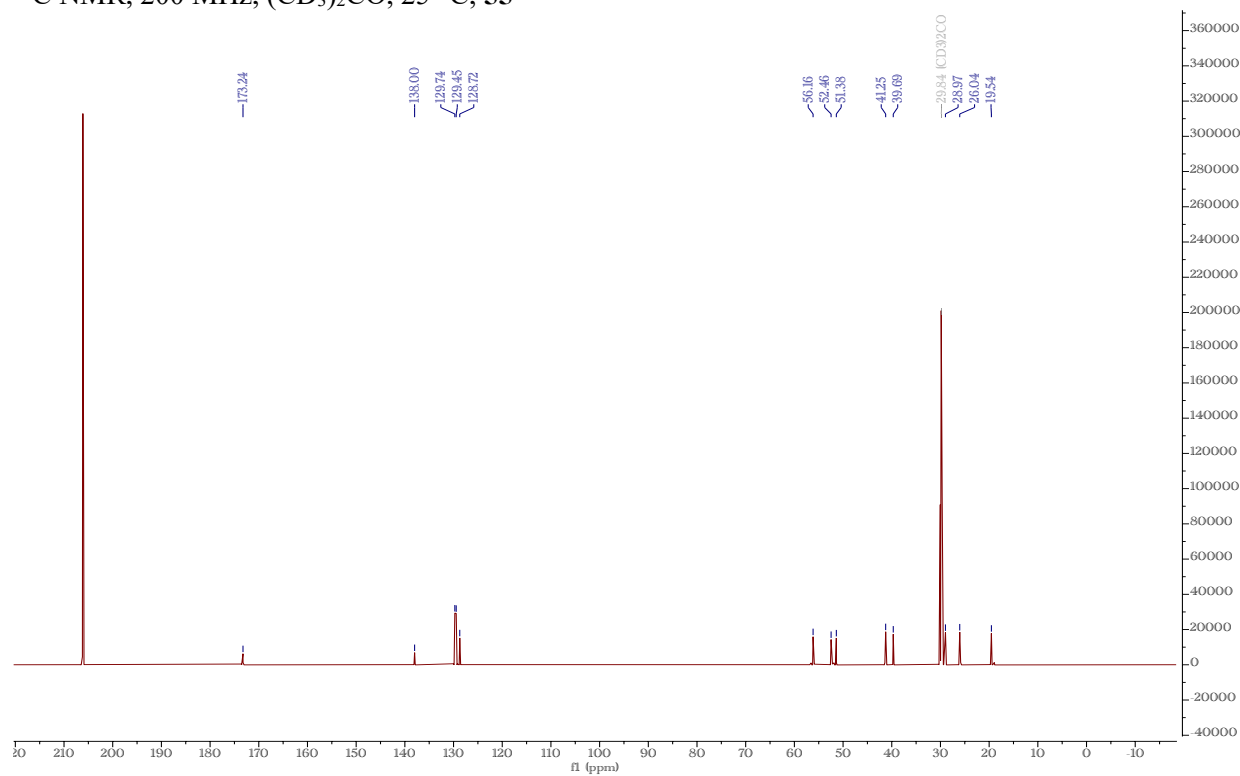




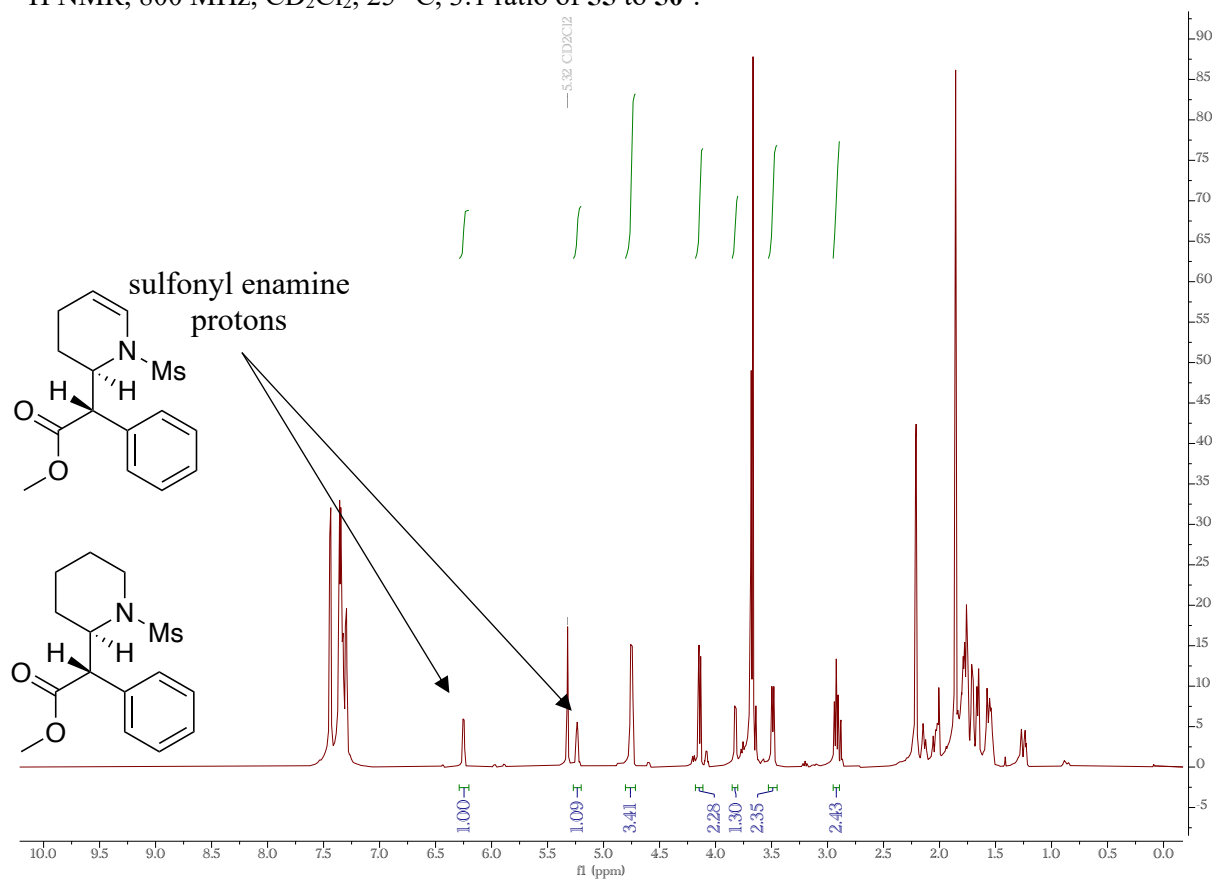
$^1\text{H}$  NMR, 800 MHz,  $(\text{CD}_3)_2\text{CO}$ , 25 °C, **55**



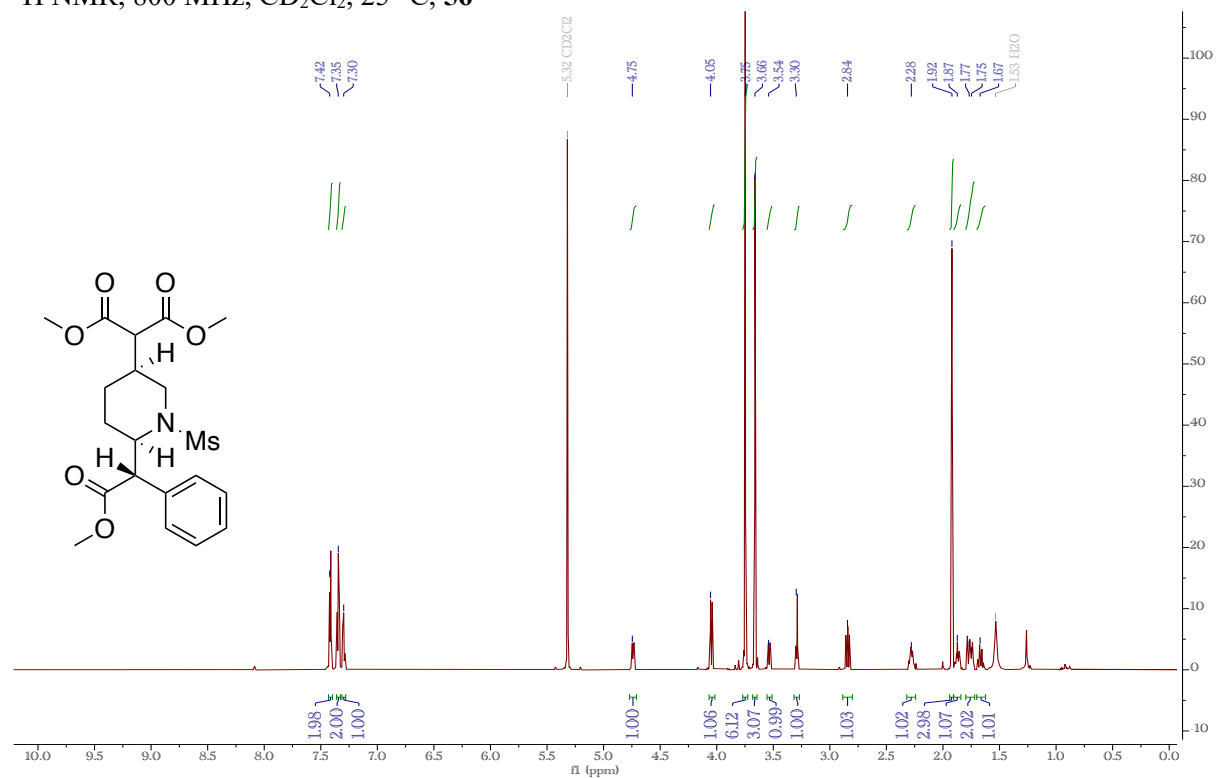
$^{13}\text{C}$  NMR, 200 MHz,  $(\text{CD}_3)_2\text{CO}$ , 25 °C, **55**



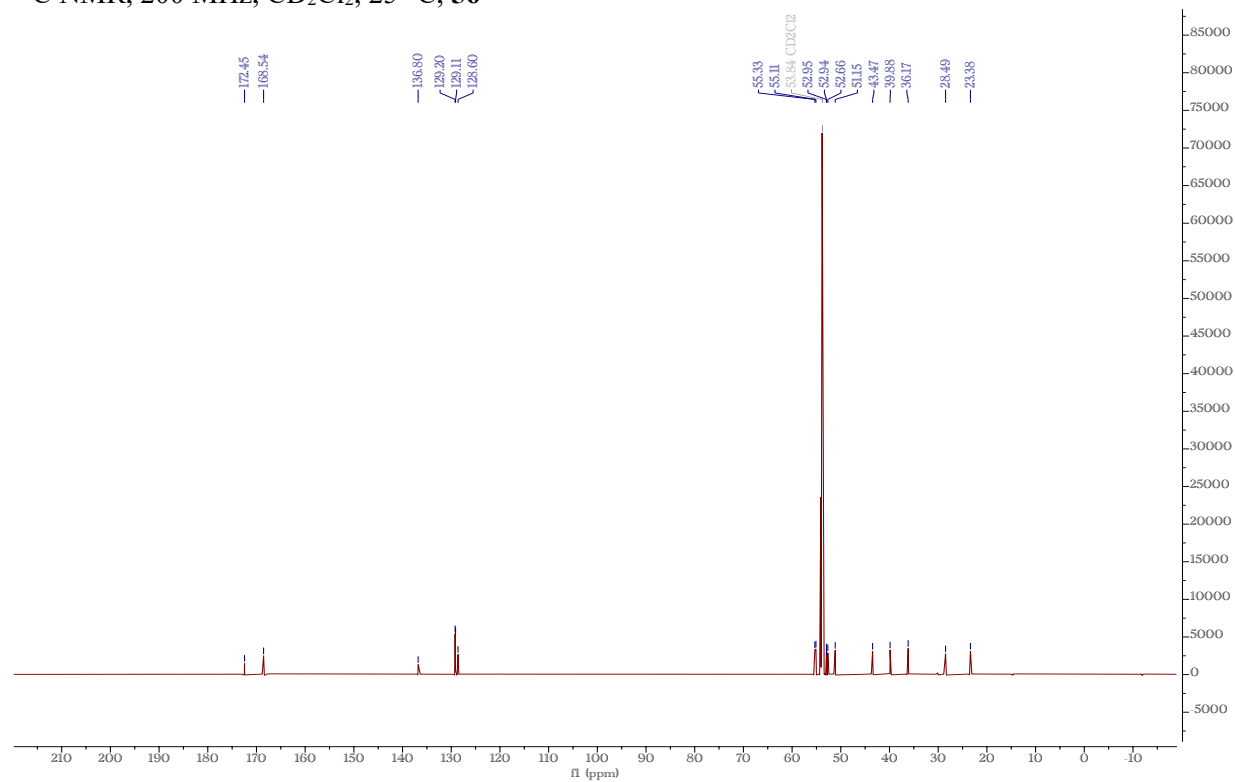
$^1\text{H}$  NMR, 800 MHz,  $\text{CD}_2\text{Cl}_2$ , 25  $^\circ\text{C}$ , 3:1 ratio of **55** to **50**.



$^1\text{H}$  NMR, 800 MHz,  $\text{CD}_2\text{Cl}_2$ , 25 °C, **56**



$^{13}\text{C}$  NMR, 200 MHz,  $\text{CD}_2\text{Cl}_2$ , 25 °C, **56**



### **Computational Methods and DFT Analysis for 35D.**

Ground-state structures were optimized at the M06 level of theory using the 6-31G\*\* [LANL2DZ for W] basis set in Gaussian 16. Conformational analysis was performed by optimizing multiple conformations and determining the lowest energy conformation. Previous literature demonstrates that this functional and basis set choice accurately corroborates experimental results. Vibrational frequency analysis verified that optimized structures were minima, and rigid-rotor-harmonic-oscillator thermochemical chemical corrections were applied at 298 K and 1 atm utilizing Gaussian's default implementation. Bond lengths were used to determine the likelihood of spatial interactions. 2D NMR analysis was performed on a 3 *erythro* : 1 *threo* sample using CD<sub>2</sub>Cl<sub>2</sub> as the solvent.

**DFT Geometry Optimization, Energies and Coordinates for erythro-35D.**

Electronic Energy: -2695.646348 Hartree  
Electronic Energy + Free Energy Correction: -2695.095613 Hartree

W	-1.277300	-0.358800	-0.127400
S	3.133200	-2.164600	0.838600
O	2.402400	3.114100	-1.759800
O	3.555700	-1.287700	1.921500
O	-0.812300	-3.271500	0.209300
O	2.635700	3.087700	0.473200
O	4.080800	-2.982800	0.095900
N	-0.871400	-2.065200	0.113500
N	2.298600	-1.207900	-0.256700
C	0.651400	0.573900	-0.489800
C	0.228400	0.027500	-1.762900
H	-0.113300	0.720500	-2.537900
C	0.987300	-1.135400	-2.253000
H	0.785800	-1.536700	-3.245700
C	2.041200	0.209100	-0.012300
H	2.184200	0.408700	1.055800
C	1.935100	-1.733100	-1.511100
H	2.494700	-2.608600	-1.830900
C	3.089800	1.073700	-0.787400
H	2.969000	0.837000	-1.852100
C	4.511300	0.775800	-0.376900
C	2.711200	2.518500	-0.592800
C	5.255800	-0.117200	-1.147900
H	4.811100	-0.543800	-2.047000
C	6.364900	0.939900	1.162800
H	6.794700	1.353000	2.072900
C	1.897900	-3.265800	1.488300
H	2.418700	-3.970700	2.141200
H	1.397000	-3.781400	0.666400
H	1.163100	-2.683100	2.049300
C	6.539700	-0.488000	-0.764800
H	7.099500	-1.198500	-1.368400
C	1.950200	4.457200	-1.636400
H	2.704700	5.082200	-1.149100
H	1.031500	4.500000	-1.039300
H	1.761700	4.810000	-2.651600
C	5.078400	1.302700	0.785800
H	4.498100	1.989300	1.397900

C	7.098100	0.042300	0.392200
H	8.101200	-0.247700	0.697200
H	0.457400	1.644000	-0.352400
P	-2.574400	-1.049400	-2.165200
C	-4.395800	-0.820100	-2.039600
H	-4.806900	-1.422700	-1.224600
H	-4.890100	-1.094100	-2.978900
H	-4.600100	0.234700	-1.816200
C	-2.286100	-0.253900	-3.796200
H	-2.493400	0.819800	-3.730900
H	-2.956700	-0.694700	-4.543000
H	-1.251100	-0.394100	-4.120500
C	-2.380700	-2.820400	-2.577300
H	-1.330300	-3.002500	-2.830300
H	-3.024800	-3.108200	-3.415800
H	-2.604500	-3.436000	-1.700600
N	-3.204800	-0.755100	0.932500
N	-2.171100	1.714000	-0.475400
N	-0.939400	0.492500	1.920100
N	-1.874400	1.292800	2.493200
N	-3.907700	0.208700	1.567100
N	-2.977800	2.273300	0.455700
C	0.055300	0.365800	2.801400
H	0.926200	-0.234800	2.562400
C	-1.459400	1.660900	3.722300
H	-2.079100	2.305500	4.332200
C	-3.850700	-1.908100	1.125800
H	-3.436100	-2.828200	0.727100
C	-2.071300	2.597500	-1.475200
H	-1.444100	2.377300	-2.332200
C	-0.226100	1.089400	3.963500
H	0.388400	1.184600	4.846400
C	-2.824300	3.740300	-1.198700
H	-2.940900	4.623800	-1.809200
B	-3.230700	1.577200	1.812100
C	-3.380200	3.488300	0.043100
H	-4.028200	4.087700	0.669400
C	-4.993200	-0.334700	2.150600
H	-5.667800	0.284500	2.727700
C	-5.006200	-1.692100	1.882200
H	-5.735700	-2.421500	2.202900
H	-3.921100	2.272800	2.509700

**DFT Geometry Optimization, Energies and Coordinates for *threo*-35D.**

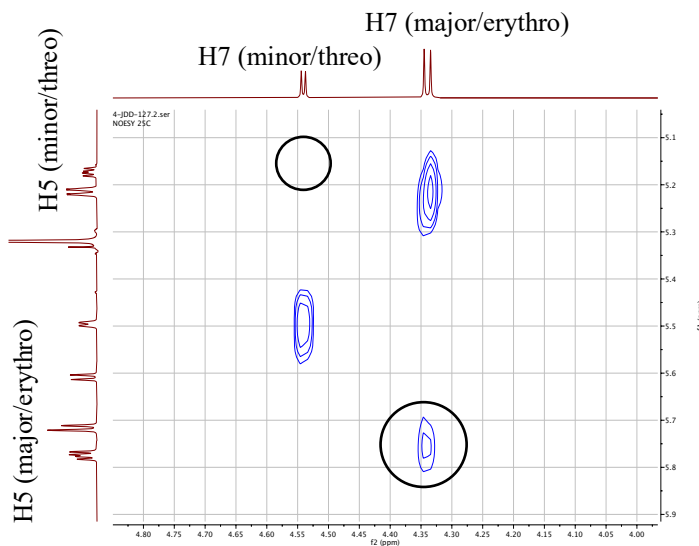
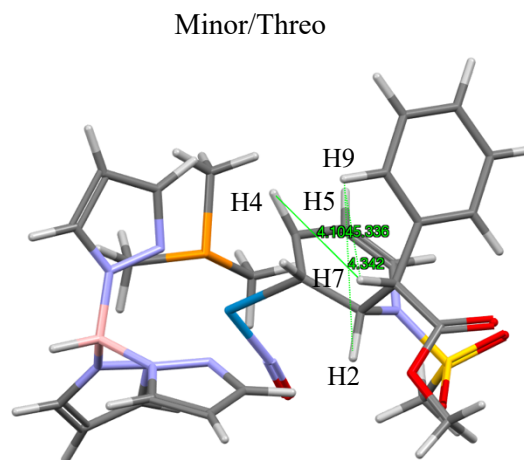
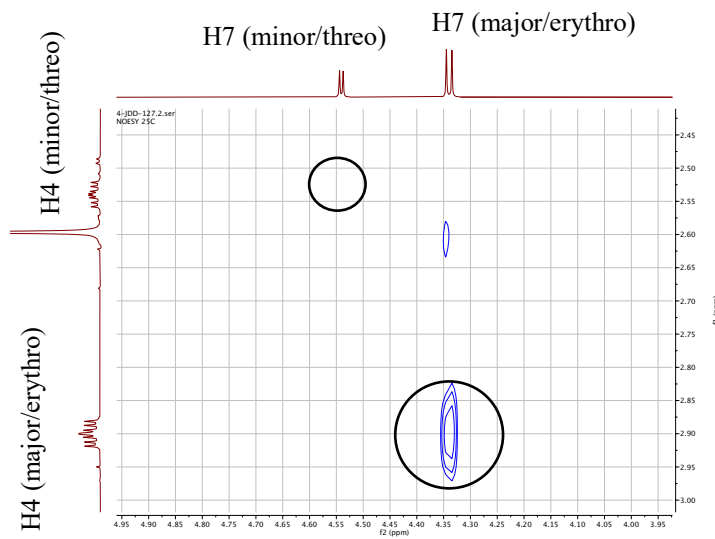
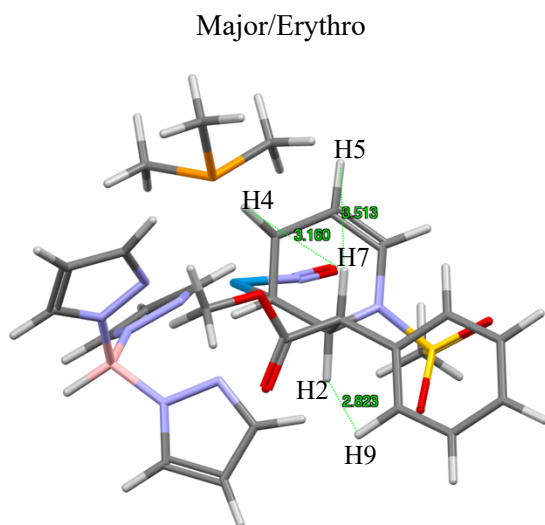
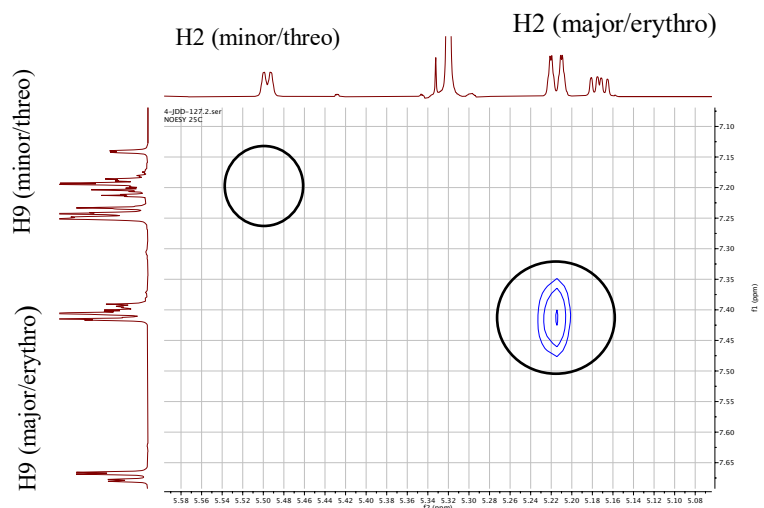
Electronic Energy: -2695.644006 Hartree

Electronic Energy + Free Energy Correction: -2695.092530 Hartree

O	-0.556500	0.328100	3.092900
N	-0.688300	0.185300	1.893500
W	-1.227500	-0.106900	0.235500
C	0.399200	-1.512200	-0.449400
C	0.721600	-0.130500	-0.720900
C	1.973600	0.501200	-0.126500
H	0.065600	-2.108100	-1.303900
H	0.575400	0.181700	-1.760500
H	1.767200	1.511900	0.242900
C	3.063300	0.647000	-1.246800
N	2.453000	-0.257900	1.039500
S	3.390000	0.477700	2.221800
O	4.606200	-0.303000	2.406400
O	3.450500	1.892200	1.875700
C	2.428500	0.305100	3.705100
H	2.231300	-0.756100	3.877400
H	3.035600	0.716100	4.515500
H	1.483500	0.839000	3.583900
C	3.636400	-0.676200	-1.674900
C	4.639400	-1.321400	-0.944200
C	3.100700	-1.321300	-2.791800
C	5.073400	-2.588000	-1.318300
H	5.079900	-0.831000	-0.080700
C	3.531900	-2.590200	-3.163100
H	2.328000	-0.820800	-3.376300
C	4.519600	-3.229800	-2.421600
H	5.853600	-3.077000	-0.738900
H	3.101200	-3.075100	-4.037000
H	4.863300	-4.221600	-2.708400
C	4.091400	1.697400	-0.875600
O	5.258200	1.524400	-0.629200
O	3.506500	2.912400	-0.885500
C	4.331900	3.968000	-0.401400
H	3.736200	4.879200	-0.479200
H	4.606000	3.774600	0.640100
H	5.242200	4.055400	-1.002500
H	2.515000	1.089200	-2.092700
C	1.258300	-2.251600	0.482500

C	2.234600	-1.640900	1.163000
H	1.167100	-3.332600	0.572800
H	2.938200	-2.167000	1.803900
N	-1.287600	1.962700	-0.709900
N	-2.422200	2.396000	-1.320700
N	-2.343800	-0.569900	-1.722000
N	-3.368300	0.221500	-2.121500
N	-3.204500	0.705500	0.898400
N	-4.126200	1.231000	0.063000
C	-2.223000	3.625800	-1.832200
C	-0.929000	4.017000	-1.552100
C	-0.386000	2.938800	-0.850300
C	-3.916900	-0.268100	-3.247000
C	-3.239900	-1.419900	-3.604300
C	-2.262700	-1.561400	-2.618300
C	-5.182700	1.670100	0.773200
C	-4.949100	1.415600	2.113100
C	-3.684200	0.821200	2.139800
B	-3.702800	1.538500	-1.386500
H	-4.577200	2.123700	-1.970400
H	-3.023700	4.128100	-2.359700
H	-0.443800	4.945400	-1.814800
H	0.614200	2.831700	-0.449900
H	-4.746200	0.246700	-3.714700
H	-3.419000	-2.056700	-4.458100
H	-1.499300	-2.323600	-2.520900
H	-6.016200	2.145100	0.271800
H	-5.593300	1.642700	2.950000
H	-3.081600	0.489700	2.979800
C	-3.952300	-2.389300	1.202300
H	-4.268300	-3.397000	1.496900
H	-4.303400	-1.667700	1.945400
H	-4.410700	-2.132800	0.238500
C	-1.499900	-2.764000	2.677100
H	-1.681700	-1.937000	3.372000
H	-1.969500	-3.682500	3.046600
H	-0.413300	-2.892100	2.609400
P	-2.122900	-2.307100	1.021400
C	-1.866800	-3.844700	0.048100
H	-2.266100	-4.701500	0.603400
H	-2.402200	-3.766800	-0.904400
H	-0.806100	-4.013600	-0.155400

# H-H Bond Lengths and NOESY Interactions.



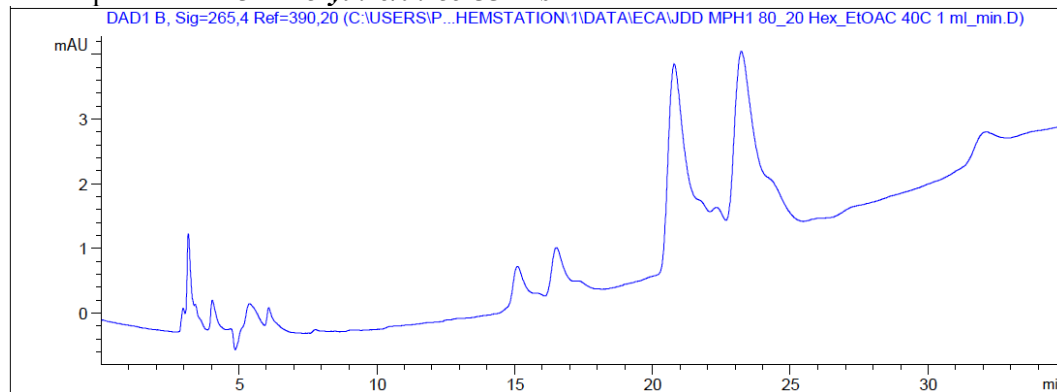
### Chiral HPLC Parameters:

Equipment: Agilent 1260 Infinity II Flexible Pump (G7104C), Agilent 1260 Vialsampler (G7129C), Agilent 1260 DAD HS (G7117C), Agilent 1260 RID (G7162A), Daicel IC-3 column, 3  $\mu$ m particle size, 4.6 mm x 250 mm

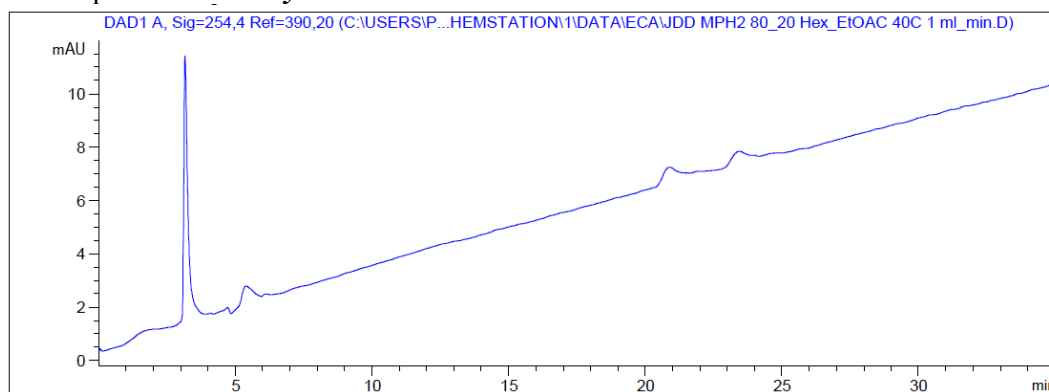
Method: 80/20 Mixed Hexanes (HPLC Grade)/Ethyl Acetate (HPLC Grade) isocratic, 1 ml/min for 35 minutes, 40 °C, 2.50  $\mu$ L injection volume

DAD: 254 nm, 265 nm with a bandwidth of 4 nm; Reference 390 nm with a bandwidth of 20 nm

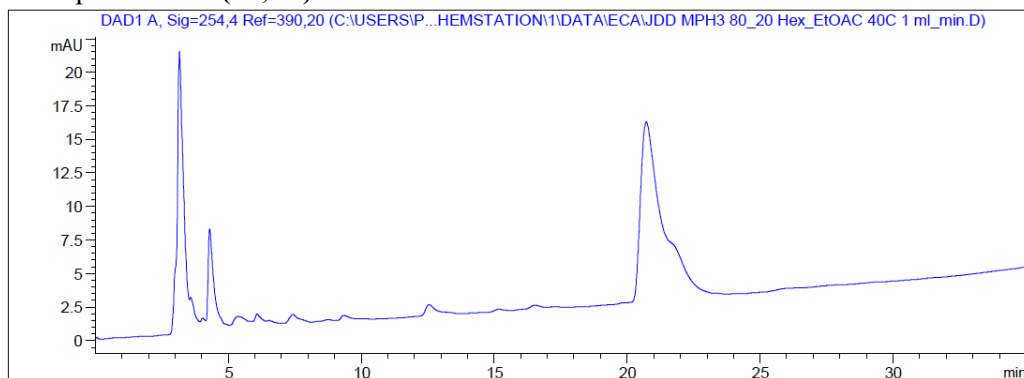
### Chiral HPLC Spectrum for 3:1 $\pm$ *erythro/threo* 55-Ms



### Chiral HPLC Spectrum for $\pm$ *erythro* 55-Ms



### Chiral HPLC Spectrum for (2*S*,7*R*)-55-Ms





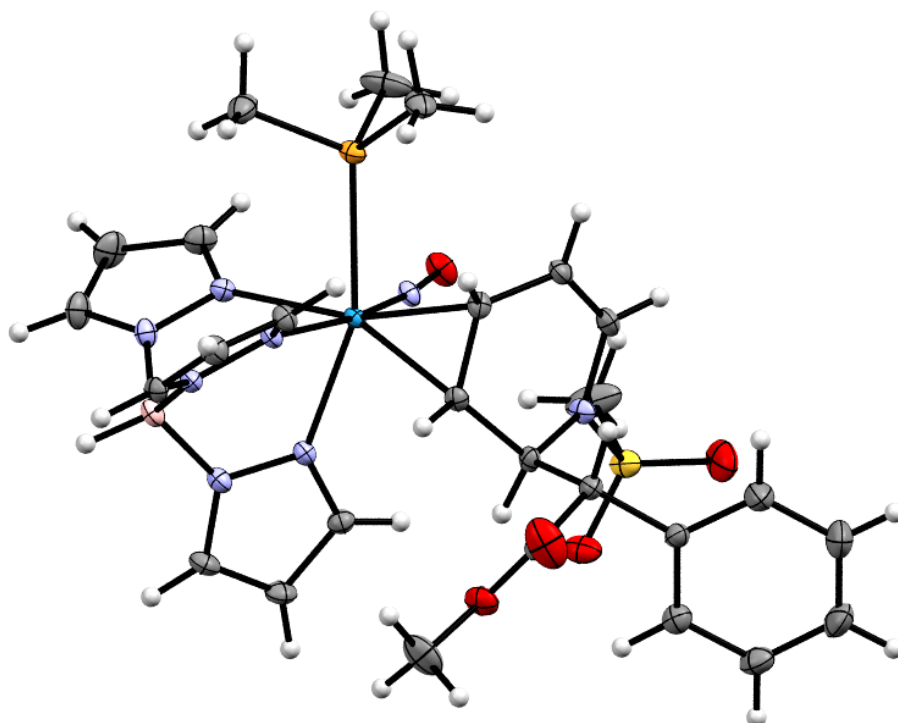
Crystallography:



ORTEP/ellipsoid diagram of **34D**.

SC-XRD data for **34D**.

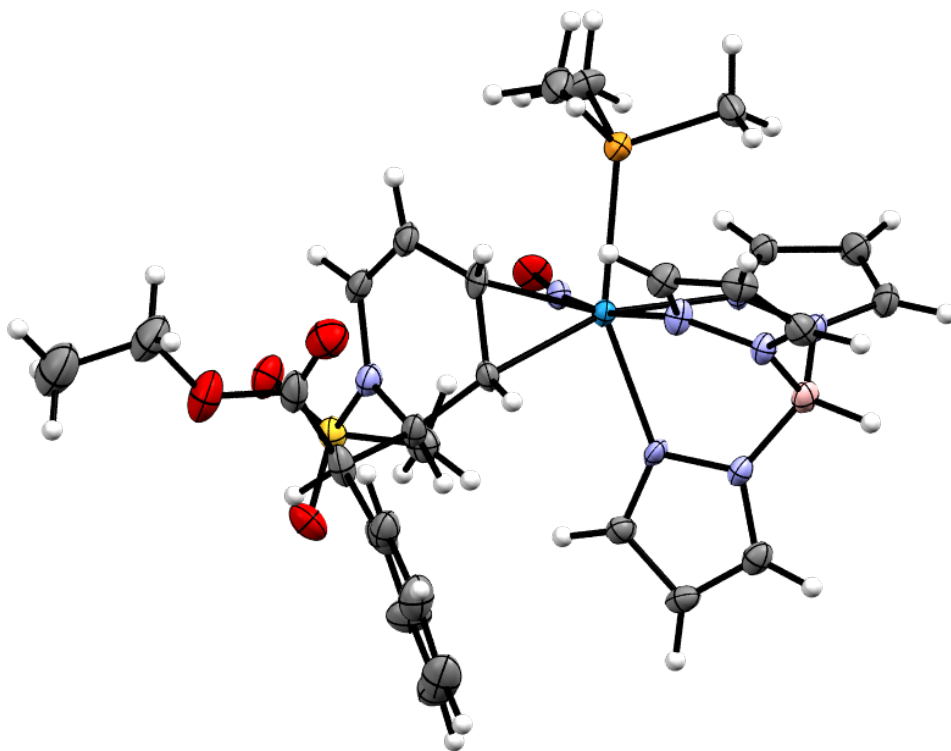
CCDC 2256163	<b>Chemical Formula</b> C <sub>21</sub> H <sub>32</sub> BN <sub>8</sub> O <sub>5</sub> PSW	<b>FW (g/mol)</b> 734.22
T (K) 100(2)	$\lambda$ (Å) 0.71073	Crystal size (mm) 0.083 x 0.090 x 0.133
Crystal habit Yellow block	Crystal system Monoclinic	Space group P 2 <sub>1/n</sub>
a (Å) 11.4488(15)	b (Å) 20.387(3)	c (Å) 12.8800(18)
$\alpha$ (°) 90	$\beta$ (°) 104.213(2)	$\gamma$ (°) 2914.3(7)
V (Å <sup>3</sup> ) 2914.3(7)	Z 2	$\rho_{\text{calc}}$ (g/cm <sup>3</sup> ) 1.770
$\mu$ (mm <sup>-1</sup> ) 4.229	F(000) 1540	$\theta$ range (°) 1.91 to 28.29
Index ranges -15 ≤ h ≤ 15 -27 ≤ k ≤ 26 -17 ≤ l ≤ 17	Data/restraints/parameters 7221 / 0 / 385	Goodness-of-fit on F <sup>2</sup> 0.976
R <sub>1</sub> [I > 2σ(I)] 0.0361	wR <sub>2</sub> [all data] 0.0706	



ORTEP/ellipsoid diagram of *erythro-35D*.

SC-XRD data for **35D**.

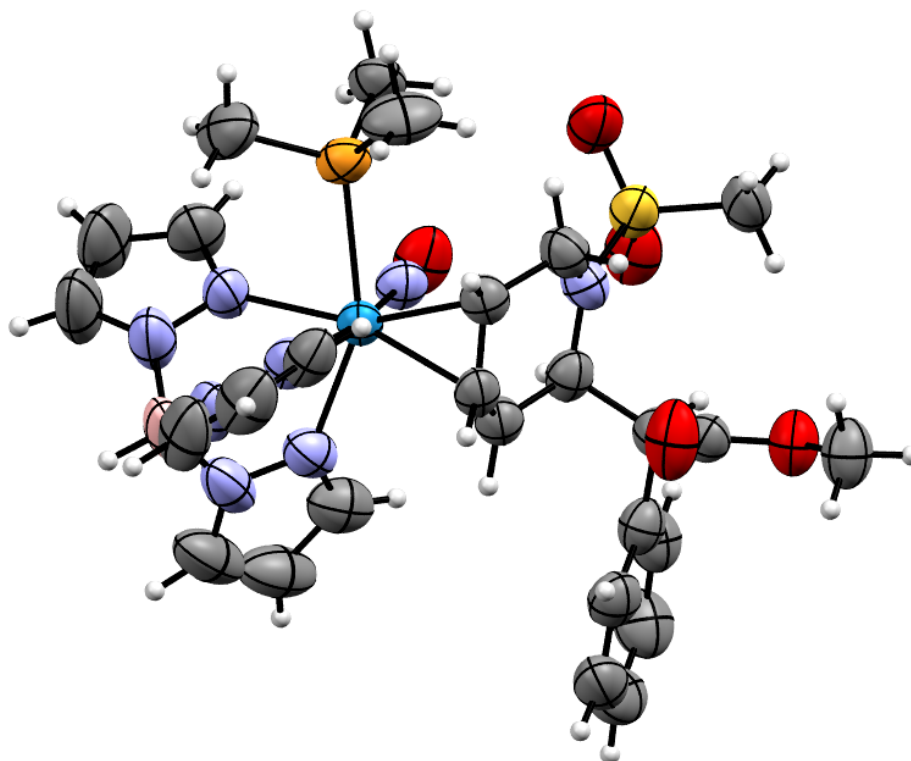
CCDC 2256164	Chemical Formula $C_{27}H_{36}BN_8O_5PSW$	FW (g/mol) 810.33
T (K) 100(2)	$\lambda$ (Å) 0.71073	Crystal size (mm) 0.070 x 0.144 x 0.164
Crystal habit Colorless plate	Crystal system Triclinic	Space group P -1
a (Å) 9.8584(12)	b (Å) 12.0339(15)	c (Å) 14.6597(17)
$\alpha$ (°) 107.053(4)	$\beta$ (°) 95.521(4)	$\gamma$ (°) 103.067(4)
V (Å <sup>3</sup> ) 1594.8(3)	Z 2	$\rho_{calc}$ (g/cm <sup>3</sup> ) 1.687
$\mu$ (mm <sup>-1</sup> ) 3.787	F(000) 808	$\theta$ range (°) 1.48 to 30.57
Index ranges -14 ≤ h ≤ 14 -17 ≤ k ≤ 17 -20 ≤ l ≤ 20	Data/restraints/parameters 9762 / 0 / 413	Goodness-of-fit on F <sup>2</sup> 1.025
R <sub>1</sub> [I > 2σ(I)] 0.0221	wR <sub>2</sub> [all data] 0.0442	



ORTEP/ellipsoid diagram of *erythro-36D*.

SC-XRD data for **36D**.

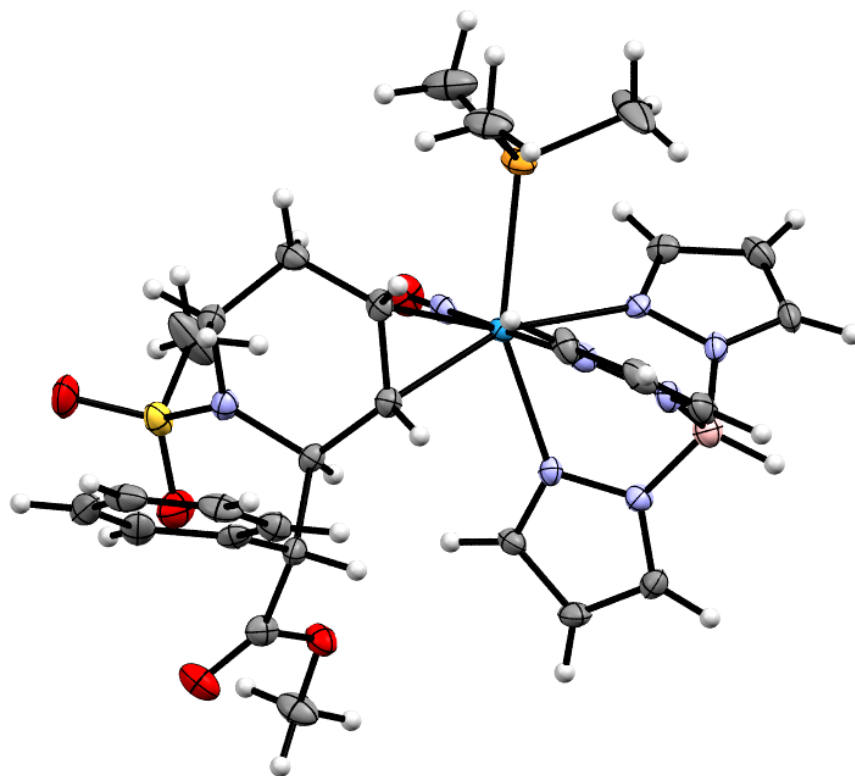
CCDC N/A	Chemical Formula $C_{28}H_{38}BN_8O_5PSW$	FW (g/mol) 824.35
T (K) 100(2)	$\lambda$ (Å) 0.71073	Crystal size (mm) 0.045 x 0.094 x 0.185
Crystal habit Yellow rod	Crystal system Monoclinic	Space group P 2 <sub>1</sub> /n
a (Å) 13.4621(13)	b (Å) 18.2186(18)	c (Å) 14.5754(15)
$\alpha$ (°) 90	$\beta$ (°) 113.609(2)	$\gamma$ (°) 90
V (Å <sup>3</sup> ) 3275.6(6)	Z 4	$\rho_{calc}$ (g/cm <sup>3</sup> ) 1.672
$\mu$ (mm <sup>-1</sup> ) 3.690	F(000) 1648	$\theta$ range (°) 1.74 to 26.48
Index ranges -16 ≤ h ≤ 16 -22 ≤ k ≤ 22 -16 ≤ l ≤ 18	Data/restraints/parameters 6761 / 0 / 421	Goodness-of-fit on F <sup>2</sup> 1.074
R <sub>1</sub> [I > 2σ(I)] 0.0387	wR <sub>2</sub> [all data] 0.1007	



ORTEP/ellipsoid diagram of **37**.

SC-XRD data for **37**.

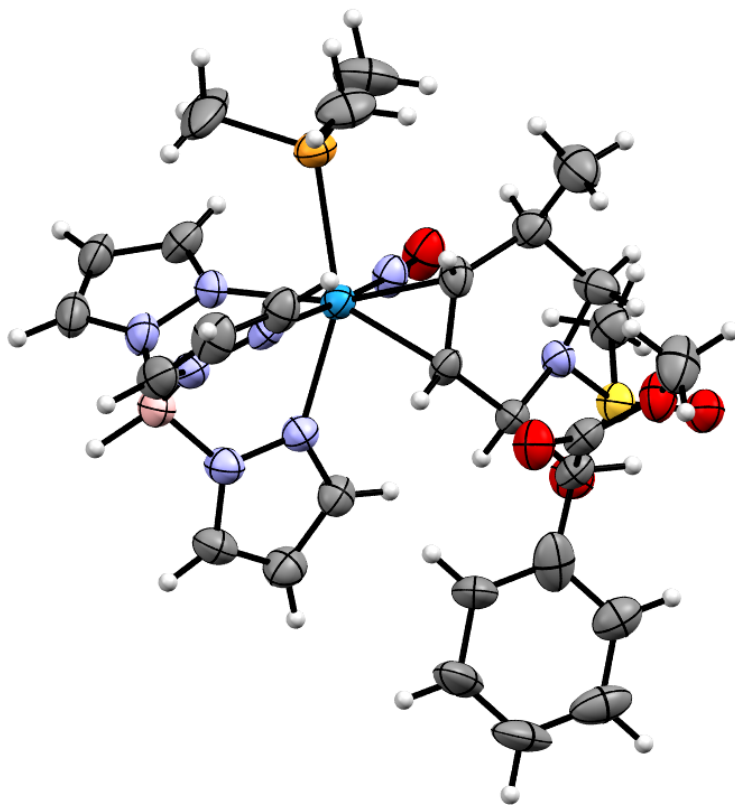
CCDC 2256165	Chemical Formula $C_{28}H_{37}BF_3N_8O_8PS_2W$	FW (g/mol) 961.52
T (K) 200(2)	$\lambda$ (Å) 1.54178	Crystal size (mm) 0.057 x 0.081 x 0.092
Crystal habit Colorless plate-like	Crystal system monoclinic	Space group P 2 <sub>1</sub> /c
a (Å) 15.1929(6)	b (Å) 16.8559(7)	c (Å) 15.1263(6)
$\alpha$ (°) 90	$\beta$ (°) 106.0660(10)	$\gamma$ (°) 90
V (Å <sup>3</sup> ) 3722.4(3)	Z 4	$\rho_{calc}$ (g/cm <sup>3</sup> ) 1.716
$\mu$ (mm <sup>-1</sup> ) 7.851	F(000) 1914	$\theta$ range (°) 3.03 to 68.420
Index ranges -18 ≤ h ≤ 17 0 ≤ k ≤ 20 0 ≤ l ≤ 18	Data/restraints/parameters 6825 / 688 / 622	Goodness-of-fit on F <sup>2</sup> 1.061
R <sub>1</sub> [I > 2σ(I)] 0.0402	wR <sub>2</sub> [all data] 0.1196	



ORTEP/ellipsoid diagram of **38**.

SC-XRD data for **38**.

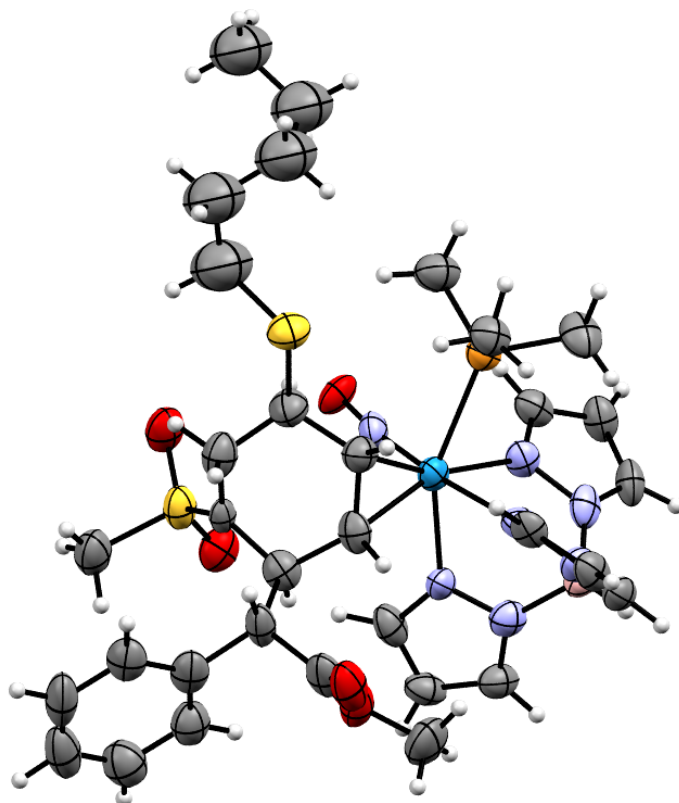
CCDC 2256166	Chemical Formula $C_{27}H_{38}BN_8O_5PSW$	FW (g/mol) 812.34
T (K) 100(2)	$\lambda$ (Å) 0.71073	Crystal size (mm) 0.055 x 0.065 x 0.073
Crystal habit Colorless plate	Crystal system triclinic	Space group P -1
a (Å) 10.8643(5)	b (Å) 12.0141(6)	c (Å) 13.3520(7)
$\alpha$ (°) 92.992(2)	$\beta$ (°) 93.154(2)	$\gamma$ (°) 113.706(2)
V (Å <sup>3</sup> ) 1588.02(14)	Z 2	$\rho_{calc}$ (g/cm <sup>3</sup> ) 1.699
$\mu$ (mm <sup>-1</sup> ) 3.804	F(000) 812	$\theta$ range (°) 2.05 to 27.89
Index ranges -14 ≤ h ≤ 12 -15 ≤ k ≤ 15 -17 ≤ l ≤ 17	Data/restraints/parameters 7570 / 0 / 413	Goodness-of-fit on F <sup>2</sup> 1.055
R <sub>1</sub> [I > 2σ(I)] 0.0396	wR <sub>2</sub> [all data] 0.0792	



ORTEP/ellipsoid diagram of **42**.

SC-XRD data for **42**.

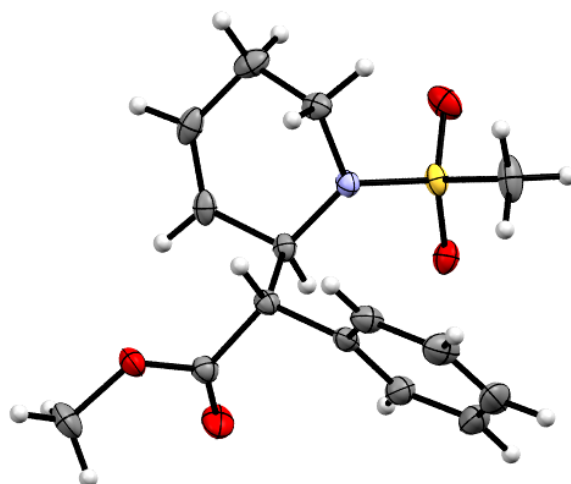
CCDC 2256167	Chemical Formula $C_{28}H_{40}BN_8O_5PSW$	FW (g/mol) 826.37
T (K) 100(2)	$\lambda$ (Å) 1.54178	Crystal size (mm) 0.037 x 0.054 x 0.070
Crystal habit clear yellow needle	Crystal system triclinic	Space group P -1
a (Å) 8.6828(4)	b (Å) 12.4253(5)	c (Å) 16.5767(8)
$\alpha$ (°) 78.170(3)	$\beta$ (°) 77.152(4)	$\gamma$ (°) 71.616(4)
V (Å <sup>3</sup> ) 1636.96(14)	Z 2	$\rho_{calc}$ (g/cm <sup>3</sup> ) 1.677
$\mu$ (mm <sup>-1</sup> ) 8.020	F(000) 828	$\theta$ range (°) 2.76 to 67.72
Index ranges -10 ≤ h ≤ 10 -14 ≤ k ≤ 14 -19 ≤ l ≤ 19	Data/restraints/parameters 5819 / 162 / 454	Goodness-of-fit on F <sup>2</sup> 0.997
R <sub>1</sub> [I > 2σ(I)] 0.0457	wR <sub>2</sub> [all data] 0.1192	



ORTEP/ellipsoid diagram of **48**.

SC-XRD data for **48**.

CCDC 2256168	Chemical Formula $C_{32}H_{48}BN_8O_5PS_2W$	FW (g/mol) 914.53
T (K) 100(2)	$\lambda$ (Å) 0.71073	Crystal size (mm) 0.043 x 0.047 x 0.071
Crystal habit translucent colorless needle	Crystal system orthorhombic	Space group P 2 <sub>1</sub> 2 <sub>1</sub> 2 <sub>1</sub>
a (Å) 10.6315(5)	b (Å) 20.7318(12)	c (Å) 21.6035(12)
$\alpha$ (°) 90	$\beta$ (°) 90	$\gamma$ (°) 90
V (Å <sup>3</sup> ) 4761.6(4)	Z 4	$\rho_{calc}$ (g/cm <sup>3</sup> ) 1.273
$\mu$ (mm <sup>-1</sup> ) 2.586	F(000) 1844	$\theta$ range (°) 1.97 to 25.69
Index ranges -12 ≤ h ≤ 12 -25 ≤ k ≤ 25 -26 ≤ l ≤ 26	Data/restraints/parameters 9030 / 28 / 459	Goodness-of-fit on F <sup>2</sup> 1.058
R <sub>1</sub> [I > 2σ(I)] 0.0422	wR <sub>2</sub> [all data] 0.1021	

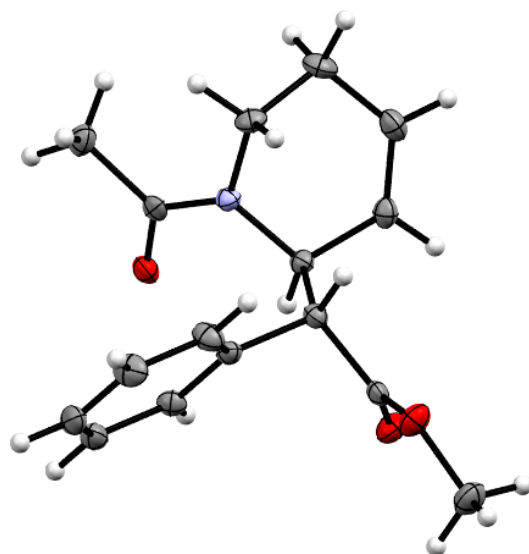


ORTEP/ellipsoid diagram of **50-Ms**.

SC-XRD data for **50-Ms**.

CCDC 2256169	Chemical Formula $C_{15}H_{19}NO_4S$	FW (g/mol) 309.37
T (K) 100(2)	$\lambda$ (Å) 1.54178	Crystal size (mm) 0.100 x 0.222 x 0.438
Crystal habit Colorless plate	Crystal system monoclinic	Space group P 2 <sub>1</sub> /c
a (Å) 13.4105(4)	b (Å) 8.4916(3)	c (Å) 13.0180(4)
$\alpha$ (°) 90	$\beta$ (°) 94.6520(10)	$\gamma$ (°) 90
V (Å <sup>3</sup> ) 1477.56(8)	Z 4	$\rho_{\text{calc}}$ (g/cm <sup>3</sup> ) 1.391
$\mu$ (mm <sup>-1</sup> ) 2.090	F(000) 656	$\theta$ range (°) 3.31 to 72.31
Index ranges -16 ≤ h ≤ 16 -10 ≤ k ≤ 10 -16 ≤ l ≤ 16	Data/restraints/parameters 2912 / 0 / 192	Goodness-of-fit on F <sup>2</sup> 1.052
R <sub>1</sub> [I > 2σ(I)] 0.0297	wR <sub>2</sub> [all data] 0.0797	

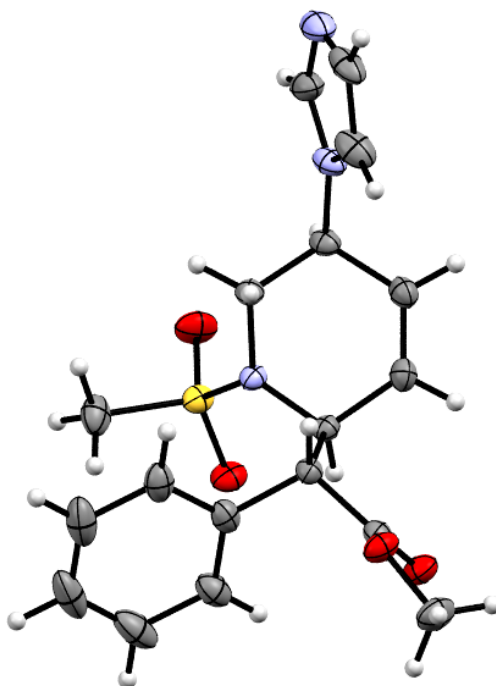




ORTEP/ellipsoid diagram of **50-Ac**.

SC-XRD data for **50-Ac**.

CCDC 2260260	Chemical Formula $C_{16}H_{19}NO_3$	FW (g/mol) 273.32
T (K) 100(2)	$\lambda$ (Å) 1.54178	Crystal size (mm) 0.076 x 0.081 x 0.422
Crystal habit colorless rod	Crystal system monoclinic	Space group C 2/c
a (Å) 22.6503(8)	b (Å) 5.8701(2)	c (Å) 21.6027(8)
$\alpha$ (°) 90	$\beta$ (°) 96.692(3)	$\gamma$ (°) 90
V (Å <sup>3</sup> ) 2852.72(18)	Z 8	$\rho_{\text{calc}}$ (g/cm <sup>3</sup> ) 1.273
$\mu$ (mm <sup>-1</sup> ) 0.711	F(000) 1168	$\theta$ range (°) 3.93 to 68.30
Index ranges -27 ≤ h ≤ 27 -7 ≤ k ≤ 7 -23 ≤ l ≤ 26	Data/restraints/parameters 2596 / 0 / 183	Goodness-of-fit on F <sup>2</sup> 1.047
R <sub>1</sub> [I > 2σ(I)] 0.0382	wR <sub>2</sub> [all data] 0.1003	



ORTEP/ellipsoid diagram of **51**.

SC-XRD data for **51**.

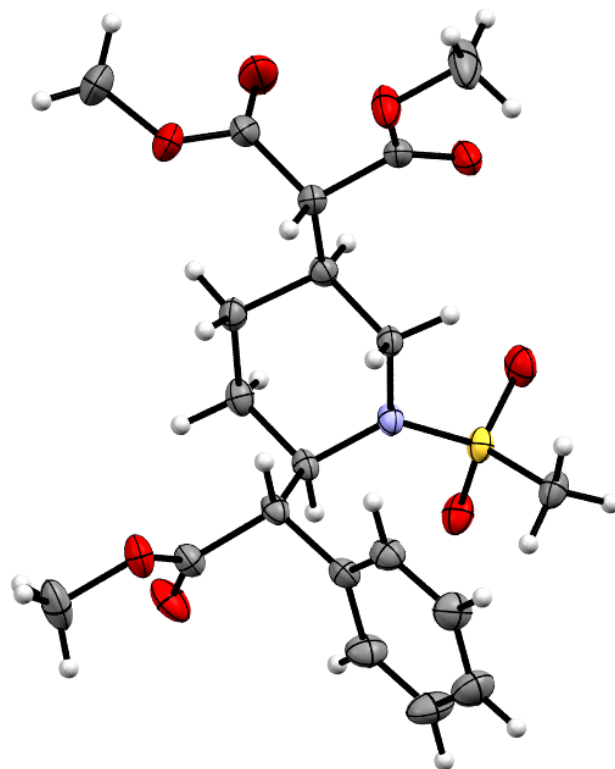
CCDC 2256170	Chemical Formula $C_{18}H_{21}N_3O_4S$	FW (g/mol) 375.44
T (K) 100.0	$\lambda$ (Å) 0.71073	Crystal size (mm) $0.163 \times 0.1 \times 0.076$
Crystal habit yellow plate	Crystal system monoclinic	Space group $P2_1/c$
a (Å) 10.9884(3)	b (Å) 13.2829(4)	c (Å) 12.9404(3)
$\alpha$ (°) 90	$\beta$ (°) 91.6820(10)	$\gamma$ (°) 90
V (Å <sup>3</sup> ) 1887.94(9)	Z 4	$\rho_{\text{calc}}$ (g/cm <sup>3</sup> ) 1.321
$\mu$ (mm <sup>-1</sup> ) 0.199	F(000) 792.0	$\theta$ range (°) 4.396 to 56.574
Index ranges -14 ≤ h ≤ 14 -17 ≤ k ≤ 17 -15 ≤ l ≤ 17	Data/restraints/parameters 4683 / 0 / 237	Goodness-of-fit on F <sup>2</sup> 1.050
R <sub>1</sub> [I > 2σ(I)] 0.0466	wR <sub>2</sub> [all data] 0.1331	



ORTEP/ellipsoid diagram of **55**.

SC-XRD data for **55**.

CCDC 2256171	Chemical Formula $C_{15}H_{21}NO_4S$	FW (g/mol) 311.39
T (K) 100(2)	$\lambda$ (Å) 0.71073	Crystal size (mm) 0.096 x 0.155 x 0.261
Crystal habit colorless block	Crystal system triclinic	Space group P -1
a (Å) 8.7149(3)	b (Å) 9.2516(3)	c (Å) 10.3319(4)
$\alpha$ (°) 89.9360(10)	$\beta$ (°) 67.2660(10)	$\gamma$ (°) 80.0590(10)
V (Å <sup>3</sup> ) 754.80(5)	Z 2	$\rho_{\text{calc}}$ (g/cm <sup>3</sup> ) 1.370
$\mu$ (mm <sup>-1</sup> ) 0.230	F(000) 332	$\theta$ range (°) 2.14 to 29.59
Index ranges -12 ≤ h ≤ 12 -12 ≤ k ≤ 12 -14 ≤ l ≤ 14	Data/restraints/parameters 4232 / 0 / 192	Goodness-of-fit on F <sup>2</sup> 1.024
R <sub>1</sub> [I > 2σ(I)] 0.0326	wR <sub>2</sub> [all data] 0.0851	



ORTEP/ellipsoid diagram of **56**.

SC-XRD data for **56**.

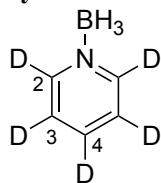
CCDC 2256172	Chemical Formula $C_{20}H_{27}NO_8S$	FW (g/mol) 441.48
T (K) 100(2)	$\lambda$ (Å) 1.54178	Crystal size (mm) 0.027 x 0.049 x 0.249
Crystal habit colorless needle	Crystal system monoclinic	Space group I a
a (Å) 13.1713(3)	b (Å) 8.4679(2)	c (Å) 19.5697(7)
$\alpha$ (°) 90	$\beta$ (°) 90.4740(10)	$\gamma$ (°) 90
V (Å <sup>3</sup> ) 2182.60(11)	Z 4	$\rho_{\text{calc}}$ (g/cm <sup>3</sup> ) 1.344
$\mu$ (mm <sup>-1</sup> ) 1.721	F(000) 936	$\theta$ range (°) 6.21 to 72.12
Index ranges -16 ≤ h ≤ 14 -10 ≤ k ≤ 10 -23 ≤ l ≤ 24	Data/restraints/parameters 4215 / 2 / 275	Goodness-of-fit on F <sup>2</sup> 1.035
R <sub>1</sub> [I > 2σ(I)] 0.0306	wR <sub>2</sub> [all data] 0.0812	

# Appendix D

## Chapter 4 Data

## Compound Synthetic Methodologies and Characterizations

### Synthesis and Characterization of $d_5$ -pyridine borane



Conditions adapted from Ramachandran *et al.*<sup>1</sup> on page S6

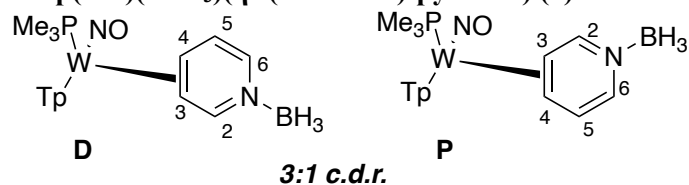
A 1 L Erlenmeyer flask was set up on a hot plate in a fume hood with a 2" stir bar, and stirring was commenced. Finely ground NaBH<sub>4</sub> (33.7 g; 0.89 mol) was added to the flask followed by NaHCO<sub>3</sub> powder (150 g; 1.79 mol) and  $d_5$ -pyridine (50 g; 0.59 mol). This slurry was then diluted with 550 mL of dried THF. A 75 mL addition funnel was positioned over the top of the large flask and filled with dH<sub>2</sub>O (32.5 g; 1.80 mol), which was then added dropwise to the slurry. Bubbling should occur quickly after the dH<sub>2</sub>O begins adding. After all the dH<sub>2</sub>O is added, the slurry was stirred for 23 hours. A 150 mL C frit was set up over a 1 L filter flask and filled with 1" of anhydrous Na<sub>2</sub>SO<sub>4</sub>. The slurry was filtered through this plug, which was then washed an additional 100 mL of dry THF to rinse any residue off the plug. This solution was transferred to a 2L round-bottom flask and reduced to ~60 mL. This solution was added to a 1L separatory funnel, diluted with 300 mL of Et<sub>2</sub>O, and washed 3x with 300 mL of brine. The combined aqueous layers were then back extracted with another 200 mL of Et<sub>2</sub>O. The combined organic layers were then flushed through a silica plug. The silica plug was then washed with an additional 50 mL of Et<sub>2</sub>O. These combined organic layers were dried with anhydrous Na<sub>2</sub>SO<sub>4</sub> and then reduced *in vacuo*. The remaining liquid was then dried under 4Å molecular sieves in an inert N<sub>2</sub> atmosphere. (35.37 g; 60% yield).

<sup>1</sup>H NMR (CD<sub>2</sub>Cl<sub>2</sub>, δ, 25 °C): 2.35-2.86 (q, BH<sub>3</sub>).

<sup>13</sup>C NMR (CD<sub>2</sub>Cl<sub>2</sub>, δ, 25 °C): 146.9 (*t*,  $J_{DC}$  = 28.1 Hz, 2C, C2), 139.1 (*t*,  $J_{DC}$  = 25.6 Hz, 1C, C4), 125.2 (*t*,  $J_{DC}$  = 25.8 Hz, 2C, C3).

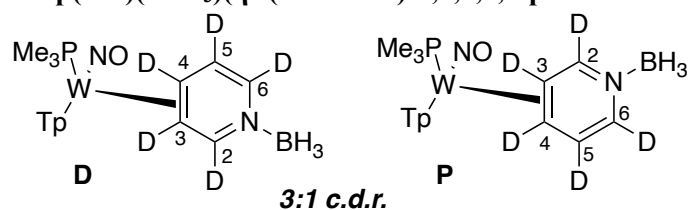
## Synthesis and Characterization of [W] pyridine borane Complexes

### WTP(NO)(PMe<sub>3</sub>)(η<sup>2</sup>-(N-borane)-pyridine) (**2**)



Previously described by Harrison et al.<sup>2</sup> on page S4

### WTP(NO)(PMe<sub>3</sub>)(η<sup>2</sup>-(N-borane)-2,3,4,5,6-pentadeuteropyridine) (*d*<sub>5</sub>-**2**)



An oven-dried round 100 mL bottom flask with a 1" stir egg was charged with **59** (10.4 g, 17.02 mmol), *d*<sub>5</sub>-pyridine borane (50 g, 0.51 mol), and TEA (3.1 g, 30.6 mmol). A yellow slurry was formed initially that gradually turned into a dark green/brown solution, which was stirred for 68 hours and monitored by <sup>31</sup>P NMR. After stirring, the solution was added to a 2L filter flask containing a 2" stir bar. To this filter flask was added 100 mL of dry THF, 400 mL of Et<sub>2</sub>O, and 1 L of hexanes. This solution was stirred for 5 minutes and then allowed to settle for 15 minutes. Separately, a 2" celite plug was set up in a 150 mL C frit over another 2 L filter flask. After settling, the solution was then slowly poured through the celite plug taking care not to pour the lower thick oily layer. The eluent of the solution was discarded. This constituted 1x "dilution," which was designed to remove excess pyridine borane ligand away from the coordinated complex. Dilutions were repeated until a yellow powder is precipitated, which required 3x total dilutions. This yellow powder is then collected a 150 mL M frit. The oily residue on the celite plug was then dissolved off the celite plug with 100 mL of DCM. This solution was reduced to ~30 mL added to 200 mL of a 10:1 hexanes/Et<sub>2</sub>O mixture, which precipitated a yellow powder that was isolated on the same frit as the previous fraction. The combined powders were then dried in a desiccator. (7.60 g; 74% yield)

<sup>1</sup>H NMR (CD<sub>2</sub>Cl<sub>2</sub>, δ, 25 °C):

**D**: 7.99 (d, *J* = 1.7 Hz, 1H, Pz3/5), 7.90 (d, *J* = 1.6 Hz, 1H, Pz3/5), 7.85 (d, *J* = 2.3 Hz, 1H, Pz3/5), 7.83 (d, *J* = 2.1 Hz, 1H, Pz3/5), 7.71 (d, *J* = 2.2 Hz, 1H, Pz3/5), 7.16 (d, *J* = 1.8 Hz, 1H, Pz3/5), 6.35 (t, *J* = 2.3 Hz, 1H, Pz4), 6.32 (t, *J* = 2.2 Hz, 1H, Pz4), 6.28 (t, *J* = 2.2 Hz, 1H, Pz4), 1.25 (d, *J*<sub>PH</sub> = 8.4 Hz, 9H, PMe<sub>3</sub>).

**P**: 8.14 (s, 1H, Pz3/5), 7.91 (s, 1H, Pz3/5), 7.85 (s, 1H, Pz3/5), 7.84 (buried, 1H, Pz3/5), 7.73 (s, 1H, Pz3/5), 7.16 (s, 1H, Pz3/5), 6.35 (s, 1H, Pz4), 6.30 (s, 1H, Pz4), 6.27 (s, 1H, Pz4), 1.31 (d, *J*<sub>PH</sub> = 8.2 Hz, 9H, PMe<sub>3</sub>).

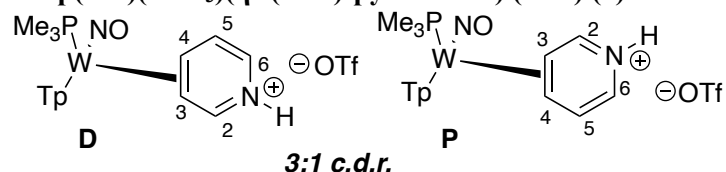
<sup>13</sup>C NMR (CD<sub>2</sub>Cl<sub>2</sub>, δ, 25 °C):

**D**: 169.4 (t, *J*<sub>DC</sub> = 26.5 Hz, C2), 144.5 (d, *J*<sub>PC</sub> = 1.5 Hz, PzB3), 144.4 (Pz3/5), 140.6 (Pz3/5), 137.5 (Pz3/5), 137.1 (Pz3/5), 136.2 (Pz3/5), 126.5 (t, *J*<sub>DC</sub> = 27.7 Hz, C6), 125.0 (t, *J*<sub>DC</sub> = 24.0 Hz, C5), 107.1 (Pz4), 106.8 (Pz4), 106.7 (Pz4), 60.4 (t, *J*<sub>DC</sub> = 20.6 Hz, C4), 57.4 (t, *J*<sub>DC</sub> = 23.6 Hz, C3), 13.1 (d, *J*<sub>PC</sub> = 28.7 Hz, 3C, PMe<sub>3</sub>).

**P**: <Not reported due to peaks being too small in the baseline or ambiguous>

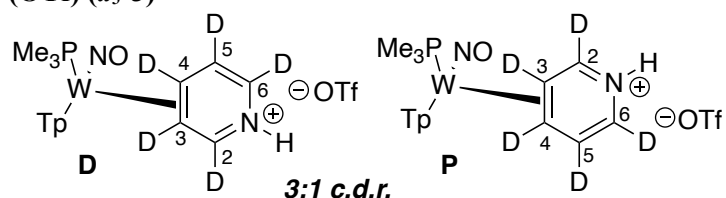
## Synthesis and Characterization of [W] pyridinium Complexes

### WTP(NO)(PMe<sub>3</sub>)(η<sup>2</sup>-(N-H)-pyridinium) (OTf) (**3**)



Previously synthesized by Harrison *et al.*<sup>2</sup> on page S5 and characterized by Delafuente *et al.*<sup>3</sup> on page 415

### Synthesis and characterization of WTP(NO)(PMe<sub>3</sub>)(η<sup>2</sup>-(N-H)-2,3,4,5,6-pentadeuteropyridinium) (OTf) (*d*<sub>5</sub>-**3**)



A 1 L Erlenmeyer flask containing a 2" stir bar was set up over a hot plate. 400 mL of Et<sub>2</sub>O and **2** (7.6 g; 12.65 mmol) were added to the flask and stirred for 1 hour to loosen the clumps of tungsten in an evenly stirred slurry. DPhAT (4.24 g, 13.28 mmol) to a tared 4-dram vial along with acetone (22 g, 378.79 mmol). This solution was pipetted until homogenous and then slowly added to the slurry. Bubbling commenced immediately followed by a gradual color change from a yellow slurry to an orange slurry. This was stirred for 90 minutes. Upon completion, this powder was collected on a 150 mL M frit and dried in a desiccator. (9.035 g; 97% yield)

<sup>1</sup>H NMR (CD<sub>2</sub>Cl<sub>2</sub>, δ, 25 °C):

**D**: 11.96 (br s, 1H, N-H), 8.21 (s, 1H, Pz3/5), 8.19 (s, 1H, Pz3/5), 8.08 (s, 1H, Pz3/5), 8.04 (s, 1H, Pz3/5), 8.02 (s, 1H, Pz3/5), 7.78 (s, 1H, Pz3/5), 6.48 (t, *J* = 2.0 Hz, 1H, Pz4), 6.45 (t, *J* = 2.0 Hz, 1H, Pz4), 6.44 (t, *J* = 2.1 Hz, 1H, Pz4), 1.18 (d, *J*<sub>PH</sub> = 9.1 Hz, 9H, PMe<sub>3</sub>).

**P**: 12.38 (br s, 1H, N-H), 8.21 (s, 1H, Pz3/5), 8.19 (s, 1H, Pz3/5), 8.08 (s, 1H, Pz3/5), 8.03 (s, 1H, Pz3/5), 7.97 (s, 1H, Pz3/5), 7.74 (s, 1H, Pz3/5), 6.47 (t, *J* = 2.0 Hz, 1H, Pz4), 6.43 (t, *J* = 2.1 Hz, 1H, Pz4), 6.40 (t, *J* = 2.1 Hz, 1H, Pz4), 1.23 (d, *J* = 8.9 Hz, 9H, PMe<sub>3</sub>).

<sup>13</sup>C NMR (CD<sub>2</sub>Cl<sub>2</sub>, δ, 25 °C):

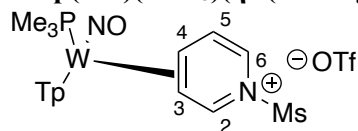
**D**: 168.1 (t, *J*<sub>DC</sub> = 25.9 Hz, C2), 145.3 (Pz3/5), 144.8 (Pz3/5), 141.9 (Pz3/5), 138.1 (Pz3/5), 137.6 (Pz3/5), 136.8 (Pz3/5), 125.9 (t, *J*<sub>DC</sub> = 23.3 Hz, C5), 120.7 (q, *J*<sub>FC</sub> = 322.1 Hz, -OTf), 115.7 (t, *J*<sub>DC</sub> = 26.7 Hz, C6), 107.5 (Pz4), 107.1 (Pz4), 106.8 (Pz4), 64.9 (br s, C4), 57.0 (br s, C3), 11.8 (d, *J*<sub>PC</sub> = 29.9 Hz, 3C, PMe<sub>3</sub>).

**P**: 163.2 (br s, C2), 144.5 (Pz3/5), 141.8 (Pz3/5), 140.7 (Pz3/5), 138.0 (Pz3/5), 137.4 (Pz3/5), 136.7 (Pz3/5), 128.5 (br s, C5), 113.5 (br s, C6), 107.3 (Pz4), 107.0 (Pz4), 106.4 (Pz4), 61.9 (br s, C4), 59.0 (br s, C3), 12.2 (d, *J*<sub>PC</sub> = 29.4 Hz, 3C, PMe<sub>3</sub>).



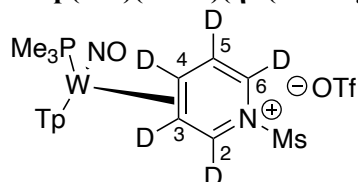
## Synthesis and Characterization of [W] (*N*-mesyl) pyridinium Complexes

### WTP(NO)(PMe<sub>3</sub>)(η<sup>2</sup>-(*N*-mesyl)-pyridinium) (OTf) (33D)



Previously described on page 196.

### WTP(NO)(PMe<sub>3</sub>)(η<sup>2</sup>-(*N*-mesyl)-2,3,4,5,6-pentadeuteropyridinium) (OTf) (*d*<sub>5</sub>-33D)



Ms<sub>2</sub>O (5.36g, 30.77 mmol), **3** (9.035 g, 12.26 mmol), and EtCN (30 mL) were charged to a flame-dried 100 mL round-bottom flask with a 1 inch stir bar. Lutidine (3.36 g, 31.36 mmol) was added to initiate the reaction, and the flask was submerged in a pre-heated oil bath set to 55 °C. After stirring the solution for ~2 hours, the solution was diluted with 150 mL of DCM and added to a separatory funnel. This solution was washed 3x with 200 mL of saturated aqueous NaHCO<sub>3</sub>. The organic layer was isolated and set aside. The combined aqueous layers were combined and back-extracted with 50 mL of DCM to prevent loss of product. The organic layers were combined in a single flask and dried with anhydrous MgSO<sub>4</sub>. This powder was then filtered off into a 60 mL coarse porosity fritted funnel and washed with DCM. The dried organic layers were then reduced *in vacuo* down to dryness. The residue in the flask was redissolved in minimal DCM (approximately 10 mL). The solution was then slowly added to 500mL of stirring Et<sub>2</sub>O. An orange precipitate formed immediately and was allowed to stir for ~10 minutes to ensure total precipitation. This powder was collected on a 60 mL medium porosity frit and washed 2x with 30 mL of ether. This powder was dried in a desiccator under vacuum for ~30 minutes. The dried powder was gently added to a stirring solution of 150 mL of HPLC grade EtOAc and triturated overnight. The final orange precipitate was collected on the F frit, washed 2x with 30 mL of ethyl acetate and 2x with 30 mL of Et<sub>2</sub>O, and dried in the desiccator overnight under vacuum. (5.3 g, 53% yield)

<sup>1</sup>H NMR (CD<sub>2</sub>Cl<sub>2</sub>, δ, 25 °C): 7.96 (d, *J* = 2.2 Hz, 1H, PzB3), 7.96 (d, *J* = 2.3 Hz, 1H, PzC5), 7.93 (d, *J* = 2.4 Hz, 1H, PzB5), 7.90 (d, *J* = 2.1 Hz, 1H, PzA3), 7.76 (d, *J* = 2.3 Hz, 1H, PzA5), 7.64 (d, *J* = 2.0 Hz, 1H, PzC3), 6.47 (t, *J* = 2.3 Hz, 1H, PzC4), 6.44 (t, *J* = 2.3 Hz, 1H, PzB4), 6.37 (t, *J* = 2.3 Hz, 1H, PzA4), 3.61 (s, 3H, Ms), 1.25 (d, *J*<sub>PH</sub> = 9.2 Hz, 9H, PMe<sub>3</sub>).

<sup>13</sup>C NMR (CD<sub>2</sub>Cl<sub>2</sub>, δ, 25 °C): 167.2 (t, *J*<sub>CD</sub> = 27.6 Hz, C2), 146.5 (PzA3), 145.6 (d, *J*<sub>PC</sub> = 1.9 Hz, PzB3), 141.7 (PzC3), 138.7 (PzC5), 138.5 (PzB5), 137.6 (A5), 123.3 (t, *J*<sub>CD</sub> = 25.1 Hz, C5), 121.3 (q, *J*<sub>CF</sub> = 322.1 Hz, OTf), 114.7 (t, *J*<sub>CD</sub> = 29.2 Hz, C6), 108.2 (PzC4), 108.1 (PzB4), 107.8 (PzA4), 66.1-66.5 (m, C4), 65.4 (t, *J*<sub>CD</sub> = 26.3 Hz, C3), 43.9 (Ms), 12.9 (d, *J*<sub>PC</sub> = 31.5 Hz, 3C, PMe<sub>3</sub>).

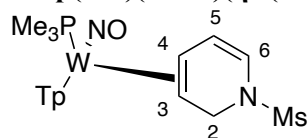
HRMS (ESI) *m/z*: [M]<sup>+</sup> Calcd for C<sub>18</sub>H<sub>22</sub>D<sub>5</sub>BN<sub>8</sub>O<sub>3</sub>PSW<sup>+</sup> 666.1575; Found 666.1581

## Synthesis and Characterization of [W] 1,2-DHP Complexes

### General Synthesis

Two separate solutions were prepared in two 30 mL glass screw-cap test tubes. Tube A was comprised of **33D/d<sub>5</sub>-33D** (967 mg, 1.19 mmol) dissolved in EtCN and Tube B was a heterogeneous slurry of NaBH<sub>4</sub>/NaBD<sub>4</sub> (4.49 mmol) in dry THF (2 mL). After both tubes were chilled in a 0 °C toluene bath for 15 minutes, Tube B slurry was added to Tube A, and the tube sat for 30 minutes. The solution was diluted with 150 mL of DCM and added to a separatory funnel. This solution was washed 3x with 200 mL of saturated aqueous NaHCO<sub>3</sub>. The organic layer was isolated and set aside. The combined aqueous layers were combined and back-extracted with 50 mL of DCM to prevent loss of product. The organic layers were combined in a single flask and dried with anhydrous MgSO<sub>4</sub>. This powder was then filtered off into a 60 mL coarse porosity fritted funnel and washed with DCM. The dried organic layers were then reduced *in vacuo* to dryness. The residue in the flask was redissolved in minimal DCM (approximately 10 mL). The solution was then slowly added to a stirring 200mL solution of 9:1 pentane/Et<sub>2</sub>O. A tan precipitate formed immediately and was allowed to stir for ~10 minutes to ensure total precipitation. This powder was collected on a 60 mL medium porosity frit and washed 2x with 30 mL of pentane. This powder was dried in a desiccator under vacuum overnight. (625 mg, 79% yield)

### WTp(NO)(PMe<sub>3</sub>)(η<sup>2</sup>-(*N*-mesyl)-1,2-dihydropyridine) (**60D**)



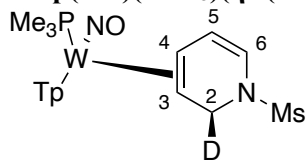
<sup>1</sup>H NMR (CD<sub>2</sub>Cl<sub>2</sub>, δ, 25 °C): 8.09 (d, *J* = 1.8 Hz, 1H, PzA3), 8.03 (d, *J* = 1.8 Hz, 1H, PzB3), 7.77 (d, *J* = 2.3 Hz, 1H, PzB5), 7.75 (d, *J* = 2.2 Hz, 1H, PzC5), 7.67 (d, *J* = 2.3 Hz, 1H, PzA5), 7.31 (d, *J* = 2.0 Hz, 1H, PzC3), 6.34 (t, *J* = 2.2 Hz, 1H, PzB4), 6.27 (t, *J* = 2.2 Hz, 1H, PzA4), 6.23 (t, *J* = 2.2 Hz, 1H, PzC4), 6.01 (d, *J* = 7.8 Hz, 1H, H6), 5.78 (dd, *J* = 4.4, 7.8 Hz, 1H, H5), 4.60 (dd, *J* = 2.6, 11.6 Hz, 1H, H2), 4.58 (dd, *J* = 4.6, 11.6 Hz, 1H, H2'), 2.95 (s, 3H, Ms), 2.72 (ddd, *J* = 4.4, 10.4, 12.4 Hz, 1H, H4), 1.53-1.57 (m, 1H, H3), 1.24 (d, *J*<sub>PH</sub> = 8.4 Hz, 9H, PMe<sub>3</sub>).

<sup>13</sup>C NMR (CD<sub>2</sub>Cl<sub>2</sub>, δ, 25 °C): 143.7 (d, *J*<sub>PC</sub> = 2.2 Hz, PzB3), 143.1 (PzA3), 140.5 (PzC3), 137.0 (PzB5), 136.5 (PzC5), 136.0 (PzA5), 119.0 (C6), 114.6 (d, *J*<sub>PC</sub> = 3.6 Hz, C5), 106.8 (PzB4), 106.3 (PzA4/C4), 106.2 (PzA4/C4), 52.3 (*J*<sub>WC</sub> = 16.4 Hz, C3), 47.2, (C2), 46.5 (*J*<sub>PC</sub> = 10.8 Hz, C4), 37.9 (Ms), 13.7 (d, *J*<sub>PC</sub> = 28.1 Hz, 3C, PMe<sub>3</sub>).

IR ν(NO) = 1567 cm<sup>-1</sup>

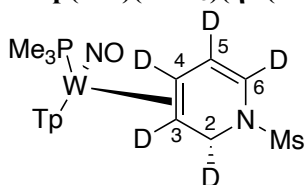
CV (DMA; 100 mV/s) *E*<sub>pa</sub> = +0.45 V (NHE)

SC-XRD Data on page 359

**WTp(NO)(PMe<sub>3</sub>)(η<sup>2</sup>-(*N*-mesyl)-2-*anti*-deutero-1,2-dihydropyridine) (*d*<sub>1</sub>-60D)**

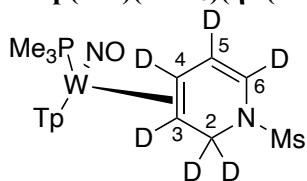
<sup>1</sup>H NMR (CD<sub>2</sub>Cl<sub>2</sub>, δ, 25 °C): 8.09 (d, *J* = 2.0 Hz, 1H, PzA3), 8.03 (d, *J* = 2.0 Hz, 1H, PzB3), 7.77 (d, *J* = 2.3 Hz, 1H, PzB5), 7.75 (d, *J* = 2.3 Hz, 1H, PzC5), 7.67 (d, *J* = 2.4 Hz, 1H, PzA5), 7.31 (d, *J* = 2.2 Hz, 1H, PzC3), 6.34 (t, *J* = 2.2 Hz, 1H, PzB4), 6.27 (t, *J* = 2.2 Hz, 1H, PzA4), 6.23 (t, *J* = 2.2 Hz, 1H, PzC4), 6.01 (d, *J* = 7.8 Hz, 1H, H6), 5.78 (dd, *J* = 4.4, 7.8 Hz, 1H, H5), 4.58 (s, 1H, H2), 2.95 (s, 3H, Ms), 2.72 (ddd, *J* = 4.4, 10.3, 12.3 Hz, 1H, H4), 1.52-1.56 (m, 1H, H3), 1.24 (d, *J*<sub>PH</sub> = 8.4 Hz, 9H, PMe<sub>3</sub>).

<sup>13</sup>C NMR (CD<sub>2</sub>Cl<sub>2</sub>, δ, 25 °C): 143.7 (d, *J*<sub>PC</sub> = 2.2 Hz, PzB3), 143.2 (PzA3), 140.5 (PzC3), 137.0 (PzB5), 136.5 (PzC5), 136.0 (PzA5), 119.1 (C6), 114.7 (d, *J*<sub>PC</sub> = 3.0 Hz, C5), 106.8 (PzB4), 106.3 (PzA4/C4), 106.2 (PzA4/C4), 52.0 (*J*<sub>WC</sub> = 32.8 Hz, C3), 46.9 (t, *J*<sub>DC</sub> = 21.0 Hz, C2), 46.6 (d, *J*<sub>PC</sub> = 10.8 Hz, C4), 37.9 (Ms), 13.7 (d, *J*<sub>PC</sub> = 28.0 Hz, 3C, PMe<sub>3</sub>).

**WTp(NO)(PMe<sub>3</sub>)(η<sup>2</sup>-(*N*-mesyl)-2-*syn*-3,4,5,6-pentadeutero-1,2-dihydropyridine) (*d*<sub>5</sub>-60D)**

<sup>1</sup>H NMR (CD<sub>2</sub>Cl<sub>2</sub>, δ, 25 °C): 8.10 (d, *J* = 1.7 Hz, 1H, PzA3), 8.04 (d, *J* = 1.9 Hz, 1H, PzB3), 7.78 (d, *J* = 2.2 Hz, 1H, PzB5), 7.76 (d, *J* = 2.1 Hz, 1H, PzC5), 7.68 (d, *J* = 2.3 Hz, 1H, PzA5), 7.31 (d, *J* = 2.0 Hz, 1H, PzC3), 6.34 (t, *J* = 2.1 Hz, 1H, PzB4), 6.26 (t, *J* = 2.2 Hz, 1H, PzA4), 6.24 (t, *J* = 2.1 Hz, 1H, PzC4), 4.56 (s, 1H, H2), 2.96 (s, 3H, Ms), 1.24 (d, *J*<sub>PH</sub> = 8.4 Hz, 9H, PMe<sub>3</sub>).

<sup>13</sup>C NMR (CD<sub>2</sub>Cl<sub>2</sub>, δ, 25 °C): 143.7 (d, *J*<sub>PC</sub> = 2.0 Hz, PzB3), 143.1 (PzA3), 140.5 (PzC3), 137.0 (PzB5), 136.5 (PzC5), 136.0 (PzA5), 118.5 (t, *J*<sub>DC</sub> = 27.7 Hz, C6), 114.1 (t, *J*<sub>DC</sub> = 24.0 Hz, C5), 106.7 (PzB4), 106.3 (PzA4/C4), 106.2 (PzA4/C4), 51.7 (t, *J*<sub>DC</sub> = 21.9 Hz, C3), 46.7 (t, *J*<sub>DC</sub> = 21.7 Hz, C2), 45.5-45.9 (m, C4), 37.8 (Ms), 13.7 (d, *J*<sub>PC</sub> = 28.1 Hz, 9H, PMe<sub>3</sub>).

**WTp(NO)(PMe<sub>3</sub>)(η<sup>2</sup>-(*N*-mesyl)-2,2,3,4,5,6-hexadeutero-1,2-dihydropyridine) (*d*<sub>6</sub>-60D)**

<sup>1</sup>H NMR (CD<sub>2</sub>Cl<sub>2</sub>, δ, 25 °C): 8.10 (s, 3H, PzA3), 8.03 (s, 3H, PzB3), 7.78 (d, *J* = 1.9 Hz, 1H, PzB5), 7.76 (d, *J* = 1.8 Hz, 1H, PzC5), 7.68 (d, *J* = 2.0 Hz, 1H, PzA5), 7.32 (s, 1H, PzC3), 6.34 (t, *J* = 2.0 Hz, 1H, PzB4), 6.26 (t, *J* = 2.0 Hz, 1H, PzA4), 6.24 (t, *J* = 1.9 Hz, 1H, PzC4), 2.96 (s, 3H, Ms), 1.24 (d, *J*<sub>PH</sub> = 8.5 Hz, 9H, PMe<sub>3</sub>).

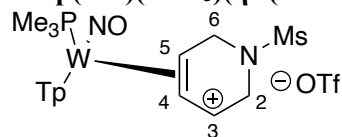
<sup>13</sup>C NMR (CD<sub>2</sub>Cl<sub>2</sub>, δ, 25 °C): 143.6 (d, *J*<sub>PC</sub> = 2.2 Hz, 1C, PzB3), 143.1 (PzA3), 140.5 (PzC3), 137.0 (PzB5), 136.4 (PzC5), 135.9 (PzA5), 118.6 (t, *J*<sub>DC</sub> = 27.4 Hz, 1C, C6), 114.1 (t, *J*<sub>DC</sub> = 23.6 Hz, 1C, C5), 106.7 (PzB4), 106.3 (PzA4/C4), 106.2 (PzA4/C4), 51.2 (t, *J*<sub>DC</sub> = 22.1 Hz, 1C, C3), 46.4 (t, *J*<sub>DC</sub> = 21.2, C2), 45.7-46.0 (m, C4), 37.9 (Ms), 13.7 (d, *J*<sub>PC</sub> = 27.9 Hz, 3C, PMe<sub>3</sub>).

## Synthesis and Characterization of [W] 1,2,6-allyl Complexes

### General Synthesis

An oven-dried 4-dram vial containing a stir pea was tared, and ***d<sub>x</sub>*-60D** (275 mg, 0.41 mmol) was massed out and diluted with dried MeCN (2 mL). To a separate 4-dram vial was added dried MeCN (1 mL) and TfOH<sup>x</sup> (63 mg, 0.42 mmol). The acid/MeCN solution was slowly added to the ***d<sub>x</sub>*-60D**/MeCN solution and stirred until solution was homogenous (about 2 minutes). The reaction was then slowly added to 100 mL of stirring Et<sub>2</sub>O, which immediately formed a tan precipitate. This powder was triturated for 5 minutes and then collected on a 30 mL medium porosity frit. The collected powder was then washed 2x with 20 mL of Et<sub>2</sub>O and dried overnight in a desiccator. (300 mg, 89% yield)

### WTp(NO)(PMe<sub>3</sub>)(η<sup>3</sup>-(*N*-mesyl)-1,2,3,6-tetrahydropyridinium (OTf) (61)



<sup>1</sup>H NMR (CD<sub>2</sub>Cl<sub>2</sub>, δ, 25 °C): 8.35 (d, *J* = 2.1 Hz, 1H, PzB3), 8.13 (d, *J* = 2.2 Hz, 1H, PzC3), 7.98 (d, *J* = 2.2 Hz, 1H, PzA3), 7.94 (d, *J* = 2.3 Hz, 1H, PzC5), 7.87 (d, *J* = 2.4 Hz, 1H, PzB5), 7.71 (d, *J* = 2.4 Hz, 1H, PzA5), 6.58 (t, *J* = 2.3 Hz, 1H, PzC4), 6.52 (t, *J* = 2.3 Hz, 1H, PzB4), 6.44 (d, *J* = 7.2 Hz, 1H, H3), 6.31 (t, *J* = 2.3 Hz, 1H, PzA4), 5.10 (t, *J* = 7.7 Hz, 2H, H4), 4.90 (d, *J* = 18.1 Hz, 1H, H2), 4.81 (dd, *J* = 3.0, 12.6 Hz, 1H, H6), 4.52 (d, *J* = 18.1 Hz, 1H, H2), 4.43-4.47 (m, 1H, H5), 4.00 (dd, *J* = 2.0, 12.7 Hz, 1H, H6), 2.90 (s, 3H, Ms), 1.27 (d, *J<sub>PH</sub>* = 9.7 Hz, 9H, PMe<sub>3</sub>).

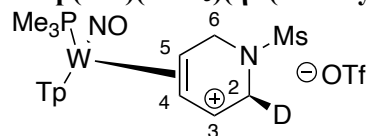
<sup>13</sup>C NMR (CD<sub>2</sub>Cl<sub>2</sub>, δ, 25 °C): 147.9 (PzA3), 144.9 (d, *J<sub>PC</sub>* = 2.2 Hz, PzB3), 142.8 (PzC3), 139.0 (PzC5), 138.8 (PzA5/B5), 138.7 (PzA5/B5), 127.4 (C3), 121.2 (q, *J<sub>FC</sub>* = 321.8 Hz, -OTf), 109.0 (PzB4/C4), 108.9 (PzB4/C4), 107.7 (PzA4), 95.7 (d, *J<sub>PC</sub>* = 2.8 Hz, C4), 65.7 (d, *J<sub>PC</sub>* = 15.3 Hz, C5), 44.7 (C2), 44.1 (d, *J<sub>PC</sub>* = 2.8 Hz, C6), 36.0 (Ms), 13.4 (d, *J<sub>PC</sub>* = 32.4 Hz, 3C, PMe<sub>3</sub>).

IR: ν(NO) = 1651 cm<sup>-1</sup>

CV: (MeCN; 100 mV/s) *E*<sub>1/2</sub> = -0.78 V (NHE)

Unable to obtain EA, SC-XRD, or HRMS data for compound. Full 2D NMR provided below.

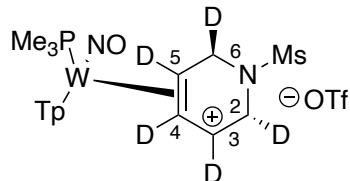
### WTp(NO)(PMe<sub>3</sub>)(η<sup>3</sup>-(*N*-mesyl)-2-*anti*-deutero-1,2,3,6-tetrahydropyridinium (OTf) (*d<sub>T</sub>*-61)



<sup>1</sup>H NMR (d<sub>6</sub>-acetone, δ, 25 °C): 8.61 (d, *J* = 2.2 Hz, 1H, Pz3/5), 8.41-8.42 (m, 2H, Pz3/5), 8.22 (d, *J* = 2.5 Hz, 1H, Pz3/5), 8.16 (d, *J* = 2.4 Hz, 1H, Pz3/5), 7.97 (d, *J* = 2.4 Hz, 1H, Pz3/5), 6.8 (d, *J* = 7.8 Hz, 1H, H3), 6.65 (t, *J* = 2.3 Hz, 1H, Pz4), 6.64 (t, *J* = 2.3 Hz, 1H, Pz4), 6.39 (t, *J* = 2.4 Hz, 1H, Pz4), 5.32 (t, *J* = 7.6 Hz, 1H, H4), 4.92 (s, 1H, H2), 4.88 (dd, *J* = 3.6, 12.8 Hz, 1H, C6), 4.65-4.69 (m, 1H, H5), 4.06 (dd, *J* = 1.9, 12.8 Hz, 1H, H6), 2.96 (s, 3H, Ms), 1.38 (d, *J<sub>PH</sub>* = 9.9 Hz, 9H, PMe<sub>3</sub>).

<sup>13</sup>C NMR (d<sub>6</sub>-acetone, δ, 25 °C): 149.1 (Pz3/5), 146.1 (Pz3/5), 143.6 (Pz3/5), 139.7 (Pz3/5), 139.5 (Pz3/5), 139.4 (Pz3/5), 129.6 (C3), 122.3 (q, *J<sub>FC</sub>* = 322.4 Hz, -OTf), 109.5 (Pz4), 109.1 (Pz4), 108.1 (Pz4), 96.2 (C4), 66.2 (d, *J<sub>PC</sub>* = 14.8 Hz, C5), 44.9 (d, *J<sub>DC</sub>* = 21.1 Hz, C2), 44.7 (d, *J<sub>PC</sub>* = 2.9 Hz, C6), 35.6 (Ms), 13.05 (d, *J<sub>PC</sub>* = 33.1 Hz, 3C, PMe<sub>3</sub>).

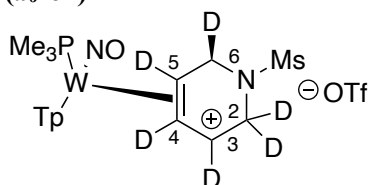
**WTp(NO)(PMe<sub>3</sub>)(η<sup>3</sup>-(*N*-mesyl)-2-*syn*-6-*anti*-3,4,5-pentadeutero-1,2,3,6-tetrahydropyridinium (OTf) (d<sub>5</sub>-61)**



<sup>1</sup>H NMR (CD<sub>2</sub>Cl<sub>2</sub>, δ, 25 °C): 8.35 (d, *J* = 2.1 Hz, 1H, PzB3), 8.12 (d, *J* = 2.2 Hz, 1H, PzC3), 7.99 (d, *J* = 2.2 Hz, 1H, PzA3), 7.94 (d, *J* = 2.3 Hz, 1H, PzC5), 7.87 (d, *J* = 2.4 Hz, 1H, PzB5), 7.71 (d, *J* = 2.4 Hz, 1H, PzA5), 6.57 (t, *J* = 2.3 Hz, 1H, PzC4), 6.52 (t, *J* = 2.3 Hz, 1H, PzB4), 6.31 (t, *J* = 2.3 Hz, 1H, PzA4), 4.52 (s, 1H, H2), 3.97 (s, 1H, H6), 2.90 (s, 3H, Ms), 1.26 (d, *J*<sub>PH</sub> = 9.6 Hz, 9H, PMe<sub>3</sub>).

<sup>13</sup>C NMR (CD<sub>2</sub>Cl<sub>2</sub>, δ, 25 °C): 148.0 (PzA3), 144.9 (PzB3), 142.8 (PzC3), 139.0 (PzC5), 138.8 (PzA5/B5), 138.7 (PzA5/B5), 126.5 (t, *J*<sub>DC</sub> = 25.4 Hz, C3), 121.3 (q, *J*<sub>FC</sub> = 320.7 Hz, -OTf), 108.9 (PzB4/C4), 107.7 (PzA4), 95.4 (t, *J*<sub>DC</sub> = 24.8 Hz, C4), 64.9-65.3 (m, C5), 44.3 (t, *J*<sub>DC</sub> = 22.1 Hz, C2), 43.7 (t, *J*<sub>DC</sub> = 20.8 Hz, C6), 36.0 (Ms), 13.4 (d, *J*<sub>PH</sub> = 33.0 Hz, 3C, PMe<sub>3</sub>).

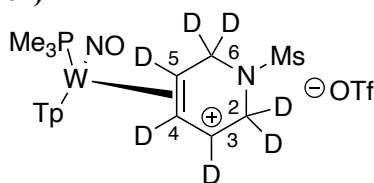
**WTp(NO)(PMe<sub>3</sub>)(η<sup>3</sup>-(*N*-mesyl)-6-*anti*-2,2,3,4,5-hexadeutero-1,2,3,6-tetrahydropyridinium (OTf) (d<sub>6</sub>-61)**



<sup>1</sup>H NMR (CD<sub>2</sub>Cl<sub>2</sub>, δ, 25 °C): 8.36 (d, *J* = 2.1 Hz, 1H, PzB3), 8.14 (d, *J* = 2.1 Hz, 1H, PzC3), 7.96 (d, *J* = 2.2 Hz, 1H, PzA3), 7.94 (d, *J* = 2.2 Hz, 1H, PzC5), 7.86 (d, *J* = 2.4 Hz, 1H, PzB5), 7.71 (d, *J* = 2.4 Hz, 1H, PzA5), 6.58 (t, *J* = 2.3 Hz, 1H, PzC4), 6.52 (t, *J* = 2.3 Hz, 1H, PzB4), 6.32 (t, *J* = 2.4 Hz, 1H, PzA4), 3.98 (s, 1H, H6), 2.90 (s, 3H, Ms), 1.27 (d, *J*<sub>PH</sub> = 9.6 Hz, 9H, PMe<sub>3</sub>).

<sup>13</sup>C NMR (CD<sub>2</sub>Cl<sub>2</sub>, δ, 25 °C): 147.9 (PzA3), 144.9 (d, *J*<sub>PC</sub> = 2.5 Hz, PzB3), 142.8 (PzC3), 139.0 (PzC5), 138.8 (PzB5), 138.7 (PzA5), 121.3 (q, *J*<sub>FC</sub> = 320.2 Hz, TfO<sup>-</sup>), 125.9-126.5 (m, C3), 108.9 (2C, PzB4/C4), 107.7 (PzA4), 95.2-95.9 (m, C4), 64.9-65.4 (m, C5), 43.9-44.3 (m, C2), 43.5-43.9 (m, C6), 36.1 (Ms), 13.4 (d, *J*<sub>PC</sub> = 33.0 Hz, 3C, PMe<sub>3</sub>).

**WTp(NO)(PMe<sub>3</sub>)(η<sup>3</sup>-(*N*-mesyl)-2,2,3,4,5,6,6-heptadeutero-1,2,3,6-tetrahydropyridinium (OTf) (d<sub>7</sub>-61)**



<sup>1</sup>H NMR (CD<sub>2</sub>Cl<sub>2</sub>, δ, 25 °C): 8.35 (d, *J* = 2.0 Hz, 1H, PzB3), 8.11 (d, *J* = 2.0 Hz, 1H, PzC3), 8.00 (d, *J* = 1.9 Hz, 1H, PzA3), 7.94 (d, *J* = 2.2 Hz, 1H, PzC5), 7.87 (d, *J* = 2.2 Hz, 1H, PzB5), 7.71 (d, *J* = 2.1 Hz, 1H, PzA5), 6.57 (t, *J* = 2.3 Hz, 1H, PzC4), 6.52 (t, *J* = 2.3 Hz, 1H, PzB4), 6.31 (t, *J* = 2.3, 1H, PzA4), 2.90 (s, 3H, Ms), 1.26 (d, *J*<sub>PH</sub> = 9.7 Hz, 9H, PMe<sub>3</sub>).

<sup>13</sup>C NMR (CD<sub>2</sub>Cl<sub>2</sub>, δ, 25 °C): 148.0 (PzA3), 144.9 (PzB3), 142.7 (PzC3), 139.0 (PzC5), 138.8 (PzA5/B5), 138.7 (PzA5/B5), 126.2-126.7 (m, C3), 121.2 (q, *J*<sub>FC</sub> = 320.8 Hz, -OTf), 109.0 (Pz4), 108.9 (Pz4), 107.7 (Pz4), 95.3-95.8 (m, C4), 64.8-65.3 (m, C5), 43.9-44.4 (m, C2), 43.5-43.8 (m, C6), 36.0 (Ms), 13.3 (d, *J*<sub>PC</sub> = 32.7 Hz, 3C, PMe<sub>3</sub>).

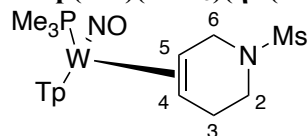
## Synthesis and Characterization of [W] 1,2,3,6-THP Complexes

### General Synthesis

Two separate solutions were prepared in two 30 mL glass screw-cap test tubes. Tube A was comprised of  $d_x$ -**61** (444 mg, 0.55 mmol) dissolved in EtCN (3 mL) and Tube B was a heterogeneous slurry of  $\text{NaBH}_4$  (207 mg, 5.47 mmol) in dry THF (2 mL). After both tubes were chilled in a  $-50\text{ }^\circ\text{C}$  toluene bath for 20 minutes, Tube B slurry was added to Tube A, and the tube sat for 16 hours. The solution was diluted with 150 mL of DCM and added to a separatory funnel. This solution was washed 3x with 200 mL of saturated aqueous  $\text{NaHCO}_3$ . The organic layer was isolated and set aside. The combined aqueous layers were combined and back-extracted with 50 mL of DCM to prevent loss of product. The organic layers were combined in a single flask and dried with anhydrous  $\text{MgSO}_4$ . This powder was then filtered off into a 60 mL coarse porosity fritted funnel and washed with DCM. The dried organic layers were then reduced *in vacuo* to dryness. The residue in the flask was redissolved in minimal DCM (approximately 10 mL). The solution was then slowly added to a stirring 200mL solution of 3:1 pentane/ $\text{Et}_2\text{O}$ . A tan precipitate formed immediately and was allowed to stir for  $\sim 10$  minutes to ensure total precipitation. This powder was collected on a 60 mL medium porosity frit and washed 2x with 30 mL of pentane. This powder was dried in a desiccator under vacuum overnight.

Highly purified material can be obtained by performing the following extra steps. The complex was eluted off of a basic alumina column with 100% ethyl acetate. The fraction was reduced to dryness and redissolved in minimal DCM, which was then slowly added to a 50 mL solution of stirring pentane. A white precipitate was then formed and collected on a 15 mL F frit. This powder, after drying in a desiccator for 1 hour, was then added to a 4 dram vial containing 1 mL of  $d_6$ -acetone and was then stirred for 1 hour. The white powder was then collected in a 2 mL F frit and then dried in a desiccator overnight. (317 mg, 87% yield)

### WTp(NO)(PMe<sub>3</sub>)( $\eta^2$ -(*N*-mesyl)-1,2,3,6-tetrahydropyridine) (**62**)



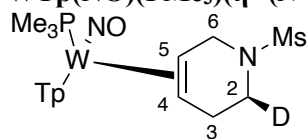
$^1\text{H}$  NMR ( $\text{CD}_2\text{Cl}_2$ ,  $\delta$ ,  $25\text{ }^\circ\text{C}$ ): 8.09 (d,  $J = 1.8$  Hz, 1H, PzA3), 8.03 (d,  $J = 1.9$  Hz, 1H, PzB3), 7.79 (d,  $J = 2.4$  Hz, 1H, PzB5), 7.72 (d,  $J = 2.2$  Hz, 1H, PzC5), 7.67 (d,  $J = 2.4$  Hz, 1H, PzA5), 7.21 (d,  $J = 2.0$  Hz, 1H, PzC3), 6.36 (t,  $J = 2.2$  Hz, 1H, PzB4), 6.27 (t,  $J = 2.2$  Hz, 1H, PzA4), 6.19 (t,  $J = 2.2$  Hz, 1H, PzC4), 4.31 (dd,  $J = 7.4, 12.6$  Hz, 1H, H6), 3.77 (dd,  $J = 8.9, 12.6$  Hz, 1H, H6), 3.49 (dt,  $J = 4.6, 10.7$  Hz, 1H, H2), 3.25 (td,  $J = 4.9, 10.7$  Hz, 1H, H'), 2.85-2.91 (m, 1H, H5), 2.84 (s, 3H, Ms), 2.78-2.83 (m, 2H, H3), 1.27-1.30 (m, 1H, H4), 1.23 (d,  $J_{\text{PH}} = 8.2$  Hz, 9H,  $\text{PMe}_3$ ).

$^{13}\text{C}$  NMR ( $\text{CD}_2\text{Cl}_2$ ,  $\delta$ ,  $25\text{ }^\circ\text{C}$ ): 144.0 (d,  $J_{\text{PC}} = 2.1$  Hz, PzB3), 143.2 (PzA3), 140.8 (PzC3), 136.9 (PzC5), 136.5 (PzB5), 135.8 (PzA5), 106.8 (PzB4), 106.2 (PzC4), 106.0 (PzA4), 51.0 (2C, C4/C5), 48.9 (d,  $J_{\text{PC}} = 2.1$  Hz, C6), 47.1 (C2), 35.7 (Ms), 28.7 (C3), 14.3 (d,  $J_{\text{PC}} = 28.1$ , 3C,  $\text{PMe}_3$ ).

IR:  $\nu(\text{NO}) = 1537\text{ cm}^{-1}$

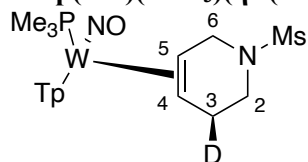
CV (DMA; 50 mV/s):  $E_{\text{pa}} = +0.49\text{ V}$  (NHE)

SC-XRD Data on page 360

**WTp(NO)(PMe<sub>3</sub>)(η<sup>2</sup>-(*N*-mesyl)-2-*anti*-deutero-1,2,3,6-tetrahydropyridine) (±(2*S*)-*d*<sub>1</sub>-62)**

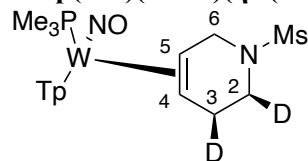
<sup>1</sup>H NMR (CD<sub>2</sub>Cl<sub>2</sub>, δ, 25 °C): 8.09 (d, *J* = 1.8 Hz, 1H, PzA3), 8.03 (d, *J* = 1.8 Hz, 1H, PzB3), 7.79 (d, *J* = 2.2 Hz, 1H, PzB5), 7.72 (d, *J* = 2.2 Hz, 1H, PzC5), 7.68 (d, *J* = 2.2 Hz, 1H, PzA5), 7.21 (d, *J* = 1.8 Hz, 1H, PzC3), 6.36 (t, *J* = 2.1 Hz, 1H, PzB4), 6.26 (t, *J* = 2.1 Hz, 1H, PzA4), 6.19 (t, *J* = 2.2 Hz, 1H, PzC4), 4.32 (dd, *J* = 7.6, 12.5 Hz, 1H, H6), 3.78 (dd, *J* = 8.8, 12.5 Hz, 1H, H6), 3.46 (t, *J* = 4.4 Hz, 1H, H2), 2.86-2.91 (m, 1H, H5), 2.84 (s, 3H, Ms), 2.77-2.83 (m, 2H, H3), 1.26-1.30 (m, 1H, H4), 1.24 (d, *J*<sub>PH</sub> = 8.3 Hz, 9H, PMe<sub>3</sub>).

<sup>13</sup>C NMR (CD<sub>2</sub>Cl<sub>2</sub>, δ, 25 °C): 144.0 (d, *J*<sub>PC</sub> = 1.9 Hz, PzB3), 143.2 (PzA3), 140.8 (PzC3), 136.9 (PzC5), 136.5 (PzB5), 135.8 (PzA5), 106.8 (PzB4), 106.2 (PzC4), 106.0 (PzA4), 50.9 (d, *J*<sub>PC</sub> = 12.7 Hz, C5), 50.9 (C4), 48.9 (d, *J*<sub>PC</sub> = 2.2 Hz, C6), 46.7 (t, *J*<sub>CD</sub> = 21.3 Hz, C2), 35.7 (Ms), 28.6 (C3), 14.3 (d, *J*<sub>PC</sub> = 27.7 Hz, 9H, PMe<sub>3</sub>).

**WTp(NO)(PMe<sub>3</sub>)(η<sup>2</sup>-(*N*-mesyl)-3-*anti*-deutero-1,2,3,6-tetrahydropyridine) (±(3*S*)-*d*<sub>1</sub>-62)**

<sup>1</sup>H NMR (CD<sub>2</sub>Cl<sub>2</sub>, δ, 25 °C): 8.09 (d, *J* = 1.9 Hz, 1H, PzA3), 8.03 (d, *J* = 1.8 Hz, 1H, PzB3), 7.79 (d, *J* = 2.2 Hz, 1H, PzB5), 7.72 (d, *J* = 2.2 Hz, 1H, PzC5), 7.67 (d, *J* = 2.2 Hz, 1H, PzA5), 7.21 (d, *J* = 1.8 Hz, 1H, PzC3), 6.36 (t, *J* = 2.1 Hz, 1H, PzB4), 6.26 (t, *J* = 2.1 Hz, 1H, PzA4), 6.19 (t, *J* = 2.2 Hz, 1H, PzC4), 4.31 (dd, *J* = 7.5, 12.6 Hz, 1H, H6), 3.77 (dd, *J* = 8.9, 12.6 Hz, 1H, H6), 3.48 (dd, *J* = 4.8, 10.8 Hz, 1H, H2), 3.24 (t, *J* = 10.8 Hz, 1H, H2), 2.85-2.91 (m, 1H, H5), 2.84 (s, 3H, Ms), 2.75-2.80 (m, 1H, H3), 1.26-1.29 (m, 1H, H4), 1.24 (*J*<sub>PH</sub> = 8.3 Hz, 9H, PMe<sub>3</sub>).

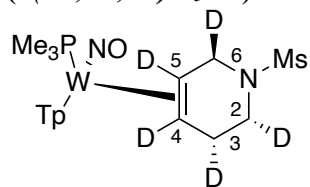
<sup>13</sup>C NMR (CD<sub>2</sub>Cl<sub>2</sub>, δ, 25 °C): 144.0 (d, *J*<sub>PC</sub> = 2.0 Hz, PzB3), 143.2 (PzA3), 140.8 (PzC3), 136.9 (PzC5), 136.5 (PzB5), 135.8 (PzA5), 106.8 (PzB4), 106.2 (PzC4), 106.0 (PzA4), 51.0 (d, *J*<sub>PC</sub> = 12.7 Hz, C5), 50.9 (C4), 48.9 (d, *J*<sub>PC</sub> = 1.8 Hz, C6), 47.0 (C2), 35.7 (Ms), 28.4 (t, *J*<sub>DC</sub> = 19.5 Hz, C3), 14.3 (d, *J*<sub>PC</sub> = 28.2 Hz, 9H, PMe<sub>3</sub>).

**WTp(NO)(PMe<sub>3</sub>)(η<sup>2</sup>-(*N*-mesyl)-2,3-*anti*-dideutero-1,2,3,6-tetrahydropyridine) (±(2*S*,3*S*)-*d*<sub>2</sub>-62)**

<sup>1</sup>H NMR (CD<sub>2</sub>Cl<sub>2</sub>, δ, 25 °C): 8.09 (d, *J* = 2.0 Hz, 1H, PzA3), 8.03 (d, *J* = 2.0 Hz, 1H, PzB3), 7.79 (d, *J* = 2.3 Hz, 1H, PzB5), 7.72 (d, *J* = 2.2 Hz, 1H, PzC5), 7.67 (d, *J* = 2.3 Hz, 1H, PzA5), 7.21 (d, *J* = 2.0 Hz, 1H, PzC3), 6.36 (t, *J* = 2.2 Hz, 1H, PzB4), 6.26 (t, *J* = 2.2 Hz, 1H, PzA4), 6.19 (t, *J* = 2.2 Hz, 1H, PzC4), 4.31 (dd, *J* = 7.5, 12.6 Hz, 1H, H6), 3.77 (dd, *J* = 9.0, 12.6 Hz, 1H, H6), 3.46 (d, *J* = 4.5 Hz, 1H, H2), 2.85-2.90 (m, 1H, H5), 2.84 (s, 3H, Ms), 2.75-2.79 (m, 1H, H3), 1.27 (ddd, *J* = 1.1, 7.6, 9.9 Hz, 1H, H4), 1.24 (d, *J*<sub>PH</sub> = 8.2 Hz, 9H, PMe<sub>3</sub>).

<sup>13</sup>C NMR (CD<sub>2</sub>Cl<sub>2</sub>, δ, 25 °C): 144.0 (d, *J*<sub>PC</sub> = 2.1 Hz, PzB3), 143.2 (PzA3), 140.8 (PzC3), 136.9 (PzC5), 136.5 (PzB5), 135.8 (PzA5), 106.8 (PzB4), 106.2 (PzC4), 106.0 (PzA4), 51.0 (d, *J*<sub>PC</sub> = 12.6 Hz, C5), 50.8 (C4), 48.9 (d, *J*<sub>PC</sub> = 2.1 Hz, C6), 46.7 (t, *J*<sub>DC</sub> = 21.6 Hz, C2), 35.7 (Ms), 28.4 (t, *J*<sub>DC</sub> = 19.5 Hz, 1C, C3), 14.3 (d, *J*<sub>PC</sub> = 28.2 Hz, 3C, PMe<sub>3</sub>).

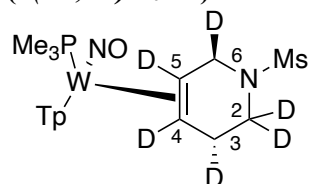
**WTp(NO)(PMe<sub>3</sub>)(η<sup>2</sup>-(*N*-mesyl)-6-*syn*-2,3-*anti*-4,5-pentadeutero-1,2,3,6-tetrahydropyridine)**  
**(±(2*R*,3*R*,6*R*)-*d*<sub>5</sub>-62)**



<sup>1</sup>H NMR (CD<sub>2</sub>Cl<sub>2</sub>, δ, 25 °C): 8.09 (d, *J* = 1.9 Hz, 1H, PzA3), 8.03 (d, *J* = 2.0 Hz, 1H, PzB3), 7.79 (d, *J* = 2.2 Hz, 1H, PzB5), 7.72 (d, *J* = 2.2 Hz, 1H, PzC5), 7.68 (d, *J* = 2.2 Hz, 1H, PzA5), 7.21 (d, *J* = 1.8 Hz, 1H, PzC3), 6.36 (t, *J* = 2.1 Hz, 1H, PzB4), 6.26 (t, *J* = 2.1 Hz, 1H, PzA4), 6.20 (t, *J* = 2.1 Hz, 1H, PzC4), 3.76 (s, 1H, H6), 3.23 (d, *J* = 4.1 Hz, 1H, H2), 2.84 (s, 3H, Ms), 2.80 (d, *J* = 4.5 Hz, 1H, H3), 1.23 (d, *J*<sub>PH</sub> = 8.2 Hz, 9H, PMe<sub>3</sub>).

<sup>13</sup>C NMR (CD<sub>2</sub>Cl<sub>2</sub>, δ, 25 °C): 144.0 (d, *J*<sub>PC</sub> = 1.9 Hz, PzB3), 143.2 (PzA3), 140.7 (PzC3), 136.9 (PzC5), 136.5 (PzB5), 135.8 (PzA5), 106.8 (PzB4), 106.2 (PzC4), 106.0 (PzA4), 50.0-50.4 (m, 2C, C4/C5), 48.5 (t, *J*<sub>DC</sub> = 20.8 Hz, C6), 46.4-46.7 (m, C2), 35.7 (Ms), 28.1 (t, *J*<sub>PC</sub> = 19.5 Hz, C3), 14.3 (d, *J*<sub>PC</sub> = 28.6 Hz, 3C, PMe<sub>3</sub>).

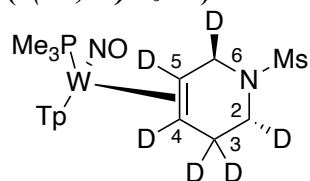
**WTp(NO)(PMe<sub>3</sub>)(η<sup>2</sup>-(*N*-mesyl)-3-*syn*-6-*anti*-2,2,4,5-hexadeutero-1,2,3,6-tetrahydropyridine)**  
**(±(3*R*,6*R*)-*d*<sub>6</sub>-62)**



<sup>1</sup>H NMR (CD<sub>2</sub>Cl<sub>2</sub>, δ, 25 °C): 8.09 (d, *J* = 1.8 Hz, 1H, PzA3), 8.03 (d, *J* = 1.9 Hz, 1H, PzB3), 7.79 (d, *J* = 2.2 Hz, 1H, PzB5), 7.72 (d, *J* = 2.2 Hz, 1H, PzC5), 7.67 (d, *J* = 2.2 Hz, 1H, PzA5), 7.20 (d, *J* = 1.9 Hz, 1H, PzC3), 6.36 (t, *J* = 2.1 Hz, 1H, PzB4), 6.26 (t, *J* = 2.1 Hz, 1H, PzA4), 6.19 (t, *J* = 2.1 Hz, 1H, PzC4), 3.75 (s, 1H, H6), 2.84 (s, 3H, Ms), 2.79 (s, 1H, H3), 1.23 (d, *J*<sub>PH</sub> = 8.2 Hz, 9H, PMe<sub>3</sub>).

<sup>13</sup>C NMR (CD<sub>2</sub>Cl<sub>2</sub>, δ, 25 °C): 144.0 (d, *J*<sub>PC</sub> = 1.5 Hz, PzB3), 143.2 (PzA3), 140.7 (PzC3), 136.9 (PzC5), 136.5 (PzB5), 135.8 (PzA5), 106.8 (PzB4), 106.2 (PzC4), 106.0 (PzA4), 50.0-50.5 (m, 2C, C4/C5), 48.5 (t, *J*<sub>DC</sub> = 20.8 Hz, C6), 46.4-46.7 (m, C2), 35.7 (Ms), 27.8-28.2 (m, C3), 14.3 (d, *J*<sub>PC</sub> = 27.9 Hz, 3C, PMe<sub>3</sub>).

**WTp(NO)(PMe<sub>3</sub>)(η<sup>2</sup>-(*N*-mesyl)-2-*syn*-6-*anti*-3,3,4,5-hexadeutero-1,2,3,6-tetrahydropyridine)**  
**(±(2*R*,6*R*)-*d*<sub>6</sub>-62)**

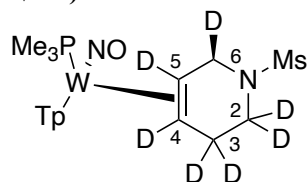


<sup>1</sup>H NMR (CD<sub>2</sub>Cl<sub>2</sub>, δ, 25 °C): 8.09 (d, *J* = 1.9 Hz, 1H, PzA3), 8.03 (d, *J* = 2.0 Hz, 1H, PzB3), 7.79 (d, *J* = 2.3 Hz, 1H, PzB5), 7.72 (d, *J* = 2.2 Hz, 1H, PzC5), 7.68 (d, *J* = 2.2 Hz, 1H, PzA5), 7.20 (d, *J* = 1.9 Hz, 1H, PzC3), 6.36 (t, *J* = 2.1 Hz, 1H, PzB4), 6.26 (t, *J* = 2.1 Hz, 1H, PzA4), 6.19 (t, *J* = 2.2 Hz, 1H, PzC4), 3.75 (s, 1H, H6), 3.22 (s, 1H, H2), 2.84 (s, 3H, Ms), 1.24 (d, *J*<sub>PH</sub> = 8.2 Hz, 9H, PMe<sub>3</sub>).

<sup>13</sup>C NMR (CD<sub>2</sub>Cl<sub>2</sub>, δ, 25 °C): 144.0 (d, *J*<sub>PC</sub> = 1.5 Hz, PzB3), 143.2 (PzA3), 140.7 (PzC3), 136.9 (PzC5), 136.5 (PzB5), 135.8 (PzA5), 106.8 (PzB4), 106.2 (PzC4), 106.0 (PzA4), 49.9-50.4 (m, 2C, C4/C5), 48.5 (t, *J*<sub>DC</sub> = 20.7 Hz, C6), 46.3-46.7 (m, C2), 35.7 (Ms), 27.5-28.2 (m, C3), 14.3 (d, *J*<sub>PC</sub> = 28.5 Hz, 3C, PMe<sub>3</sub>).



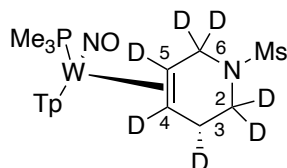
**WTp(NO)(PMe<sub>3</sub>)(η<sup>2</sup>-(*N*-mesyl)-6-*anti*-2,2,3,3,4,5-heptadeutero-1,2,3,6-tetrahydropyridine) (±(*6R*)-*d*<sub>7</sub>-62)**



<sup>1</sup>H NMR (CD<sub>2</sub>Cl<sub>2</sub>, δ, 25 °C): 8.09 (d, *J* = 1.9 Hz, 1H, PzA3), 8.03 (d, *J* = 1.8 Hz, 1H, PzB3), 7.80 (d, *J* = 2.2 Hz, 1H, PzB5), 7.72 (d, *J* = 2.2 Hz, 1H, PzPzC5), 7.68 (d, *J* = 2.2 Hz, 1H, PzA5), 7.21 (d, *J* = 1.9 Hz, 1H, PzC3), 6.36 (t, *J* = 2.1 Hz, 1H, PzB4), 6.26 (t, *J* = 2.2 Hz, 1H, PzA4), 6.20 (t, *J* = 2.2 Hz, PzC4), 3.76 (s, 1H, H6), 2.84 (s, 3H, Ms), 1.23 (d, *J*<sub>PH</sub> = 8.2 Hz, 9H, PMe<sub>3</sub>).

<sup>13</sup>C NMR (CD<sub>2</sub>Cl<sub>2</sub>, δ, 25 °C): 144.0 (d, *J*<sub>PC</sub> = 1.7 Hz, PzB3), 143.1 (PzA3), 140.7 (PzC3), 136.9 (PzC5), 136.5 (PzB5), 135.8 (PzA5), 106.8 (PzB4), 106.2 (PzC4), 106.0 (PzA4), 49.9-50.4 (m, 2C, C4/C5), 48.5 (t, *J*<sub>CD</sub> = 20.6 Hz, C6), 45.9-46.7 (m, C2), 35.7 (Ms), 27.4-28.1 (m, C3), 14.2 (d, *J*<sub>PC</sub> = 28.2 Hz, 3C, PMe<sub>3</sub>).

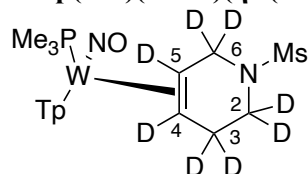
**WTp(NO)(PMe<sub>3</sub>)(η<sup>2</sup>-(*N*-mesyl)-3-*syn*-2,2,4,5,6,6-heptadeutero-1,2,3,6-tetrahydropyridine) (±(*3R*)-*d*<sub>7</sub>-62)**



<sup>1</sup>H NMR (CD<sub>2</sub>Cl<sub>2</sub>, δ, 25 °C): 8.10 (d, *J* = 1.9 Hz, 1H, PzA3), 8.04 (d, *J* = 1.9 Hz, 1H, PzB3), 7.80 (d, *J* = 2.3 Hz, 1H, PzB5), 7.73 (d, *J* = 2.3 Hz, 1H, PzC5), 7.68 (d, *J* = 2.3 Hz, 1H, PzA5), 7.21 (d, *J* = 1.9 Hz, 1H, PzC3), 6.36 (t, *J* = 2.2 Hz, 1H, PzB4), 6.26 (t, *J* = 2.2 Hz, 1H, PzA4), 6.20 (t, *J* = 2.2 Hz, 1H, PzC4), 2.85 (s, 3H, Ms), 2.80 (s, 1H, H3), 1.24 (d, *J*<sub>PH</sub> = 8.3 Hz, 9H, PMe<sub>3</sub>).

<sup>13</sup>C NMR (CD<sub>2</sub>Cl<sub>2</sub>, δ, 25 °C): 144.0 (d, *J*<sub>PC</sub> = 1.9 Hz, PzB3), 143.1 (PzA3), 140.7 (PzC3), 136.9 (PzC5), 136.5 (PzB5), 135.8 (PzA5), 106.8 (PzB4), 106.2 (PzC4), 106.0 (PzA4), 49.8-50.4 (m, 2C, C4/C5), 47.9-48.6 (C6), 45.9-46.4 (m, C2), 35.7 (s, 3H, Ms), 28.0 (t, *J*<sub>DC</sub> = 19.5 Hz, C3), 14.2 (d, *J*<sub>PC</sub> = 28.0 Hz, 3C, PMe<sub>3</sub>).

**WTp(NO)(PMe<sub>3</sub>)(η<sup>2</sup>-(*N*-mesyl)-2,2,3,3,4,5,6,6-octadeutero-1,2,3,6-tetrahydropyridine) (*d*<sub>8</sub>-62)**



<sup>1</sup>H NMR (CD<sub>2</sub>Cl<sub>2</sub>, δ, 25 °C): 8.09 (d, *J* = 1.6 Hz, PzA3), 8.03 (d, *J* = 1.7 Hz, PzB3), 7.80 (d, *J* = 2.2 Hz, PzB5), 7.73 (d, *J* = 2.1 Hz, PzC5), 7.68 (d, *J* = 2.3 Hz, PzA5), 6.36 (t, *J* = 2.2 Hz, PzB4), 6.26 (t, *J* = 2.2 Hz, PzA4), 6.20 (t, *J* = 2.2 Hz, PzC4), 2.84 (s, 3H, Ms), 1.24 (d, *J*<sub>PH</sub> = 8.3 Hz, 9H, PMe<sub>3</sub>).

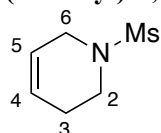
<sup>13</sup>C NMR (CD<sub>2</sub>Cl<sub>2</sub>, δ, 25 °C): 143.6 (d, *J*<sub>PC</sub> = 1.7 Hz, PzB3), 142.8 (PzA3), 140.4 (PzC3), 136.6 (PzB5), 136.1 (PzC5), 135.4 (PzA5), 106.5 (PzB4), 105.9 (PzC4), 105.7 (PzA4), 49.5-50.0 (m, 2C, C4/C5), 47.6-48.3 (m, C6), 45.5-46.1 (m, C2), 35.4 (Ms), 27.0-27.5 (m, C3), 13.88 (d, *J*<sub>PC</sub> = 27.9 Hz, 3C, PMe<sub>3</sub>).

## Synthesis and Characterization of 1,2,3,6-THPs

### General Synthesis

Acetone (3 mL), DDQ (200 mg, 0.88 mmol), and **d<sub>x</sub>-62** (130 mg, 0.20 mmol) were added to a 4-dram vial containing a stir pea. The reaction was stirred in a fume hood for 4 hours. This solution was diluted with 30 mL of DCM and was washed 3x with 50 mL of saturated aqueous NaHCO<sub>3</sub>. The organic layer was isolated and set aside. The combined aqueous layers were combined and back-extracted with 30 mL of DCM to prevent loss of product. The organic layers were combined in a single round-bottom flask to which 5 grams of basic alumina powder were added. The solution was then reduced off *in vacuo*, bringing the eluted organic into the basic alumina powder. This powder was then dry loaded onto an 8 gram Teledyne basic alumina column, upon which clean product was eluted off of with 40% EtOAc in hexanes. The tubes containing organic were combined and reduced *in vacuo*, yielding a colorless residue. (14 mg, 44% isolated yield)

### (*N*-mesyl)-1,2,3,6-tetrahydropyridine (**65**)

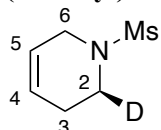


<sup>1</sup>H NMR (CD<sub>2</sub>Cl<sub>2</sub>, δ, 25 °C): 5.84-5.88 (m, 1H, H4), 5.69-5.73 (m, 1H, H5), 3.71-3.74 (m, 2H, H6), 3.33 (dt, *J* = 1.2, 5.7 Hz, 2H, H2), 2.77 (s, 3H, Ms), 2.23-2.27 (m, 2H, H3).

<sup>13</sup>C NMR (CD<sub>2</sub>Cl<sub>2</sub>, δ, 25 °C): 125.7 (C4), 123.4 (C5), 45.1 (C6), 42.8 (C2), 35.3 (Ms), 25.6 (C3).

SC-XRD Data on page 361

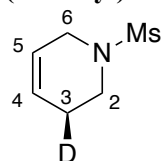
### (*N*-mesyl)-2-deutero-1,2,3,6-tetrahydropyridine (±(2*S*)-*d*<sub>1</sub>-**65**)



<sup>1</sup>H NMR (CD<sub>2</sub>Cl<sub>2</sub>, δ, 25 °C): 5.85-5.89 (m, 1H, H4), 5.70-5.73 (m, 1H, H5), 3.72-3.74 (m, 2H, H6), 3.31 (tt, *J* = 1.7, 5.8 Hz, 1H, H2), 2.77 (s, 3H, Ms), 2.23-2.26 (m, 2H, H3).

<sup>13</sup>C NMR (CD<sub>2</sub>Cl<sub>2</sub>, δ, 25 °C): 125.8 (C4), 123.4 (C5), 45.0 (C6), 42.5 (t, *J*<sub>DC</sub> = 21.3 Hz, C2), 35.4 (Ms), 25.5 (C3).

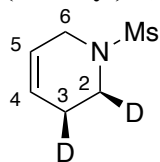
### (*N*-mesyl)-3-deutero-1,2,3,6-tetrahydropyridine (±(3*S*)-*d*<sub>1</sub>-**65**)



<sup>1</sup>H NMR (CD<sub>2</sub>Cl<sub>2</sub>, δ, 25 °C): 5.85-5.89 (m, 1H, H4), 5.72 (dq, *J* = 3.2, 10.2 Hz, 1H, H5), 3.73 (q, *J* = 2.8 Hz, 2H, H6), 3.31-3.35 (m, 2H, H2), 2.78 (s, 3H, Ms), 2.22-2.26 (m, 1H, H3).

<sup>13</sup>C NMR (CD<sub>2</sub>Cl<sub>2</sub>, δ, 25 °C): 125.7 (C4), 123.5 (C5), 45.1 (C6), 42.7 (C2), 35.3 (Ms), 25.3 (t, *J*<sub>DC</sub> = 19.8 Hz, C3).

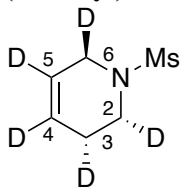
**(*N*-mesyl)-2,3-*cis*-dideutero-1,2,3,6-tetrahydropyridine ( $\pm(2S,3S)$ -*d*<sub>2</sub>-65)**



<sup>1</sup>H NMR (CD<sub>2</sub>Cl<sub>2</sub>,  $\delta$ , 25 °C): 5.85-5.88 (m, 1H, H5), 5.72 (dq,  $J$  = 3.0, 10.2 Hz, 1H, H4), 3.73 (s, 2H, H6), 3.30 (s, 1H, H2), 2.77 (s, 3H, Ms), 2.23 (s, 1H, H3).

<sup>13</sup>C NMR (CD<sub>2</sub>Cl<sub>2</sub>,  $\delta$ , 25 °C): 125.7 (C4), 123.5 (C5), 45.0 (C6), 42.4 (t,  $J_{DC}$  = 21.4 Hz, C2), 35.4 (Ms), 25.1 (t,  $J_{DC}$  = 19.8 Hz, C3).

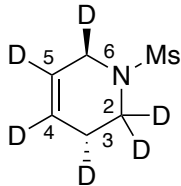
**(*N*-mesyl)-2,3-*cis*-6-*trans*-4,5-pentadeutero-1,2,3,6-tetrahydropyridine ( $\pm(2R,3R,6R)$ -*d*<sub>5</sub>-65)**



<sup>1</sup>H NMR (CD<sub>2</sub>Cl<sub>2</sub>,  $\delta$ , 25 °C): 3.69-3.71 (m, 1H, H6), 3.27-3.33 (m, 1H, H2), 2.77 (s, 3H, Ms), 2.22 (br s, 1H, H3).

<sup>13</sup>C NMR (CD<sub>2</sub>Cl<sub>2</sub>,  $\delta$ , 25 °C): 125.3 (t,  $J_{DC}$  = 24.6 Hz, C4), 123.0 (t,  $J_{DC}$  = 24.6 Hz, C5), 44.6 (t,  $J_{DC}$  = 21.4 Hz, C6), 42.4 (t,  $J_{DC}$  = 21.3 Hz, C2), 35.4 (Ms), 25.0 (t,  $J_{DC}$  = 19.9 Hz, C3).

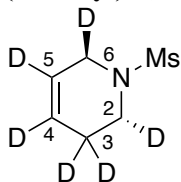
**(*N*-mesyl)-3,6-*trans*-2,2,4,5-hexadeutero-1,2,3,6-tetrahydropyridine ( $\pm(3R,6R)$ -*d*<sub>6</sub>-65)**



<sup>1</sup>H NMR (CD<sub>2</sub>Cl<sub>2</sub>,  $\delta$ , 25 °C): 3.69 (s, 1H, H3), 2.77 (s, 3H, Ms), 2.22 (s, 1H, H6).

<sup>13</sup>C NMR (CD<sub>2</sub>Cl<sub>2</sub>,  $\delta$ , 25 °C): 125.3 (t,  $J_{DC}$  = 24.6 Hz, C4), 123.0 (t,  $J_{DC}$  = 24.9 Hz, C5), 44.6 (t,  $J_{DC}$  = 21.3 Hz, C6), 41.8-42.5 (m, C2), 35.4 (Ms), 24.9 (t,  $J_{DC}$  = 19.9 Hz, C3).

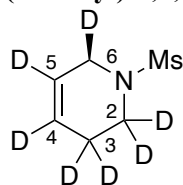
**(*N*-mesyl)-2,6-*trans*-3,3,4,5-hexadeutero-1,2,3,6-tetrahydropyridine ( $\pm(2R,6R)$ -*d*<sub>6</sub>-65)**



<sup>1</sup>H NMR (CD<sub>2</sub>Cl<sub>2</sub>,  $\delta$ , 25 °C): 3.70 (t,  $J$  = 2.4 Hz, 1H, H6), 3.31 (s, 1H, H2), 2.77 (s, 3H, Ms).

<sup>13</sup>C NMR (CD<sub>2</sub>Cl<sub>2</sub>,  $\delta$ , 25 °C): 125.3 (t,  $J_{DC}$  = 24.6 Hz, C4), 123.1 (t,  $J_{DC}$  = 24.6 Hz, C5), 44.6 (t,  $J_{DC}$  = 21.3 Hz, C6), 42.3 (t,  $J_{DC}$  = 21.6 Hz, C2), 35.4 (Ms), 24.6 (q,  $J_{DC}$  = 19.9 Hz, C3).

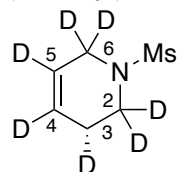
**(*N*-mesyl)-2,2,3,3,4,5,6-heptadeutero-1,2,3,6-tetrahydropyridine ( $\pm(6R)$ -*d*<sub>7</sub>-65)**



<sup>1</sup>H NMR (CD<sub>2</sub>Cl<sub>2</sub>, δ, 25 °C): 3.70 (s, 1H, H<sub>6</sub>), 2.78 (s, 3H, Ms).

<sup>13</sup>C NMR (CD<sub>2</sub>Cl<sub>2</sub>, δ, 25 °C): 125.2 (t, *J*<sub>DC</sub> = 24.7 Hz, C<sub>4</sub>), 123.1 (t, *J*<sub>DC</sub> = 24.8 Hz, C<sub>5</sub>), 44.6 (t, *J*<sub>DC</sub> = 21.4 Hz, C<sub>6</sub>), 41.7-42.4 (m, C<sub>2</sub>), 35.4 (Ms), 24.3-25.0 (m, C<sub>3</sub>).

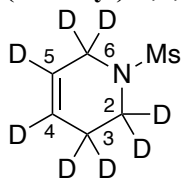
**(*N*-mesyl)-2,2,3,4,5,6,6-heptadeutero-1,2,3,6-tetrahydropyridine ( $\pm(3R)$ -*d*<sub>7</sub>-65)**



<sup>1</sup>H NMR (CD<sub>2</sub>Cl<sub>2</sub>, δ, 25 °C): 2.77 (s, 3H, Ms), 2.21 (s, 1H, H<sub>3</sub>).

<sup>13</sup>C NMR (CD<sub>2</sub>Cl<sub>2</sub>, δ, 25 °C): 125.4 (t, *J*<sub>DC</sub> = 24.7 Hz, C<sub>4</sub>), 122.9 (t, *J*<sub>DC</sub> = 24.7 Hz, C<sub>5</sub>), 44.1-44.7 (m, C<sub>6</sub>), 41.8-42.5 (m, C<sub>2</sub>), 35.4 (Ms), 24.9 (t, *J*<sub>DC</sub> = 19.9 Hz, C<sub>3</sub>).

**(*N*-mesyl)-2,2,3,3,4,5,6,6-octadeutero-1,2,3,6-tetrahydropyridine (*d*<sub>8</sub>-65)**

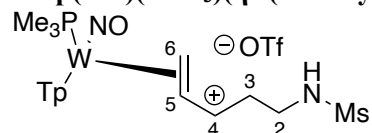


<sup>1</sup>H NMR (CD<sub>2</sub>Cl<sub>2</sub>, δ, 25 °C): 2.77 (s, 3H, Ms).

<sup>13</sup>C NMR (CD<sub>2</sub>Cl<sub>2</sub>, δ, 25 °C): 125.3 (t, *J*<sub>DC</sub> = 24.8 Hz, C<sub>4</sub>), 123.0 (t, *J*<sub>DC</sub> = 24.3 Hz, C<sub>5</sub>), 43.9-44.7 (m, C<sub>6</sub>), 41.7-42.4 (m, C<sub>2</sub>), 35.4 (Ms), 24.4-24.8 (m, C<sub>3</sub>).

## Synthesis and Characterization of [W] THP ring-opened Complexes

### WTp(NO)(PMe<sub>3</sub>)(η<sup>2</sup>-(*N*-mesyl)-1-amino-5-pentenylium)(OTf) (63)



An oven-dried 4-dram vial and stir pea were set up on a stir plate. EtCN and **7** (60 mg, 0.09 mmol) were charged into the vial followed by DPhAT (34 mg, 0.11 mmol). The homogenous solution was stirred for 3 minutes, and then the reaction mixture was added to 50 mL of a stirring 4:1 Et<sub>2</sub>O/hexanes solution. A tan precipitate was formed and collected on a 15 mL F frit. This was washed 2x with 10 mL of hexanes and dried in a desiccator. (60 mg, 82% yield)

<sup>1</sup>H NMR (CD<sub>2</sub>Cl<sub>2</sub>, δ, 25 °C): 8.33 (d, *J* = 2.1 Hz, 1H, PzB3), 8.09 (d, *J* = 2.0 Hz, 1H, PzA3), 7.91 (d, *J* = 2.2 Hz, 1H, PzC5), 7.89 (d, *J* = 2.1 Hz, 1H, PzC3), 7.86 (d, *J* = 2.1 Hz, 1H, PzB5), 7.68 (d, *J* = 2.1 Hz, 1H, PzA5), 6.52 (t, *J* = 2.3 Hz, 1H, PzC4), 6.50 (t, *J* = 2.3 Hz, 1H, PzA4), 6.31 (t, *J* = 2.3 Hz, 1H, PzB4), 6.06-6.10 (m, 1H, H3), 5.87 (t, *J* = 6.0 Hz, 1H, *N*-H), 4.99 (dt, *J* = 8.4, 13.7 Hz, 1H, H4), 3.41-3.47 (m, 2H, H5/H1), 3.32-3.37 (m, 1H, H1), 3.11-3.16 (m, 1H, H2), 2.96 (s, 3H, Ms), 2.71 (ddd, *J* = 4.7, 8.9, 13.8 Hz, 1H, H5), 2.20-2.26 (m, 1H, H2), 1.26 (d, *J*<sub>PH</sub> = 9.9 Hz, 9H, PMe<sub>3</sub>).

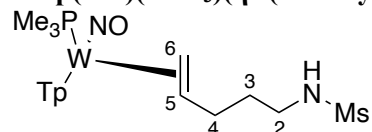
<sup>13</sup>C NMR (CD<sub>2</sub>Cl<sub>2</sub>, δ, 25 °C): 148.2 (PzA3), 145.6 (d, *J*<sub>PC</sub> = 2.2 Hz, PzB3), 142.0 (PzC3), 138.9 (PzB5), 138.8 (PzC5), 138.5 (PzA5), 132.5 (C3), 121.2 (q, *J*<sub>FC</sub> = 320.2 Hz, -OTf), 108.7 (PzB4), 108.4 (PzC4), 107.6 (PzA4), 105.1 (d, *J*<sub>PC</sub> = 5.6 Hz, C4), 52.9 (d, *J*<sub>PC</sub> = 12.9 Hz, C5), 45.0 (C2), 40.0 (Ms), 31.9 (C1), 13.6 (d, *J*<sub>PC</sub> = 33.1 Hz, 3C, PMe<sub>3</sub>).

IR: ν(NO) = 1634 cm<sup>-1</sup>

CV (MeCN; 100 mV/s): *E*<sub>1/2</sub> = -801 mV, *E*<sub>1/2</sub> = -1507 mV, (NHE)

Unable to obtain EA, SC-XRD, or HRMS data for compound. Full 2D NMR provided below.

### WTp(NO)(PMe<sub>3</sub>)(η<sup>2</sup>-(*N*-mesyl)-1-amino-5-pentene) (64D)



A test tube containing **8** (167 mg, 0.21 mmol) with EtCN (3 mL) was cooled in a toluene bath set to -50 °C. A separate tube was set up in the cold bath containing NaBH<sub>4</sub> (143 mg, 3.78 mmol) and dried THF (2 mL). Both tubes were chilled for 15 minutes, after which the NaBH<sub>4</sub> slurry was added to the solution of **8**. This solution was washed 3x with 200 mL of saturated aqueous NaHCO<sub>3</sub>. The organic layer was isolated and set aside. The combined aqueous layers were combined and back-extracted with 50 mL of DCM to prevent loss of product. The organic layers were combined in a single flask and dried with anhydrous MgSO<sub>4</sub>. This powder was then filtered off into a 60 mL coarse porosity fritted funnel and washed with DCM. The dried organic layers were then reduced *in vacuo* to dryness. The residue in the flask was redissolved in minimal DCM (approximately 10 mL). The solution was then slowly added to a stirring 50 mL solution of pentane. A tan precipitate formed immediately and was allowed to stir for ~10 minutes to ensure total precipitation. This powder was collected on a 60 mL medium porosity frit and washed 2x with 30 mL of pentane. This powder was dried in a desiccator under vacuum overnight.

<sup>1</sup>H NMR (CD<sub>2</sub>Cl<sub>2</sub>, δ, 25 °C): 8.19 (d, *J* = 1.2 Hz, 1H, PzA3), 8.04 (d, *J* = 1.2 Hz, 1H, PzB3), 7.76 (d, *J* = 2.0 Hz, 1H, PzB5), 7.70 (d, *J* = 1.6 Hz, 1H, PzC5), 7.67 (d, *J* = 2.1 Hz, 1H, PzA5), 7.33 (d, *J* = 1.6 Hz, 1H, PzC3), 6.32 (t, *J* = 2.1 Hz, 1H, PzB4), 6.25 (t, *J* = 2.1 Hz, 1H, PzA4), 6.18 (t, *J* = 2.1 Hz, 1H, PzC4), 4.46-4.51 (b, 1H, NH), 3.20-3.27 (m, 2H, H2), 2.91 (s, 3H, Ms), 2.52-2.59 (m, 1H, H4), 1.78-1.84 (m, 2H, H3), 1.71-1.78 (m, 4H, H4/H6), 1.53-1.57 (m, 1H, H6), 1.28 (d, *J*<sub>PH</sub> = 8.16 Hz, 9H, PMe<sub>3</sub>), 1.05-1.10 (m, 1H, H5).

$^{13}\text{C}$  NMR ( $\text{CD}_2\text{Cl}_2$ ,  $\delta$ , 25 °C): 144.4 (d,  $J_{PC} = 1.9$  Hz, PzB3), 142.9 (PzA3), 141.1 (PzC3), 136.7 (PzC5), 136.3 (PzB5), 135.8 (PzA5), 106.3 (PzB4), 105.9 (PzA4), 105.8 (PzC4), 52.8 (C5), 44.1 (C2), 43.9 (d,  $J_{PC} = 10.7$  Hz, C6), 40.3 (Ms), 37.4 (C3), 34.9 (C4), 14.2 (d,  $J_{PC} = 28.6$  Hz, 3C,  $\text{PMe}_3$ ).

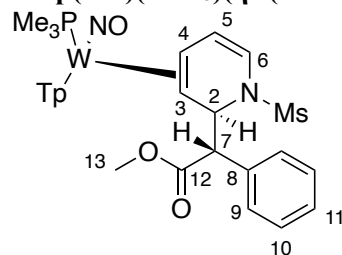
IR:  $\nu(\text{NO}) = 1532 \text{ cm}^{-1}$

CV, (MeCN; 100 mV/s):  $E_{p,a} = +0.65 \text{ V}$

*Unable to obtain EA, SC-XRD, or HRMS data for compound. Full 2D NMR provided below.*

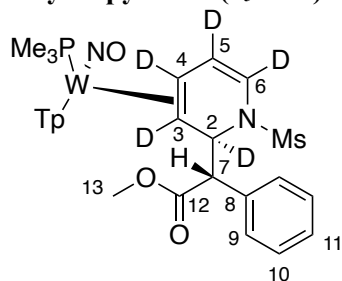
## Synthesis and Characterization of [W] MPH 1,2-DHP Complexes

### WTp(NO)(PMe<sub>3</sub>)(η<sup>2</sup>-(*N*-mesyl)-2-(methyl- $\alpha$ -phenylacetate)-1,2-dihydropyridine (35D)



Previously described on page 198-199

### WTp(NO)(PMe<sub>3</sub>)(η<sup>2</sup>-(*N*-mesyl)-2-(methyl- $\alpha$ -phenylacetate)-2-*syn*-3,4,5,6-pentadeutero-1,2-dihydropyridine (*d*<sub>5</sub>-35D)



Methyl  $\alpha$ -phenylbromoacetate (1.35 g, 5.89 mmol), *d*<sub>5</sub>-33D (1.95 g, 2.39 mmol), and THF (10 mL) were charged to a flame-dried 50 mL round-bottom flask with a 1 inch stir bar. Zinc powder (684 mg, 10.46 mmol) was added to initiate the reaction, and the heterogenous solution was stirred for 1 hour. The zinc was removed by filtering the solution through a celite plug set up in a 60 mL coarse porosity frit with 1 inch of celite, which was then washed with residual DCM to prevent loss of product. The solution was diluted with 150 mL of DCM and added to a separatory funnel. This solution was washed 3x with 200 mL of saturated aqueous NaHCO<sub>3</sub>. The organic layer was isolated and set aside. The combined aqueous layers were combined and back-extracted with 50 mL of DCM to prevent loss of product. The organic layers were combined in a single flask and dried with anhydrous MgSO<sub>4</sub>. This powder was then filtered off into a 60 mL coarse porosity fritted funnel and washed with DCM. The dried organic layers were then reduced *in vacuo* to dryness. The residue in the flask was redissolved in minimal DCM (approximately 10 mL). The solution was then slowly added to 200mL of stirring pentane. A tan precipitate formed immediately and was allowed to stir for ~10 minutes to ensure total precipitation. This powder was collected on a 60 mL medium porosity frit and washed 2x with 30 mL of pentane. This powder was dried in a desiccator under vacuum for ~30 minutes. The dried powder was gently added to a 4-dram vial and stir pea filled with 15 mL of stirring MeOH and triturated overnight. The tan precipitate was collected on a 15 mL fine porosity frit and washed 2x with 10 mL of MeOH. The highly pure tan precipitate, after drying in a desiccator for 2 hours, was added to a 4-dram vial and stir pea filled with 15 mL of DME and triturated overnight. The highly enriched tan powder was collected on a 15 mL fine porosity frit and washed 1x with 10 mL of DME and 2x with 10 mL of diethyl ether. This powder was then dried in the desiccator. (700 mg, 36% yield)

<sup>1</sup>H NMR (CD<sub>2</sub>Cl<sub>2</sub>,  $\delta$ , 25 °C): 8.16 (d, *J* = 1.8 Hz, 1H, PzA3), 8.10 (d, *J* = 1.9 Hz, 1H, PzB3), 7.79 (d, *J* = 2.4 Hz, 1H, PzB5), 7.75 (d, *J* = 2.2 Hz, 1H, PzC5), 7.67 (d, *J* = 2.3 Hz, 1H, PzA5), 7.41 (d, *J* = 7.1 Hz, 2H, H9), 7.25 (t, *J* = 7.1 Hz, 2H, H10), 7.24 (d, *J* = 2.2 Hz, 1H, PzC3), 7.21 (tt, *J* = 1.3, 7.1 Hz, 1H, H11), 6.35 (t, *J* = 2.2 Hz, 1H, PzB4), 6.29 (t, *J* = 2.2 Hz, 1H, PzA4), 6.23 (t, *J* = 2.2 Hz, 1H, PzC4), 4.33 (s, 1H, H7), 3.42 (s, 3H, H13), 2.59 (Ms), 1.19 (d, *J*<sub>PC</sub> = 8.5 Hz, 9H, PMe<sub>3</sub>).

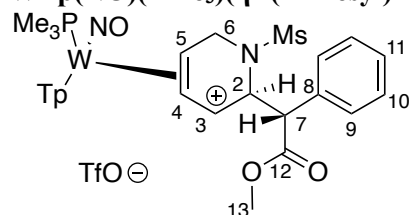
$^{13}\text{C}$  NMR ( $\text{CD}_2\text{Cl}_2$ ,  $\delta$ , 25 °C): 173.5 (C12), 143.9 (PzA3), 142.8 (d,  $J_{PC}$  = 2.0 Hz, PzB3), 139.9 (PzC3), 137.6 (C8), 137.0 (PzC5), 136.4 (PzB5), 135.9 (PzA5), 130.1 (2C, C9), 128.3 (2C, C10), 127.7 (C11), 115.4 (t,  $J_{DC}$  = 26.4 Hz, C6), 114.2 (t,  $J_{DC}$  = 22.5 Hz, C5), 106.8 (PzB4), 106.4 (PzC4), 106.2 (PzA4), 63.3 (t,  $J_{DC}$  = 21.2 Hz, C3), 59.8 (C7), 58.7 (t,  $J_{DC}$  = 22.3 Hz, C2), 51.8 (C13), 43.5-43.8 (m, C4), 41.9 (Ms), 13.0 (d,  $J_{PC}$  = 28.3, 3C,  $\text{PMe}_3$ ).

## Synthesis and Characterization of [W] MPH 1,2,6-allyl Complexes

### General Synthesis

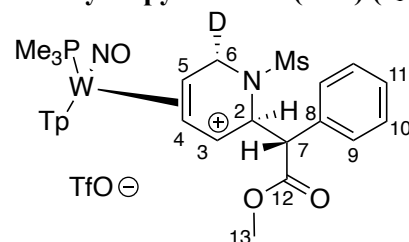
An oven-dried 4-dram vial containing a stir pea was set up on a hot plate. To this vial, *d<sub>x</sub>*-**35D** (643 mg, 0.79 mmol) was added followed by 3 mL of EtCN. A separate oven-dried 4-dram vial was tared and filled with 1 mL of EtCN. To this was then added  $^x\text{HOTf}$  (153 mg, 1.02 mmol), and the combined solution was then added to the *d<sub>x</sub>*-**35D**/EtCN solution, which was stirred until homogenous (about 1 minute). This solution was then added to a 150 mL stirring solution of Et<sub>2</sub>O in a 300 mL Erlenmeyer flask with a 1" stir bar. A tan precipitate immediately formed, and the slurry was triturated for 10 minutes. The powder was then collected in a 30 mL F frit, washed 2x with 20 mL of Et<sub>2</sub>O, and dried in a desiccator. (768 mg, 95% yield)

### WTp(NO)(PMe<sub>3</sub>)( $\eta^3$ -(*N*-mesyl)-2-(methyl- $\alpha$ -phenylacetate)-1,2,3,6-tetrahydropyridinium (OTf) (**37**))



Previously described on page 200

### WTp(NO)(PMe<sub>3</sub>)( $\eta^3$ -(*N*-mesyl)-2-(methyl- $\alpha$ -phenylacetate)-6-*syn*-deutero-1,2,3,6-tetrahydropyridinium (OTf) (*d<sub>T</sub>*-**37**))

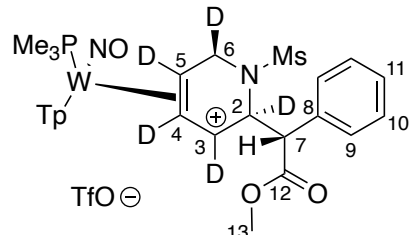


$^1\text{H}$  NMR ( $\text{CD}_2\text{Cl}_2$ ,  $\delta$ , 25 °C): 8.31 (d,  $J$  = 2.2 Hz, 1H, PzB3), 8.11 (d,  $J$  = 2.2 Hz, 1H, PzC3), 7.90 (d,  $J$  = 2.3 Hz, 1H, PzC5), 7.80 (d,  $J$  = 2.3 Hz, 1H, PzB5), 7.59 (d,  $J$  = 2.3 Hz, 1H, PzA5), 7.53 (d,  $J$  = 7.4 Hz, 2H, H9), 7.46 (t,  $J$  = 7.8 Hz, 2H, H10), 7.42 (t,  $J$  = 7.4 Hz, 1H, H11), 6.86 (d,  $J$  = 2.2 Hz, 1H, PzA3), 6.58 (t,  $J$  = 2.4 Hz, 1H, PzC4), 6.47 (t,  $J$  = 2.4 Hz, 1H, PzB4), 5.98 (t,  $J$  = 2.4 Hz, 1H, PzA4), 5.89 (d,  $J$  = 7.9 Hz, 1H, H3), 5.46-5.48 (m, 1H, H2), 5.23 (t,  $J$  = 8.0 Hz, 1H, H4), 4.77-4.79 (m, 2H, H7, H6), 4.49-4.54 (m, 1H, H5), 3.84 (s, 3H, H13), 2.95 (s, 3H, Ms), 1.26 (d,  $J_{PH}$  = 9.7 Hz, 9H,  $\text{PMe}_3$ ).

$^{13}\text{C}$  NMR ( $\text{CD}_2\text{Cl}_2$ ,  $\delta$ , 25 °C): 171.4 (C12), 146.4 (PzA3), 144.5 (d,  $J_{PC}$  = 2.1 Hz, PzB3), 142.7 (PzC3), 138.9 (PzC5), 138.7 (PzA5/B5), 138.6 (PzA5/B5), 134.6 (C8), 129.7 (2C, C10), 129.0 (2C, C9), 128.9 (C11), 121.4 (q,  $J_{FC}$  = 321.7 Hz, TfO<sup>-</sup>), 120.2 (C3), 109.1 (PzB4/C4), 108.9 (PzB4/C4), 107.3 (PzA4), 98.3 (d,  $J_{PC}$  = 3.0 Hz, C4), 65.1 (d,  $J_{PC}$  = 14.6 Hz, C5), 58.6 (C2), 55.9 (C7), 53.0 (C13), 42.7 (d,  $J_{DC}$  = 20.1 Hz, C6), 41.2 (Ms), 13.5 (d,  $J_{PC}$  = 32.9 Hz, 3C,  $\text{PMe}_3$ ).



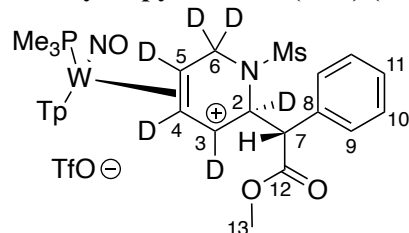
**WTp(NO)(PMe<sub>3</sub>)(η<sup>3</sup>-(*N*-mesyl)-2-(methyl- $\alpha$ -phenylacetate)-2-*syn*-6-*anti*-3,4,5-pentadeutero-1,2,3,6-tetrahydropyridinium (OTf) (*d*<sub>5</sub>-37)**



<sup>1</sup>H NMR (CD<sub>2</sub>Cl<sub>2</sub>,  $\delta$ , 25 °C): 8.30 (d,  $J$  = 2.1 Hz, 1H, PzB3), 8.13 (d,  $J$  = 2.1 Hz, 1H, PzC3), 7.91 (d,  $J$  = 2.3 Hz, 1H, PzC5), 7.83 (d,  $J$  = 2.2 Hz, 1H, PzB5), 7.61 (d,  $J$  = 2.3 Hz, 1H, PzA5), 7.54 (d,  $J$  = 7.6 Hz, 2H, H9), 7.46 (t,  $J$  = 7.6 Hz, 2H, H10), 7.42 (d,  $J$  = 7.4 Hz, 1H, H11), 6.84 (d,  $J$  = 2.1 Hz, 1H, PzA3), 6.57 (t,  $J$  = 2.3 Hz, 1H, PzC4), 6.48 (t,  $J$  = 2.3 Hz, 1H, PzB4), 5.98 (t,  $J$  = 2.3 Hz, 1H, PzA4), 4.78 (s, 1H, H7), 4.10 (s, 1H, H6<sup>syn</sup>), 3.84 (s, 3H, H13), 2.96 (s, 3H, Ms), 1.27 (t,  $J_{PH}$  = 9.7 Hz, 9H, PMe<sub>3</sub>).

<sup>13</sup>C NMR (CD<sub>2</sub>Cl<sub>2</sub>,  $\delta$ , 25 °C): 171.3 (C12), 146.3 (PzA3), 144.4 (d,  $J_{PC}$  = 2.2 Hz, PzB3), 142.7 (PzC3), 138.9 (PzC5), 138.7 (PzA5/B5), 138.6 (PzA5/B5), 134.6 (C8), 129.7 (2C, C10), 129.0 (2C, C9), 128.8 (C11), 121.4 (q,  $J_{FC}$  = 320 Hz, TfO<sup>-</sup>), 118.9 (t,  $J_{DC}$  = 23.5 Hz, C3), 109.0 (PzB4/C4), 108.9 (PzB4/C4), 107.3 (PzA4), 98.1 (t,  $J_{DC}$  = 25.7 Hz, C4), 64.6-65.0 (m, C5), 58.3 (t,  $J_{DC}$  = 22.4 Hz, C2), 55.8 (C7), 53.0 (C13), 42.6 (t,  $J_{DC}$  = 21.5 Hz, C6), 41.1 (Ms), 13.50 (d,  $J_{PC}$  = 32.9 Hz, 3C, PMe<sub>3</sub>).

**WTp(NO)(PMe<sub>3</sub>)(η<sup>3</sup>-(*N*-mesyl)-2-(methyl- $\alpha$ -phenylacetate)-2-*syn*-3,4,5,6,6-hexadeutero-1,2,3,6-tetrahydropyridinium (OTf) (*d*<sub>6</sub>-37)**



<sup>1</sup>H NMR (CD<sub>2</sub>Cl<sub>2</sub>,  $\delta$ , 25 °C): 8.30 (d,  $J$  = 2.1 Hz, 1H, PzB3), 8.13 (d,  $J$  = 2.2 Hz, 1H, PzC3), 7.91 (d,  $J$  = 2.2 Hz, 1H, PzC5), 7.82 (d,  $J$  = 2.3 Hz, 1H, PzB5), 7.60 (d,  $J$  = 2.3 Hz, 1H, PzA5), 7.54 (d,  $J$  = 7.4 Hz, 2H, H9), 7.46 (t,  $J$  = 7.6 Hz, 2H, H10), 7.42 (t,  $J$  = 7.3 Hz, 1H, H11), 6.84 (t,  $J$  = 2.1 Hz, 1H, PzA3), 6.57 (t,  $J$  = 2.3 Hz, 1H, PzC4), 6.47 (t,  $J$  = 2.4 Hz, 1H, PzB4), 5.98 (t,  $J$  = 2.4 Hz, 1H, PzA4), 4.77 (s, 1H, H7), 3.84 (s, 3H, H13), 2.96 (s, 3H, Ms), 1.27 (d,  $J_{PC}$  = 9.7 Hz, 9H, PMe<sub>3</sub>).

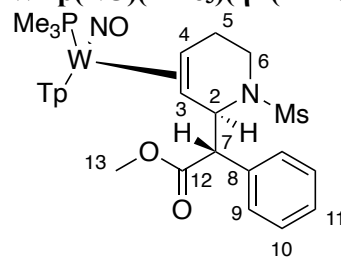
<sup>13</sup>C NMR (CD<sub>2</sub>Cl<sub>2</sub>,  $\delta$ , 25 °C): 171.3 (C12), 146.4 (PzA3), 144.4 (d,  $J_{PC}$  = 2.4 Hz, PzB3), 142.8 (PzC3), 138.9 (PzC5), 138.7 (PzA5/B5), 138.6 (PzA5/B5), 134.6 (C8), 129.7 (2C, C10), 129.0 (2C, C9), 128.8 (C11), 121.4 (q,  $J_{FC}$  = 320.8 Hz, TfO<sup>-</sup>), 119.0 (t,  $J_{DC}$  = 26.3 Hz, C3), 109.1 (PzB4/C4), 108.9 (PzB4/C4), 107.3 (PzA4), 98.1 (t,  $J_{DC}$  = 25.7, C4), 64.5-64.9 (m, C5), 58.2 (t,  $J_{DC}$  = 22.2 Hz, C2), 55.9 (C7), 53.0 (C13), 42.1-42.5 (m, C6), 41.2 (Ms), 13.5 (d,  $J_{PC}$  = 32.9 Hz, 3C, PMe<sub>3</sub>).

## Synthesis and Characterization of [W] MPH 1,2,5,6-THP Complexes

### General Synthesis

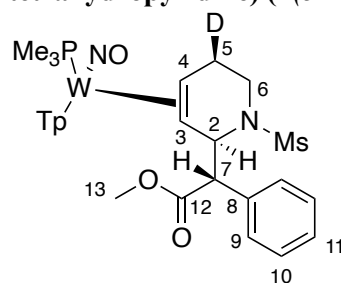
NaCNB<sup>X</sup>H<sub>3</sub> (340 mg, 5.4 mmol) and dry THF (2.0 mL) were added to a screw-cap test tube that was placed in a cold bath set at -50 °C. To another tube was added **d<sub>x</sub>-37** (518 mg, 0.54 mmol) and propionitrile (3 mL). Both tubes were chilled for 15 minutes before the NaCNB<sup>X</sup>H<sub>3</sub>/THF solution was added to the solution of **d<sub>x</sub>-37**, which sat in the cold bath for 16 hours. This solution was diluted with 50 mL of DCM and was washed 3x with 50 mL of saturated aqueous NaHCO<sub>3</sub>. The organic layer was isolated and set aside. The combined aqueous layers were combined and back-extracted with 50 mL of DCM to prevent loss of product. The organic layers were combined in a single flask and dried with anhydrous MgSO<sub>4</sub>. This powder was then filtered off into a 60 mL coarse porosity fritted funnel and washed with DCM. The dried organic layers were then reduced *in vacuo* down to dryness. The residue in the flask was redissolved in minimal DCM (approximately 10 mL). The solution was then slowly added to 100 mL of stirring pentane. A light tan precipitate formed immediately and was allowed to stir for ~10 minutes to ensure total precipitation. This powder was collected on a 15 mL fine porosity frit and washed 2x with 10 mL of pentane. This powder was dried in a desiccator under vacuum overnight. (202 mg, 46% yield)

### WTp(NO)(PMe<sub>3</sub>)(η<sup>2</sup>-(*N*-mesyl)-2-(methyl- $\alpha$ -phenylacetate)-1,2,5,6-tetrahydropyridine) (**38**)



Previously described on page 202

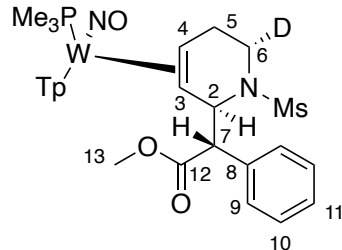
### WTp(NO)(PMe<sub>3</sub>)(η<sup>2</sup>-(*N*-mesyl)-2-(methyl- $\alpha$ -phenylacetate)-5-*anti*-deutero-1,2,5,6-tetrahydropyridine) ( $\pm$ (5'*R*)-**d<sub>1</sub>-38**)



<sup>1</sup>H NMR (CD<sub>2</sub>Cl<sub>2</sub>,  $\delta$ , 25 °C): 8.31 (d,  $J$  = 1.8 Hz, 1H, PzA3), 8.04 (d,  $J$  = 1.8 Hz, 1H, PzB3), 7.75 (d,  $J$  = 2.3 Hz, 1H, PzC5), 7.73 (d,  $J$  = 2.3 Hz, 1H, PzB5), 7.69 (d,  $J$  = 2.3 Hz, 1H, PzA5), 7.38 (d,  $J$  = 7.1 Hz, 2H, H9), 7.24 (tt,  $J$  = 1.5, 7.1 Hz, 2H, H10), 7.21 (tt,  $J$  = 1.5, 7.1 Hz, 1H, H11), 7.20 (d,  $J$  = 1.6 Hz, 1H, PzC3), 6.32 (t,  $J$  = 2.2 Hz, 1H, PzB4), 6.31 (t,  $J$  = 2.2 Hz, 1H, PzA4), 6.24 (t,  $J$  = 2.2 Hz, 1H, PzC4), 5.54 (dd,  $J$  = 1.8, 8.3 Hz, 1H, H2), 4.07 (d,  $J$  = 8.3 Hz, H7), 3.39 (dd,  $J$  = 4.9, 13.1 Hz, 1H, H6), 3.06 (s, 3H, H13), 2.98 (dd,  $J$  = 11.8, 12.9 Hz, 1H, H6), 2.84 (ddd,  $J$  = 4.9, 10.4, 20.7 Hz, 1H, H4), 2.66 (dt,  $J$  = 5.0, 11.5 Hz, 1H, H5), 2.19 (s, 3H, Ms), 1.22 (d,  $J_{PH}$  = 8.3 Hz, 9H, PMe<sub>3</sub>), 0.73 (d,  $J$  = 11.7 Hz, 1H, H3).

<sup>13</sup>C NMR (CD<sub>2</sub>Cl<sub>2</sub>,  $\delta$ , 25 °C): 172.7 (C12), 144.0 (PzA3), 143.2 (d,  $J_{PC}$  = 2.1 Hz, PzB3), 140.0 (PzC3), 137.7 (C8), 136.6 (PzB5/C5), 136.4 (PzB5/C5), 136.0 (PzA5), 130.1 (2C, C9), 128.6 (2C, C10), 127.9 (C11), 106.6 (PzA4/B4/C4), 106.4 (PzA4/B4/C4), 106.3 (PzA4/B4/C4), 62.8 (C7), 59.7 (C2), 54.3 ( $J_{WC}$  = 32.9 Hz, C3), 51.4 (C13), 46.0 (d,  $J_{PC}$  = 12.6 Hz, C4), 41.2 (C6), 40.6 (Ms), 27.9 (t,  $J_{DC}$  = 18.6 Hz, C5), 13.8 (d,  $J_{PC}$  = 27.9 Hz, 3C, PMe<sub>3</sub>).

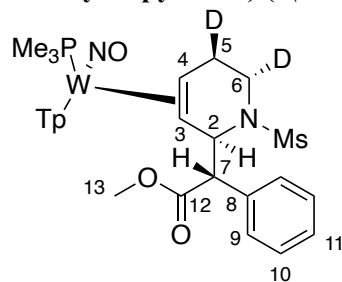
**WTp(NO)(PMe<sub>3</sub>)(η<sup>2</sup>-(*N*-mesyl)-2-(methyl- $\alpha$ -phenylacetate)-6-*syn*-deutero-1,2,5,6-tetrahydropyridine) ( $\pm$ (6'*S*)-*d*<sub>1</sub>-38)**



<sup>1</sup>H NMR (CD<sub>2</sub>Cl<sub>2</sub>,  $\delta$ , 25 °C): 8.33 (s, 1H, PzA3), 8.05 (d,  $J$  = 1.7 Hz, 1H, PzB3), 7.76 (d,  $J$  = 2.2 Hz, 1H, PzB5), 7.75 (d,  $J$  = 2.2 Hz, 1H, PzC5), 7.70 (d,  $J$  = 2.2 Hz, 1H, PzA5), 7.40 (d,  $J$  = 7.3 Hz, 2H, H9), 7.25 (t,  $J$  = 7.0 Hz, 2H, H10), 7.20-7.23 (m, 2H, H11 & PzC3), 6.33 (t,  $J$  = 2.1 Hz, 1H, PzB4), 6.31 (t,  $J$  = 2.1 Hz, 1H, PzA4), 6.25 (t,  $J$  = 2.1 Hz, 1H, PzC4), 5.56 (dd,  $J$  = 1.7, 8.3 Hz, 1H, H2), 4.09 (d,  $J$  = 8.2 Hz, 1H, H7), 3.08 (s, 3H, H13), 2.96-3.00 (m, 1H, H6), 2.82-2.89 (m, 1H, H4), 2.67-2.72 (m, 1H, H5), 2.51-2.55 (m, 1H, H5), 2.22 (s, 3H, Ms), 1.22 (d,  $J_{PH}$  = 8.3 Hz, 9H, PMe<sub>3</sub>), 0.76 (d,  $J$  = 11.7 Hz, 1H, H3).

<sup>13</sup>C NMR (CD<sub>2</sub>Cl<sub>2</sub>,  $\delta$ , 25 °C): 172.6 (C12), 143.9 (PzA3), 143.1 (d,  $J_{PC}$  = 1.8 Hz, PzB3), 140.0 (PzC3), 137.6 (C8), 136.6 (PzB5/C5), 136.4 (PzB5/C5), 136.0 (PzA5), 130.1 (2C, C9), 128.5 (2C, C10), 127.8 (C11), 106.6 (PzA4/B4/C4), 106.4 (PzA4/B4/C4), 106.3 (PzA4/B4/C4), 62.7 (C7), 59.7 (C2), 54.3 (C3), 51.4 (C13), 46.0 (d,  $J_{PC}$  = 12.5 Hz, C4), 40.9 (t,  $J_{PC}$  = 20.5 Hz, C6), 40.5 (Ms), 28.2 (d,  $J_{PC}$  = 1.9 Hz, C5), 13.7 (d,  $J_{PC}$  = 27.8 Hz, 3C, PMe<sub>3</sub>).

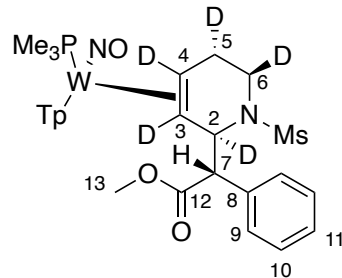
**WTp(NO)(PMe<sub>3</sub>)(η<sup>2</sup>-(*N*-Mesyl)-2-(methyl- $\alpha$ -phenylacetate)-6-*syn*-5-*anti*-dideutero-1,2,5,6-tetrahydropyridine) ( $\pm$ (5'*R*,6'*S*)-*d*<sub>2</sub>-38)**



<sup>1</sup>H NMR (CD<sub>2</sub>Cl<sub>2</sub>,  $\delta$ , 25 °C): 8.32 (s, 1H, PzA3), 8.05 (s, 1H, PzB3), 7.76 (d,  $J$  = 2.2 Hz, 1H, PzB5), 7.74 (d,  $J$  = 2.2 Hz, 1H, PzC5), 7.69 (d,  $J$  = 2.2 Hz, 1H, PzA5), 7.40 (d,  $J$  = 7.2 Hz, 2H, C9), 7.25 (t,  $J$  = 7.6 Hz, 2H, C10), 7.20-7.23 (m, 2H, C11 & PzC3), 6.32 (t,  $J$  = 2.1 Hz, 1H, PzB4), 6.31 (t,  $J$  = 2.1 Hz, 1H, PzA4), 6.24 (t,  $J$  = 2.0 Hz, 1H, PzC4), 5.55 (dd,  $J$  = 1.5, 8.2 Hz, 1H, H2), 4.08 (d,  $J$  = 8.2 Hz, 1H, H7), 3.08 (H13), 2.95-3.00 (m, 1H, H6), 2.82-2.88 (m, 1H, H4), 2.65-2.69 (m, 1H, H5), 2.21 (s, 3H, Ms), 1.22 (d,  $J_{PH}$  = 8.3 Hz, 9H, PMe<sub>3</sub>), 0.75 (d,  $J$  = 11.7 Hz, 1H, H3).

<sup>13</sup>C NMR (CD<sub>2</sub>Cl<sub>2</sub>,  $\delta$ , 25 °C): 172.6 (C12), 143.9 (PzA3), 143.1 (d,  $J_{PC}$  = 2.2 Hz, PzB3), 140.0 (PzC3), 137.7 (C8), 136.6 (PzB5/C5), 136.4 (PzB5/C5), 136.0 (PzA5), 130.1 (2C, C9), 128.5 (2C, C10), 127.8 (C11), 106.6 (PzA4/B4/C4), 106.3 (PzA4/B4/C4), 106.2 (PzA4/B4/C4), 62.8 (C7), 59.7 (C2), 54.3 (C3), 51.4 (C13), 46.0 (d,  $J_{PC}$  = 12.5 Hz, C4), 40.9 (t,  $J_{DC}$  = 20.9 Hz, C6), 40.6 (Ms), 27.8 (t,  $J_{DC}$  = 18.3 Hz, C5), 13.7 (d,  $J_{PC}$  = 27.8 Hz, 3C, PMe<sub>3</sub>).

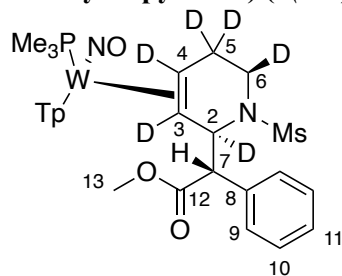
**WTp(NO)(PMe<sub>3</sub>)( $\eta^2$ -(*N*-mesyl)-2-(methyl- $\alpha$ -phenylacetate)-2,5-*syn*-6-*anti*-3,4-pentadeutero-1,2,5,6-tetrahydropyridine) ( $\pm$ (5'*S*,6'*R*)-*d*<sub>5</sub>-38)**



<sup>1</sup>H NMR (CD<sub>2</sub>Cl<sub>2</sub>,  $\delta$ , 25 °C): 8.31 (s, 1H, PzA3), 8.04 (s, 1H, PzB3), 7.75 (d,  $J$  = 1.9 Hz, 1H, PzB5), 7.74 (d,  $J$  = 1.9 Hz, 1H, PzC5), 7.69 (d,  $J$  = 1.9 Hz, 1H, PzA5), 7.38 (d,  $J$  = 7.4 Hz, 2H, H9), 7.24 (t,  $J$  = 7.4 Hz, 2H, H10), 7.21 (d,  $J$  = 7.4 Hz, 1H, H11), 7.19 (s, 1H, PzC3), 6.32 (t,  $J$  = 2.0 Hz, 1H, PzB4), 6.31 (t,  $J$  = 2.0 Hz, 1H, PzA4), 6.24 (t,  $J$  = 2.0 Hz, 1H, PzC4), 4.06 (s, 1H, H7), 3.37 (d,  $J$  = 2.2 Hz, 1H, H6), 3.05 (s, 3H, H13), 2.48 (d,  $J$  = 2.2 Hz, 1H, H5), 2.18 (s, 3H, Ms), 1.22 (d,  $J_{PH}$  = 8.3 Hz, 9H, PMe<sub>3</sub>).

<sup>13</sup>C NMR (CD<sub>2</sub>Cl<sub>2</sub>,  $\delta$ , 25 °C): 172.7 (C12), 144.0 (PzA3), 143.2 (d,  $J_{PC}$  = 2.0 Hz, PzB3), 140.0 (PzC3), 137.7 (C8), 136.6 (PzB5/C5), 136.4 (PzB5/C5), 136.0 (PzA5), 130.1 (2C, C9), 128.6 (2C, C10), 127.9 (C11), 106.6 (PzA4/B4/C4), 106.4 (PzA4/B4/C4), 106.3 (PzA4/B4/C4), 62.7 (C7), 59.3 (t,  $J_{DC}$  = 21.9 Hz, C2), C3 buried under solvent peak, 51.4 (C13), 45.1-45.5 (m, C4), 40.8 (t,  $J_{DC}$  = 21.2 Hz, C6), 40.6 (Ms), 27.7 (t,  $J_{DC}$  = 19.6 Hz, C5), 13.8 (d,  $J_{PC}$  = 27.9 Hz, 3C, PMe<sub>3</sub>).

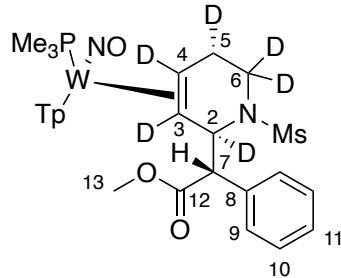
**WTp(NO)(PMe<sub>3</sub>)( $\eta^2$ -(*N*-mesyl)-2-(methyl- $\alpha$ -phenylacetate)-2-*syn*-6-*anti*-3,4,5,5-hexadeutero-1,2,5,6-tetrahydropyridine) ( $\pm$ (6'*R*)-*d*<sub>6</sub>-38)**



<sup>1</sup>H NMR (CD<sub>2</sub>Cl<sub>2</sub>,  $\delta$ , 25 °C): 8.31 (s, 1H, PzA3), 8.04 (s, 1H, PzB3), 7.75 (d,  $J$  = 1.9 Hz, 1H, PzB5), 7.73 (d,  $J$  = 1.9 Hz, 1H, PzC5), 7.69 (d,  $J$  = 1.9 Hz, 1H, PzA5), 7.38 (d,  $J$  = 7.4 Hz, 2H, H9), 7.24 (t,  $J$  = 7.4 Hz, 2H, H10), 7.21 (d,  $J$  = 7.3 Hz, 1H, H11), 7.19 (d,  $J$  = 1.6 Hz, 1H, PzC3), 6.32 (t,  $J$  = 2.1 Hz, 1H, PzB4), 6.31 (t,  $J$  = 2.0 Hz, 1H, PzA4), 6.24 (t,  $J$  = 2.0 Hz, 1H, PzC4), 4.05 (s, 1H, H7), 3.37 (s, 1H, H6), 3.05 (s, 3H, H13), 2.18 (s, 3H, Ms), 1.22 (d,  $J_{PH}$  = 8.2 Hz, 9H, PMe<sub>3</sub>).

<sup>13</sup>C NMR (CD<sub>2</sub>Cl<sub>2</sub>,  $\delta$ , 25 °C): 172.7 (C12), 144.0 (PzA3), 143.2 (d,  $J_{PC}$  = 2.2 Hz, PzB3), 140.0 (PzC3), 137.7 (C8), 136.6 (PzB5/C5), 136.4 (PzB5/C5), 136.0 (PzA5), 130.1 (2C, C9), 128.6 (2C, C10), 127.9 (C11), 106.6 (PzA4/B4/C4), 106.4 (PzA4/B4/C4), 106.3 (PzA4/B4/C4), 62.7 (C7), 59.3 (t,  $J_{DC}$  = 21.4 Hz, C2), C3 buried under solvent peak, 51.4 (C13), 45.1-45.5 (m, C4), 40.7 (t,  $J_{DC}$  = 20.5 Hz, C6), 40.6 (Ms), 27.1-27.4 (m, C5), 13.8 (d,  $J_{PC}$  = 27.9 Hz, 3C, PMe<sub>3</sub>).

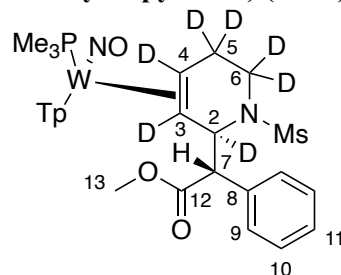
**WTP(NO)(PMe<sub>3</sub>)(η<sup>2</sup>-(*N*-mesyl)-2-(methyl- $\alpha$ -phenylacetate)-2,5-*syn*-3,4,6,6-hexadeutero-1,2,5,6-tetrahydropyridine) ( $\pm$ (5'*S*)-*d*<sub>6</sub>-38)**



<sup>1</sup>H NMR (CD<sub>2</sub>Cl<sub>2</sub>,  $\delta$ , 25 °C): 8.41 (s, 1H, PzA3), 8.07 (s, 1H, PzB3), 7.79 (s, 1H, PzB5), 7.76 (s, 1H, PzC5), 7.75 (s, 1H, PzA5), 7.47 (d,  $J = 7.4$  Hz, 2H, H9), 7.38 (t,  $J = 7.4$ , 2H, H10), 7.32 (t,  $J = 7.2$  Hz, 1H, H11), 7.21 (s, 1H, PzC3), 6.42 (s, 1H, PzA4/B4/C4), 6.37 (s, 1H, PzA4/B4/C4), 6.27 (s, 1H, PzA4/B4/C4), 4.12 (s, 1H, H7), 2.99 (s, 3H, H13), 2.76 (s, 1H, H5), 1.64 (s, 3H, Ms), 1.26 (d,  $J_{PH} = 8.6$  Hz, 9H, PMe<sub>3</sub>).

<sup>13</sup>C NMR (CD<sub>2</sub>Cl<sub>2</sub>,  $\delta$ , 25 °C): 172.1 (C12), 144.5 (PzA3), 143.3 (PzB3), 140.3 (PzC3), 137.9 (C8), 137.2 (PzB5/C5), 136.9 (PzB5/C5), 136.7 (PzA5), 129.5 (2C, C9), 129.4 (2C, C10), 128.8 (C11), 107.4 (PzA4/B4/C4), 107.0 (PzA4/B4/C4), 106.7 (PzA4/B4/C4), 61.6 (C7), 58.5-58.8 (C2), 56.5-56.8 (m, C3), 51.8 (C13), 45.9-46.2 (m, C4), 39.5 (Ms), 38.8-39.1 (m, C6), 26.8-27.1 (m, C5), 13.6 (d,  $J_{PC} = 29.3$  Hz, 3C, PMe<sub>3</sub>).

**WTP(NO)(PMe<sub>3</sub>)(η<sup>2</sup>-(*N*-mesyl)-2-(methyl- $\alpha$ -phenylacetate)-2-*syn*-3,4,5,5,6,6-heptadeutero-1,2,5,6-tetrahydropyridine) (*d*<sub>7</sub>-38)**



<sup>1</sup>H NMR (CD<sub>2</sub>Cl<sub>2</sub>,  $\delta$ , 25 °C): 8.35 (s, 1H, PzA3), 8.03 (s, 1H, PzB3), 7.75 (d,  $J = 2.1$  Hz, 1H, PzB5), 7.73 (d,  $J = 1.8$  Hz, 1H, PzC5), 7.70 (d,  $J = 1.8$  Hz, 1H, PzA5), 7.40 (d,  $J = 7.5$  Hz, 2H, H9), 7.27 (t,  $J = 7.5$  Hz, 2H, H10), 7.22 (t,  $J = 7.2$  Hz, 1H, H11), 7.16 (s, 1H, PzC3), 6.35 (s, 1H, PzB4), 6.32 (s, 1H, PzA4), 6.22 (s, 1H, PzC4), 4.01 (s, 1H, H7), 2.97 (s, 3H, H13), 2.02 (s, 3H, Ms), 1.20 (d,  $J_{PH} = 8.2$  Hz, 9H, PMe<sub>3</sub>).

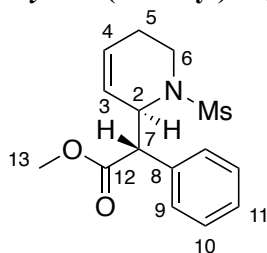
<sup>13</sup>C NMR (CD<sub>2</sub>Cl<sub>2</sub>,  $\delta$ , 25 °C): 172.5 (C12), 143.9 (PzA3), 143.0 (d,  $J_{PC} = 1.6$  Hz, PzB3), 139.7 (PzC3), 137.5 (C8), 136.4 (PzB5/C5), 136.3 (PzB5/C5), 135.9 (PzA5), 129.9 (2C, C9), 128.6 (2C, C10), 127.9 (C11), 106.5 (PzA4/B4/C4), 106.2 (2C, PzA4/B4/C4), 62.4 (C7), 58.9-59.1 (m, C2), C3 buried under solvent peak, 51.3 (C13), 44.6-44.9 (m, C4), 40.3 (Ms), 40.0-40.3 (m, C6), 26.7-27.3 (m, C5), 13.6 (d,  $J_{PC} = 27.9$  Hz, 3C, PMe<sub>3</sub>).

## Synthesis and Characterization of MPH 1,2,5,6-THPs

### General Synthesis

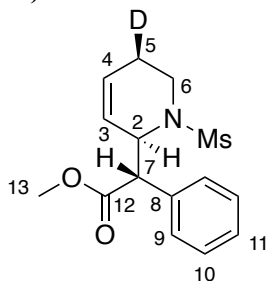
Acetone (3 mL), DDQ (170 mg, 0.75 mmol), and *d<sub>r</sub>*-**38** (200 mg, 0.25 mmol) were added to a 4-dram vial containing a stir pea. The reaction was stirred in a fume hood for 4 hours. The solution was flushed through a 1 cm basic alumina plug set up in a 30 mL coarse porosity frit. This solution was diluted with 30 mL of DCM and was washed 3x with 50 mL of saturated aqueous NaHCO<sub>3</sub>. The organic layer was isolated and set aside. The combined aqueous layers were combined and back-extracted with 30 mL of DCM to prevent loss of product. The organic layers were combined in a single round-bottom flask to which 5 grams of basic alumina powder were added. The solution was then reduced off *in vacuo* and then dry loaded onto a 8 gram Teledyne basic alumina column, upon which clean product was eluted off with 40% ethyl acetate in hexanes. The tubes containing organic were combined and reduced *in vacuo*, yielding a white residue. (949 mg, 64% isolated yield)

### Erythro-(*N*-mesyl)-2-(methyl- $\alpha$ -phenylacetate)-1,2,5,6-tetrahydropyridine (**50**)



Previously described on page 214

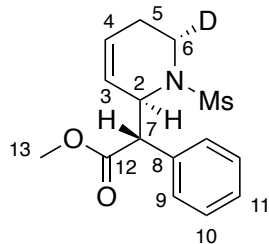
### Erythro-(*N*-mesyl)-2-(methyl- $\alpha$ -phenylacetate)-5-*cis*-deutero-1,2,5,6-tetrahydropyridine ( $\pm(5'R)$ -*d<sub>1</sub>*-**50**)



<sup>1</sup>H NMR (d<sub>6</sub>-acetone,  $\delta$ , 25 °C): 7.45 (d,  $J$  = 7.6 Hz, 2H, H9), 7.36 (t,  $J$  = 7.6 Hz, 1H, H10), 7.31 (t,  $J$  = 7.6 Hz, 1H, H11), 5.96 (d,  $J$  = 10.5 Hz, 1H, H4), 5.87 (ddd,  $J$  = 2.9, 4.0, 10.5 Hz, 1H, H3), 4.90 (d,  $J$  = 10.5 Hz, 1H, H2), 3.89 (d,  $J$  = 10.7 Hz, 1H, H7), 3.68 (s, 3H, H13), 3.60 (dd,  $J$  = 6.5, 14.4 Hz, 1H, H6), 3.26 (dd,  $J$  = 12.0, 14.4 Hz, 1H, H6), 2.29-2.34 (m, 1H, H5), 2.06 (s, 3H, Ms).

<sup>13</sup>C NMR (d<sub>6</sub>-acetone,  $\delta$ , 25 °C): 172.8 (C12), 137.6 (C8), 129.8 (2C, C9), 129.4 (2C, C10), 128.7 (C11), 128.4 (C4), 127.3 (C3), 56.5 (C7), 56.1 (C2), 52.5 (C13), 39.8 (Ms), 39.0 (C6), 24.4 (t,  $J_{DC}$  = 19.6 Hz, C5).

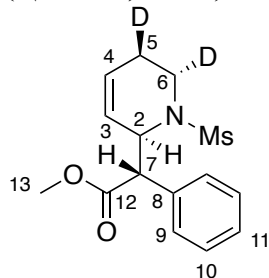
***Erythro-(N-mesyl)-2-(methyl- $\alpha$ -phenylacetate)-6-*trans*-deutero-1,2,5,6-tetrahydropyridine ( $\pm(6'S)$ -*d*<sub>1</sub>-50)***



<sup>1</sup>H NMR (d<sub>6</sub>-acetone,  $\delta$ , 25 °C): 7.45 (d,  $J$  = 7.2 Hz, 2H, H<sub>9</sub>), 7.36 (tt,  $J$  = 1.4, 7.8 Hz, 2H, H<sub>10</sub>), 7.31 (tt,  $J$  = 1.4, 7.4 Hz, 1H, H<sub>11</sub>), 5.97 (ddt,  $J$  = 1.9, 5.5, 10.4 Hz, 1H, H<sub>4</sub>), 5.85-5.88 (m, 1H, H<sub>3</sub>), 4.90 (d,  $J$  = 10.7 Hz, 1H, H<sub>2</sub>), 3.89 (d,  $J$  = 10.7 Hz, 1H, H<sub>7</sub>), 3.68 (s, 3H, H<sub>13</sub>), 3.25 (d,  $J$  = 11.8 Hz, 1H, H<sub>6</sub>), 2.33 (ddq,  $J$  = 2.4, 11.8, 18.0 Hz, 1H, H<sub>5</sub>), 2.06 (s, 3H, Ms), 1.99 (dt,  $J$  = 4.6, 18.0 Hz, 1H, H<sub>5</sub>).

<sup>13</sup>C NMR (d<sub>6</sub>-acetone,  $\delta$ , 25 °C): 172.8 (C<sub>12</sub>), 137.6 (C<sub>8</sub>), 129.8 (2C, C<sub>9</sub>), 129.4 (2C, C<sub>10</sub>), 128.7 (C<sub>11</sub>), 128.4 (C<sub>4</sub>), 127.3 (C<sub>3</sub>), 56.5 (C<sub>7</sub>), 56.1 (C<sub>2</sub>), 52.5 (C<sub>13</sub>), 39.8 (Ms), 38.7 (d,  $J_{DC}$  = 21.5 Hz, C<sub>6</sub>), 24.6 (C<sub>5</sub>).

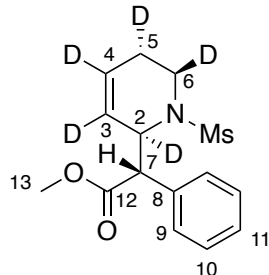
***Erythro-(N-mesyl)-2-(methyl- $\alpha$ -phenylacetate)-5-*cis*-6-*trans*-dideutero-1,2,5,6-tetrahydropyridine ( $\pm(5'R,6'S)$ -*d*<sub>2</sub>-50)***



<sup>1</sup>H NMR (d<sub>6</sub>-acetone,  $\delta$ , 25 °C): 7.45 (d,  $J$  = 7.3 Hz, 2H, H<sub>9</sub>), 7.36 (tt,  $J$  = 1.7, 7.8 Hz, 2H, H<sub>10</sub>), 7.31 (tt,  $J$  = 1.7, 7.4 Hz, 1H, H<sub>11</sub>), 5.96 (d,  $J$  = 10.4 Hz, 1H, H<sub>4</sub>), 5.87 (ddd,  $J$  = 2.7, 4.1, 10.4 Hz, 1H, H<sub>3</sub>), 4.90 (d,  $J$  = 10.7 Hz, 1H, H<sub>2</sub>), 3.88 (d,  $J$  = 10.7 Hz, 1H, H<sub>7</sub>), 3.67 (s, 3H, H<sub>13</sub>), 3.24 (d,  $J$  = 11.9 Hz, 1H, H<sub>6</sub>), 2.31 (d,  $J$  = 11.9 Hz, 1H, H<sub>5</sub>), 2.06 (s, 3H, Ms).

<sup>13</sup>C NMR (d<sub>6</sub>-acetone,  $\delta$ , 25 °C): 172.8 (C<sub>12</sub>), 137.6 (C<sub>8</sub>), 129.8 (2C, C<sub>9</sub>), 129.4 (2C, C<sub>10</sub>), 128.7 (C<sub>11</sub>), 128.4 (C<sub>4</sub>), 127.3 (C<sub>3</sub>), 56.5 (C<sub>7</sub>), 56.0 (C<sub>2</sub>), 52.5 (C<sub>13</sub>), 39.8 (Ms), 38.7 (t,  $J_{DC}$  = 21.7, C<sub>6</sub>), 24.3 (t,  $J_{DC}$  = 19.6 Hz, C<sub>5</sub>).

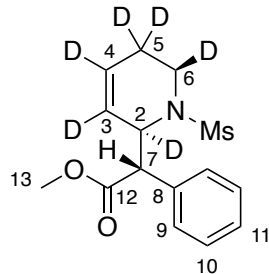
***Erythro-(N-mesyl)-2-(methyl- $\alpha$ -phenylacetate)-2,5-*trans*-6-*cis*-3,4-pentadeutero-1,2,5,6-tetrahydropyridine ( $\pm(5'S,6'R)$ -*d*<sub>5</sub>-50)***



<sup>1</sup>H NMR (d<sub>6</sub>-acetone,  $\delta$ , 25 °C): 7.45 (d,  $J$  = 7.5 Hz, 2H, H<sub>9</sub>), 7.36 (t,  $J$  = 7.3 Hz, 2H, H<sub>10</sub>), 7.31 (tt,  $J$  = 1.2, 7.3 Hz, 1H, H<sub>11</sub>), 3.88 (s, 1H, H<sub>7</sub>), 3.67 (s, 3H, H<sub>13</sub>), 3.58 (s, 1H, H<sub>6</sub>), 2.06 (s, 3H, Ms), 1.96 (s, 1H, H<sub>5</sub>).

<sup>13</sup>C NMR (d<sub>6</sub>-acetone,  $\delta$ , 25 °C): 172.8 (C<sub>12</sub>), 137.6 (C<sub>8</sub>), 129.8 (2C, C<sub>9</sub>), 129.4 (2C, C<sub>10</sub>), 128.7 (C<sub>11</sub>), 128.0 (t,  $J_{DC}$  = 24.5 Hz, C<sub>4</sub>), 126.8 (t,  $J_{DC}$  = 24.6 Hz, C<sub>3</sub>), 56.4 (C<sub>7</sub>), 55.6 (t,  $J_{DC}$  = 22.0 Hz, C<sub>2</sub>), 52.5 (C<sub>13</sub>), 39.8 (Ms), 38.6 (t,  $J_{DC}$  = 21.4 Hz, C<sub>6</sub>), 24.0 (t,  $J_{DC}$  = 19.7 Hz, C<sub>5</sub>).

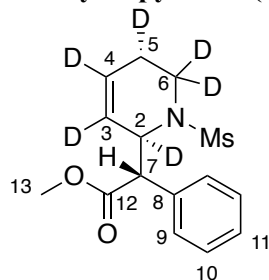
***Erythro-(N-mesyl)-2-(methyl- $\alpha$ -phenylacetate)-6-cis-2-trans-3,4,5,5-hexadeutero-1,2,5,6-tetrahydropyridine ( $\pm(6'R)$ - $d_6$ -50)***



$^1\text{H}$  NMR ( $d_6$ -acetone,  $\delta$ , 25 °C): 7.45 (d,  $J$  = 7.5 Hz, 2H, H9), 7.36 (t,  $J$  = 7.8 Hz, 2H, H10), 7.31 (tt,  $J$  = 1.9, 7.3 Hz, 1H, H11), 3.88 (s, 1H, H7), 3.67 (s, 3H, H13), 3.57 (s, 1H, H6), 2.06 (s, 3H, Ms).

$^{13}\text{C}$  NMR ( $d_6$ -acetone,  $\delta$ , 25 °C): 172.8 (C12), 137.5 (C8), 129.7 (2C, C9), 129.4 (2C, C10), 128.7 (C11), 127.9 (t,  $J_{DC}$  = 24.6 Hz, C4), 126.9 (t,  $J_{DC}$  = 24.2 Hz, C3), 56.4 (C7), 55.6 (t,  $J_{DC}$  = 22.1 Hz, C2), 52.5 (C13), 39.8 (Ms), 38.5 (t,  $J_{DC}$  = 21.2 Hz, C6), 23.5-24.2 (m, C5).

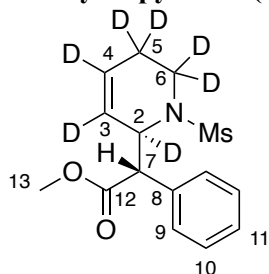
***Erythro-(N-mesyl)-2-(methyl- $\alpha$ -phenylacetate)-2,5-trans-3,4,6,6-hexadeutero-1,2,5,6-tetrahydropyridine ( $\pm(5'S)$ - $d_6$ -50)***



$^1\text{H}$  NMR ( $d_6$ -acetone,  $\delta$ , 25 °C): 7.45 (d,  $J$  = 7.2 Hz, 2H, H9), 7.36 (tt,  $J$  = 1.5 Hz, 2H, H10), 7.31 (tt,  $J$  = 1.3 Hz, 1H, H11), 3.88 (s, 1H, H7), 3.67 (s, 3H, H13), 2.06 (s, 3H, Ms), 1.96 (s, 1H, H5).

$^{13}\text{C}$  NMR ( $d_6$ -acetone,  $\delta$ , 25 °C): 172.8 (C12), 137.6 (C8), 129.8 (2C, C9), 129.4 (2C, C10), 128.7 (C11), 128.0 (t,  $J_{DC}$  = 24.7 Hz, C4), 126.9 (t,  $J_{DC}$  = 24.8 Hz, C3), 56.4 (C7), 55.6 (t,  $J_{DC}$  = 21.9 Hz, C2), 52.5 (C13), 39.8 (Ms), 38.1-38.7 (m, C6), 23.9 (t,  $J_{DC}$  = 19.8 Hz, C5).

***Erythro-(N-mesyl)-2-(methyl- $\alpha$ -phenylacetate)-2,3,4,5,5,6,6-heptadeutero-1,2,5,6-tetrahydropyridine ( $d_7$ -50)***



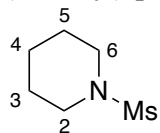
$^1\text{H}$  NMR ( $d_6$ -acetone,  $\delta$ , 25 °C): 7.45 (d,  $J$  = 7.4 Hz, 2H, H9), 7.36 (t,  $J$  = 7.3 Hz, 2H, H10), 7.31 (t,  $J$  = 7.3 Hz, 1H, H11), 3.88 (s, 1H, H7), 3.67 (s, 3H, H13), 2.06 (s, 3H, Ms).

$^{13}\text{C}$  NMR ( $d_6$ -acetone,  $\delta$ , 25 °C): 172.8 (C12), 137.6 (C8), 129.8 (2C, C9), 129.4 (2C, C10), 128.7 (C11), 127.9 (t,  $J_{DC}$  = 24.3 Hz, C4), 126.9 (t,  $J_{DC}$  = 24.6 Hz, C3), 56.5 (C7), 55.61 (t,  $J_{DC}$  = 22.2 Hz, C2), 52.5 (C13), 39.8 (Ms), 38.1-38.7 (m, C6), 23.4-24.0 (m, C5).



## Synthesis and Characterization of Hydrogenated Piperidines

### (*N*-mesyl)-piperidine (**66**)



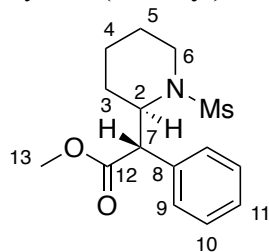
THP **65** (57 mg, 35 mmol) was dissolved in methanol (3 mL) and added to a 4-dram vial. This solution was then circulated through a ThalesNano H-Cube flow hydrogenator for 5 hours. The temperature was set to 50 °C, the H<sub>2</sub> pressure to 25 bars, and the catalyst cartridge used contained 5% Pd on carbon. After circulation, the solution was collected and reduced to dryness (38 mg 66% yield).

<sup>1</sup>H NMR (d<sub>6</sub>-CD<sub>2</sub>Cl<sub>2</sub>, δ, 25 °C): 3.14 (t, *J* = 5.4 Hz, 4H, H<sub>2</sub>), 2.71 (s, 3H, Ms), 1.66 (q, *J* = 5.6 Hz, 4H, H<sub>3</sub>), 1.53-1.57 (m, 2H, H<sub>4</sub>).

<sup>13</sup>C NMR (d<sub>6</sub>-CD<sub>2</sub>Cl<sub>2</sub>, δ, 25 °C): 46.8 (2C, C<sub>2</sub>), 34.0 (Ms), 25.4 (2C, C<sub>3</sub>), 23.7 (C<sub>4</sub>).

*SC-XRD Data on page 362*

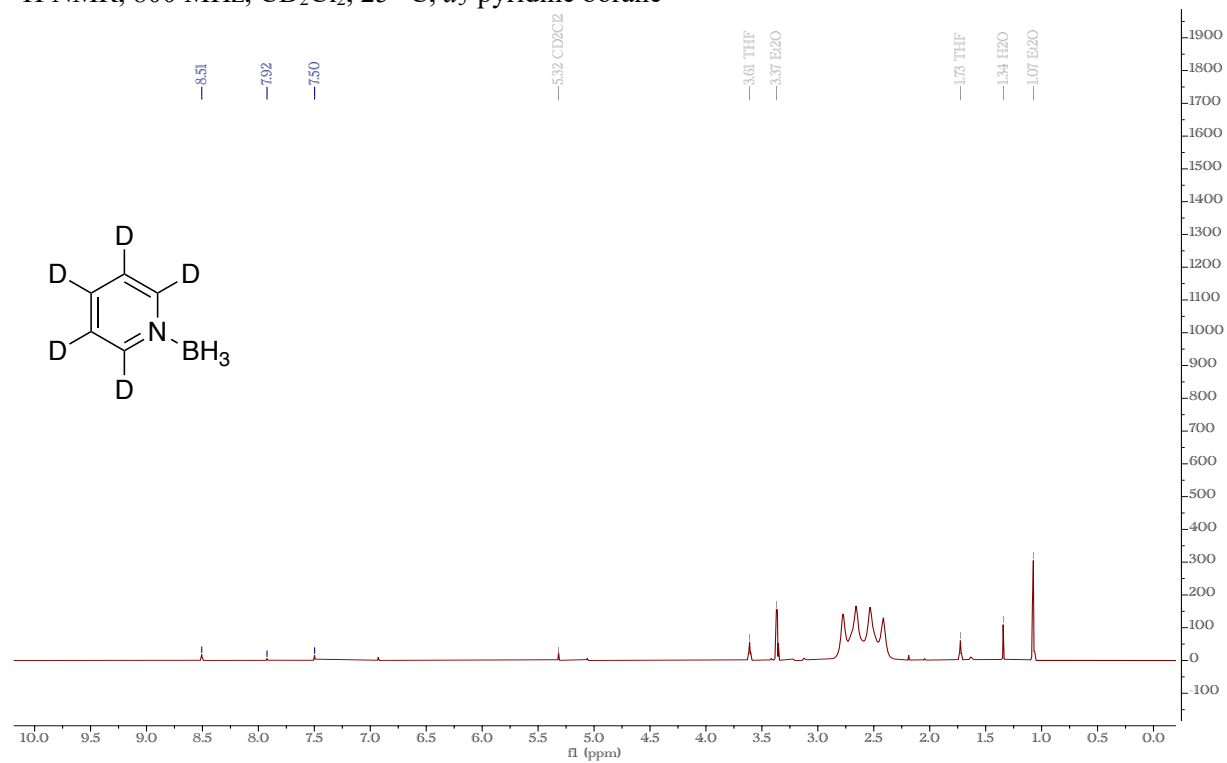
### *erythro*-(*N*-mesyl)-methylphenidate (**55**)



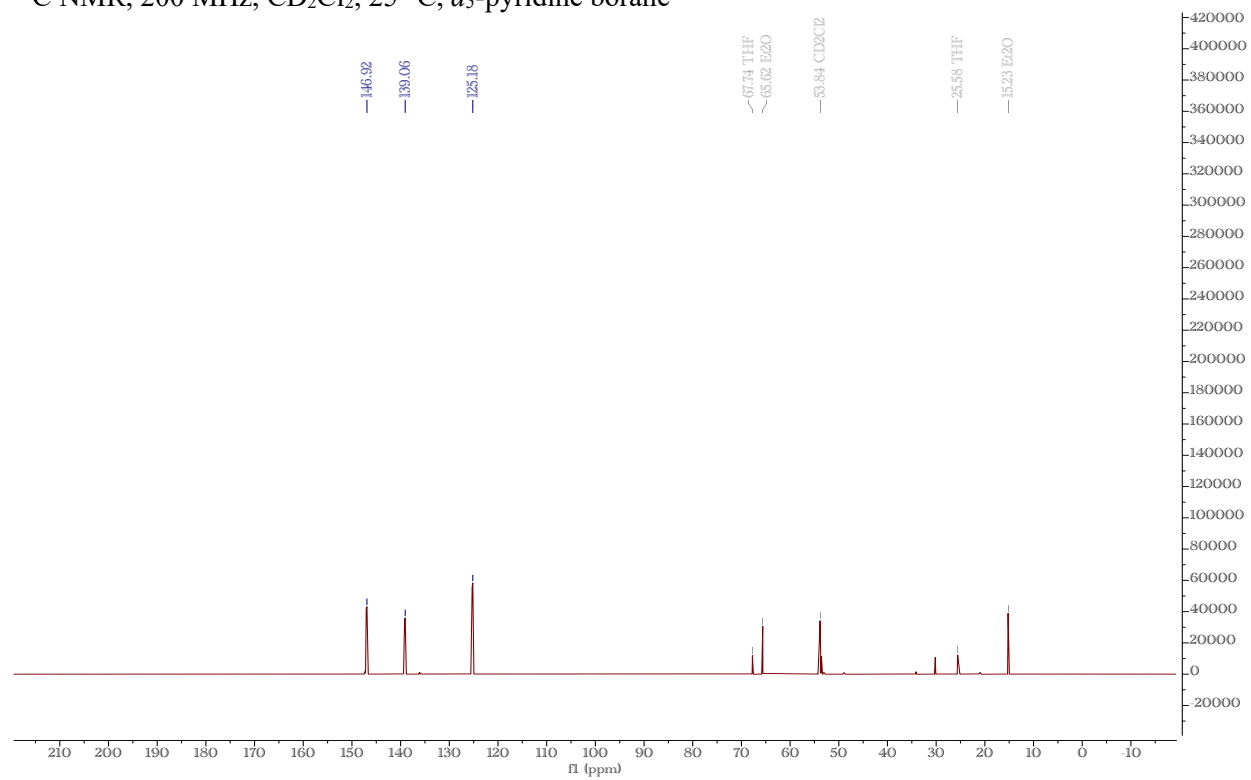
*Previously described on page 221*

# NMR Spectroscopy

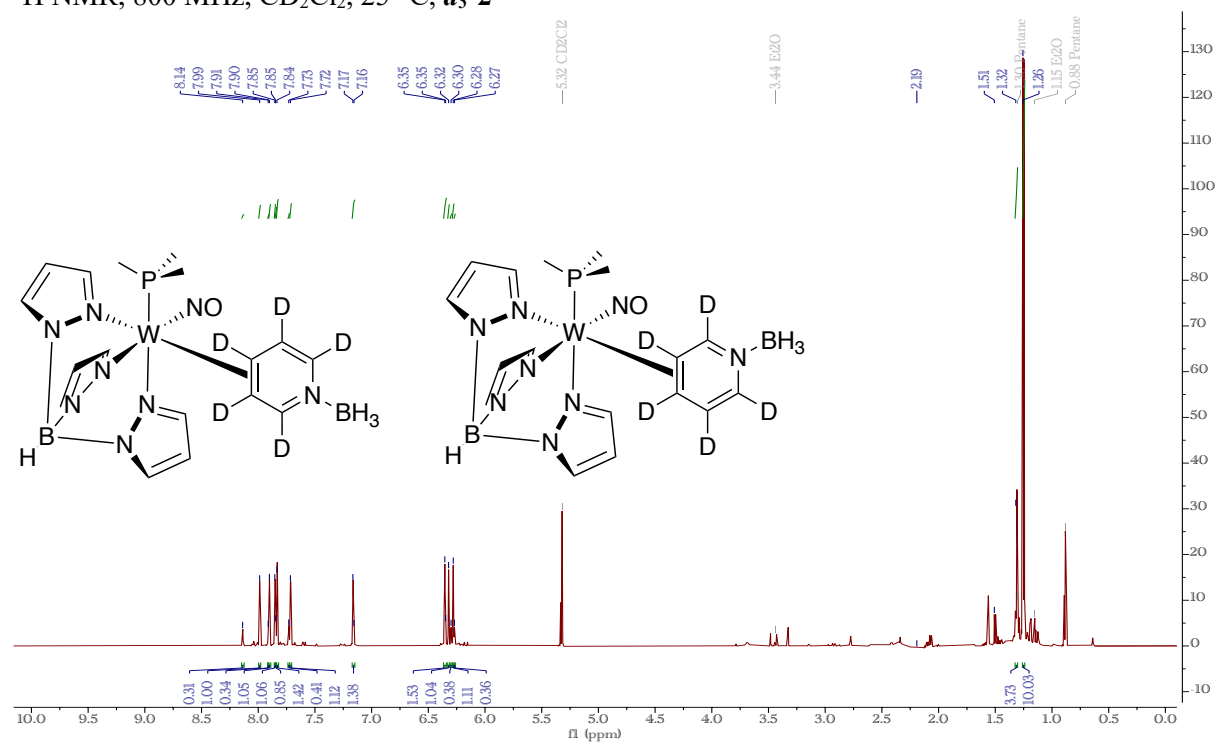
$^1\text{H}$  NMR, 800 MHz,  $\text{CD}_2\text{Cl}_2$ , 25 °C,  $d_5$ -pyridine borane



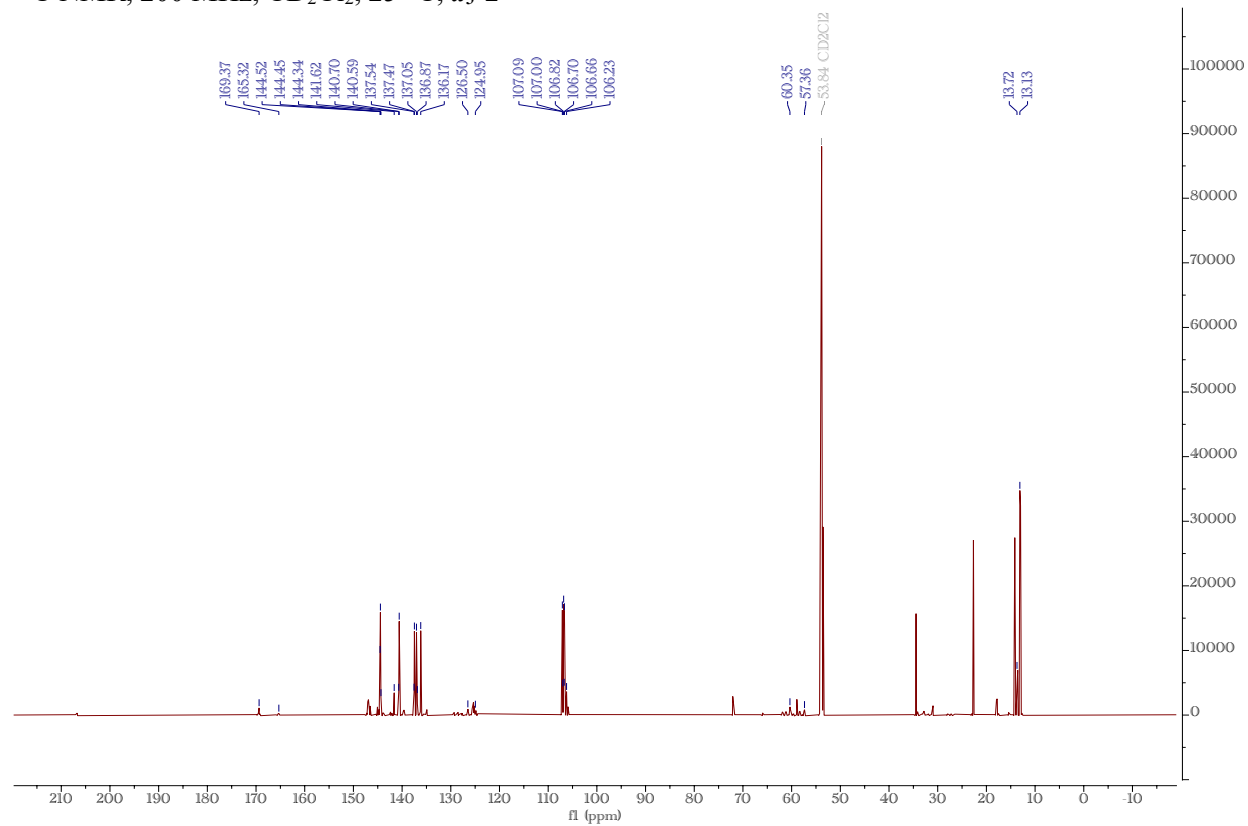
$^{13}\text{C}$  NMR, 200 MHz,  $\text{CD}_2\text{Cl}_2$ , 25 °C,  $d_5$ -pyridine borane



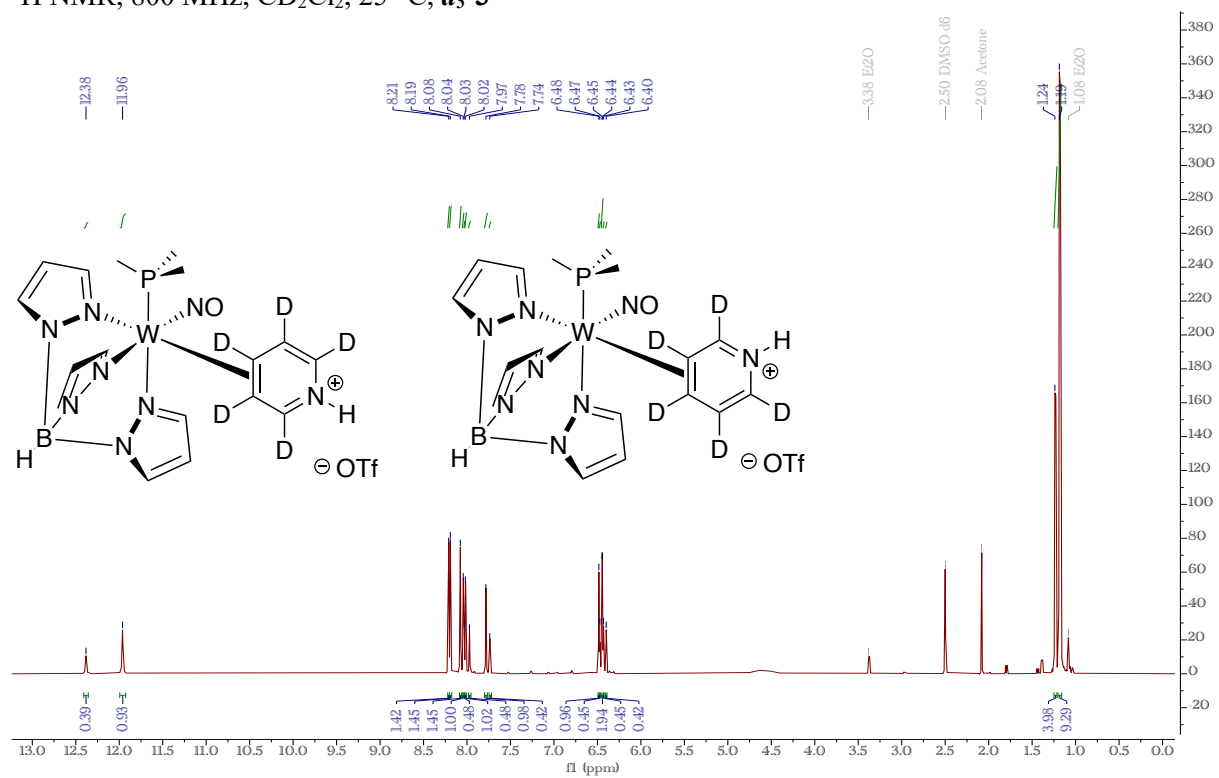
$^1\text{H}$  NMR, 800 MHz,  $\text{CD}_2\text{Cl}_2$ , 25 °C,  $d_5$ -2



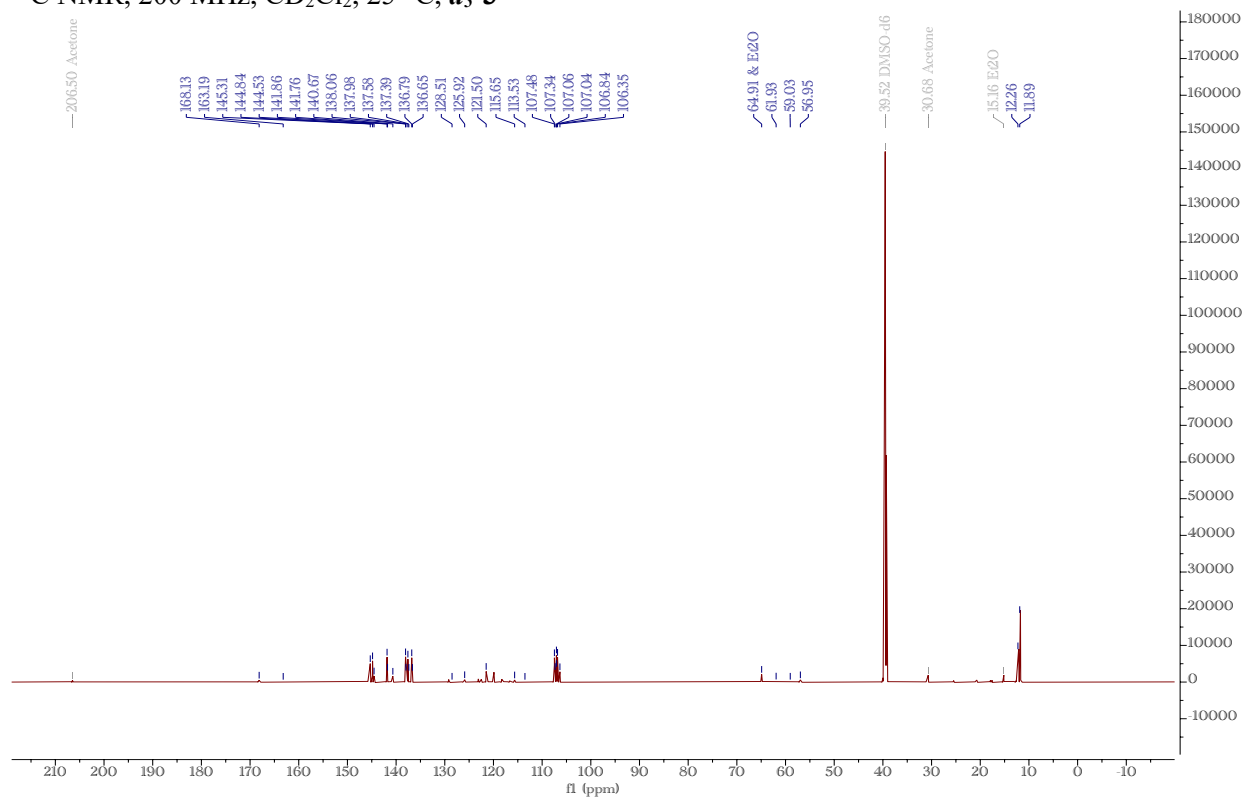
$^{13}\text{C}$  NMR, 200 MHz,  $\text{CD}_2\text{Cl}_2$ , 25 °C,  $d_5$ -2



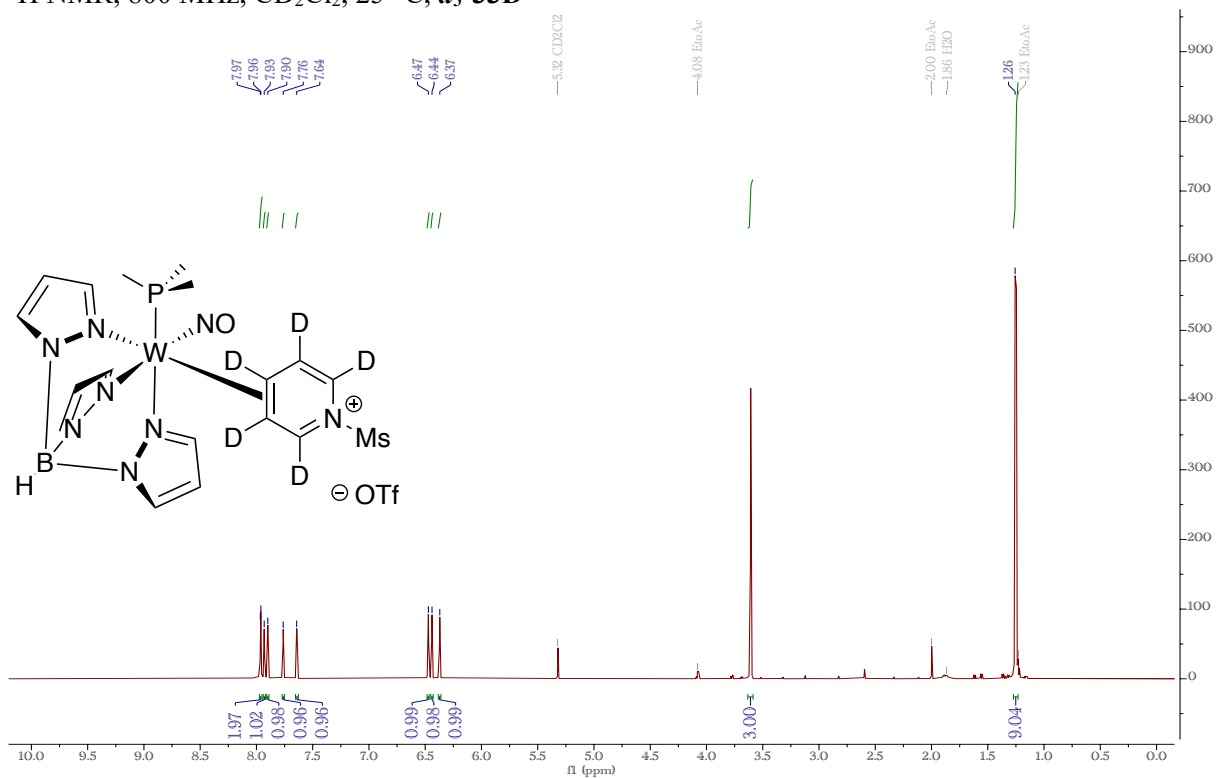
$^1\text{H}$  NMR, 800 MHz,  $\text{CD}_2\text{Cl}_2$ , 25 °C,  $d_5\text{-3}$



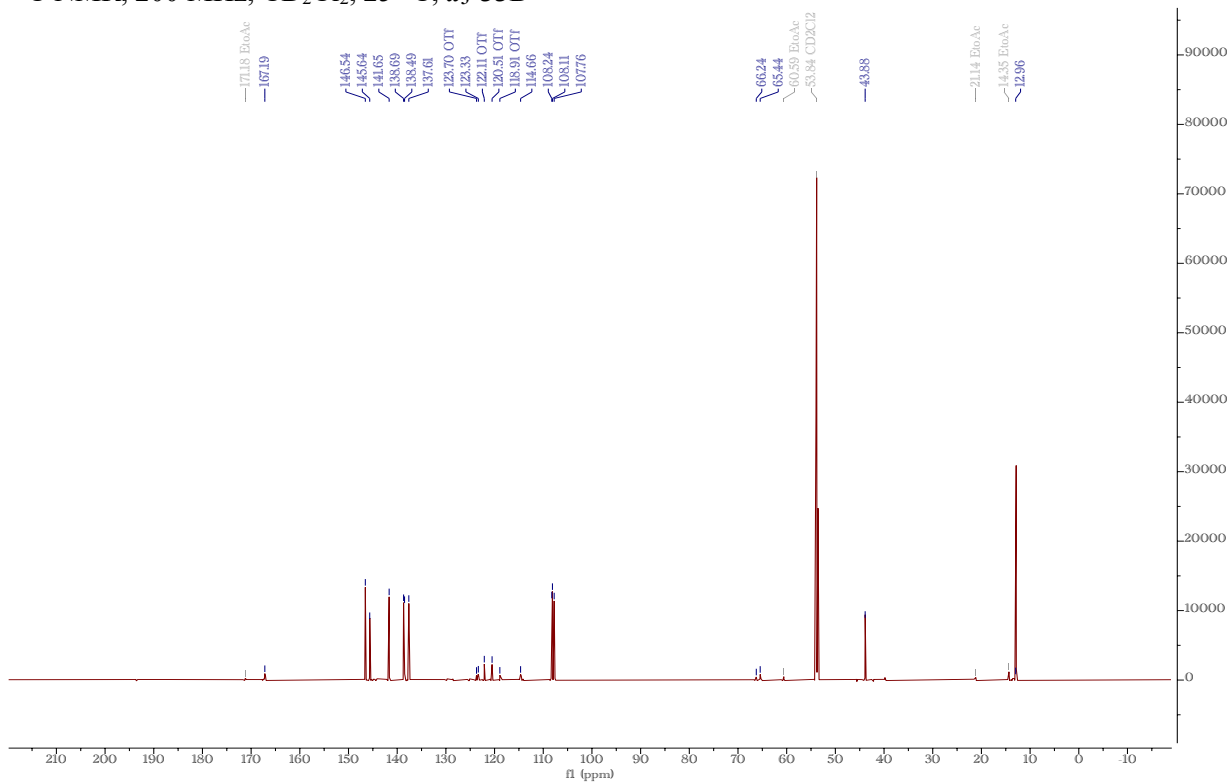
$^{13}\text{C}$  NMR, 200 MHz,  $\text{CD}_2\text{Cl}_2$ , 25 °C,  $d_5\text{-3}$



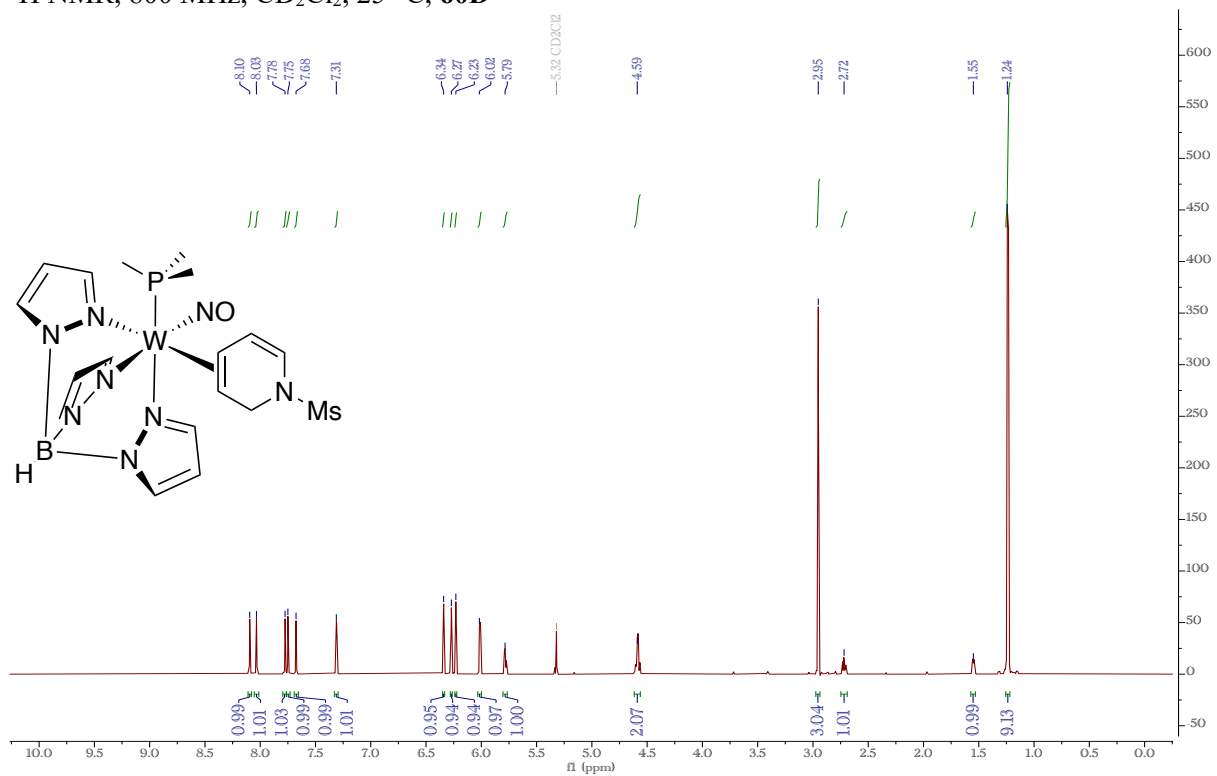
$^1\text{H}$  NMR, 800 MHz,  $\text{CD}_2\text{Cl}_2$ , 25 °C,  $d_5$ -**33D**



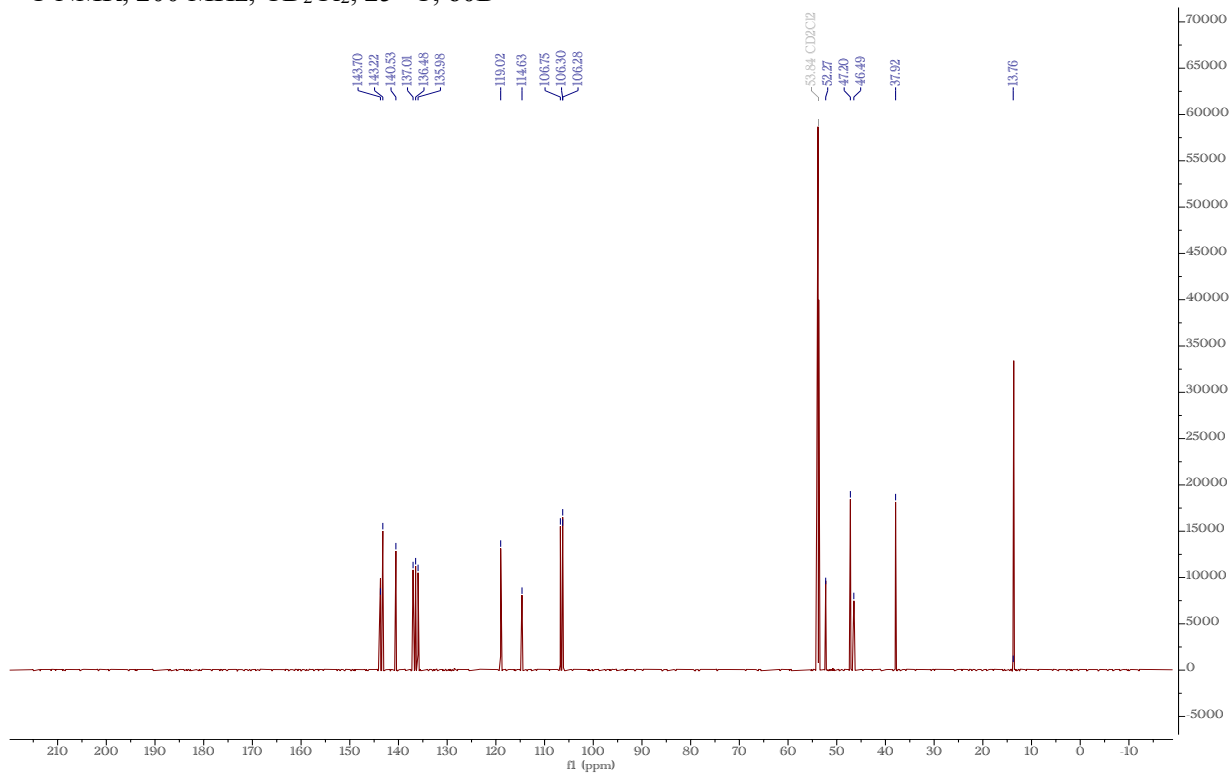
$^{13}\text{C}$  NMR, 200 MHz,  $\text{CD}_2\text{Cl}_2$ , 25 °C,  $d_5$ -**33D**



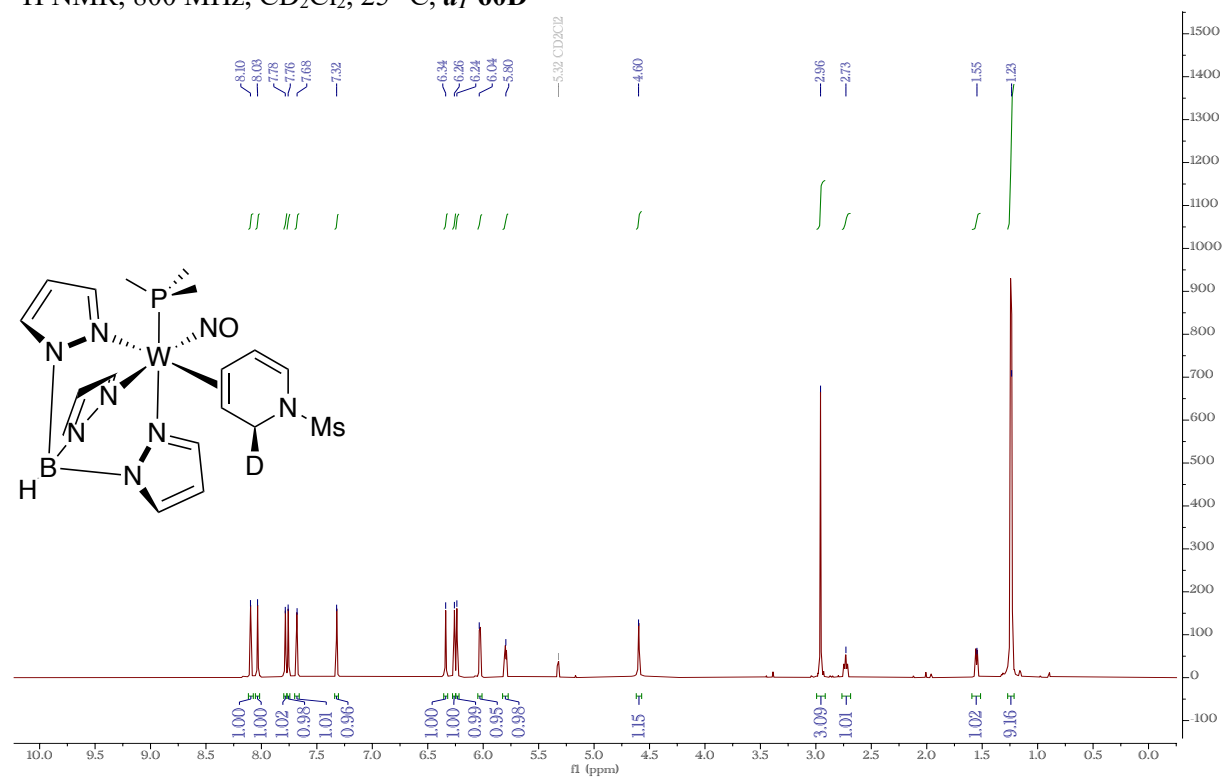
$^1\text{H}$  NMR, 800 MHz,  $\text{CD}_2\text{Cl}_2$ , 25 °C, **60D**



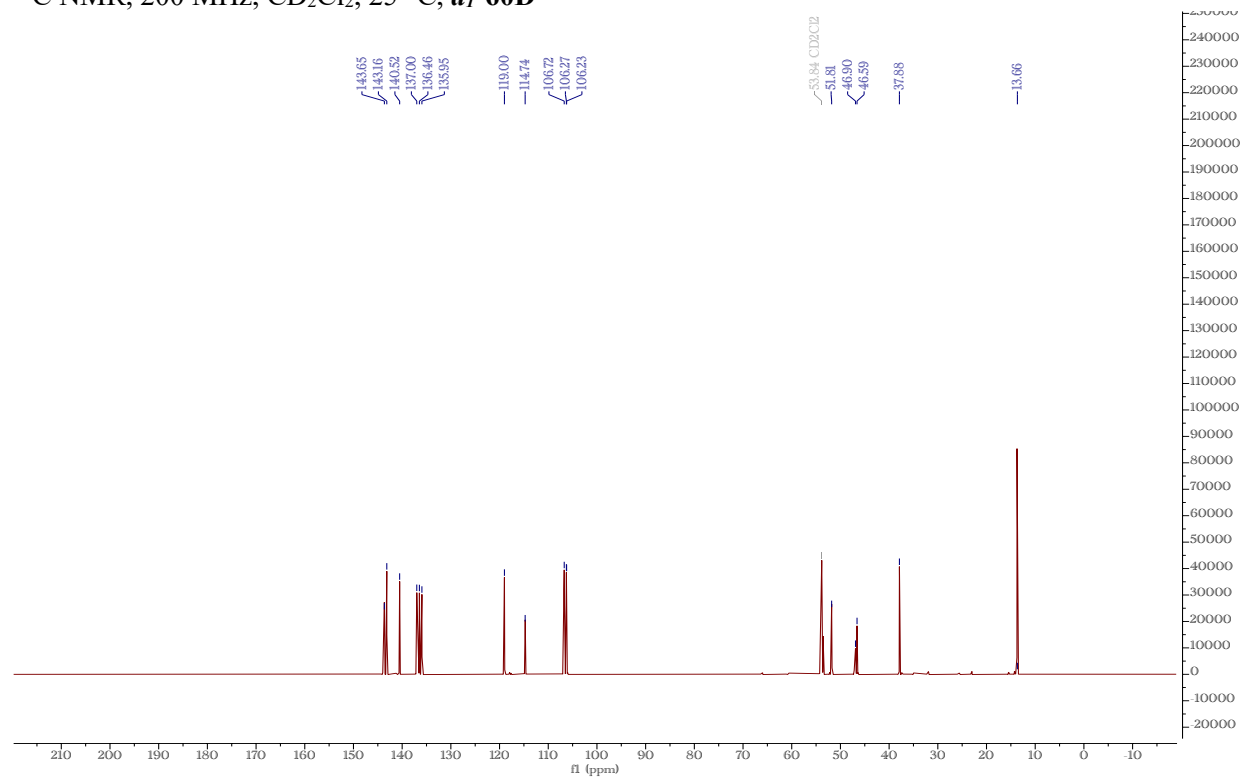
$^{13}\text{C}$  NMR, 200 MHz,  $\text{CD}_2\text{Cl}_2$ , 25 °C, **60D**



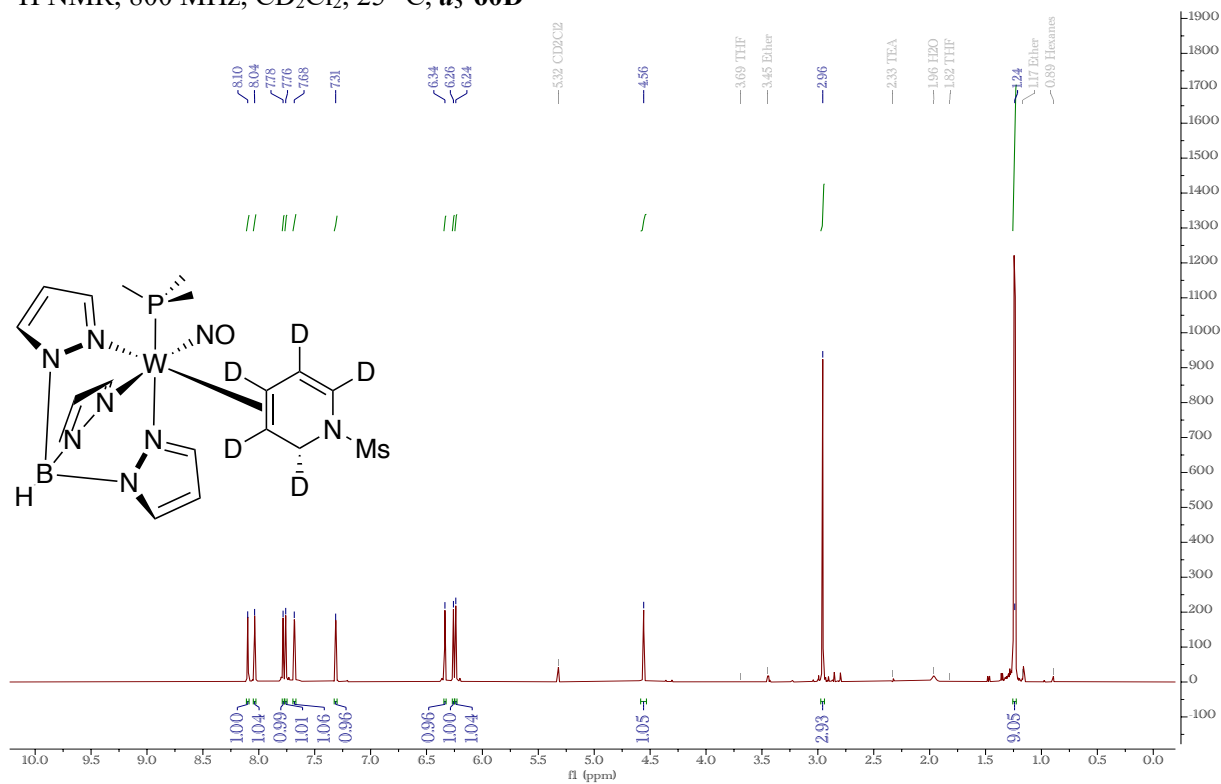
$^1\text{H}$  NMR, 800 MHz,  $\text{CD}_2\text{Cl}_2$ , 25 °C,  $d_1$ -60D



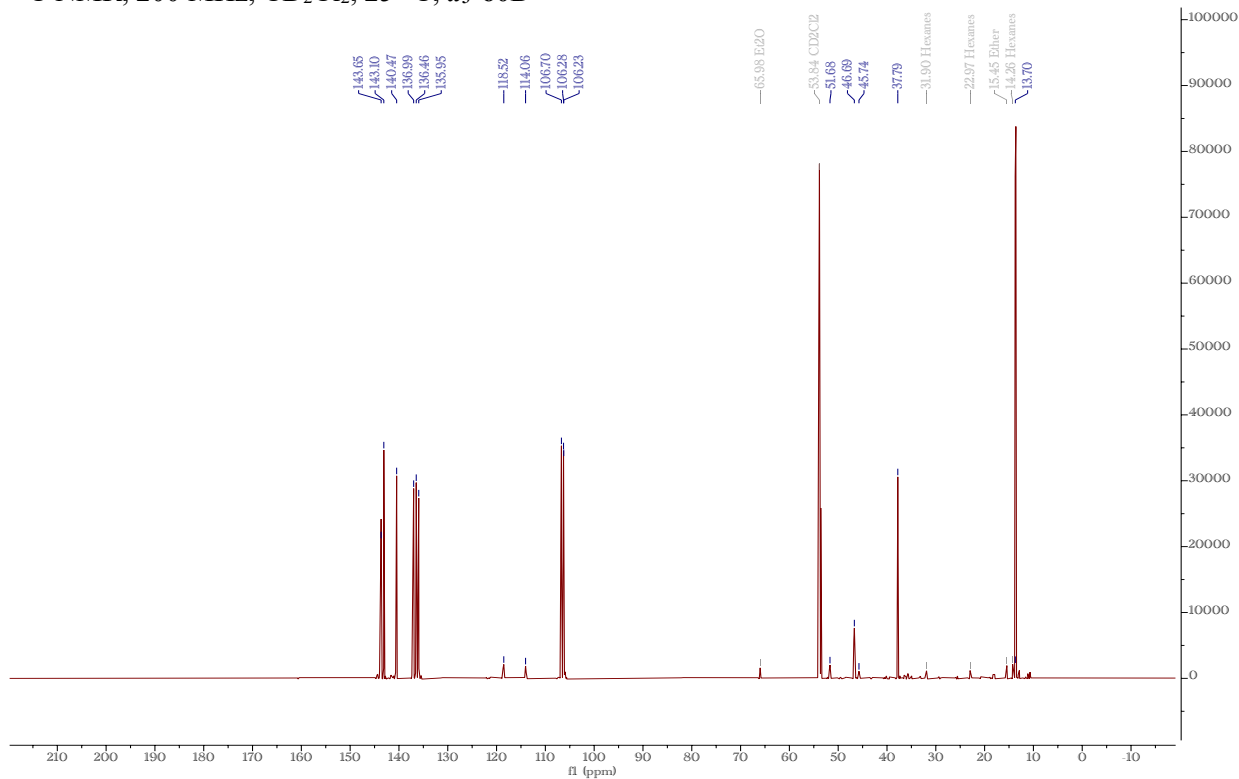
$^{13}\text{C}$  NMR, 200 MHz,  $\text{CD}_2\text{Cl}_2$ , 25 °C,  $d_1$ -60D



$^1\text{H}$  NMR, 800 MHz,  $\text{CD}_2\text{Cl}_2$ , 25 °C,  $d_5$ -60D

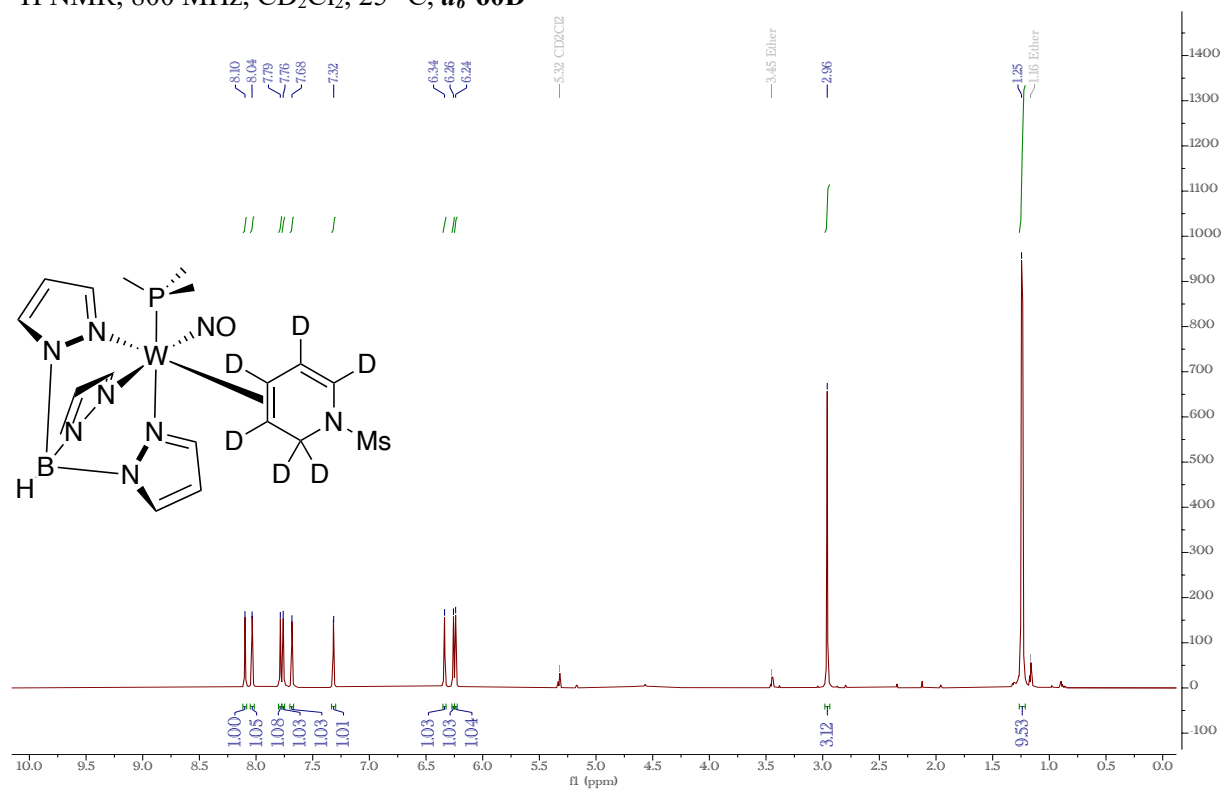


$^{13}\text{C}$  NMR, 200 MHz,  $\text{CD}_2\text{Cl}_2$ , 25 °C,  $d_5$ -60D

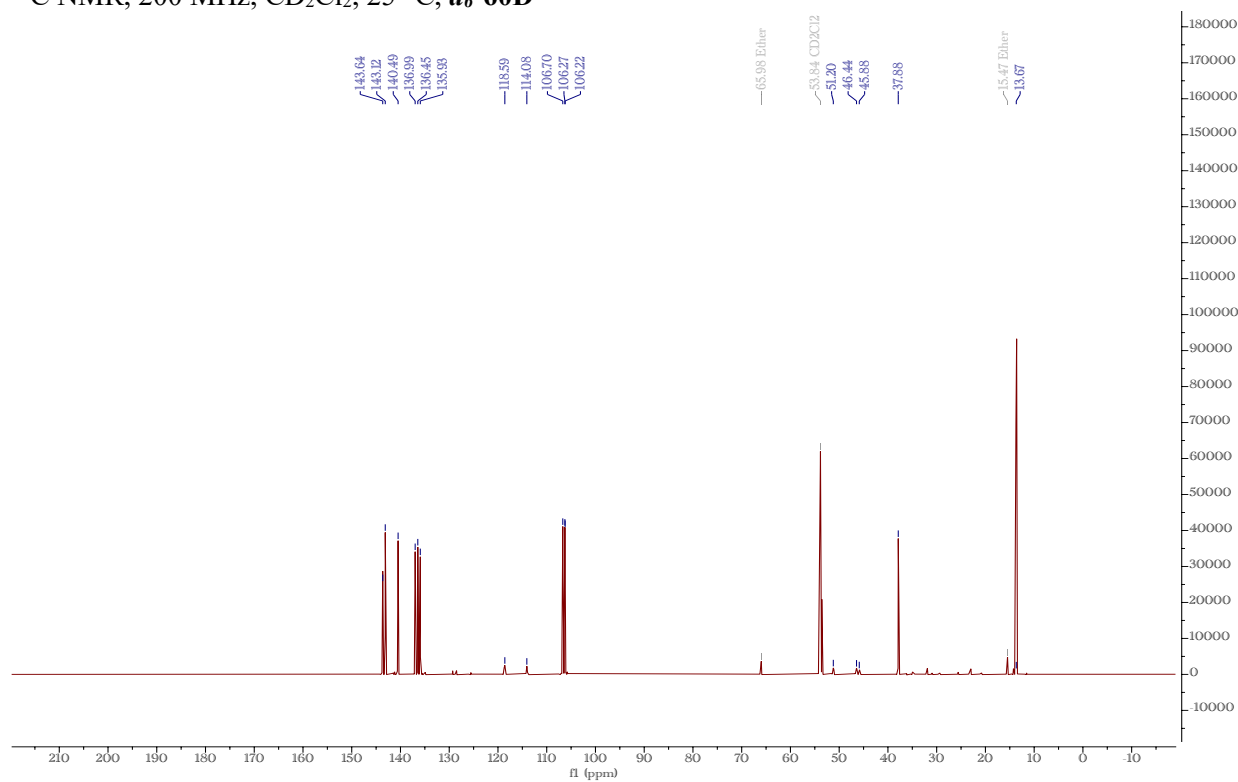




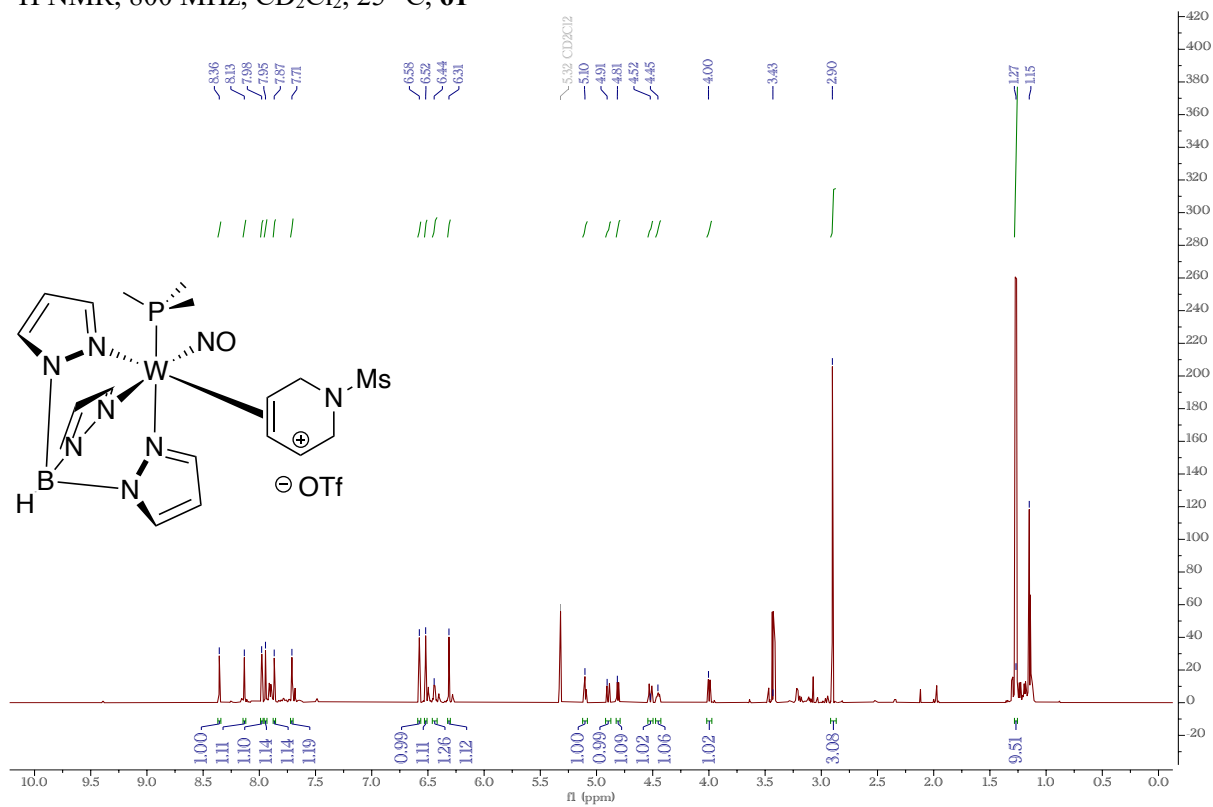
$^1\text{H}$  NMR, 800 MHz,  $\text{CD}_2\text{Cl}_2$ , 25 °C,  $d_6$ -60D



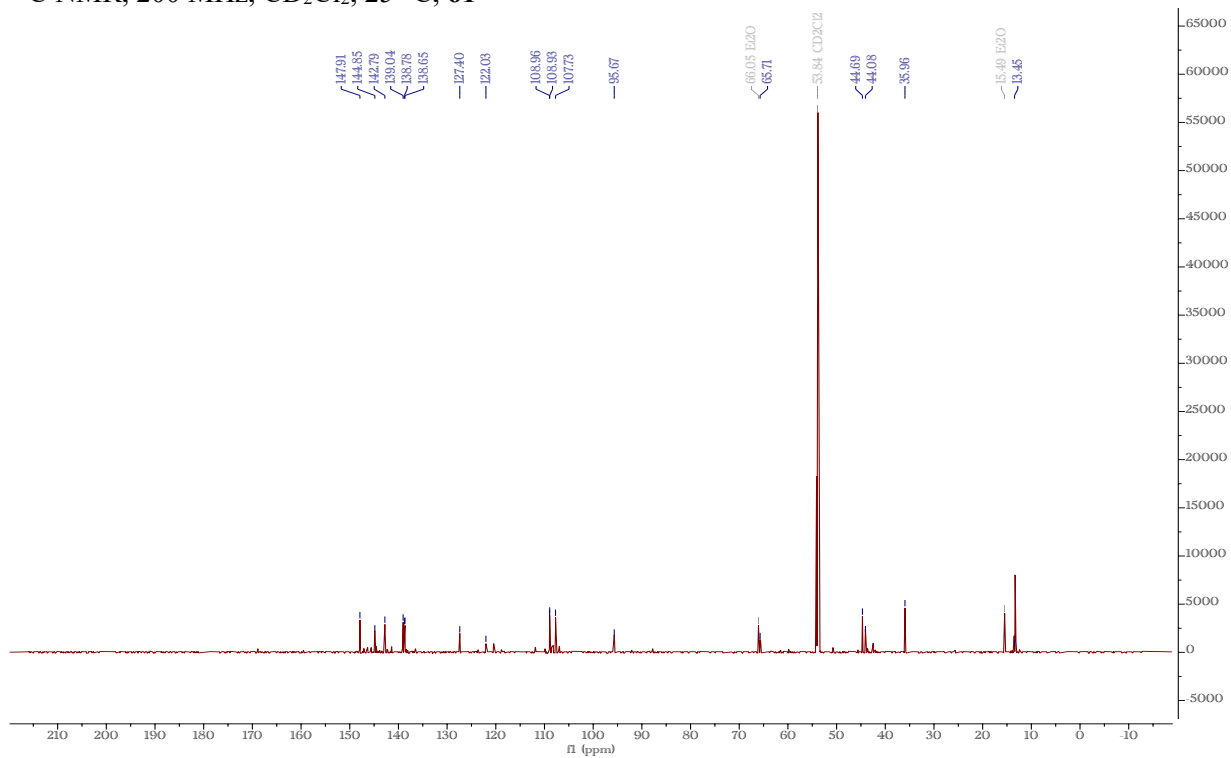
$^{13}\text{C}$  NMR, 200 MHz,  $\text{CD}_2\text{Cl}_2$ , 25 °C,  $d_6$ -60D



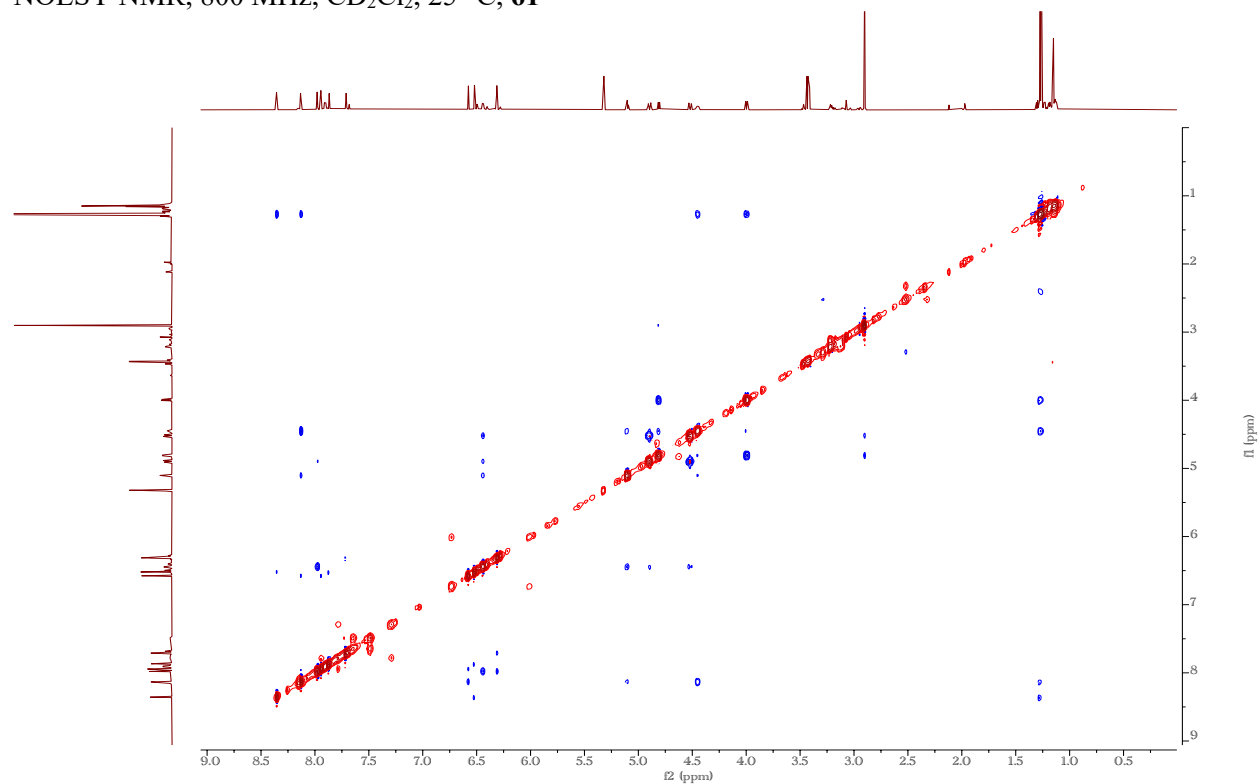
$^1\text{H}$  NMR, 800 MHz,  $\text{CD}_2\text{Cl}_2$ , 25 °C, **61**



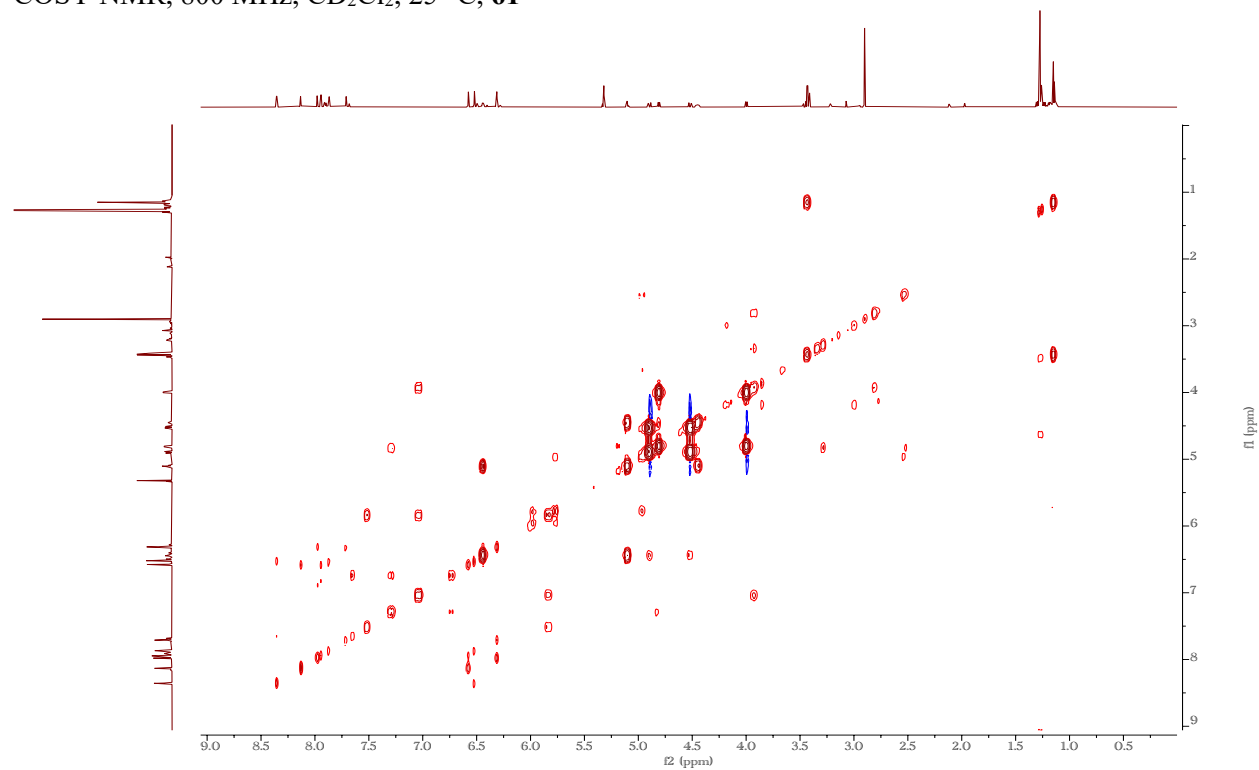
$^{13}\text{C}$  NMR, 200 MHz,  $\text{CD}_2\text{Cl}_2$ , 25 °C, **61**



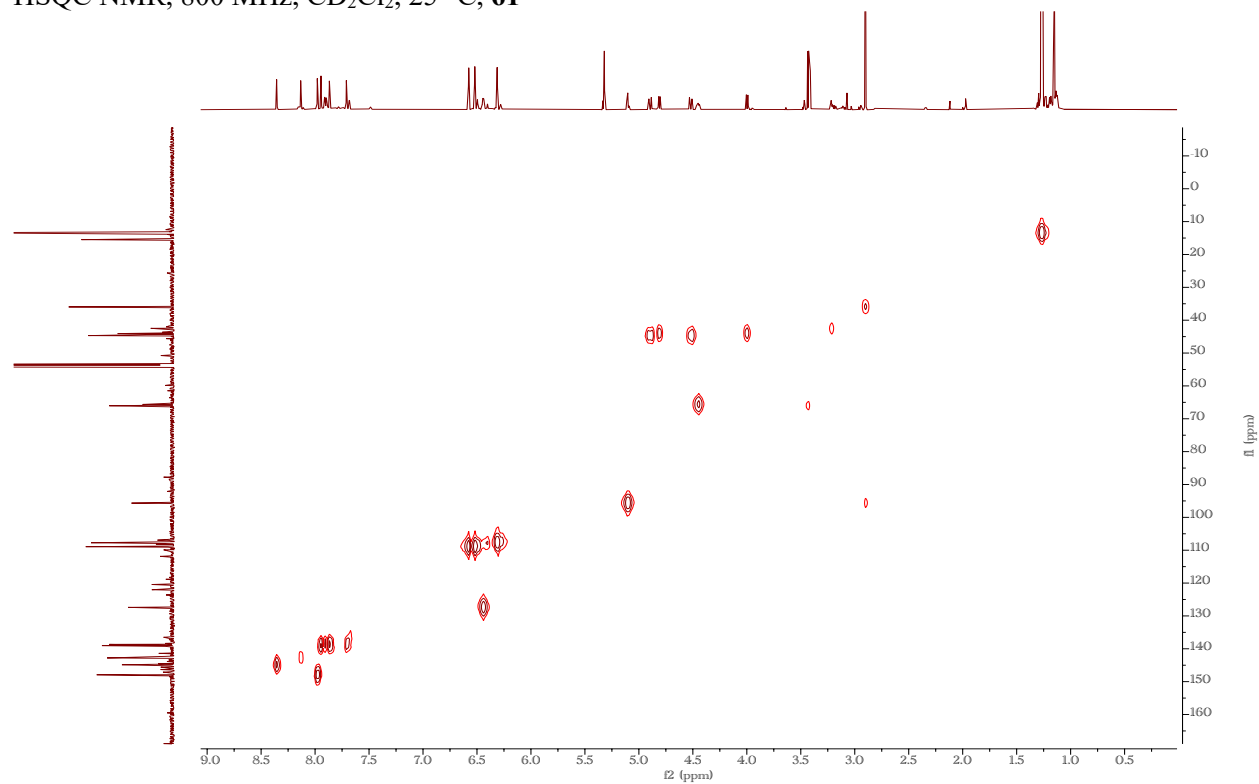
NOESY NMR, 800 MHz, CD<sub>2</sub>Cl<sub>2</sub>, 25 °C, **61**



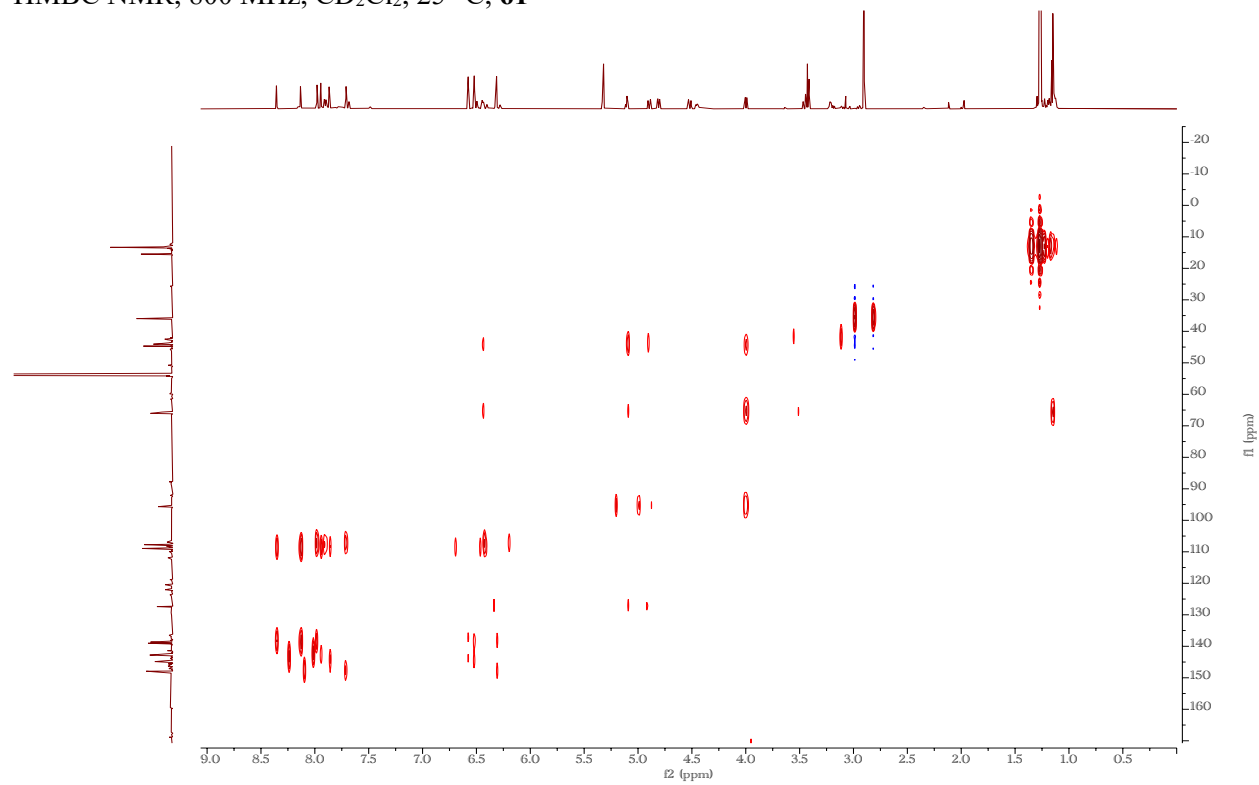
COSY NMR, 800 MHz, CD<sub>2</sub>Cl<sub>2</sub>, 25 °C, **61**



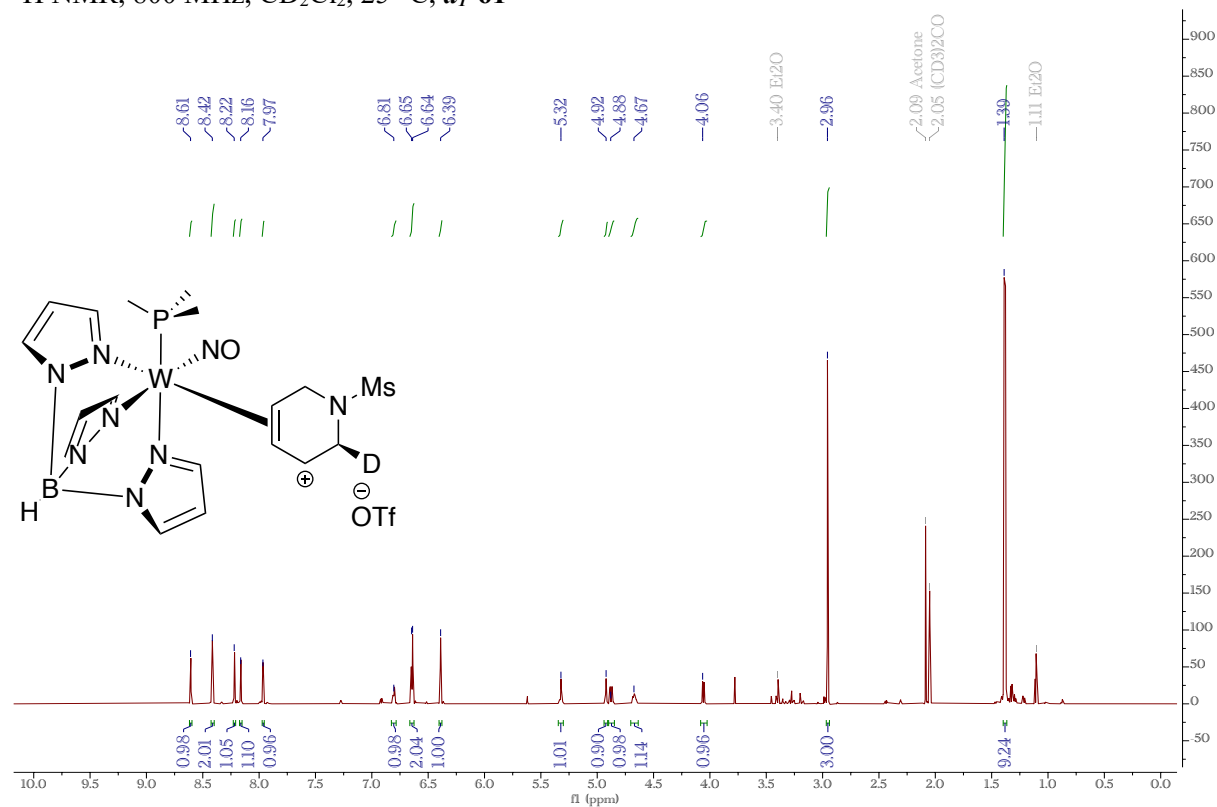
HSQC NMR, 800 MHz, CD<sub>2</sub>Cl<sub>2</sub>, 25 °C, **61**



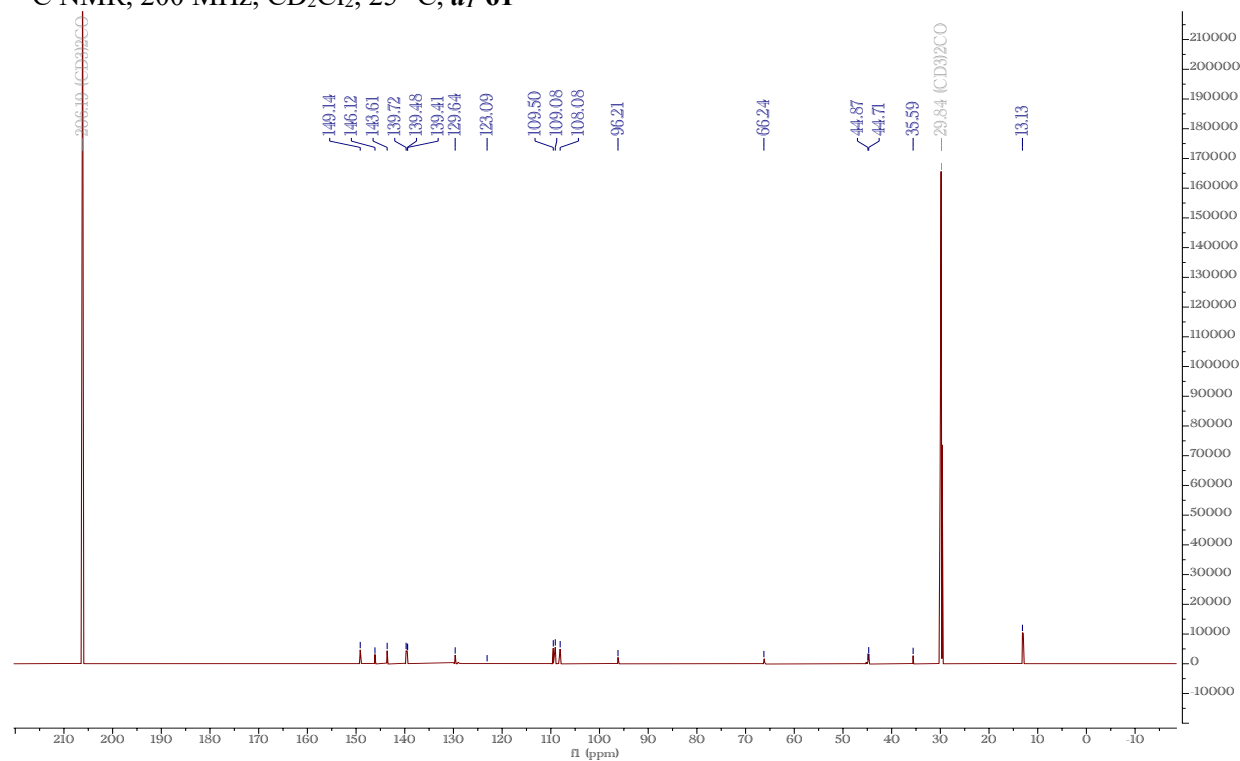
HMBC NMR, 800 MHz, CD<sub>2</sub>Cl<sub>2</sub>, 25 °C, **61**



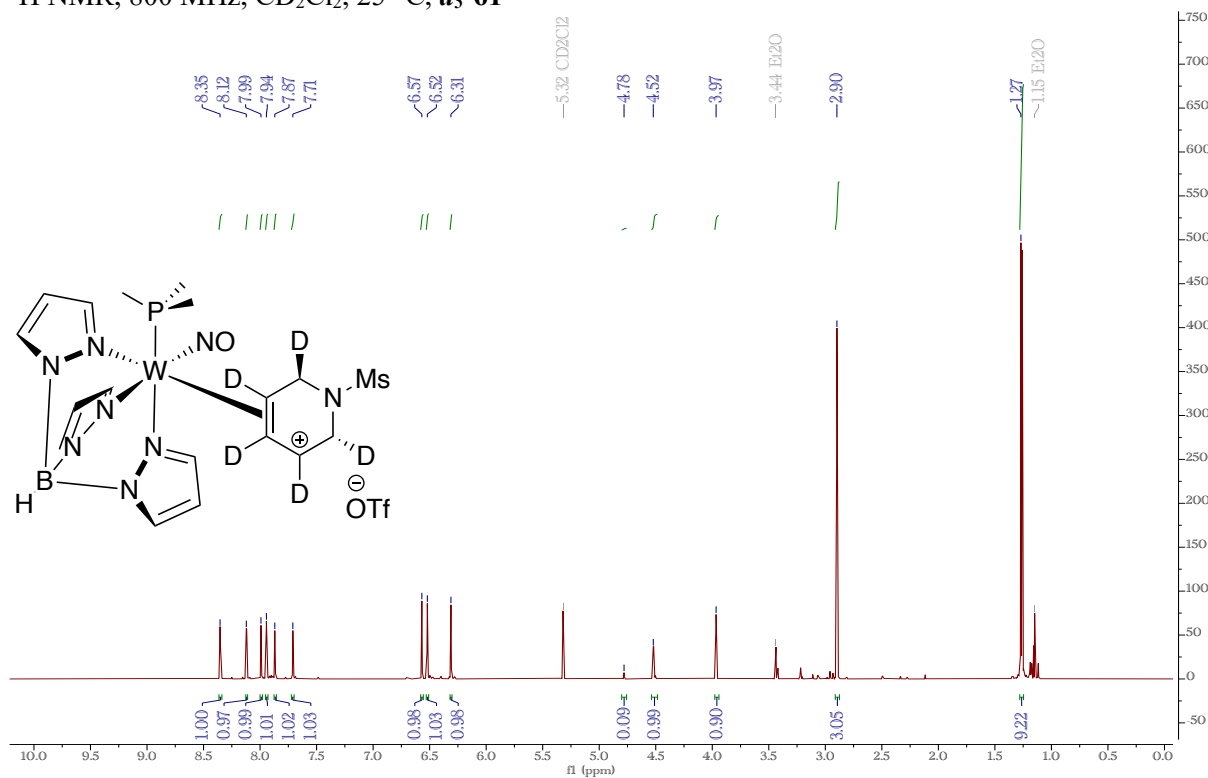
$^1\text{H}$  NMR, 800 MHz,  $\text{CD}_2\text{Cl}_2$ , 25 °C, *d*<sub>1</sub>-61



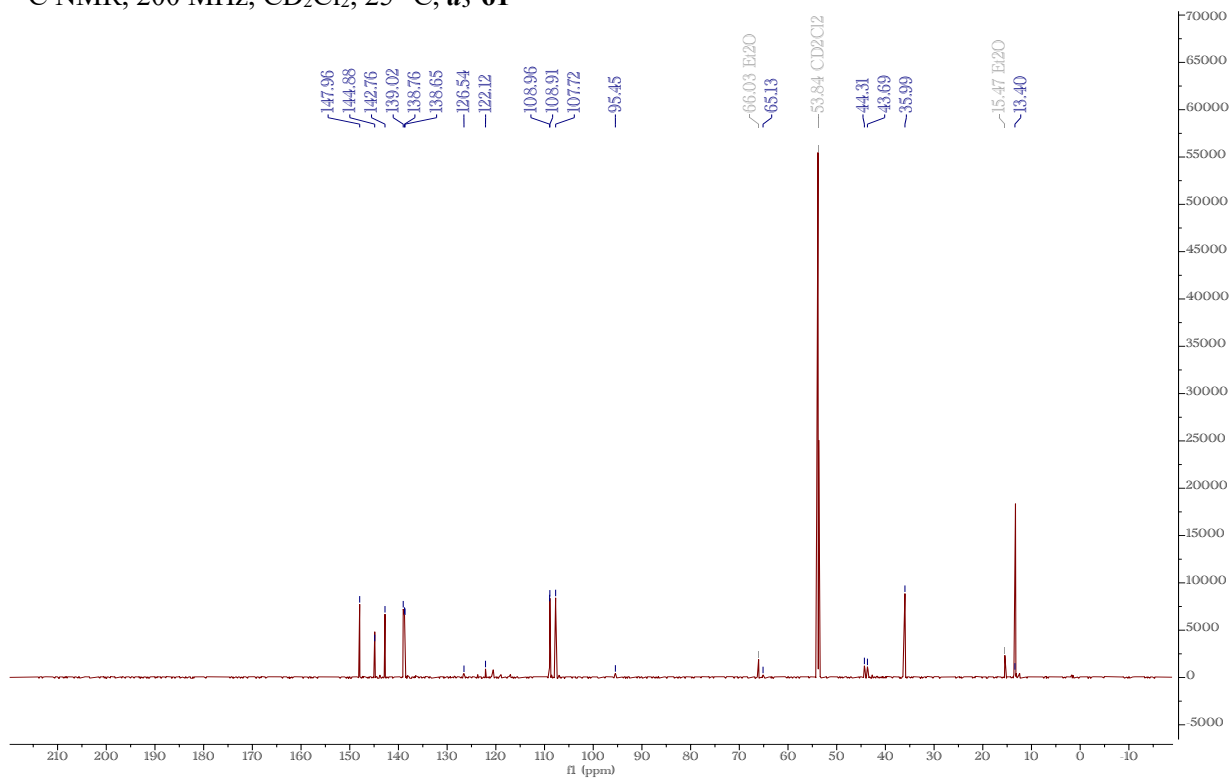
$^{13}\text{C}$  NMR, 200 MHz,  $\text{CD}_2\text{Cl}_2$ , 25 °C, *d*<sub>1</sub>-61



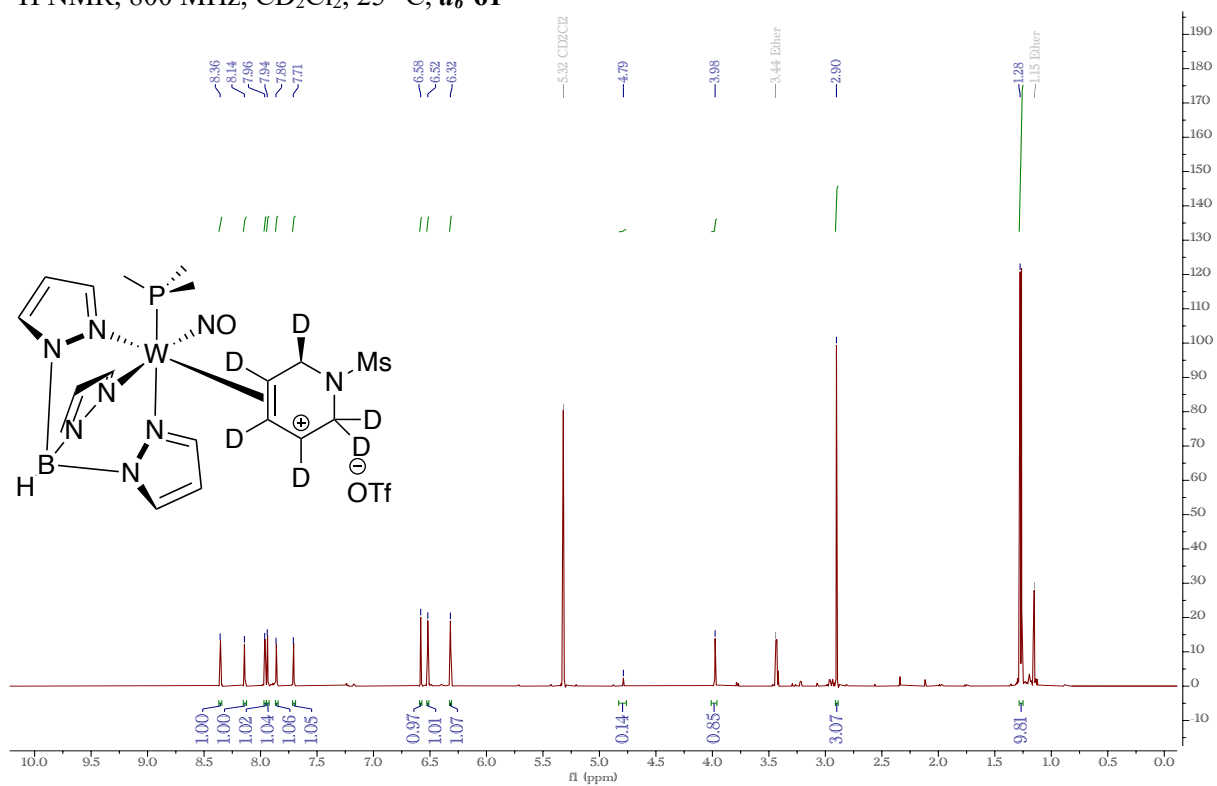
$^1\text{H}$  NMR, 800 MHz,  $\text{CD}_2\text{Cl}_2$ , 25 °C, *d*<sub>5</sub>-61



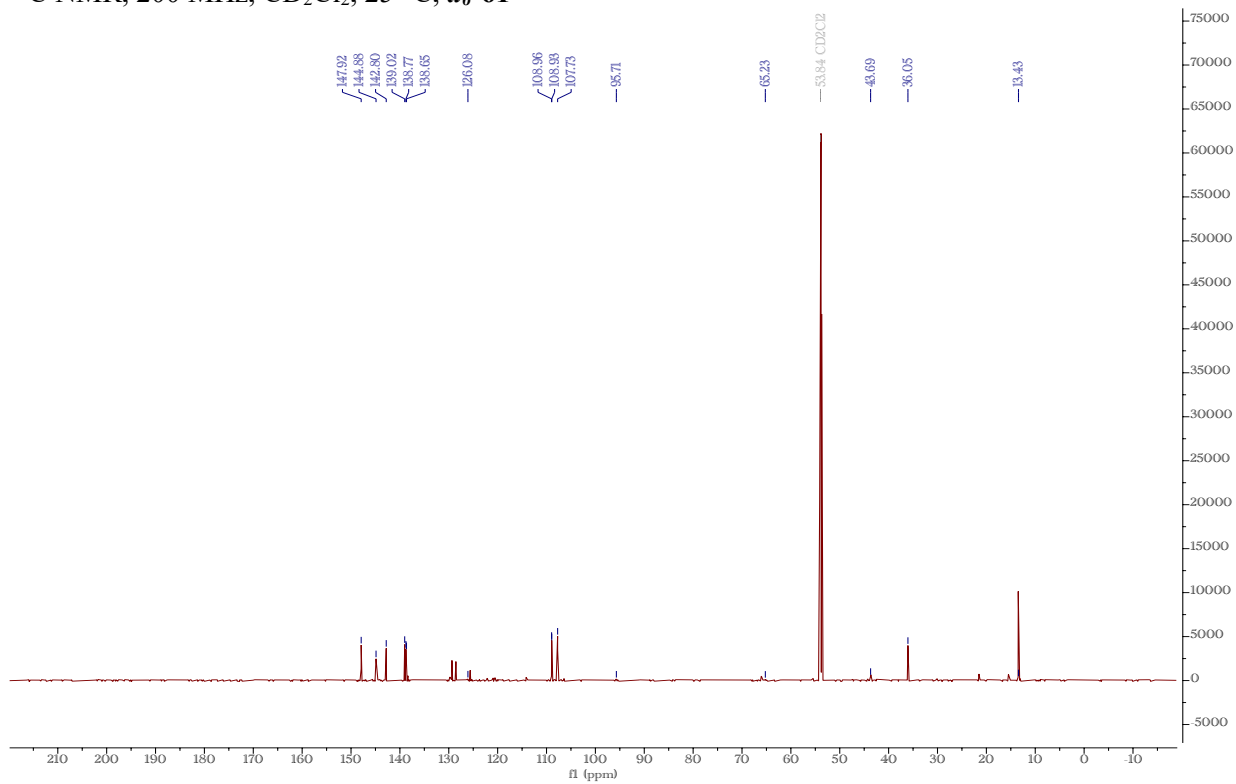
$^{13}\text{C}$  NMR, 200 MHz,  $\text{CD}_2\text{Cl}_2$ , 25 °C, *d*<sub>5</sub>-61



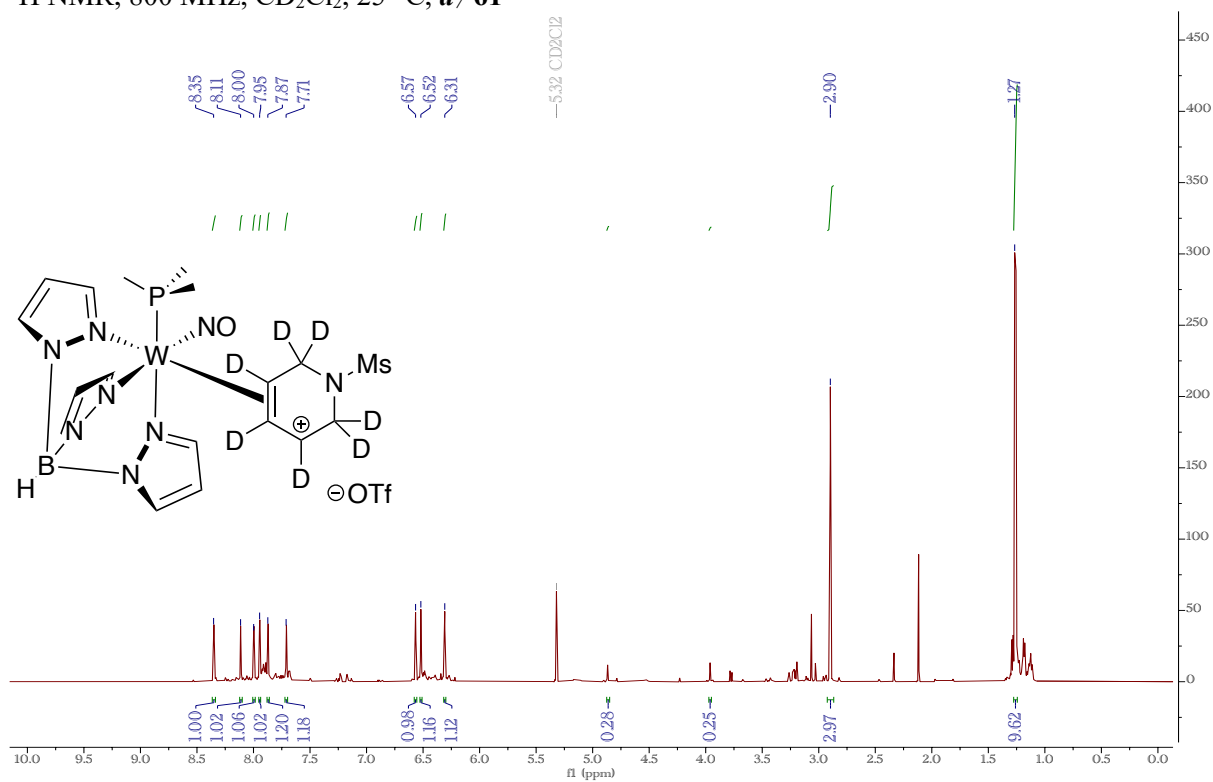
$^1\text{H}$  NMR, 800 MHz,  $\text{CD}_2\text{Cl}_2$ , 25 °C,  $d_6$ -**61**



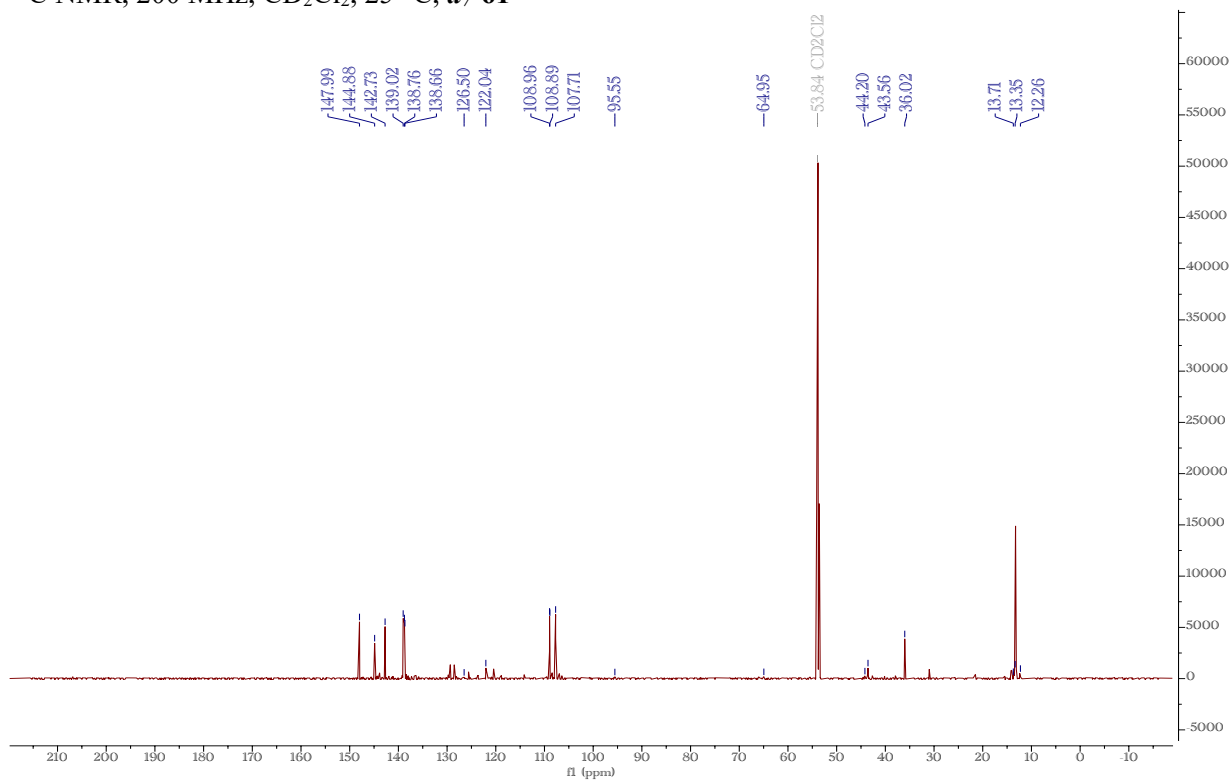
$^{13}\text{C}$  NMR, 200 MHz,  $\text{CD}_2\text{Cl}_2$ , 25 °C,  $d_6$ -**61**



$^1\text{H}$  NMR, 800 MHz,  $\text{CD}_2\text{Cl}_2$ , 25 °C, *d*<sub>7</sub>-**61**

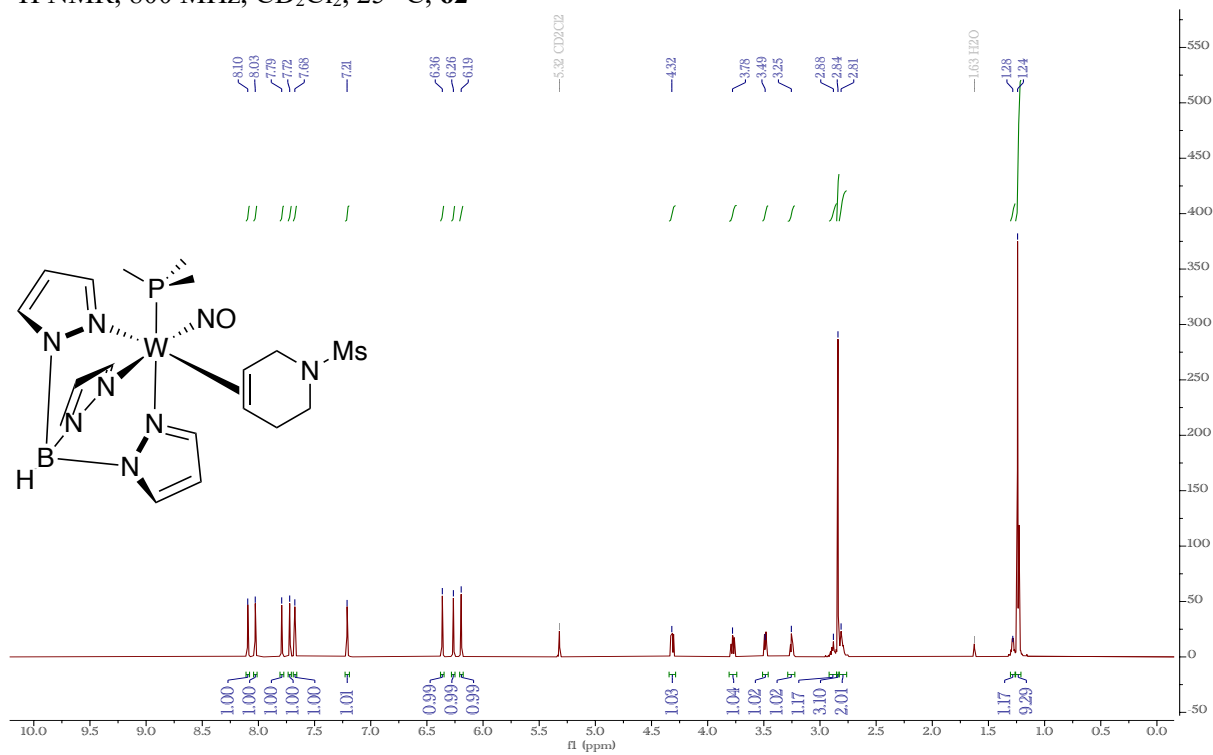


$^{13}\text{C}$  NMR, 200 MHz,  $\text{CD}_2\text{Cl}_2$ , 25 °C, *d*<sub>7</sub>-**61**





$^1\text{H}$  NMR, 800 MHz,  $\text{CD}_2\text{Cl}_2$ , 25 °C, **62**



$^{13}\text{C}$  NMR, 200 MHz,  $\text{CD}_2\text{Cl}_2$ , 25 °C, **62**

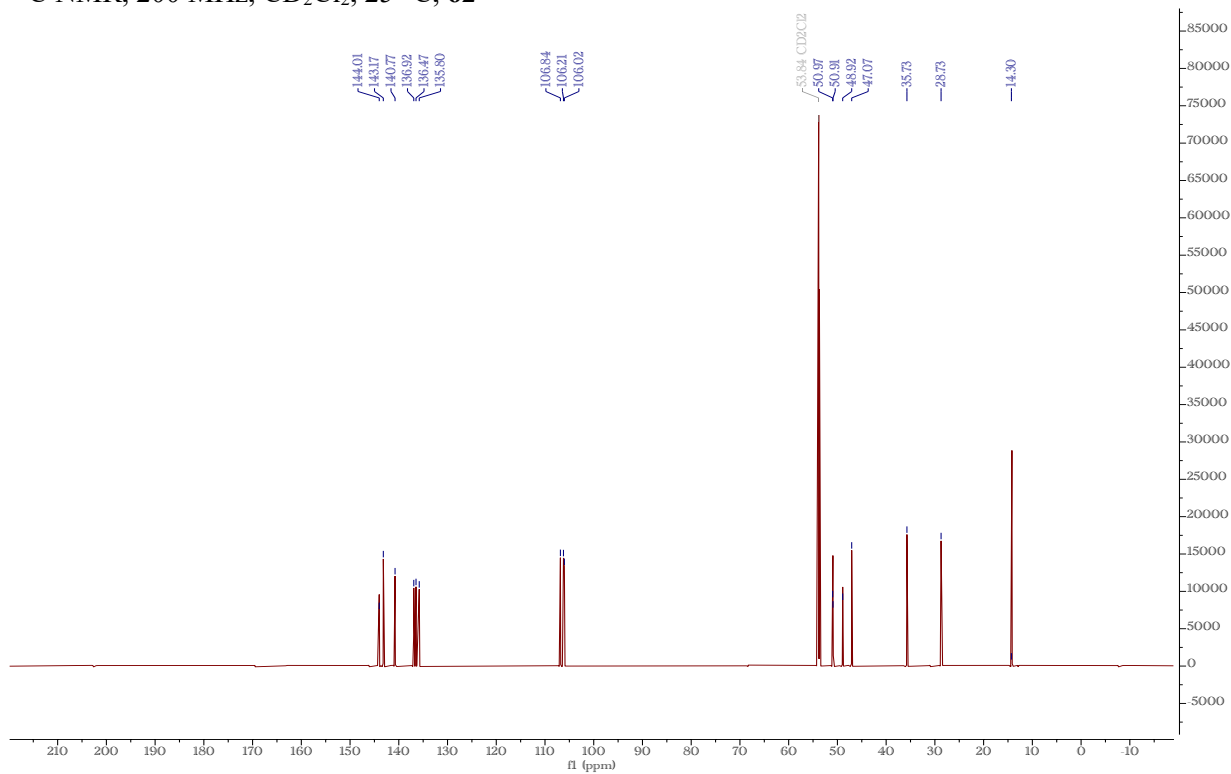


Figure S33:  $^1\text{H}$  NMR, 800 MHz,  $\text{CD}_2\text{Cl}_2$ , 25  $^\circ\text{C}$ ,  $\pm(2S)\text{-}d_1\text{-}62$

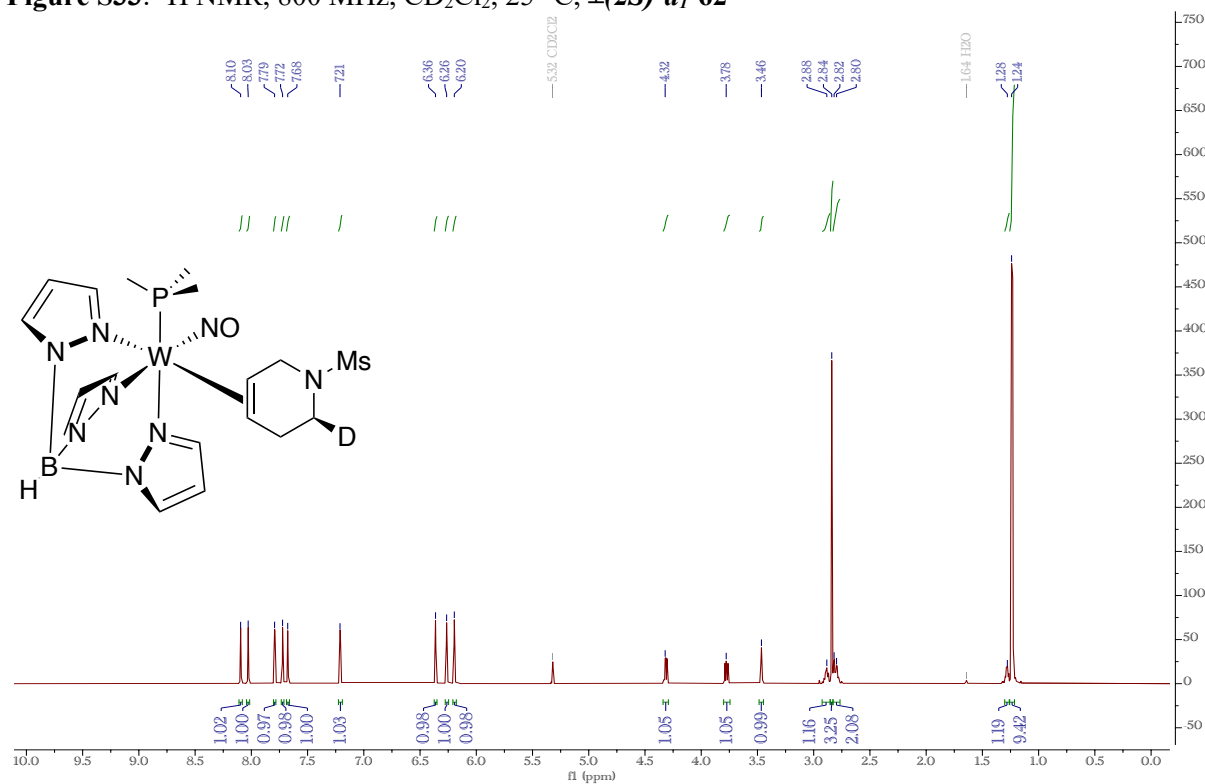


Figure S34:  $^{13}\text{C}$  NMR, 200 MHz,  $\text{CD}_2\text{Cl}_2$ , 25  $^\circ\text{C}$ ,  $\pm(2S)\text{-}d_1\text{-}62$

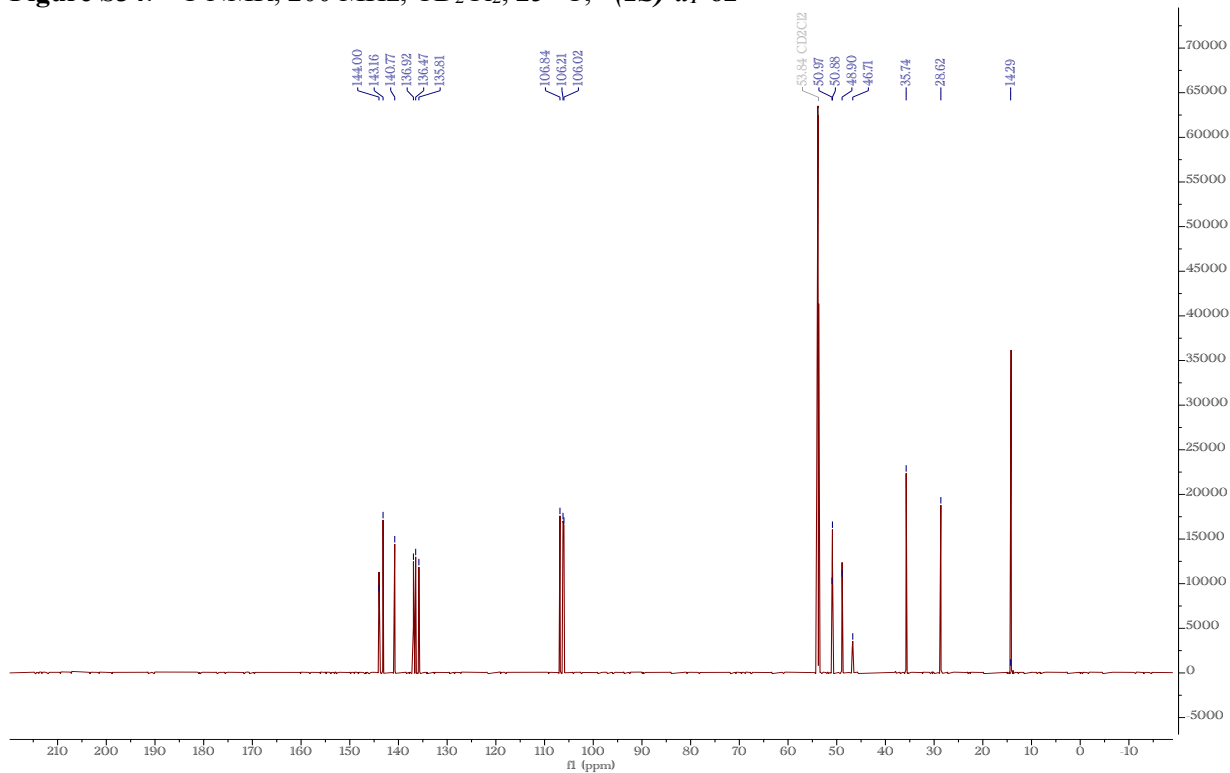
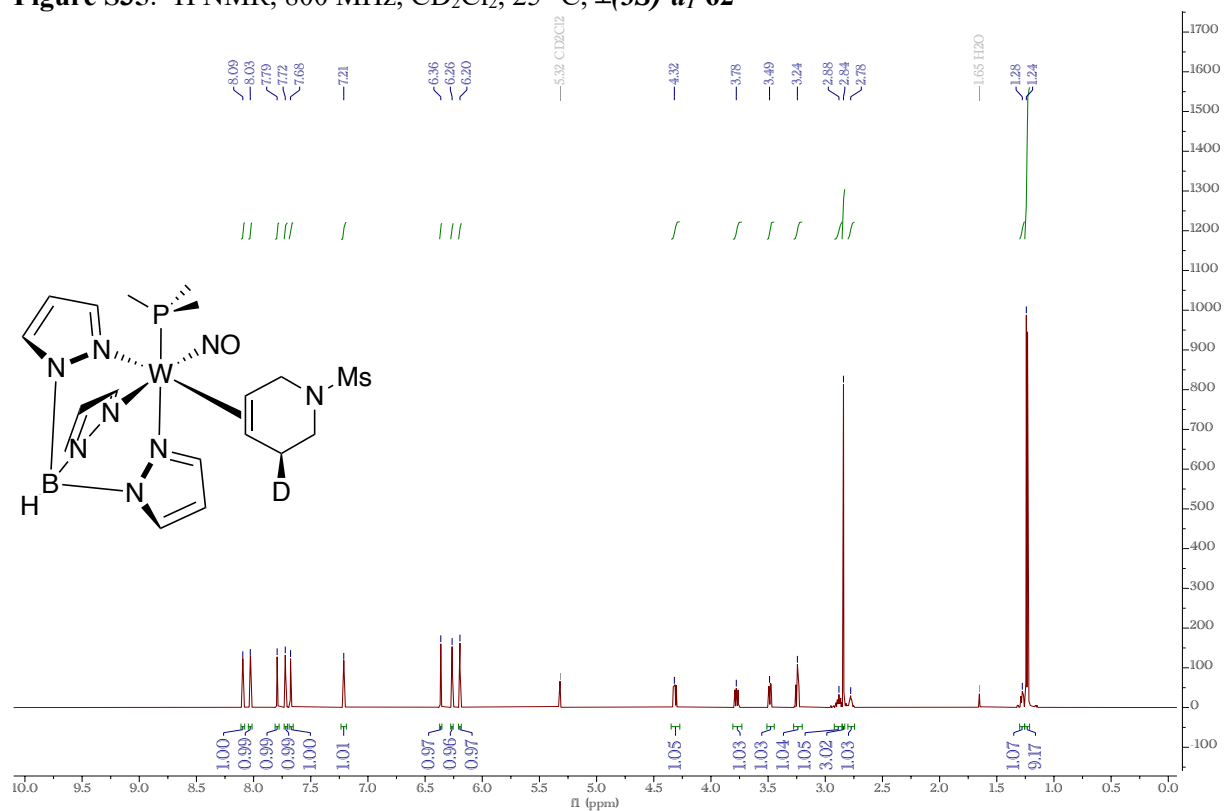
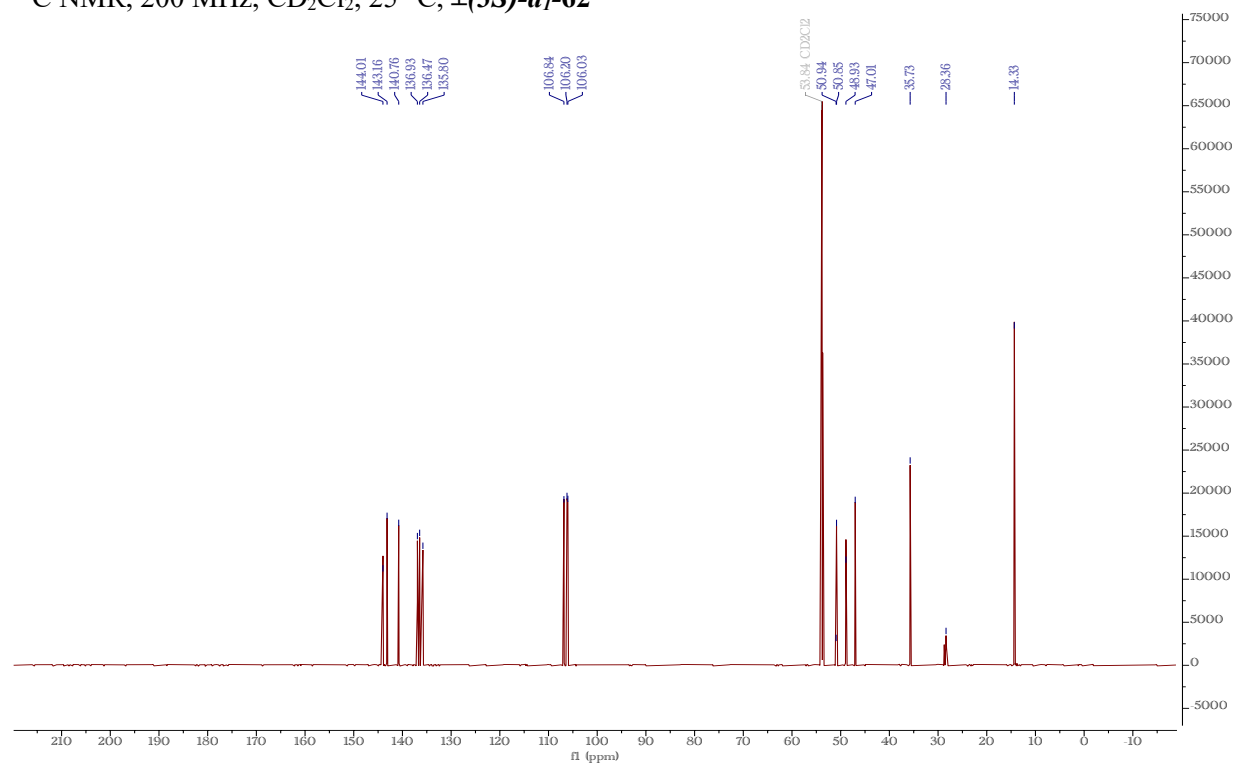


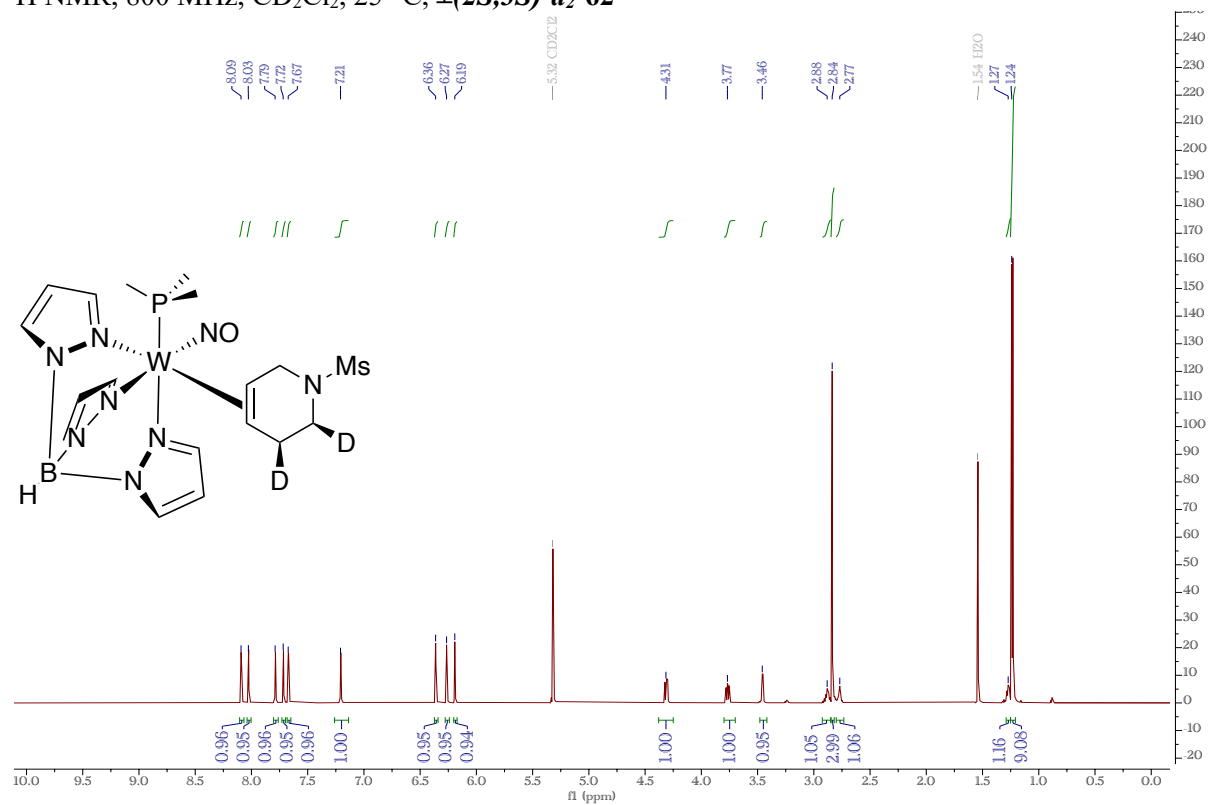
Figure S35:  $^1\text{H}$  NMR, 800 MHz,  $\text{CD}_2\text{Cl}_2$ , 25  $^\circ\text{C}$ ,  $\pm(3S)\text{-}d_1\text{-}62$



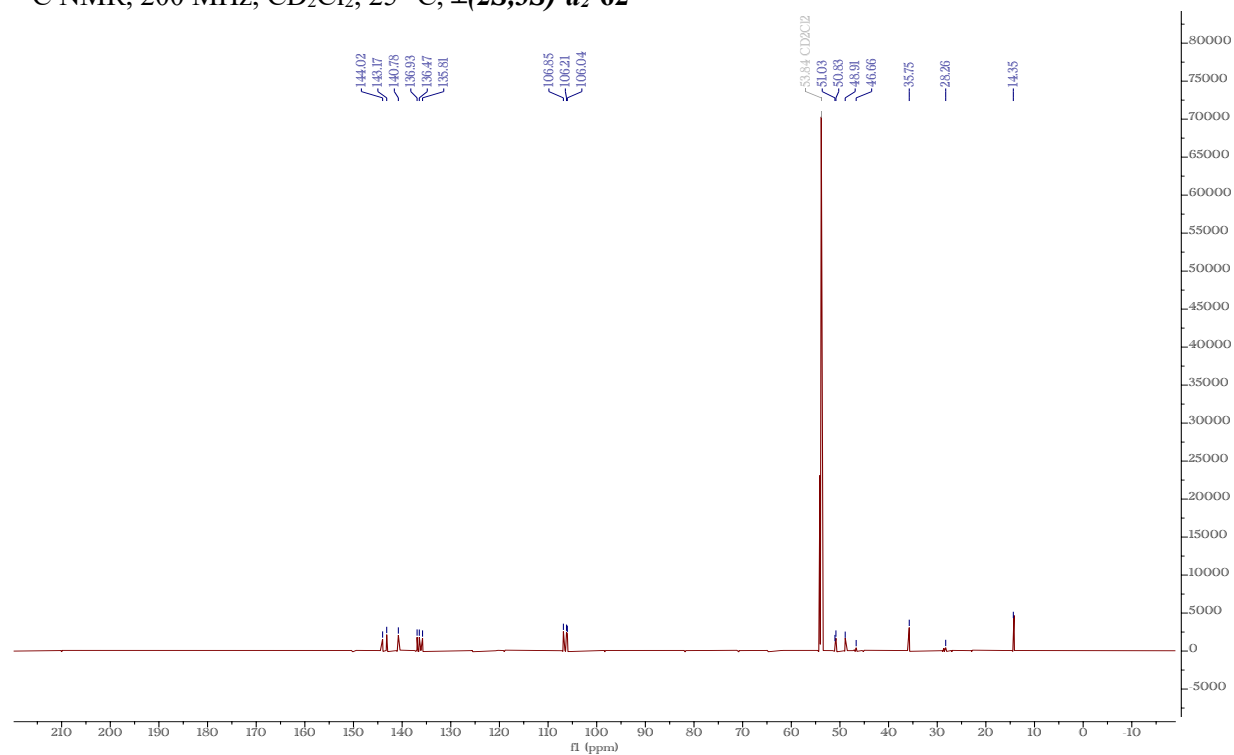
$^{13}\text{C}$  NMR, 200 MHz,  $\text{CD}_2\text{Cl}_2$ , 25  $^\circ\text{C}$ ,  $\pm(3S)\text{-}d_1\text{-}62$



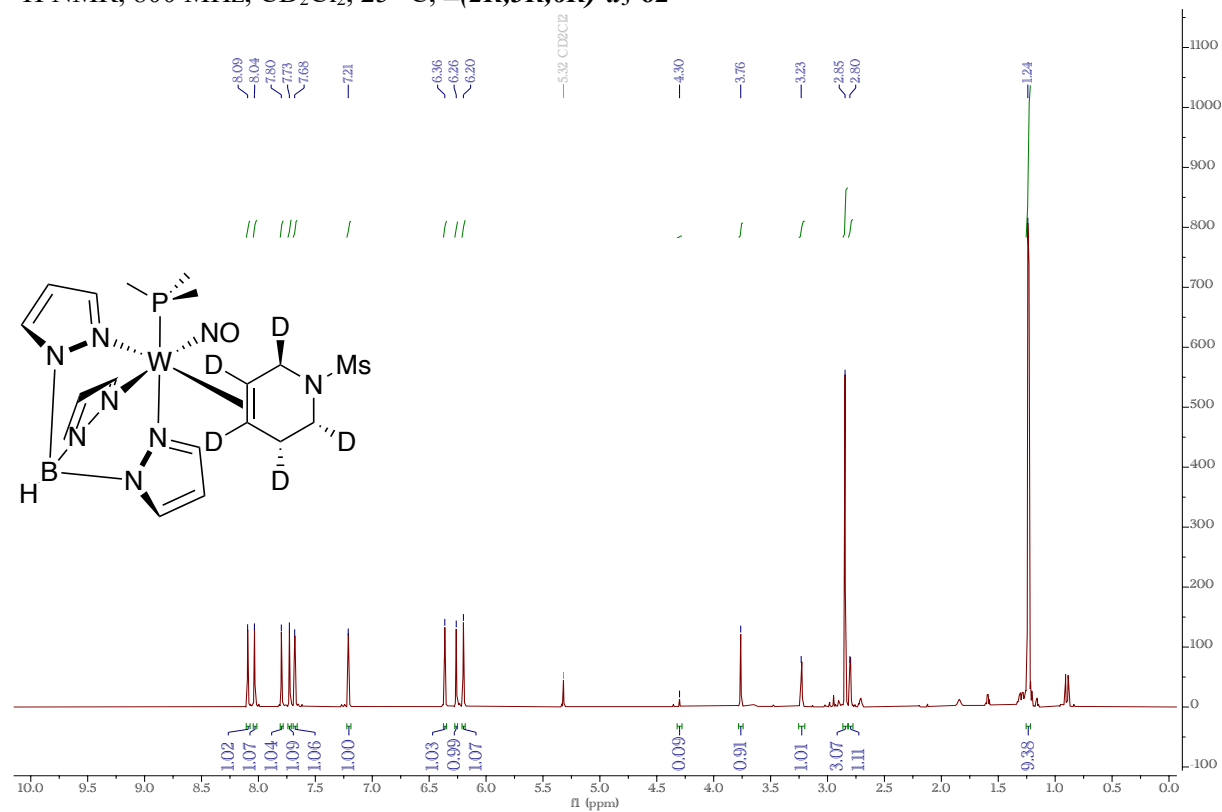
$^1\text{H}$  NMR, 800 MHz,  $\text{CD}_2\text{Cl}_2$ , 25 °C,  $\pm(2S,3S)\text{-}d_2\text{-62}$



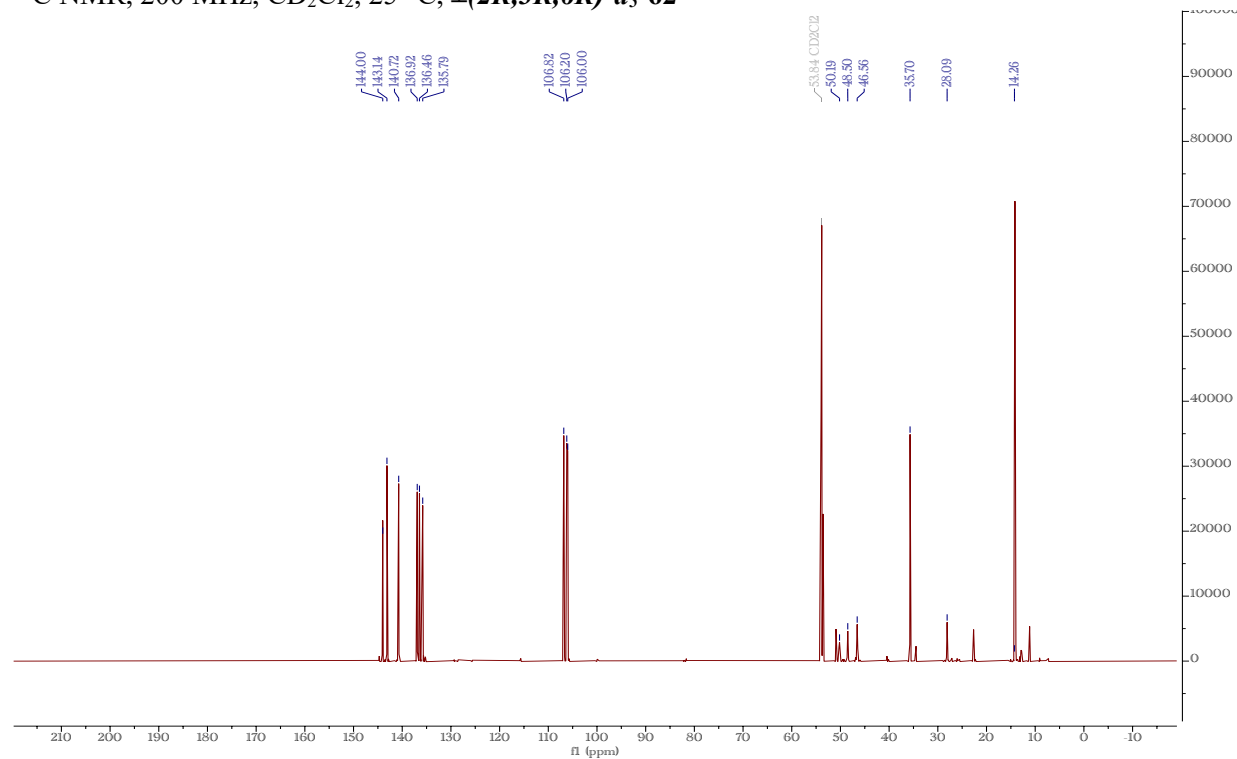
$^{13}\text{C}$  NMR, 200 MHz,  $\text{CD}_2\text{Cl}_2$ , 25 °C,  $\pm(2S,3S)\text{-}d_2\text{-62}$



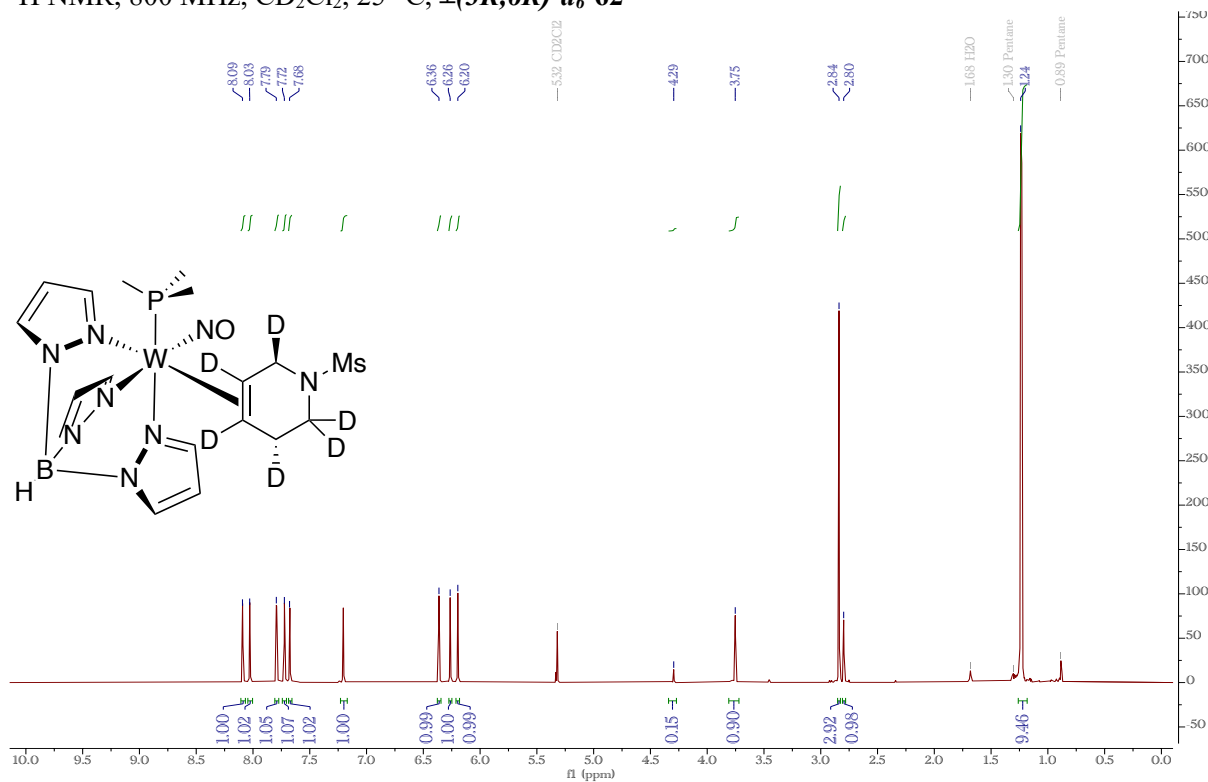
$^1\text{H}$  NMR, 800 MHz,  $\text{CD}_2\text{Cl}_2$ , 25 °C,  $\pm(2R,3R,6R)\text{-}d_5\text{-62}$



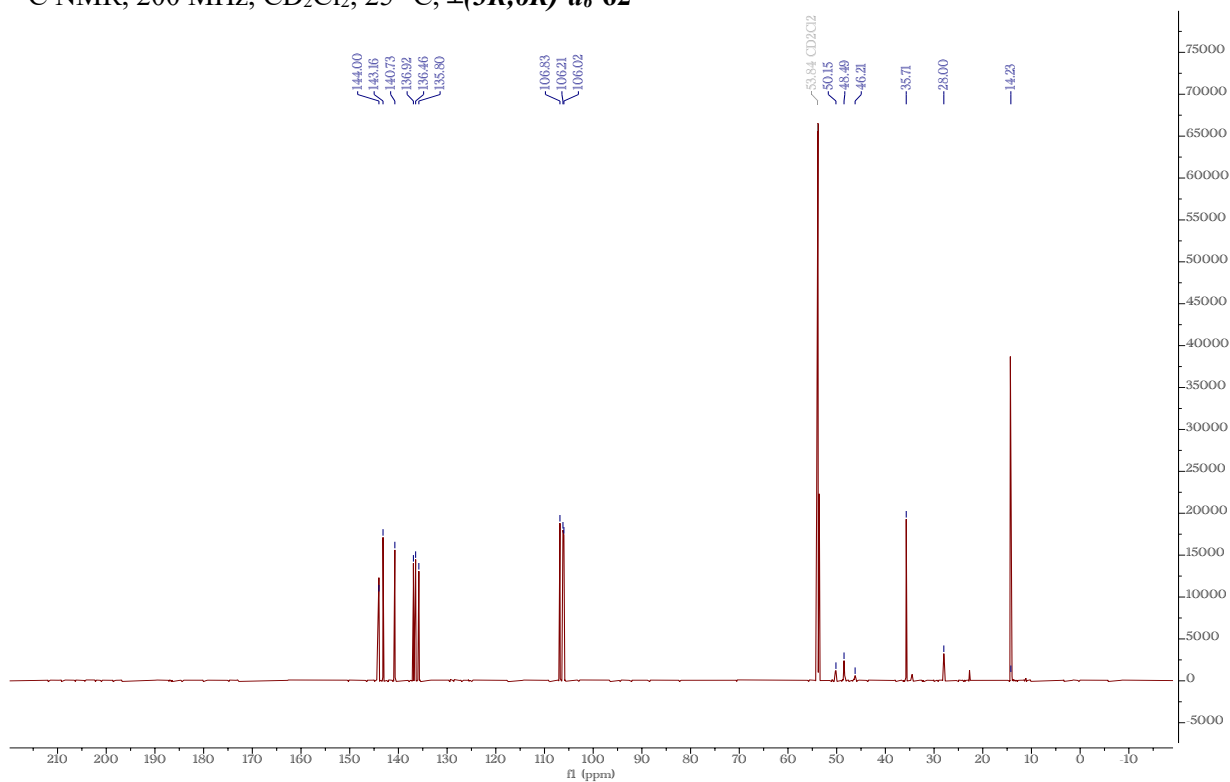
$^{13}\text{C}$  NMR, 200 MHz,  $\text{CD}_2\text{Cl}_2$ , 25 °C,  $\pm(2R,3R,6R)\text{-}d_5\text{-62}$



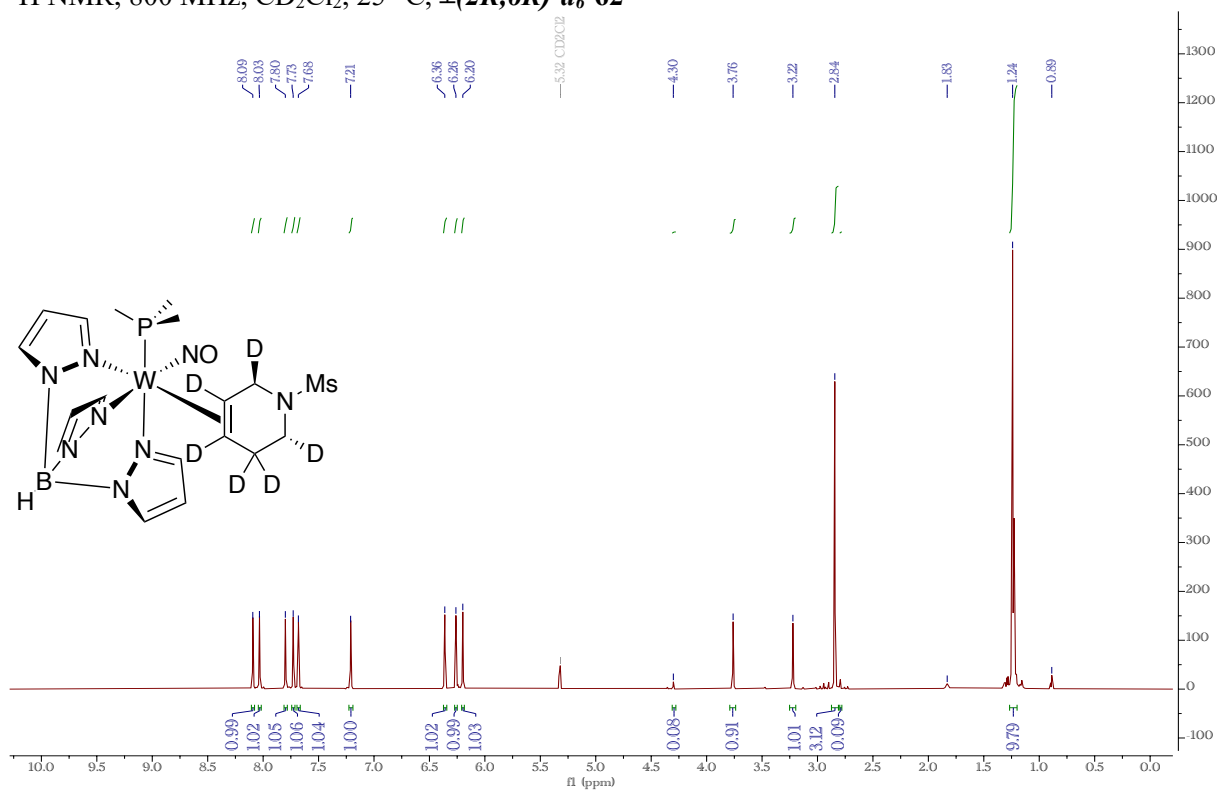
$^1\text{H}$  NMR, 800 MHz,  $\text{CD}_2\text{Cl}_2$ , 25 °C,  $\pm(3R,6R)\text{-}d_6\text{-}62$



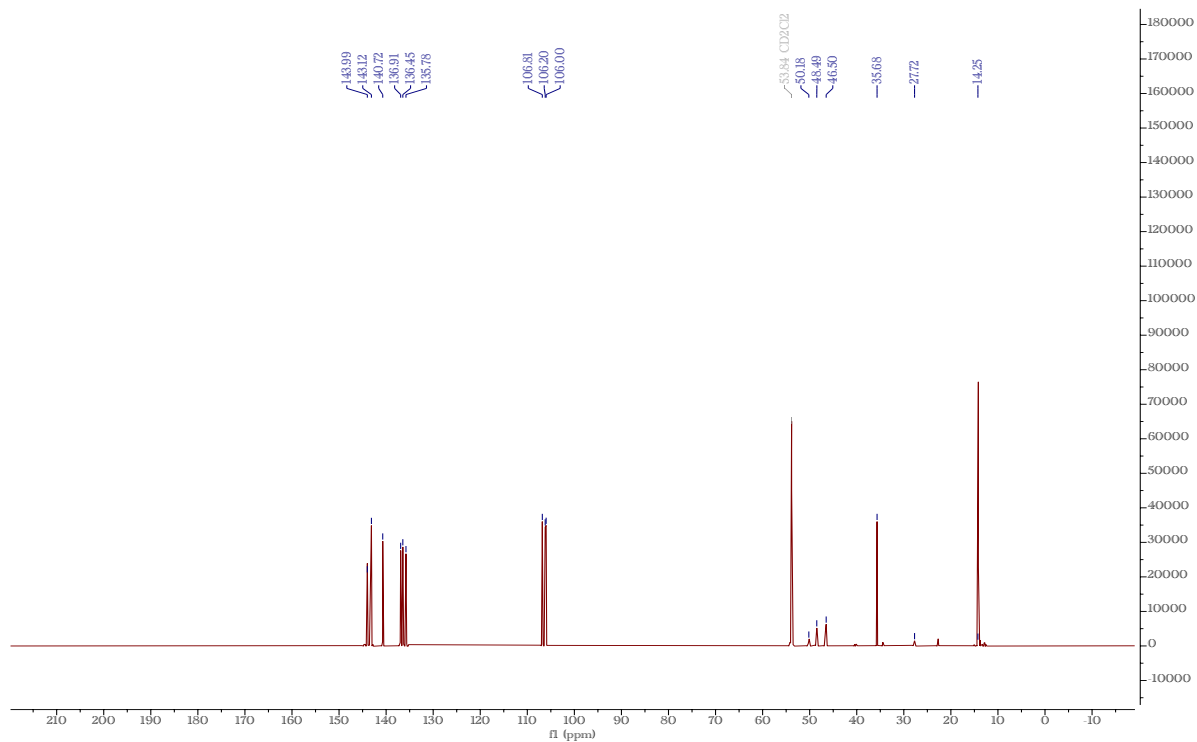
$^{13}\text{C}$  NMR, 200 MHz,  $\text{CD}_2\text{Cl}_2$ , 25 °C,  $\pm(3R,6R)\text{-}d_6\text{-}62$



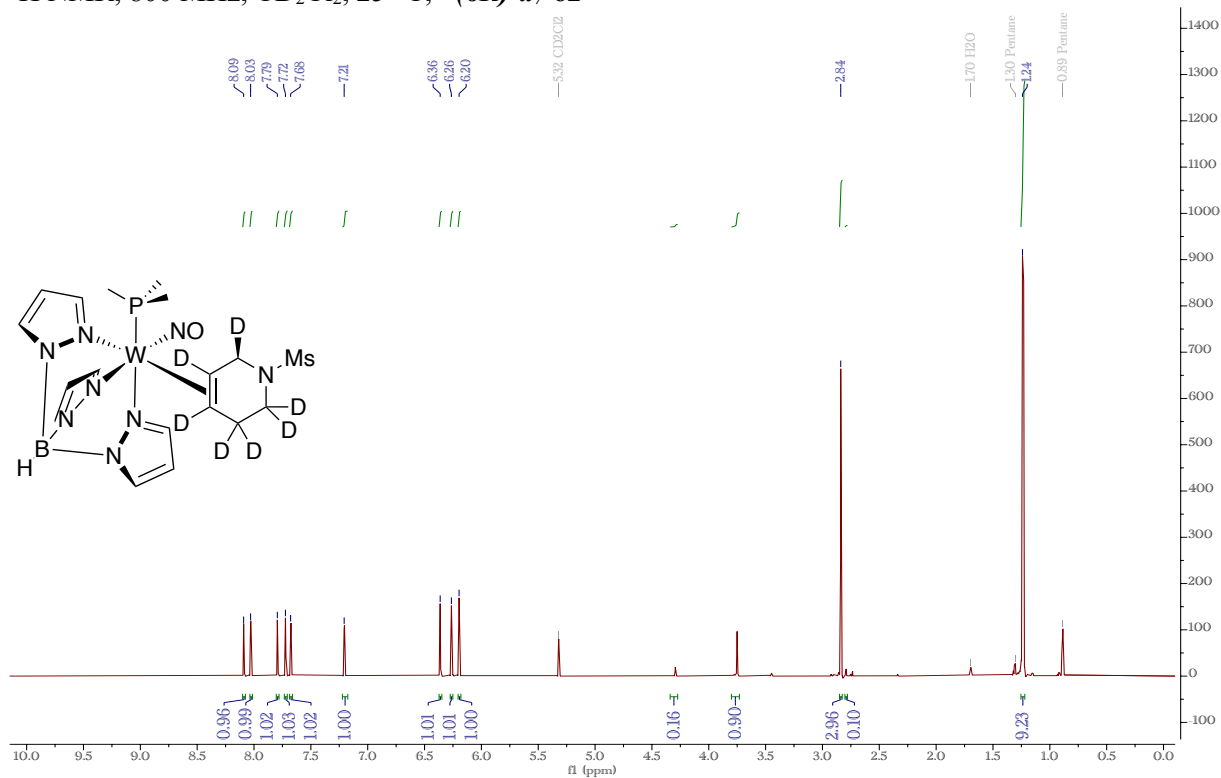
$^1\text{H}$  NMR, 800 MHz,  $\text{CD}_2\text{Cl}_2$ , 25 °C,  $\pm(2R,6R)\text{-}d_6\text{-}62$



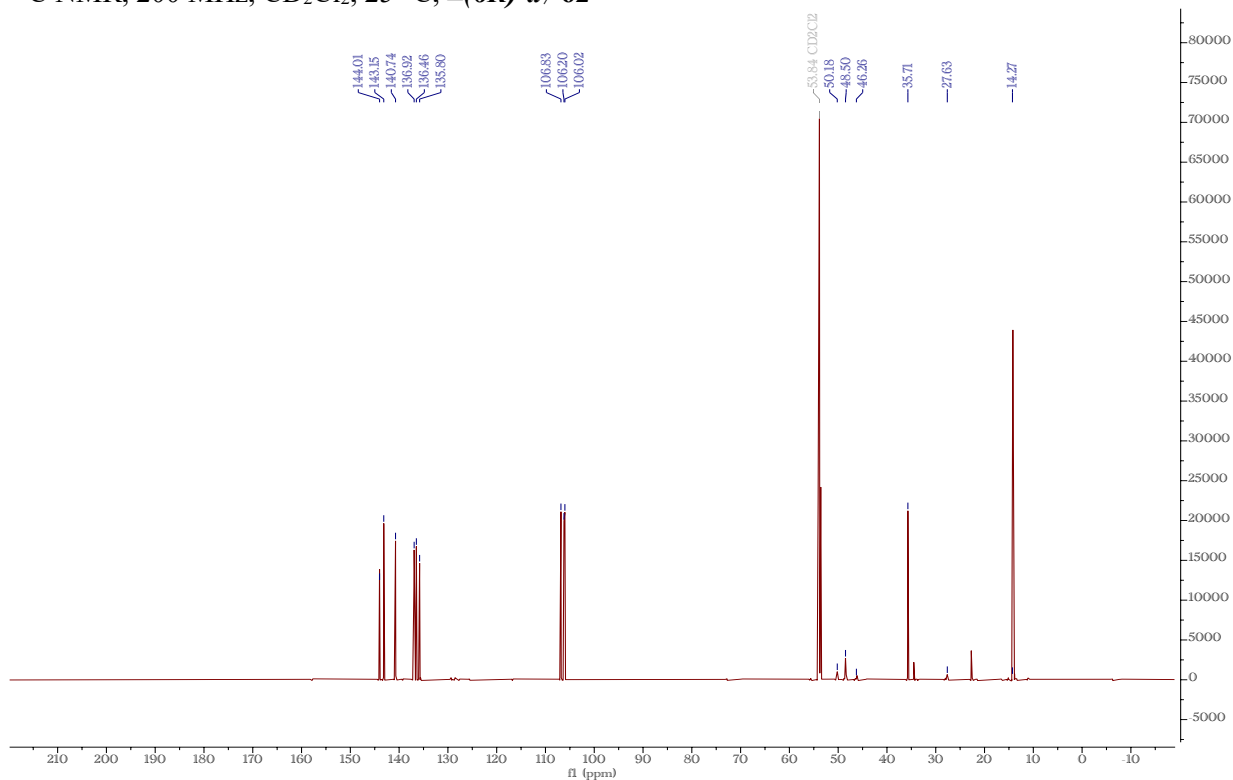
$^{13}\text{C}$  NMR, 200 MHz,  $\text{CD}_2\text{Cl}_2$ , 25 °C,  $\pm(2R,6R)\text{-}d_6\text{-}62$



$^1\text{H}$  NMR, 800 MHz,  $\text{CD}_2\text{Cl}_2$ , 25 °C,  $\pm(6R)\text{-}d_7\text{-}62$

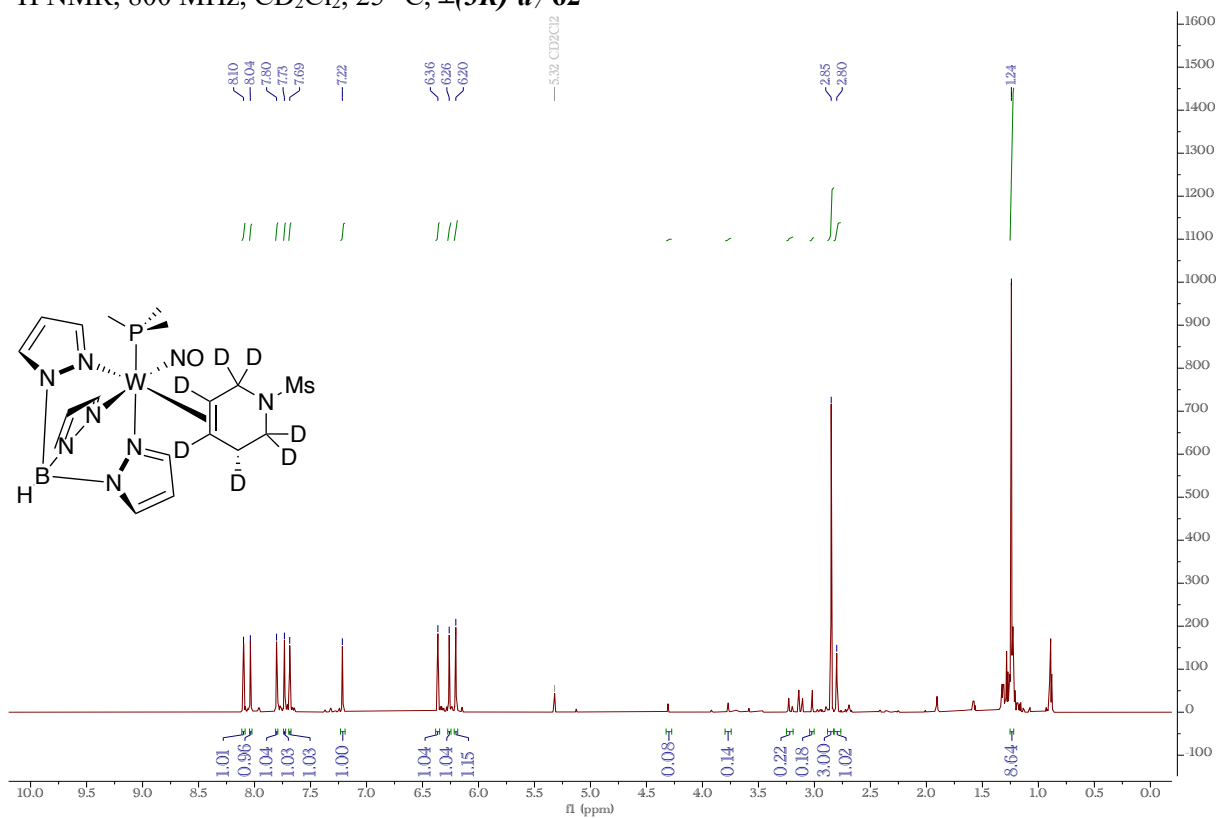


$^{13}\text{C}$  NMR, 200 MHz,  $\text{CD}_2\text{Cl}_2$ , 25 °C,  $\pm(6R)\text{-}d_7\text{-}62$

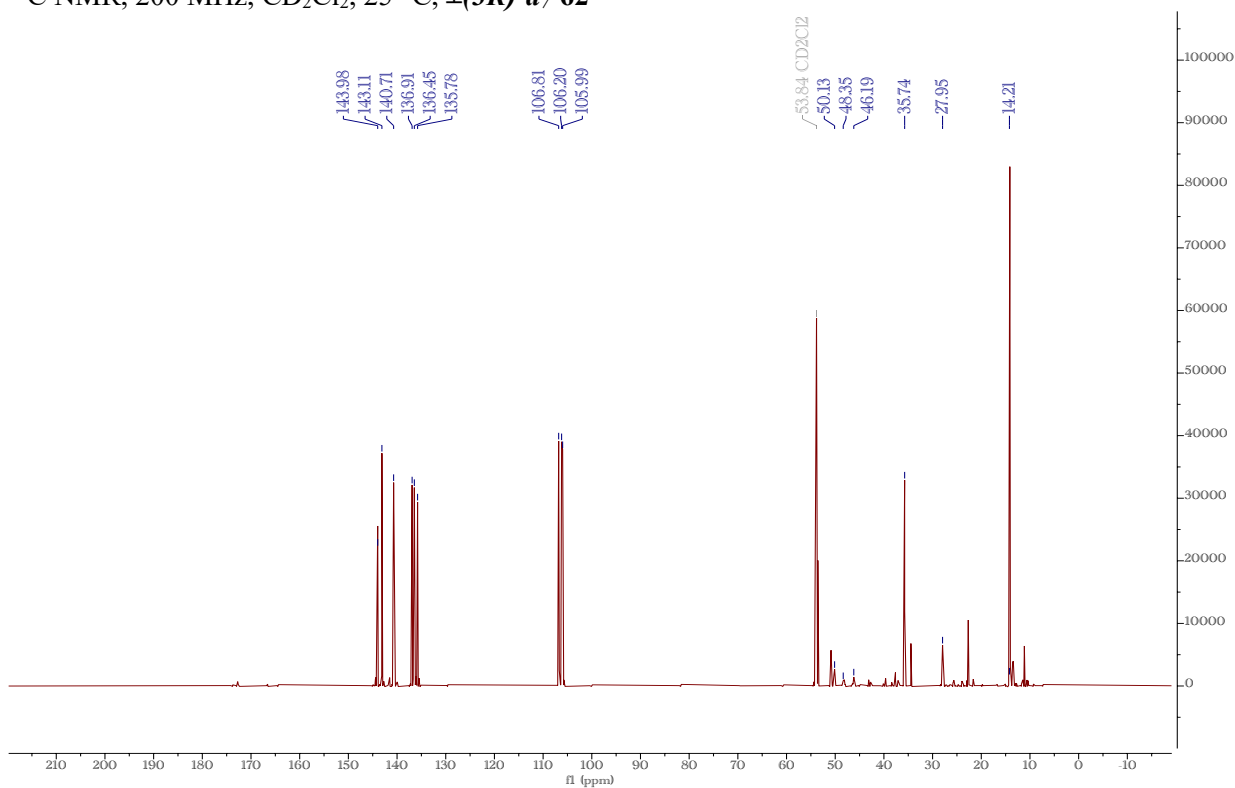




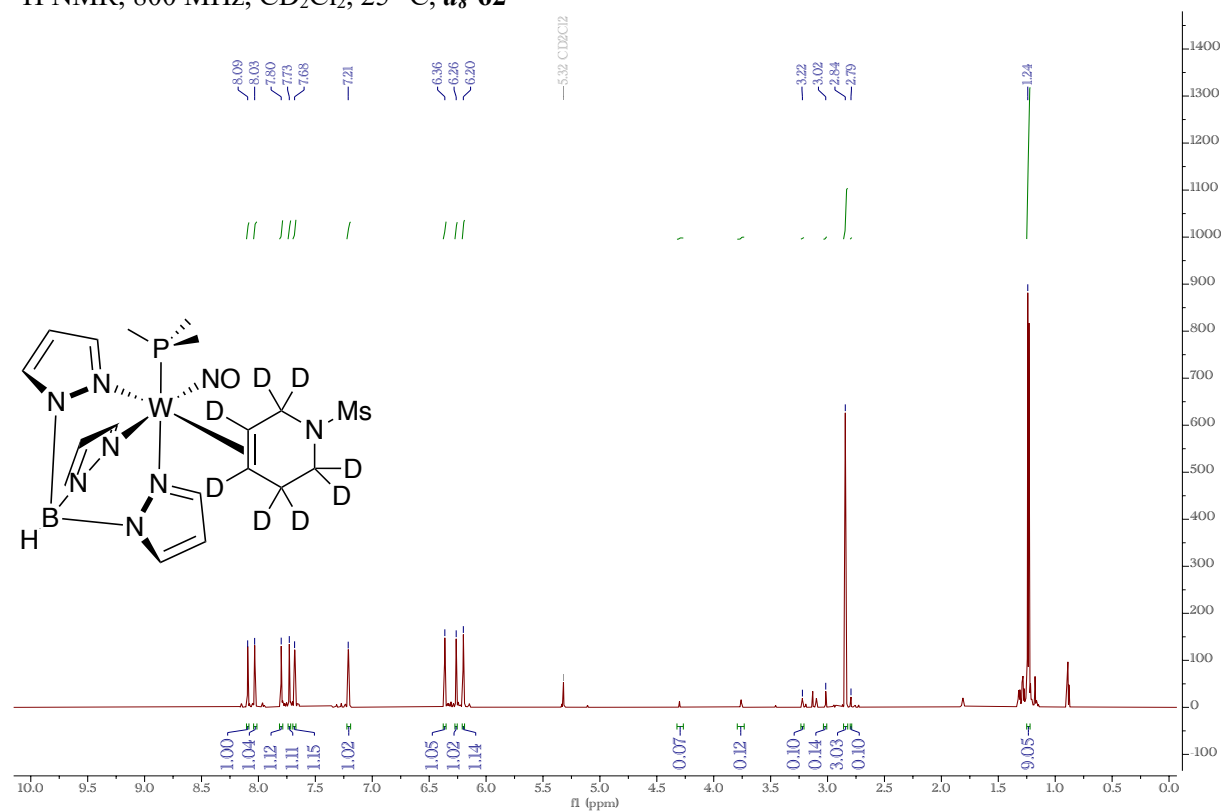
$^1\text{H}$  NMR, 800 MHz,  $\text{CD}_2\text{Cl}_2$ , 25 °C,  $\pm(3R)\text{-}d_7\text{-}62$



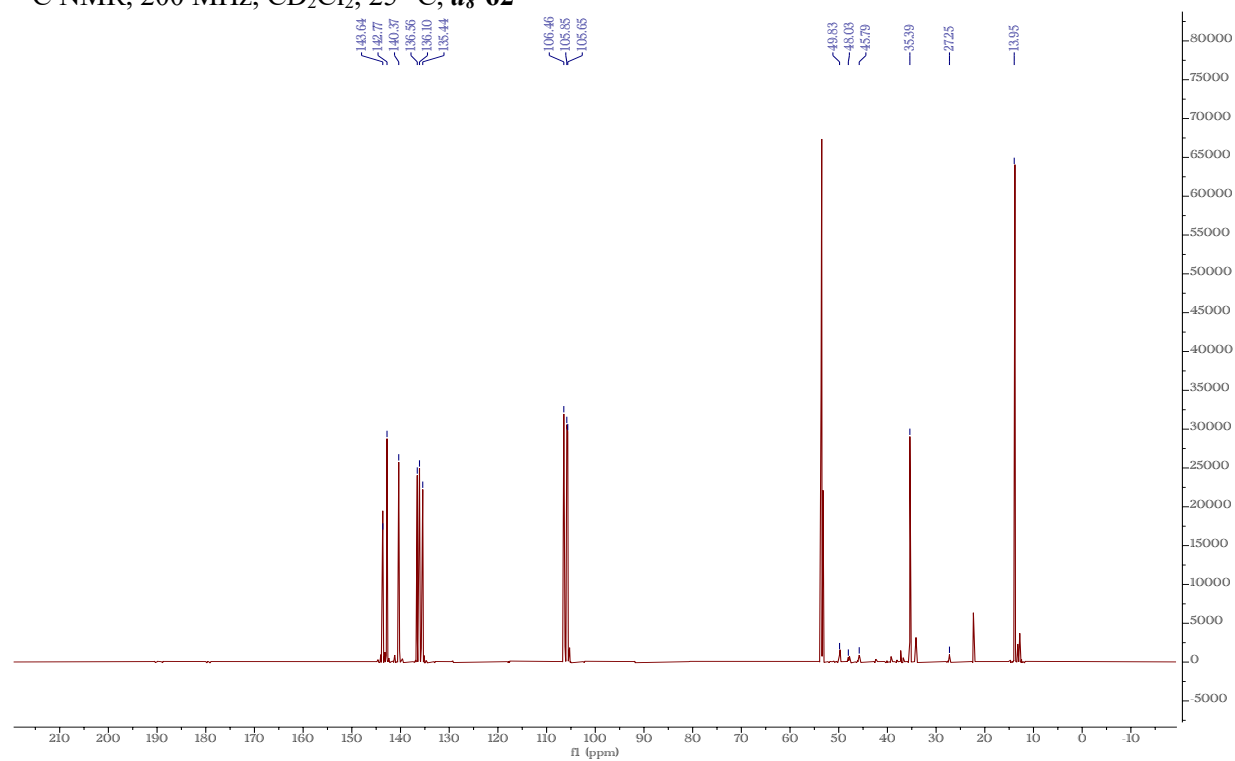
$^{13}\text{C}$  NMR, 200 MHz,  $\text{CD}_2\text{Cl}_2$ , 25 °C,  $\pm(3R)\text{-}d_7\text{-}62$



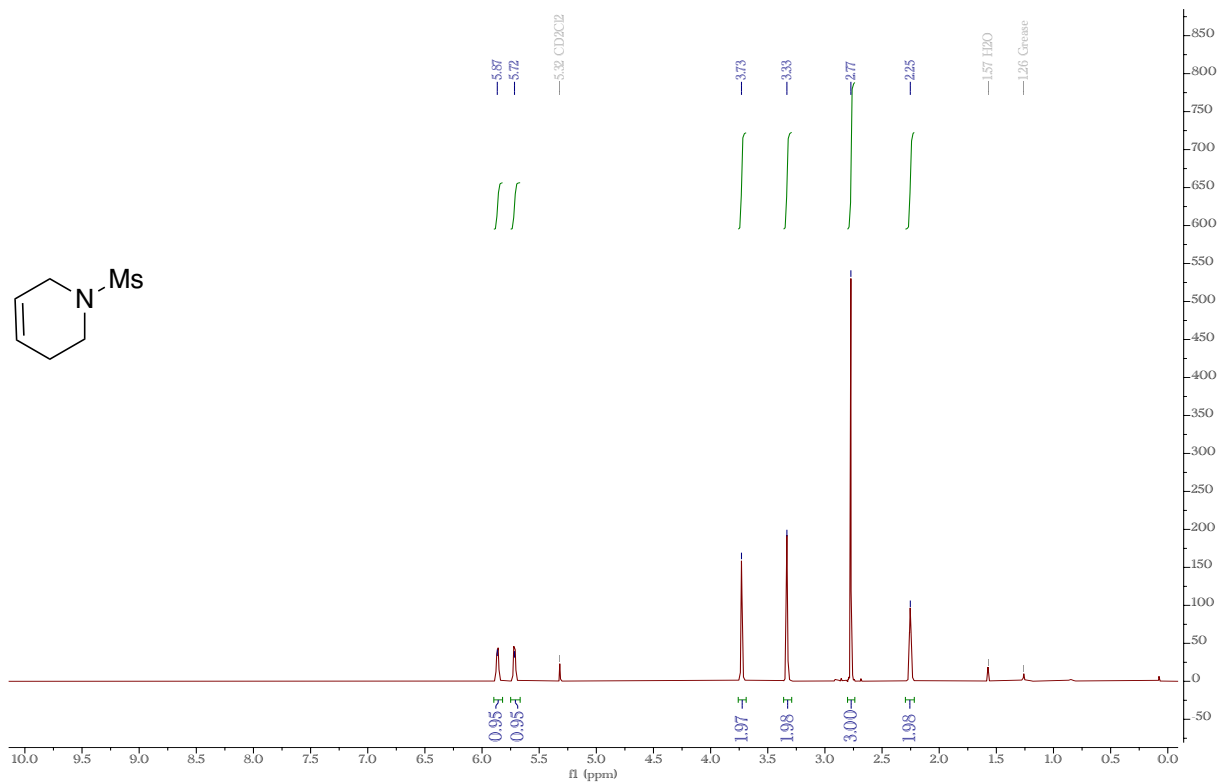
$^1\text{H}$  NMR, 800 MHz,  $\text{CD}_2\text{Cl}_2$ , 25 °C, *d*<sub>8</sub>-62



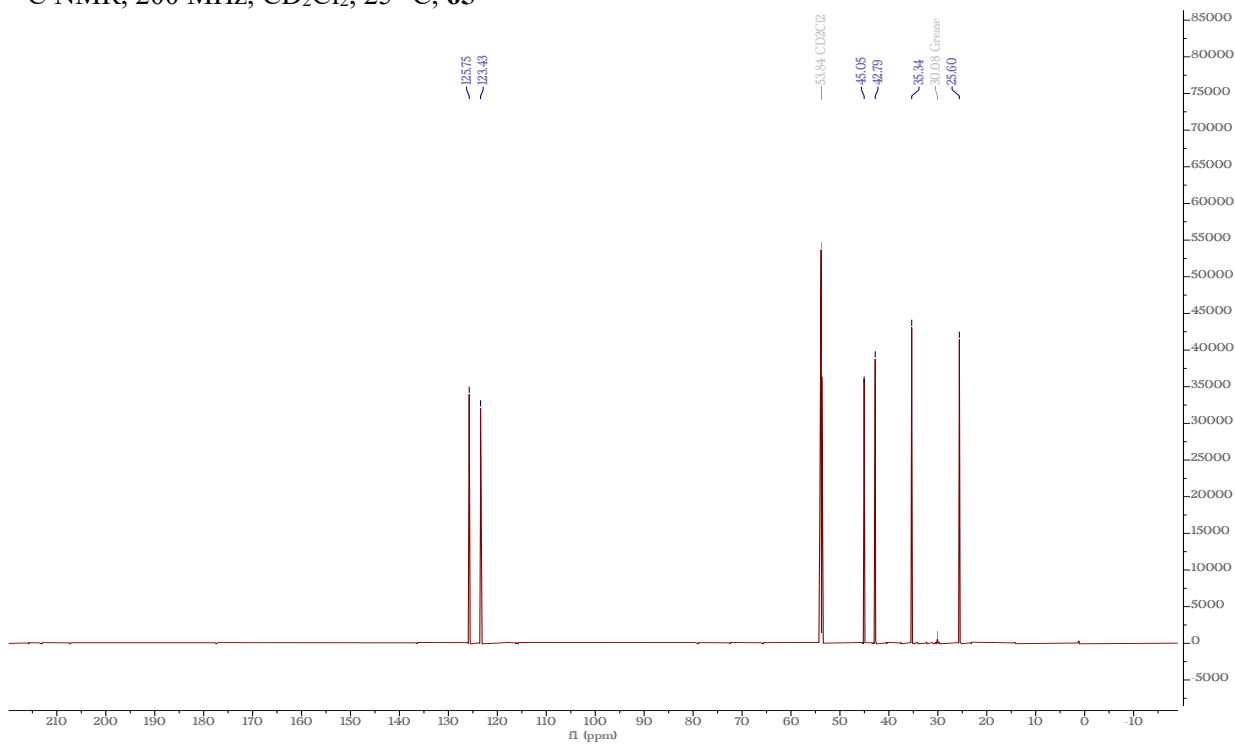
$^{13}\text{C}$  NMR, 200 MHz,  $\text{CD}_2\text{Cl}_2$ , 25 °C, *d*<sub>8</sub>-62



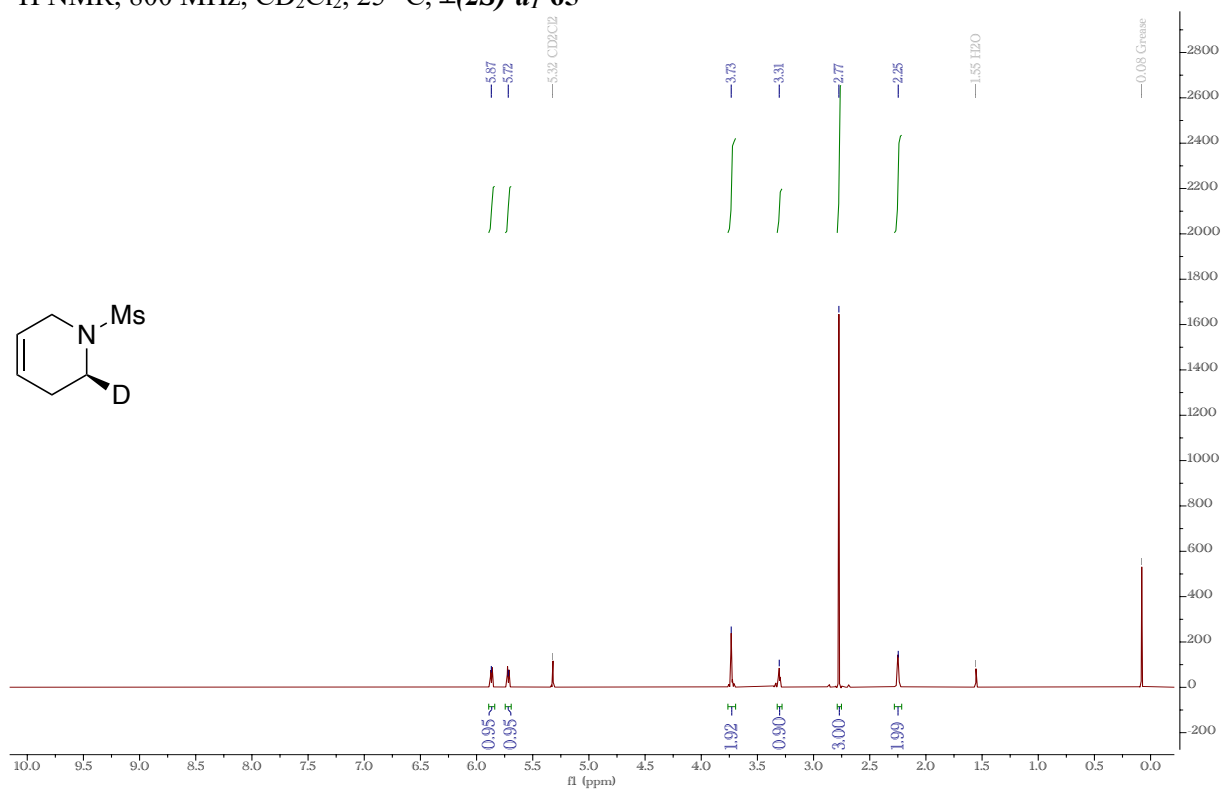
$^1\text{H}$  NMR, 800 MHz,  $\text{CD}_2\text{Cl}_2$ , 25 °C, **65**



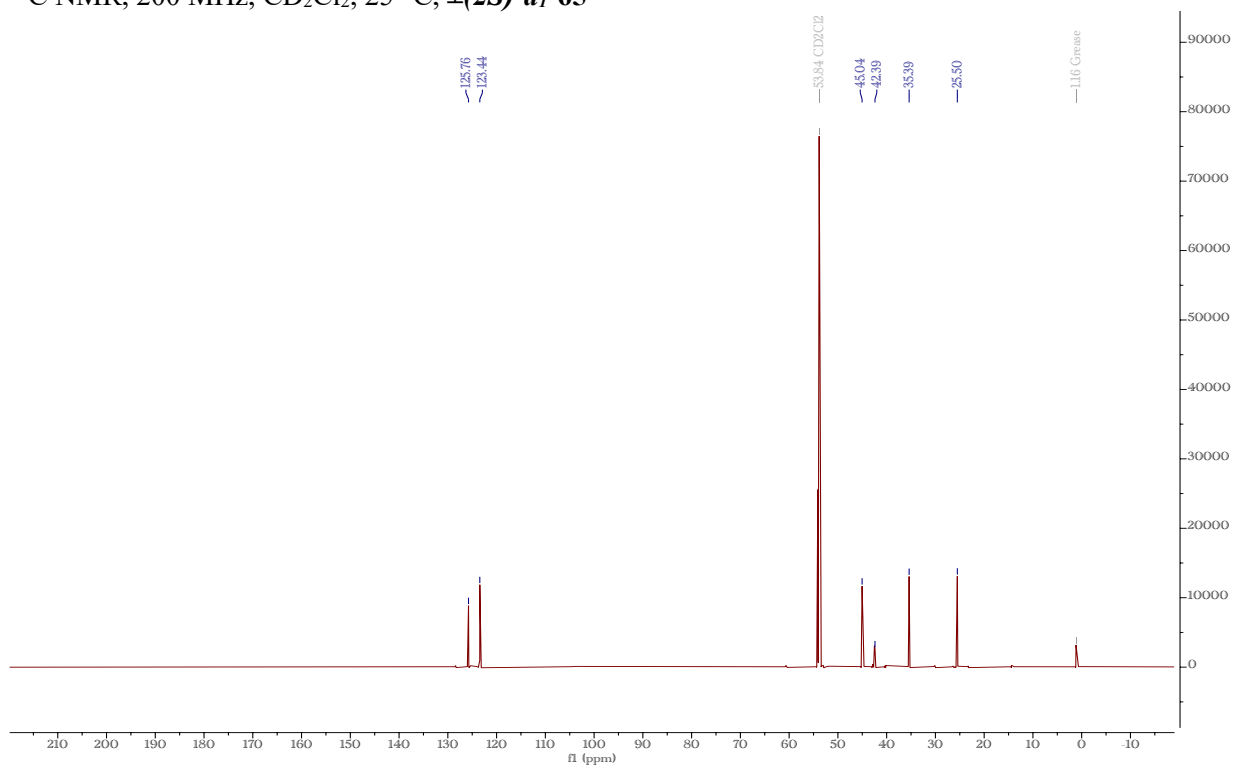
$^{13}\text{C}$  NMR, 200 MHz,  $\text{CD}_2\text{Cl}_2$ , 25 °C, **65**



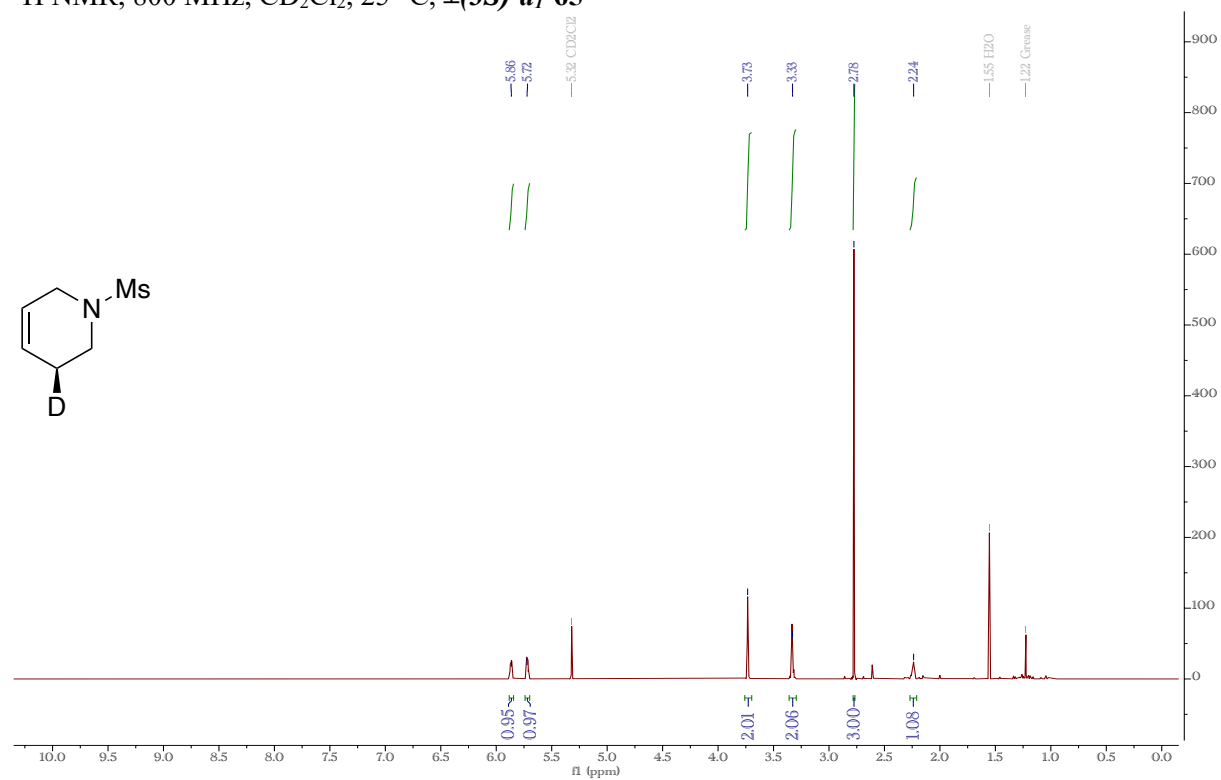
$^1\text{H}$  NMR, 800 MHz,  $\text{CD}_2\text{Cl}_2$ , 25 °C,  $\pm(2S)\text{-}d_1\text{-}65$



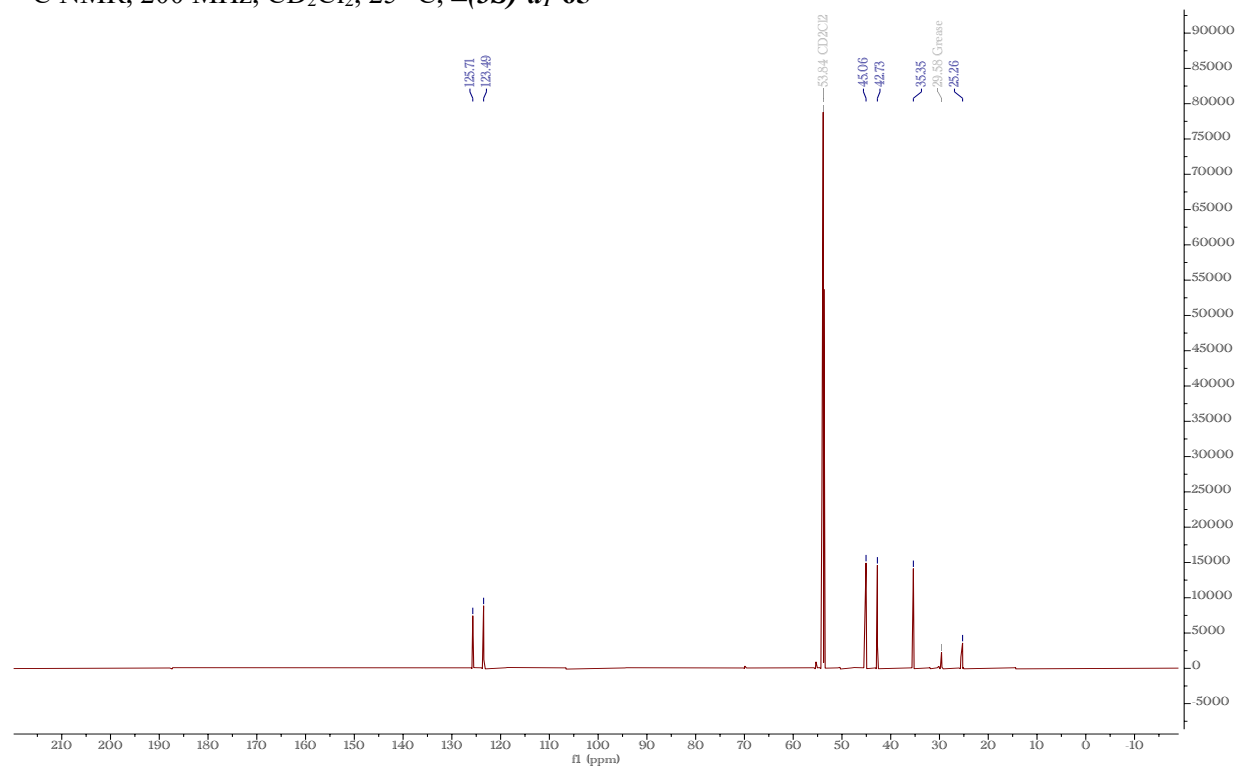
$^{13}\text{C}$  NMR, 200 MHz,  $\text{CD}_2\text{Cl}_2$ , 25 °C,  $\pm(2S)\text{-}d_1\text{-}65$



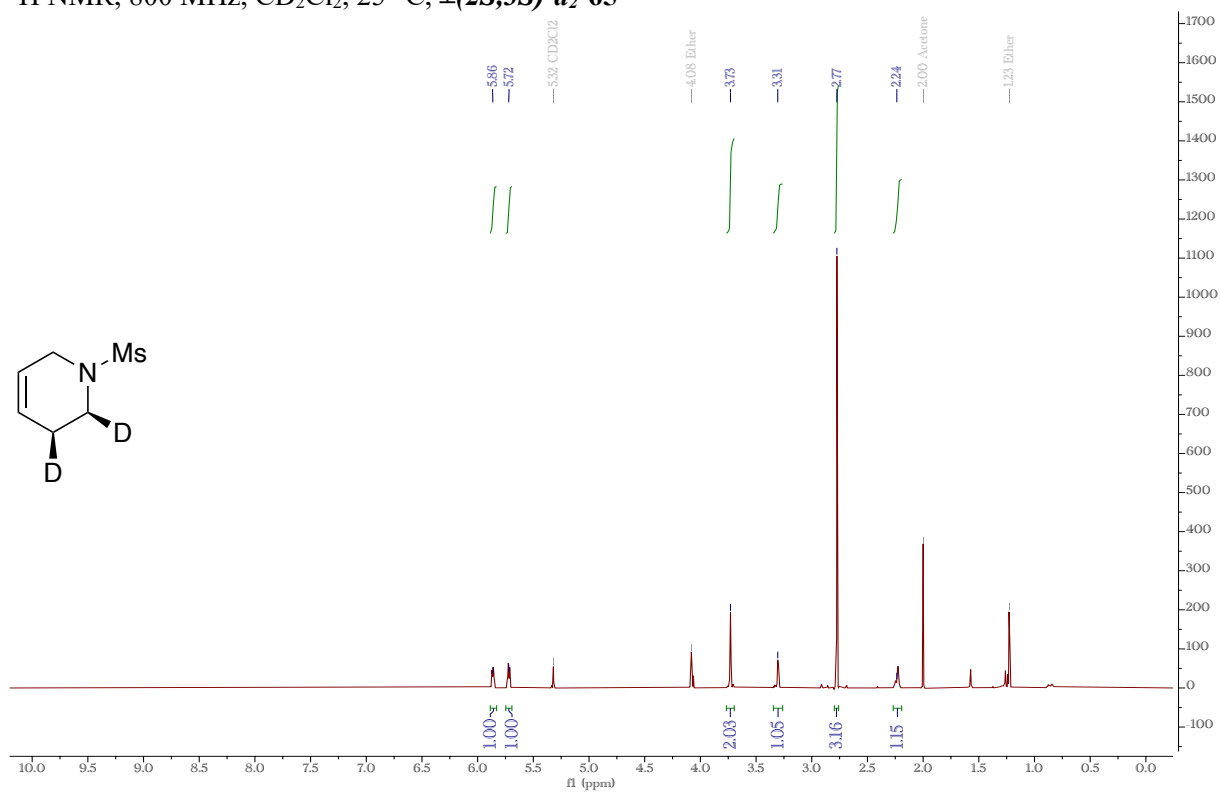
$^1\text{H}$  NMR, 800 MHz,  $\text{CD}_2\text{Cl}_2$ , 25 °C,  $\pm(3S)\text{-}d_1\text{-}65$



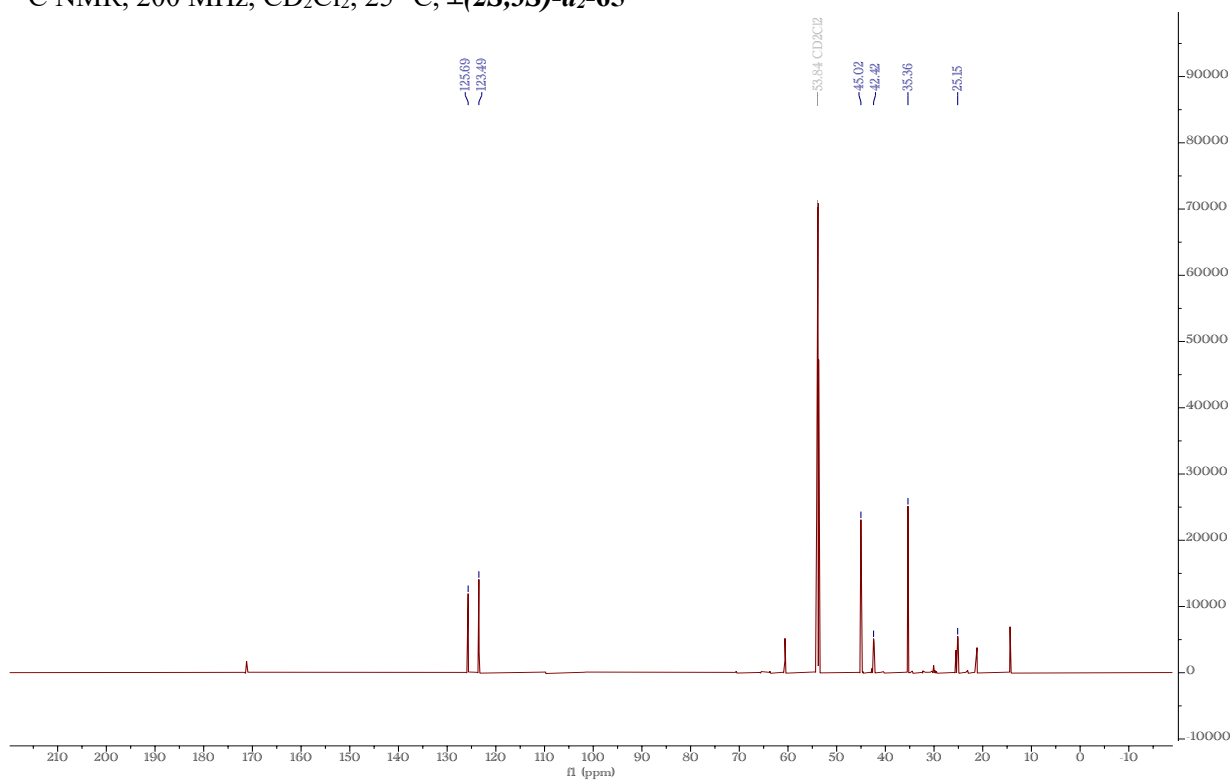
$^{13}\text{C}$  NMR, 200 MHz,  $\text{CD}_2\text{Cl}_2$ , 25 °C,  $\pm(3S)\text{-}d_1\text{-}65$



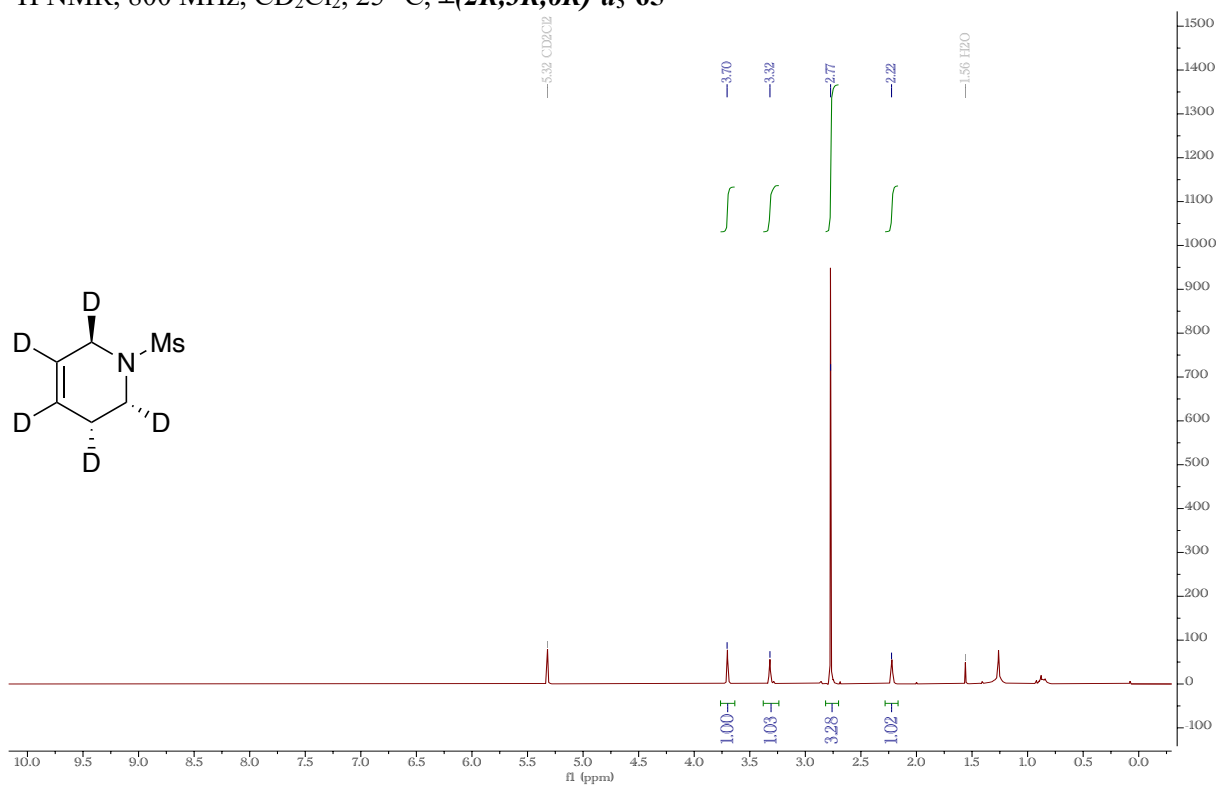
$^1\text{H}$  NMR, 800 MHz,  $\text{CD}_2\text{Cl}_2$ , 25 °C,  $\pm(2S,3S)\text{-}d_2\text{-65}$



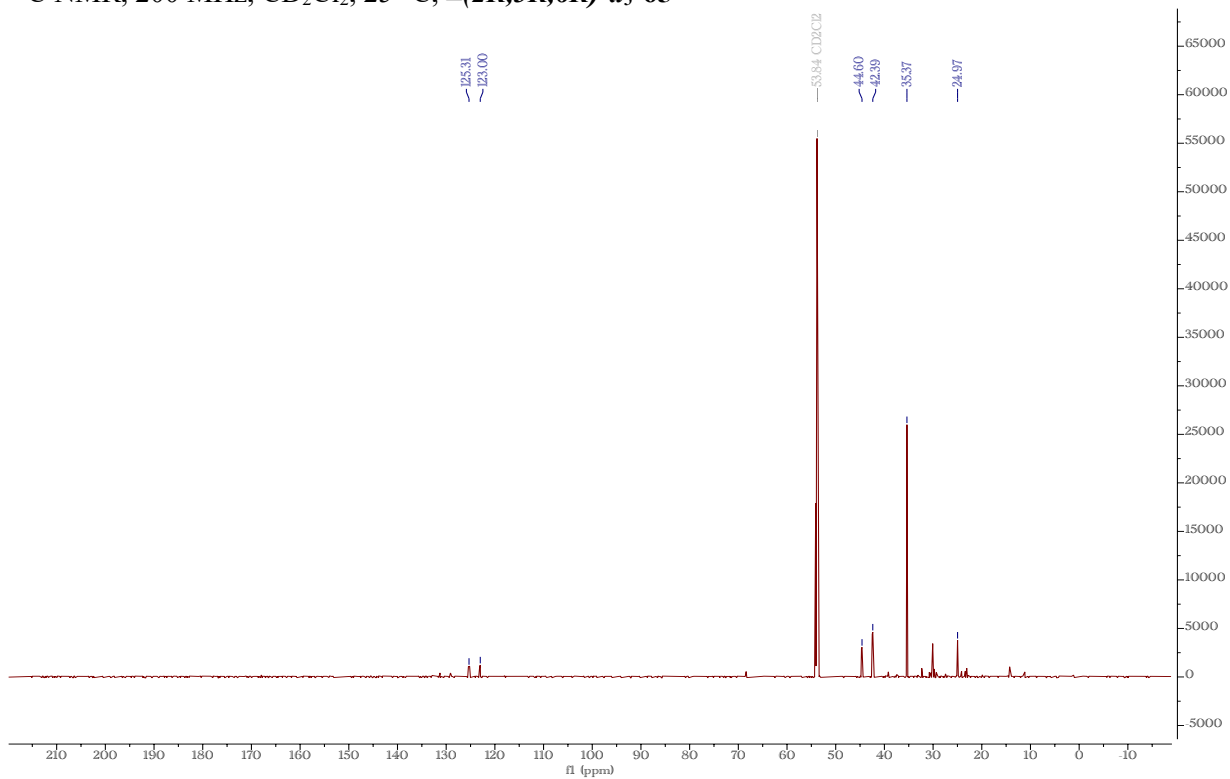
$^{13}\text{C}$  NMR, 200 MHz,  $\text{CD}_2\text{Cl}_2$ , 25 °C,  $\pm(2S,3S)\text{-}d_2\text{-65}$



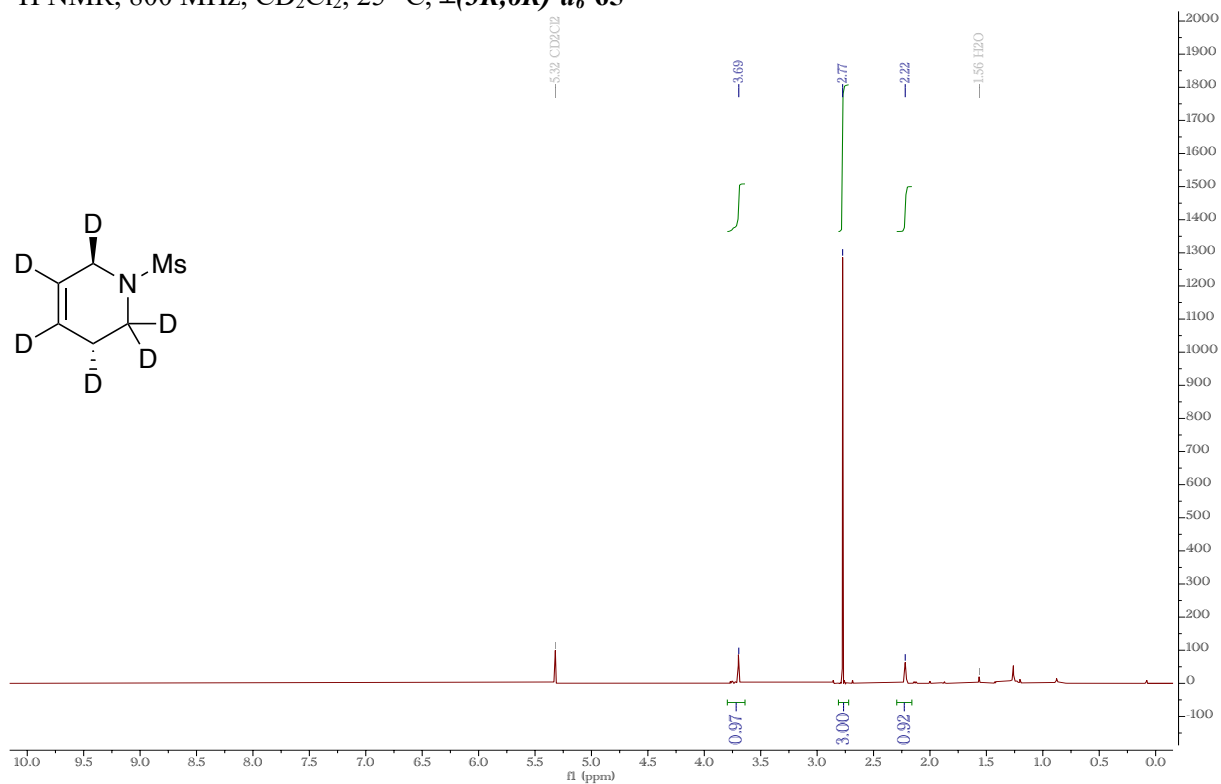
$^1\text{H}$  NMR, 800 MHz,  $\text{CD}_2\text{Cl}_2$ , 25 °C,  $\pm(2R,3R,6R)\text{-}d_5\text{-65}$



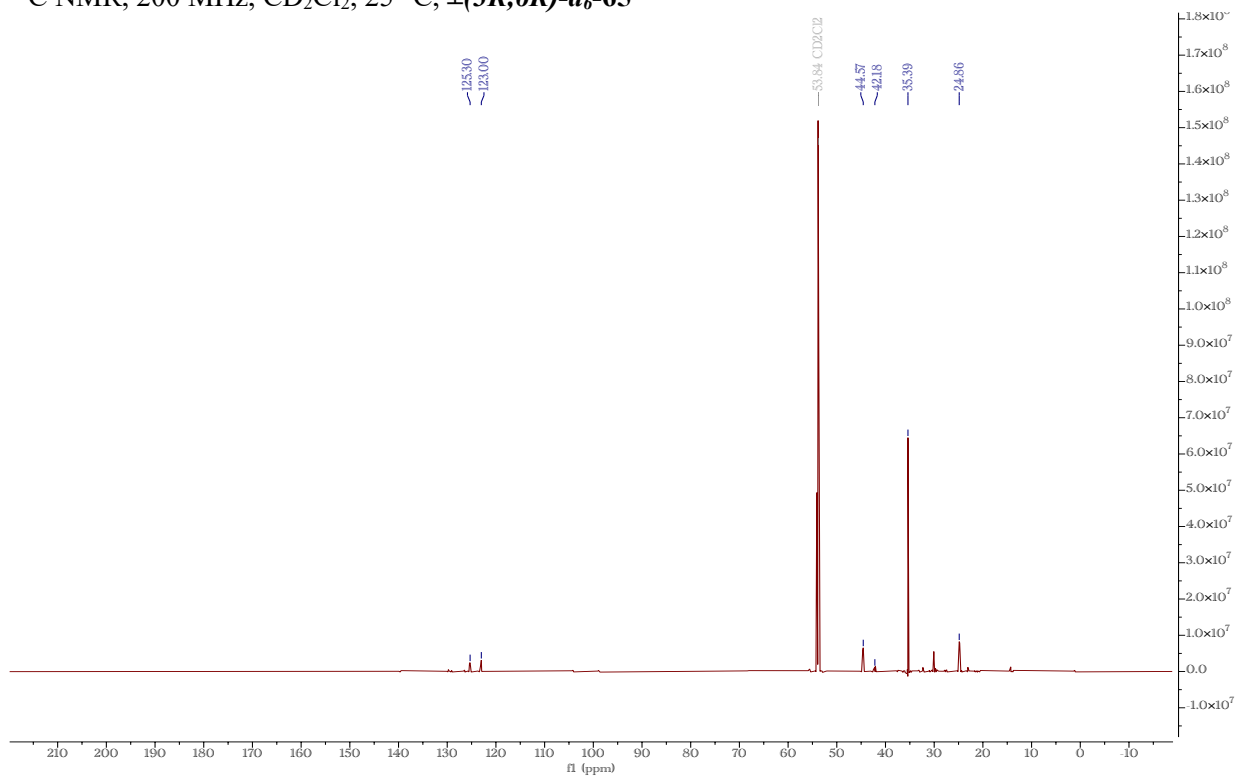
$^{13}\text{C}$  NMR, 200 MHz,  $\text{CD}_2\text{Cl}_2$ , 25 °C,  $\pm(2R,3R,6R)\text{-}d_5\text{-65}$



$^1\text{H}$  NMR, 800 MHz,  $\text{CD}_2\text{Cl}_2$ , 25 °C,  $\pm(3R,6R)\text{-}d_6\text{-}65$

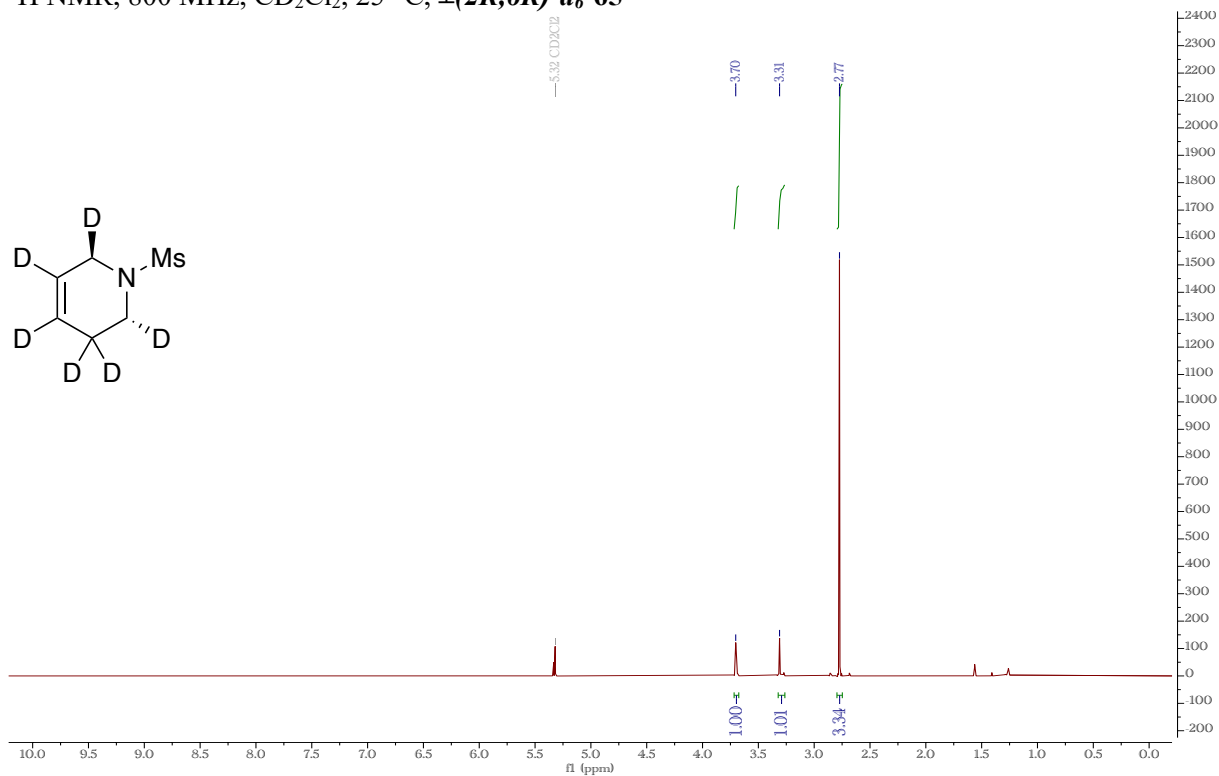


$^{13}\text{C}$  NMR, 200 MHz,  $\text{CD}_2\text{Cl}_2$ , 25 °C,  $\pm(3R,6R)\text{-}d_6\text{-}65$

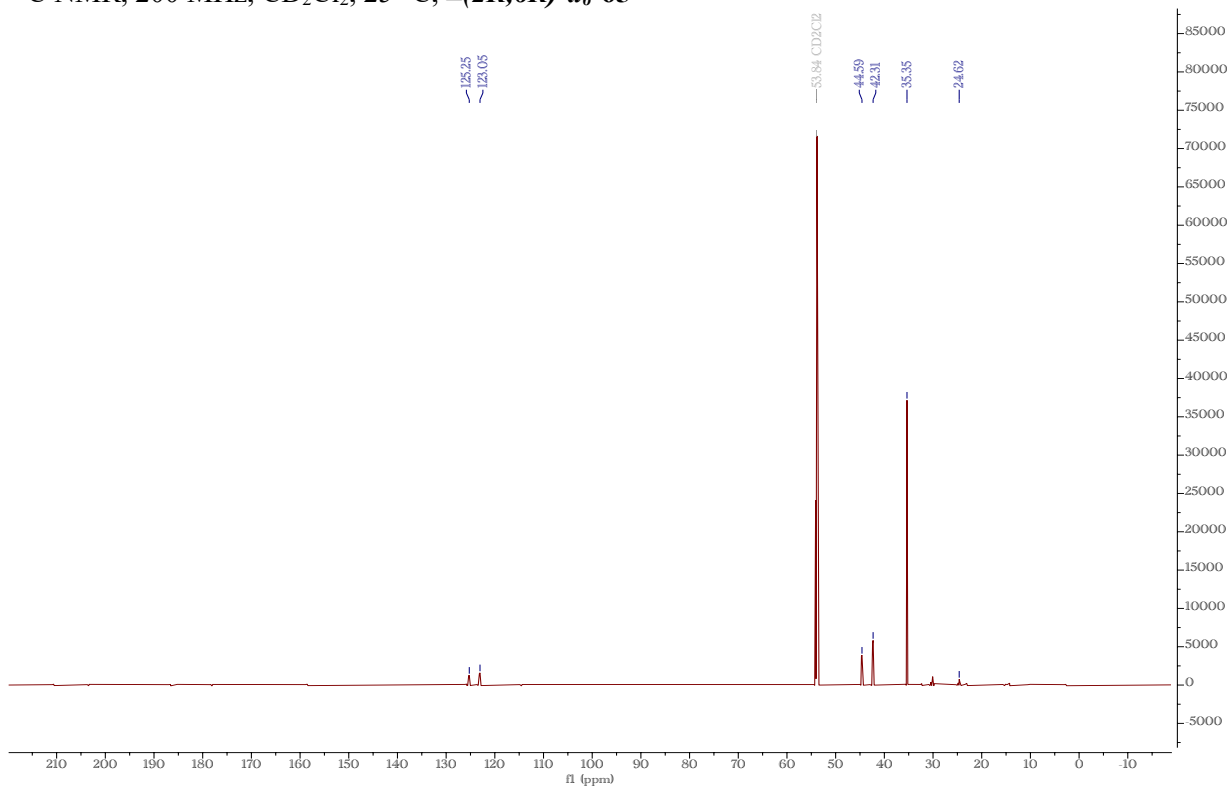




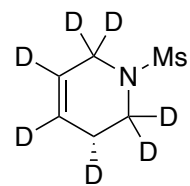
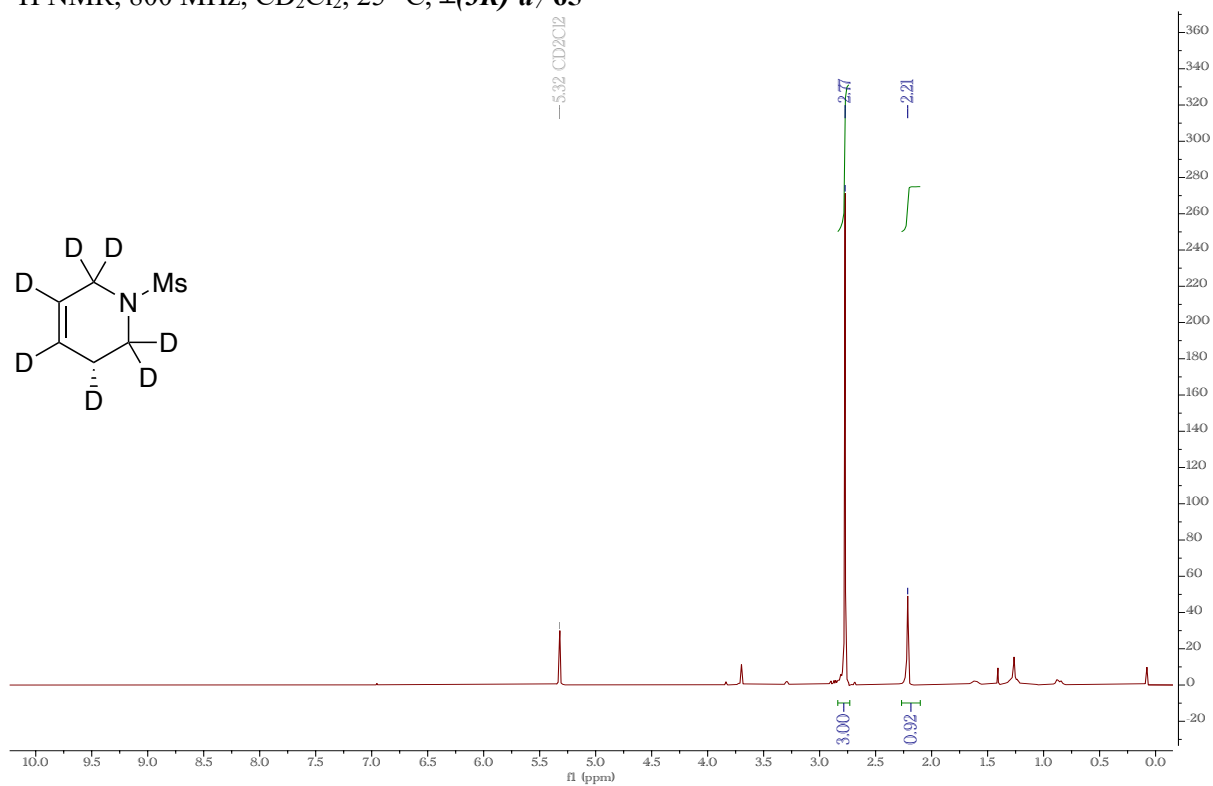
$^1\text{H}$  NMR, 800 MHz,  $\text{CD}_2\text{Cl}_2$ , 25 °C,  $\pm(2R,6R)\text{-}d_6\text{-}65$



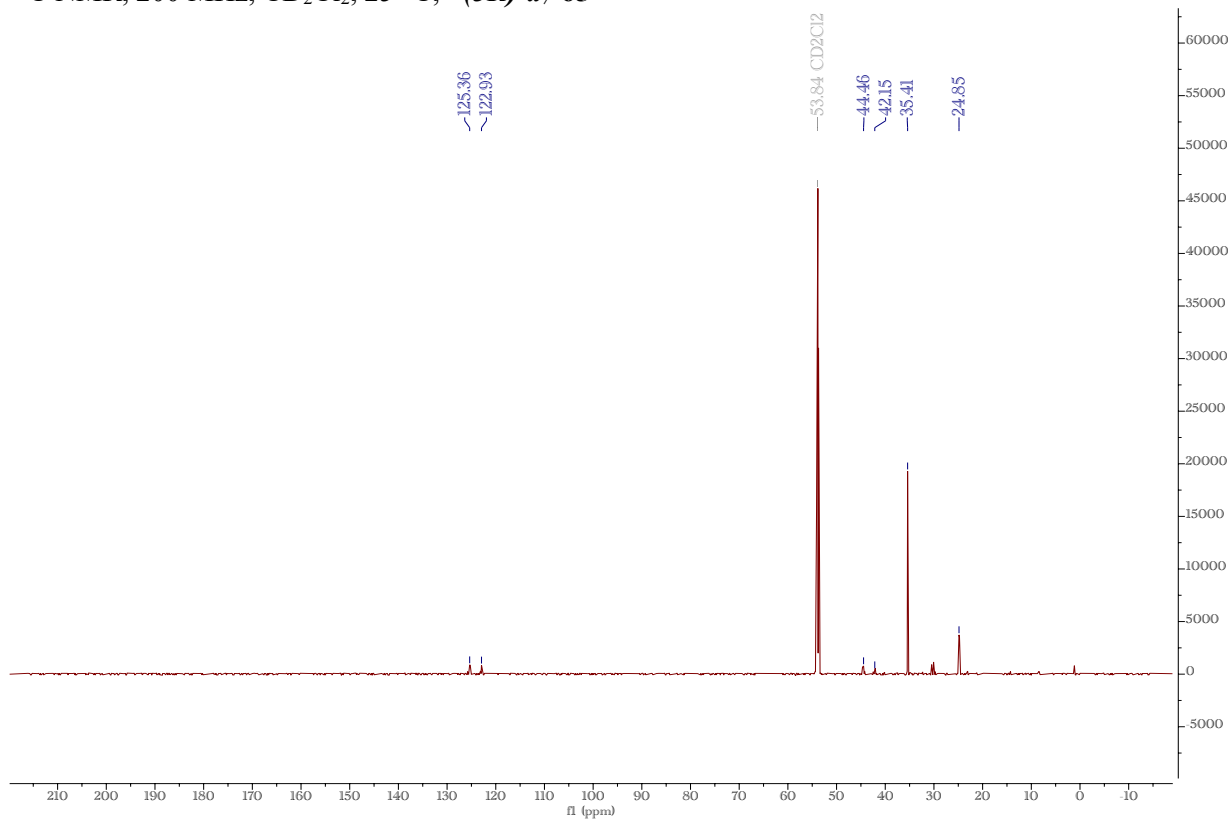
$^{13}\text{C}$  NMR, 200 MHz,  $\text{CD}_2\text{Cl}_2$ , 25 °C,  $\pm(2R,6R)\text{-}d_6\text{-}65$



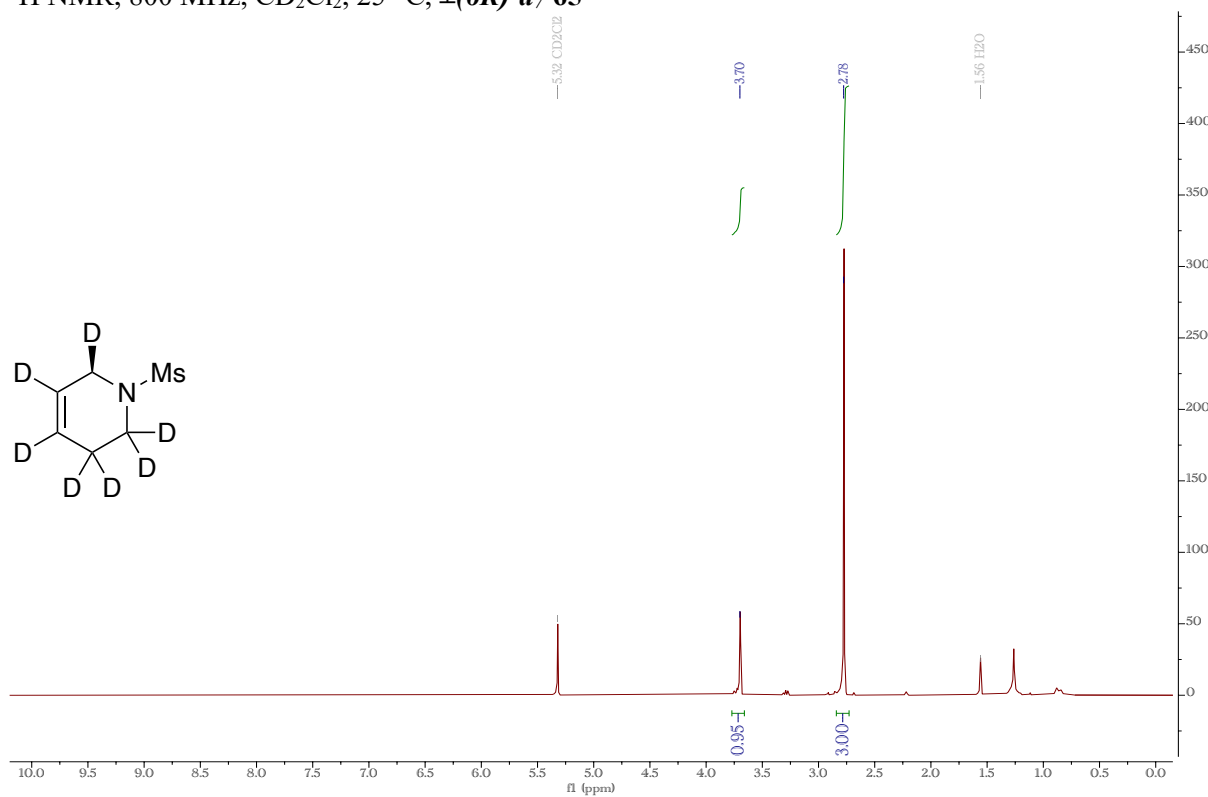
$^1\text{H}$  NMR, 800 MHz,  $\text{CD}_2\text{Cl}_2$ , 25 °C,  $\pm(3R)\text{-}d_7\text{-}65$



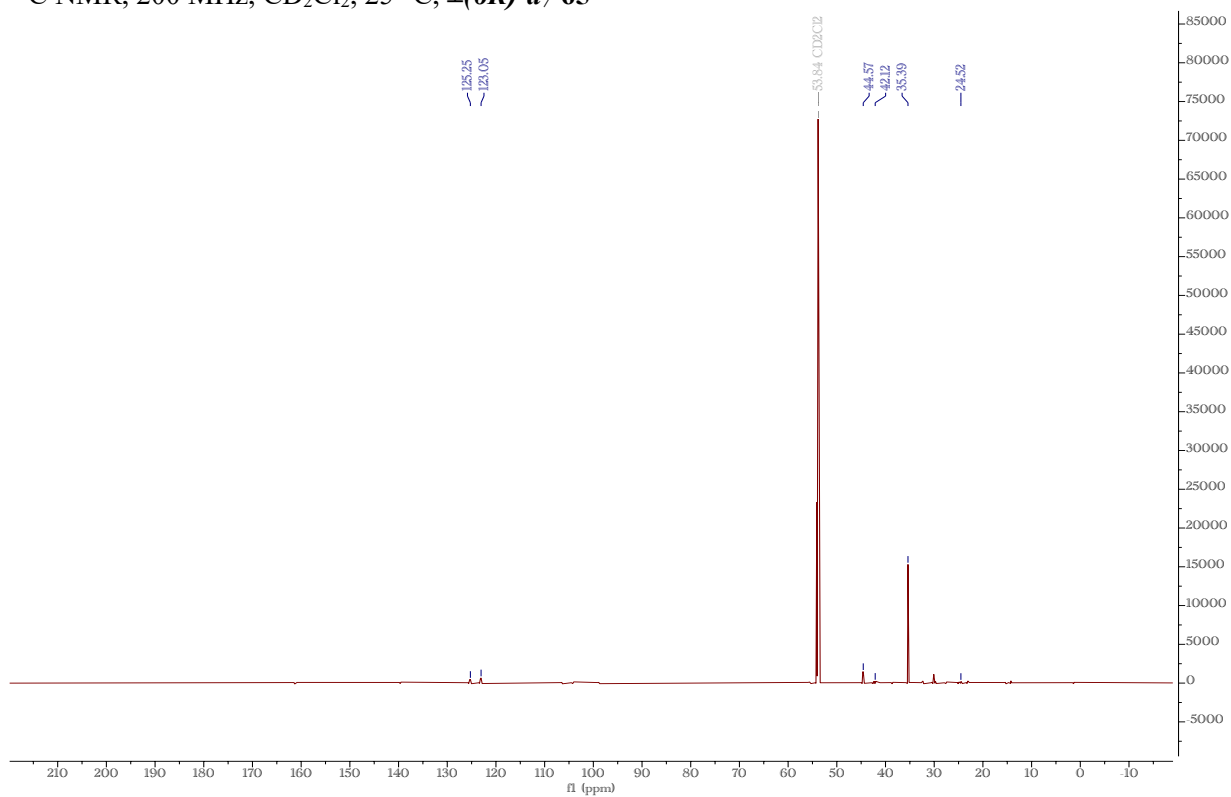
$^{13}\text{C}$  NMR, 200 MHz,  $\text{CD}_2\text{Cl}_2$ , 25 °C,  $\pm(3R)\text{-}d_7\text{-}65$



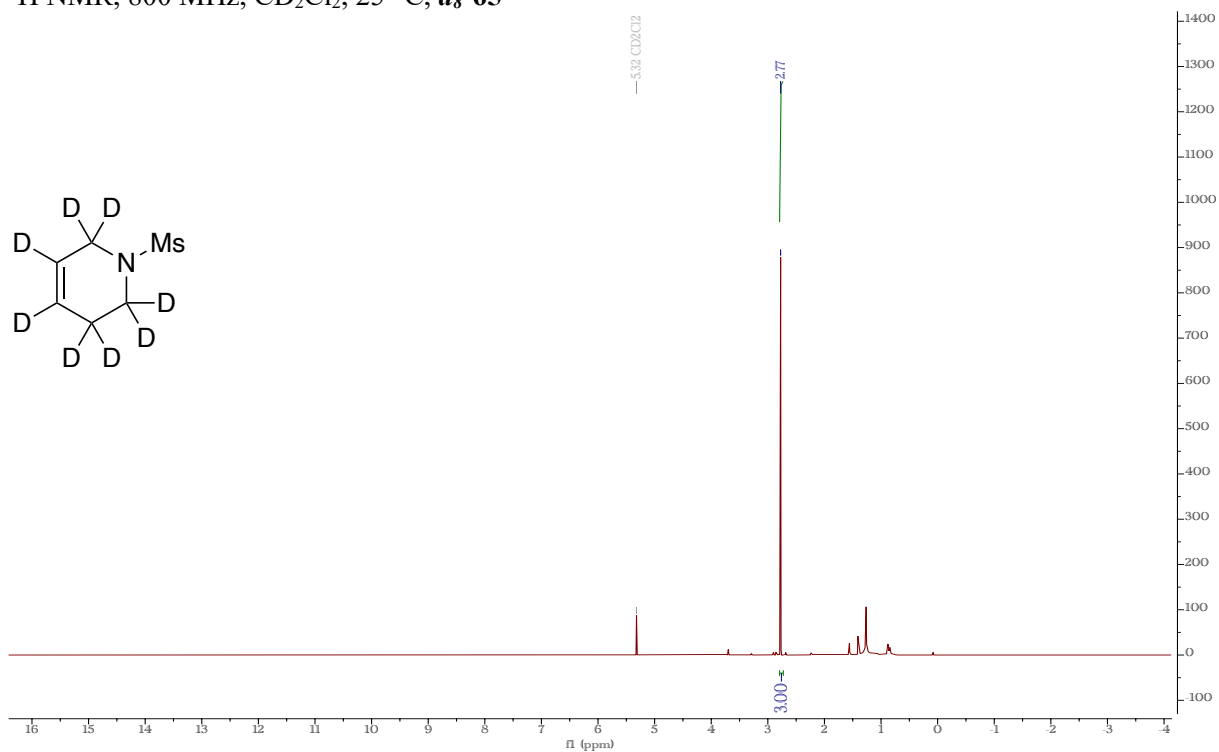
$^1\text{H}$  NMR, 800 MHz,  $\text{CD}_2\text{Cl}_2$ , 25 °C,  $\pm(6R)\text{-}d_7\text{-}65$



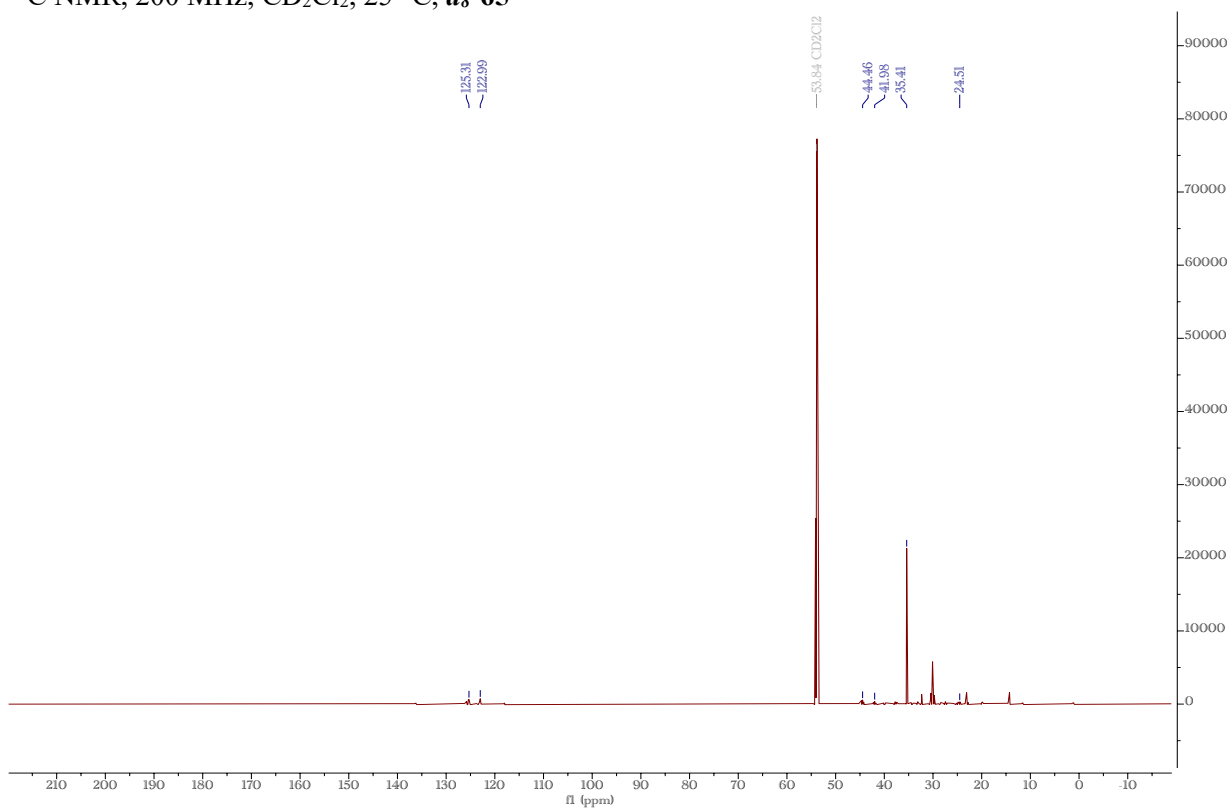
$^{13}\text{C}$  NMR, 200 MHz,  $\text{CD}_2\text{Cl}_2$ , 25 °C,  $\pm(6R)\text{-}d_7\text{-}65$



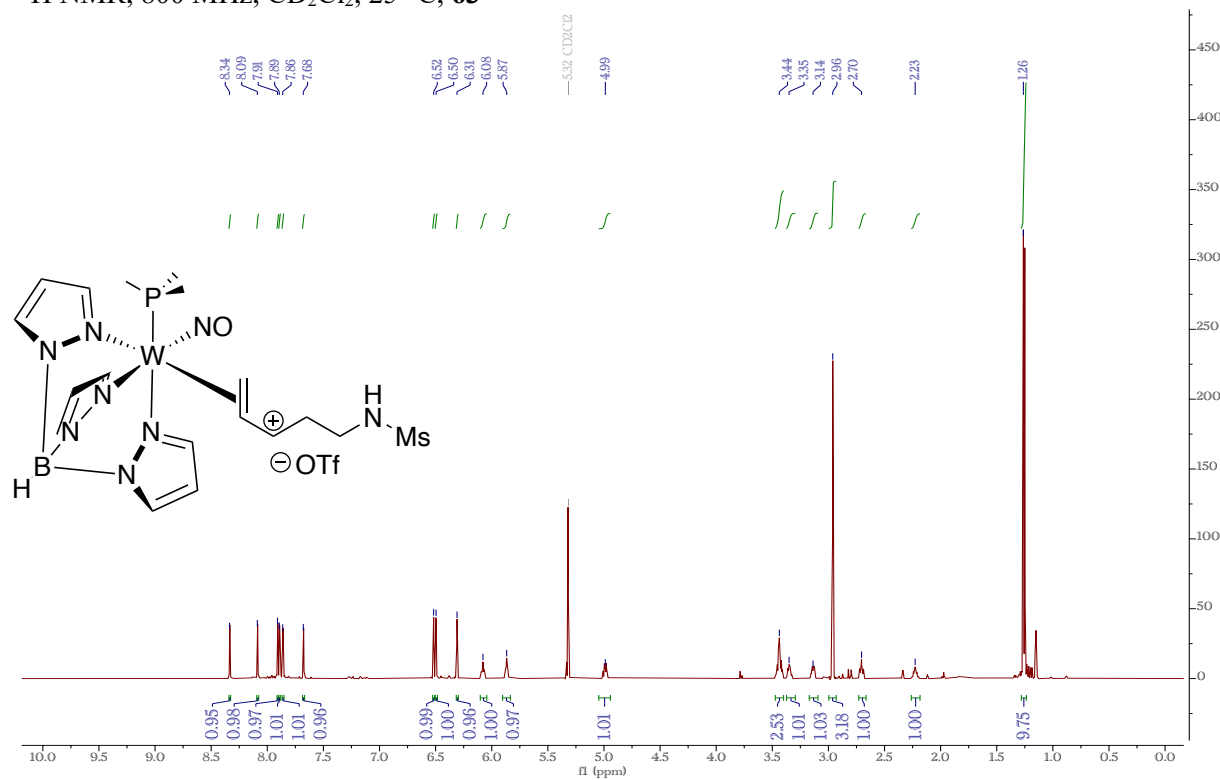
$^1\text{H}$  NMR, 800 MHz,  $\text{CD}_2\text{Cl}_2$ , 25 °C, *d*<sub>8</sub>-65



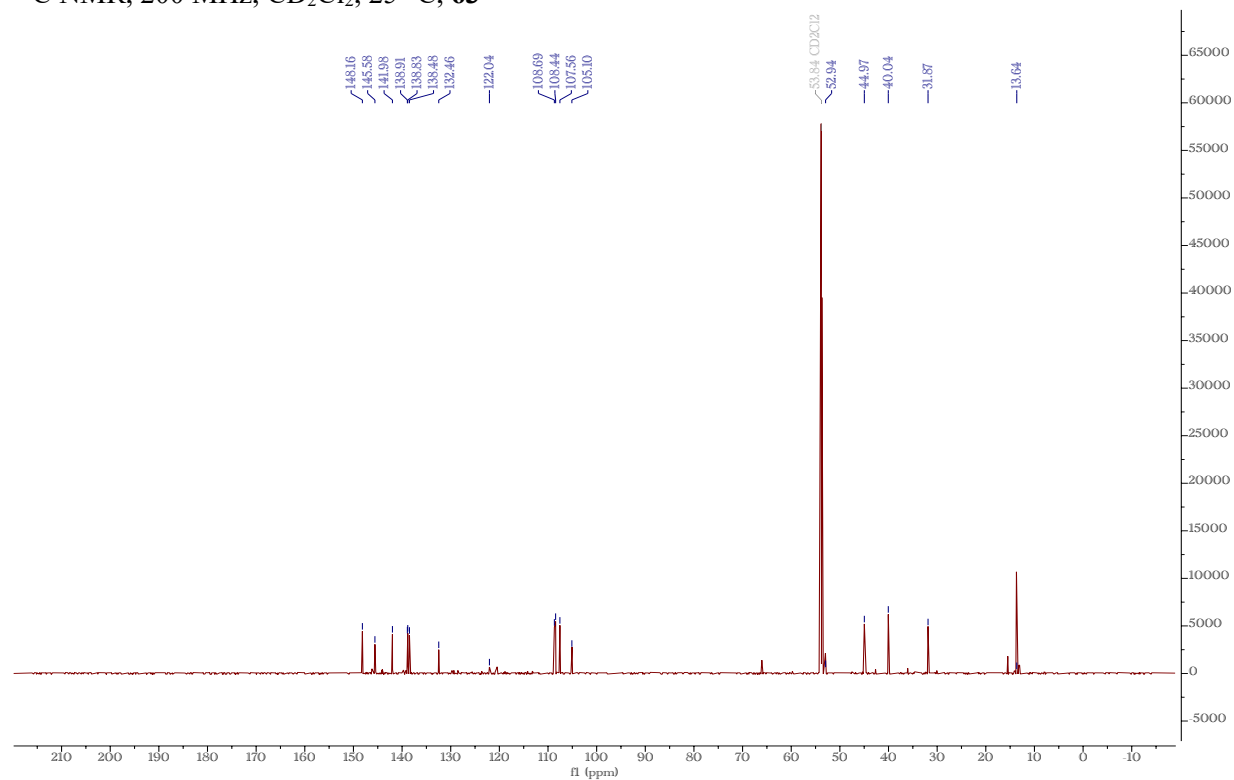
$^{13}\text{C}$  NMR, 200 MHz,  $\text{CD}_2\text{Cl}_2$ , 25 °C, *d*<sub>8</sub>-65



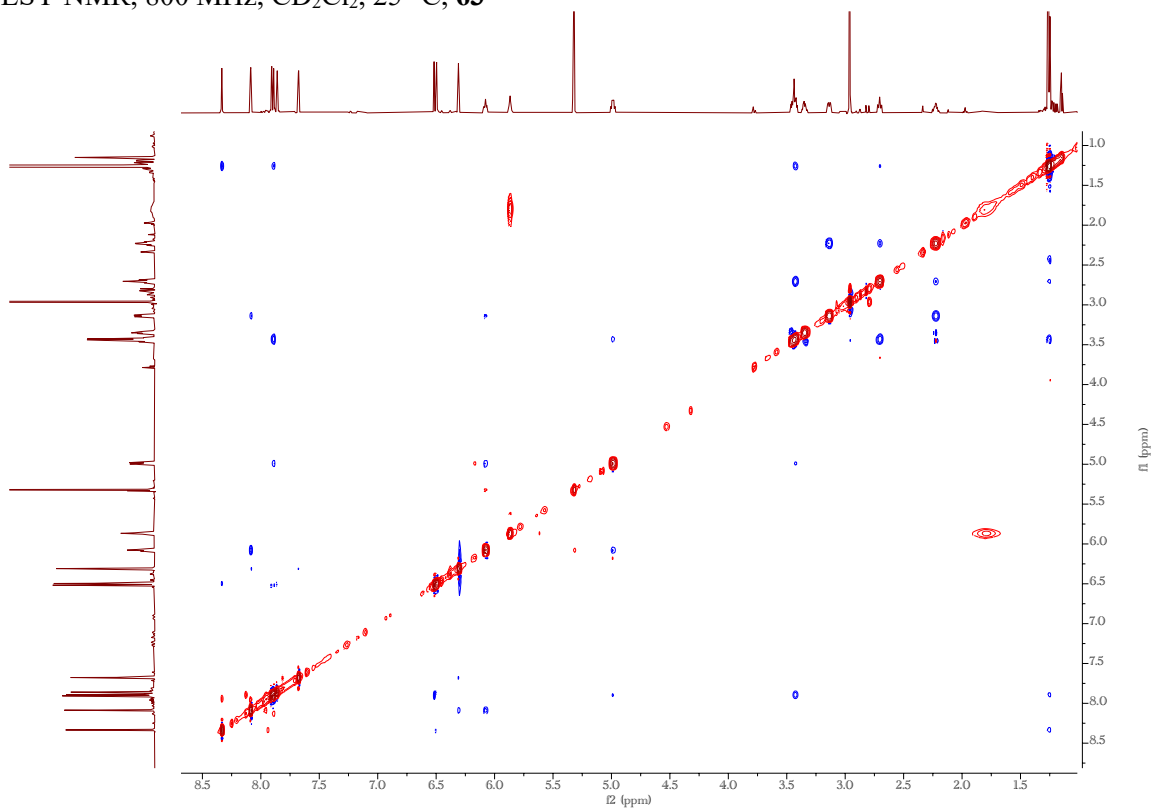
$^1\text{H}$  NMR, 800 MHz,  $\text{CD}_2\text{Cl}_2$ , 25 °C, **63**



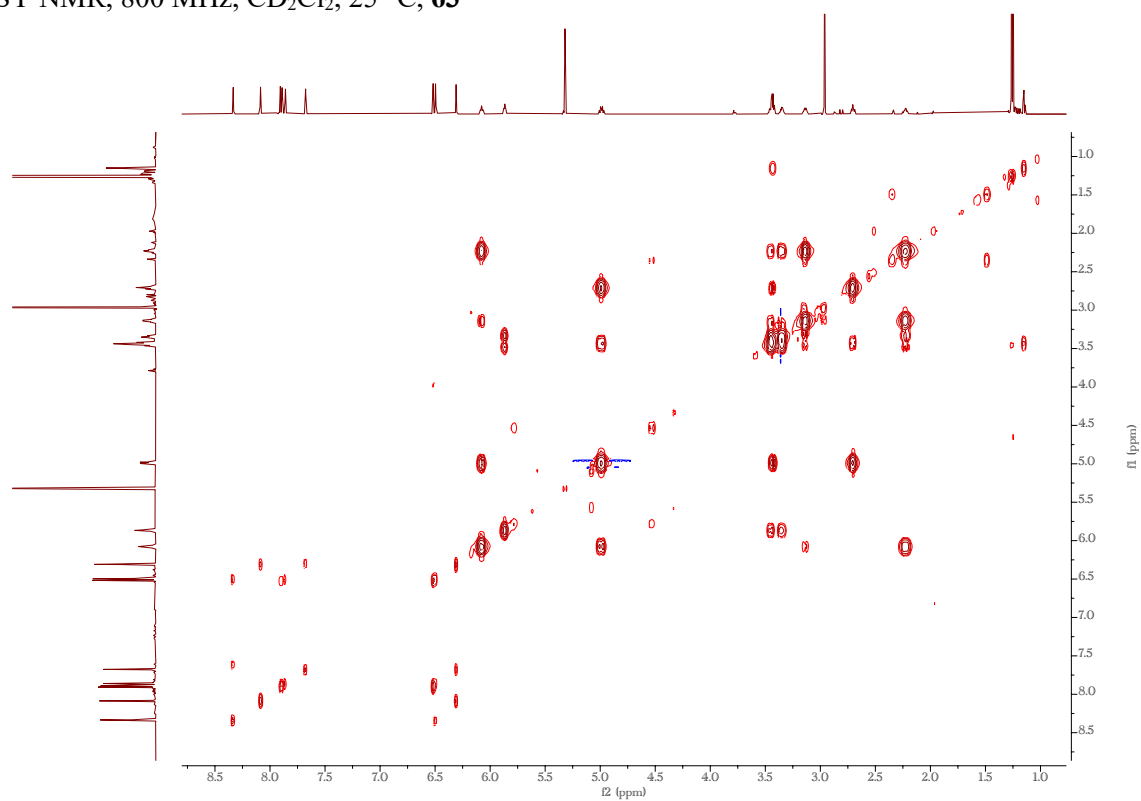
$^{13}\text{C}$  NMR, 200 MHz,  $\text{CD}_2\text{Cl}_2$ , 25 °C, **63**



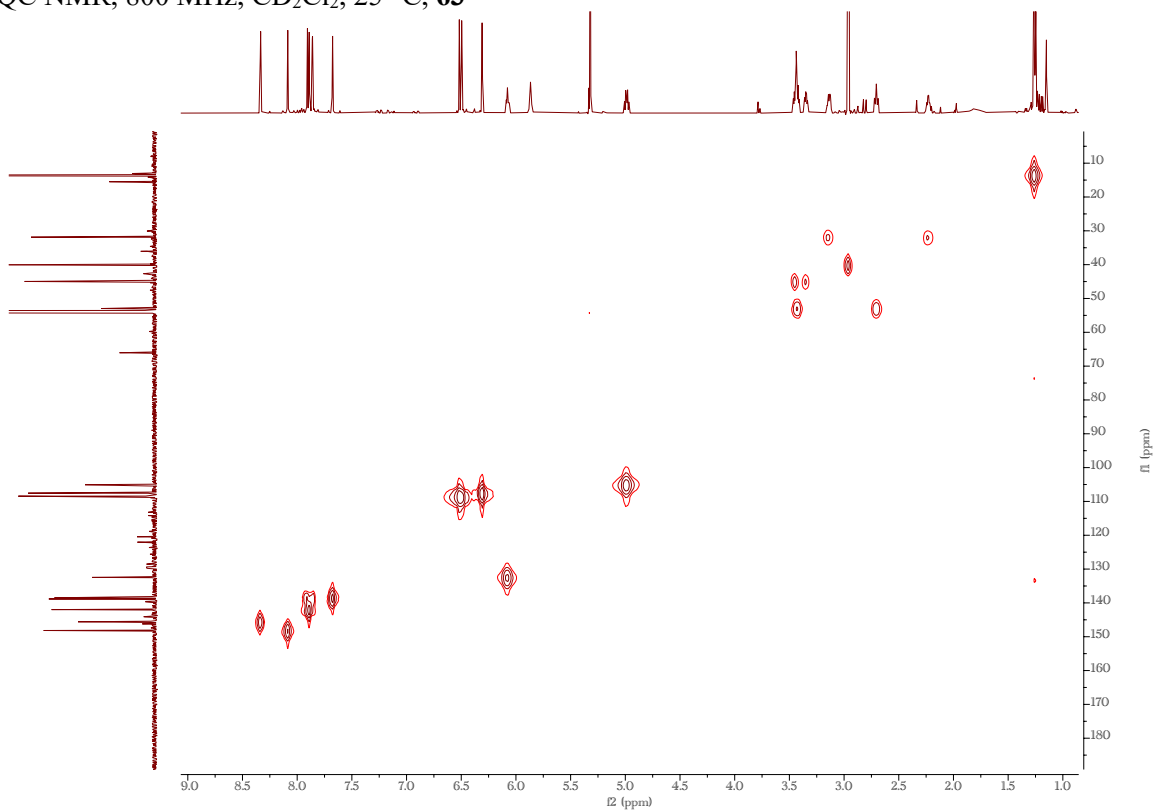
NOESY NMR, 800 MHz, CD<sub>2</sub>Cl<sub>2</sub>, 25 °C, **63**



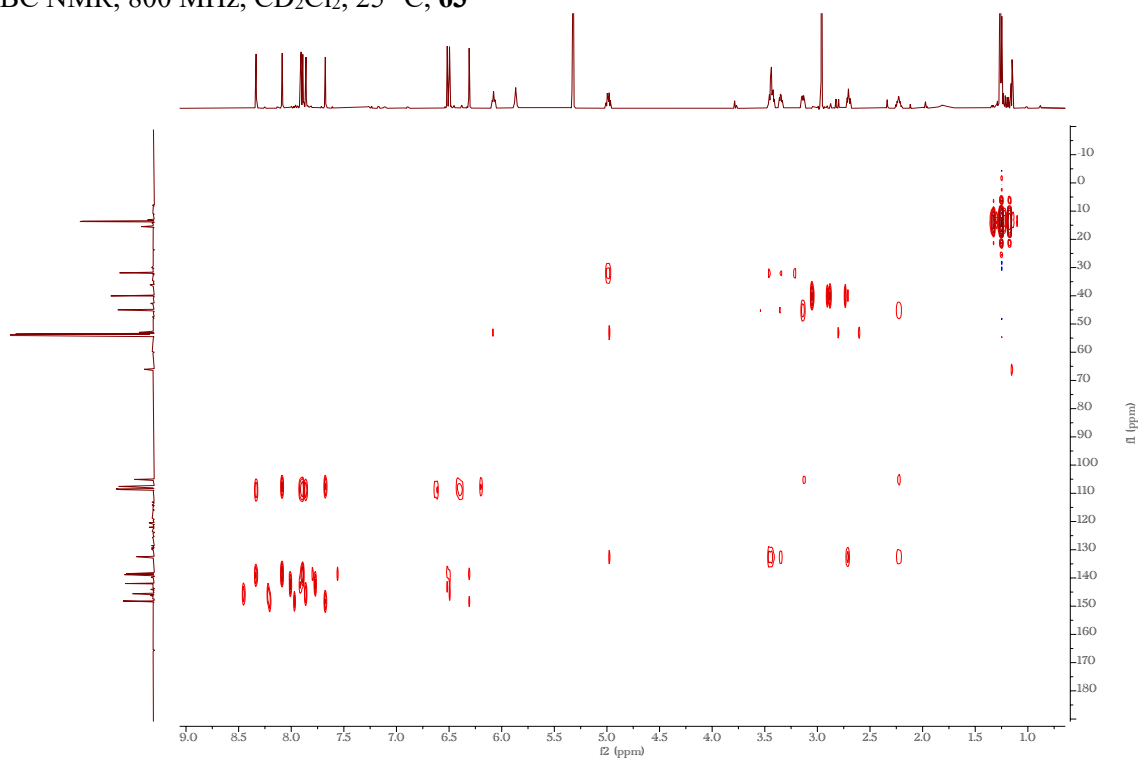
COSY NMR, 800 MHz, CD<sub>2</sub>Cl<sub>2</sub>, 25 °C, **63**



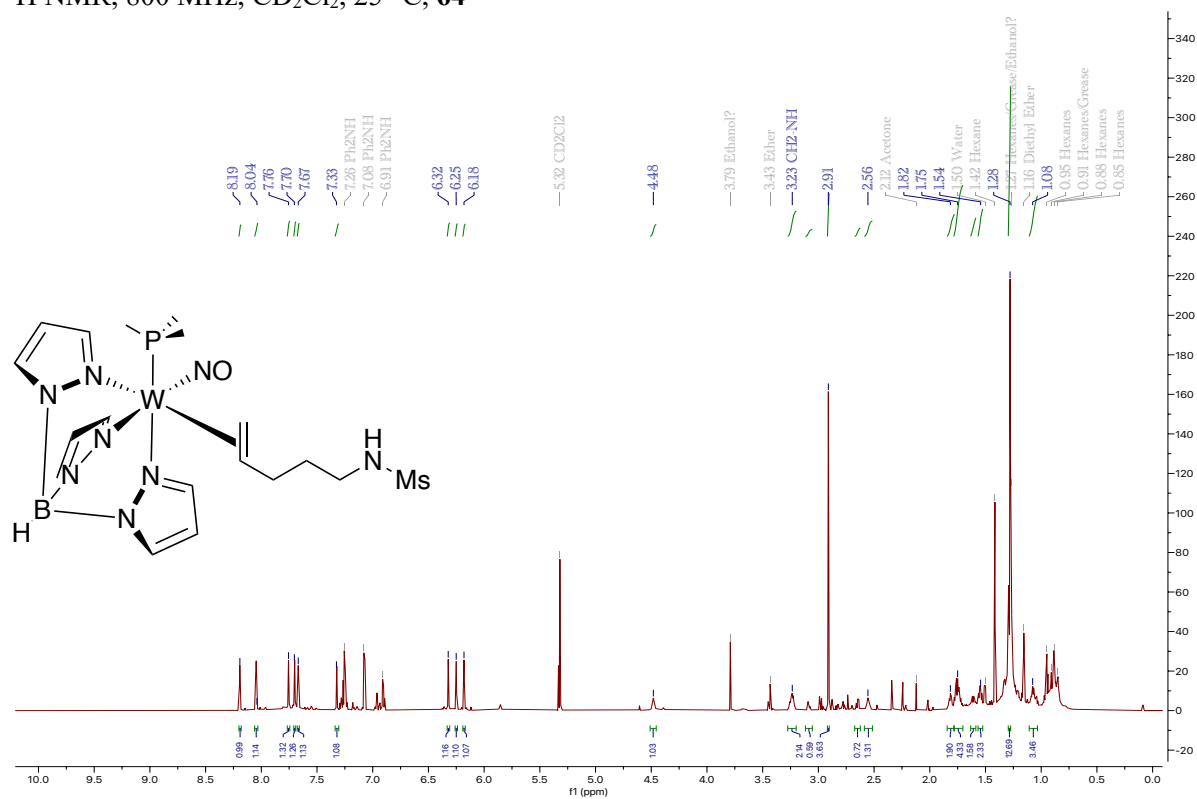
HSQC NMR, 800 MHz, CD<sub>2</sub>Cl<sub>2</sub>, 25 °C, **63**



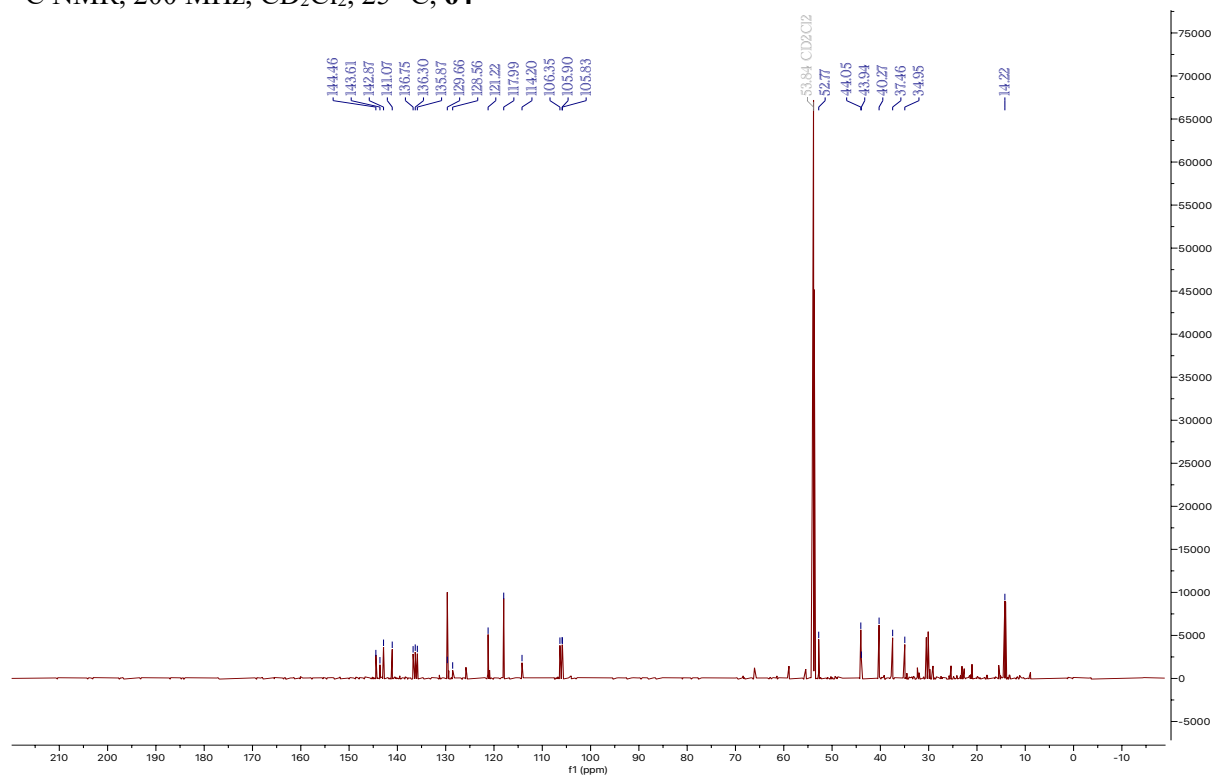
HMBC NMR, 800 MHz, CD<sub>2</sub>Cl<sub>2</sub>, 25 °C, **63**



$^1\text{H}$  NMR, 800 MHz,  $\text{CD}_2\text{Cl}_2$ , 25 °C, **64**

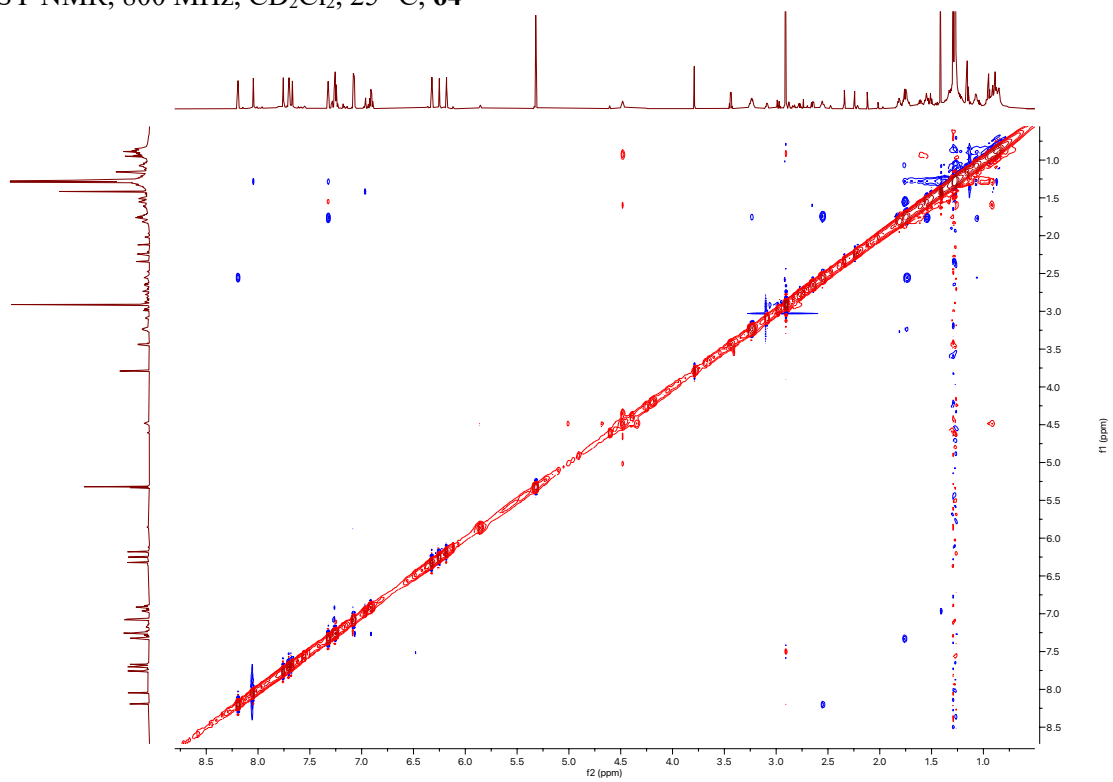


$^{13}\text{C}$  NMR, 200 MHz,  $\text{CD}_2\text{Cl}_2$ , 25 °C, **64**

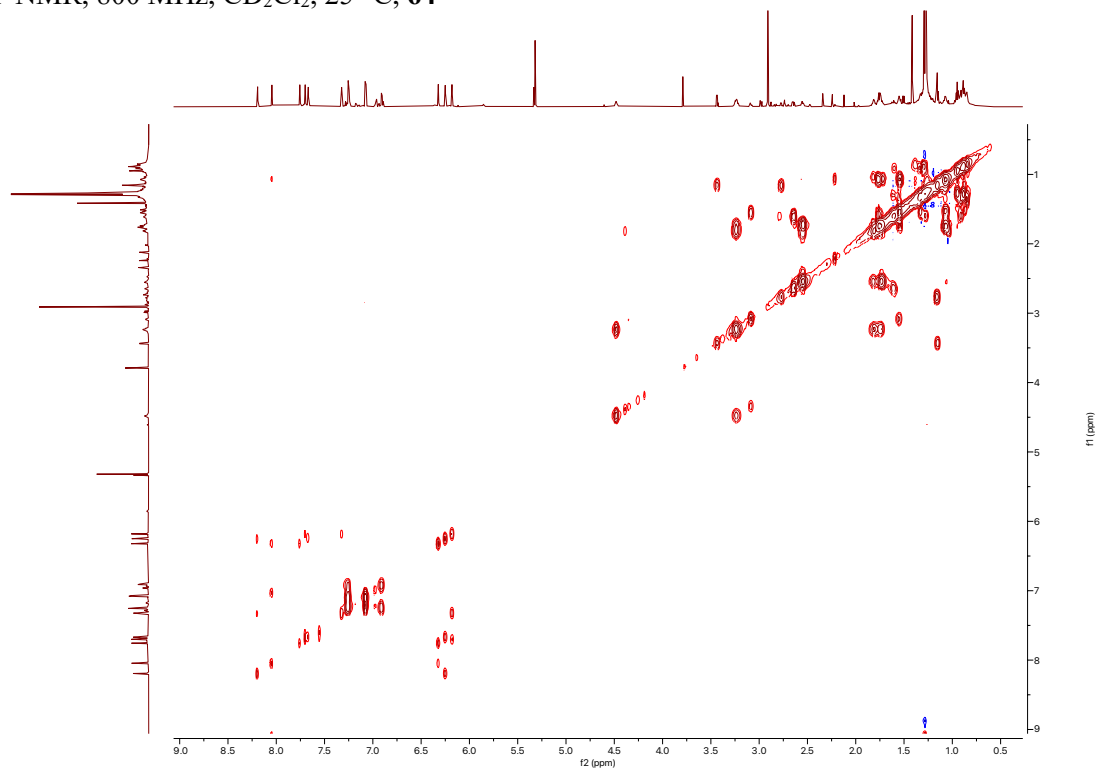




NOESY NMR, 800 MHz, CD<sub>2</sub>Cl<sub>2</sub>, 25 °C, **64**



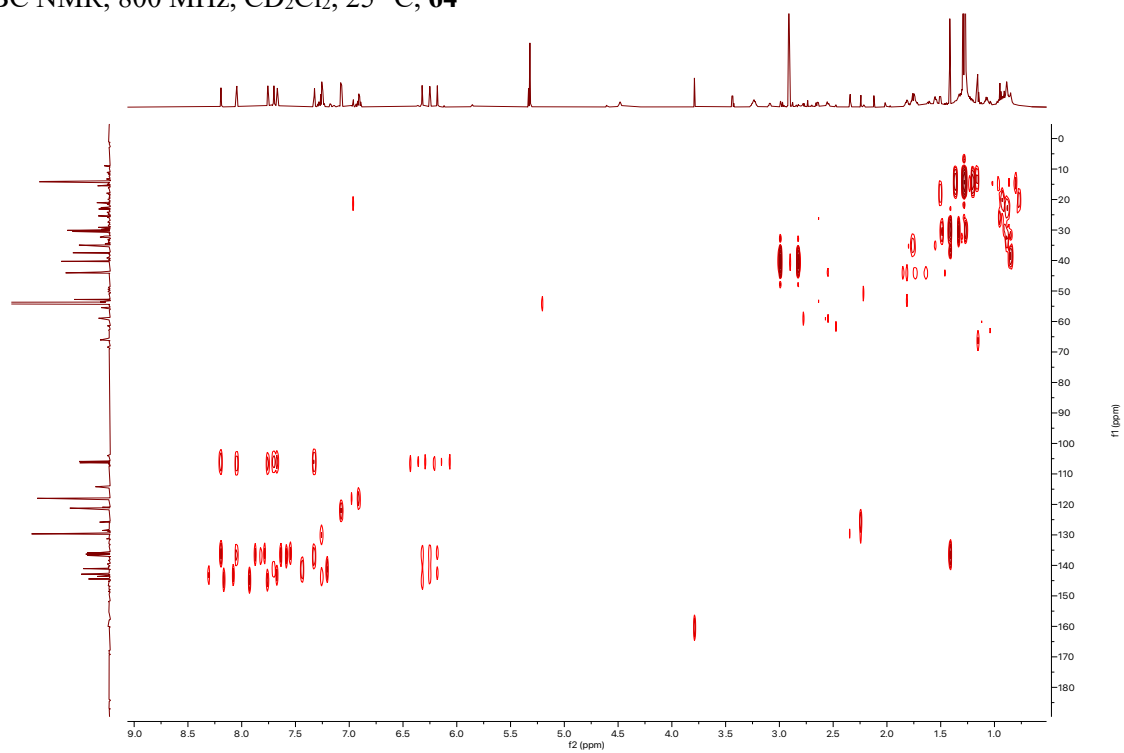
COSY NMR, 800 MHz, CD<sub>2</sub>Cl<sub>2</sub>, 25 °C, **64**



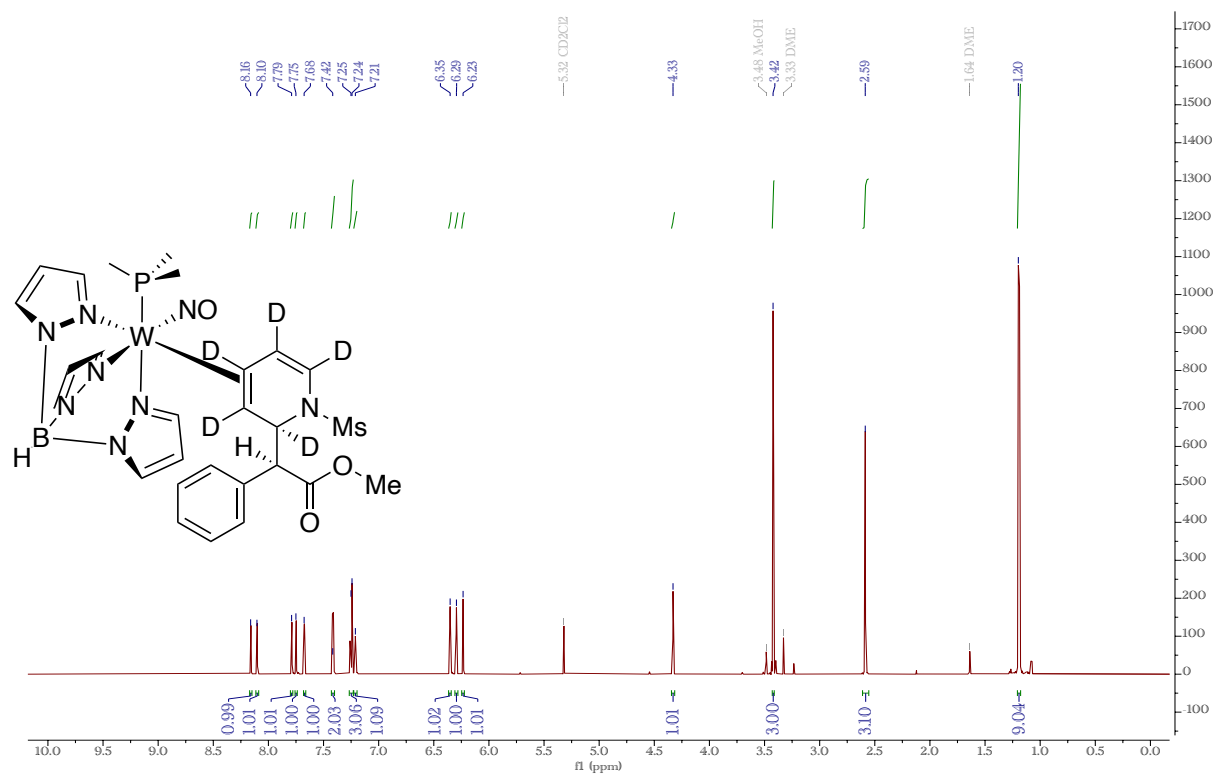
HSQC NMR, 800 MHz, CD<sub>2</sub>Cl<sub>2</sub>, 25 °C, **64**



HMBC NMR, 800 MHz, CD<sub>2</sub>Cl<sub>2</sub>, 25 °C, **64**



$^1\text{H}$  NMR, 800 MHz,  $\text{CD}_2\text{Cl}_2$ , 25 °C,  $d_5$ -**35D**



$^{13}\text{C}$  NMR, 200 MHz,  $\text{CD}_2\text{Cl}_2$ , 25 °C,  $d_5$ -**35D**

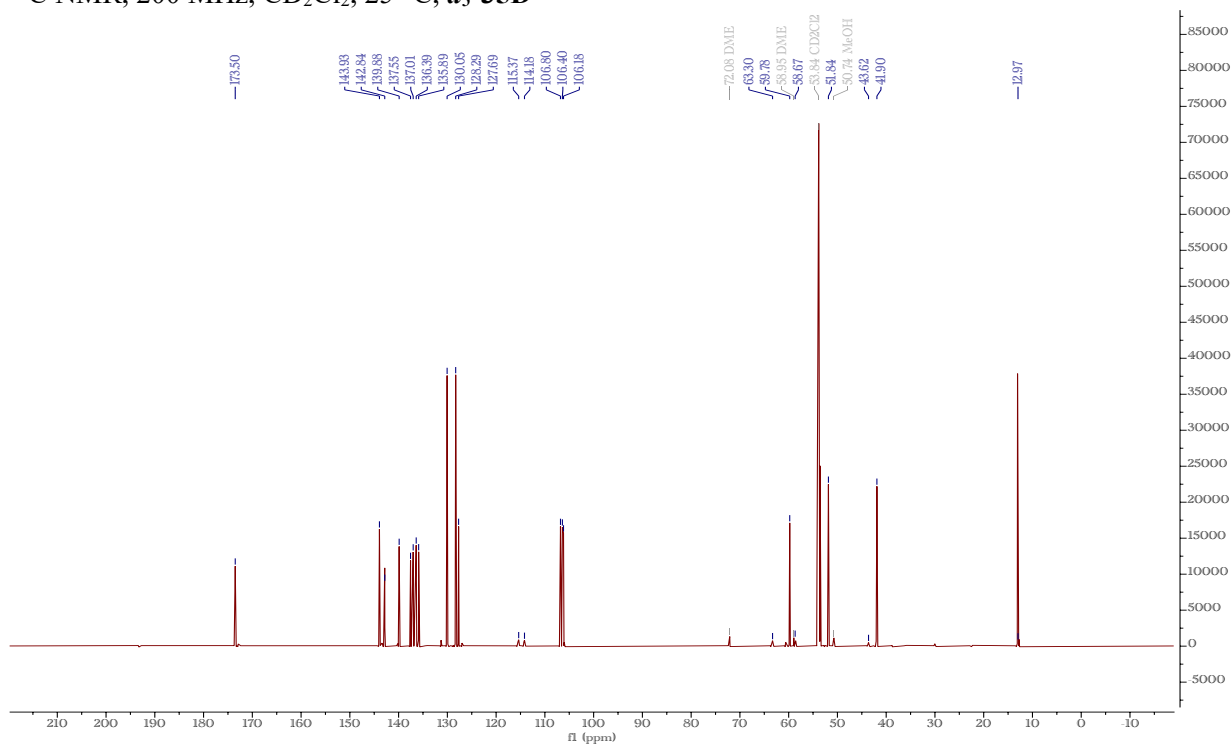
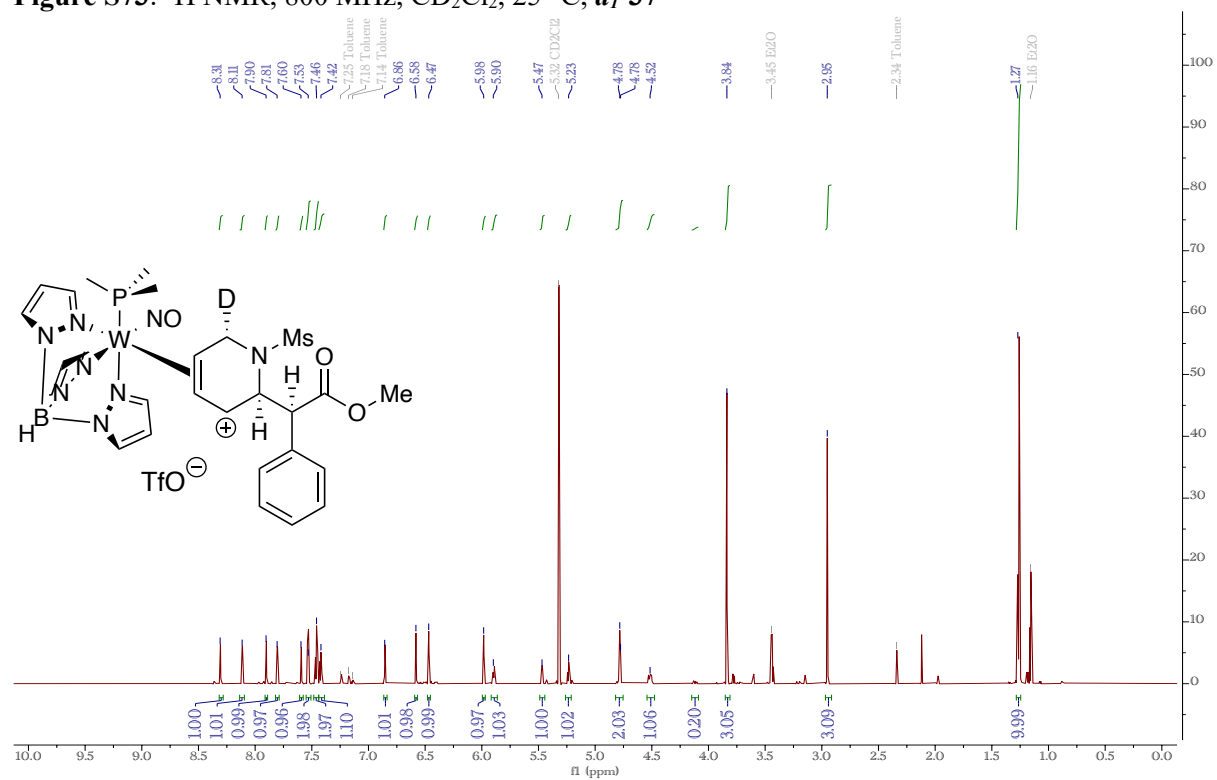
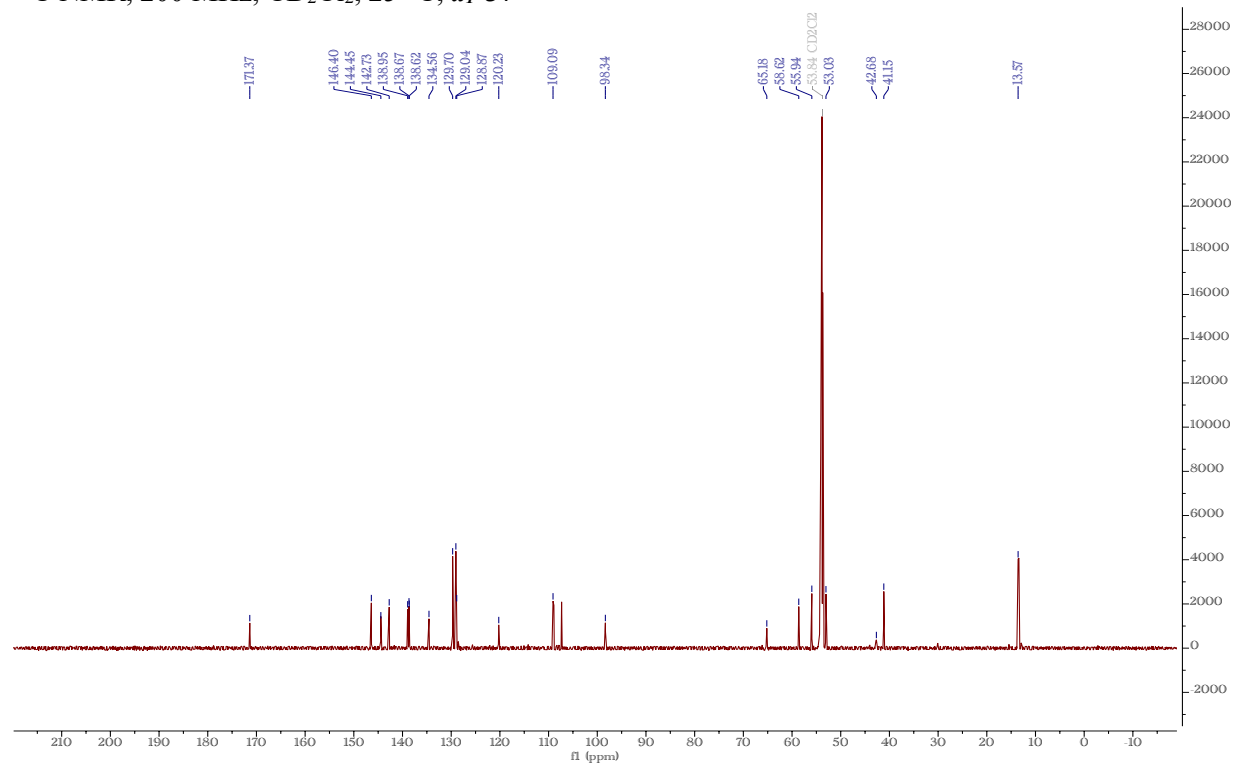


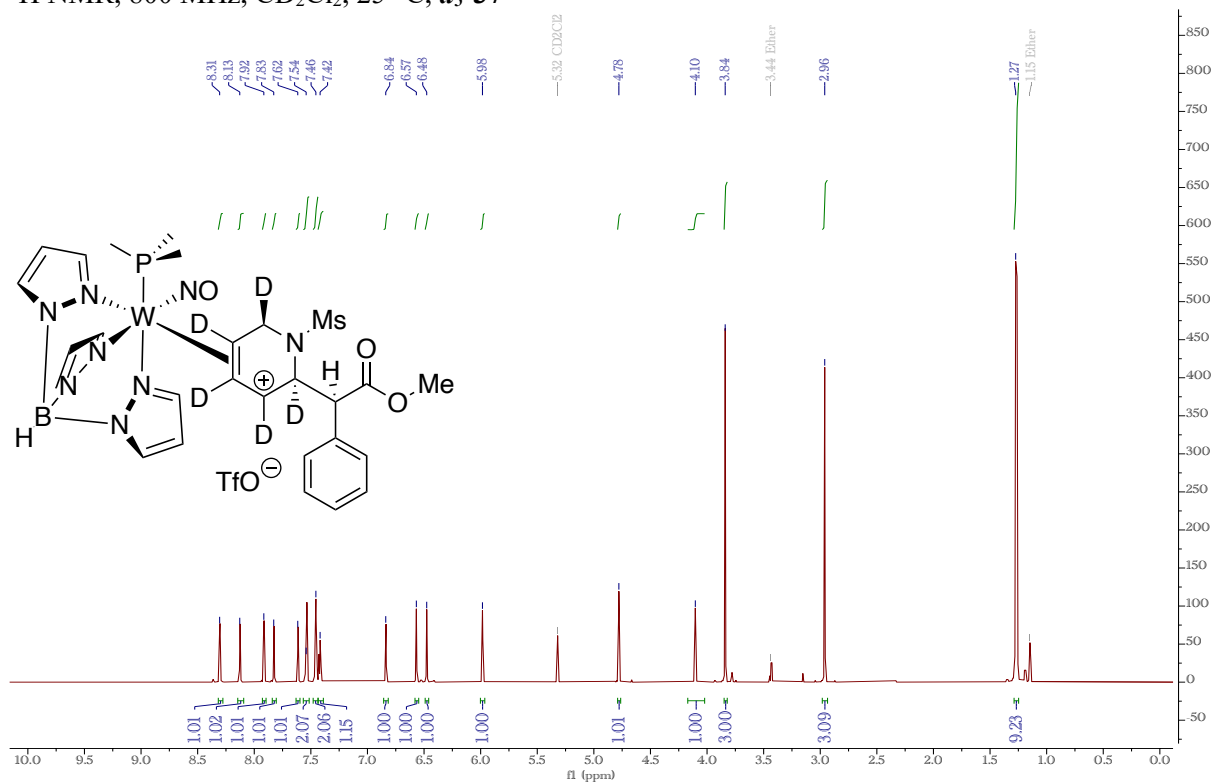
Figure S73:  $^1\text{H}$  NMR, 800 MHz,  $\text{CD}_2\text{Cl}_2$ , 25  $^\circ\text{C}$ ,  $d_1$ -37



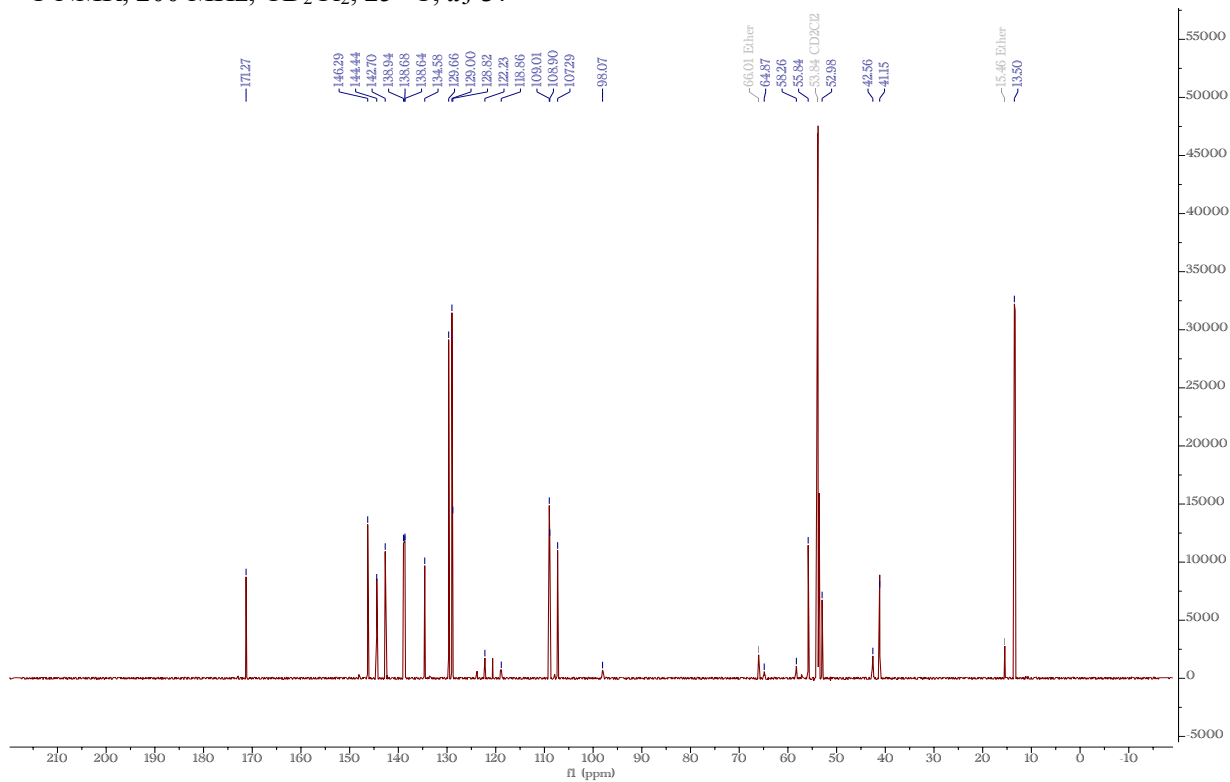
$^{13}\text{C}$  NMR, 200 MHz,  $\text{CD}_2\text{Cl}_2$ , 25  $^\circ\text{C}$ ,  $d_1$ -37



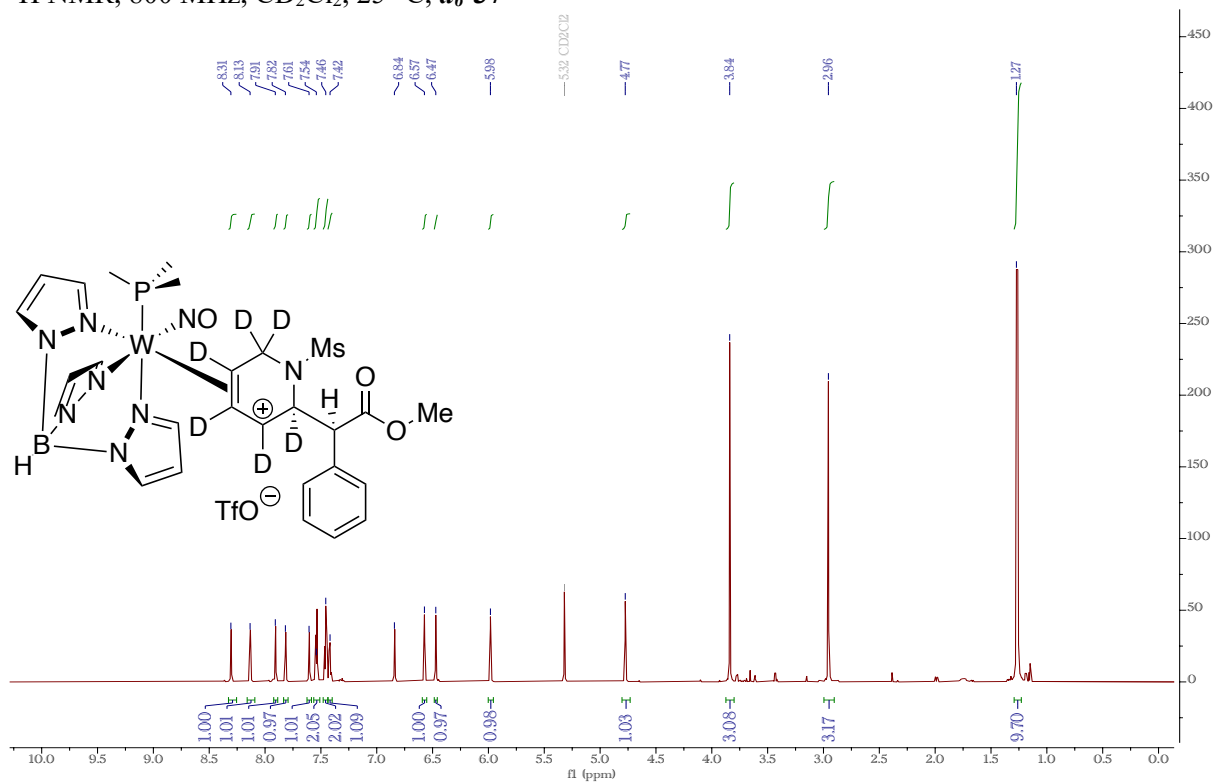
$^1\text{H}$  NMR, 800 MHz,  $\text{CD}_2\text{Cl}_2$ , 25 °C,  $d_5$ -**37**



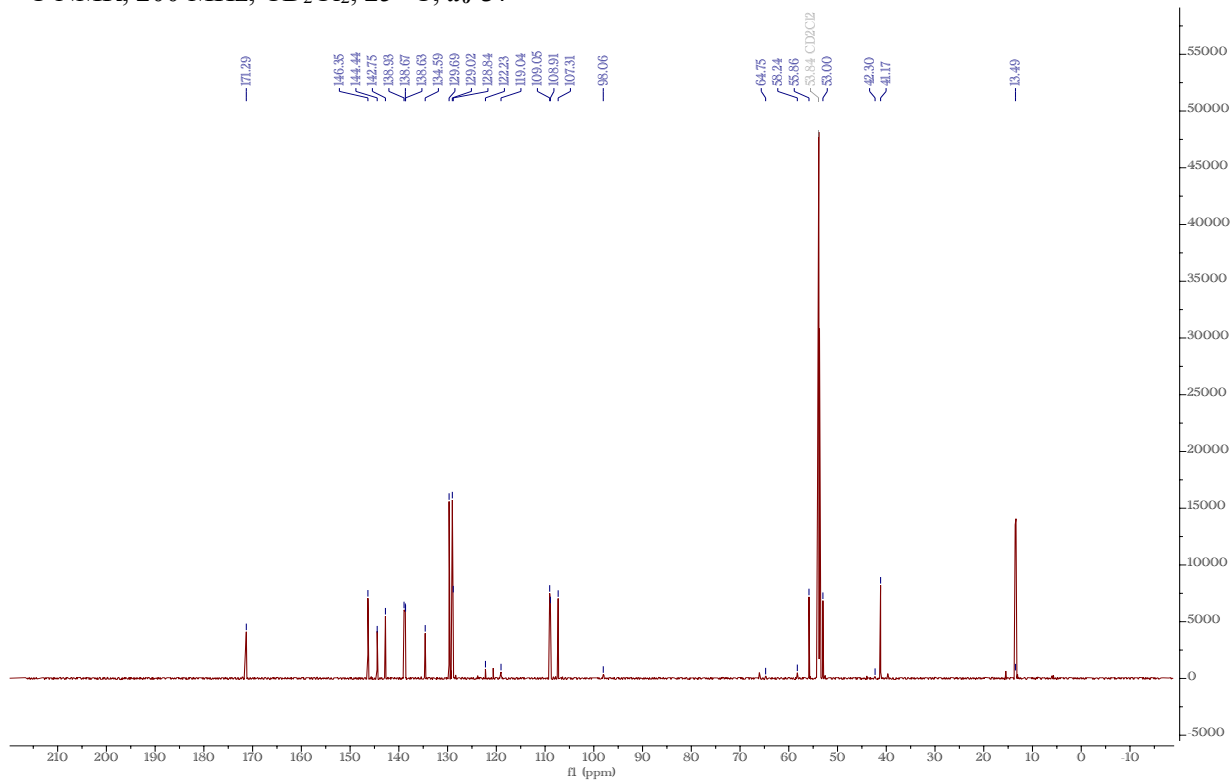
$^{13}\text{C}$  NMR, 200 MHz,  $\text{CD}_2\text{Cl}_2$ , 25 °C,  $d_5$ -**37**



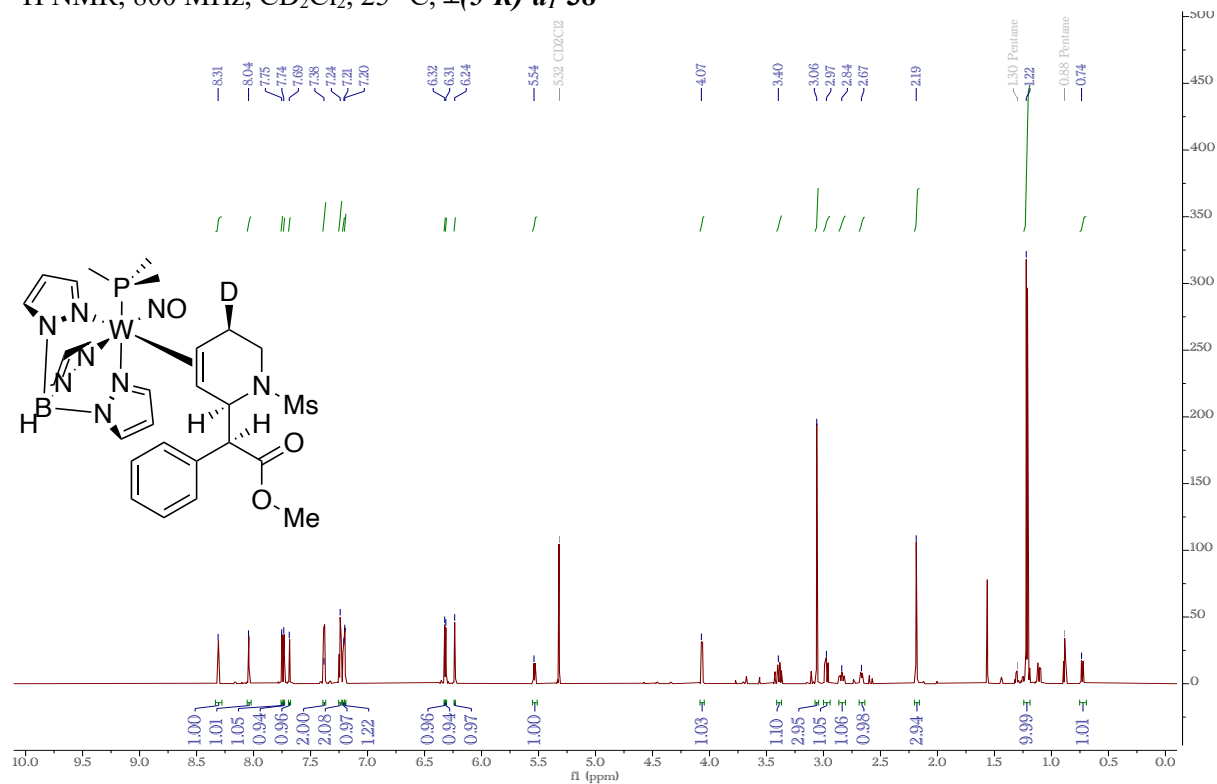
$^1\text{H}$  NMR, 800 MHz,  $\text{CD}_2\text{Cl}_2$ , 25 °C,  $d_6$ -37



$^{13}\text{C}$  NMR, 200 MHz,  $\text{CD}_2\text{Cl}_2$ , 25 °C,  $d_6$ -37



$^1\text{H}$  NMR, 800 MHz,  $\text{CD}_2\text{Cl}_2$ , 25 °C,  $\pm(5'R)\text{-d}_1\text{-38}$



$^{13}\text{C}$  NMR, 200 MHz,  $\text{CD}_2\text{Cl}_2$ , 25 °C,  $\pm(5'R)\text{-d}_1\text{-38}$

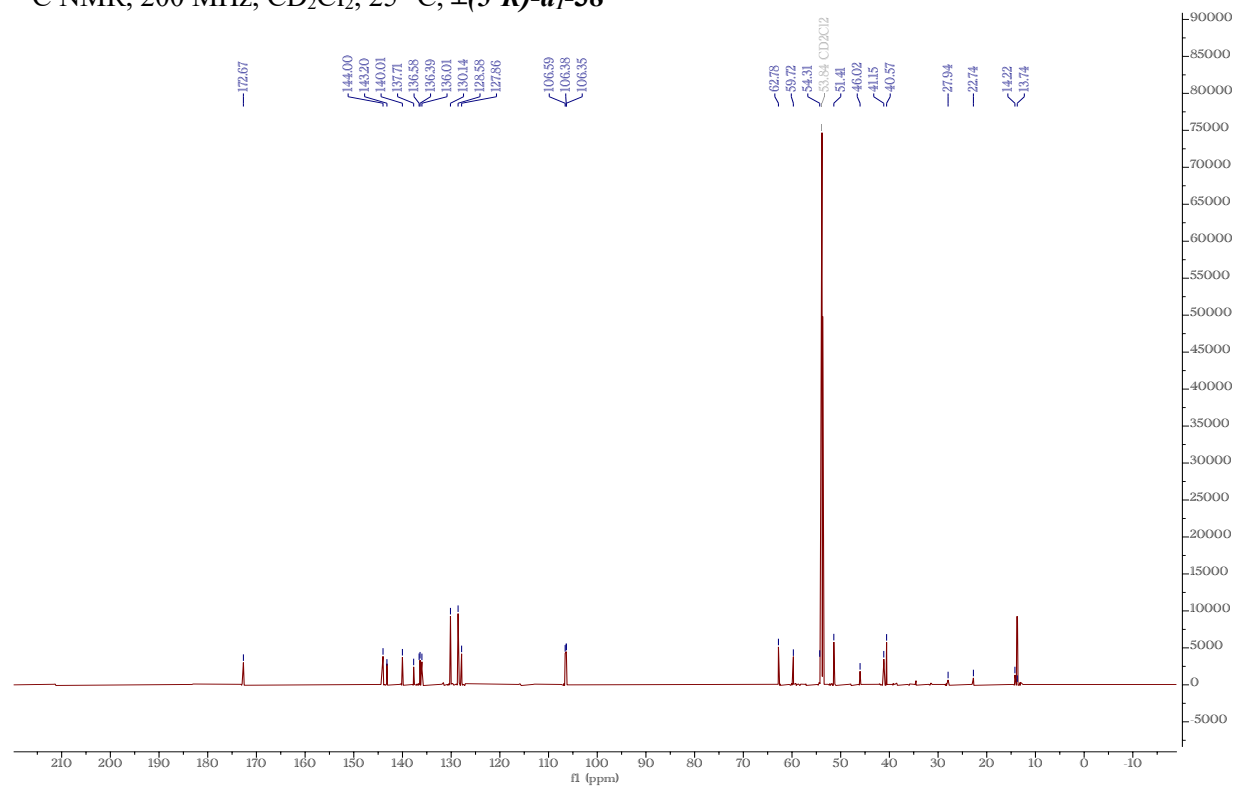


Figure S81:  $^1\text{H}$  NMR, 800 MHz,  $\text{CD}_2\text{Cl}_2$ , 25  $^\circ\text{C}$ ,  $\pm(6'S)\text{-d}_1\text{-38}$

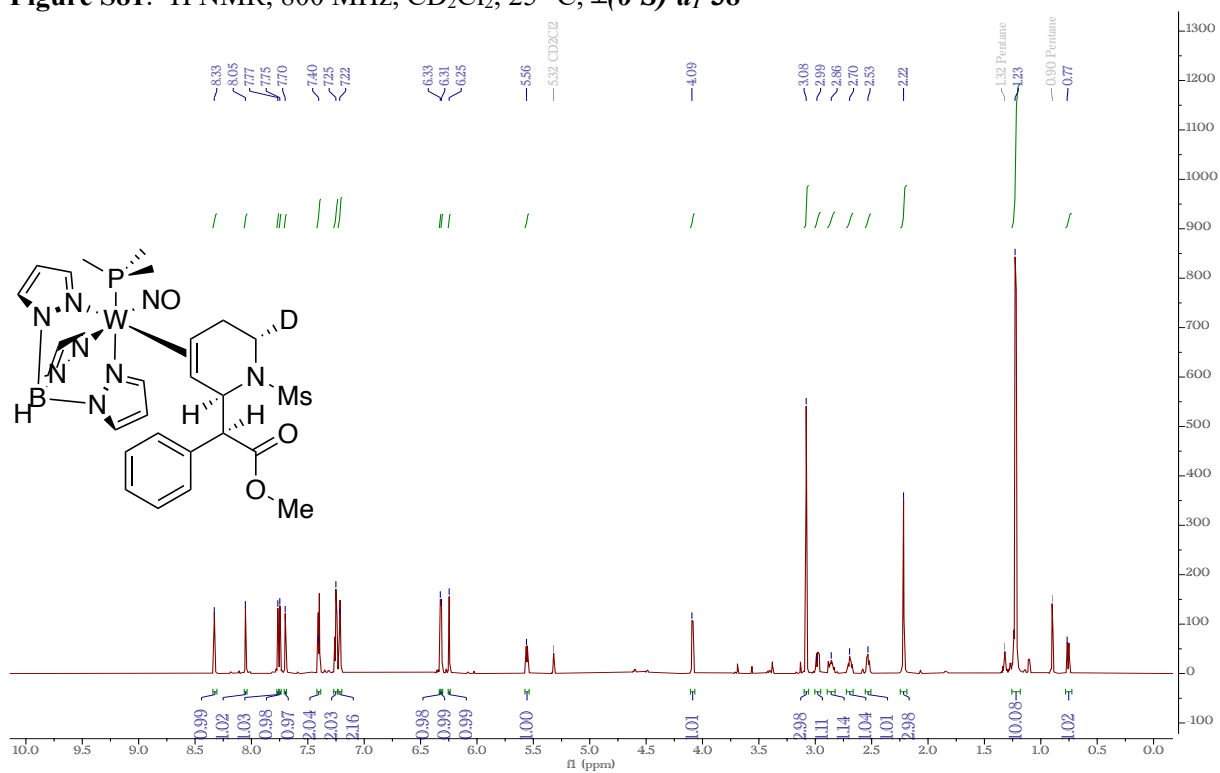
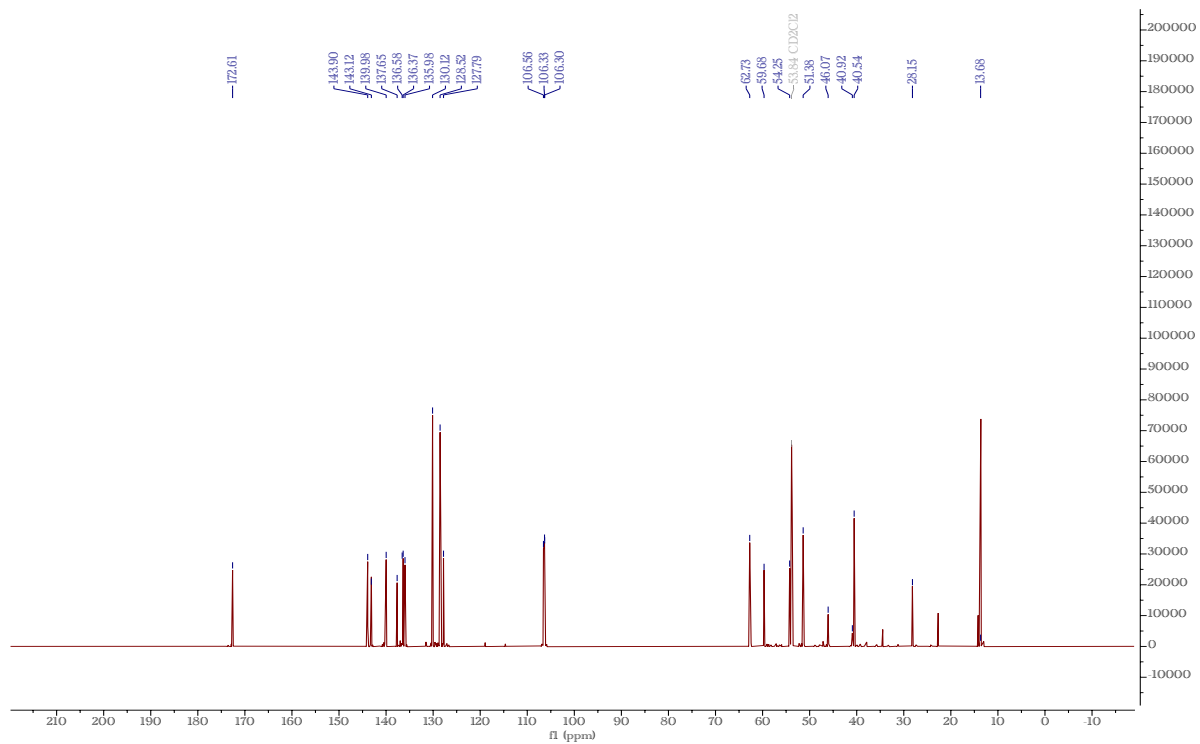
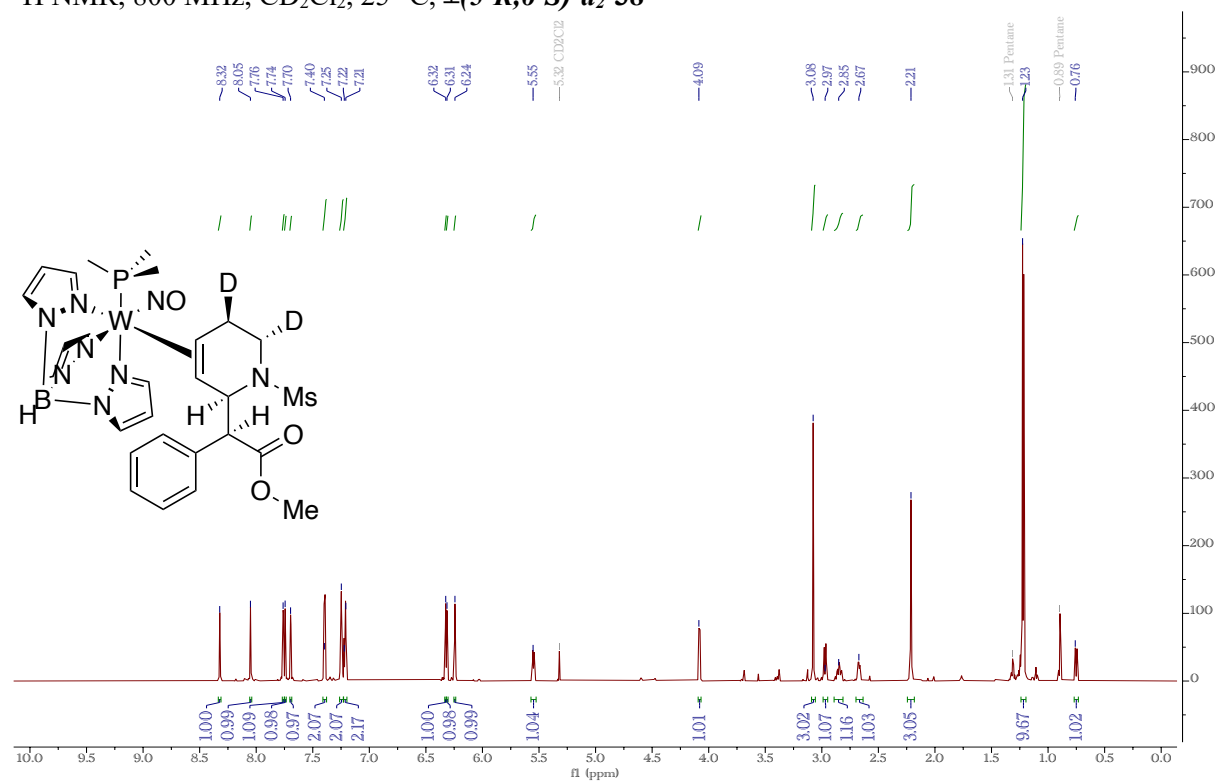


Figure S82:  $^{13}\text{C}$  NMR, 200 MHz,  $\text{CD}_2\text{Cl}_2$ , 25  $^\circ\text{C}$ ,  $\pm(6'S)\text{-d}_1\text{-38}$

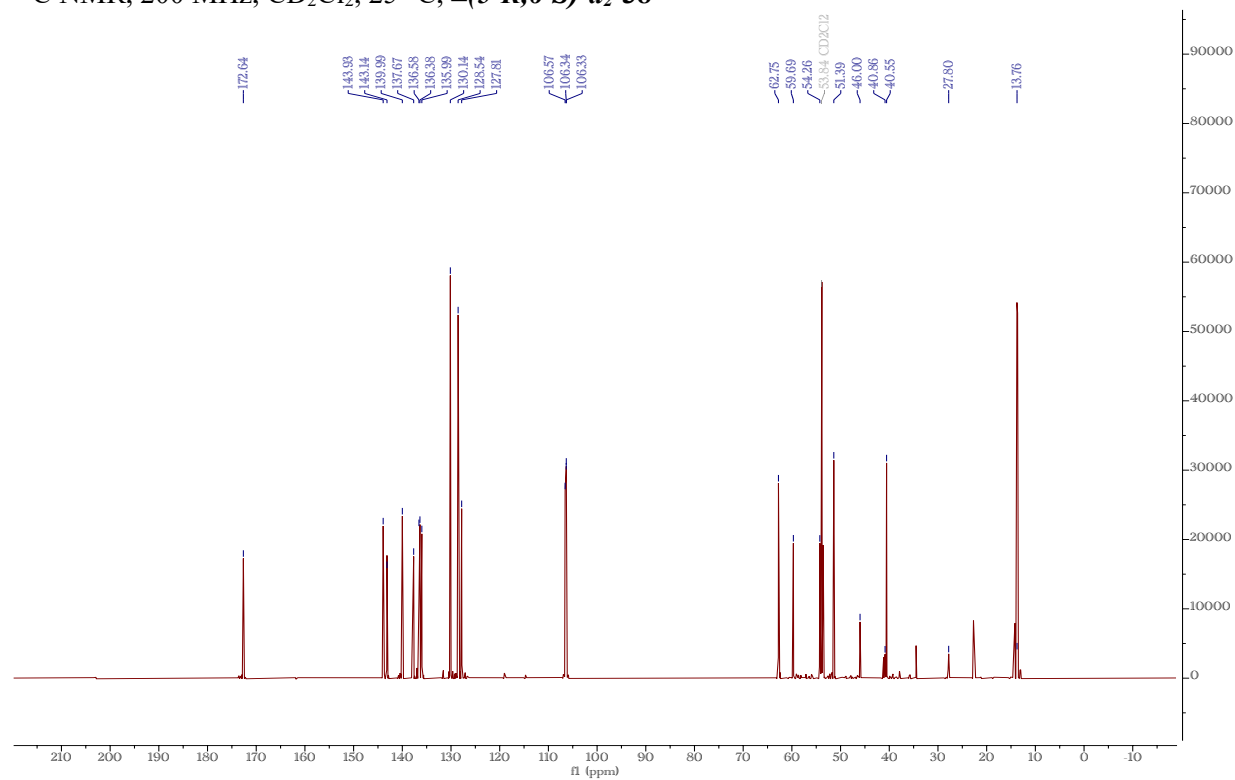




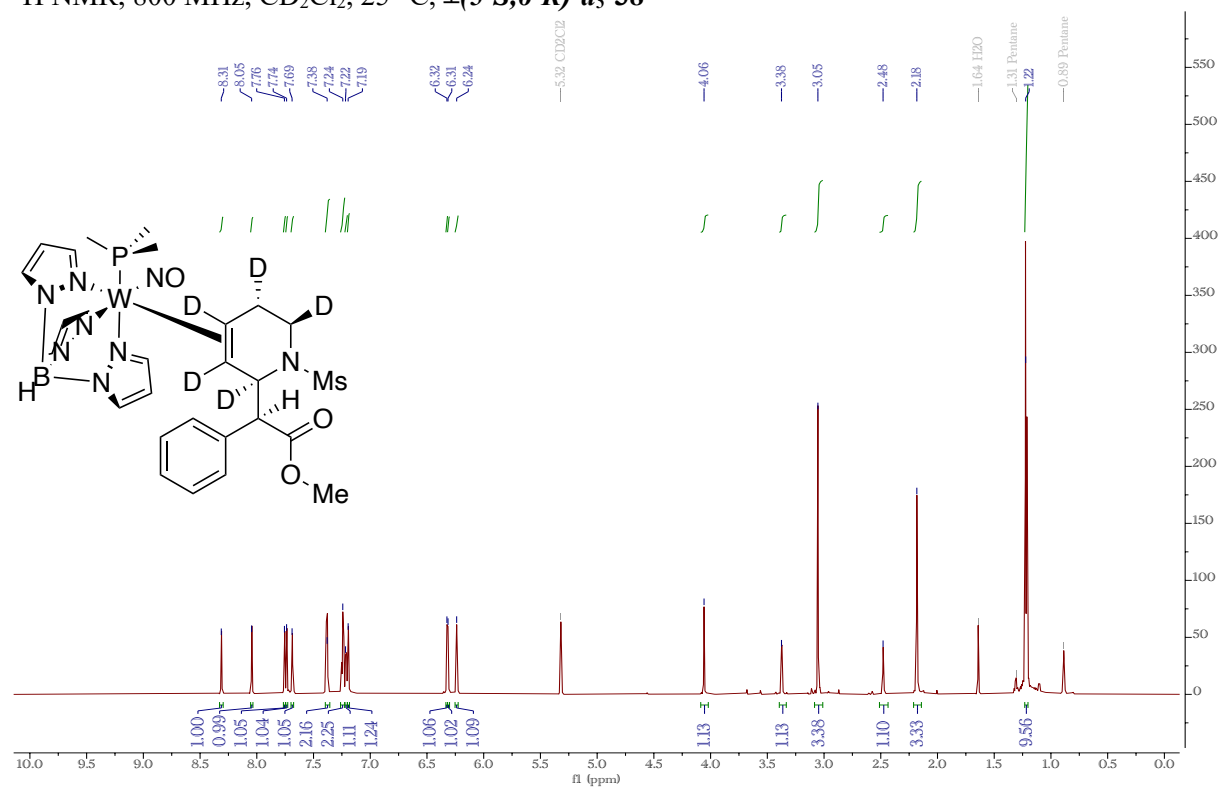
$^1\text{H}$  NMR, 800 MHz,  $\text{CD}_2\text{Cl}_2$ , 25 °C,  $\pm(5'R,6'S)\text{-}d_2\text{-}38$



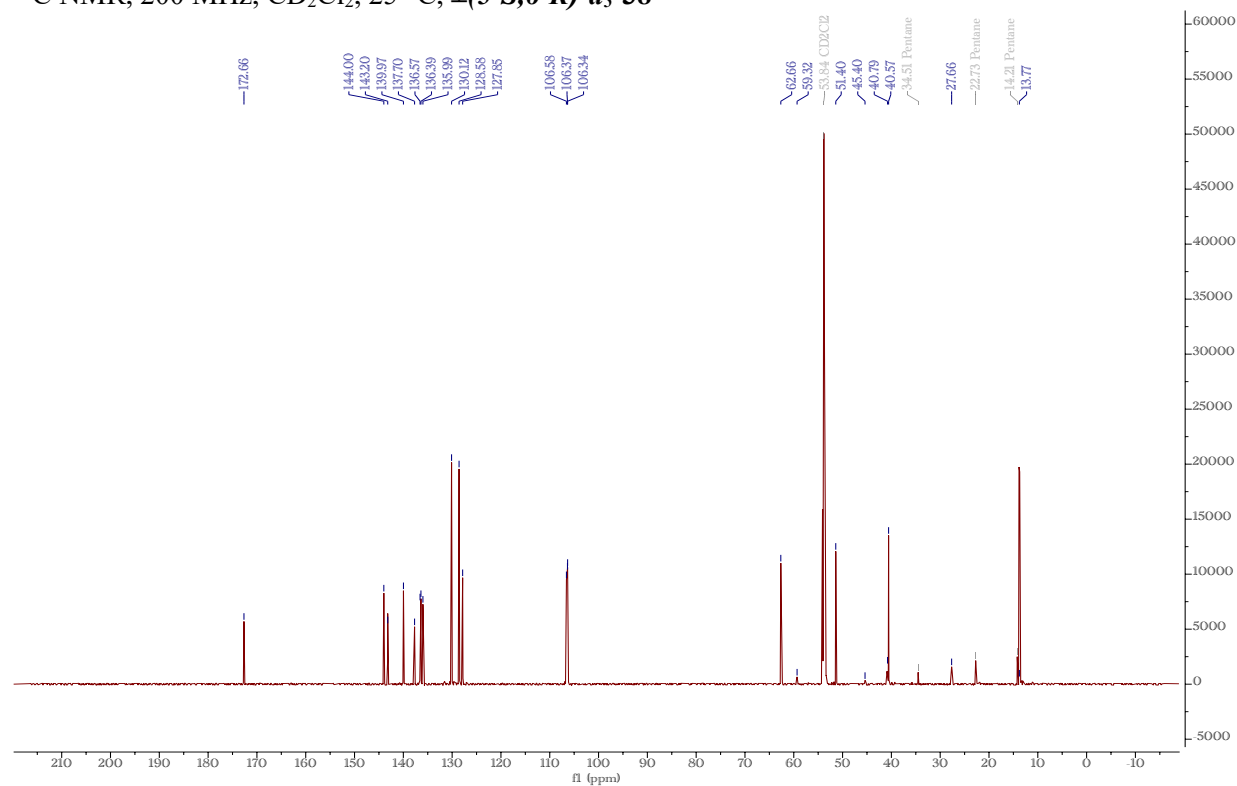
$^{13}\text{C}$  NMR, 200 MHz,  $\text{CD}_2\text{Cl}_2$ , 25 °C,  $\pm(5'R,6'S)\text{-}d_2\text{-}38$



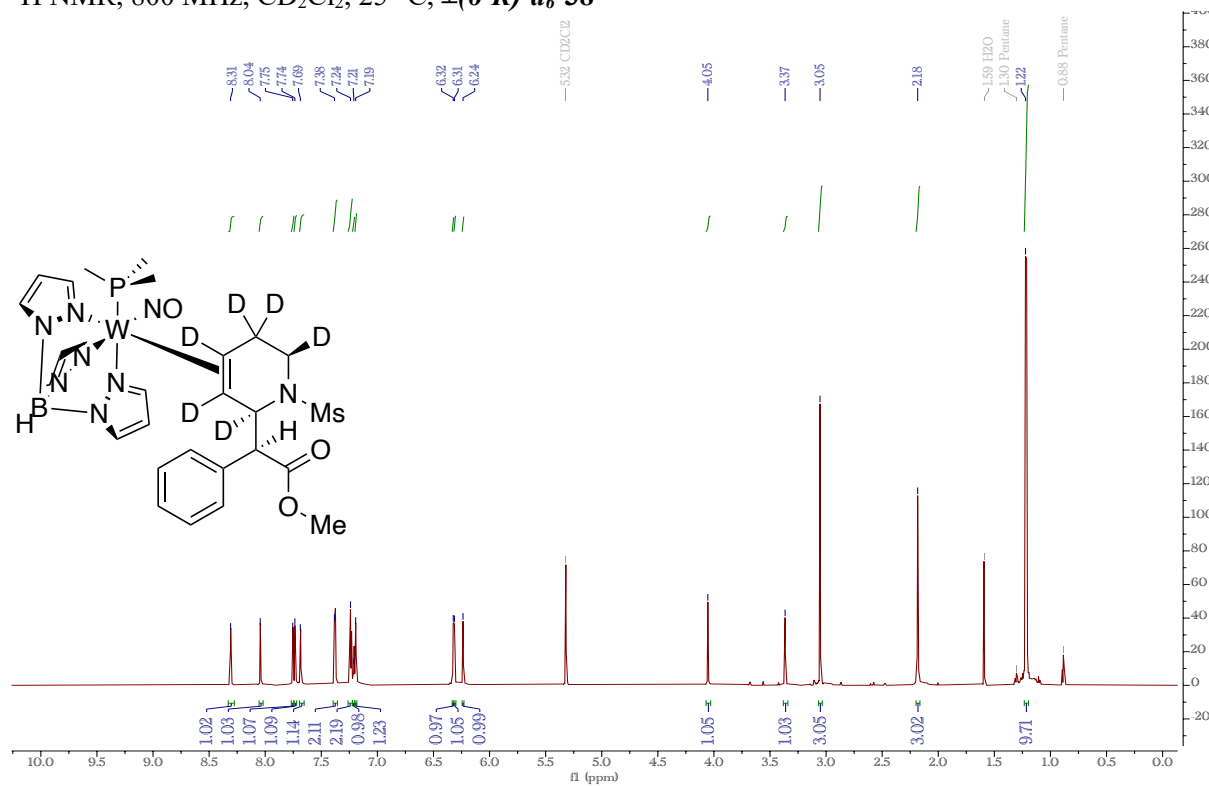
$^1\text{H}$  NMR, 800 MHz,  $\text{CD}_2\text{Cl}_2$ , 25 °C,  $\pm(5'S,6'R)\text{-}d_5\text{-}38$



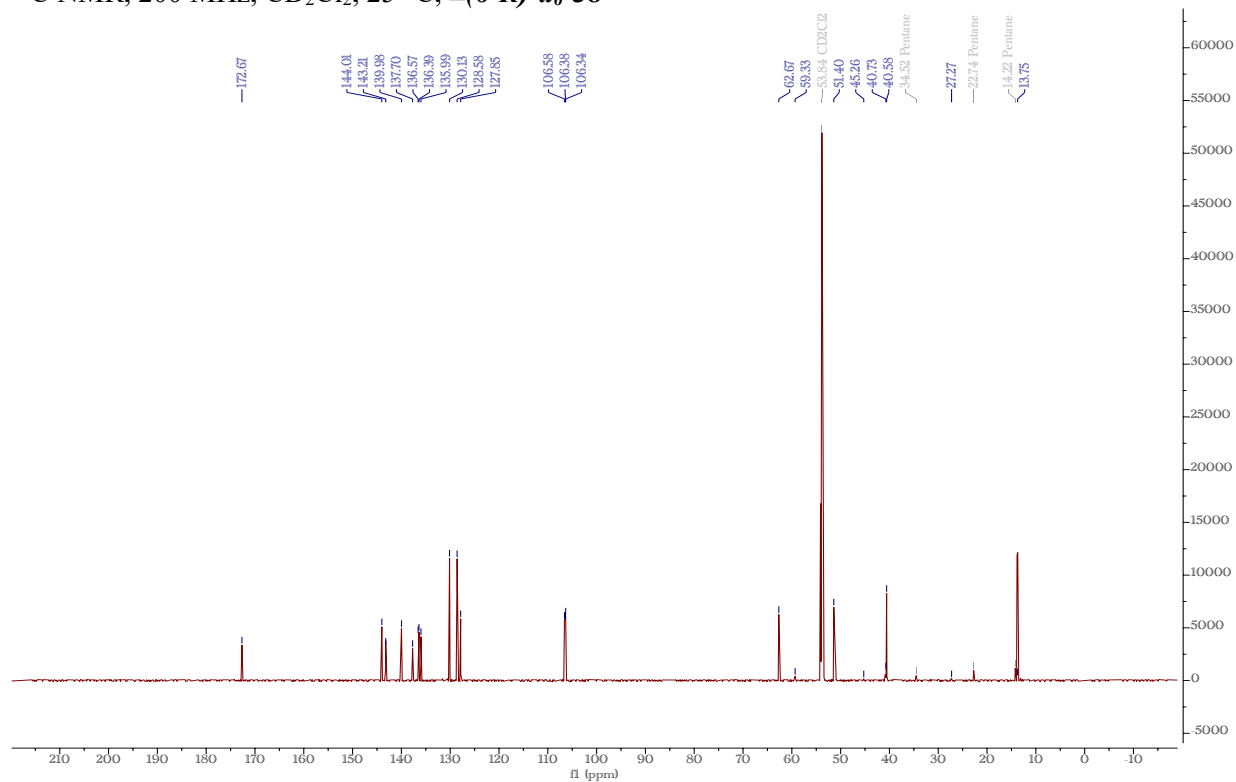
$^{13}\text{C}$  NMR, 200 MHz,  $\text{CD}_2\text{Cl}_2$ , 25 °C,  $\pm(5'S,6'R)\text{-}d_5\text{-}38$



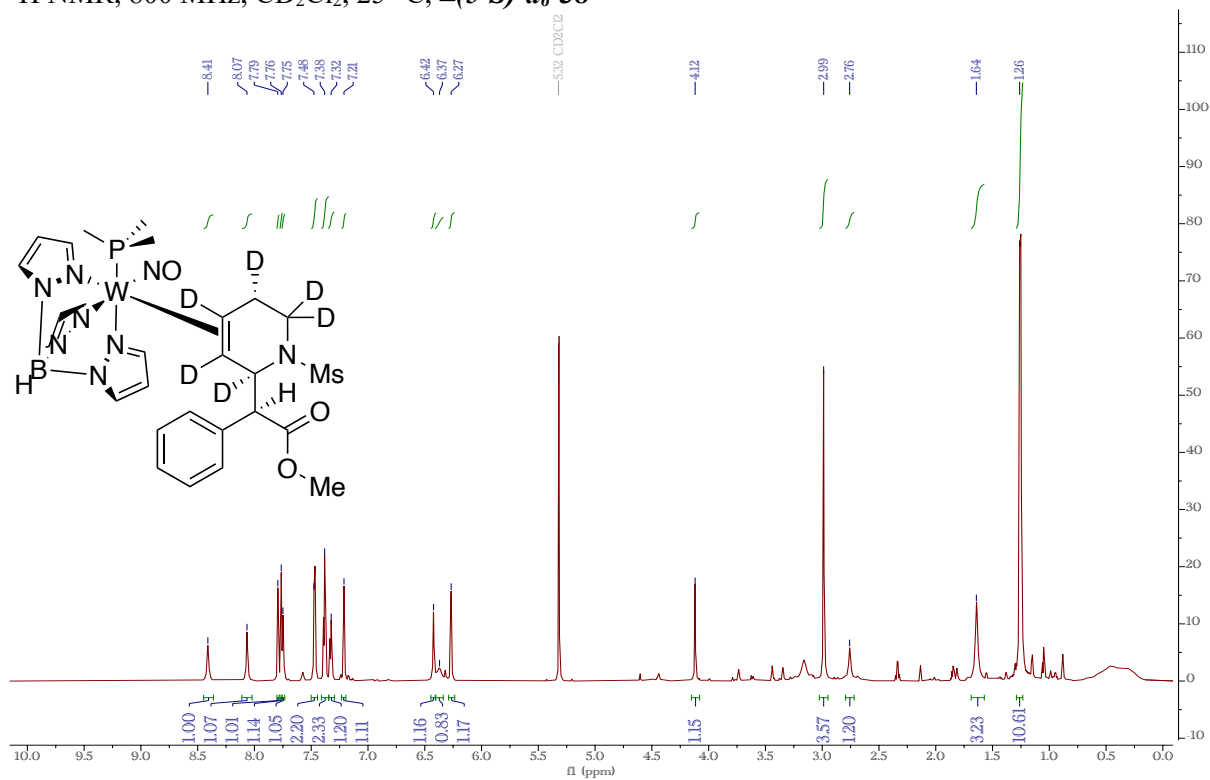
$^1\text{H}$  NMR, 800 MHz,  $\text{CD}_2\text{Cl}_2$ , 25 °C,  $\pm(6'R)\text{-}d_6\text{-}38$



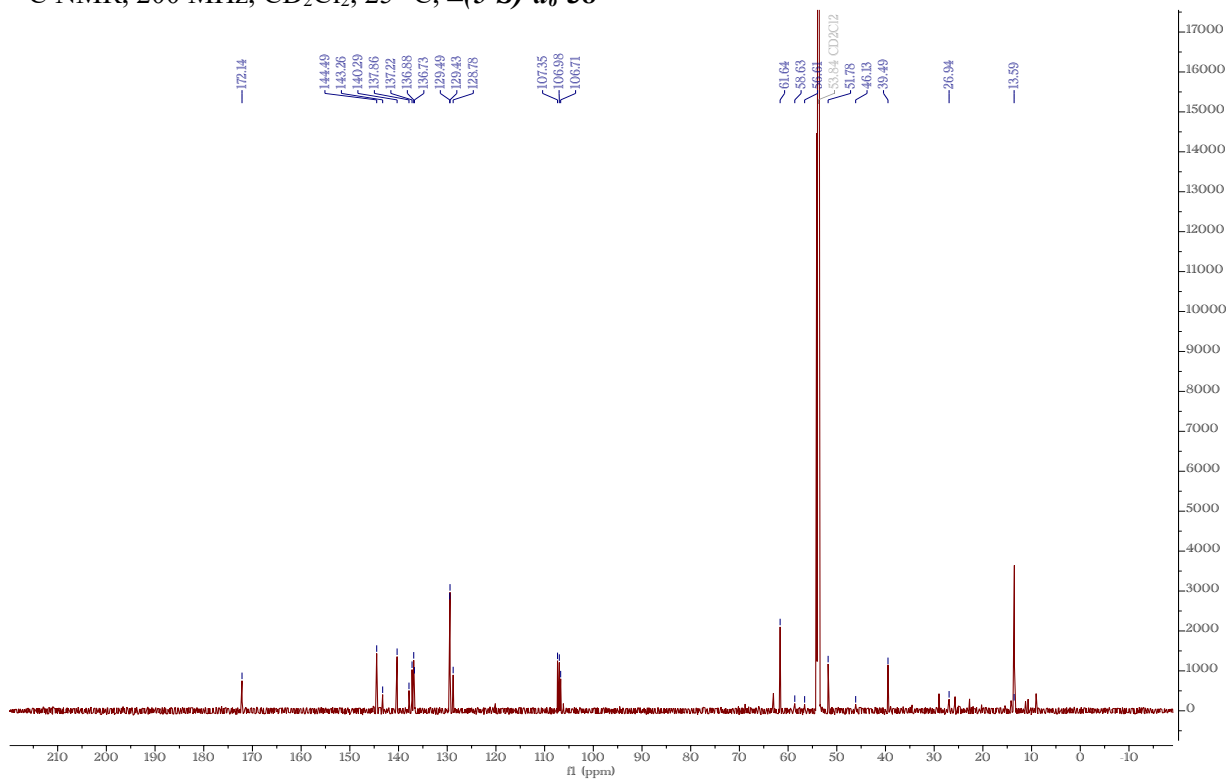
$^{13}\text{C}$  NMR, 200 MHz,  $\text{CD}_2\text{Cl}_2$ , 25 °C,  $\pm(6'R)\text{-}d_6\text{-}38$



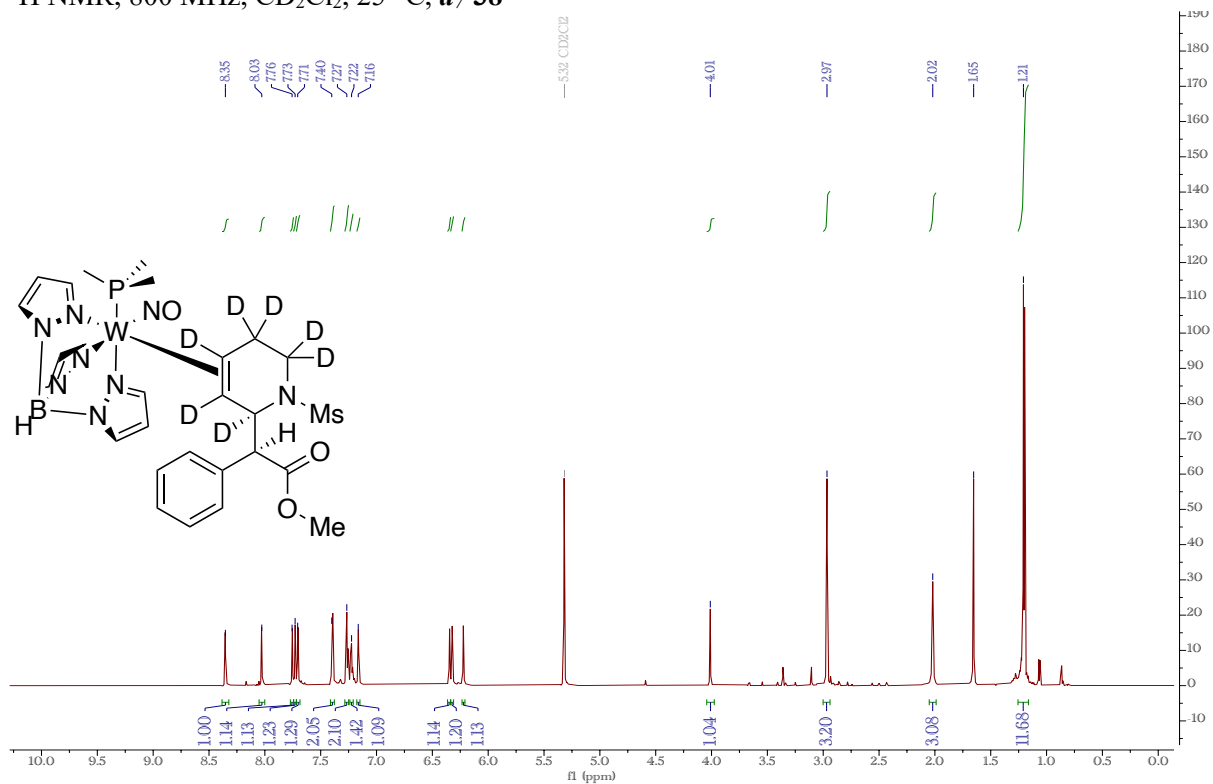
$^1\text{H}$  NMR, 800 MHz,  $\text{CD}_2\text{Cl}_2$ , 25 °C,  $\pm(5'S)\text{-}d_6\text{-}38$



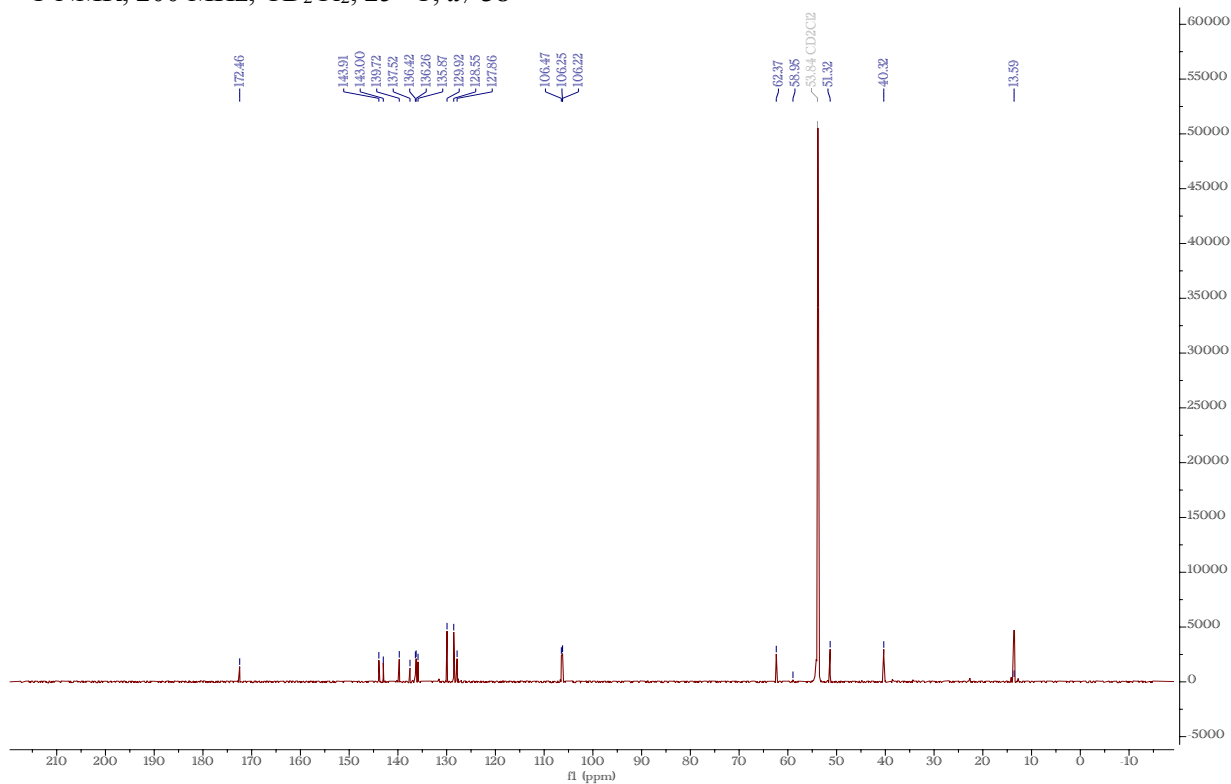
$^{13}\text{C}$  NMR, 200 MHz,  $\text{CD}_2\text{Cl}_2$ , 25 °C,  $\pm(5'S)\text{-}d_6\text{-}38$



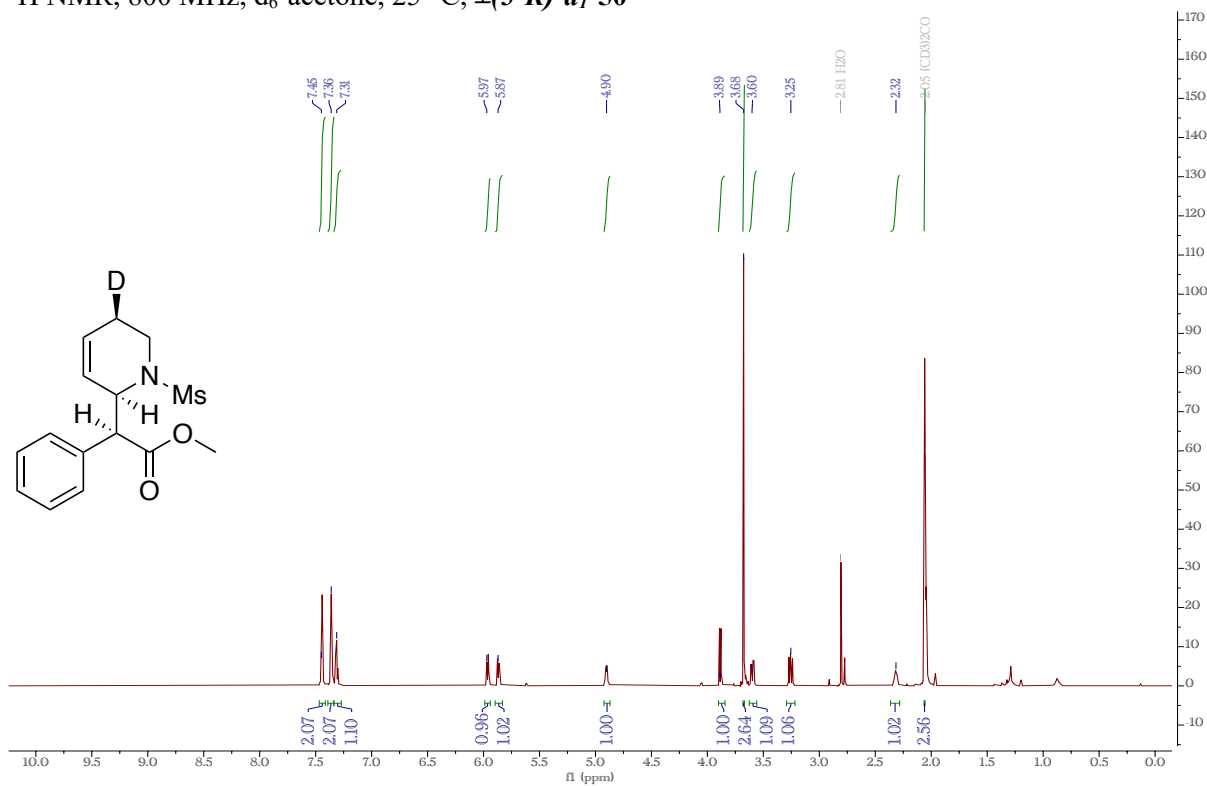
$^1\text{H}$  NMR, 800 MHz,  $\text{CD}_2\text{Cl}_2$ , 25 °C,  $d_7\text{-38}$



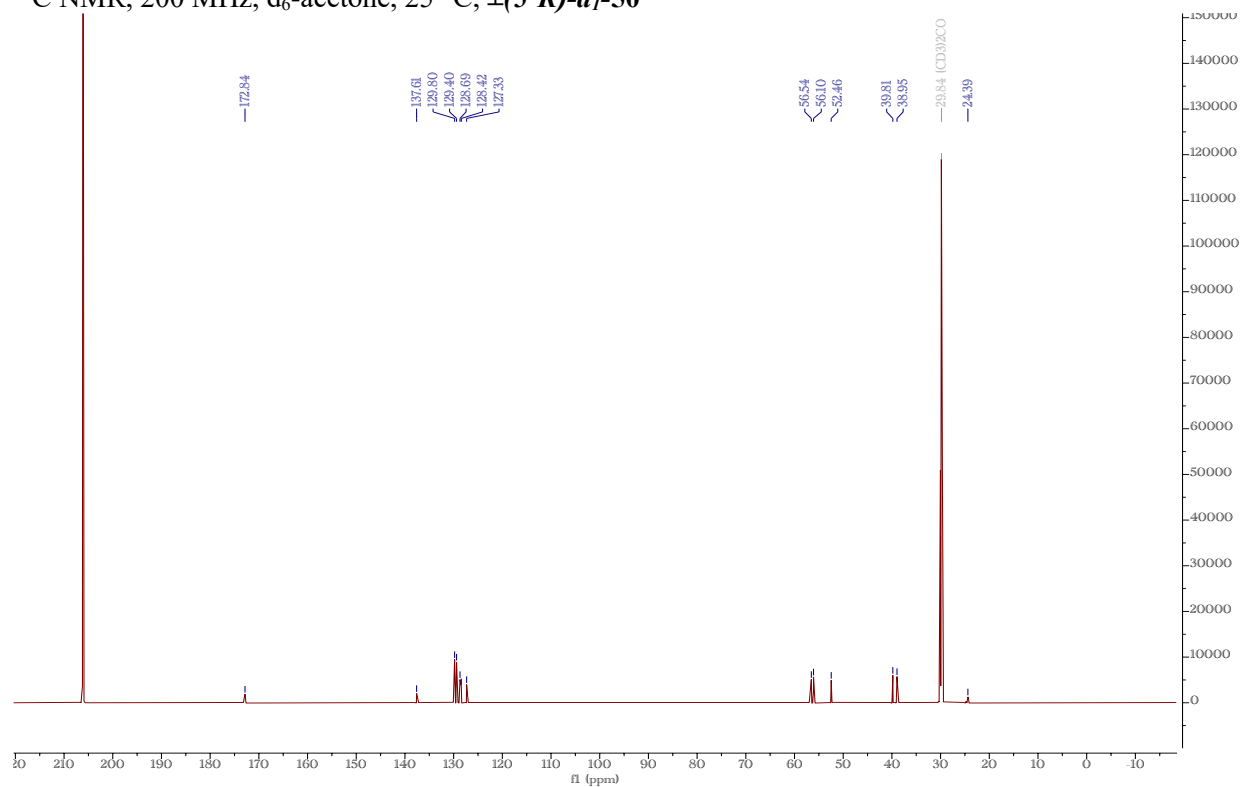
$^{13}\text{C}$  NMR, 200 MHz,  $\text{CD}_2\text{Cl}_2$ , 25 °C,  $d_7\text{-38}$



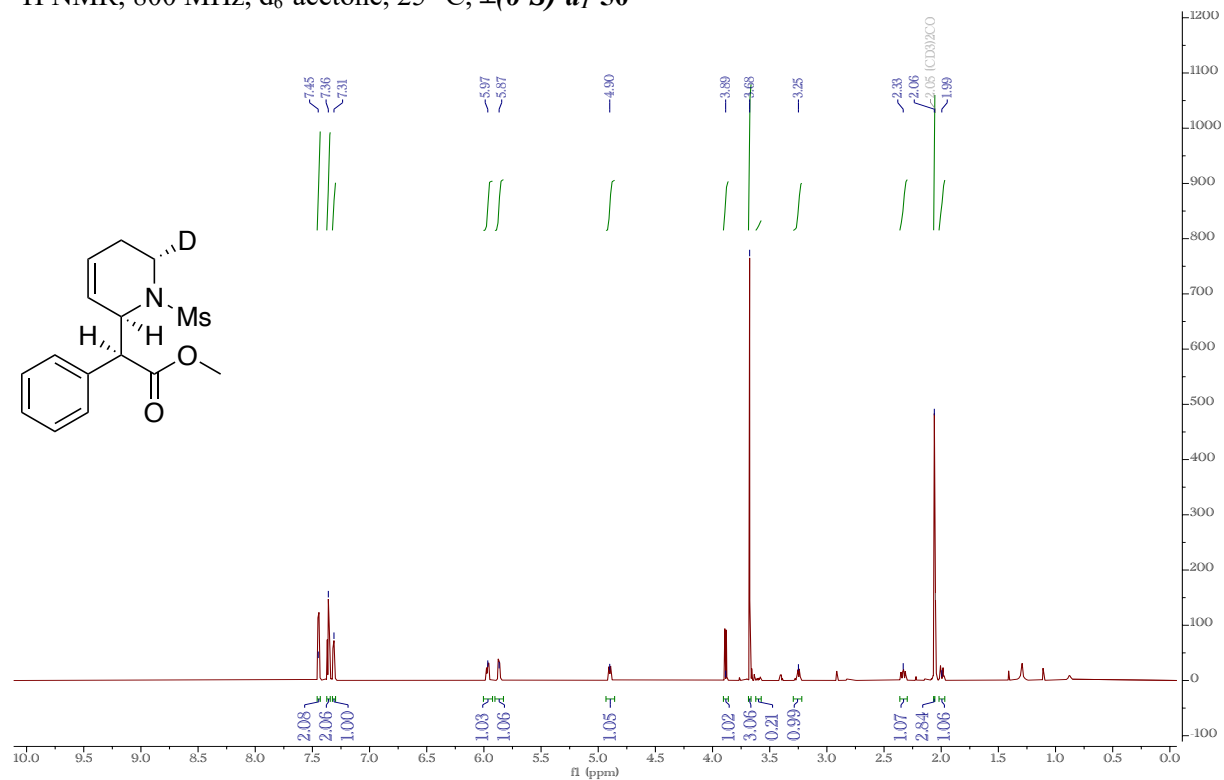
$^1\text{H}$  NMR, 800 MHz,  $\text{d}_6$ -acetone, 25 °C,  $\pm(5'R)\text{-d}_1\text{-50}$



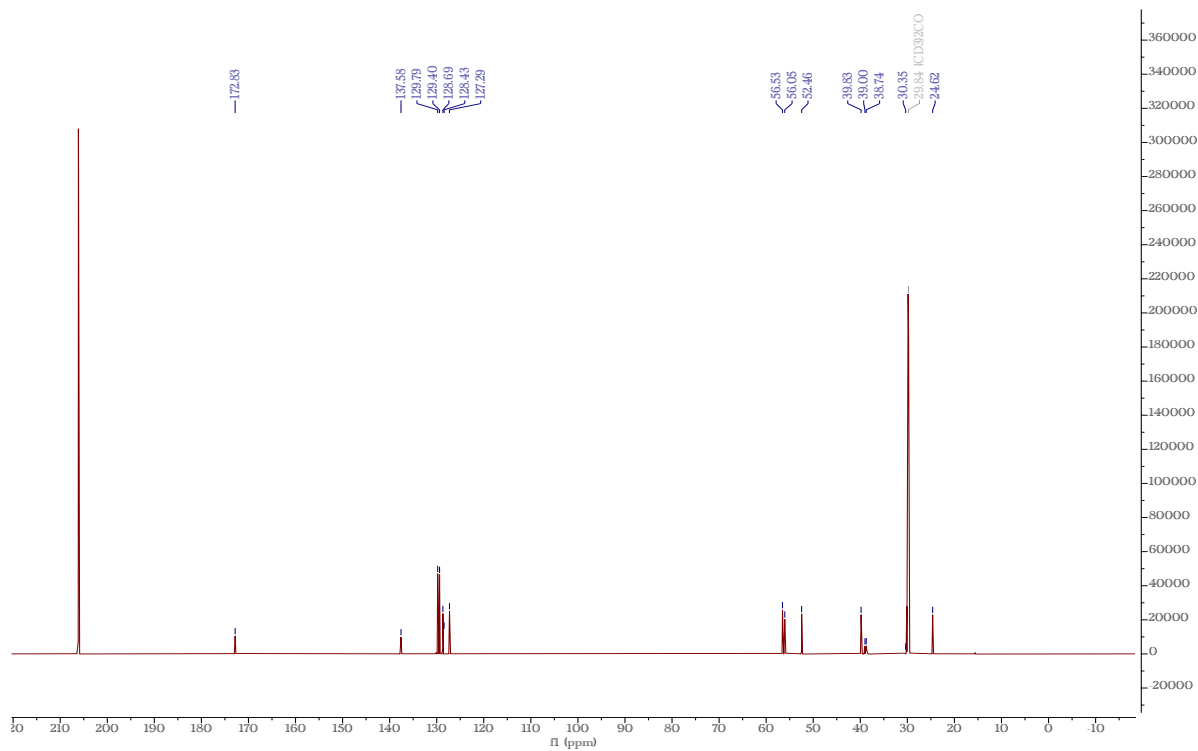
$^{13}\text{C}$  NMR, 200 MHz,  $\text{d}_6$ -acetone, 25 °C,  $\pm(5'R)\text{-d}_1\text{-50}$



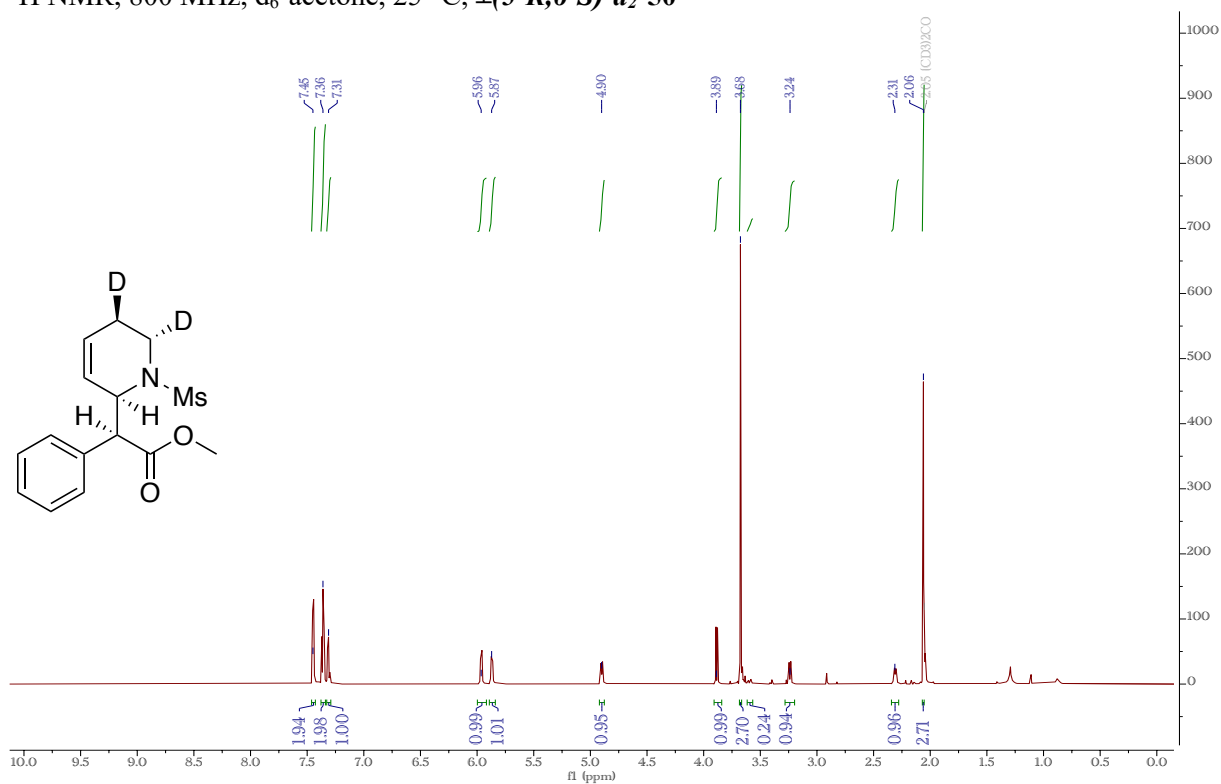
$^1\text{H}$  NMR, 800 MHz,  $\text{d}_6$ -acetone, 25 °C,  $\pm(6'S)\text{-d}_1\text{-50}$



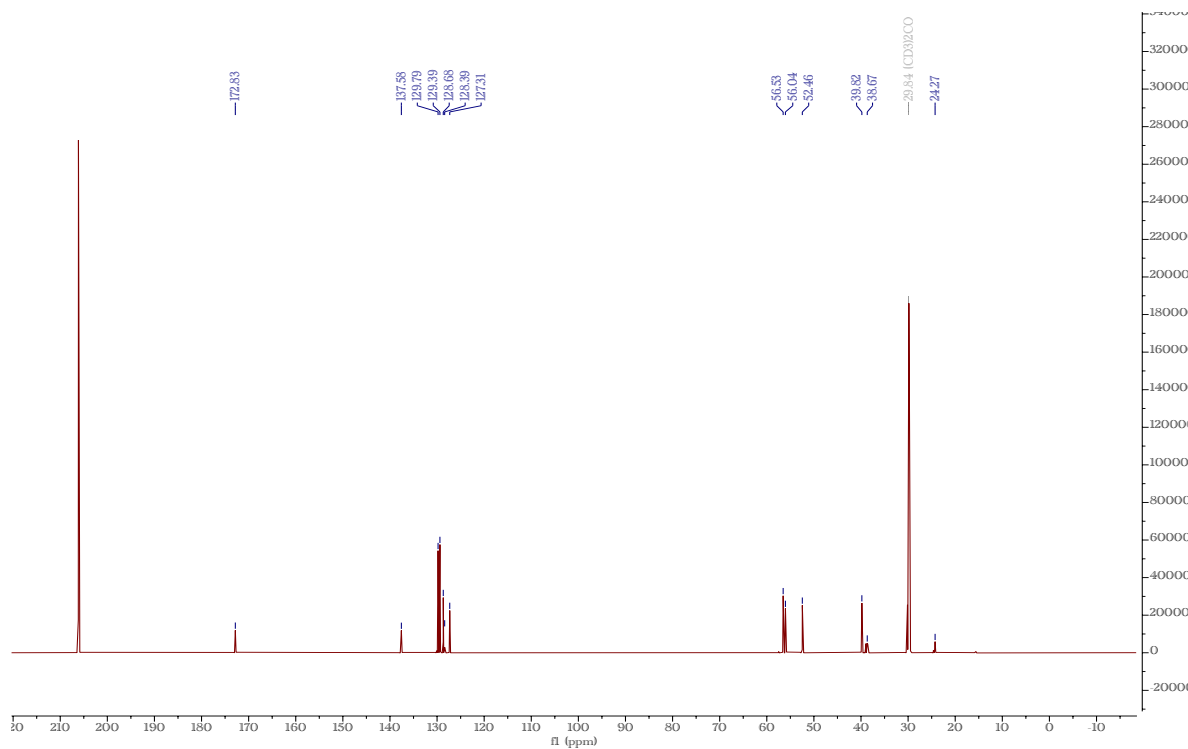
$^{13}\text{C}$  NMR, 200 MHz,  $\text{d}_6$ -acetone, 25 °C,  $\pm(6'S)\text{-d}_1\text{-50}$



$^1\text{H}$  NMR, 800 MHz,  $\text{d}_6$ -acetone, 25 °C,  $\pm(5'R,6'S)\text{-d}_2\text{-50}$

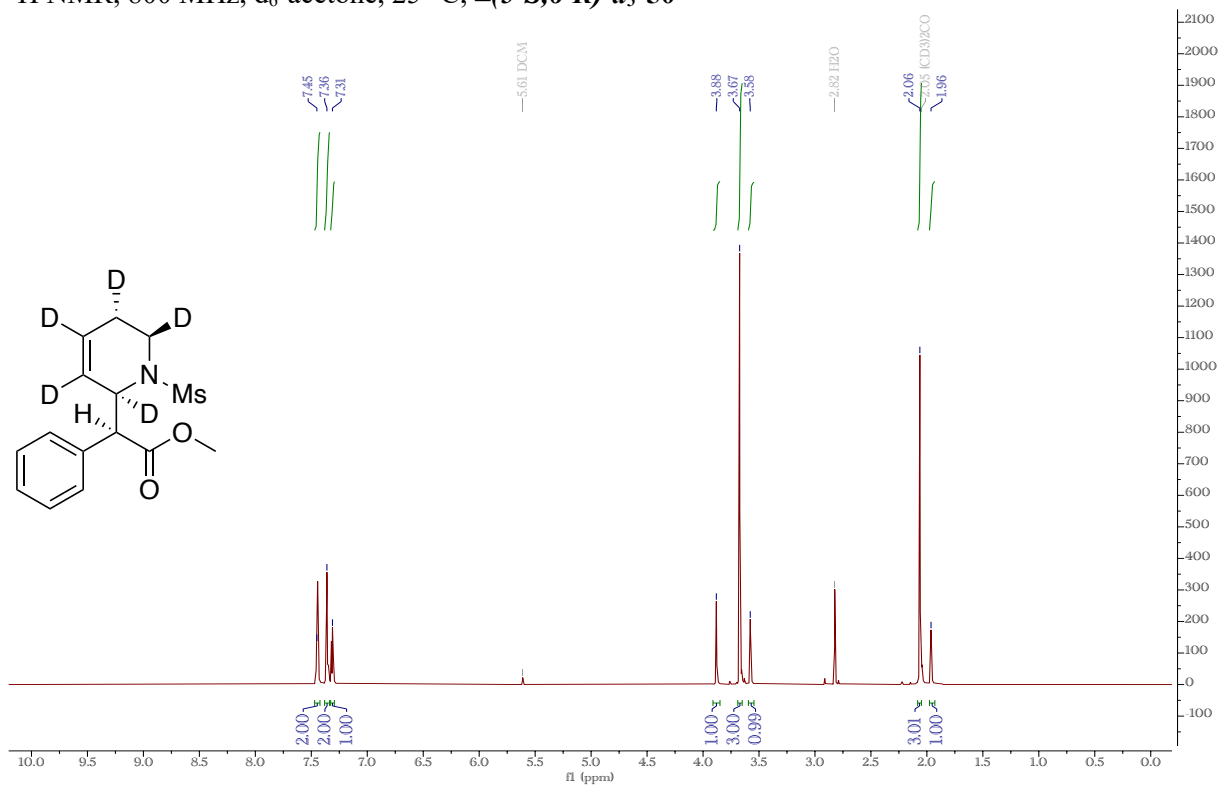


$^{13}\text{C}$  NMR, 200 MHz,  $\text{d}_6$ -acetone, 25 °C,  $\pm(5'R,6'S)\text{-d}_2\text{-50}$

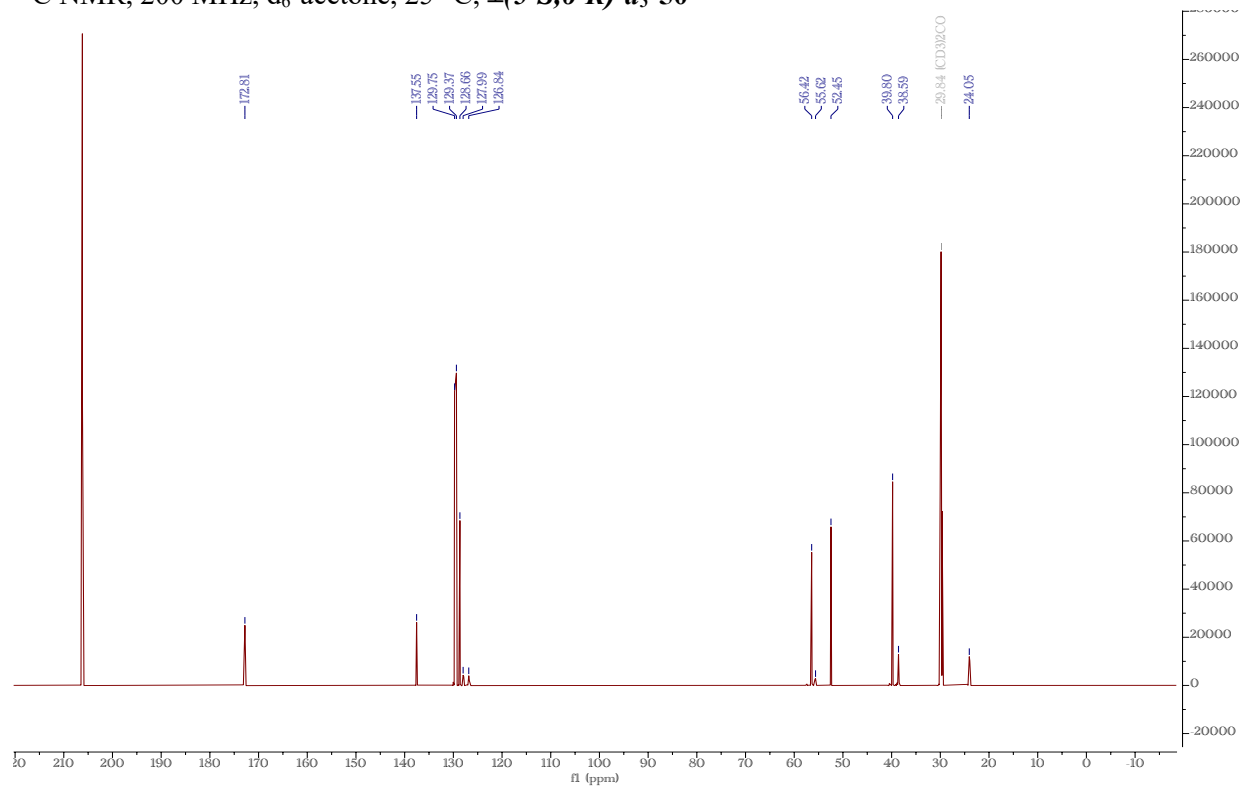




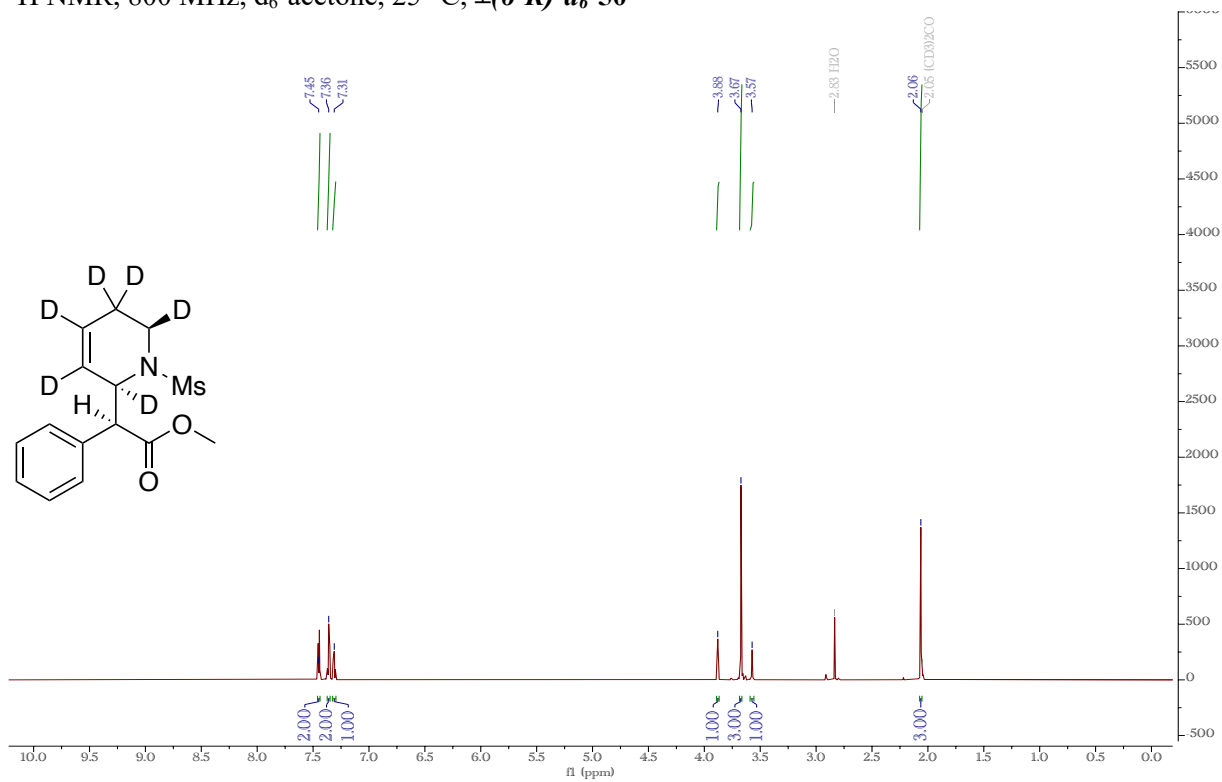
$^1\text{H}$  NMR, 800 MHz,  $d_6$ -acetone, 25 °C,  $\pm(5'S,6'R)$ - $d_5$ -50



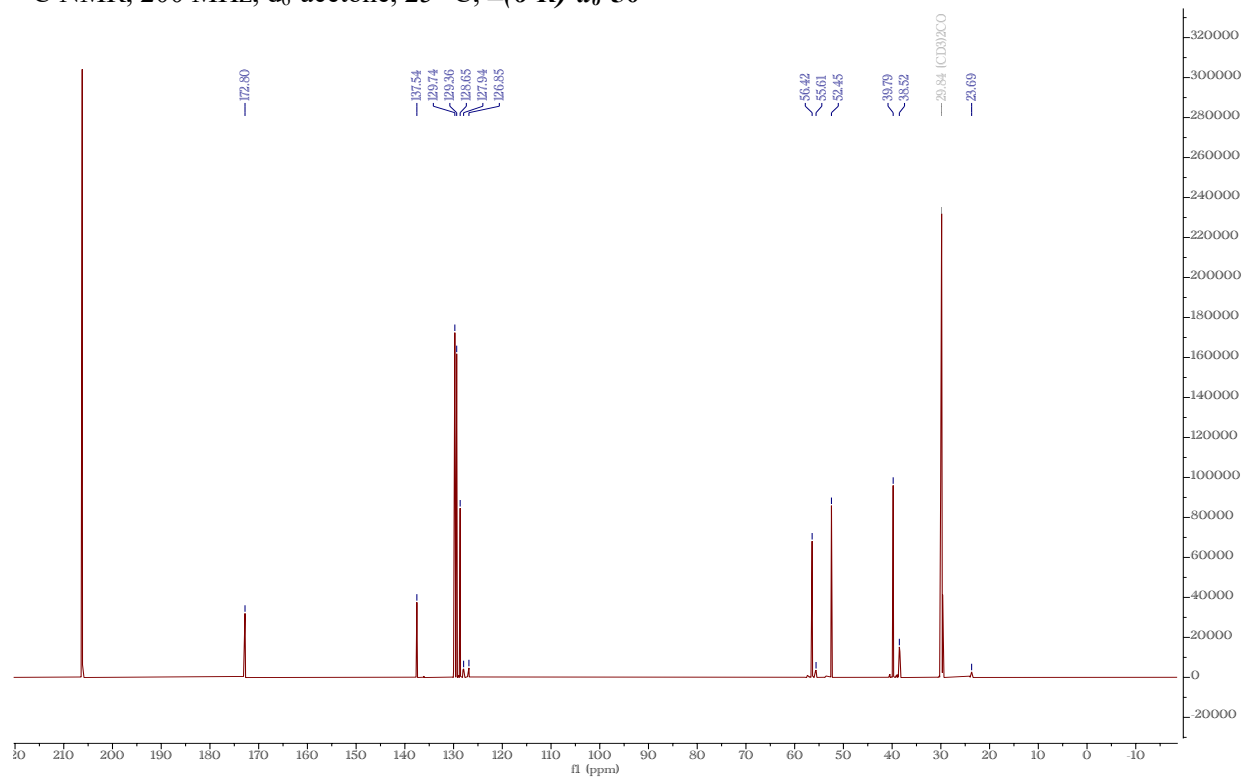
$^{13}\text{C}$  NMR, 200 MHz,  $d_6$ -acetone, 25 °C,  $\pm(5'S,6'R)$ - $d_5$ -50



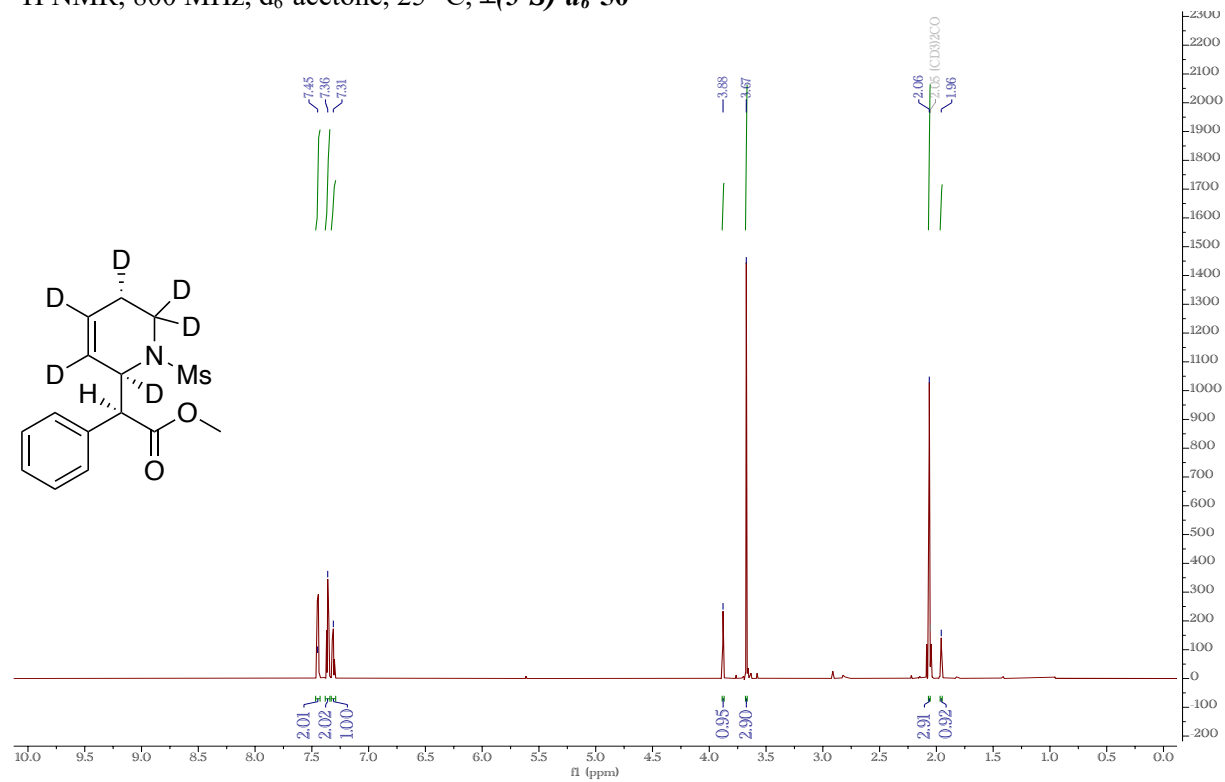
$^1\text{H}$  NMR, 800 MHz,  $d_6$ -acetone, 25 °C,  $\pm(6'R)$ - $d_6$ -50



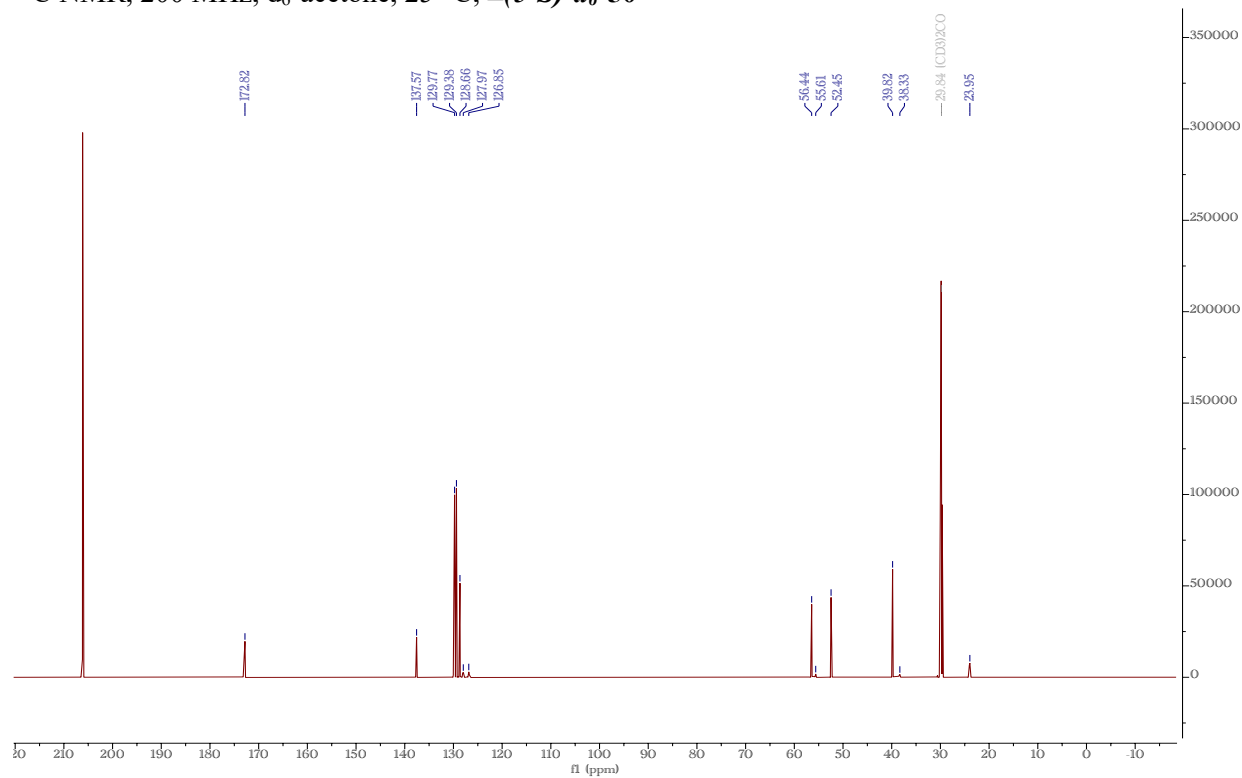
$^{13}\text{C}$  NMR, 200 MHz,  $d_6$ -acetone, 25 °C,  $\pm(6'R)$ - $d_6$ -50



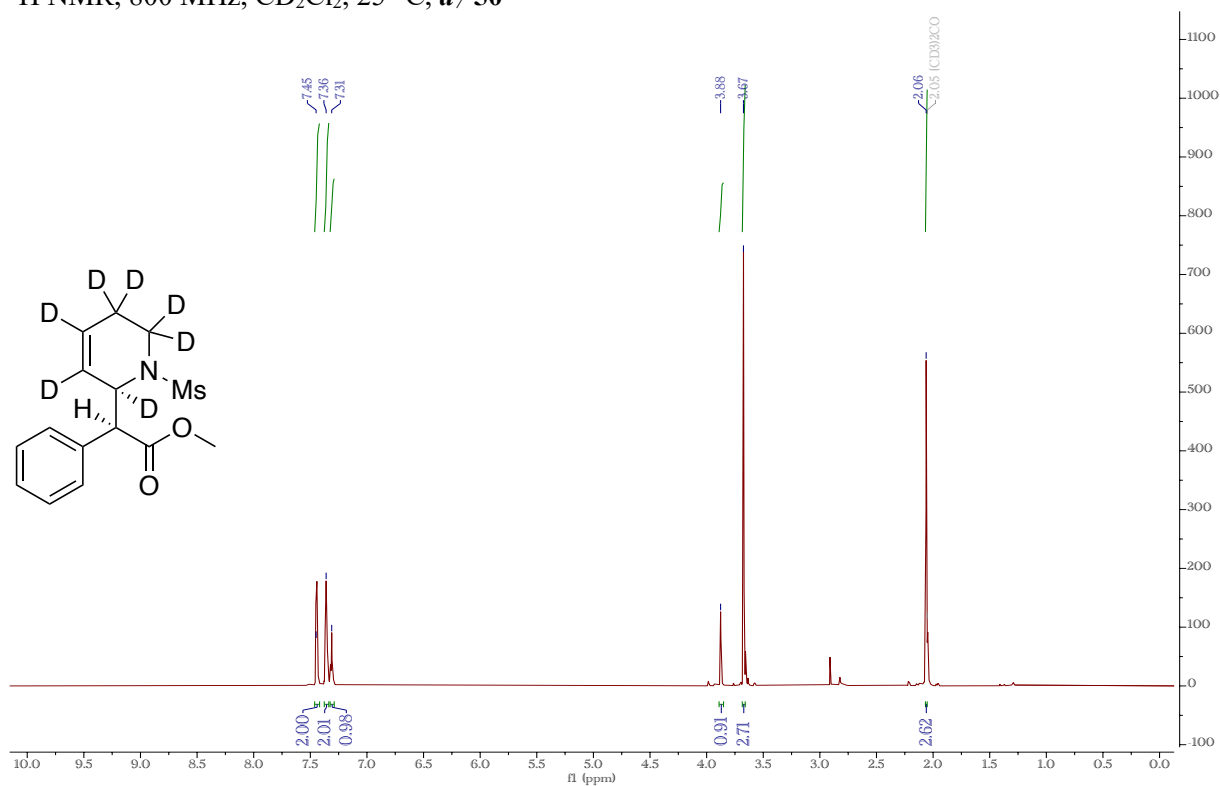
$^1\text{H}$  NMR, 800 MHz,  $d_6$ -acetone, 25 °C,  $\pm(5'S)\text{-}d_6\text{-50}$



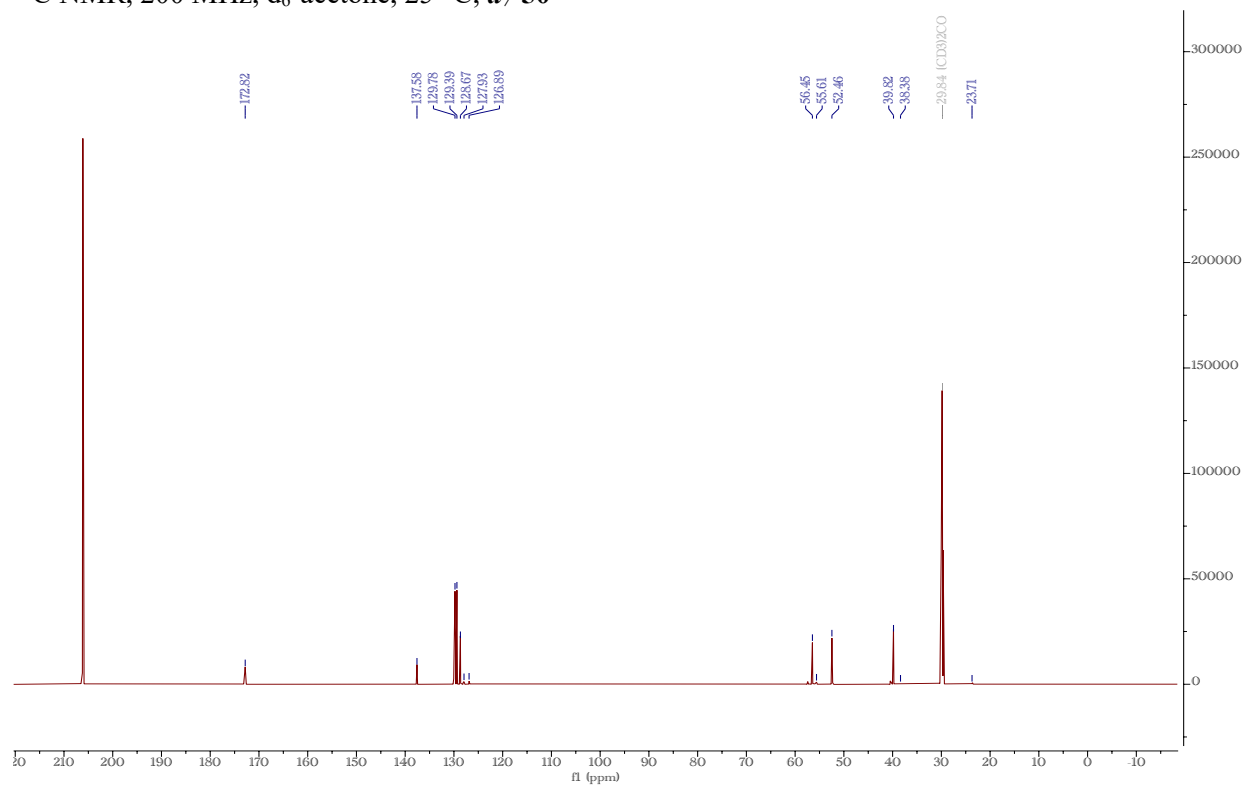
$^{13}\text{C}$  NMR, 200 MHz,  $d_6$ -acetone, 25 °C,  $\pm(5'S)\text{-}d_6\text{-50}$



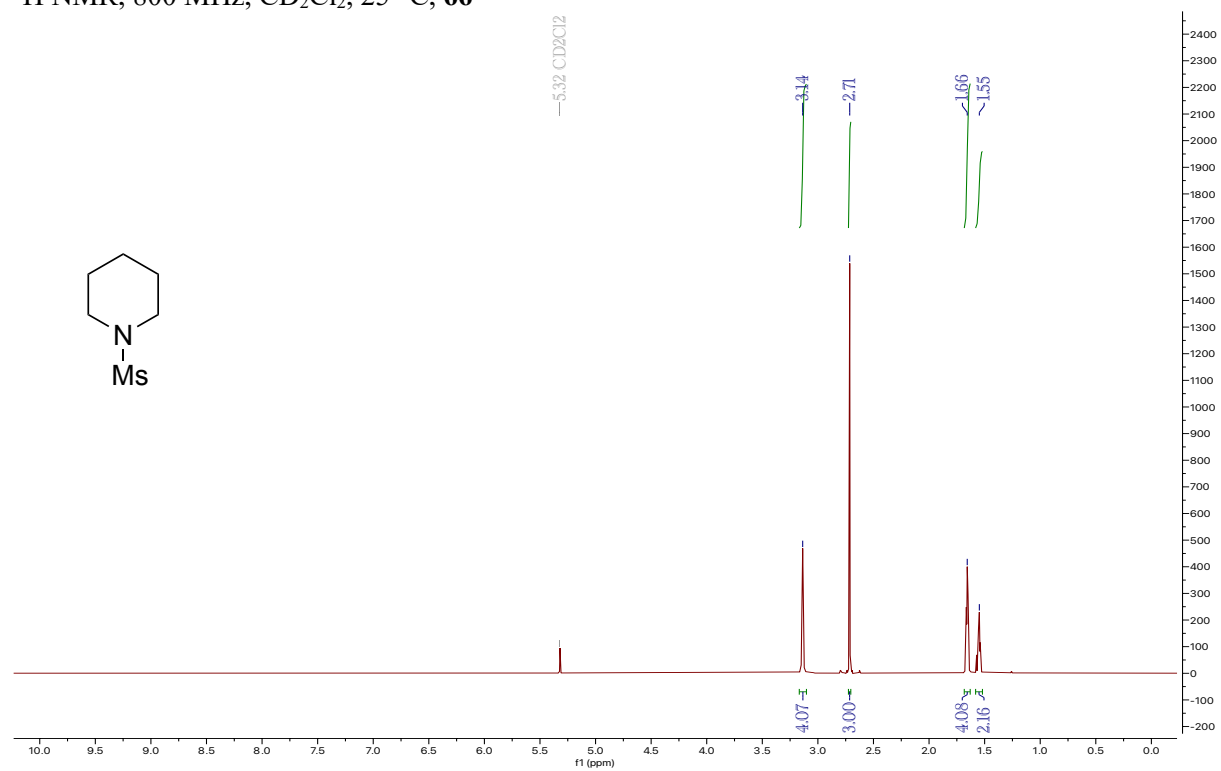
$^1\text{H}$  NMR, 800 MHz,  $\text{CD}_2\text{Cl}_2$ , 25 °C, *d*<sub>7</sub>-50



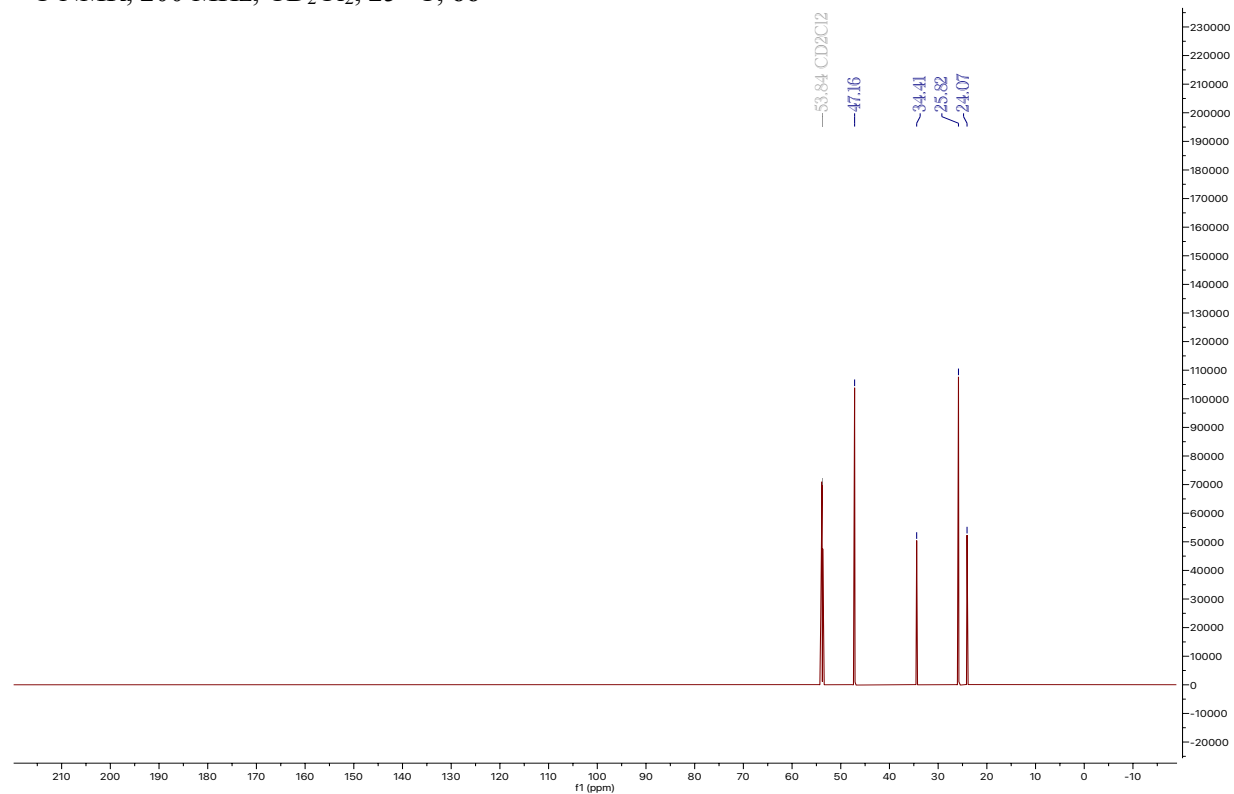
$^{13}\text{C}$  NMR, 200 MHz,  $d_6$ -acetone, 25 °C, *d*<sub>7</sub>-50



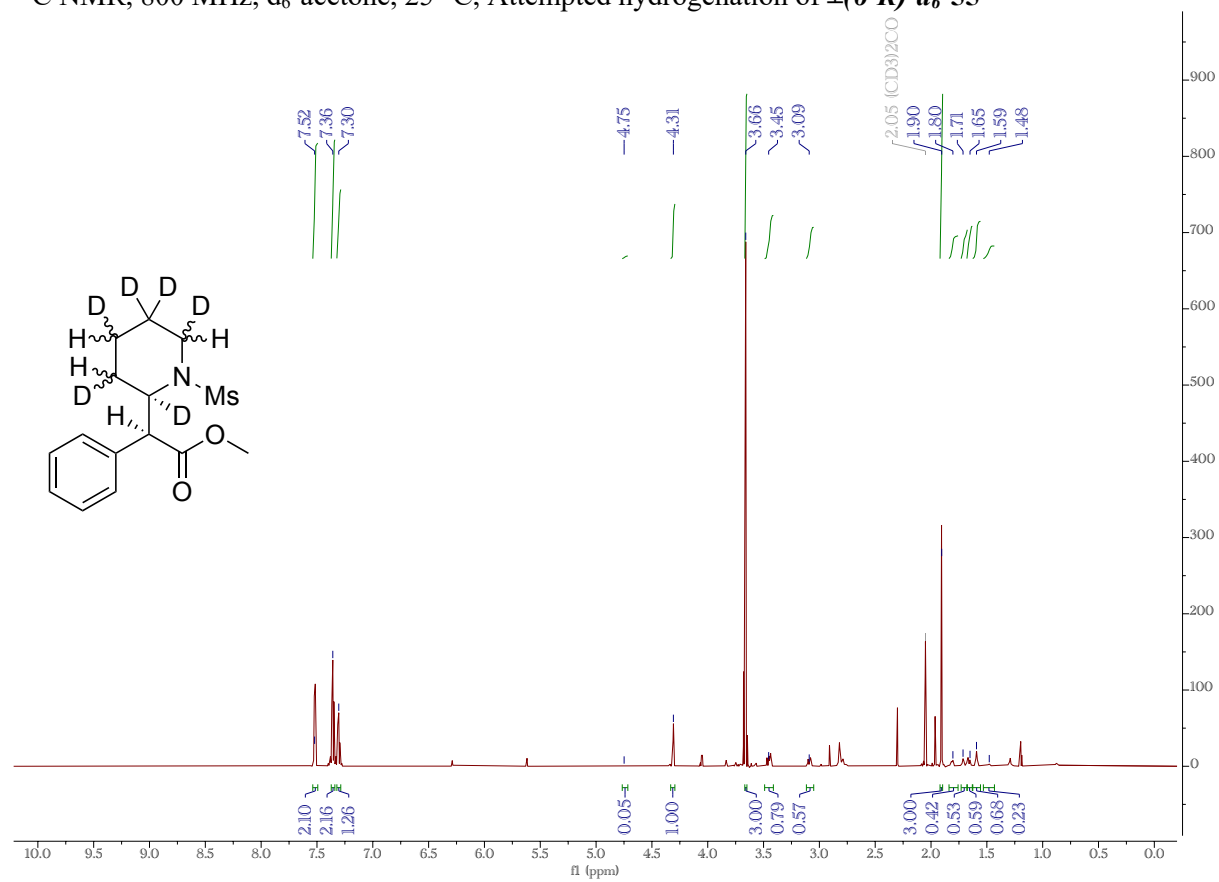
$^1\text{H}$  NMR, 800 MHz,  $\text{CD}_2\text{Cl}_2$ , 25 °C, **66**



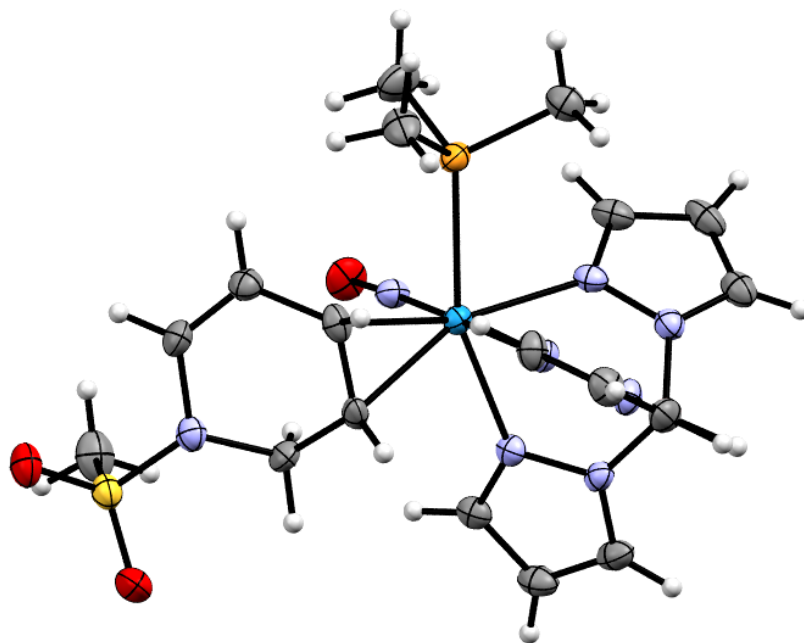
$^{13}\text{C}$  NMR, 200 MHz,  $\text{CD}_2\text{Cl}_2$ , 25 °C, **66**



$^{13}\text{C}$  NMR, 800 MHz,  $d_6$ -acetone, 25 °C, Attempted hydrogenation of  $\pm(6'R)$ - $d_6$ -55



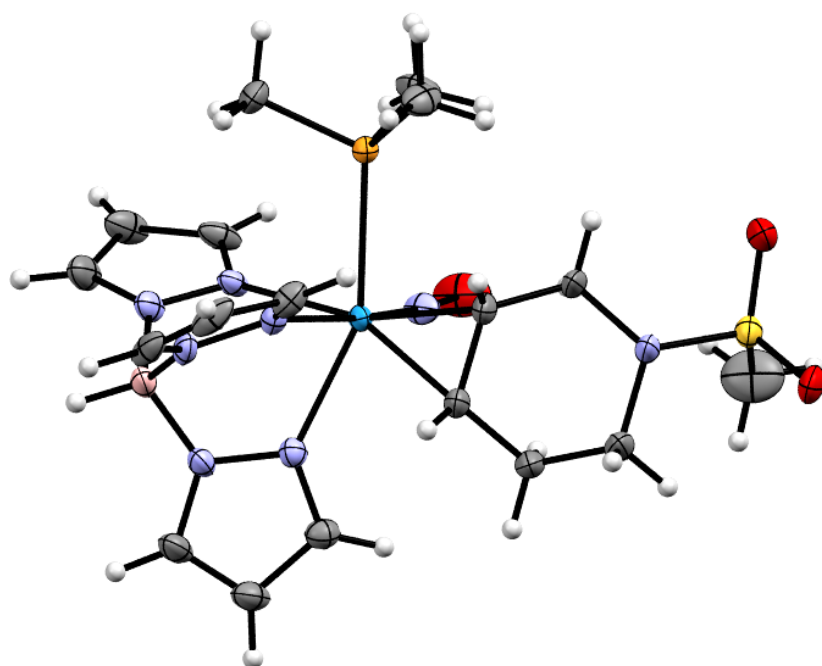
SC-XRD Data:



ORTEP/ellipsoid diagram of **60D**.

SC-XRD data for **60D**.

CCDC 2298721	Chemical Formula $C_{18}H_{28}BN_8O_3PSW$	FW (g/mol) 662.17
T (K) 100(2)	$\lambda$ (Å) 0.71073	Crystal size (mm) 0.056 x 0.129 x 0.159
Crystal habit Colorless plate	Crystal system Monoclinic	Space group $P2_1/n$
a (Å) 9.8554(10)	b (Å) 19.675(2)	c (Å) 13.2017(13)
$\alpha$ (°) 90	$\beta$ (°) 106.438(3)	$\gamma$ (°) 90
V (Å <sup>3</sup> ) 2455.2(4)	Z 4	$\rho_{calc}$ (g/cm <sup>3</sup> ) 1.791
$\mu$ (mm <sup>-1</sup> ) 4.892	F(000) 1304	$\theta$ range (°) 1.91 to 28.35
Index ranges -13 ≤ h ≤ 13 -26 ≤ k ≤ 26 -17 ≤ l ≤ 17	Data/restraints/parameters 6127 / 0 / 314	Goodness-of-fit on F <sup>2</sup> 1.011
R <sub>1</sub> [I > 2σ(I)] 0.0348	wR <sub>2</sub> [all data] 0.0672	

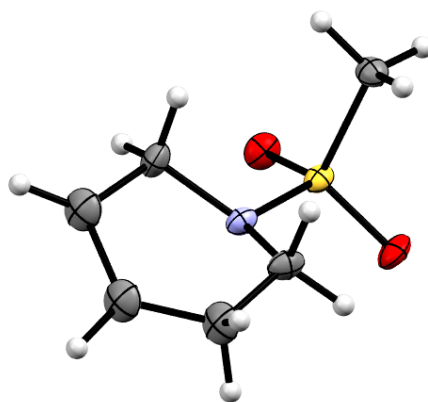


ORTEP/ellipsoid diagram of **62**.

SC-XRD data for **62**.

CCDC 2298722	Chemical Formula $C_{18}H_{30}BN_8O_3PSW$	FW (g/mol) 664.19
T (K) 100(2)	$\lambda$ (Å) 0.71073	Crystal size (mm) 0.077 x 0.129 x 0.141
Crystal habit Yellow prism	Crystal system Monoclinic	Space group P 2 <sub>1</sub> /c
a (Å) 7.9593(4)	b (Å) 25.6443(14)	c (Å) 12.5253(7)
$\alpha$ (°) 90	$\beta$ (°) 103.734(2)	$\gamma$ (°) 90
V (Å <sup>3</sup> ) 2483.5(2)	Z 4	$\rho_{calc}$ (g/cm <sup>3</sup> ) 1.776
$\mu$ (mm <sup>-1</sup> ) 4.837	F(000) 1312	$\theta$ range (°) 2.31 to 30.05
Index ranges -11 ≤ h ≤ 11 -36 ≤ k ≤ 35 -17 ≤ l ≤ 16	Data/restraints/parameters 7241 / 0 / 314	Goodness-of-fit on F <sup>2</sup> 1.229
R <sub>1</sub> [I > 2σ(I)] 0.0277	wR <sub>2</sub> [all data] 0.0527	

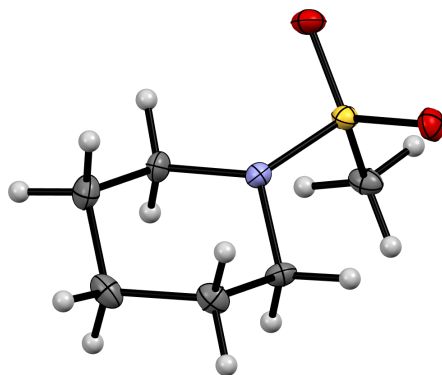




ORTEP/ellipsoid diagram of **65**.

SC-XRD data for **65**.

CCDC 2298723	Chemical Formula $C_6H_{11}NO_2S$	FW (g/mol) 161.22
T (K) 100(2)	$\lambda$ (Å) 0.71073	Crystal size (mm) 0.087 x 0.095 x 0.266
Crystal habit Colorless plate	Crystal system Monoclinic	Space group P 2 <sub>1</sub> /c
a (Å) 14.2783(10)	b (Å) 5.6636(4)	c (Å) 9.7732(6)
$\alpha$ (°) 90	$\beta$ (°) 100.875(3)	$\gamma$ (°) 90
V (Å <sup>3</sup> ) 776.13(9)	Z 4	$\rho_{\text{calc}}$ (g/cm <sup>3</sup> ) 1.380
$\mu$ (mm <sup>-1</sup> ) 0.357	F(000) 344	$\theta$ range (°) 2.90 to 30.54
Index ranges -20 ≤ h ≤ 19 -7 ≤ k ≤ 8 -13 ≤ l ≤ 13	Data/restraints/parameters 2356 / 0 / 90	Goodness-of-fit on F <sup>2</sup> 1.163
R <sub>1</sub> [I > 2σ(I)] 0.0583	wR <sub>2</sub> [all data] 0.1178	



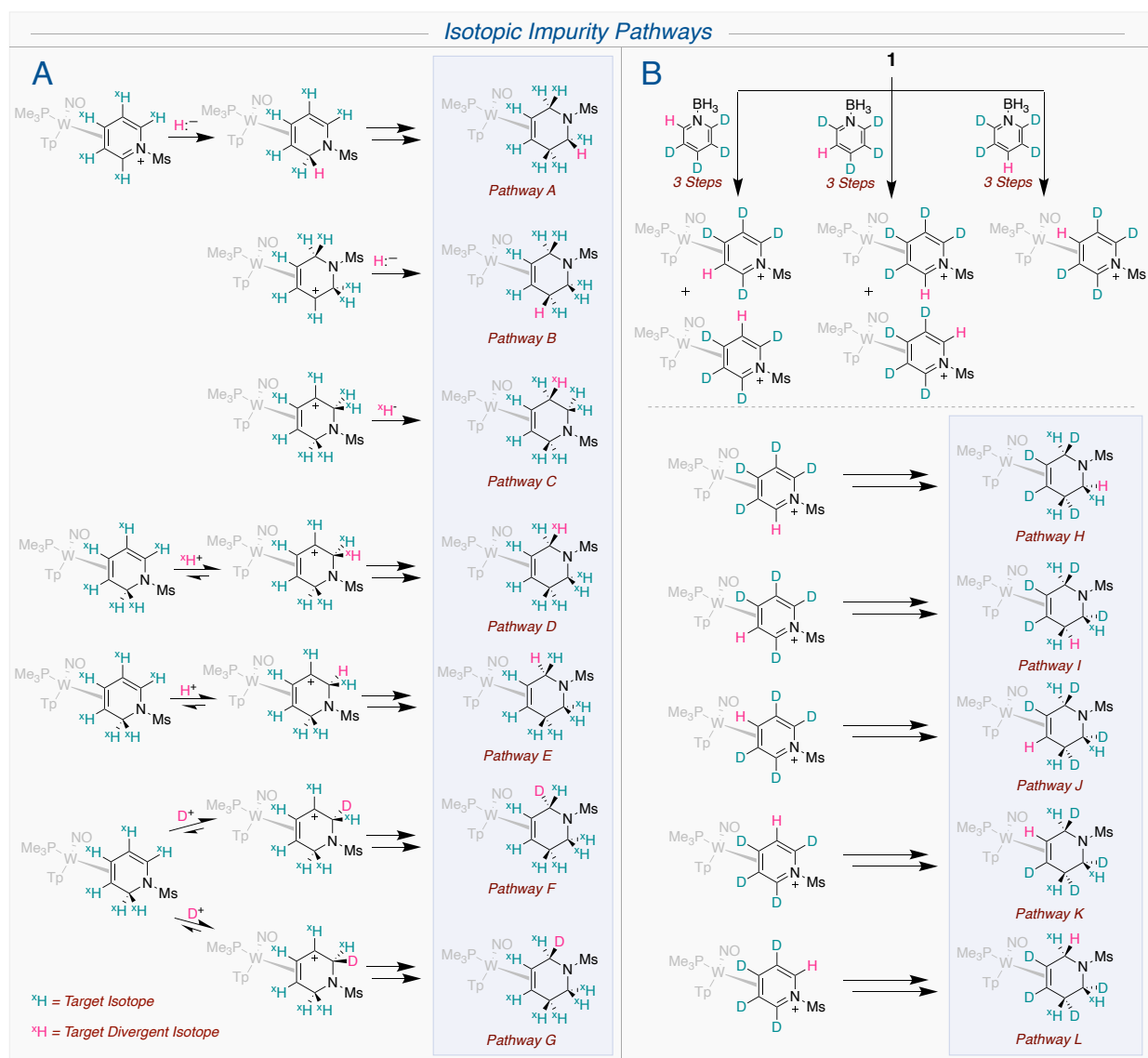
ORTEP/ellipsoid diagram of **66**.

SC-XRD data for **66**.

CCDC 2298724	Chemical Formula $C_6H_{13}NO_2S$	FW (g/mol) 163.23
T (K) 100(2)	$\lambda$ (Å) 0.71073	Crystal size (mm) 0.046 x 0.150 x 0.195
Crystal habit Colorless plate	Crystal system Monoclinic	Space group P 2 <sub>1</sub> /c
a (Å) 14.2951(7)	b (Å) 5.6581(2)	c (Å) 10.0681(5)
$\alpha$ (°) 90	$\beta$ (°) 100.777(2)	$\gamma$ (°) 90
V (Å <sup>3</sup> ) 799.98(6)	Z 4	$\rho_{calc}$ (g/cm <sup>3</sup> ) 1.355
$\mu$ (mm <sup>-1</sup> ) 0.347	F(000) 352	$\theta$ range (°) 2.90 to 28.26
Index ranges -19 ≤ h ≤ 19 -7 ≤ k ≤ 6 -13 ≤ l ≤ 13	Data/restraints/parameters 1980 / 0 / 92	Goodness-of-fit on F <sup>2</sup> 1.264
R <sub>1</sub> [I > 2σ(I)] 0.0521	wR <sub>2</sub> [all data] 0.0964	

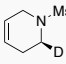
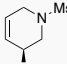
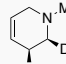
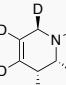
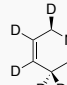
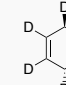
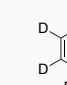
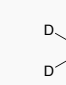
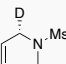
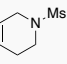
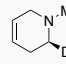
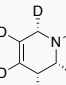
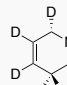
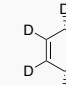
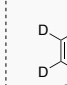
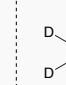
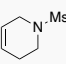
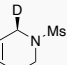
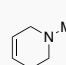
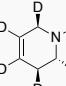
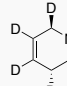
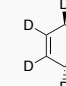
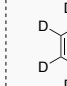
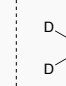
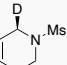
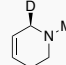
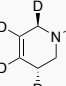
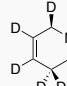
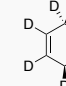
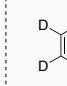
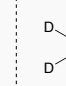
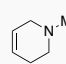
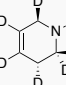
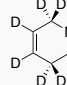
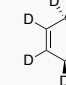
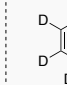
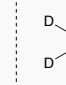
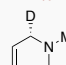
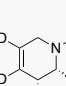
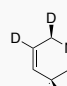
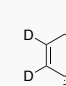
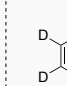
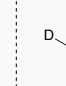
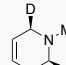
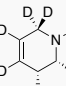
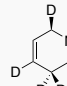
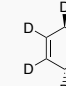
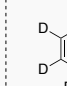
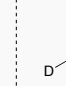
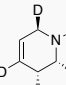
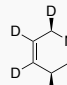
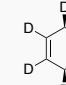
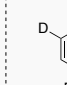
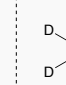
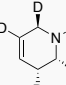
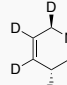
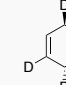
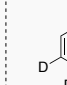
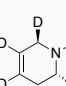
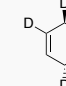
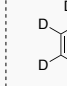
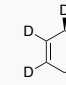
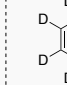
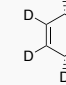
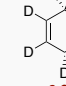
## Molecular Rotational Resonance Spectroscopy Results

After subjecting each sample of **65** to MRR, analysis of each spectrum was then thoroughly conducted and observed peaks were matched to computational simulated peaks, which were in excellent agreement. The composition of each sample was conclusively determined with a detection limit of 0.2% of the overall sample for each impurity. Based on these results, several common impurity pathways were proposed to account for each of these impurities. A sample-by-sample breakdown of species sought, detected, mechanistically explained follows.

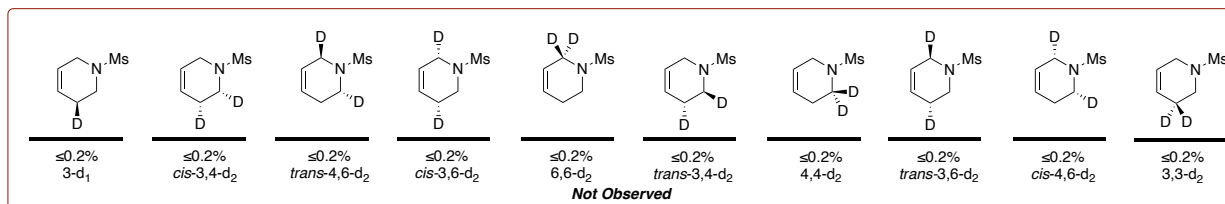
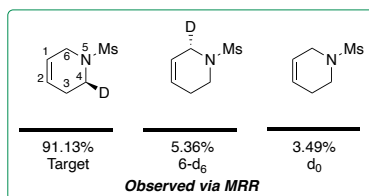


(A) Various impurity pathways observed across samples. (B) Impurities generated stemming from the coordination of various  $d_4$ -pyridine borane species to [W].

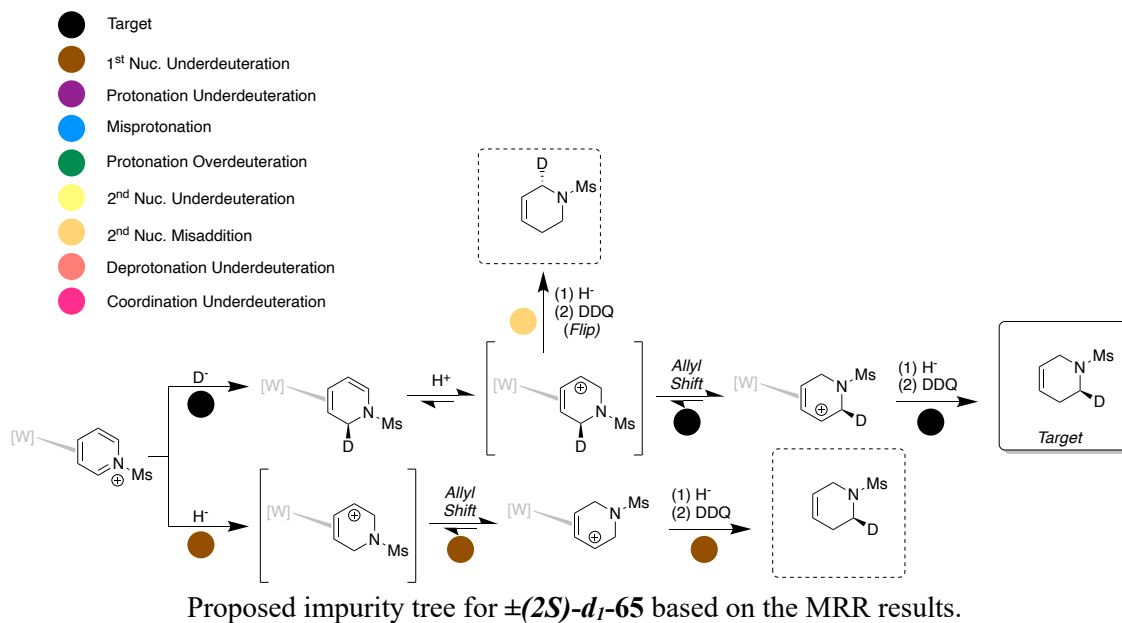
Compounds detected via MRR for each deuterated analogue of **65**. The detection limit is  $\geq 0.2\%$  of the overall sample composition.

 91.13% Target	 94.28% Target	 75.34% Target	 82.36% Target	 85.26% Target	 72.50% Target	 81.89% Target	 72.09% Target
 5.36%	 4.022%	 14.37%	 7.95%	 7.87%	 13.39%	 4.21%	 18.78%
 3.49%	 1.04%	 6.23%	 3.68%	 2.39%	 4.37%	 4.18%	 4.32%
	 0.64%	 1.72%	 1.57%	 1.80%	 2.67%	 3.55%	 2.34%
		 1.47%	 1.18%	 0.76%	 1.39%	 1.75%	 0.85%
		 0.49%	 0.76%	 0.62%	 1.18%	 1.10%	 0.62%
		 0.35%	 0.70%	 0.56%	 1.14%	 1.04%	 0.51%
			 0.66%	 0.49%	 0.88%	 0.62%	 0.47%
			 0.56%	 0.21%	 0.69%	 0.62%	
			 0.52%		 0.64%	 0.54%	
					 0.47%	 0.41%	
					 0.36%		
					 0.25%		

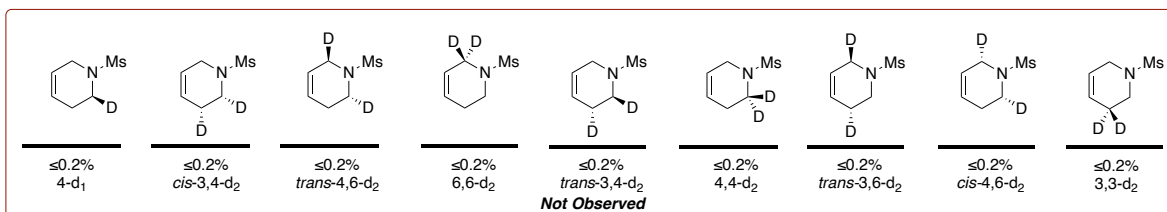
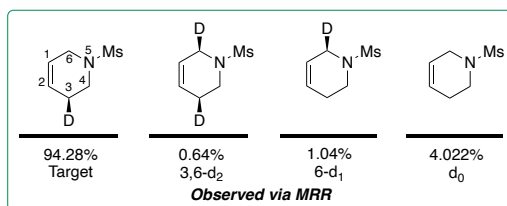
Sample:  $\pm(2S)$ - $d_1$ -65



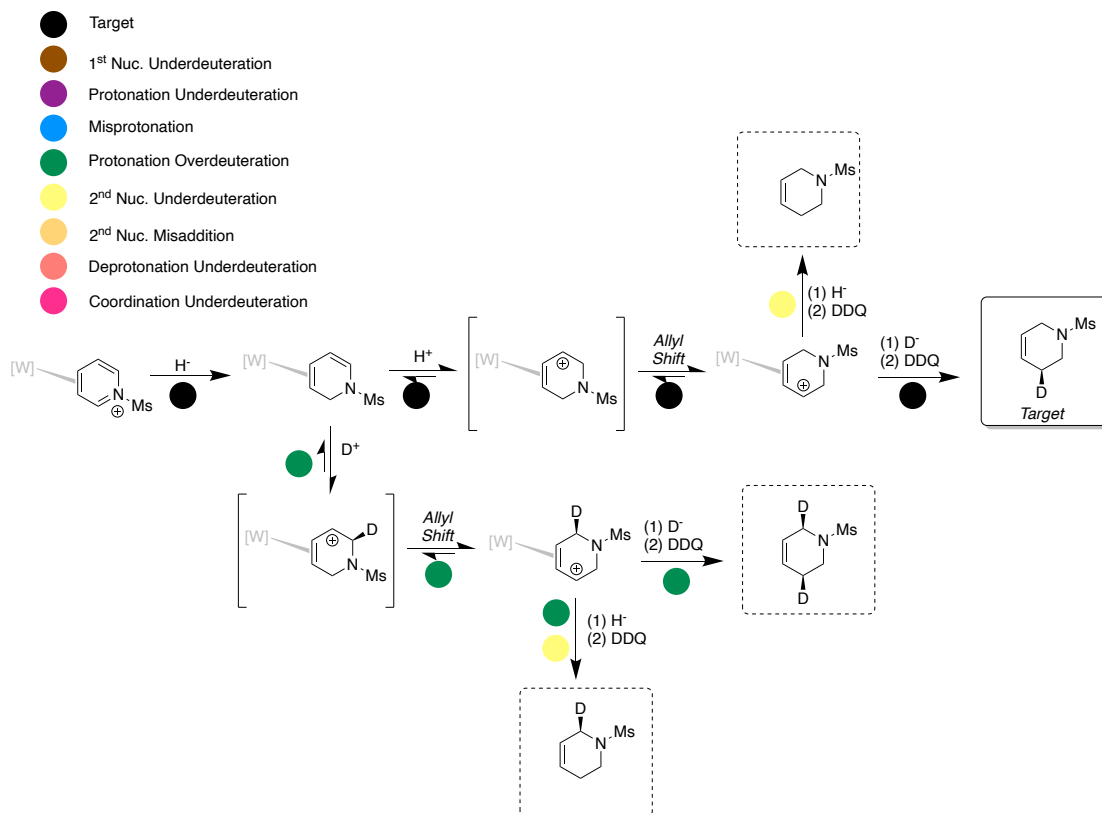
MRR revealed the presence of 3 species (2  $d_1$  and  $d_0$ ) within a 0.2% minimum threshold of the overall mixture. Approximately 91% of the mixture was the target  $\pm(2S)$ - $d_1$ -65. The observed isotopic impurities can be generated via the general impurity pathways originating from **33D**. Other possible  $d_1$  and  $d_2$  impurities were screened but not identified within the detection limit.



Sample:  $\pm(3S)$ -*d*<sub>1</sub>-65

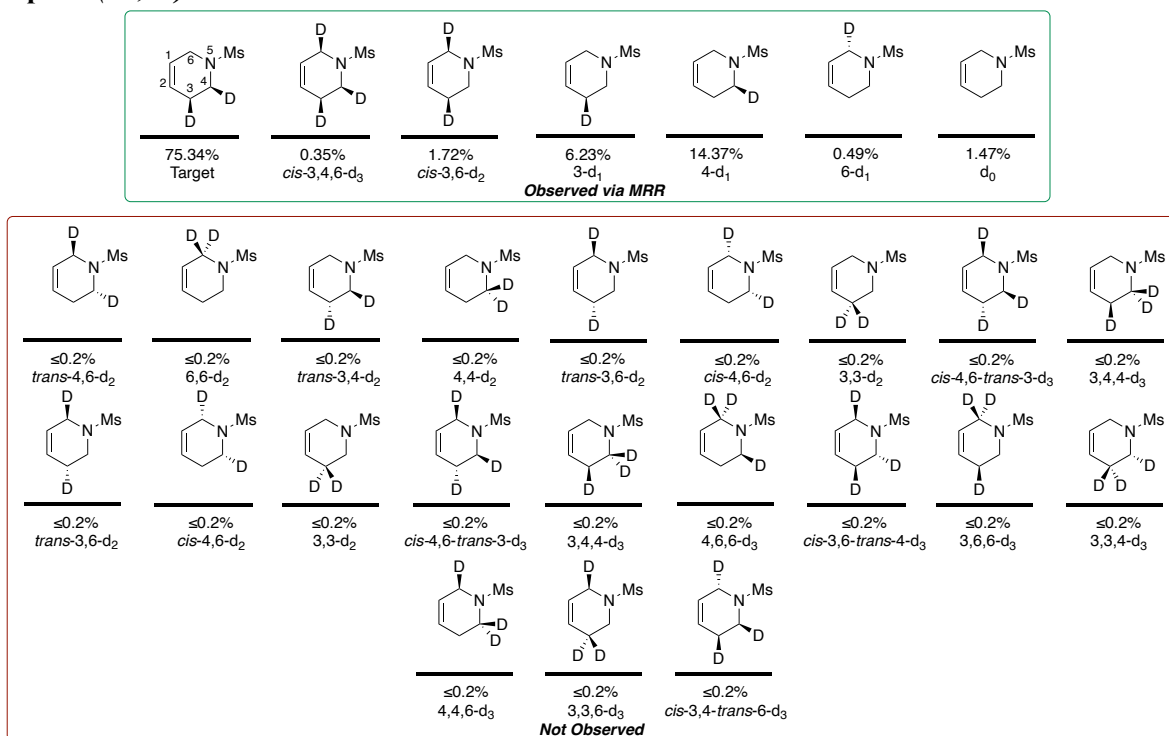


MRR revealed the presence of 4 species (1 d<sub>2</sub>, 2 d<sub>1</sub>, and d<sub>0</sub> compounds) within a 0.2% minimum threshold of the overall mixture. Approximately 94% of the mixture was the target  $\pm(3S)$ -*d*<sub>1</sub>-65. The observed isotopic impurities can be generated via the general impurity pathways originating from **33D**. Impurities 3,6-d<sub>2</sub> and 6-d<sub>1</sub> are likely sourced from a 6-d<sub>1</sub> allyl undergoing a deuteride and hydride addition respectively. Generation of this 6-d<sub>1</sub> allyl is challenging since this complex was not introduced to deuterium until the final deuteride addition, suggesting that perhaps residual BD<sub>3</sub>, formed after successful incorporation of deuteride, may facilitate an H/D exchange with remaining allyl in solution. Other possible d<sub>1</sub> and d<sub>2</sub> impurities were screened but not identified within the detection limit.

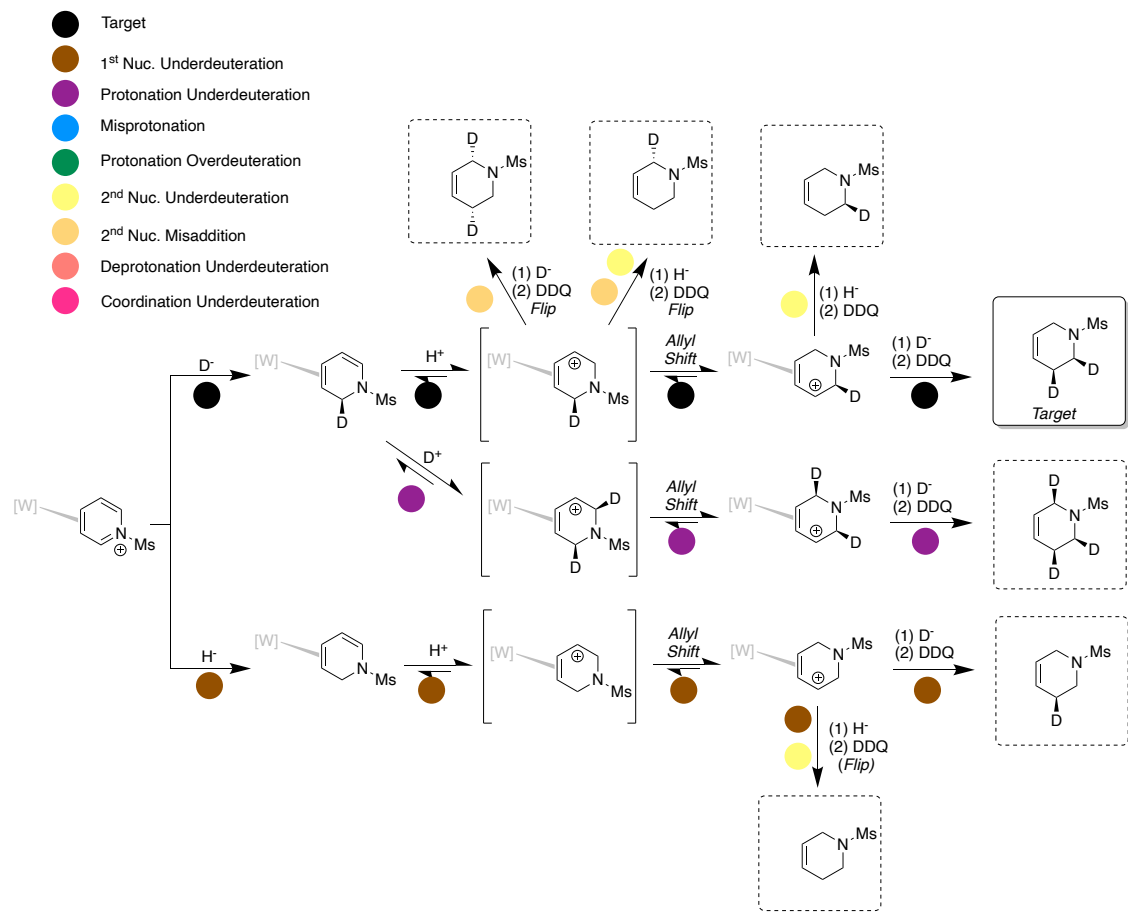


Proposed impurity tree for  $\pm(3S)$ -*d*<sub>1</sub>-65 based on the MRR results.

Sample:  $\pm(2S,3S)$ - $d_2$ -65

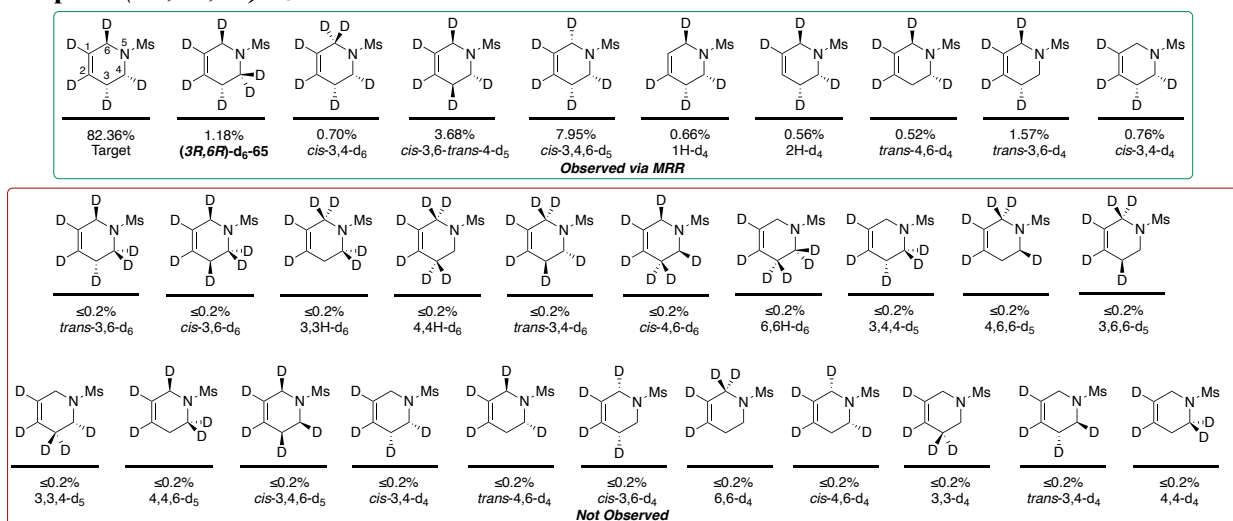


MRR revealed the presence of 7 species (1  $d_3$ , 2  $d_2$ , 3  $d_3$ , and  $d_0$  compounds detected) within a 0.2% minimum threshold of the overall mixture. Approximately 75% of the mixture was the target  $\pm(2S,3S)$ - $d_2$ -65. The observed isotopic impurities can be generated via the general impurity pathways originating from 33D. While the most likely impurity pathways for each sample are proposed, it is likely that multiple impurity pathways aggregate in the formation of these samples. These samples were prepared in racemic mixtures, and conventional MRR cannot distinguish between enantiomers; therefore, impurity pathways that generate enantiomers will be indistinguishable. The common impurity pathways observed in this sample include 1<sup>st</sup> and 2<sup>nd</sup> deuteride underdeuteration, misaddition of the second deuteride, and protonation overdeuteration. Like with the previous sample, the speculated source of  $D^+$  is residually formed  $BD_3$  following successfully incorporated deuteride. Other possible  $d_3$  and  $d_2$  impurities were screened but not identified within the detection limit.

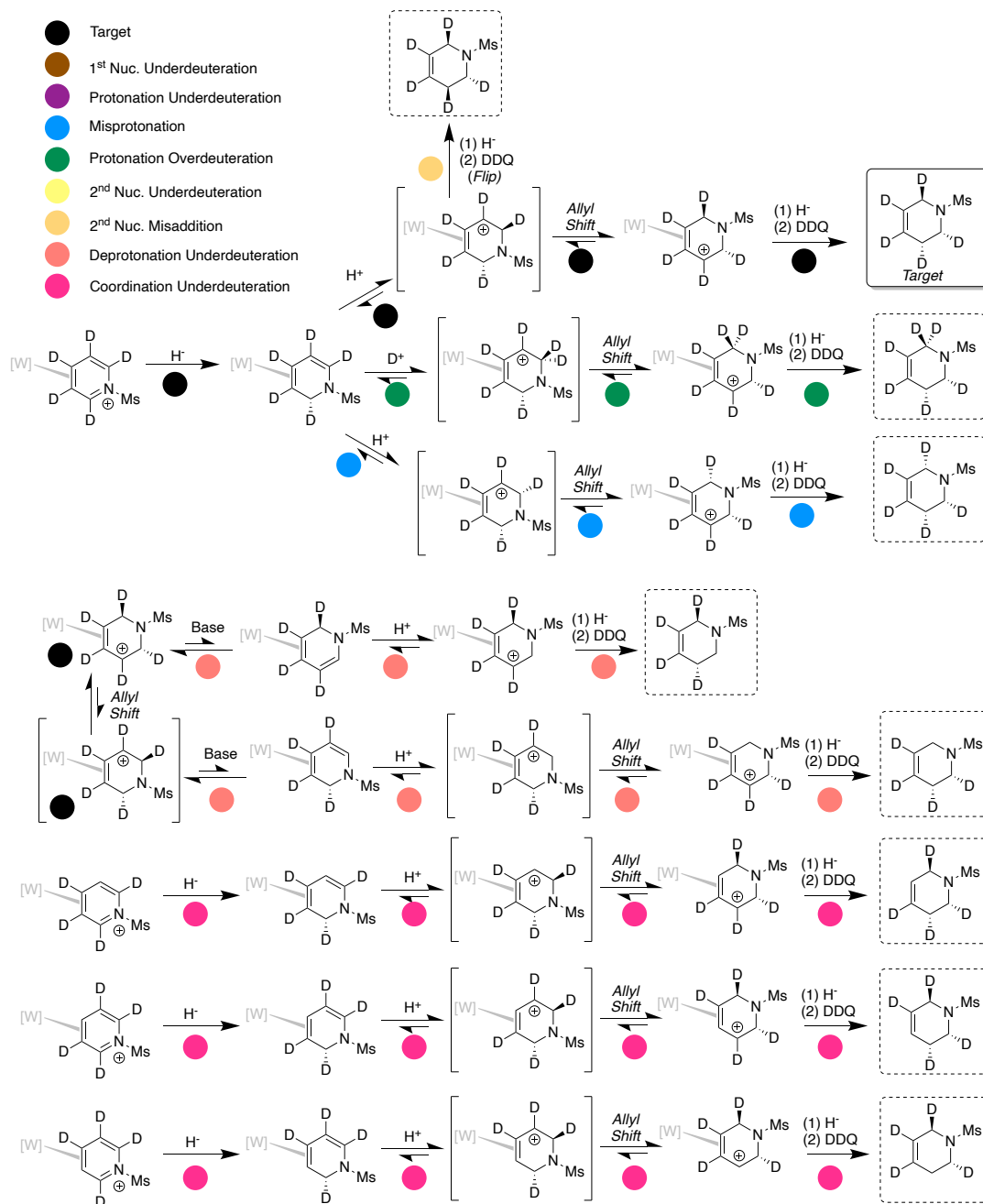




**Sample:  $\pm(2R,3R,6R)$ - $d_5$ -65**

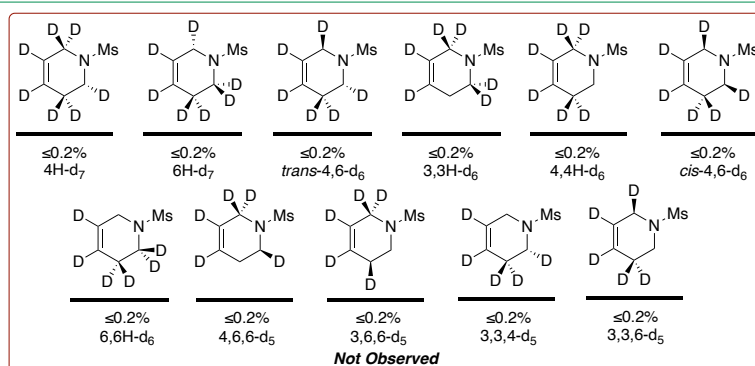
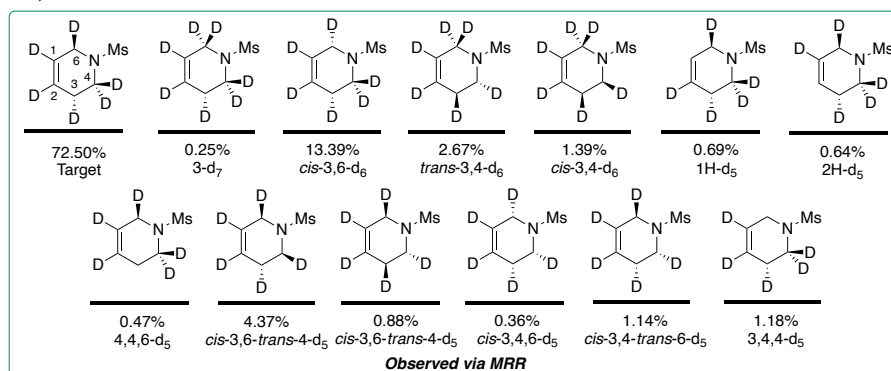


MRR revealed the presence of 10 species (2  $d_6$ , 3  $d_5$ , and 5  $d_4$  compounds detected) within a 0.2% minimum threshold of the overall mixture. Approximately 82% of the mixture was the target  $\pm(2R,3R,6R)$ - $d_5$ -65. Sample  $\pm(3R,6R)$ - $d_6$ -65 was analyzed immediately before this sample, and thus we believe leftover residue accounts for its presence in this sample. The remaining observed isotopic impurities can be generated via the general impurity pathways originating from  $d_5$ -33D. While the most likely impurity pathways for each sample are proposed, it is likely that multiple impurity pathways aggregate in the formation of these samples. These samples were prepared in racemic mixtures, and conventional MRR cannot distinguish between enantiomers; therefore, impurity pathways that generate enantiomers will be indistinguishable. The common impurity pathways observed in this sample include misaddition of the second hydride, misprotonation, protonation overdeuteration, base-promoted elimination underdeuteration, and coordination underdeuteration. Other possible  $d_4$ ,  $d_5$ , and  $d_6$  impurities were screened but not identified within the detection limit.

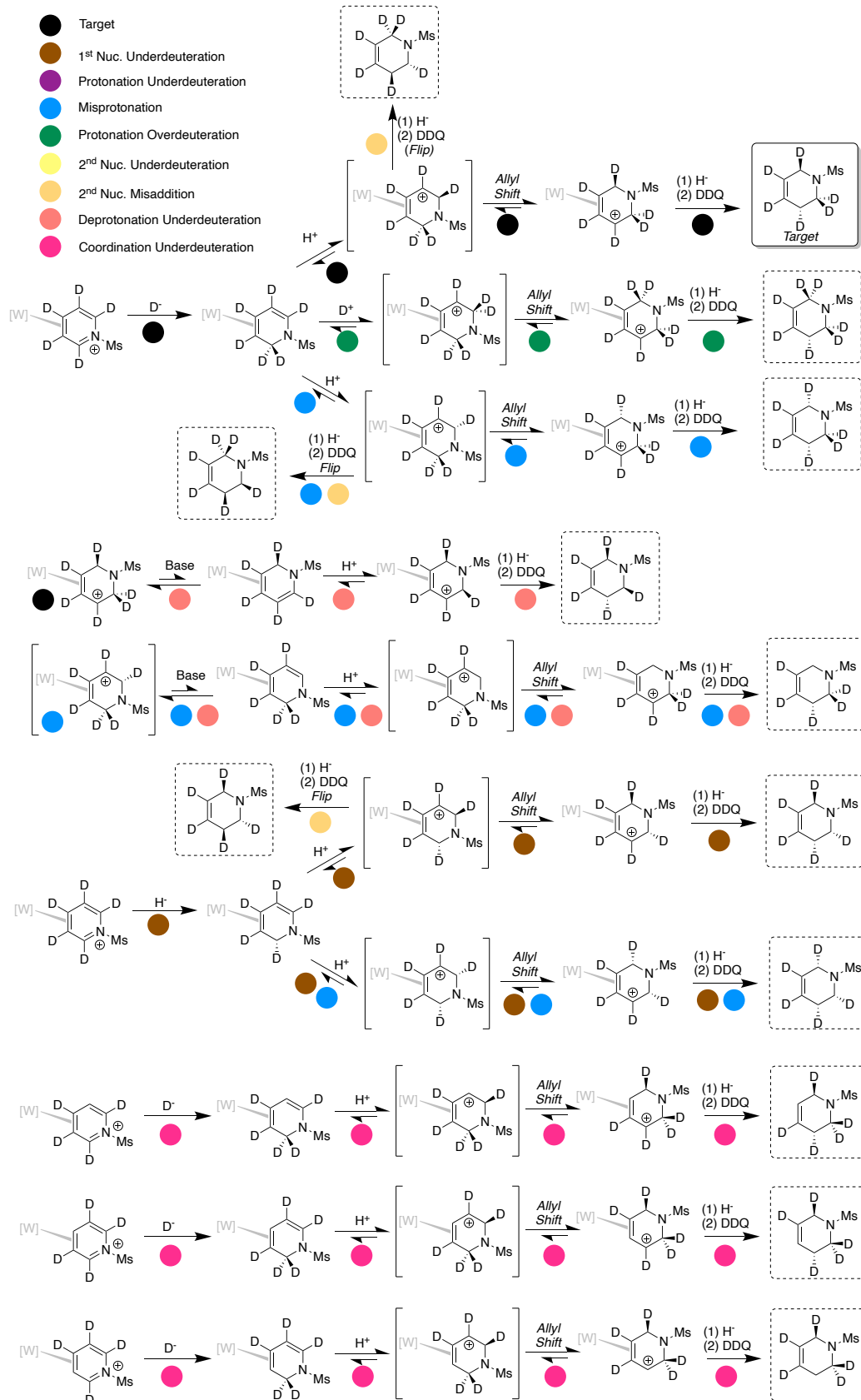


Proposed impurity tree for  $\pm(2R,3R,6R)$ - $d_5$ -65 based on the MRR results.

**Sample:  $\pm(3R,6R)$ -*d*<sub>6</sub>-65**

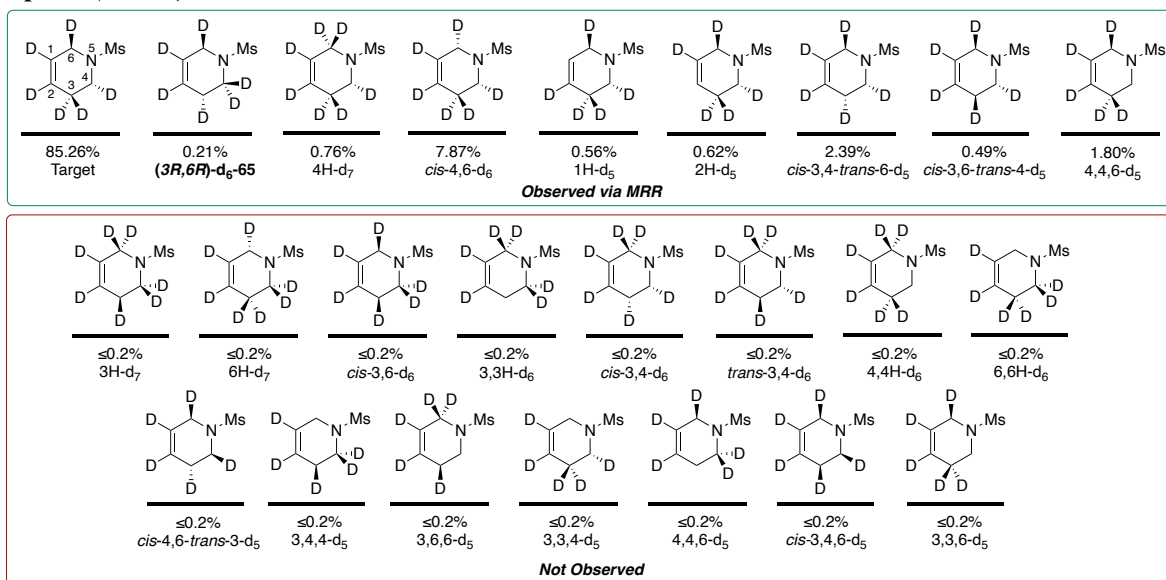


MRR revealed the presence of 13 species (1 d<sub>7</sub>, 4 d<sub>6</sub>, and 8 d<sub>5</sub> compounds detected) within a 0.2% minimum threshold of the overall mixture. Approximately 72% of the mixture was the target  $\pm(3R,6R)$ -*d*<sub>6</sub>-65. This sample was analyzed first, and correspondingly, no other previously analyzed samples were detected, supporting the theory that the presence of previously analyzed targets in other samples are likely carried-over residue. The remaining observed isotopic impurities can be generated via the general impurity pathways originating from *d*<sub>5</sub>-33D. While the most likely impurity pathways for each sample are proposed, it is likely that multiple impurity pathways aggregate in the formation of these samples. These samples were prepared in racemic mixtures, and conventional MRR cannot distinguish between enantiomers; therefore, impurity pathways that generate enantiomers will be indistinguishable. The common impurity pathways observed in this sample include 1<sup>st</sup> nucleophile underdeuteration, misaddition of the second hydride, misprotonation, protonation overdeuteration, base-promoted elimination underdeuteration, and coordination underdeuteration. Other possible d<sub>7</sub>, d<sub>6</sub>, and d<sub>5</sub> impurities were screened but not identified within the detection limit.

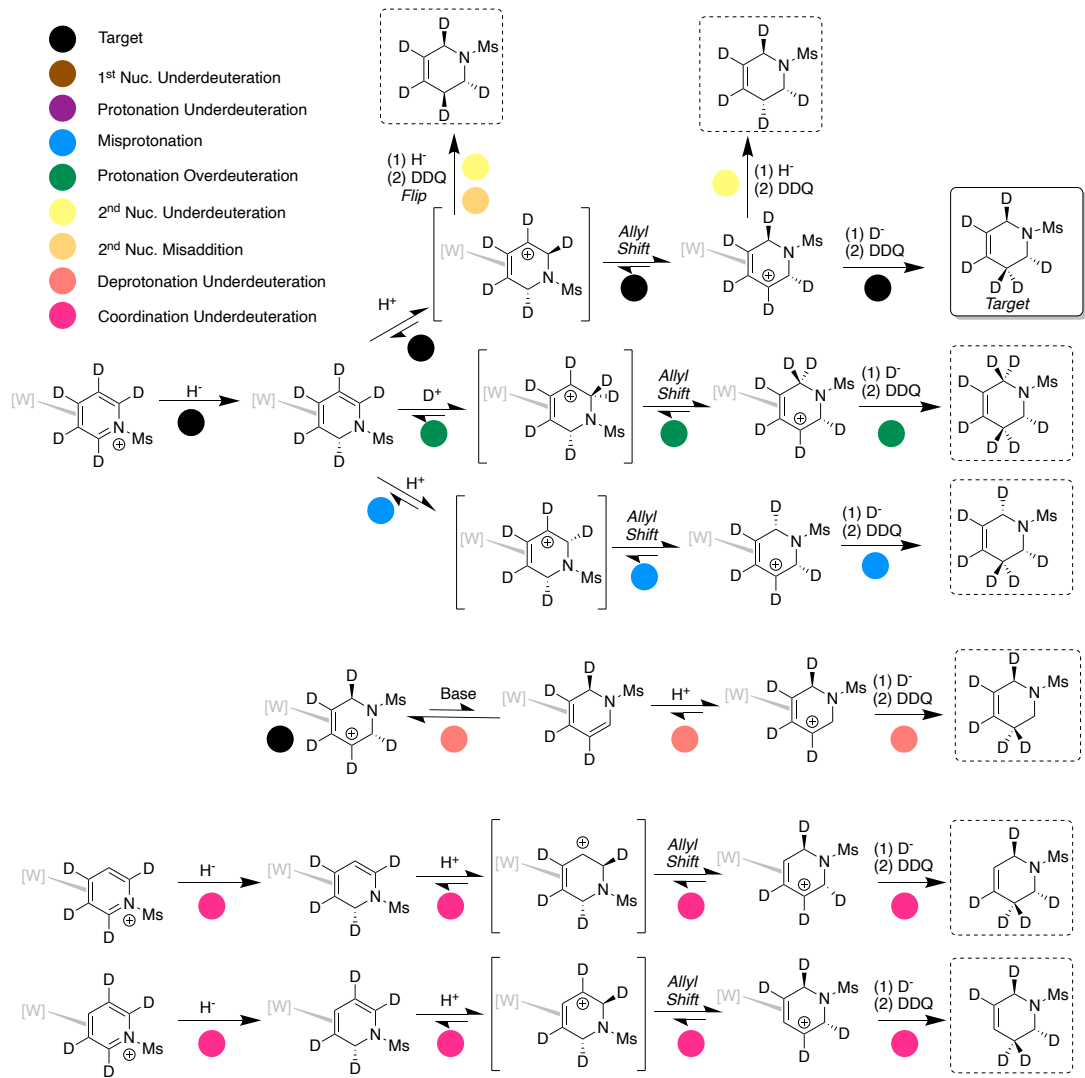


Proposed impurity tree for  $\pm(3R,6R)$ - $d_6$ -65 based on the MRR results.

**Sample:  $\pm(2R,6R)$ - $d_6$ -65**

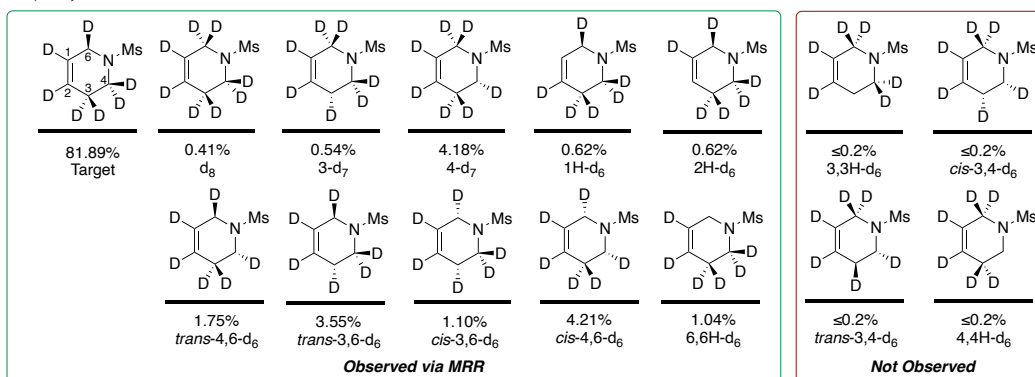


MRR revealed the presence of 9 species (1  $d_7$ , 3  $d_6$ , and 5  $d_5$  compounds detected) within a 0.2% minimum threshold of the overall mixture. Approximately 85% of the mixture was the target  $\pm(2R,6R)$ - $d_6$ -65. Sample  $\pm(3R,6R)$ - $d_6$ -65 was analyzed immediately before this sample, and thus we believe leftover residue accounts for its presence in this sample. The remaining observed isotopic impurities can be generated via the general impurity pathways originating from  $d_5$ -33D. While the most likely impurity pathways for each sample are proposed, it is likely that multiple impurity pathways aggregate in the formation of these samples. These samples were prepared in racemic mixtures, and conventional MRR cannot distinguish between enantiomers; therefore, impurity pathways that generate enantiomers will be indistinguishable. The common impurity pathways observed in this sample include 2<sup>nd</sup> nucleophile underdeuteration/misaddition, misprotonation, protonation overdeuteration, base-promoted elimination underdeuteration, and coordination underdeuteration. However, 2<sup>nd</sup> addition deuterium misaddition simply  $\pm(3R,6R)$ - $d_6$ -65, making this pathway invisible by MRR for this sample. Other possible  $d_7$ ,  $d_6$ , and  $d_5$  impurities were screened but not identified within the detection limit.

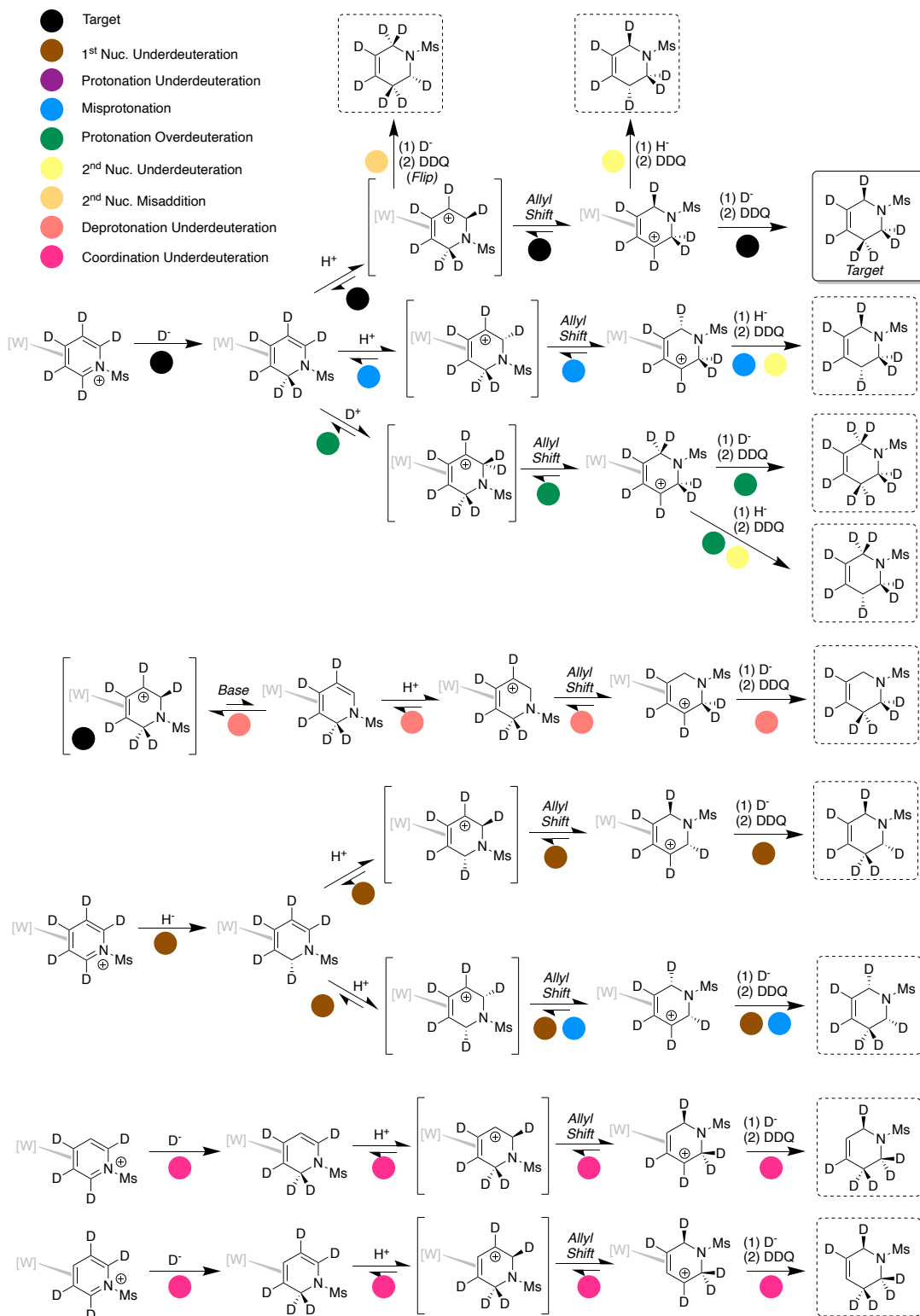


Proposed impurity tree for  $\pm(2R,6R)$ - $d_6$ -65 based on the MRR results.

Sample:  $\pm(6R)$ -*d*<sub>7</sub>-65



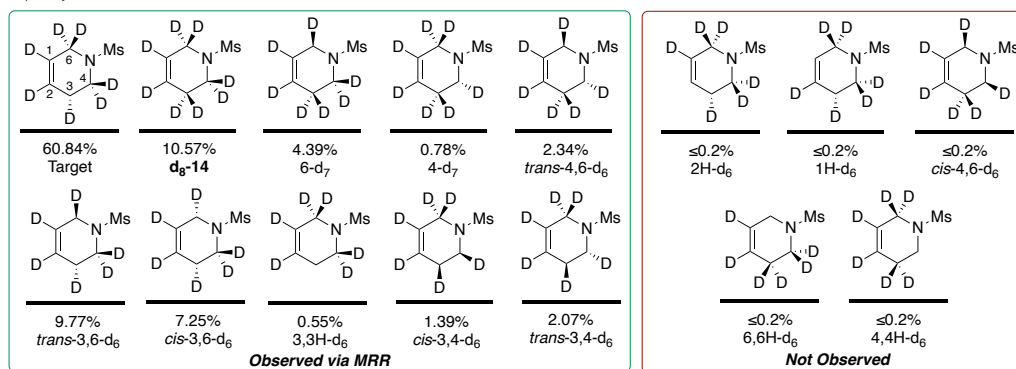
MRR revealed the presence of 11 species (1 *d*<sub>8</sub>, 3 *d*<sub>7</sub>, and 7 *d*<sub>6</sub> compounds detected) within a 0.2% minimum threshold of the overall mixture. Approximately 82% of the mixture was the target  $\pm(6R)$ -*d*<sub>7</sub>-65. Sample *d*<sub>8</sub>-65 was analyzed immediately before this sample, and thus we believe leftover residue accounts for a portion of its presence in this sample. The remaining observed isotopic impurities can be generated via the general impurity pathways originating from *d*<sub>5</sub>-33D. While the most likely impurity pathways for each sample are proposed, it is likely that multiple impurity pathways aggregate in the formation of these samples. These samples were prepared in racemic mixtures, and conventional MRR cannot distinguish between enantiomers; therefore, impurity pathways that generate enantiomers will be indistinguishable. The common impurity pathways observed in this sample include 1<sup>st</sup> nucleophile underdeuteration, 2<sup>nd</sup> nucleophile underdeuteration/misaddition, misprotonation, protonation overdeuteration, base-promoted elimination underdeuteration, and coordination underdeuteration. Other possible *d*<sub>6</sub> impurities were screened but not identified within the detection limit.



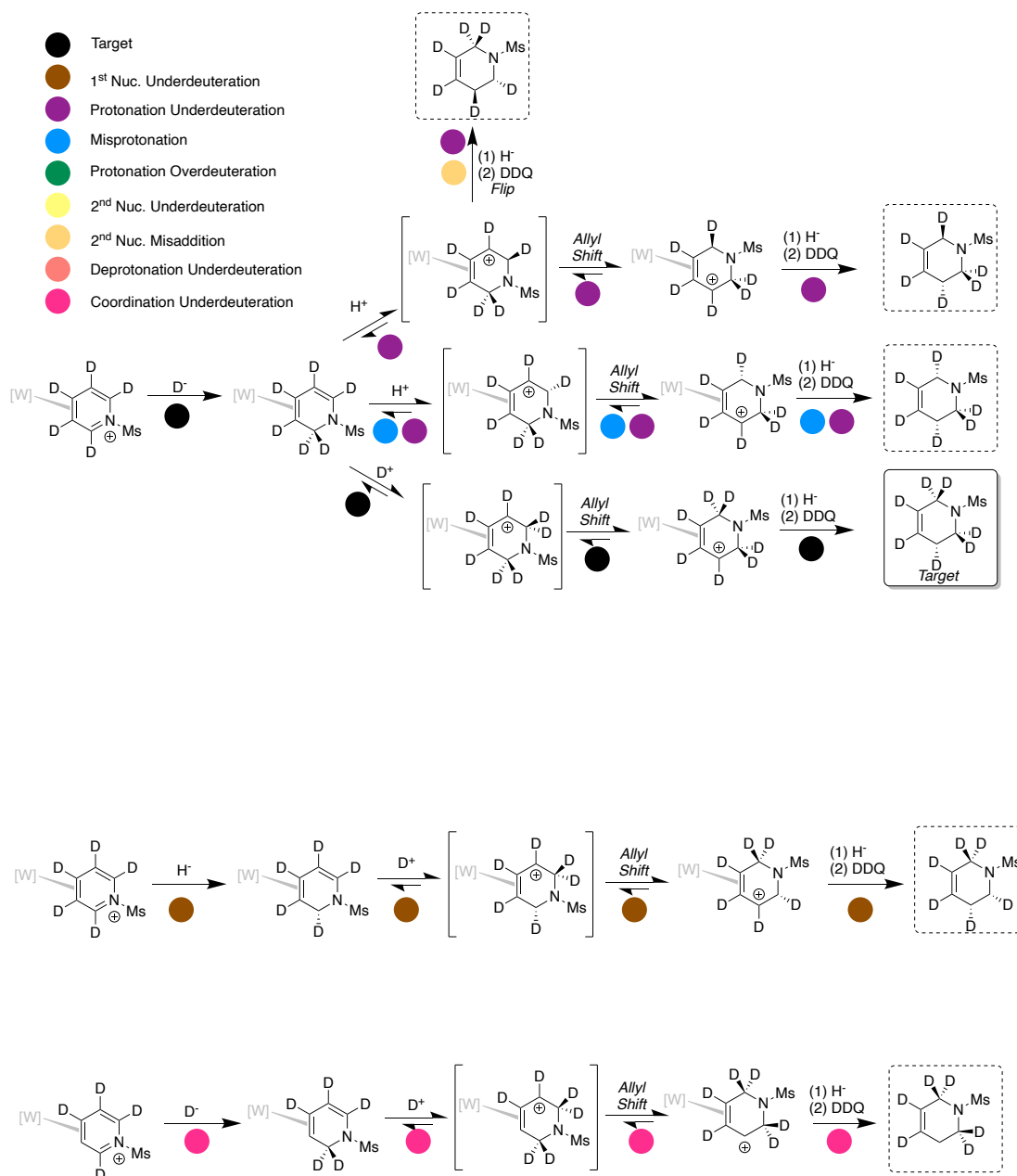
Proposed impurity tree for  $\pm(6R)\text{-}d_7\text{-}65$  based on the MRR results.



Sample:  $\pm(3R)$ -*d*<sub>7</sub>-65

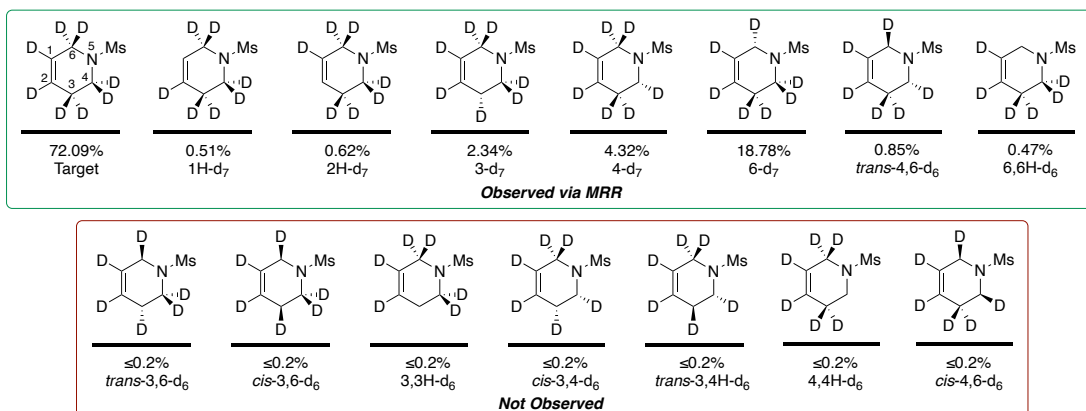


MRR revealed the presence of 10 species (1 *d*<sub>8</sub>, 3 *d*<sub>7</sub>, and 6 *d*<sub>6</sub> compounds detected) within a 0.2% minimum threshold of the overall mixture. Approximately 61% of the mixture was the target  $\pm(3R)$ -*d*<sub>7</sub>-65. The presence of *d*<sub>8</sub>, 6-*d*<sub>7</sub>, 4-*d*<sub>7</sub>, and *trans*-4,6-*d*<sub>6</sub> were particularly enigmatic as they could only be formed from deuteride adding a second nucleophile. This should not occur given that the precursor allyl was in the presence of excess borohydride which, even if it could exchange with residual deuterium to render a deuteride source, would need to overcome the kinetic isotope effect to outcompete addition of the remaining hydride. Alternatively, the *d*<sub>8</sub>-65 was analyzed directly before this sample, and each of these impurities were present in this sample. It is possible that each of these samples carried over from the previous analysis; however, the ratio between these compounds in this sample is not the same as in the *d*<sub>8</sub>-65 sample. Furthermore, carryover in previous samples was observed ≤1% the total composition, each of these impurities carrying over would comprise ≥16% of the entire sample. The remaining observed isotopic impurities can be generated via the general impurity pathways originating from *d*<sub>5</sub>-33D. While the most likely impurity pathways for each sample are proposed, it is likely that multiple impurity pathways aggregate in the formation of these samples. These samples were prepared in racemic mixtures, and conventional MRR cannot distinguish between enantiomers; therefore, impurity pathways that generate enantiomers will be indistinguishable. The common impurity pathways observed in this sample include 1<sup>st</sup> nucleophile underdeuteration, 2<sup>nd</sup> nucleophile misaddition, misprotonation, protonation underdeuteration, and coordination underdeuteration. Other possible *d*<sub>6</sub> impurities were screened but not identified within the detection limit.

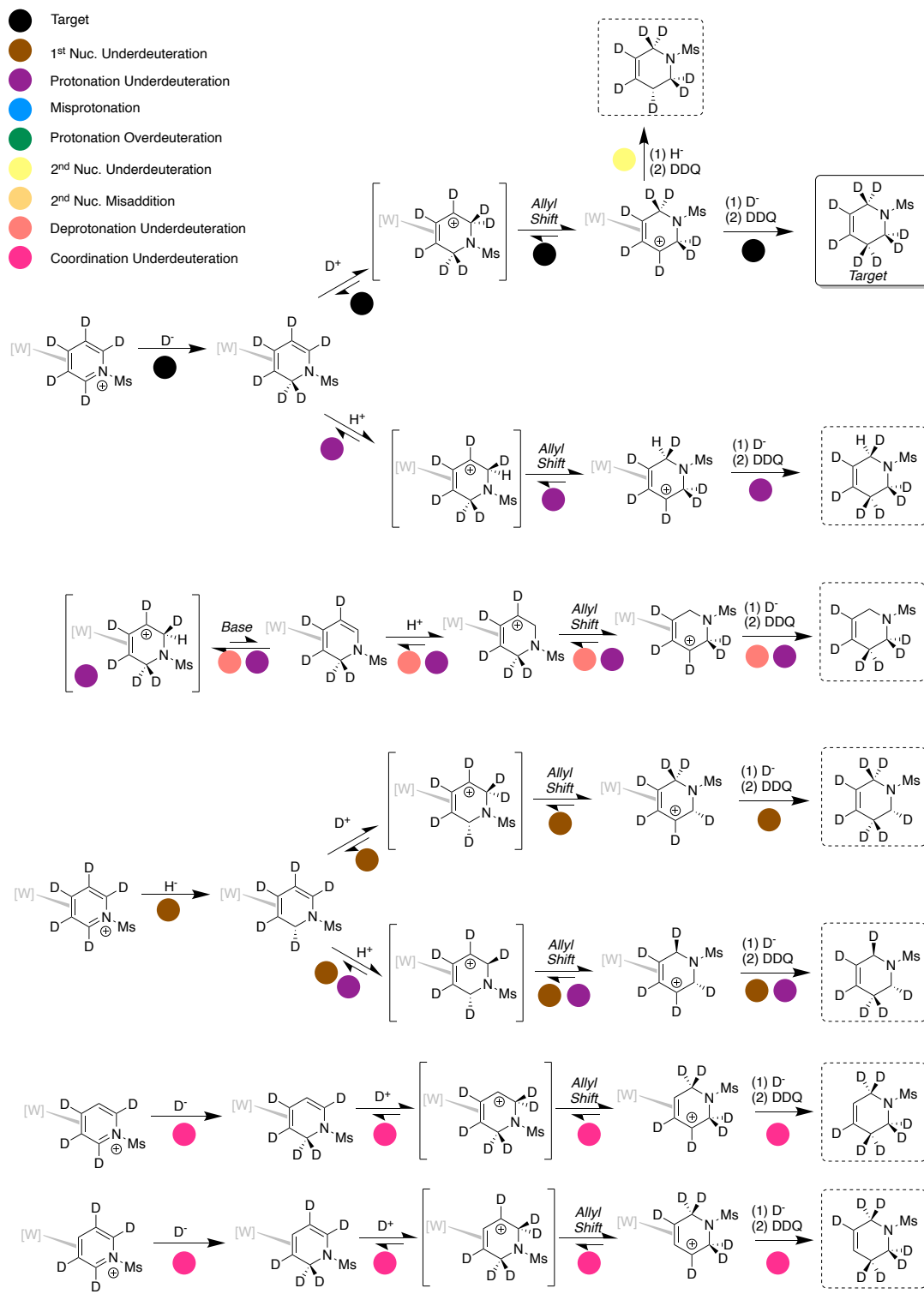


Proposed impurity tree for  $\pm(3R)$ -d-65 based on the MRR results.

Sample: *d*<sub>8</sub>-65



MRR revealed the presence of 8 species (1 *d*<sub>8</sub>, 5 *d*<sub>7</sub>, and 2 *d*<sub>6</sub> compounds detected) within a 0.2% minimum threshold of the overall mixture. Approximately 72% of the mixture was the target *d*<sub>8</sub>-65. Previously analyzed samples were not detected within this sample. The remaining observed isotopic impurities can be generated via the general impurity pathways originating from *d*<sub>5</sub>-33D. While the most likely impurity pathways for each sample are proposed, it is likely that multiple impurity pathways aggregate in the formation of these samples. These samples were prepared in racemic mixtures, and conventional MRR cannot distinguish between enantiomers; therefore, impurity pathways that generate enantiomers will be indistinguishable. The common impurity pathways observed in this sample include 1<sup>st</sup> nucleophile underdeuteration, 2<sup>nd</sup> nucleophile underdeuteration, misprotonation, protonation underdeuteration, base-promoted elimination underdeuteration, and coordination underdeuteration. However, misaddition impurities also form *d*<sub>8</sub>-65, making this pathway invisible in this sample. Other possible *d*<sub>7</sub> and *d*<sub>6</sub> impurities were screened but not identified within the detection limit.



Proposed impurity tree for  $d_8$ -65 based on the MRR results.

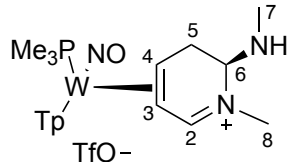
## References:

- (1) Ramachandran, P. V.; Kulkarni, A. S.; Zhao, Y.; Mei, J. Amine-boranes bearing borane-incompatible functionalities: application to selective amine protection and surface functionalization. *Chem. Commun. (Camb.)* **2016**, 52 (80), 11885-11888.
- (2) Harrison, D. P.; Welch, K. D.; Nielander, A. C.; Sabat, M.; Myers, W. H.; Harman, W. D. Efficient synthesis of an  $\eta^2$ -pyridine complex and a preliminary investigation of the bound heterocycle's reactivity. *J. Am. Chem. Soc.* **2008**, 130 (50), 16844-16845.
- (3) Delafuente, D. A.; Kosturko, G. W.; Graham, P. M.; Harman, W. H.; Myers, W. H.; Surendranath, Y.; Klet, R. C.; Welch, K. D.; Trindle, C. O.; Sabat, M.; Harman, W. D. Isomerization dynamics and control of the  $\eta^2/N$  equilibrium for pyridine complexes. *J. Am. Chem. Soc.* **2007**, 129 (2), 406-416.

# Appendix E

## Chapter 5 Data

**Synthesis and characterization of  $W\text{Tp}(\text{NO})(\text{PMe}_3)(\eta^2\text{-}N\text{-methyl-6-methylamino-5,6-dihydropyridin-2-ium})(\text{OTf})$  (**70**)**



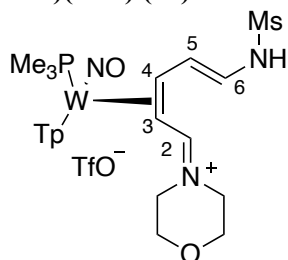
To an oven-dried 4-dram vial was added a stir pea, **5D** (101 mg, 0.11 mmol), 2.0M methylamine in THF (0.2 mL, 0.40 mmol), EtCN (1 mL), and DCM (2 mL). The solution was stirred for 5 minutes and then added to a 50 mL of stirring Et<sub>2</sub>O. A tan powder was precipitated, collected on a 15 mL F frit, washed 2x with 10 mL of Et<sub>2</sub>O, and dried in a desiccator (77 mg, 87% yield).

<sup>1</sup>H NMR (CD<sub>3</sub>CN, δ, 25 °C): 8.82 (d, *J* = 5.0 Hz, 1H, H2), 8.07 (d, *J* = 2.0 Hz, 1H, Tp3/5), 7.99 (d, *J* = 2.1 Hz, 1H, Tp3/5), 7.95 (d, *J* = 2.3 Hz, 2H, Tp3/5), 7.78 (d, *J* = 2.4 Hz, 1H, Tp3/5), 7.73 (d, *J* = 2.2 Hz, 1H, Tp3/5), 6.48 (t, *J* = 2.3 Hz, 1H, Tp4), 6.42 (t, *J* = 2.3 Hz, 1H, Tp4), 6.38 (t, *J* = 2.3 Hz, 1H, Tp4), 4.54 (dd, *J* = 6.4, 11.1 Hz, 1H, H6), 4.19-4.24 (m, 1H, H5), 3.61 (s, 3H, H9), 3.25-3.29 (m, 1H, H4), 3.18 (dd, *J* = 6.4, 14.7 Hz, 1H, H5), 2.48 (s, 3H, H8), 2.29 (dd, *J* = 5.0, 8.1 Hz, 1H, H3), 1.22 (d, *J*<sub>PH</sub> = 9.2 Hz, 9H, PMe<sub>3</sub>).

<sup>13</sup>C NMR (CD<sub>3</sub>CN, δ, 25 °C): 181.5 (C2), 148.8 (Tp3/5), 145.4 (Tp3/5), 142.5 (Tp3/5), 139.2 (Tp3/5), 138.8 (Tp3/5), 137.7 (Tp3/5), 122.1 (q, *J*<sub>FC</sub> = 321.7 Hz, OTf), 108.6 (Tp4), 107.9 (Tp4), 107.8 (Tp4), 74.0 (C6), 59.6 (d, *J*<sub>PC</sub> = 15.1 Hz, C4), 50.8 (C3), 40.3 (C9), 35.1 (C5), 31.5 (C8), 12.9 (d, *J*<sub>PC</sub> = 31.3 Hz, 3C, PMe<sub>3</sub>).

HRMS (ESI) *m/z*: [M]<sup>+</sup> Calcd for C<sub>19</sub>H<sub>32</sub>BN<sub>9</sub>OPW<sup>+</sup> 628.2064; Found 628.2064

**Synthesis and characterization of  $W\text{Tp}(\text{NO})(\text{PMe}_3)(\eta^2\text{-}N\text{-mesyl-1-morpholino-3,5-dienylimin-1-ium})(\text{OTf})$  (**71**)**



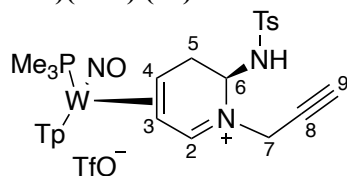
To an oven-dried 10 mL test tube was added, **33D** (56 mg, 0.06 mmol) and DCM (2 mL). To a separate dried 10 mL tube was added morpholine (45 mg, 0.52 mmol) and DCM. Both solutions were chilled at -20 °C for 15 minutes, and then the amine solution was added to the solution of **33D**. The solution was then manually swirled, sat in the bath for 15 minutes, and then added to a 50 mL of stirring Et<sub>2</sub>O. A tan powder was precipitated, collected on a 15 mL F frit, washed 2x with 10 mL of Et<sub>2</sub>O, and dried in a desiccator (45 mg, 79% yield).

<sup>1</sup>H NMR (CD<sub>3</sub>CN, δ, 25 °C): 8.05 (m, 1H, Tp3/5), 7.97 (d, *J* = 2.1 Hz, 1H, Tp3/5), 7.94 (d, *J* = 2.2 Hz, 1H, Tp3/5), 7.92 (m, 1H, Tp3/5), 7.88 (m, 1H, Tp3/5), 7.65 (d, *J* = 11.8 Hz, 1H, H2), 7.49 (m, 1H, Tp3/5), 6.40-6.48 (m, 3H, Tp4), 6.13 (d, *J* = 8.6 Hz, 1H, H6), 5.68 (dd, *J* = 8.7, 10.7 Hz, 1H, H5), 3.98-4.04 (m, 1H, H4), 3.20-3.96 (m, 8H, morpholine), 3.09 (s, 3H, Ms), 2.56 (dd, *J* = 8.9, 11.8 Hz, 1H, H3), 1.17 (d, *J*<sub>PH</sub> = 9.4 Hz, 9H, PMe<sub>3</sub>).

HRMS (ESI) *m/z*: [M]<sup>+</sup> Calcd for C<sub>22</sub>H<sub>36</sub>BN<sub>9</sub>O<sub>4</sub>PSW<sup>+</sup> 748.1945; Found 748.1952



**Synthesis and characterization of WTp(NO)(PMe<sub>3</sub>)(η<sup>2</sup>-*N*-propargyl-6-tosyl)-5,6-dihydropyridin-2-ium)(OTf) (72)**



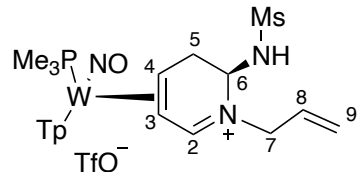
To an oven-dried 4-dram vial was added a stir pea, **5D** (231 mg, 0.26 mmol), propargylamine (61 mg, 1.11 mmol), EtCN (2 mL), and DCM (3 mL). The solution was stirred for 20 seconds and then added to a 50 mL of stirring Et<sub>2</sub>O. A tan powder was precipitated, collected on a 15 mL F frit, washed 2x with 10 mL of Et<sub>2</sub>O, and dried in a desiccator (181 mg, 74% yield).

<sup>1</sup>H NMR (CD<sub>3</sub>CN, δ, 25 °C): 9.12 (d, *J* = 5.4 Hz, 1H, H2), 8.00-8.01 (m, 2H, Tp3/5), 7.93-7.95 (m, 2H, Tp3/5), 7.86 (d, *J* = 8.1 Hz, 2H, Ts), 7.76-7.77 (m, 1H, Tp3/5), 7.66-7.68 (m, 1H, Tp3/5), 7.45 (d, *J* = 8.1 Hz, Ts), 6.44 (t, *J* = 2.2 Hz, Tp4), 6.39 (t, *J* = 2.3 Hz, Tp4), 6.35 (t, *J* = 2.3 Hz, Tp4), 5.07 (dd, *J* = 6.6, 11.2 Hz, 1H, H6), 4.74 (q, *J* = 18.1 Hz, 2H, H7), 3.22-3.27 (m, 1H, H4), 3.08 (t, *J* = 2.5 Hz, 1H, H9), 2.65 (dd, *J* = 6.5, 14.4 Hz, 1H, H5), 2.45 (s, 3H, Ts), 2.42 (obscured, H3), 0.91 (d, *J*<sub>PH</sub> = 9.3 Hz, 9H, PMe<sub>3</sub>).

<sup>13</sup>C NMR (CD<sub>3</sub>CN, δ, 25 °C): 181.5 (C2), 149.1 (Tp3/5), 145.7 (Ts), 145.2 (Tp3/5), 142.4 (Tp3/5), 139.3 (Tp3/5), 139.1 (Tp3/5), 138.0 (Ts), 137.8 (Tp3/5), 131.2 (2C, Ts), 128.3 (2C, Ts), 122.9 (q, *J*<sub>FC</sub> = 320.4 Hz, OTf), 108.8 (Tp4), 108.1 (Tp4), 108.0 (Tp4), 79.4 (d, *J*<sub>PC</sub> = 3.7 Hz, C9), 77.6 (C8), 67.2 (C6), 59.9 (d, *J*<sub>PC</sub> = 15.5 Hz, C4), 52.7 (C3), 41.8 (C7), 37.4 (C5), 21.6 (Ts), 12.6 (d, *J*<sub>PC</sub> = 31.6 Hz, 3C, PMe<sub>3</sub>).

HRMS (ESI) *m/z*: [M]<sup>+</sup> Calcd for C<sub>27</sub>H<sub>36</sub>BN<sub>9</sub>O<sub>3</sub>PSW<sup>+</sup> 792.1996; Found 792.2002

**Synthesis and characterization of WTp(NO)(PMe<sub>3</sub>)(η<sup>2</sup>-N-allyl-6-tosyl)-5,6-dihydropyridin-2-ium)(OTf) (73)**

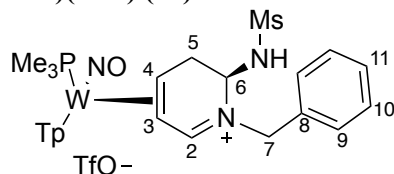


To an oven-dried 10 mL test tube was added, **33D** (46 mg, 0.06 mmol) and DCM (2 mL). To a separate dried 10 mL tube was added allylamine (16 mg, 0.28 mmol) and DCM. Both solutions were chilled at -20 °C for 15 minutes, and then the amine solution was added to the solution of **33D**. The solution was then manually swirled, sat in the bath for 15 minutes, and then added to a 50 mL of stirring Et<sub>2</sub>O. A tan powder was precipitated, collected on a 15 mL F frit, washed 2x with 10 mL of Et<sub>2</sub>O, and dried in a desiccator (24 mg, 49% yield).

<sup>1</sup>H NMR (CD<sub>3</sub>CN, δ, 25 °C): See below. Not assigned due to lack of 2D

HRMS (ESI) m/z: [M]<sup>+</sup> Calcd for C<sub>21</sub>H<sub>34</sub>BN<sub>9</sub>O<sub>3</sub>PSW<sup>+</sup> 718.1840; Found 718.1848

**Synthesis and characterization of WTp(NO)(PMe<sub>3</sub>)( $\eta^2$ -*N*-benzyl-6-mesyl)-5,6-dihydropyridin-2-ium)(OTf) (74)**



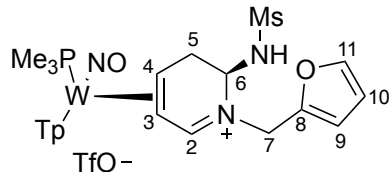
To an oven-dried 4-dram vial was added a stir pea, **33D** (46 mg, 0.06 mmol), benzylamine (32 mg, 0.30 mmol), EtCN (1 mL), and DCM (2 mL). The solution was stirred for 10 seconds and then added to a 50 mL of stirring Et<sub>2</sub>O. A tan powder was precipitated, collected on a 15 mL F frit, washed 2x with 10 mL of Et<sub>2</sub>O, and dried in a desiccator (44 mg, 84% yield).

<sup>1</sup>H NMR (CD<sub>3</sub>CN,  $\delta$ , 25 °C): 8.62 (d,  $J$  = 5.3 Hz, 1H, H2), 8.11 (d,  $J$  = 1.9 Hz, 1H, Tp3/5), 7.94 (d,  $J$  = 2.3 Hz, 1H, Tp3/5), 7.93 (d,  $J$  = 2.2 Hz, 1H, Tp3/5), 7.72 (d,  $J$  = 1.9 Hz, 1H, Tp3/5), 7.69 (d,  $J$  = 2.3 Hz, 1H, Tp3/5), 7.57 (d,  $J$  = 7.7 Hz, 2H, H9), 7.44-7.50 (m, 3H, H10 & 11), 6.89 (d,  $J$  = 1.8 Hz, 1H, Tp3/5), 6.46 (t,  $J$  = 2.2 Hz, 1H, Tp4), 6.39 (t,  $J$  = 2.3 Hz, 1H, Tp4), 6.09 (t,  $J$  = 2.2 Hz, 1H, Tp4), 5.41 (dd,  $J$  = 6.2, 10.8 Hz, 1H, H6), 5.21 (d,  $J$  = 14.7 Hz, 1H, H7), 4.98 (d,  $J$  = 14.7 Hz, 1H, H7), 4.31-4.35 (m, 1H, H5), 3.35-3.39 (m, 2H, H4 & H5), 3.07 (s, 3H, Ms), 2.37 (dd,  $J$  = 5.8, 7.4 Hz, 1H, H3), 1.20 (d,  $J_{PH}$  = 9.3 Hz, 9H, PMe<sub>3</sub>).

<sup>13</sup>C NMR (CD<sub>3</sub>CN,  $\delta$ , 25 °C): 181.8 (C2), 148.7 (Tp3/5), 145.3 (Tp3/5), 142.5 (Tp3/5), 139.3 (Tp3/5), 139.0 (Tp3/5), 137.6 (Tp3/5), 135.8 (C8), 131.3 (2C, C10), 130.4 (2C, C9), 130.1 (C11), 122.1 (q,  $J_{FC}$  = 323.0 Hz, OTf), 108.7 (Tp4), 108.0 (Tp4), 107.6 (Tp4), 67.9 (C6), 59.6 (d,  $J_{PC}$  = 15.5 Hz, C4), 55.7 (C7), 52.0 (C3), 42.4 (Ms), 38.5 (C5), 12.8 (d,  $J_{PC}$  = 31.6 Hz, 3C, PMe<sub>3</sub>).

HRMS (ESI)  $m/z$ : [M]<sup>+</sup> Calcd for C<sub>25</sub>H<sub>36</sub>BN<sub>9</sub>O<sub>3</sub>PSW<sup>+</sup> 768.1996; Found 768.2002

**Synthesis and characterization of WTp(NO)(PMe<sub>3</sub>)(η<sup>2</sup>-*N*-furfuryl-6-mesyl)-5,6-dihydropyridin-2-ium)(OTf) (75)**



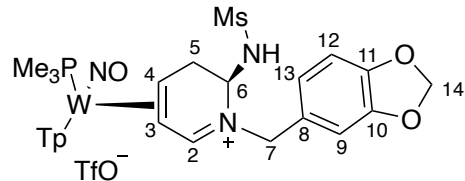
To an oven-dried 4-dram vial was added a stir pea, **33D** (57 mg, 0.70 mmol), furfurylamine (27 mg, 0.28 mmol), EtCN (1 mL), and DCM (2 mL). The solution was stirred for 10 seconds and then added to a 50 mL of stirring Et<sub>2</sub>O. A tan powder was precipitated, collected on a 15 mL F frit, washed 2x with 10 mL of Et<sub>2</sub>O, and dried in a desiccator (45 mg, 71% yield).

<sup>1</sup>H NMR (CD<sub>3</sub>CN, δ, 25 °C): 8.81 (d, *J* = 5.4 Hz, 1H, H2), 8.07 (d, *J* = 2.1 Hz, 1H, Tp3/5), 7.96 (d, *J* = 2.3 Hz, 1H, Tp3/5), 7.95 (d, *J* = 2.4 Hz, 1H, Tp3/5), 7.76 (d, *J* = 2.4 Hz, 1H, Tp3/5), 7.75 (d, *J* = 2.1 Hz, 1H, Tp3/5), 7.74 (d, *J* = 2.2 Hz, 1H, Tp3/5), 7.59 (dd, *J* = 0.8, 1.8 Hz, 1H, H11), 6.64 (d, *J* = 3.3 Hz, 1H, H10), 6.47 (dd, *J* = 1.8, 3.3 Hz, 1H, H9), 6.46 (t, *J* = 2.3 Hz, 1H, Tp4), 6.41 (t, *J* = 2.3 Hz, 1H, Tp4), 6.33 (t, *J* = 2.3 Hz, 1H, Tp4), 5.31 (dd, *J* = 6.4, 11.0 Hz, 1H, H6), 5.19 (d, *J* = 15.7 Hz, 1H, H7), 4.96 (d, *J* = 15.7 Hz, 1H, H7), 4.27-4.32 (m, 1H, H5), 3.35-3.40 (m, 2H, H4 & H5), 3.11 (s, 3H, Ms), 2.46 (dd, *J* = 5.7, 7.6 Hz, 1H, H3), 1.19 (d, *J*<sub>PH</sub> = 9.3 Hz, 9H, PMe<sub>3</sub>).

<sup>13</sup>C NMR (CD<sub>3</sub>CN, δ, 25 °C): 182.4 (C2), 148.9 (Tp3/5), 148.8 (C8), 145.3 (Tp3/5), 145.2 (C11), 142.5 (Tp3/5), 139.3 (Tp3/5), 139.0 (Tp3/5), 137.7 (Tp3/5), 122.1 (q, *J*<sub>FC</sub> = 320.4 Hz, OTf), 113.0 (C10), 112.2 (C9), 108.7 (Pz4), 108.0 (Pz4), 107.9 (Pz4), 66.9 (C6), 60.3 (d, *J*<sub>PC</sub> = 15.5 Hz, C4), 52.4 (C3), 48.5 (C7), 42.5 (Ms), 38.7 (C5), 12.8 (d, *J*<sub>PC</sub> = 31.5 Hz, 3C, PMe<sub>3</sub>).

HRMS (ESI) *m/z*: [M]<sup>+</sup> Calcd for C<sub>23</sub>H<sub>34</sub>BN<sub>9</sub>O<sub>4</sub>PSW<sup>+</sup> 758.1789; Found 758.1788

**Synthesis and characterization of  $W\text{Tp}(\text{NO})(\text{PMe}_3)(\eta^2\text{-}N\text{-piperonyl-6-mesy})\text{-5,6-dihydropyridin-2-ium}(\text{OTf})$  (**76**)**

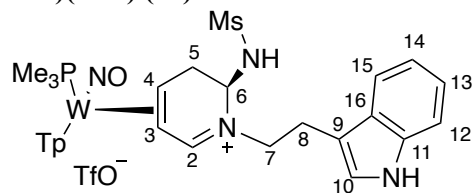


To an oven-dried 10 mL test tube was added, **33D** (52 mg, 0.06 mmol) and DCM (2 mL). To a separate oven-dried 10 mL tube was added piperonylamine (33 mg, 0.22 mmol) and DCM. Both solutions were chilled at  $-10\text{ }^\circ\text{C}$  for 15 minutes, and then the amine solution was added to the solution of **33D**. The solution was then manually swirled, sat in the bath for 15 minutes, and then added to a 50 mL of stirring  $\text{Et}_2\text{O}$ . A tan powder was precipitated, collected on a 15 mL F frit, washed 2x with 10 mL of  $\text{Et}_2\text{O}$ , and dried in a desiccator (46 mg, 74% yield).

$^1\text{H}$  NMR ( $\text{CD}_3\text{CN}$ ,  $\delta$ ,  $25\text{ }^\circ\text{C}$ ): See below. Not assigned due to lack of 2D

HRMS (ESI)  $m/z$ :  $[\text{M}]^+$  Calcd for  $\text{C}_{26}\text{H}_{36}\text{BN}_9\text{O}_5\text{PSW}^+$  812.1895; Found 812.1909

**Synthesis and characterization of WTp(NO)(PMe<sub>3</sub>)(η<sup>2</sup>-*N*-trypto-6-mesyl)-5,6-dihydropyridin-2-ium)(OTf) (**77**)**

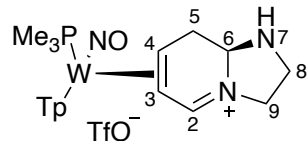


To an oven-dried 10 mL test tube was added, **33D** (46 mg, 0.06 mmol) and DCM (2 mL). To a separate dried 10 mL tube was added tryptamine (33 mg, 0.21 mmol) and DCM. Both solutions were chilled at -40 °C for 15 minutes, and then the amine solution was added to the solution of **33D**. The solution was then manually swirled, sat in the bath for 15 minutes, and then added to a 50 mL of stirring Et<sub>2</sub>O. A tan powder was precipitated, collected on a 15 mL F frit, washed 2x with 10 mL of Et<sub>2</sub>O, and dried in a desiccator (yield not obtained).

<sup>1</sup>H NMR (CD<sub>3</sub>CN, δ, 25 °C): See below. Not assigned due to lack of 2D

HRMS (ESI) m/z: [M]<sup>+</sup> Calcd for C<sub>28</sub>H<sub>39</sub>BN<sub>10</sub>O<sub>3</sub>PSW<sup>+</sup> 821.2262; Found 821.2270

**Synthesis and characterization of WTp(NO)(PMe<sub>3</sub>)( $\eta^2$ -pentahydroimidazo-[1,7]-pyridin-2-ium) (OTf) (78)**



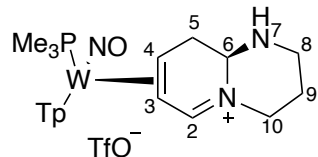
To an oven-dried 4-dram vial was added a stir pea, **5D** (202 mg, 0.23 mmol), ethylenediamine (58 mg, 0.97 mmol), EtCN (2 mL), and DCM (3 mL). The solution was stirred for 5 minutes and then added to a 50 mL of stirring Et<sub>2</sub>O. A tan powder was precipitated, collected on a 15 mL F frit, washed 2x with 10 mL of Et<sub>2</sub>O, and dried in a desiccator (149 mg, 84% yield).

<sup>1</sup>H NMR (CD<sub>3</sub>CN,  $\delta$ , 25 °C): 9.04 (d,  $J$  = 5.6 Hz, 1H, H2), 8.08 (d,  $J$  = 2.0 Hz, 1H, Tp3/5), 7.99 (d,  $J$  = 2.0 Hz, 1H, Tp3/5), 7.96 (d,  $J$  = 2.3 Hz, 1H, Tp3/5), 7.75-7.77 (m, 2H, Tp3/5), 6.46 (t,  $J$  = 2.3 Hz, 1H, Tp4), 6.40 (t,  $J$  = 2.3 Hz, 1H, Tp4), 6.33 (t,  $J$  = 2.3 Hz, 1H, Tp4), 4.39 (dd,  $J$  = 5.8, 11.2 Hz, 1H, H6), 4.19 (dd,  $J$  = 8.2, 12.4 Hz, 1H, H9), 3.80-3.84 (m, 1H, H9), 3.69-3.74 (m, 1H, H5), 3.36-3.41 (m, 2H, H5 & H8), 3.28-3.32 (m, 1H, H4), 3.05 (dt,  $J$  = 8.8, 12.4 Hz, 1H, H8), 2.33 (dd,  $J$  = 5.6, 9.2 Hz, 1H, H3), 1.19 (d,  $J_{PH}$  = 9.2 Hz, 9H, PMe<sub>3</sub>).

<sup>13</sup>C NMR (CD<sub>3</sub>CN,  $\delta$ , 25 °C): 177.2 (C2), 148.9 (Tp3/5), 145.4 (Tp3/5), 142.5 (Tp3/5), 139.2 (Tp3/5), 138.7 (Tp3/5), 137.4 (Tp3/5), 122.1 (q,  $J_{FC}$  = 321.0 Hz, OTf), 108.6 (Tp4), 107.8 (2C, Tp4), 75.5 (C6), 61.9 (d,  $J_{PC}$  = 15.4 Hz, C4), 51.5 (C9), 50.0 (C3), 44.8 (C8), 34.5 (C5), 12.82 (d,  $J_{PC}$  = 30.9 Hz, 3C, PMe<sub>3</sub>).

HRMS (ESI)  $m/z$ : [M]<sup>+</sup> Calcd for C<sub>19</sub>H<sub>30</sub>BN<sub>9</sub>OPW<sup>+</sup> 626.1908; Found 626.1928  
SC-XRD Data on page 409

### Synthesis and characterization of $\text{W}(\text{NO})(\text{PMe}_3)(\eta^2\text{-hexahydropyrimido-[1,7]-pyridin-2-ium})(\text{OTf})$ (**79**)



To an oven-dried 4-dram vial was added a stir pea, **5D** (217 mg, 0.24 mmol), diaminopropane (75 mg, 1.01 mmol), EtCN (2 mL), and DCM (3 mL). The solution was stirred for 10 minutes and then added to a 50 mL of stirring Et<sub>2</sub>O. A tan powder was precipitated, collected on a 15 mL F frit, washed 2x with 10 mL of Et<sub>2</sub>O, and dried in a desiccator (155 mg, 80% yield).

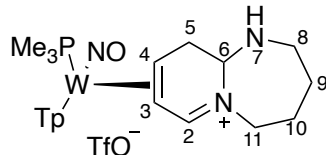
<sup>1</sup>H NMR (CD<sub>3</sub>CN, δ, 25 °C): 8.61 (d, *J* = 4.8 Hz, 1H, H2), 8.05 (d, *J* = 2.1 Hz, 1H, Tp3/5), 8.00 (d, *J* = 2.1 Hz, 1H, Tp3/5), 7.94-7.95 (m, 2H, Tp3/5), 7.78 (d, *J* = 2.4 Hz, 1H, Tp3/5), 7.72 (d, *J* = 2.2 Hz, 1H, Tp3/5), 6.45 (t, *J* = 2.3 Hz, 1H, Tp4), 6.40 (t, *J* = 2.3 Hz, 1H, Tp4), 6.36 (t, *J* = 2.3 Hz, 1H, Tp4), 4.67 (dd, *J* = 6.5, 10.8 Hz, 1H, H6), 4.48 (td, *J* = 3.6, 13.3 Hz, 1H, H10), 4.07-4.12 (m, 1H, H5), 4.03-4.06 (m, 1H, H10), 3.23-3.27 (m, 2H, H4 & H5), 3.12 (dq, *J* = 2.1, 14.1 Hz, 1H, H8), 2.85 (td, *J* = 2.8, 11.9 Hz, 1H, H8), 2.26 (dd, *J* = 4.8, 8.5 Hz, 1H, H3), 1.76-1.83 (m, 1H, H9), 1.71 (d, *J* = 13.3 Hz, 1H H9), 1.18 (d, *J*<sub>PH</sub> = 9.2 Hz, 9H, PMe<sub>3</sub>).

<sup>13</sup>C NMR (CD<sub>3</sub>CN, δ, 25 °C): 178.4 (C2), 148.8 (Tp3/5), 145.3 (Tp3/5), 142.5 (Tp3/5), 139.2 (Tp3/5), 138.8 (Tp3/5), 137.7 (Tp3/5), 122.1 (q, *J*<sub>FC</sub> = 321.5 Hz, OTf), 108.6 (Tp4), 107.9 (Tp4), 107.8 (Tp4), 71.0 (C6), 59.0 (d, *J*<sub>PC</sub> = 15.0 Hz, C4), 53.8 (C10), 50.9 (C3), 44.4 (C8), 37.0 (C5), 27.8 (C9), 12.9 (d, *J*<sub>PC</sub> = 31.0 Hz, 3C, PMe<sub>3</sub>)

HRMS (ESI) *m/z*: [M]<sup>+</sup> Calcd for C<sub>20</sub>H<sub>32</sub>BN<sub>9</sub>OPW<sup>+</sup> 640.2064; Found 640.2072  
SC-XRD Data on page 410



**Synthesis and characterization of WTp(NO)(PMe<sub>3</sub>)( $\eta^2$ -heptahydrodiazepino-[1,7]-pyridin-2-ium) (OTf) (80)**



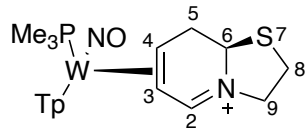
To an oven-dried 4-dram vial was added a stir pea, **5D** (251 mg, 0.28 mmol), diaminobutane (112 mg, 1.27 mmol), EtCN (2 mL), and DCM (3 mL). The solution was stirred for 5 minutes and then added to a 50 mL of stirring Et<sub>2</sub>O. A tan powder was precipitated, collected on a 15 mL F frit, washed 2x with 10 mL of Et<sub>2</sub>O, and dried in a desiccator (189 mg, 83% yield).

<sup>1</sup>H NMR (CD<sub>3</sub>CN,  $\delta$ , 25 °C): 8.90 (d,  $J$  = 5.2 Hz, 1H, H2), 8.10 (d,  $J$  = 2.0 Hz, 1H, Tp3/5), 7.96 (d,  $J$  = 2.0 Hz, 1H, Tp3/5), 7.94-7.95 (m, 2H, Tp3/5), 7.77 (d,  $J$  = 2.4 Hz, 1H, Tp3/5), 7.72 (d,  $J$  = 2.2 Hz, 1H, Tp3/5), 6.45 (t,  $J$  = 2.3 Hz, 1H, Tp4), 6.39 (t,  $J$  = 2.3 Hz, 1H, Tp4), 6.33 (d,  $J$  = 2.3 Hz, 1H, Tp4), 4.69-4.72 (m, 1H, H6), 4.02-4.07 (m, 2H, H5/11), 3.97 (dd,  $J$  = 7.3, 13.7 Hz, 1H, H11), 3.16-3.20 (m, 2H, H4), 3.00-3.06 (m, 2H, H5/8), 2.82-2.86 (m, 1H, H8), 2.45 (br s, 1H, N-H), 2.22 (dd,  $J$  = 5.4, 8.0 Hz, 1H, H3), 1.86-1.91 (m, 1H, H10), 1.78-1.84 (m, 1H, H10), 1.62-1.68 (m, 1H, H9), 1.57-1.62 (m, 1H, H9), 1.20 (d,  $J_{PH}$  = 9.2 Hz, 9H, PMe<sub>3</sub>).

<sup>13</sup>C NMR (CD<sub>3</sub>CN,  $\delta$ , 25 °C): 180.0 (C2), 148.8 (Tp3/5), 145.4 (Tp3/5), 142.5 (Tp3/5), 139.2 (Tp3/5), 138.7 (Tp3/5), 137.5 (Tp3/5), 122.1 (q,  $J_{FC}$  = 322.1 Hz, OTf), 108.5 (Tp4), 107.8 (2C, Tp4), 74.5 (C6), 60.9 (d,  $J_{PC}$  = 15.3 Hz, C4), 56.7 (C11), 49.6 (C3), 47.0 (C8), 37.4 (C5), 32.3 (C9), 29.7 (C10), 12.9 (d,  $J_{PC}$  = 25.1 Hz, 3C, PMe<sub>3</sub>).

HRMS (ESI)  $m/z$ : [M]<sup>+</sup> Calcd for C<sub>21</sub>H<sub>34</sub>BN<sub>9</sub>OPW<sup>+</sup> 654.2221; Found 654.2227

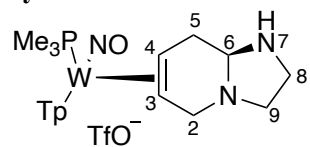
**Synthesis and characterization of  $\text{W}(\text{NO})(\text{PMe}_3)(\eta^2\text{-pentahydrothiazo-[1,7]-pyridin-2-ium}) (\text{OTf})$  (**81**)**



To an oven-dried 4-dram vial with a stir pea was added **5D** (103 mg, 0.13 mmol) and THF (2 mL). To a separate 4-dram vial was added cysteamine (45 mg, 0.58 mmol) and MeOH (1 mL). The **5D** solution was then added to the amine solution, and both were stirred for 3 hours, and then added to a 50 mL of stirring  $\text{Et}_2\text{O}$ . A tan powder was precipitated, collected on a 15 mL F frit, washed 2x with 10 mL of  $\text{Et}_2\text{O}$ , and dried in a desiccator (yield not acquired).

$^1\text{H}$  NMR ( $\text{CD}_3\text{CN}$ ,  $\delta$ , 25 °C): See below. Not assigned due to lack of 2D

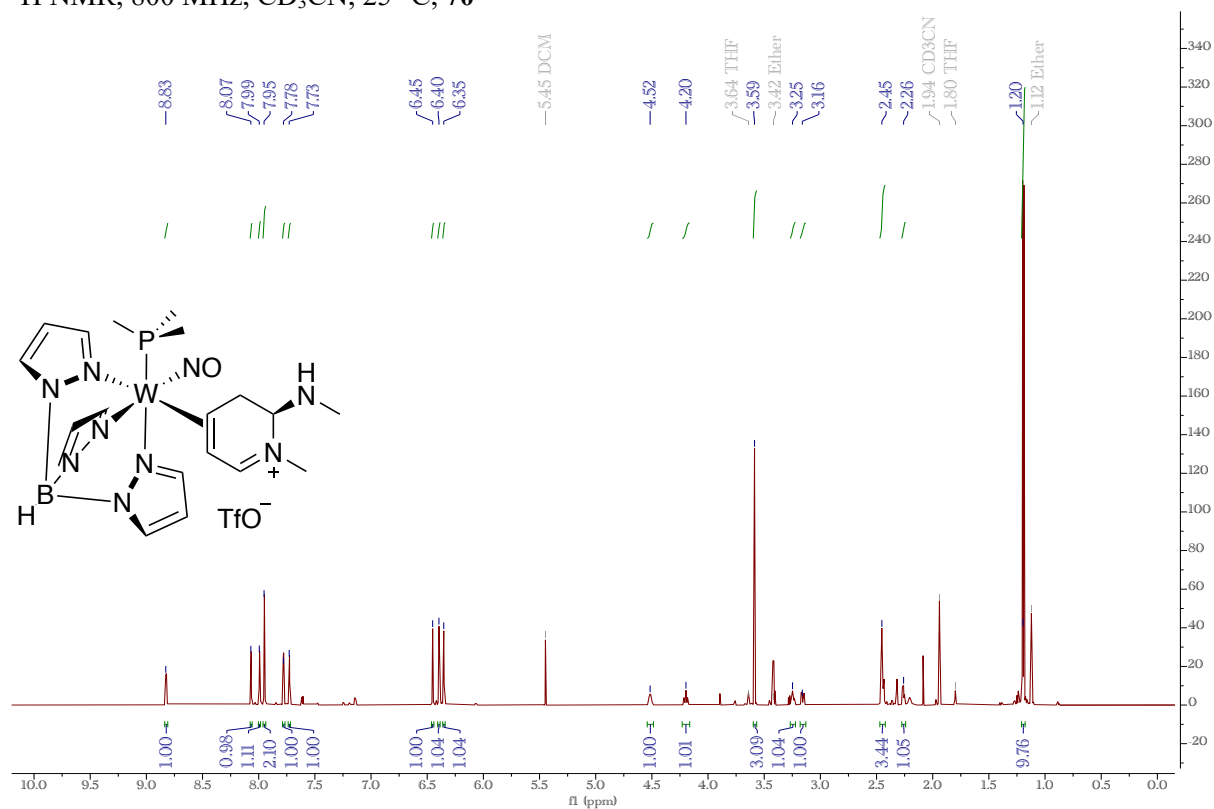
**Synthesis and characterization of  $\text{W}(\text{NO})(\text{PMe}_3)(\eta^2\text{-heptahydroimidazo-[1,7]-pyridine})$  (**82**)**



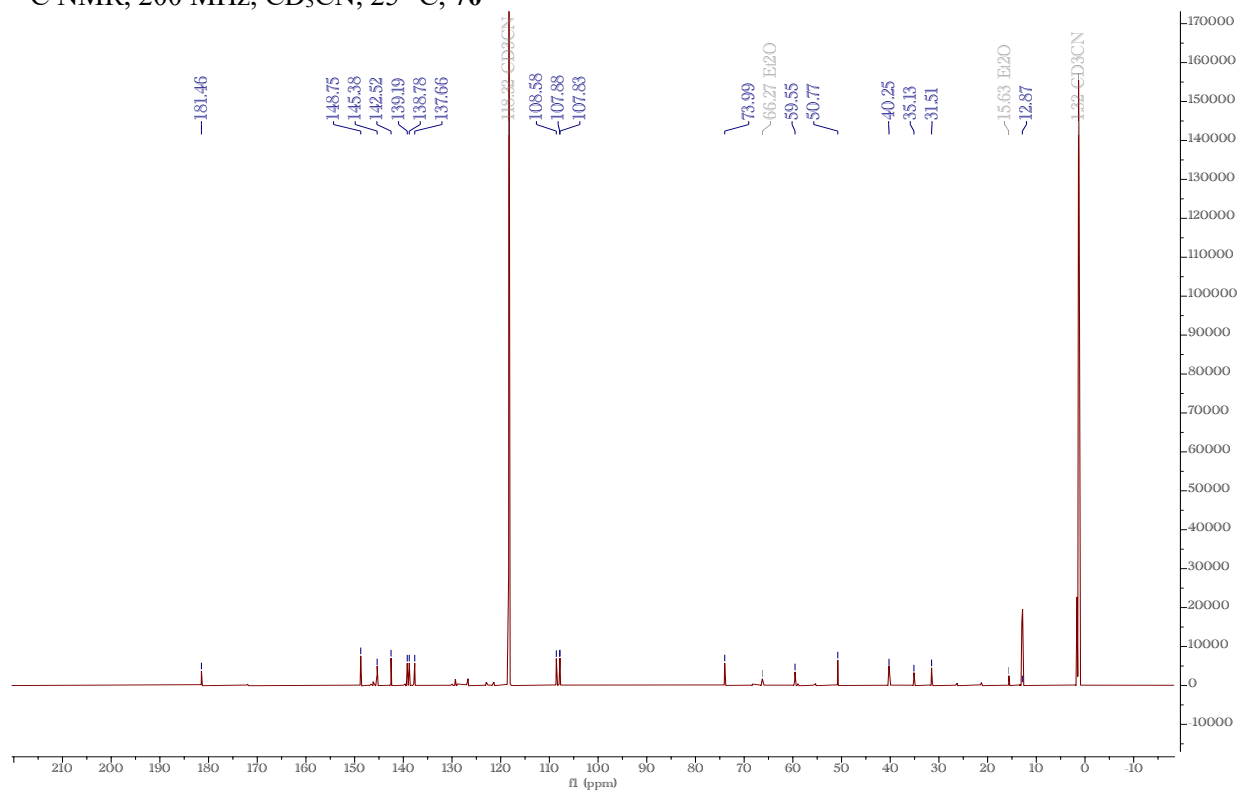
To an oven-dried NMR tube was added 7 mg of **78**, 4 mg of  $\text{NaBH}_4$ , and  $\text{d}_4\text{-MeOH}$ . Crude  $^1\text{H}$  NMR obtained after 10 minutes.

$^1\text{H}$  NMR ( $\text{d}_4\text{-MeOH}$ ,  $\delta$ , 25 °C): See below. Not assigned due to lack of 2D

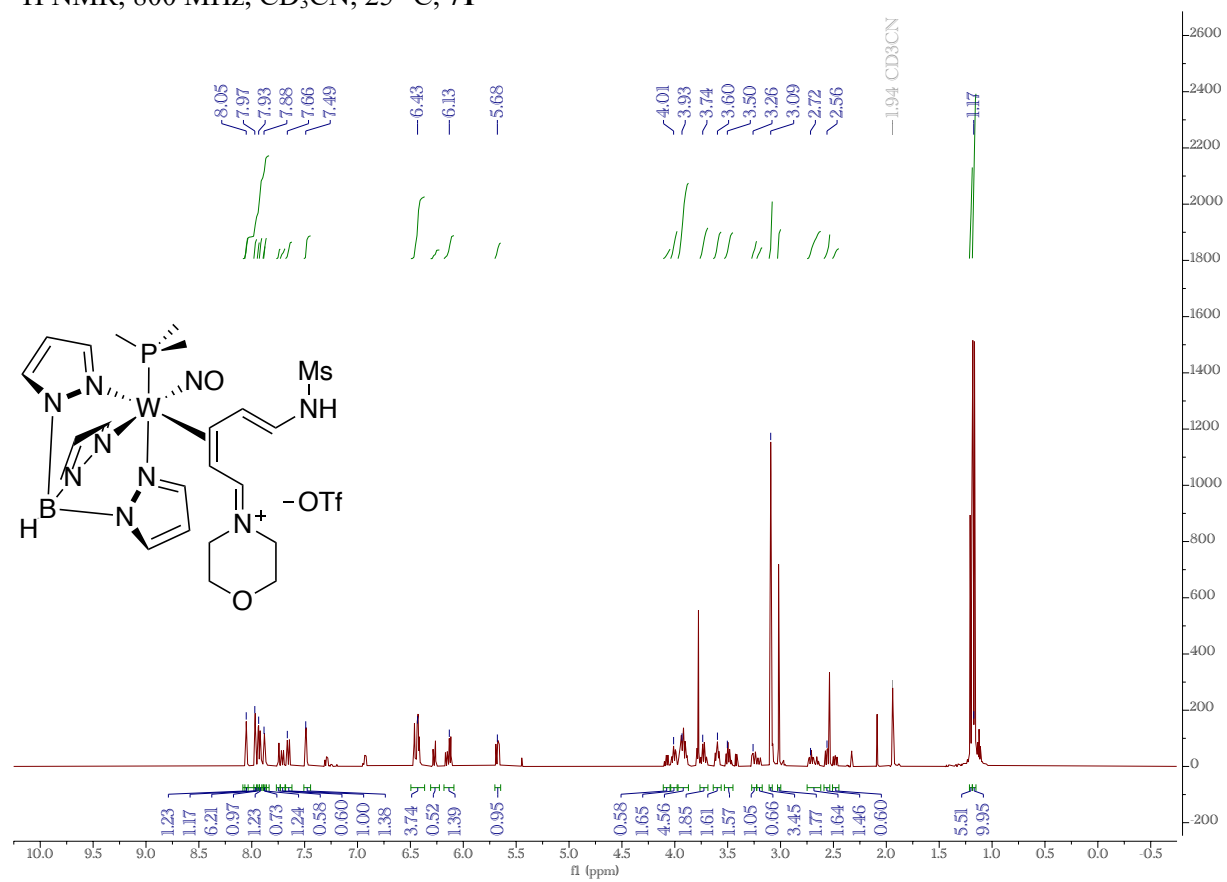
$^1\text{H}$  NMR, 800 MHz,  $\text{CD}_3\text{CN}$ , 25 °C, **70**



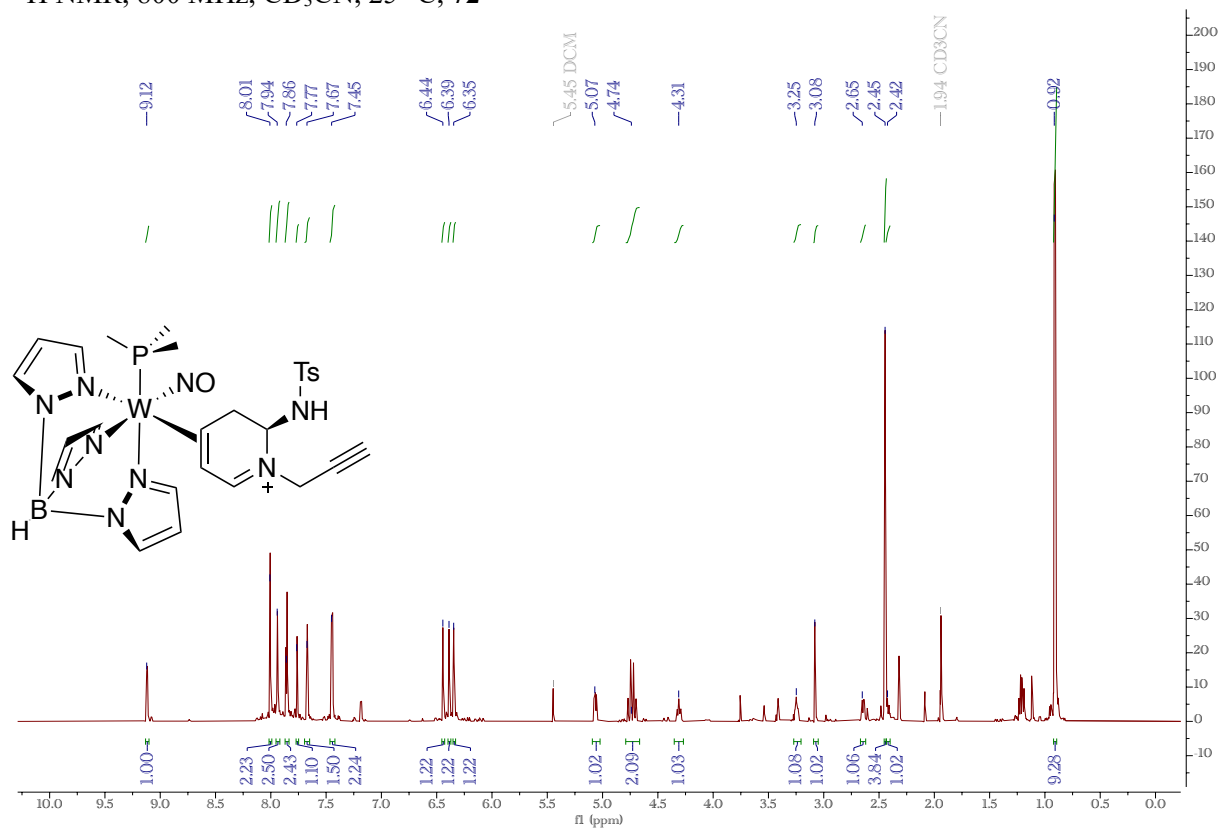
$^{13}\text{C}$  NMR, 200 MHz,  $\text{CD}_3\text{CN}$ , 25 °C, **70**



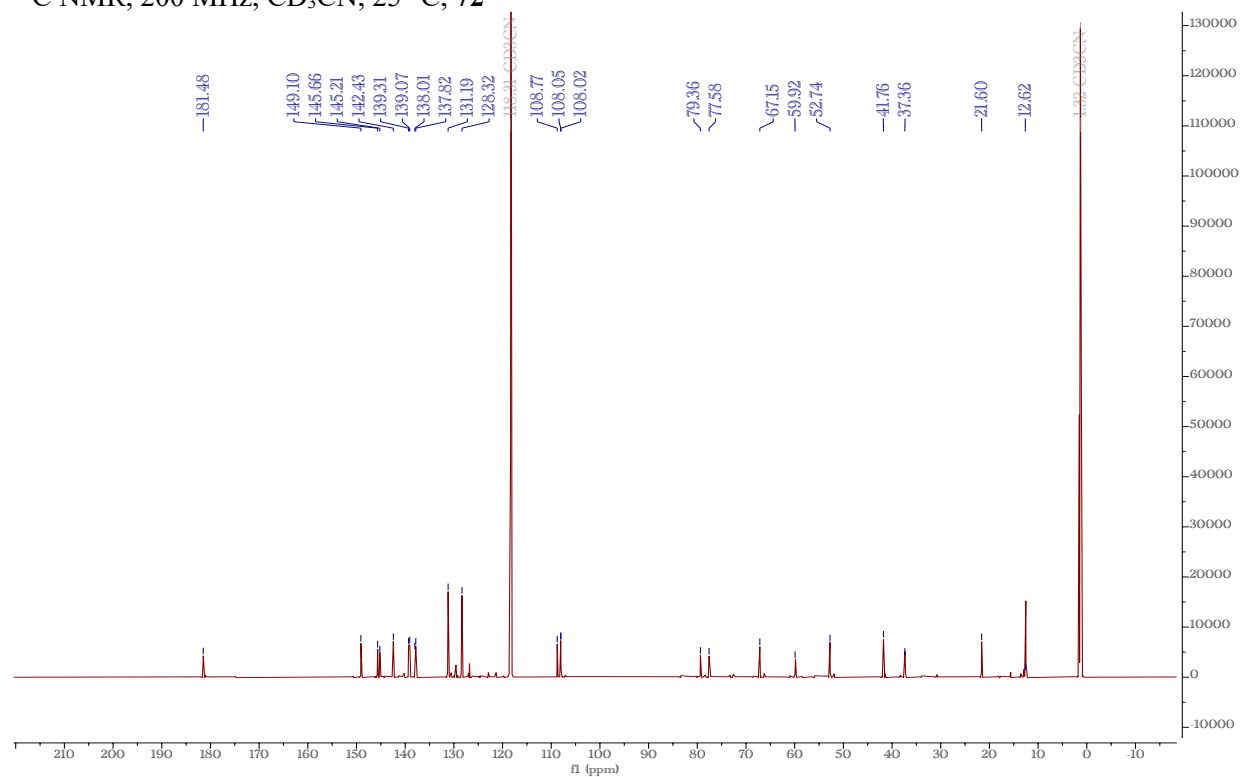
$^1\text{H}$  NMR, 800 MHz,  $\text{CD}_3\text{CN}$ , 25  $^\circ\text{C}$ , 71



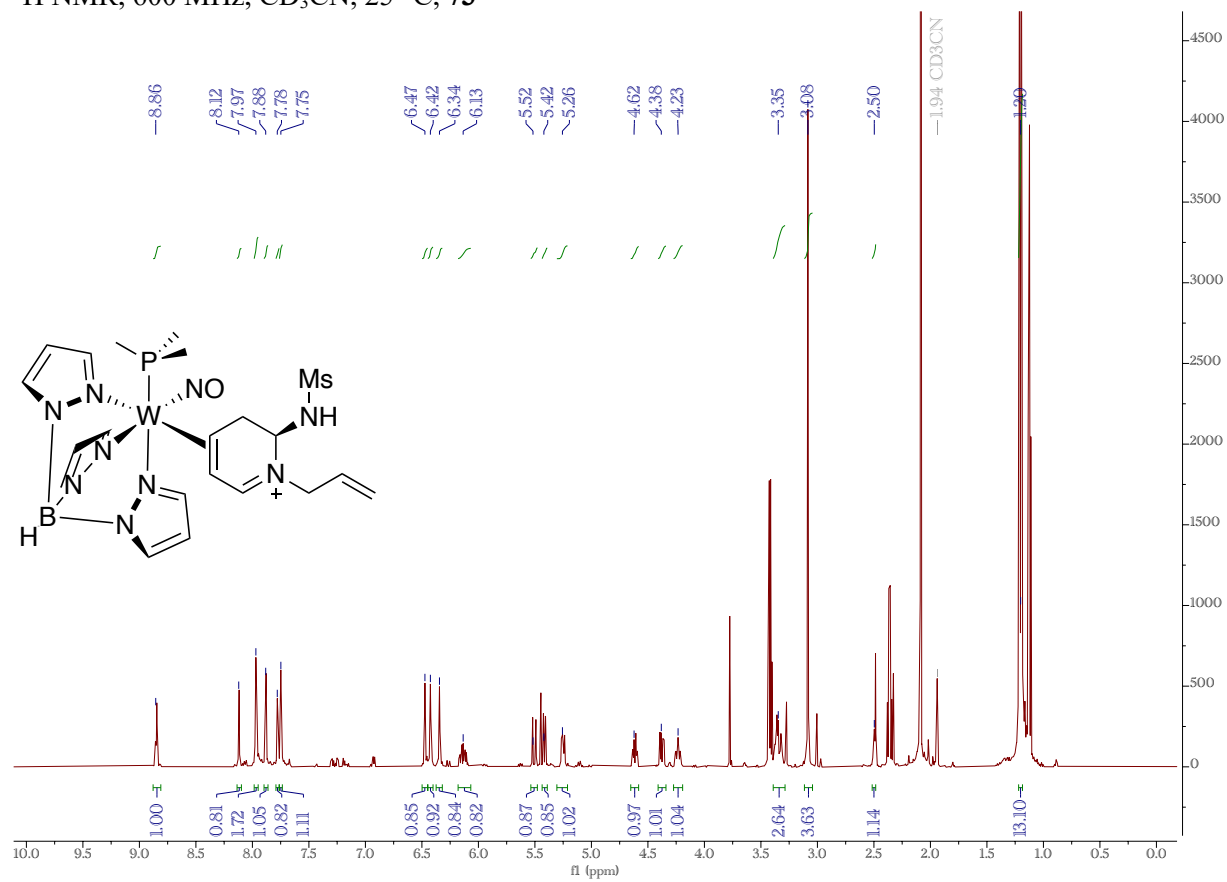
$^1\text{H}$  NMR, 800 MHz,  $\text{CD}_3\text{CN}$ , 25 °C, **72**



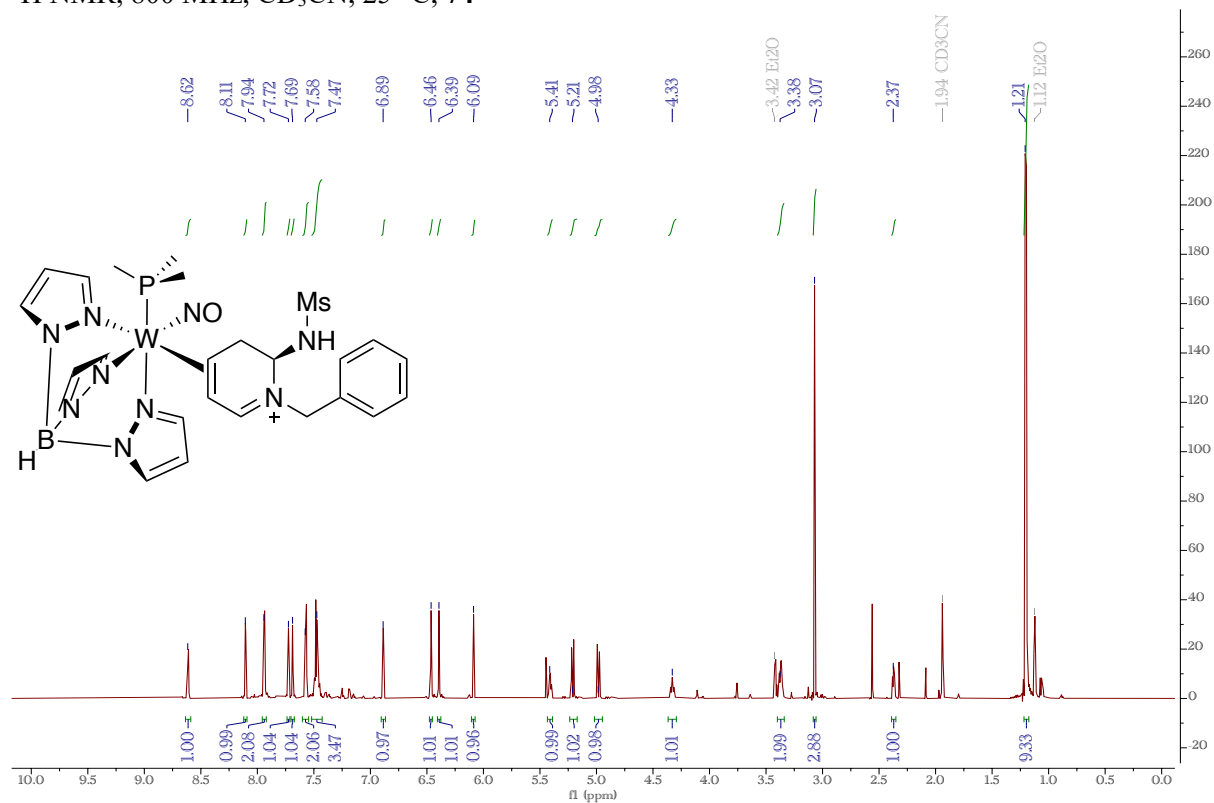
$^{13}\text{C}$  NMR, 200 MHz,  $\text{CD}_3\text{CN}$ , 25 °C, **72**



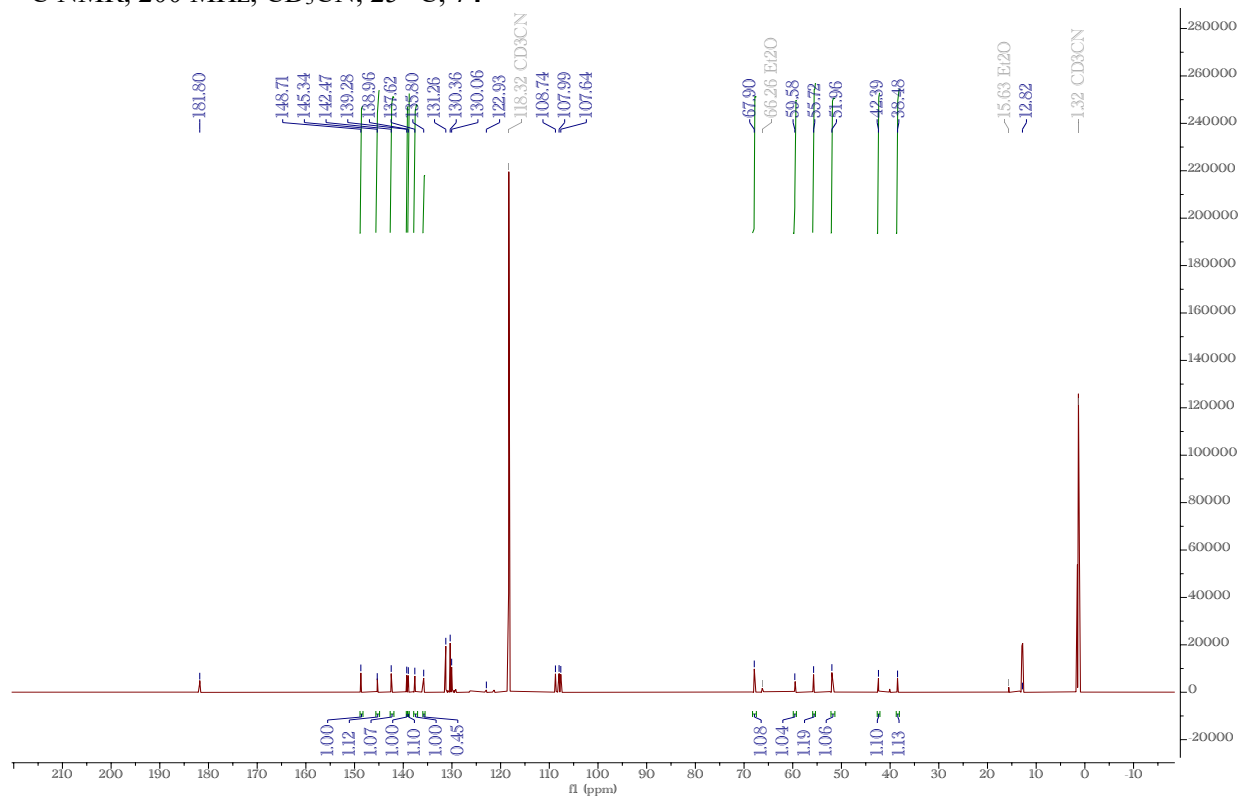
$^1\text{H}$  NMR, 600 MHz,  $\text{CD}_3\text{CN}$ , 25 °C, **73**



$^1\text{H}$  NMR, 800 MHz,  $\text{CD}_3\text{CN}$ , 25 °C, 74

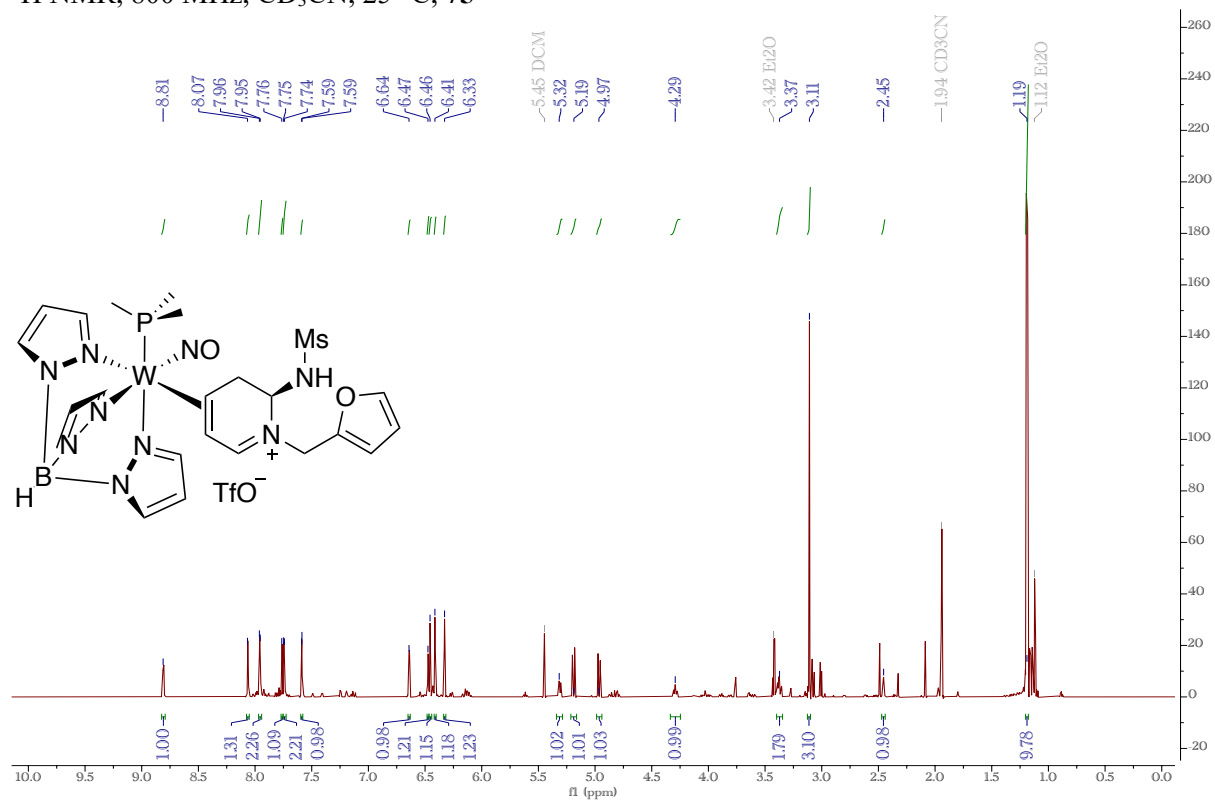


$^{13}\text{C}$  NMR, 200 MHz,  $\text{CD}_3\text{CN}$ , 25 °C, 74

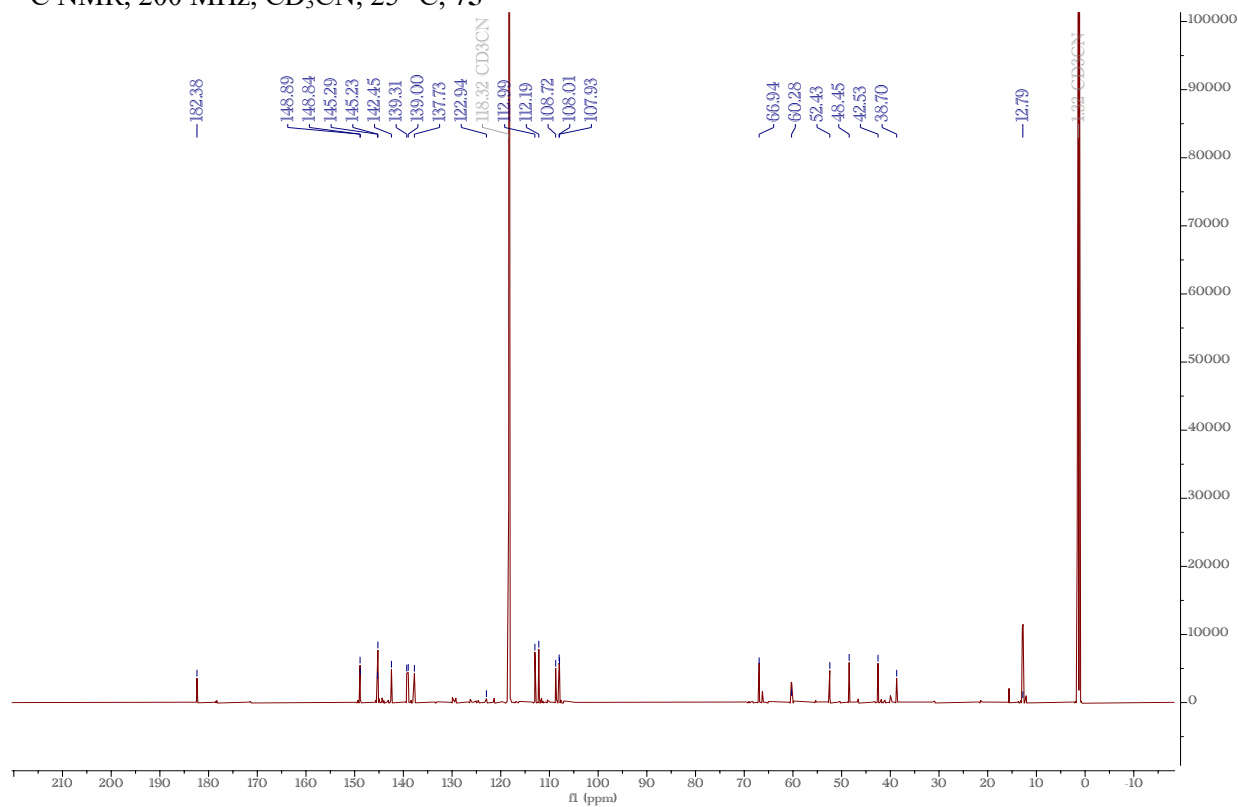




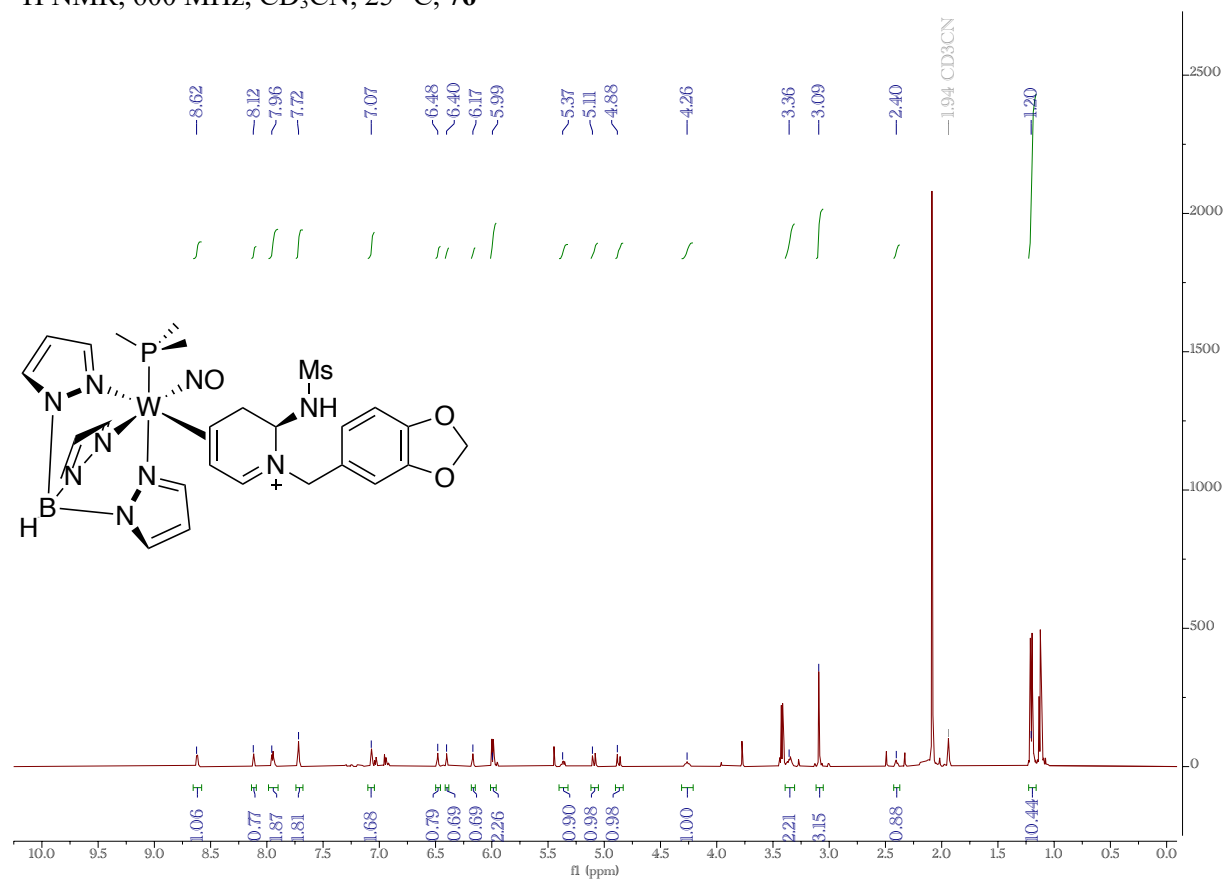
$^1\text{H}$  NMR, 800 MHz,  $\text{CD}_3\text{CN}$ , 25 °C, 75



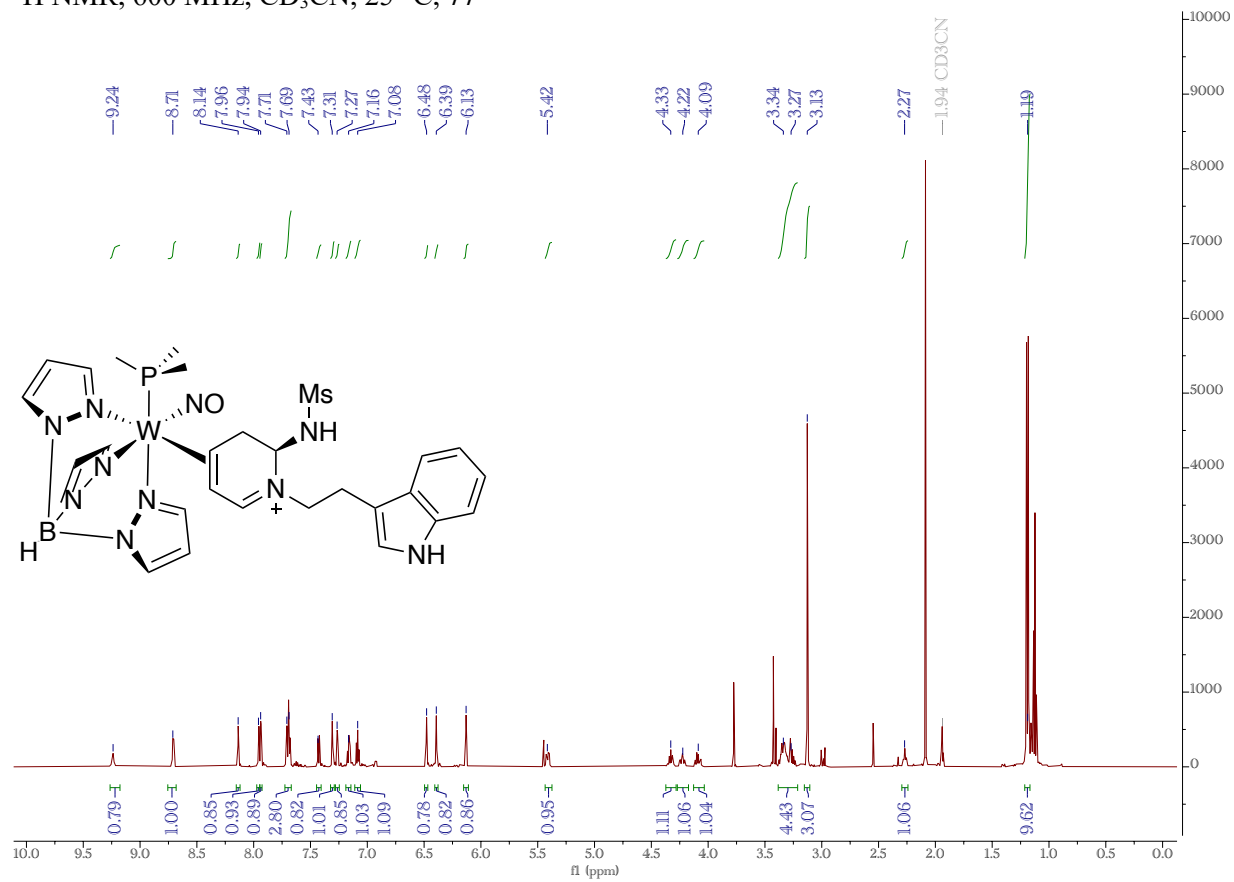
$^{13}\text{C}$  NMR, 200 MHz,  $\text{CD}_3\text{CN}$ , 25 °C, 75



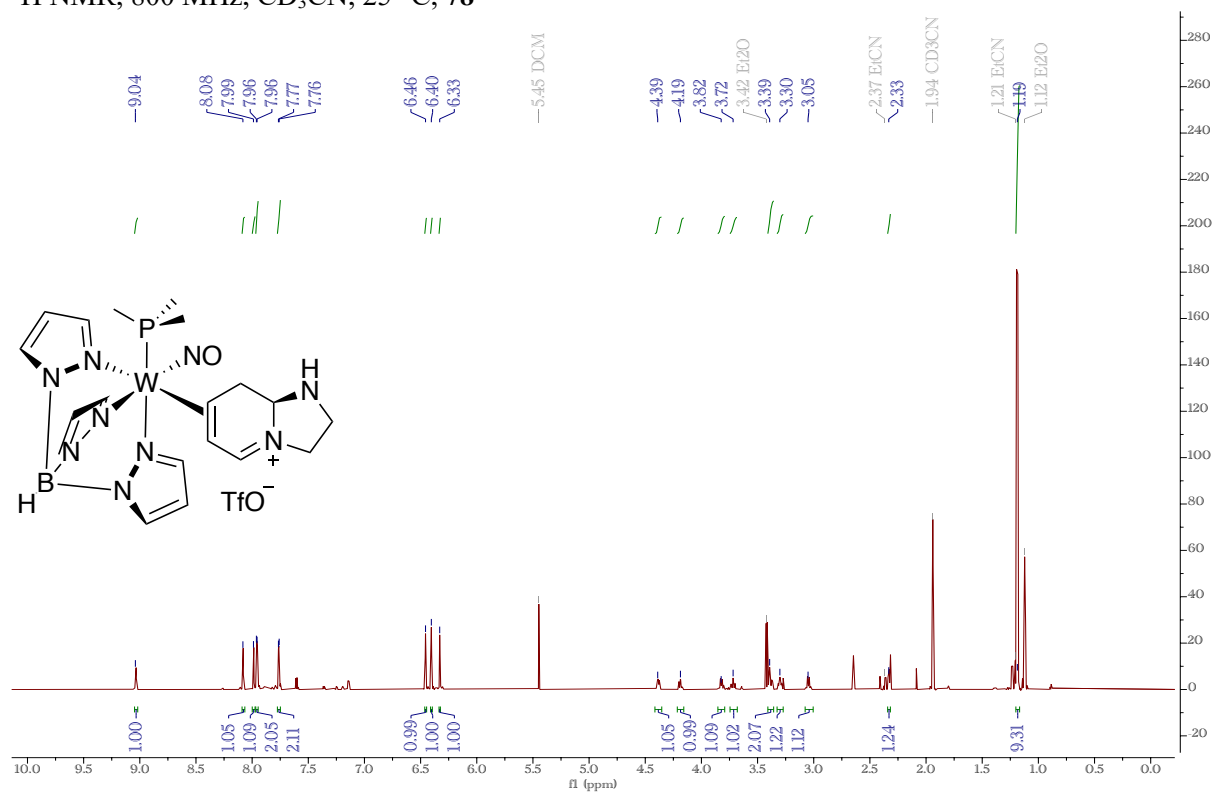
$^1\text{H}$  NMR, 600 MHz,  $\text{CD}_3\text{CN}$ , 25  $^\circ\text{C}$ , 76



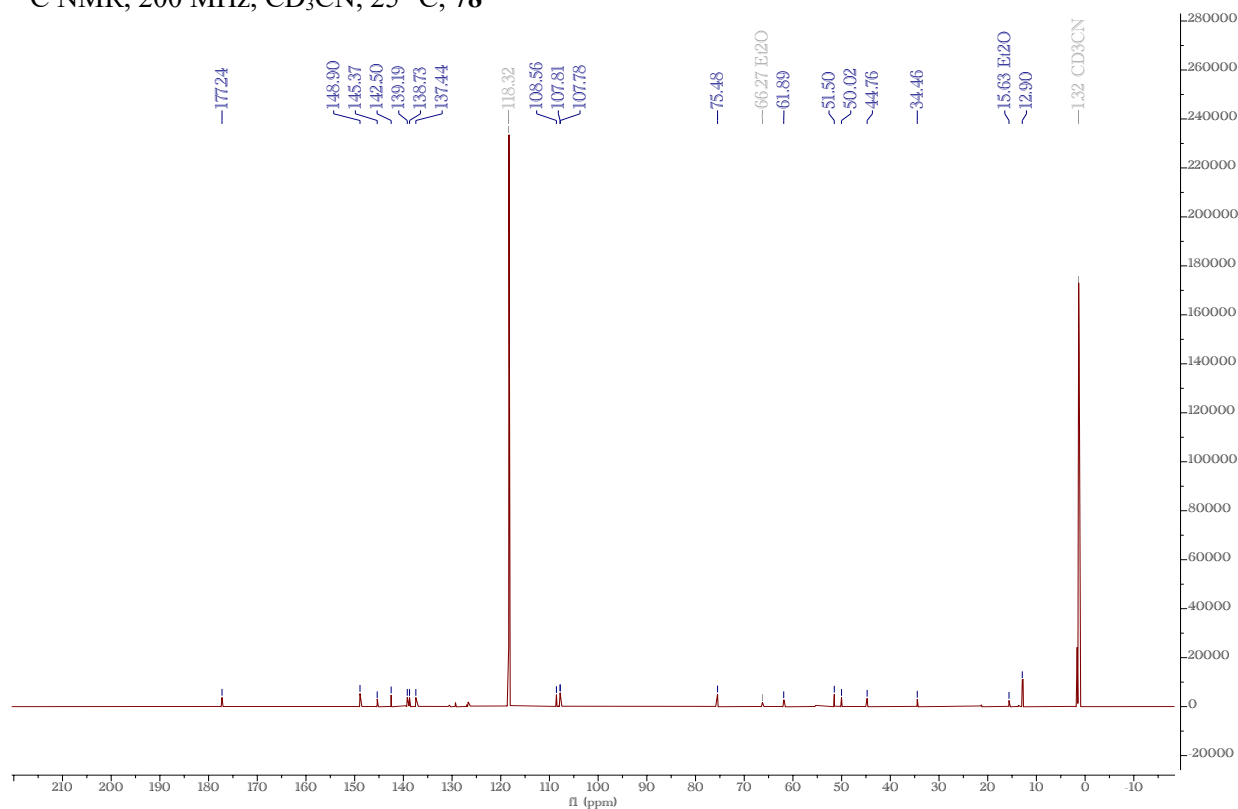
$^1\text{H}$  NMR, 600 MHz,  $\text{CD}_3\text{CN}$ , 25 °C, 77



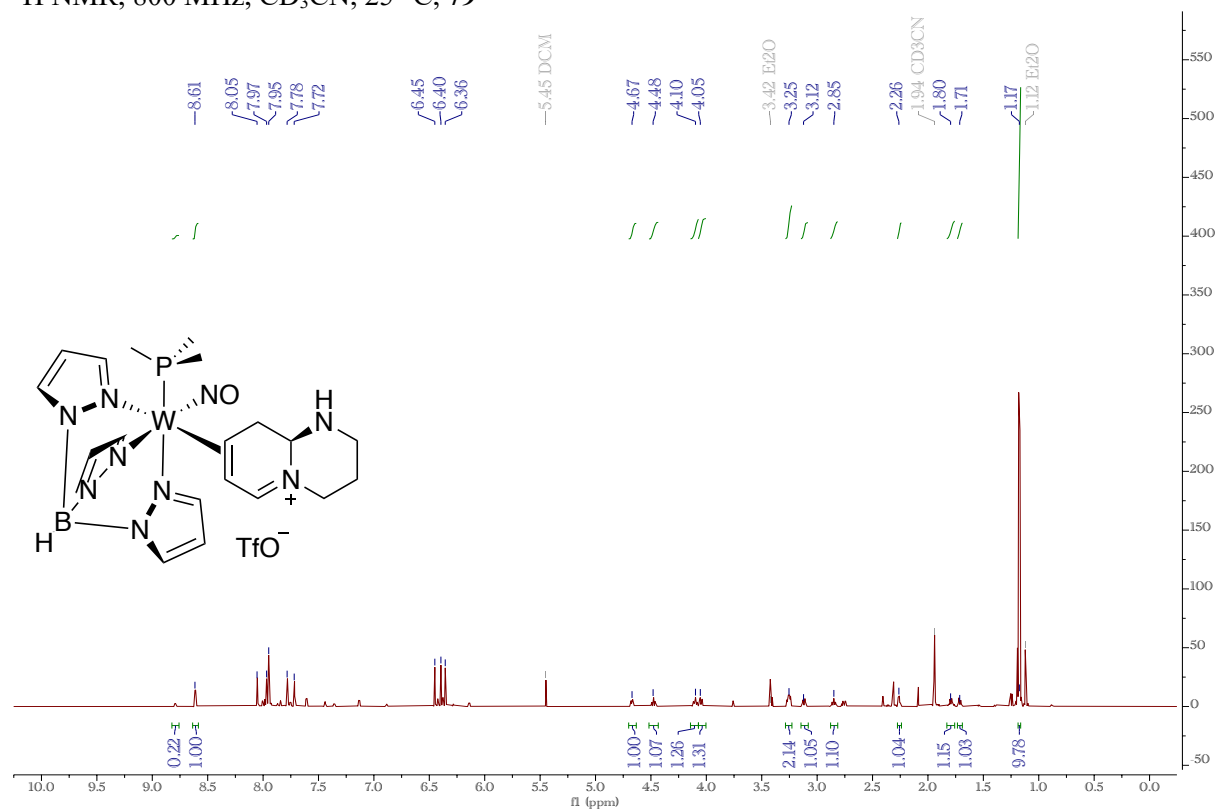
$^1\text{H}$  NMR, 800 MHz,  $\text{CD}_3\text{CN}$ , 25 °C, **78**



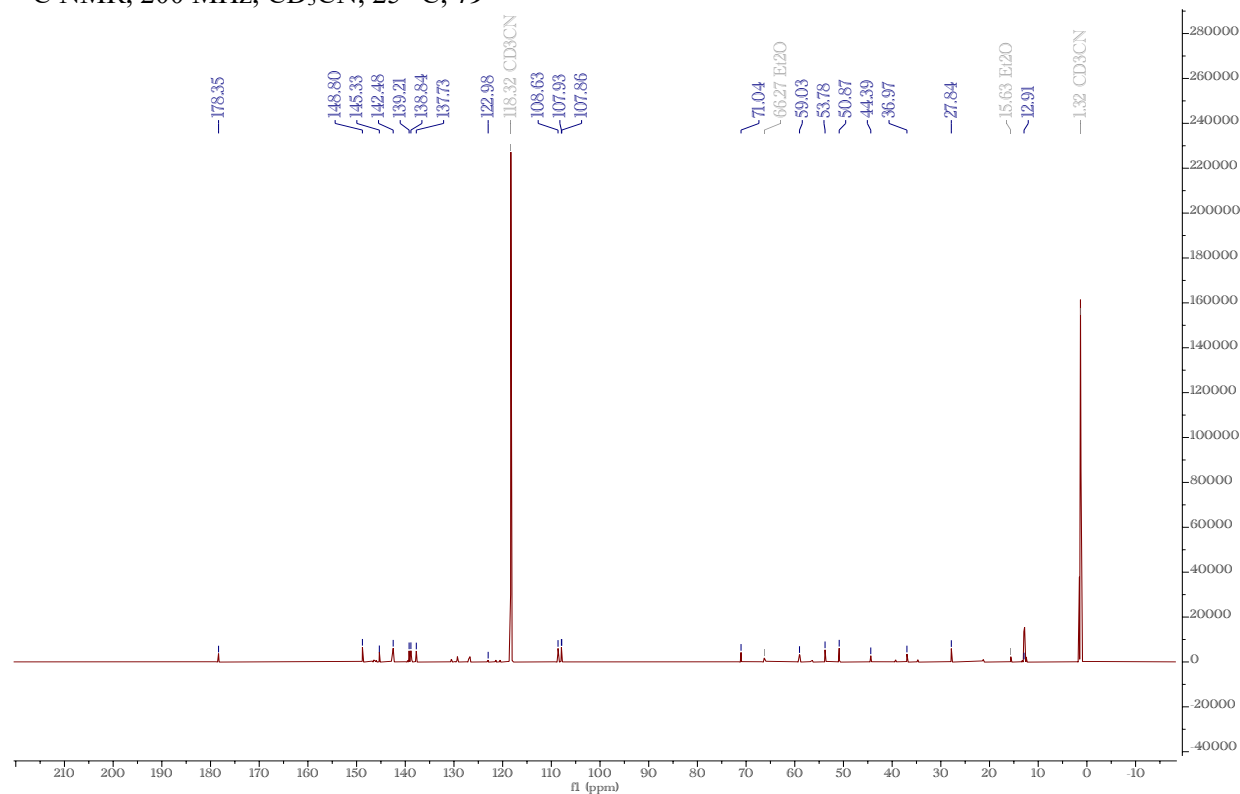
$^{13}\text{C}$  NMR, 200 MHz,  $\text{CD}_3\text{CN}$ , 25 °C, **78**



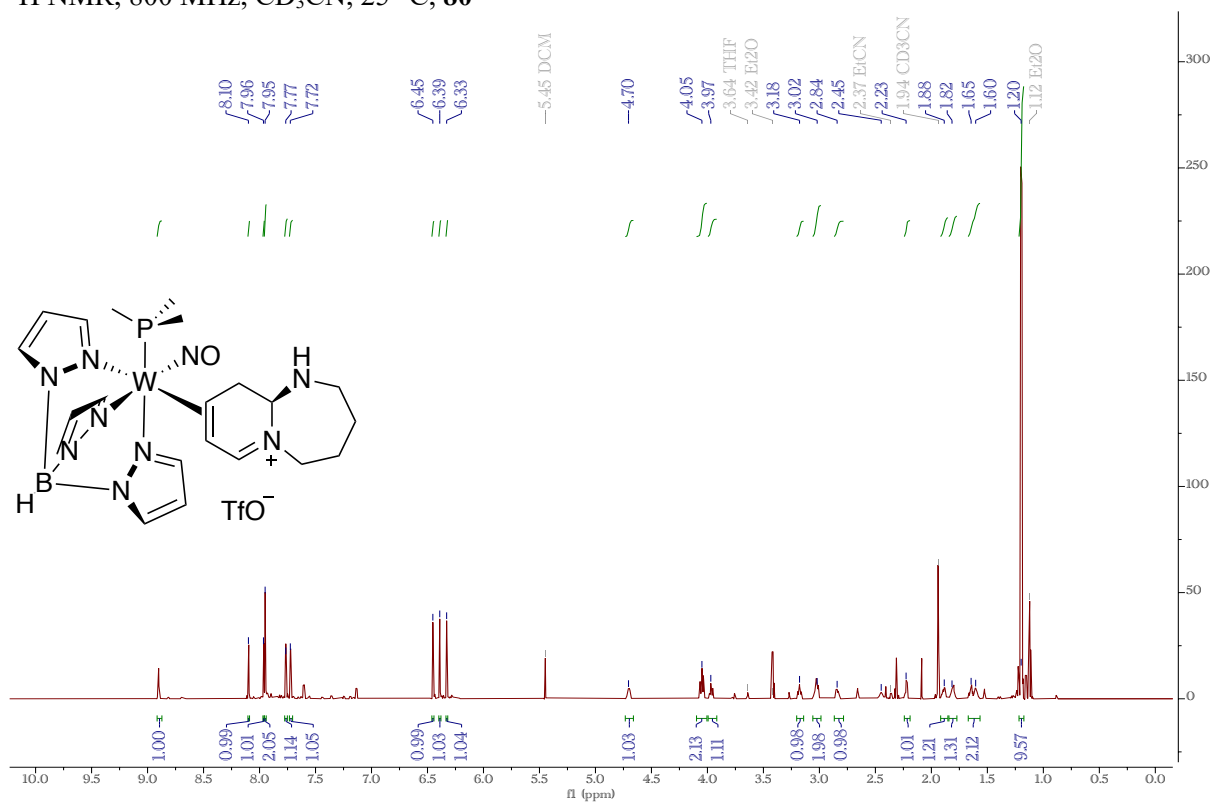
$^1\text{H}$  NMR, 800 MHz,  $\text{CD}_3\text{CN}$ , 25 °C, **79**



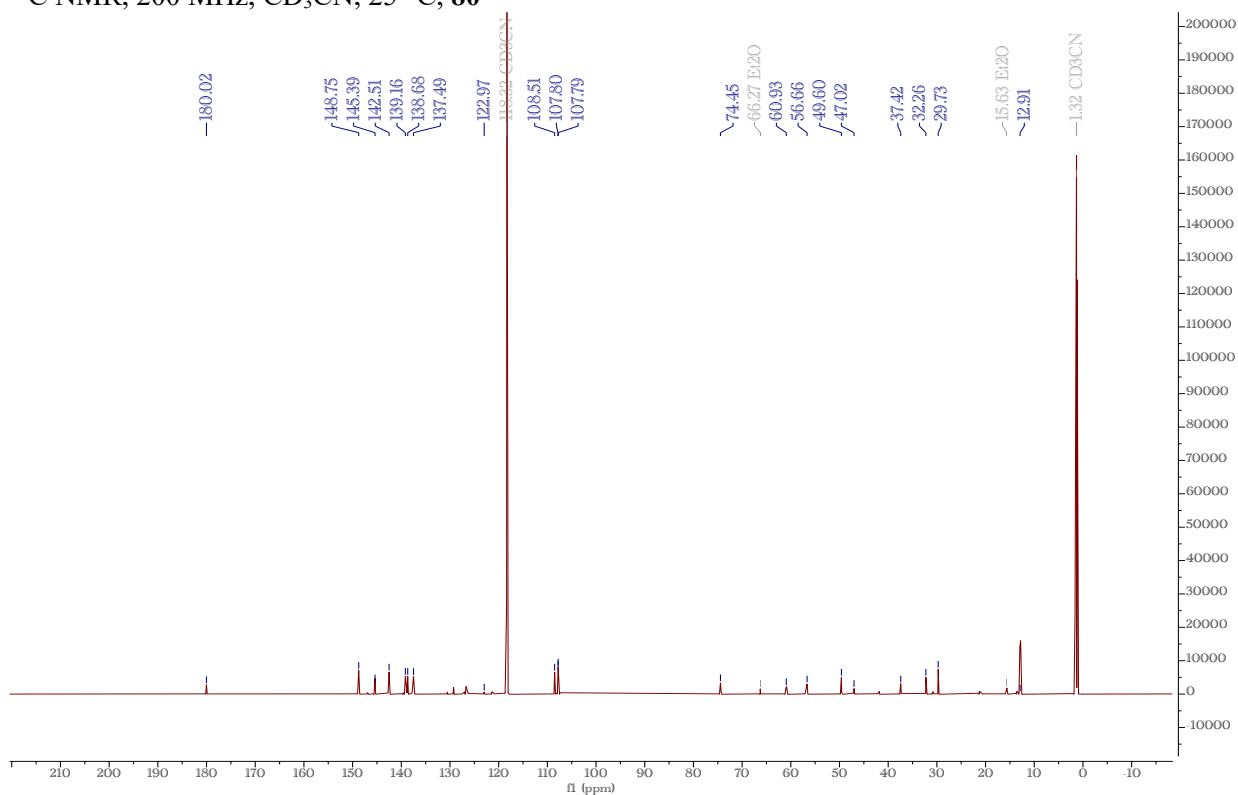
$^{13}\text{C}$  NMR, 200 MHz,  $\text{CD}_3\text{CN}$ , 25 °C, **79**



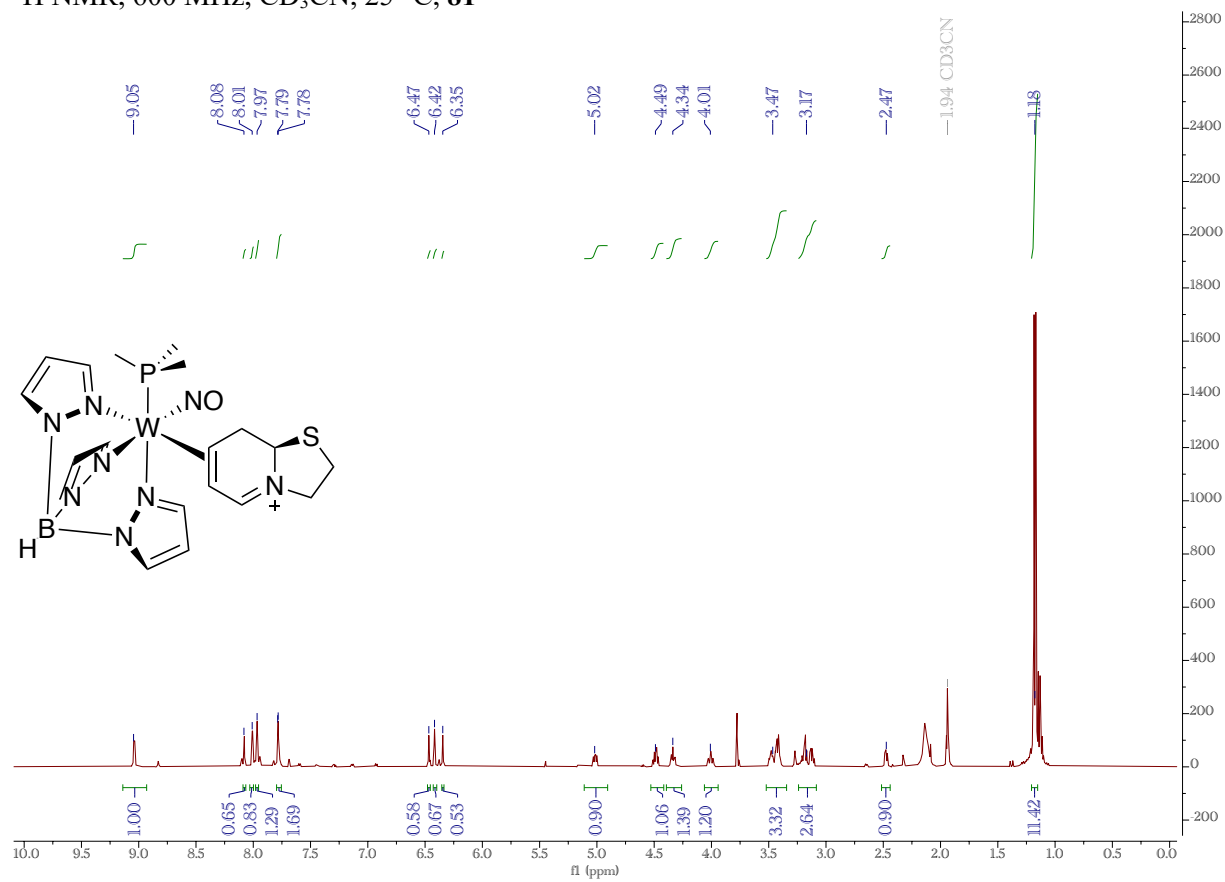
$^1\text{H}$  NMR, 800 MHz,  $\text{CD}_3\text{CN}$ , 25 °C, **80**



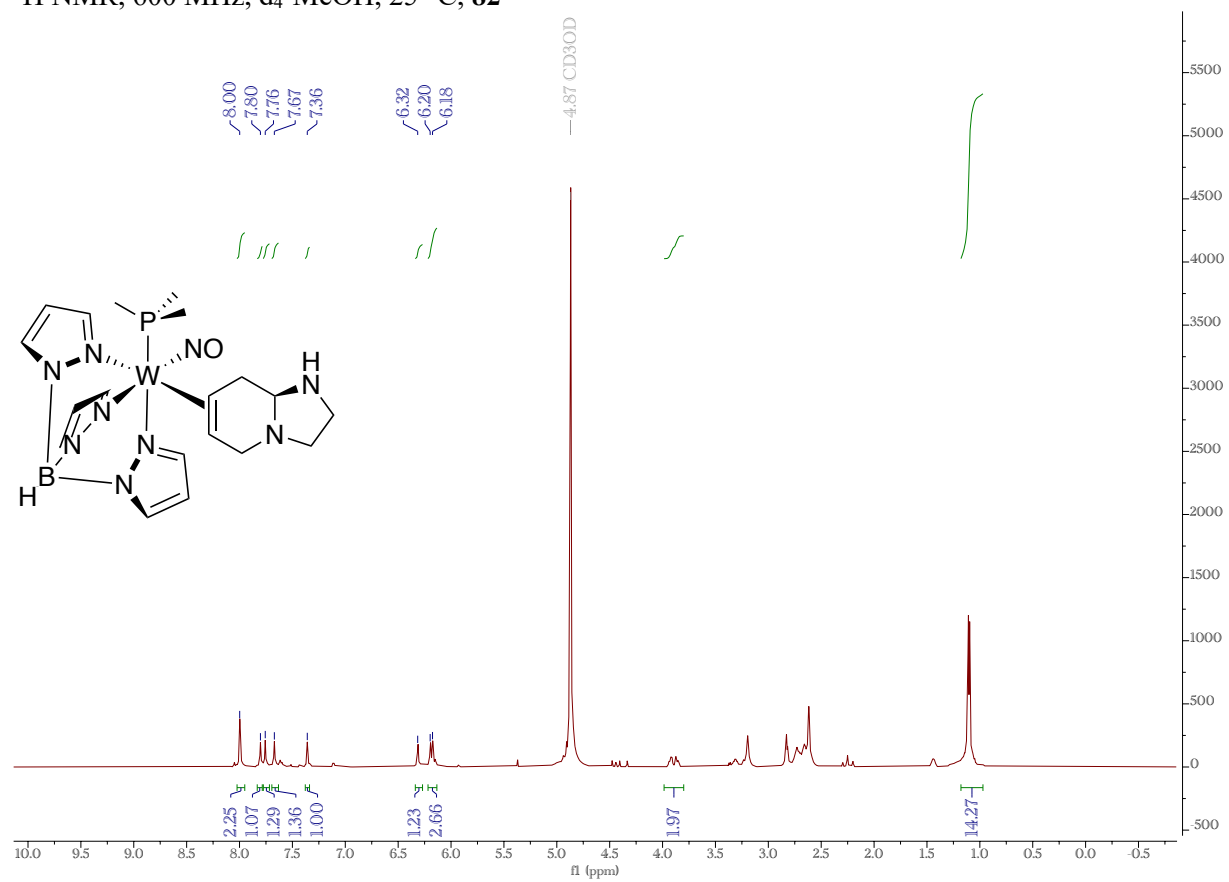
$^{13}\text{C}$  NMR, 200 MHz,  $\text{CD}_3\text{CN}$ , 25 °C, **80**



$^1\text{H}$  NMR, 600 MHz,  $\text{CD}_3\text{CN}$ , 25  $^\circ\text{C}$ , **81**

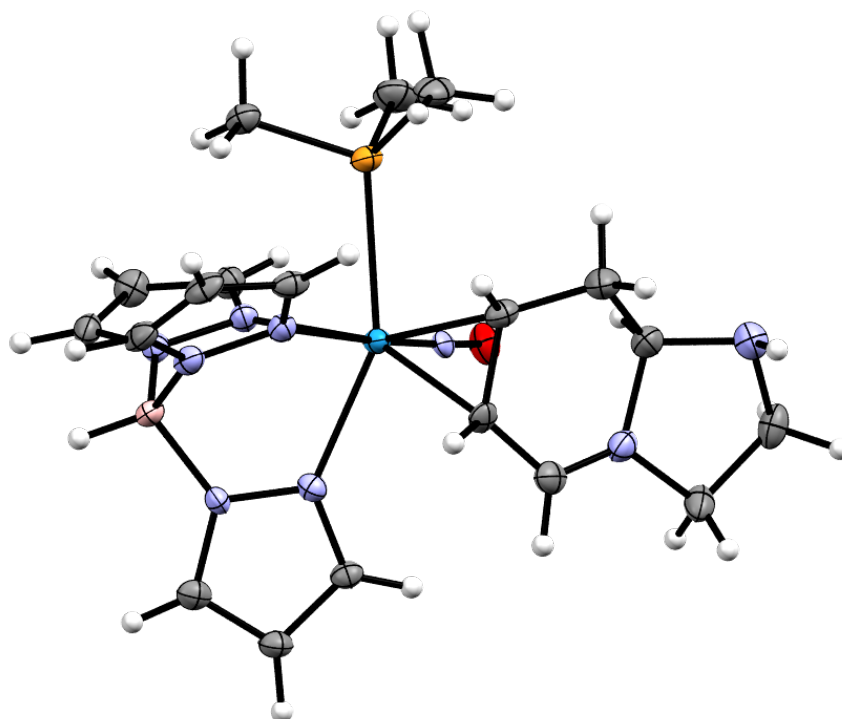


$^1\text{H}$  NMR, 600 MHz,  $\text{d}_4\text{-MeOH}$ , 25  $^\circ\text{C}$ , **82**





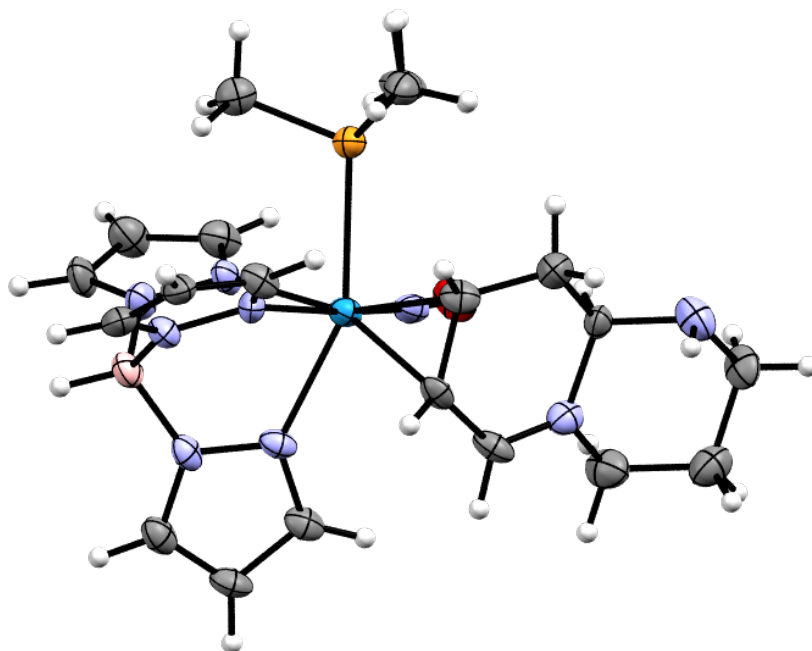
SC-XRD Data:



ORTEP/ellipsoid diagram of **78** (disordered triflate omitted).

SC-XRD data for **78**.

CCDC	Chemical Formula	FW (g/mol)
N/A	$C_{20}H_{30}BF_3N_9O_4PSW$	775.22
T (K)	$\lambda$ (Å)	Crystal size (mm)
100(2)	0.71073	0.046 x 0.067 x 0.090
Crystal habit	Crystal system	Space group
Yellow needle	Monoclinic	$P 2_1/n$
a (Å)	b (Å)	c (Å)
16.1373(6)	10.2833(3)	16.6623(6)
$\alpha$ (°)	$\beta$ (°)	$\gamma$ (°)
90	100.0990(10)	90
V (Å <sup>3</sup> )	Z	$\rho_{calc}$ (g/cm <sup>3</sup> )
2722.18(16)	4	1.892
$\mu$ (mm <sup>-1</sup> )	F(000)	$\theta$ range (°)
4.446	1528	2.34 to 28.28
Index ranges	Data/restraints/parameters	Goodness-of-fit on $F^2$
-21 $\leq h \leq$ 21	6757 / 30 / 394	1.009
-13 $\leq k \leq$ 12		
-22 $\leq l \leq$ 19		
R <sub>1</sub> [ $I > 2\sigma(I)$ ]	wR <sub>2</sub> [all data]	
0.0342	0.0717	



ORTEP/ellipsoid diagram of **79** (triflate omitted).

SC-XRD data for **79**.

CCDC N/A	Chemical Formula $C_{21}H_{32}BF_3N_9O_4PSW$	FW (g/mol) 789.24
T (K) 100(2)	$\lambda$ (Å) 0.71073	Crystal size (mm) 0.051 x 0.059 x 0.114
Crystal habit Orange block	Crystal system Monoclinic	Space group P 2 <sub>1</sub> /n
a (Å) 15.8033(7)	b (Å) 10.6246(4)	c (Å) 17.4770(9)
$\alpha$ (°) 90	$\beta$ (°) 98.4000(10)	$\gamma$ (°) 90
V (Å <sup>3</sup> ) 2903.0(2)	Z 4	$\rho_{calc}$ (g/cm <sup>3</sup> ) 1.806
$\mu$ (mm <sup>-1</sup> ) 4.171	F(000) 1560	$\theta$ range (°) 2.25 to 27.49
Index ranges -20 ≤ h ≤ 18 -12 ≤ k ≤ 13 -22 ≤ l ≤ 18	Data/restraints/parameters 6664 / 0 / 385	Goodness-of-fit on F <sup>2</sup> 1.016
R <sub>1</sub> [I > 2σ(I)] 0.0557	wR <sub>2</sub> [all data] 0.1314	